

UNIVERSAL  
LIBRARY

**OU\_166867**

UNIVERSAL  
LIBRARY







OSMANIA UNIVERSITY LIBRARY

Call No. 669 / 177417 / Accession No. 25980

Author Mondolfo, L. F.

Title Metallography of aluminum and

This book should be returned on or before the date last marked below.



# Metallography of Aluminum Alloys

*By*

Lucio F. Mondolfo

JOHN WILEY & SONS, INC. • NEW YORK

LONDON • CHAPMAN & HALL, LIMITED

THIS BOOK HAS BEEN MANUFACTURED IN  
ACCORDANCE WITH THE RECOMMENDATIONS  
OF THE WAR PRODUCTION BOARD IN THE  
INTEREST OF THE CONSERVATION OF PAPER  
AND OTHER IMPORTANT WAR MATERIALS.

COPYRIGHT, 1943  
BY  
LUCIO F. MONDOLFO

---

*All Rights Reserved*

*This book or any part thereof must not  
be reproduced in any form without the  
written permission of the publisher.*

PRINTED IN THE UNITED STATES OF AMERICA

## PREFACE

In the last few years, a continuous development in the use of aluminum alloys has steadily increased the number of metallurgists interested in them. Because of this growing interest and the fact that the most recent books on the subject are now somewhat outdated, it was believed that a new book could be useful. Since many books on the general metallurgy are available, this book has been limited purposely to aluminum alloys. It is intended for consultation by the plant metallurgist, rather than as a textbook for students. For these reasons no details are given on general metallurgy and metallography and most of the theoretical problems have not been treated at all or have been dismissed briefly.

The first part of the book illustrates the equilibrium diagrams of aluminum alloys. All information about binary, ternary, and quaternary diagrams published up to date has been sifted, coordinated, and often integrated with data from the author's experiments, to eliminate the discrepancies between the different authors. Usually the discrepancies are only minor, but at times they are so wide that it has been necessary to report two sets of diagrams. Whenever possible the equilibrium diagrams have been reported graphically, limiting the text to facts about solid solubilities, eutectic and peritectic temperatures, crystal structures, etc., which could not be represented adequately in the diagrams. Most of the diagrams are only partial, because, when the complete diagram has not been established beyond doubt, it seemed better not to crowd the book with doubtful details which have no interest for commercial alloys. The same criterion has been applied to the bibliography, which is as complete as possible for the aluminum end of the diagrams but disregards investigations limited to alloys with low aluminum contents. Data about the structures in non-equilibrium conditions caused by rapid cooling have been included whenever possible, and most of these are from experiments by the author, since very little has been published. The scarcity of published material is all the more regrettable as facts about non-equilibrium are often more useful than those about equilibrium conditions.

The second part is dedicated to the technique of macro- and micro-examination. The polishing technique, including electrolytic polishing and a new fast method developed by the author, is here described. The etching reagents and their technique are also discussed in this part, and a list of the constituents, formed by the alloying elements, is illustrated with carefully selected photo-micrographs to show their typical aspects in commercial alloys.\*

The third part shows the normal structure of the commercial alloys of aluminum. To give as complete a picture of the aluminum field as possible, the alloys commonly used abroad have been included, in addition to those used in the United States. The alloys have been grouped in accordance to their main alloying elements and their general uses and properties are briefly discussed. The eutectics commonly present in the alloys are listed. Great care has been taken to identify for each alloy the lowest melting eutectics; probably less accurate are the data about the high melting point eutectics.

The fourth part discusses the effect of fabricating on the microstructure, with references to macrostructure and actual practices, when they are necessary for a better understanding of the microstructure. Rather than a complete list of the effects of these operations on the structure, which would be almost impossible, this part is intended to show how to interpret the microscopic results and to serve as a guide in the thousands of different problems which arise every day in the aluminum industry. With the examples of normal operations, some examples of the most common defects arising from improper technique are given.

The author is fully aware that some of the parts are overemphasized and some underemphasized; this has sometimes been intentional. Some inaccurate data may have been included, and the author will appreciate being informed of any errors and of the need for additional information.

The author acknowledges with gratitude the help and collaboration received during the preparation of this book. Particular thanks are due to T. L. Fritzlen and V. F. Flaherty, Reynolds Metals Company, and to Kurt R. Gustavsen, Extruded Metals Defense Corp., for the help and constructive criticism offered; to Professor A. H. Carpenter, Illinois Institute of Technology, for reading and correcting the manuscript, and to Mrs. L. Mondolfo for the help and assistance proffered.

\* These photo-micrographs, as all other photo-micrographs in the book, are original and mostly unpublished.

Thanks are also due to the U.S. Reduction Co., East Chicago, Indiana, and to R. Lavin and Sons, Inc., Chicago, for permission to publish photo-micrographs taken in their laboratories. Grateful acknowledgment is also made to all the authors who gave permission to use data from their work and to all those authors whose permissions could not be secured because of the present war conditions.

LUCIO F. MONDOLFO

*June, 1943*





## CONTENTS

### *PART I EQUILIBRIUM DIAGRAMS*

CHAPTER	PAGE
1 Binary Diagrams . . . . .	1
2 Ternary Diagrams . . . . .	53
3 Quaternary Diagrams . . . . .	123

### *PART II POLISHING AND ETCHING*

4 Macro-Examination . . . . .	140
5 Polishing . . . . .	151
6 Etching . . . . .	164
7 Constituents. . . . .	173

### *PART III COMMERCIAL ALLOYS*

8 Master Alloys . . . . .	202
9 Aluminum-Copper Alloys . . . . .	211
10 Aluminum-Silicon Alloys . . . . .	226
11 Corrosion-Resistant Alloys . . . . .	237
12 Duralumin . . . . .	249
13 Aluminum-Copper-Nickel Alloys . . . . .	257

### *PART IV EFFECT OF FABRICATING ON THE MICROSTRUCTURE*

14 Melting, Fluxing, Pouring, Casting. . . . .	266
15 Working . . . . .	290
16 Heat Treatment . . . . .	295
17 Corrosion and Protection . . . . .	310
Bibliography . . . . .	317
Index . . . . .	345



# PART I

## EQUILIBRIUM DIAGRAMS

### CHAPTER 1

#### BINARY DIAGRAMS

##### Al-Ag

##### Aluminum-Silver

The partial equilibrium diagram (Fig. 1) is from data by Hansen (39),\* Crepaz (40), Tischenko (42), and Barrett and colleagues (49).

Silver is soluble to a large extent in aluminum at the eutectic temperature. The solid solubility decreases with decreasing temperature as reported below.

558°C	1036°F	48.00% Ag
500°C	932°F	33.00% Ag
450°C	832°F	21.00% Ag
400°C	752°F	12.00% Ag
350°C	662°F	6.50% Ag
300°C	572°F	3.25% Ag
250°C	482°F	1.75% Ag
200°C	392°F	0.75% Ag
20°C	68°F	0.50% Ag approx.

The eutectic  $E = \text{Al}-\beta(\text{AlAg})$  is at 558°C (1036°F) and contains 73.5 per cent silver. The phase  $\beta(\text{AlAg})$ , which is the constituent in equilibrium with aluminum, contains 85 to 90 per cent silver and is probably an intermediate solid solution. It has a close-packed hexagonal structure with lattice parameters  $a = 2.879 \text{ \AA}$ ,  $c = 4.573 \text{ \AA}$ , when it contains 85 per cent silver. Another form of  $\beta(\text{AlAg})$  is known, also with close-packed hexagonal structure, with lattice parameters  $a = 2.858 \text{ \AA}$ ,  $c = 4.607 \text{ \AA}$ . This phase is formed during reprecipitation and is considered a transition phase between the supersaturated solid

\* Numbers in parentheses refer to references listed in the Bibliography at the end of the book.

solution and the regular  $\beta(\text{AlAg})$ . At the silver end of the diagram several other phases are present, but, since they have not been positively identified, no further data are reported.

Aluminum-silver alloys have very little commercial importance. The slight increase in mechanical properties, obtained through additions of silver to aluminum alloys, is not sufficient to pay for the high cost of silver, especially because the same improvement can be made by the

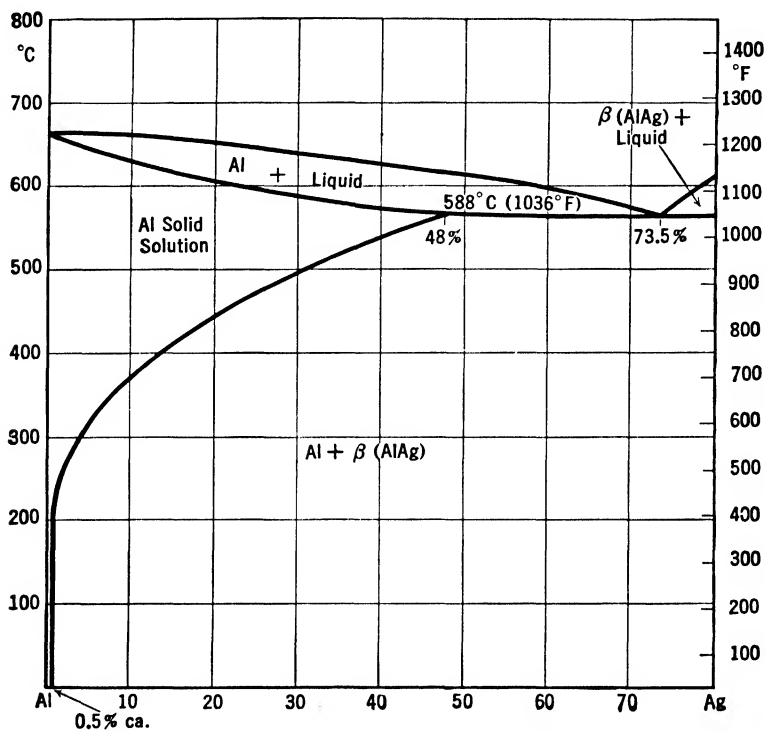


FIG. 1. System Al-Ag, aluminum end of the equilibrium diagram.

addition of copper or magnesium or any other metal soluble in solid aluminum.

### Al-As

#### Aluminum-Arsenic

A few experimenters (51-52) have tried to prepare aluminum-arsenic alloys but without success.

By reaction between molten aluminum and arsenic vapors the compound  $\text{AsAl}$  and perhaps also  $\text{As}_2\text{Al}_3$  can be formed. These compounds, however, do not dissolve in aluminum to any appreciable extent either in the liquid or in the solid state. The mixture of aluminum and the

compounds cannot be considered an alloy; moreover, the compounds are unstable and in the presence of moisture tend to decompose.

Arsenic is not used at all as an alloying element in aluminum; its presence in aluminum alloys is considered harmful but is seldom detected in very small amounts in low-grade secondary materials.

## Al-Au

### Aluminum-Gold

Figure 2 is drawn from data by Bornemann (56), Heycock and Neville (57), West and Peterson (59), and Coffinberry and Hultgren (60).

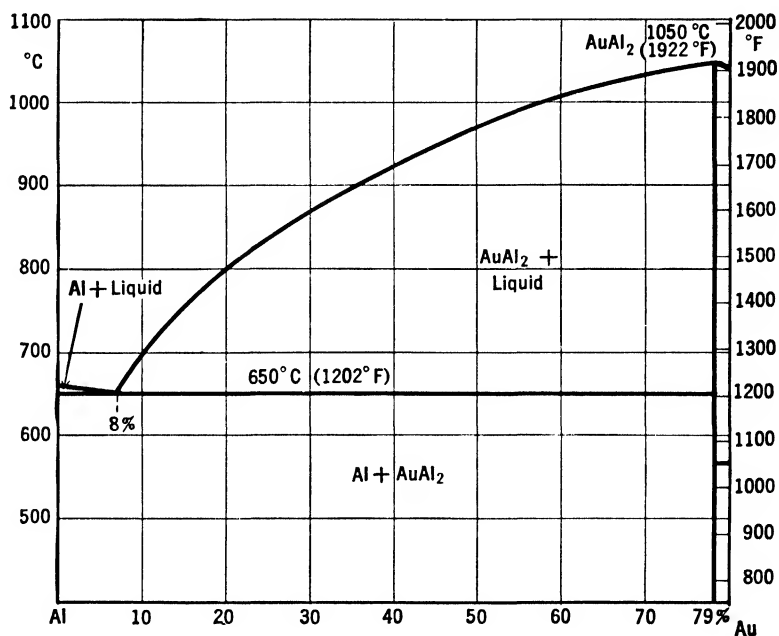


FIG. 2. System Al-Au, aluminum end of the equilibrium diagram.

Gold is not soluble in solid aluminum to any appreciable extent, the solid solubility being approximately 0.02 per cent gold at the eutectic temperature. The constituent in equilibrium with Al is AuAl<sub>2</sub>, which has a face-centered cubic structure with lattice parameter  $a = 5.9868$  Å, and 12 atoms in the unit cell. A eutectic  $E$  between Al and AuAl<sub>2</sub> is formed at 650°C (1202°F) and contains 8 per cent gold. The gold end of the diagram is rather complex and contains several phases which are not given as they are only partially known.

No aluminum-gold alloys are used commercially; the high price of gold makes its use in light alloys impossible, and alloys with high gold content have not been used to any appreciable extent.

**Al-B****Aluminum-Boron**

The diagram (Fig. 3) is from data by Hofmann and Jaeniche (64) and Halla and Weil (65).

Boron is not soluble in solid aluminum to any appreciable extent; the solid solubility at the eutectic temperature is below 0.05 per cent boron.

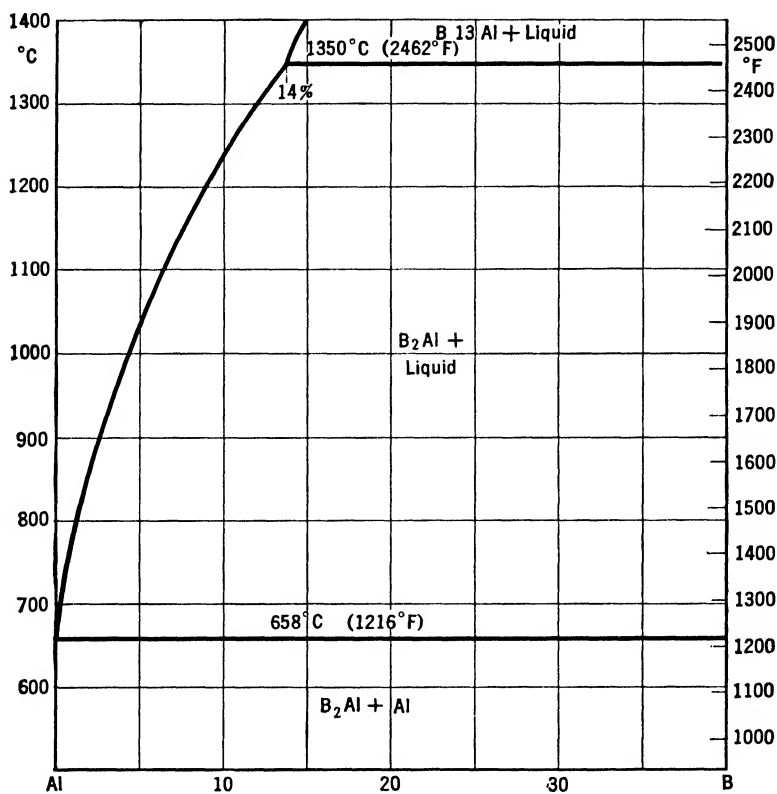


FIG. 3. System Al-B, aluminum end of the equilibrium diagram, according to Hofmann and Jaeniche.

The constituent in equilibrium with Al is B<sub>2</sub>Al, which forms hexagonal crystals with lattice parameters  $a = 3.00$  Å,  $c = 3.24$  Å, and 3 atoms in the unit cell. The eutectic Al-B<sub>2</sub>Al almost coincides with pure Al as to both composition and melting point. From the aluminum end up to 14 per cent boron, B<sub>2</sub>Al forms primary crystals at increasing temperatures; upward from 14 per cent boron, it is formed at 1350°C (2462°F) by peritectic reaction between B<sub>13</sub>Al and the liquid. B<sub>13</sub>Al forms monoclinic crystals with lattice parameters  $a = 17.01$  Å,  $b = 10.98$  Å,  $c = 18.80$  Å, and 448 atoms in the unit cell.

Another Al-B diagram (Fig. 4), completely different from the one reported above, has been published by Haenni (63).

His diagram shows a eutectic Al-B<sub>2</sub>Al at 15 to 18 per cent boron, with a melting point of 565°C (1049°F). The solid solubility of boron in aluminum is reported as 1.7 per cent at the eutectic temperature, decreasing with decreasing temperatures. B<sub>2</sub>Al is reported to form

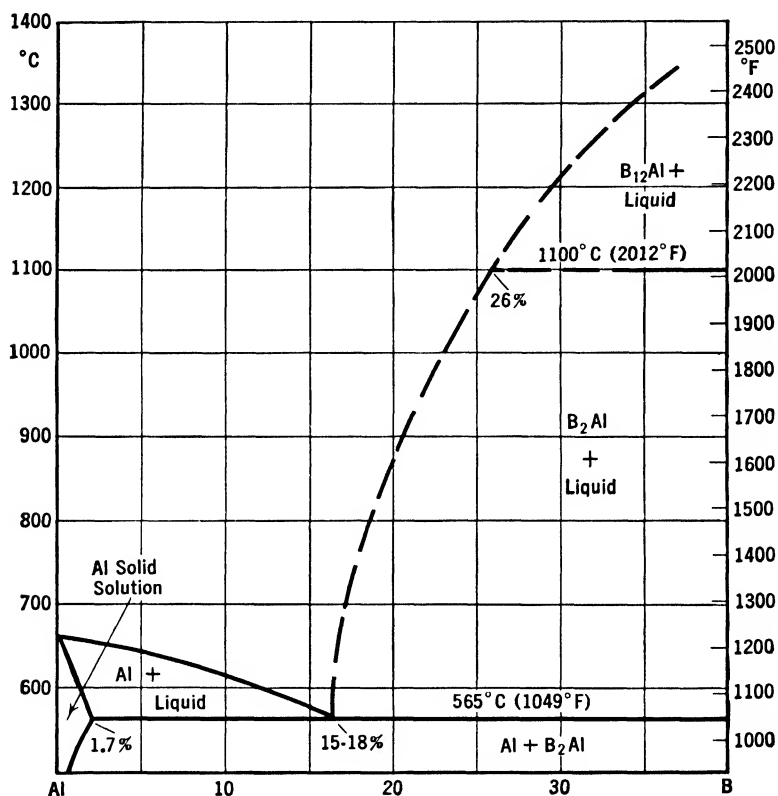


FIG. 4. System Al-B, aluminum end of the equilibrium diagram, according to Haenni.

primary crystals from the eutectic temperature to about 26 per cent boron, where it is formed by peritectic reaction between B<sub>12</sub>Al and the liquid.

Although the first diagram reported seems to be the most probable, there is not sufficient evidence to discard Haenni's diagram; additional investigations are necessary before the point can be considered as thoroughly established.

Boron as an alloying element for aluminum is used little if at all. It is difficult to alloy with aluminum and does not seem to improve aluminum alloys. Sometimes it has been used as a grain refiner and



has been claimed to modify the aluminum-silicon alloys, but there are no grounds for this assertion. At present, for patent reasons, it is added only rarely to some alloys of the aluminum-silicon type in amounts up to 0.10 per cent.

## Al-Ba

### Aluminum-Barium

The only data available on this diagram (Fig. 5) are those reported by Alberti and Andress (66-67).

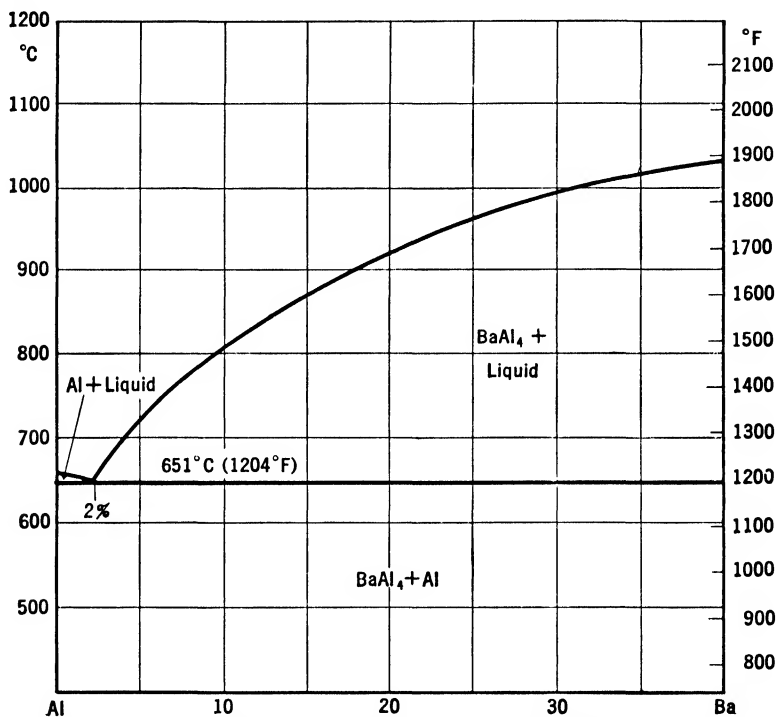


FIG. 5. System Al-Ba, aluminum end of the equilibrium diagram.

The solid solubility of barium in aluminum is negligible. The phase in equilibrium with Al is  $\text{BaAl}_4$ , which contains 56.01 per cent barium and melts at 1050°C (1922°F). It crystallizes in tetragonal form, body-centered, with lattice parameters  $a = 4.53 \text{ \AA}$ ,  $c = 11.14 \text{ \AA}$ . The eutectic  $E$  between Al and  $\text{BaAl}_4$  is formed at 2 per cent barium and has a melting point of 651°C (1204°F). No data are available for barium contents above 56 per cent.

Aluminum-barium alloys are of no practical interest. The tendency of barium to oxidize makes it difficult to handle. To the author's knowledge no aluminum-barium alloys have ever been used, although probably some hundreds of them have been patented.

**Al-Be****Aluminum-Beryllium**

The diagram (Fig. 6) is from data of Oesterheld (68), Mikheeva (77), and Sawyer (78).

No compound is formed between aluminum and beryllium, the phases present are Al and Be, forming a eutectic at 0.5 to 0.7 per cent

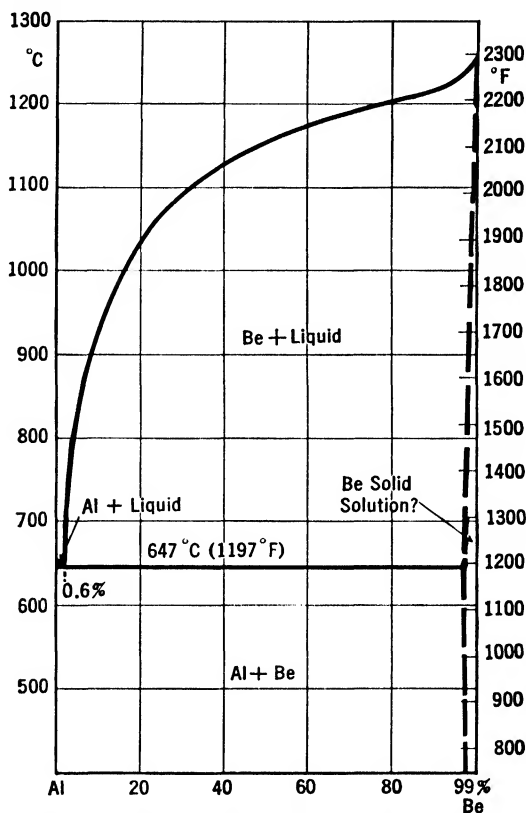


FIG. 6. System Al-Be, equilibrium diagram.

beryllium with a melting point of 647°C (1197°F). The solid solubility and eutectic composition are variably reported by different authors; the higher values reported probably resulted from the use of an erroneous method of analysis. The most reliable values for the solid solubility are:

647°C	1197°F	0.05% Be
630°C	1166°F	0.035% Be
600°C	1112°F	0.020% Be
500°C	932°F	0.005% Be

The beryllium end of the diagram is little known. According to the latest investigations aluminum is soluble in solid beryllium in amounts

of about 1 per cent, and the solid solubility probably decreases with decreasing temperatures.

No commercial aluminum-beryllium alloy is used. Wonders were expected from the addition of beryllium to aluminum and a great deal of research was expended on these alloys. Unfortunately, the hoped for improvements failed to develop because additions of beryllium increase the tensile strength of aluminum only slightly and there is a large decrease in elongation. From the equilibrium diagram it can be seen that the mechanical properties to be expected will not be much above those of the two pure metals, for the solid solubility is very limited and no compound is formed. Alloys with high beryllium contents seem to be of some interest now, but further investigation is necessary before their commercial value can be determined.

### Al-Bi

#### Aluminum-Bismuth

The partial diagram (Fig. 7) is from data by Gwyer (85) and Kempf and Van Horn (88).

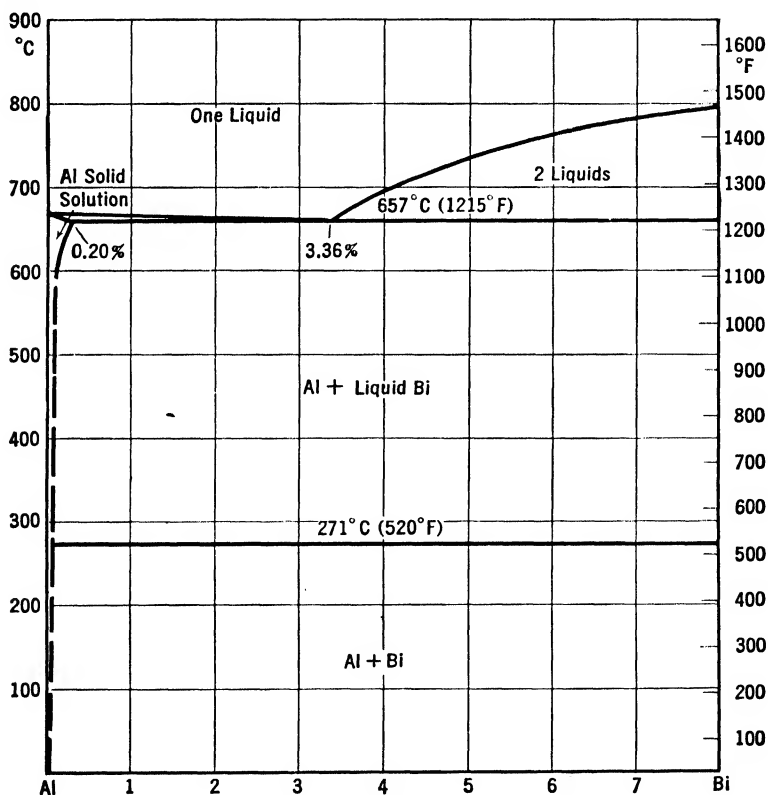


FIG. 7. System Al-Bi, aluminum end of the equilibrium diagram.

Bismuth and aluminum do not form compounds and their miscibility in the liquid state is limited. Additions of bismuth lower the melting point of aluminum from 660°C (1220°F) to 657°C (1215°F). At this temperature the solid solubility of bismuth in aluminum is about 0.20 per cent and probably decreases with decreasing temperatures. The miscibility in the molten state increases with increasing temperatures and, from a minimum of 3.36 per cent bismuth at 657°C (1215°F), reaches 15 per cent bismuth at 877°C (1611°F) and goes on, increasing rapidly. The immiscibility at lower temperatures extends almost to the bismuth end, where a limited zone of miscibility exists, similar to that at the aluminum end.

Aluminum alloys containing bismuth have only recently entered the commercial field. The addition of bismuth, which is accompanied by additions of lead, is intended to improve the machinability. Bismuth has been selected in preference to several other elements because it shrinks in melting and compensates for the dilatation of lead. For this reason the melting of the bismuth and lead during hot working does not tend to crack the alloy, for no appreciable change in volume is produced.

## Al-Ca

### Aluminum-Calcium

The diagram (Fig. 8) is from data by Doan (96) and Nowotny and colleagues (100).

Calcium is soluble in aluminum to a certain extent. The solid solubilities at various temperatures are given below.

616°C	1141°F	2.80% Ca
400°C	752°F	2.20% Ca
300°C	572°F	1.70% Ca

The constituent in equilibrium with Al is  $\text{CaAl}_4$ , tetragonal body-centered, with lattice parameters  $a = 4.35 \text{ \AA}$ ,  $c = 11.07 \text{ \AA}$ . The eutectic between Al and  $\text{CaAl}_4$  is at 8.1 per cent calcium and has a melting point of 616°C (1141°F).  $\text{CaAl}_4$  forms primary crystals from the eutectic up to 15 per cent calcium; then it is formed by peritectic reaction at 700°C (1292°F) between  $\text{CaAl}_2$  and the liquid.  $\text{CaAl}_2$  has a face-centered cubic structure with a lattice parameter  $a = 8.02 \text{ \AA}$  and 24 atoms in the unit cell.

Calcium has sometimes been used as a scavenger for aluminum alloys, but with doubtful results. Its addition has also been proposed to improve the electrical conductivity of commercial aluminum (see Al-Ca-Si diagram). Recently the use of rolled aluminum-calcium alloys for cladding duralumin has been proposed. The calcium in the

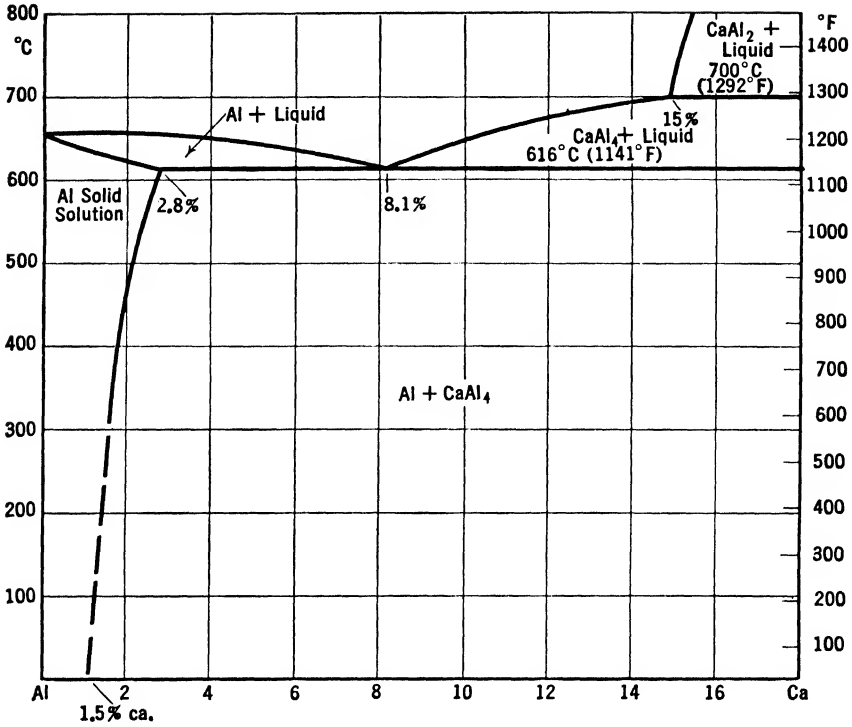


FIG. 8. System Al-Ca, aluminum end of the equilibrium diagram.

aluminum should have the effect of opposing diffusion of copper into the cladding. No reliable data are available at present on this use.

### Al-Cb

#### Aluminum-Columbium

Investigations on this system are very limited. According to Brauer (104), a compound  $\text{CbAl}_3$  is formed, which forms tetragonal crystals with lattice parameters  $a = 5.427 \text{ \AA}$ ,  $c = 8.584 \text{ \AA}$ . Probably the equilibrium diagram for aluminum-columbium is very similar to that of aluminum-titanium.

Columbium, sometimes called niobium (Nb), has been used in aluminum alloys as a grain refiner, but there seems to be no special reason to prefer it to titanium for this purpose.

### Al-Cd

#### Aluminum-Cadmium

Figure 9 is compiled from data by Hansen and Blumenthal (109).

Aluminum and cadmium are only partially miscible and do not form any compounds. Cadmium is soluble in solid aluminum up to 0.97

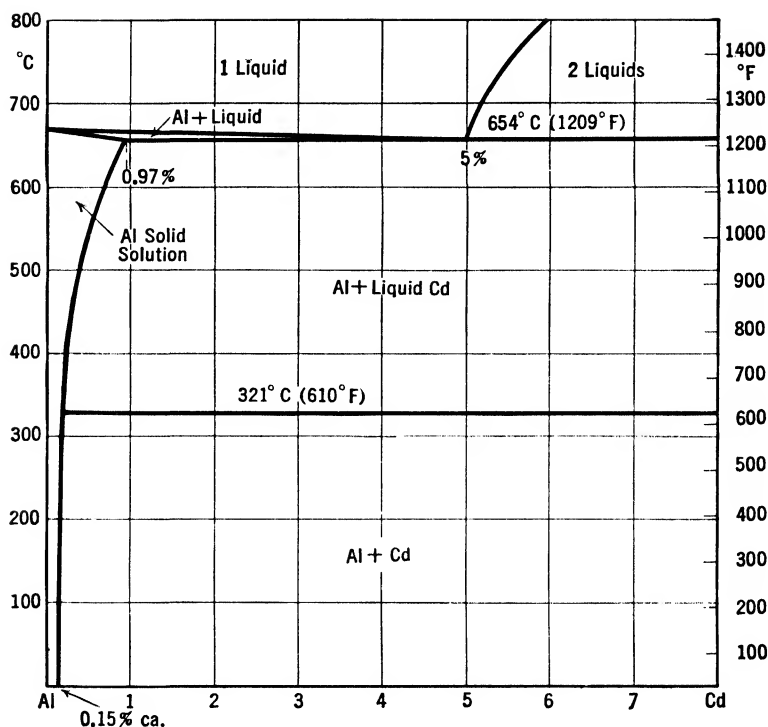


FIG. 9. System Al-Cd, aluminum end of the equilibrium diagram.

per cent cadmium at 654°C (1209°F); the solid solubility decreases with decreasing temperatures and is 0.20 per cent at 150°C (302°F). The limit of miscibility in the liquid state is 5 per cent cadmium at 654°C (1209°F) and the miscibility increases with increasing temperatures. The immiscibility extends almost to the cadmium end, where a small zone similar to the aluminum end exists.

Aluminum-cadmium alloys have been investigated mostly for soldering purposes. Owing to the difficulty of preparing them, due to the low miscibility and owing to their low corrosion resistance, these alloys have not been used commercially to any extent and probably have been completely abandoned.

## Al-Ce

### Aluminum-Cerium

The partial diagram (Fig. 10) is from data by Schulte (113) and Bosshard (116).

The solid solubility of cerium in aluminum is very low and probably about 0.05 per cent at the eutectic temperature. A eutectic, Al- $\alpha$ (CeAl<sub>4</sub>), is formed at 13 per cent cerium 638°C (1180°F). The

first phase at the aluminum end is reported as  $\alpha(\text{CeAl}_4)$ , formed at 33 per cent cerium,  $1005^\circ\text{C}$  ( $1841^\circ\text{F}$ ), by allotropic transformation from  $\beta(\text{CeAl}_4)$ . Several other constituents are present in the diagram, and the cerium end is rather complex.

Aluminum alloys containing small amounts of cerium have been proposed but, since additions of cerium do not produce appreciable

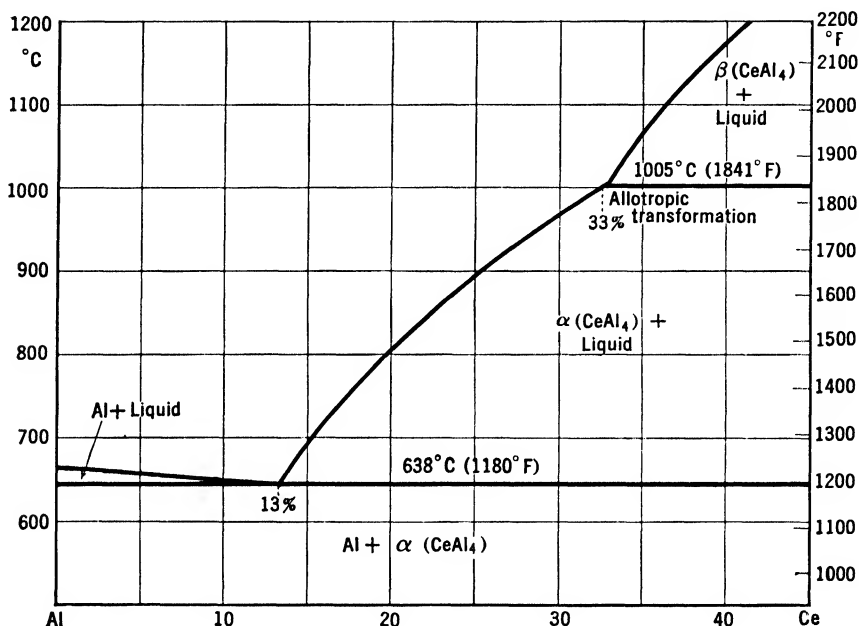


FIG. 10. System Al-Ce, aluminum end of the equilibrium diagram.

improvements, these alloys have never had wide application and, generally speaking, are no longer in use.

## Al-Co

### Aluminum-Cobalt

The partial equilibrium diagram (Fig. 11) is from data by Gwyer (120), Fink and Freche (126), and Bradley and Seager (128).

The solid solubility of cobalt in aluminum is negligible and below 0.02 per cent cobalt at the eutectic temperature  $657^\circ\text{C}$  ( $1215^\circ\text{F}$ ). The eutectic is at about 1 per cent cobalt  $657^\circ\text{C}$  ( $1215^\circ\text{F}$ ) between Al and  $\text{Co}_2\text{Al}_9$ , which is the phase in equilibrium with Al.  $\text{Co}_2\text{Al}_9$  forms primary crystals from the eutectic up to about 20 per cent cobalt and about  $1000^\circ\text{C}$  ( $1832^\circ\text{F}$ ); then it is formed by peritectic reaction from some other phase, richer in cobalt, which has been tentatively identified as  $\text{Co}_4\text{Al}_{13}$ . Above 20 per cent cobalt the diagram is complex and con-

tains several phases. Because the data about them are incomplete and doubtful, they will not be reported here.

Cobalt is used sometimes as an alloying element for aluminum, especially in aluminum-silicon alloys. The reason for its use in these alloys is that it combines with the iron to form a ternary phase (see Al-Co-Fe

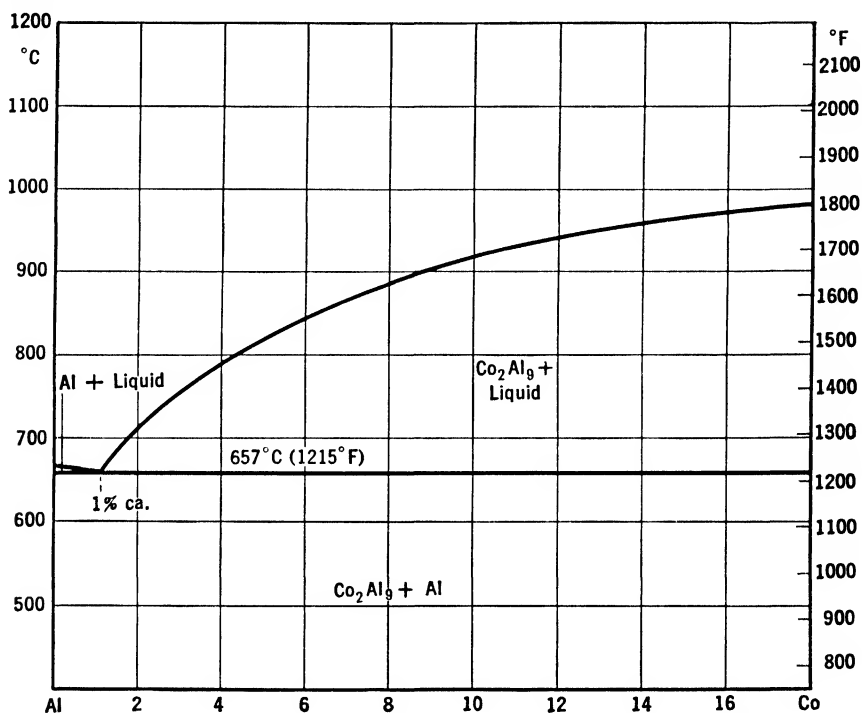


FIG. 11. System Al-Co, aluminum end of the equilibrium diagram.

diagram), hindering the formation of  $\text{FeSiAl}_5$  (see Al-Fe-Si diagram) which, when present in large amounts, makes the alloy brittle.

## Al-Cr

### Aluminum-Chromium

The partial diagram (Fig. 12) is from data by Bradley and Lu (139), Fink and Freche (136), Koch and Winterhagen (140), and Hofmann and Herzer (141).

The solid solubility of chromium in aluminum is given below.

661°C	1222°F	0.87% Cr *
600°C	1112°F	0.56% Cr
500°C	932°F	0.30% Cr
275°C	527°F	0.10% Cr

\* More recently Knappwost and Nowotny (142) have reported a solid solubility at peritectic temperature of 3.1 per cent, but this value seems excessive and needs confirmation.



In Fig. 13 the aluminum end is shown in detail, with the solid solubilities at different temperatures. Up to 0.40 per cent chromium, aluminum with chromium in solid solution forms primary crystals. From there on,  $\text{CrAl}_7$  forms primary crystals at increasing temperatures and a peritectic reaction takes place at  $661^\circ\text{C}$  ( $1222^\circ\text{F}$ ), by which some of

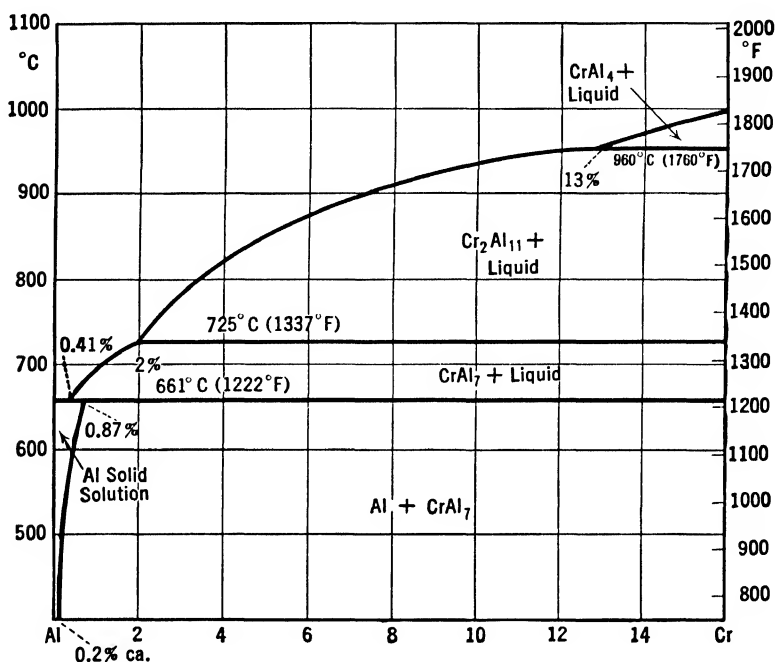


FIG. 12. System Al-Cr, aluminum end of the equilibrium diagram.

the  $\text{CrAl}_7$  goes into solid solution in the aluminum, saturating it at 0.87 per cent chromium.  $\text{CrAl}_7$  is rhombic with lattice parameters  $a = 19.99 \text{ \AA}$ ,  $b = 34.51 \text{ \AA}$ ,  $c = 12.47 \text{ \AA}$ , and contains 21.6 per cent chromium.  $\text{CrAl}_7$  forms primary crystals up to 2 per cent chromium; then it is formed at  $725^\circ\text{C}$  ( $1337^\circ\text{F}$ ) by peritectic reaction between  $\text{Cr}_2\text{Al}_{11}$  and the liquid.  $\text{Cr}_2\text{Al}_{11}$  forms primary crystals up to 13 per cent chromium; from there on it is formed at  $960^\circ\text{C}$  ( $1760^\circ\text{F}$ ) by peritectic reaction between  $\text{CrAl}_4$  and the liquid. Several other phases are present in the intermediate alloys. The system at the chromium end is complex and only partially known, and since it has no interest for aluminum alloys it is not shown here.

In non-equilibrium conditions that are due to fast cooling,  $\text{Cr}_2\text{Al}_{11}$  is present in alloys containing more than 2 per cent chromium in its typical hexagonal form. In alloys with a lower chromium content the effect of fast cooling is limited to the solid solubility.

Chromium is a minor alloying element for several commercial aluminum alloys. However, as it is accompanied by other alloying elements, the ternary diagrams should be consulted, for chromium tends to combine with other elements to form ternary or quaternary phases.

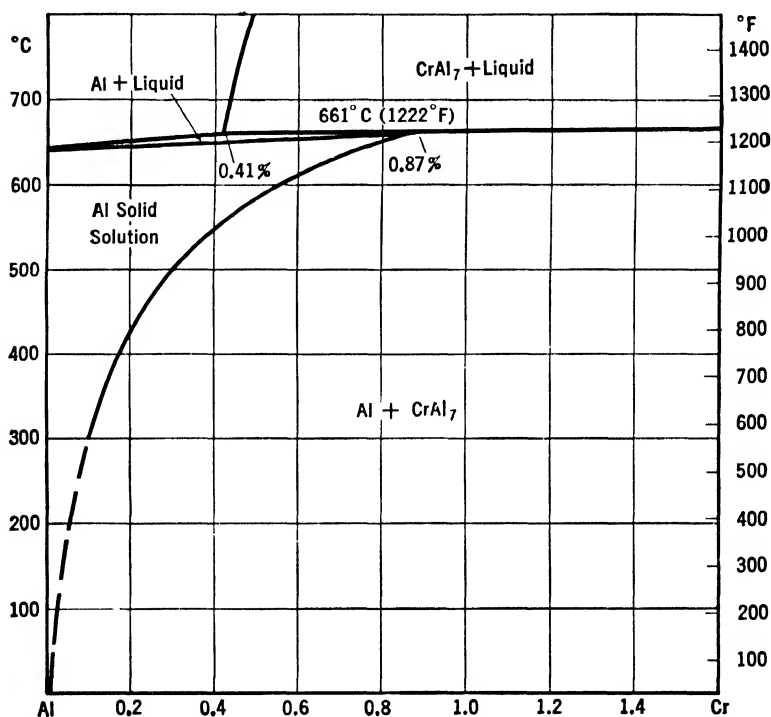


FIG. 13. System Al-Cr, detail of the aluminum end of the equilibrium diagram, showing the solid solubility of chromium in aluminum.

## Al-Cs

### Aluminum-Caesium

The equilibrium diagram (Fig. 14) is from data by Czochralski and Kakzynski (143) and the author.

Caesium and aluminum are almost immiscible in both the liquid and solid state, although a small zone of liquid miscibility exists at the aluminum end, as shown by the dashed line in the diagram.

Caesium has been tried successfully as a modifying agent for aluminum-silicon alloys, but, as it does not offer any advantage over sodium which is less expensive, it has never been used outside the laboratory.

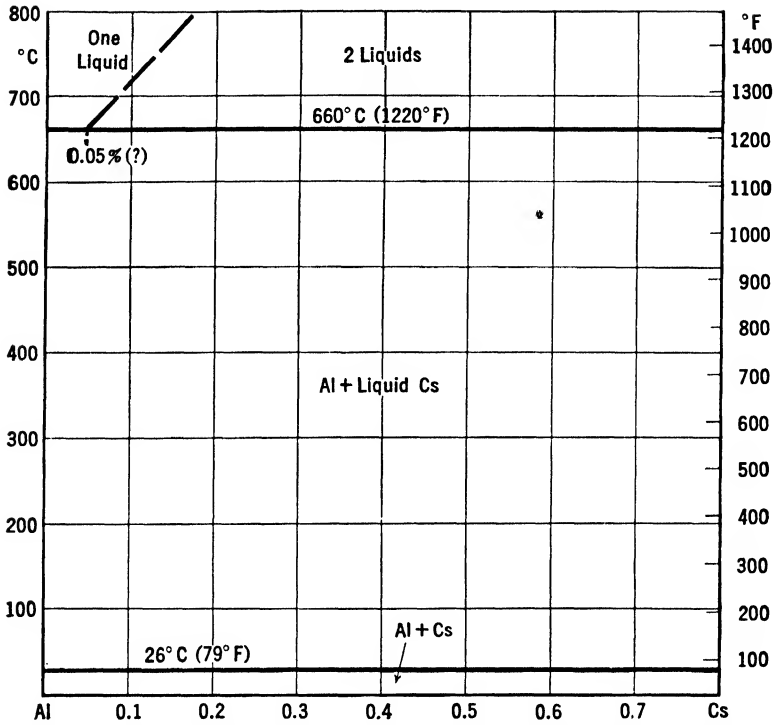


FIG. 14. System Al-Cs, aluminum end of the equilibrium diagram.

## Al-Cu

### Aluminum-Copper

The partial diagrams (Figs. 15 and 16) are from data by Stockdale (168), Bradley and Jones (169), Auer (179), Brownieski and colleagues (182), Wassermann and Weerts (178), and Preston (181).

Copper is soluble to a certain extent in solid aluminum, and its solid solubility decreases with decreasing temperatures. Reported below are the solubilities at various temperatures.

548°C	1018°F	5.65% Cu
525°C	977°F	5.00% Cu
515°C	959°F	4.65% Cu
500°C	932°F	4.00% Cu
450°C	842°F	2.80% Cu
400°C	752°F	1.30% Cu
300°C	572°F	0.50% Cu
20°C	68°F	0.10% Cu approx.*

\* The solid solubility of copper in aluminum usually is reported as 0.25 to 0.30 per cent at room temperature. Theoretical considerations, however, point to a lower value—0.08 to 0.12 per cent.

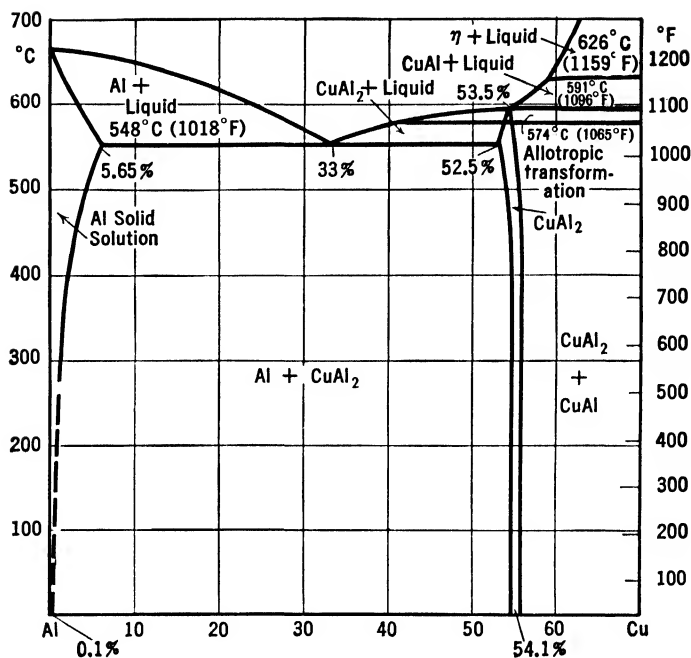


FIG. 15. System Al-Cu, aluminum end of the equilibrium diagram.

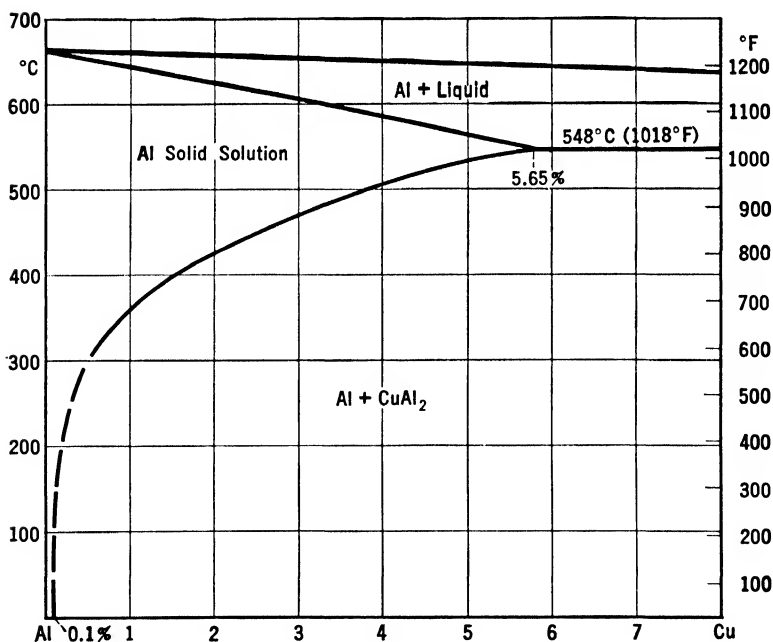


FIG. 16. System Al-Cu, detail of the aluminum end of the equilibrium diagram, showing the solid solubility of copper in aluminum.

Figure 16 gives the aluminum corner in detail, showing the solid solubilities. A eutectic is formed at 33 per cent copper, 548°C (1018°F) between Al and CuAl<sub>2</sub>, which is the first phase at the aluminum end. CuAl<sub>2</sub> at room temperature is tetragonal body-centered, with lattice parameters  $a = 6.054$  Å,  $c = 4.864$  Å, and 12 atoms in the unit cell. It undergoes an allotropic transformation at 574°C (1065°F) with change in volume. Its composition at high temperatures does not correspond with the formula CuAl<sub>2</sub>; it contains from 52.5 per cent copper at 548°C (1018°F) to 53.5 per cent at 591°C (1096°F) instead of the required 54.1 per cent. Another form of CuAl<sub>2</sub> is known: tetragonal with lattice parameters  $a = 8.20$  Å,  $c = 11.6$  Å, or  $a = 5.8$  Å,  $c = 5.71$  Å, depending on the plane considered as basis. This form is the first to precipitate during aging and usually is considered a transition phase between the supersaturated solid solution of copper in aluminum and the regular CuAl<sub>2</sub>.

The effects of non-equilibrium conditions caused by fast cooling are not impressive; the only appreciable change is the amount of copper which remains in solid solution. With commercial casting practice from 2.5 per cent to 4 per cent copper remains in solid solution at room temperature, depending upon the rate of cooling.

Copper is one of the most common alloying elements for aluminum. However, as it is never used alone in commercial alloys, the ternary or quaternary diagrams should be consulted, especially when magnesium or nickel is present.

## Al-Fe

### Aluminum-Iron

The equilibrium diagram (Fig. 17) is from data by Bradley and Taylor (200), Roth (201), and Bachemetew (199).

The solid solubility of iron in aluminum is very low: from 0.03 per cent at the eutectic temperature 655°C (1211°F) it decreases to about 0.01 per cent iron at 200°C (392°F). A eutectic is formed at about 1.8 per cent iron at 655°C (1211°F). The compound at the aluminum end, until recently reported to be FeAl<sub>3</sub>, rhombic with lattice parameters  $a = 47.43$  Å,  $b = 15.46$  Å,  $c = 8.08$  Å, and 96 atoms in the unit cell, has been proved by Bradley and Taylor to be Fe<sub>2</sub>Al<sub>7</sub> below 500°C (932°F). The crystal structure of this phase has not been determined as yet. There is evidence that it is rhombic with an atomic arrangement slightly different from FeAl<sub>3</sub>. The nature of the transformation FeAl<sub>3</sub> → Fe<sub>2</sub>Al<sub>7</sub> has not been established; investigations by the author point to the existence of a peritectic transformation close to the

eutectic temperature  $655^{\circ}\text{C}$  ( $1211^{\circ}\text{F}$ ). There is also evidence of an unstable diagram where the transformation  $\text{FeAl}_3 \rightarrow \text{Fe}_2\text{Al}_7$  is suppressed and the eutectic composition is at about 4 per cent iron, instead of about 1.8 per cent iron. Although in the literature (192–194) some irregularities are reported which could confirm the author's evidence, further investigations are necessary before the point can be considered settled. For this reason Fig. 17 does not embody the proposed changes.

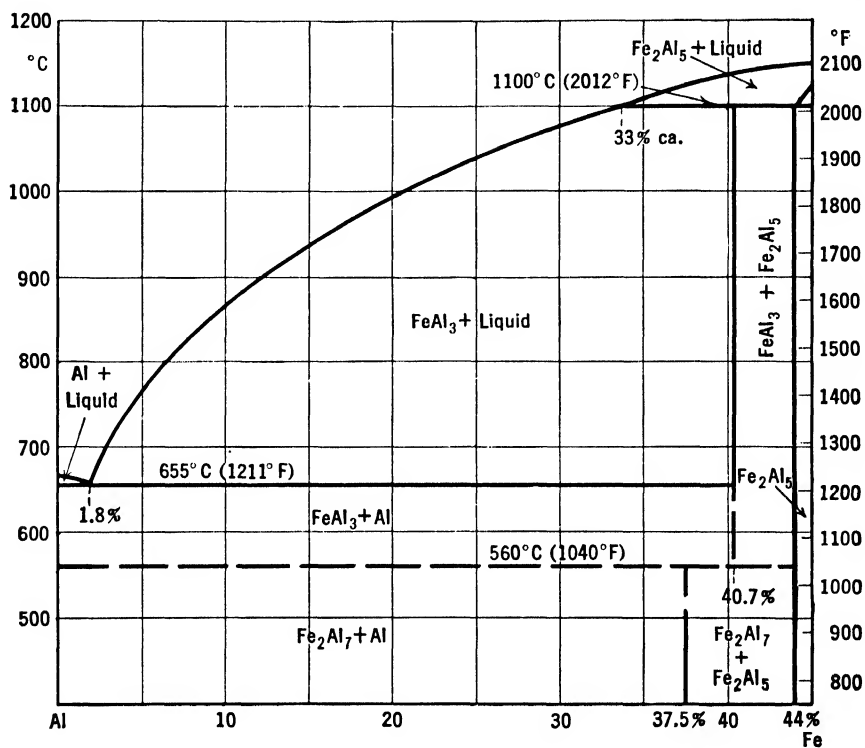


FIG. 17. System Al-Fe, aluminum end of the equilibrium diagram.

In non-equilibrium conditions caused by fast cooling, the transformation  $\text{FeAl}_3 \rightarrow \text{Fe}_2\text{Al}_7$  is commonly suppressed and the iron-containing phase can be seen in the form of star-shaped clusters, typical of  $\text{FeAl}_3$ . Alloys below the eutectic composition are not affected by the cooling rate to any appreciable extent, the only difference being in the size of the crystals.

The aluminum-iron equilibrium diagram has little commercial importance because iron is never present in aluminum alloys alone and most other elements tend to combine with it, forming ternary or quaternary phases. For this reason the ternary or, when available, the quaternary diagrams should be consulted.

**Al-Ga****Aluminum-Gallium**

The equilibrium diagram (Fig. 18) is from data by Jenckel (207), and Pushin and Micic (208).

No intermetallic compound is formed between aluminum and gallium, the eutectic Al-Ga being very near the gallium end of the diagram with

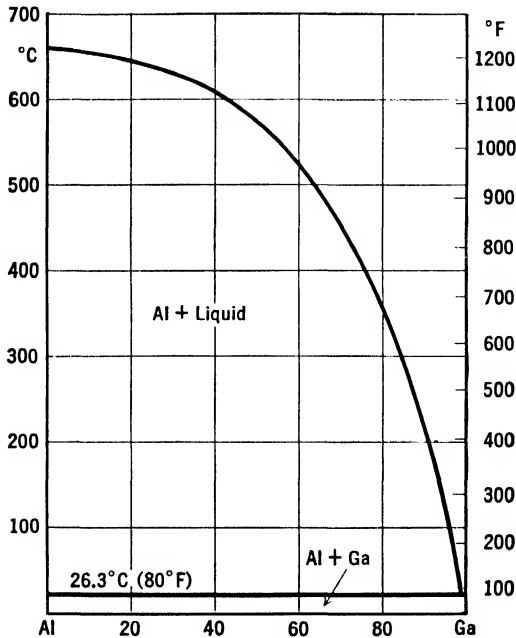


FIG. 18. System Al-Ga, equilibrium diagram.

a melting point of 26.3°C (80°F). The solid solubility of gallium in aluminum is practically zero.

No aluminum alloy containing gallium has ever been used for commercial purposes, and there is no reason to expect any application of aluminum-gallium alloys for structural purposes, for they melt almost at room temperature.

**Al-Ge****Aluminum-Germanium**

The equilibrium diagram (Fig. 19) is from data by Kroll (209) and Stoehr and Klemm (210).

No compound is formed between aluminum and germanium; an Al-Ge eutectic is formed at 53 to 55 per cent germanium, 424°C (795°F).

The solid solubilities of germanium in aluminum are given below.

424°C	795°F	5.00% Ge
393°C	740°F	3.50% Ge
295°C	563°F	0.98% Ge
177°C	351°F	0.38% Ge
20°C	68°F	0.30% Ge

The germanium end of the diagram is little known and is reported in dashed lines.

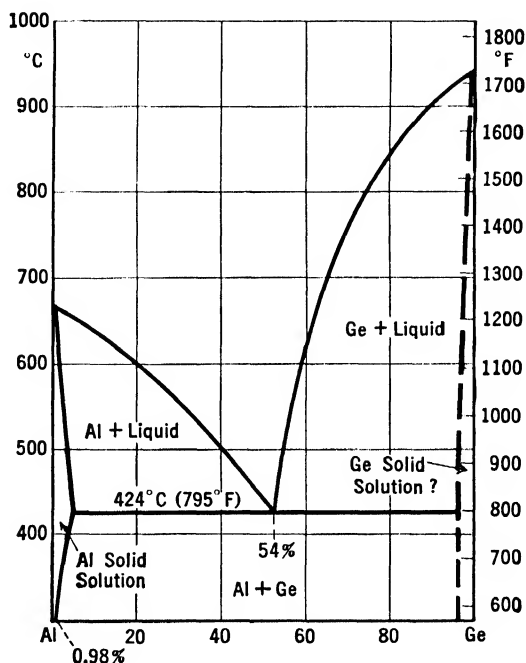


FIG. 19. System Al-Ge, equilibrium diagram.

No aluminum alloy containing germanium has ever been used commercially. The properties of these alloys are similar to those of aluminum-silicon alloys, and there is no reason to expect any commercial application of aluminum-germanium alloys because silicon is less expensive.

## Al-Hg

### Aluminum-Mercury

The equilibrium diagram (Fig. 20) is from data, which seem to be the most reliable among the contradicting material in existence, by Smits and De Gruyter (213).



No compound is formed between aluminum and mercury; the Al-Hg eutectic is almost identical with Hg as regards both composition and melting point. No solid solubility of mercury in aluminum is reported.

Aluminum-mercury alloys, however, are of only theoretical interest, if any. In the presence of moisture, mercury in contact with aluminum

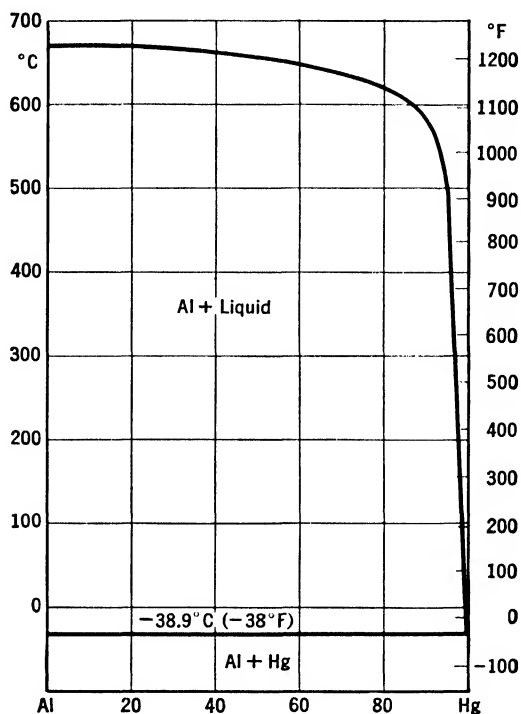


FIG. 20. System Al-Hg, equilibrium diagram.

attacks it readily, yielding  $\text{Al}(\text{OH})_3$  and Hg. For this reason industries using aluminum avoid the use of mercury thermometers as much as possible; even a few droplets of mercury in contact with aluminum destroy it or at least damage it irreparably.

## Al-K

### Aluminum-Potassium

The aluminum-potassium equilibrium diagram has not been investigated recently and the data available are not altogether reliable.

Aluminum and potassium are almost completely immiscible, both in the liquid and solid state, as shown in Fig. 21. In view of the modifying effect of potassium in aluminum-silicon alloys, there must be a

small field of miscibility in the liquid state, probably about the same as the miscibility of sodium and aluminum. The diagram shows this miscibility with a dashed line. The immiscibility extends almost to the potassium end of the diagram, where there is probably another small field of miscibility.

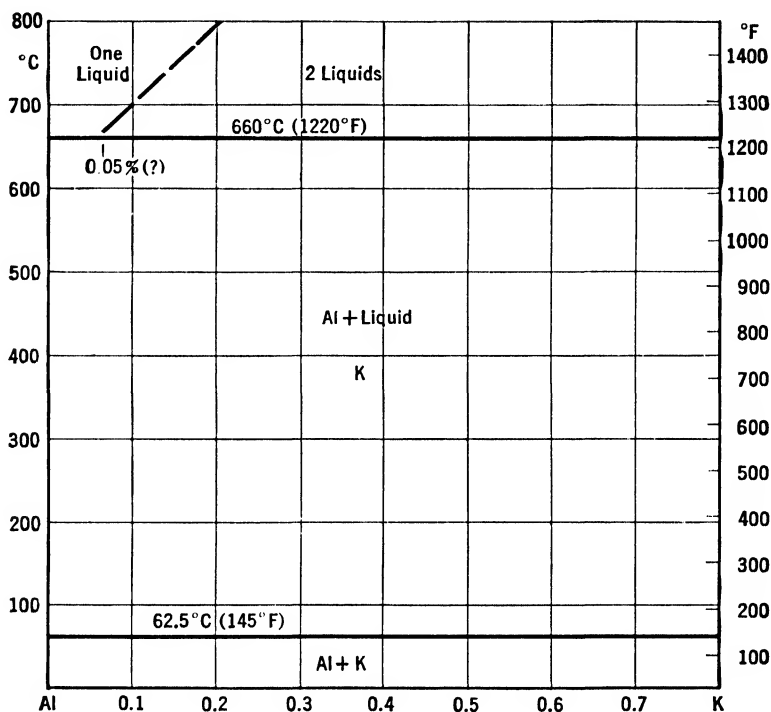


FIG. 21. System Al-K, aluminum end of the equilibrium diagram.

Potassium sometimes is used as a modifying agent for aluminum-silicon alloys but, as it does not offer any advantage over sodium and is more expensive, its use is very limited.

## Al-La

### Aluminum-Lanthanum

The equilibrium diagram (Fig. 22) is from data by Canneri (220), Rossi (221), and Weibke and Schmidt (222).

The solid solubility of lanthanum in aluminum is very limited and practically zero. At the aluminum end there is a eutectic Al-LaAl<sub>4</sub> containing 3 per cent lanthanum and melting at 639°C (1182°F). Two forms of LaAl<sub>4</sub> are reported, with an allotropic transformation taking place at 816°C (1501°F). Several other intermediate phases exist with

higher lanthanum concentrations, but they are not reported because they are of no interest.

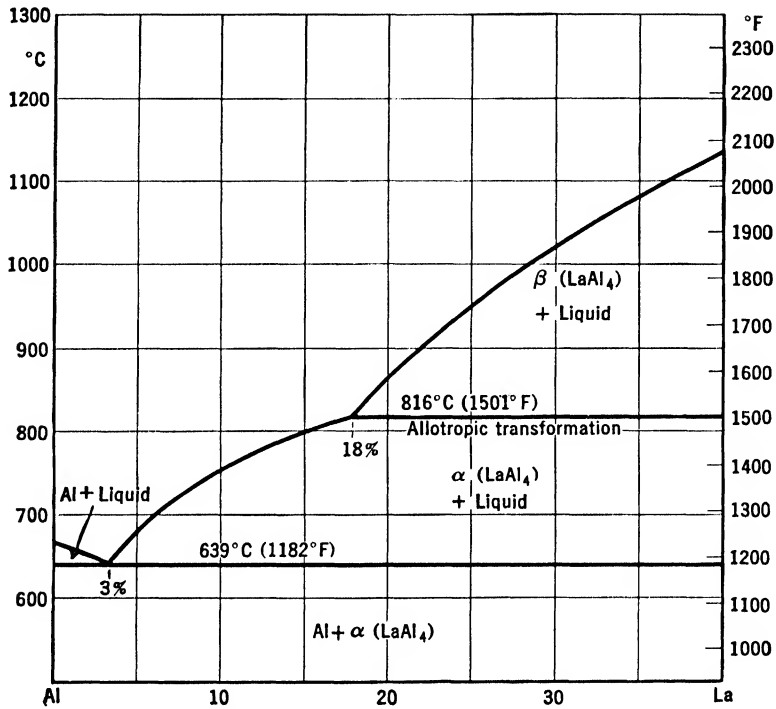


FIG. 22. System Al-La, aluminum end of the equilibrium diagram.

No commercial aluminum alloy containing lanthanum has ever been used, and it is not expected that it will find practical application unless lanthanum can be produced on an industrial scale.

**Al-Li**  
**Aluminum-Lithium**

The equilibrium diagram (Fig. 23) is from data by Assmann (223), Vosskuehler (230), Komovski and Maximow (227), and Shamray and Saldau (231).

The solid solubilities of lithium in aluminum are reported below.

602°C	1116°F	5.2% Li
550°C	1022°F	3.6% Li
500°C	932°F	2.5% Li
400°C	752°F	1.50% Li
220°C	428°F	0.90% Li
20°C	68°F	0.70% Li

A eutectic Al-LiAl is formed at 602°C (1116°F), 7.8 per cent lithium. The compound LiAl, whose field extends from 18 to 23 per cent

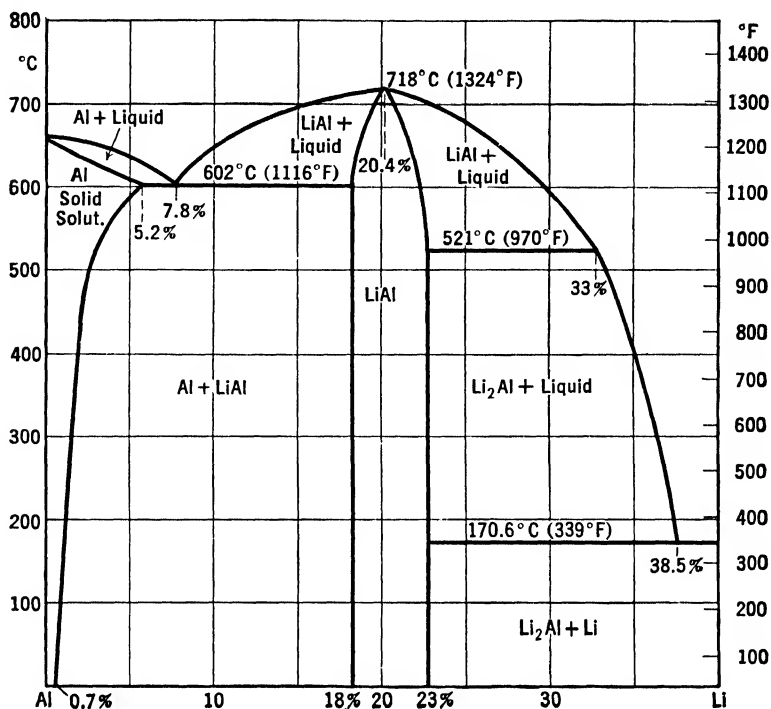


Fig. 23. System Al-Li, aluminum end of the equilibrium diagram.

lithium, has a melting point of 718°C (1324°F) and crystallizes cubic body-centered, with a lattice parameter  $a = 6.37$  Å and 16 atoms in the unit cell. The next compound is  $\text{Li}_2\text{Al}$ , formed by peritectic reaction at 521°C (970°F) from the liquid and LiAl. The eutectic  $\text{Li}_2\text{Al}$ -Li is at 38.5 per cent lithium, 170.6°C (339°F). From this point no new phases are formed and the upper melting point raises slowly until it reaches 179°C (354°F) at 100 per cent lithium.

Lithium sometimes has been used as an alloying element for aluminum; but, on account of the difficulties involved in its use and on consideration of the negligible improvement which it makes in aluminum alloys, no wide application of aluminum-lithium alloys is to be expected.

## Al-Mg

### Aluminum-Magnesium

The equilibrium diagrams (Figs. 24 and 25) have been plotted from the data by Hanson and Gayler (239), Siebel and Vosskuehler (269), and Laves and Moeller (267).

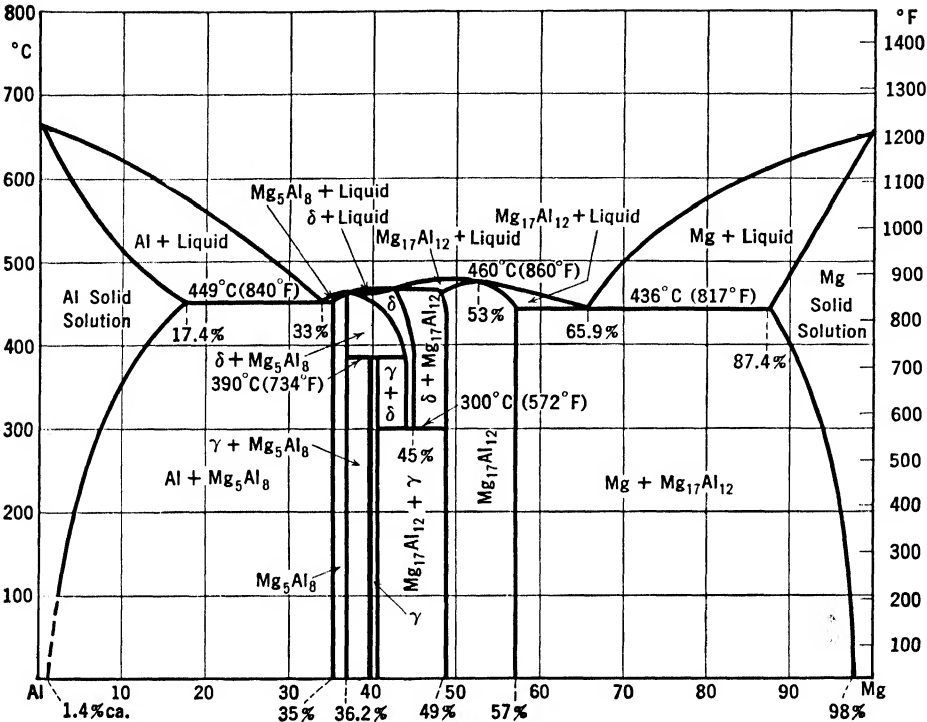


FIG. 24. System Al-Mg, equilibrium diagram.

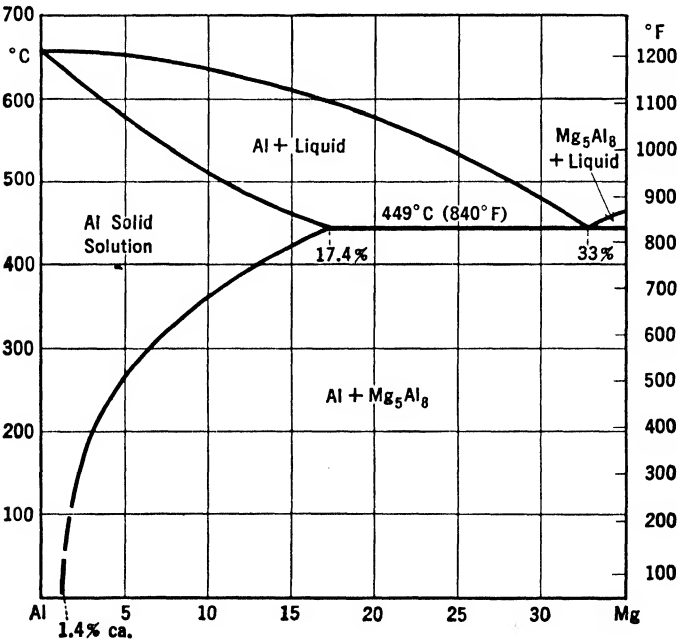


FIG. 25. System Al-Mg, detail of the aluminum end of the equilibrium diagram, showing the solid solubility of magnesium in aluminum.

The solid solubilities of magnesium in aluminum are reported below.

449°C	840°F	17.4% Mg
400°C	752°F	13.5% Mg
350°C	662°F	9.9% Mg
300°C	572°F	6.7% Mg
250°C	482°F	4.4% Mg
200°C	392°F	3.1% Mg
150°C	302°F	2.3% Mg
100°C	212°F	1.9% Mg

Figure 25 shows the aluminum corner in detail, with the solid solubilities. Magnesium and aluminum form four compounds, two of which are only partially known. The first at the aluminum end is  $\text{Mg}_5\text{Al}_8$  hexagonal, with lattice parameters  $a = 11.38 \text{ \AA}$ ,  $c = 17.88 \text{ \AA}$ , and a magnesium content of 35 to 36.2 per cent. Another crystal structure of  $\text{Mg}_5\text{Al}_8$  is formed by precipitation from a supersaturated solid solution of magnesium in aluminum. Little is known about it, and it is considered a transition phase, analogous to the one formed by  $\text{CuAl}_2$ .  $\text{Mg}_5\text{Al}_8$  forms a eutectic with Al at about 33 per cent magnesium, melting at 449°C (840°F). The next phase  $\gamma(\text{AlMg})$  is stable only below 390°C (734°F). It contains about 40 per cent magnesium and has a complex lattice which has not yet been resolved. The phase  $\delta(\text{AlMg})$  is stable above 300°C (572°F) and contains about 45 per cent magnesium. The last phase at the magnesium end, containing 49 to 57 per cent magnesium, is cubic body-centered, with lattice parameter  $a = 10.54 \text{ \AA}$ . It contains 58 atoms in the unit cell with a distribution corresponding to the formula  $\text{Mg}_{17}\text{Al}_{12}$ .

In non-equilibrium conditions created by fast cooling the two intermediate phases  $\gamma(\text{AlMg})$  and  $\delta(\text{AlMg})$  usually do not form, and the alloys consist of a mixture of  $\text{Mg}_5\text{Al}_8$  and  $\text{Mg}_{17}\text{Al}_{12}$ . Alloys lower in magnesium are less affected by fast cooling, their only difference from alloys in equilibrium being in the amount of magnesium dissolved, which, with commercial cooling rates, ranges from 3 to 6 per cent magnesium at room temperature. The reprecipitation of this amount is very slow and requires days of annealing to be completed.

Magnesium is one of the most common additions in aluminum alloys. When it is the only element added, it increases the mechanical properties to a remarkable extent, at the same time improving the corrosion resistance. In the presence of silicon it forms the compound  $\text{Mg}_2\text{Si}$  (see Al-Mg-Si diagram); in the presence of copper it forms the  $\text{AlCuMg}$  phases (see Al-Cu-Mg diagram); in the presence of both copper and silicon it may form the  $\text{CuMg}_5\text{Si}_4\text{Al}_4$  phase (see Al-Cu-Mg-Si diagram), all of which form the base for alloys susceptible to heat treatment.

However, the ternary or quaternary diagrams should be consulted for commercial alloys because magnesium is always associated with other elements.

## Al-Mn

### Aluminum-Manganese

The partial diagrams (Figs. 26 and 27) are taken from data by Von Rassow (282), Hofmann (289), and Dix, Fink, and Willey (288).

Manganese is soluble to a certain extent in solid aluminum and the solubilities at various temperatures are reported below.

658°C	1216°F	1.82% Mn
626°C	1159°F	1.35% Mn
570°C	1058°F	0.78% Mn
500°C	932°F	0.36% Mn
20°C	68°F	0.05% Mn approx.

Figure 27 shows in detail the aluminum end of the diagram, with the solid solubilities of manganese in aluminum. The compound at the aluminum end is  $\text{MnAl}_6$ , rhombic with lattice parameters  $a = 6.51$  Å,  $b = 7.54$  Å,  $c = 8.87$  Å. It forms a eutectic with Al at 1.95 per cent manganese, 658°C (1216°F); then primary crystals of  $\text{MnAl}_6$  form up to 4 per cent manganese. From there on  $\text{MnAl}_6$  is formed at 710°C (1310°F) by peritectic reaction from  $\text{MnAl}_4$  and the liquid.  $\text{MnAl}_4$  is hexagonal with lattice parameters  $a = 28.35$  Å,  $c = 12.36$  Å, and forms primary crystals from 4 to 12 per cent manganese; then it is formed by peritectic reaction from  $\text{MnAl}_3$  at 820°C (1508°F). The rest of the system contains several other phases, but the data are scanty and somewhat doubtful; for this reason it is not reported here.

The peritectic reactions



are slow, and in non-equilibrium conditions usually are not completed. At concentrations below the peritectic (4 per cent manganese), where  $\text{MnAl}_6$  forms primary crystals, the only difference usually produced by fast cooling consists in the amount of manganese in solid solution.

Manganese is one of the minor alloying elements in aluminum alloys, quite commonly used. In straight aluminum-manganese alloys manganese increases the mechanical properties of aluminum without reducing the corrosion resistance; in aluminum-silicon alloys it counteracts the damaging effect of high iron content by the formation of complex phases (see Al-Fe-Mn-Si) at the expense of  $\text{FeSiAl}_5$  (see Al-Fe-Si); in aluminum-magnesium alloys it acts as a grain refiner and probably

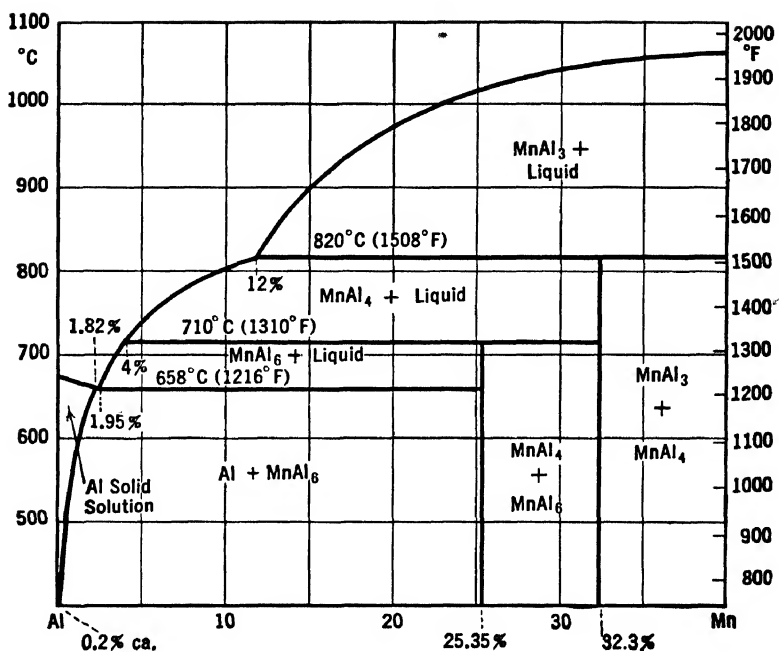


FIG. 26. System Al-Mn, aluminum end of the equilibrium diagram.

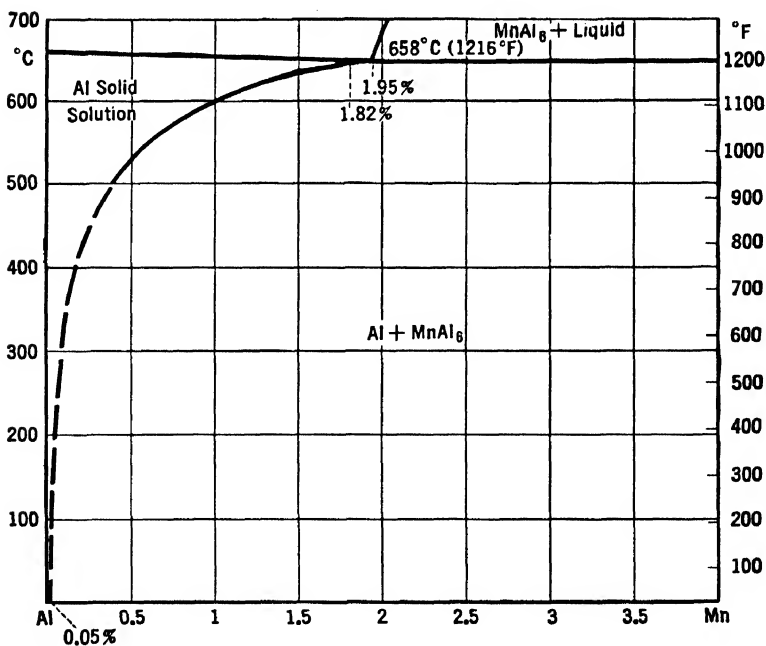


FIG. 27. System Al-Mn, detail of the aluminum end of the equilibrium diagram, showing the solid solubility of manganese in aluminum.



hinders the formation of the  $\text{AlFeMgSi}$  phase (see  $\text{Al-Fe-Mg-Si}$ ); in duralumin it hinders the formation of  $\text{AlCuFeSi}$  and probably acts as a grain refiner. For all these alloys the binary diagram is of little interest and the ternary or the quaternary should be consulted.

## Al-Mo

### Aluminum-Molybdenum

The equilibrium diagram (Fig. 28) is taken from data by Yamaguchi and Simizu (295), Roentgen and Koch (293), and the author.

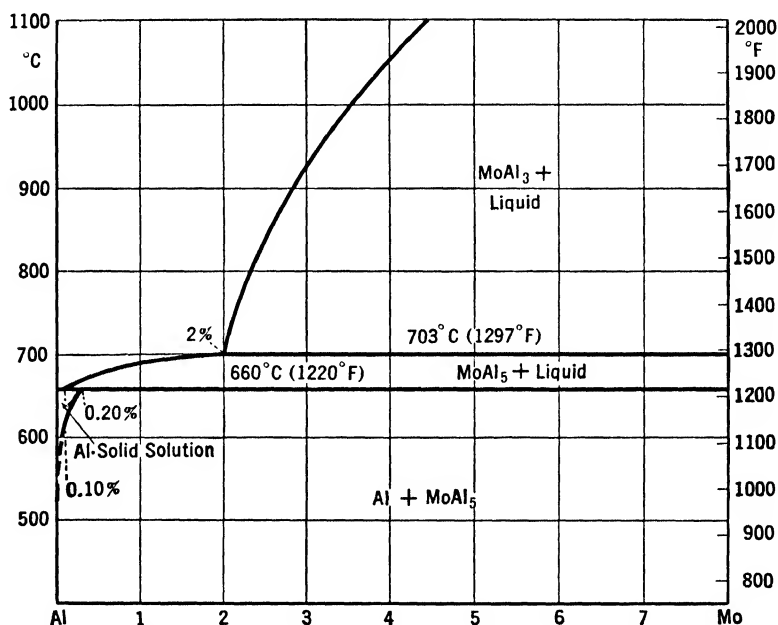


FIG. 28. System Al-Mo, aluminum end of the equilibrium diagram.

The solid solubility of molybdenum in aluminum is probably about 0.20 per cent at  $660^{\circ}\text{C}$  ( $1220^{\circ}\text{F}$ ) and decreases with decreasing temperature, being about 0.02 per cent at  $560^{\circ}\text{C}$  ( $1040^{\circ}\text{F}$ ). A peritectic reaction takes place at  $660^{\circ}\text{C}$  ( $1220^{\circ}\text{F}$ ) from about 0.10 per cent molybdenum on, between the liquid and  $\text{MoAl}_5$ , according to the equation



$\text{MoAl}_5$  is the first constituent at the aluminum end and forms primary crystals up to 2 per cent molybdenum; from there on it is formed at  $703^{\circ}\text{C}$  ( $1297^{\circ}\text{F}$ ) by peritectic reaction from  $\text{MoAl}_3$ . Data on the rest of the diagram are scanty and not altogether reliable and therefore are not reported.

Molybdenum is used occasionally in aluminum alloys, in percentages up to 0.3 per cent, as a grain refiner; but, as it is less effective than titanium, it is added mainly for patent reasons.

## Al-Na

### Aluminum-Sodium

The equilibrium diagram (Fig. 29) is composed from data by Mathewson (297) and Scheuer (298).

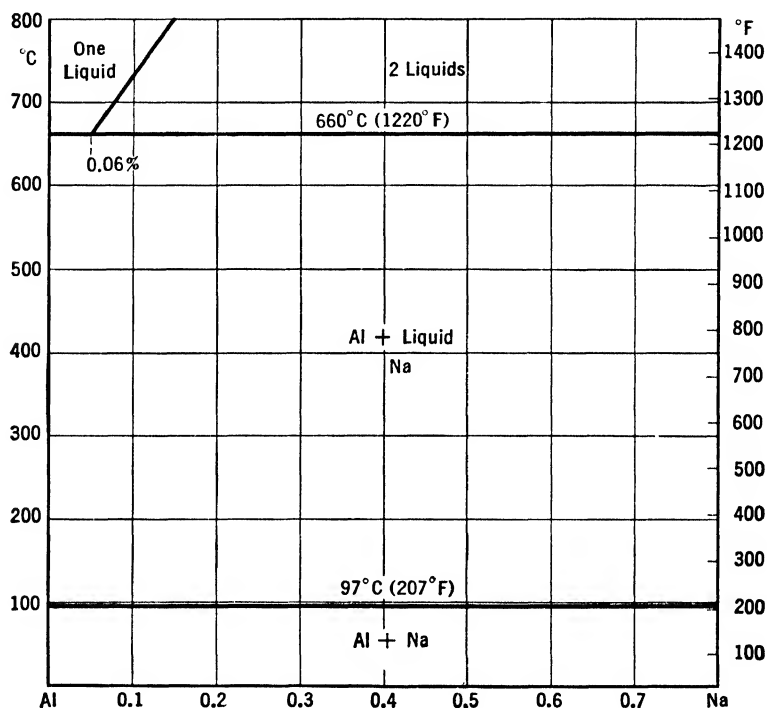


FIG. 29. System Al-Na, aluminum end of the equilibrium diagram.

Sodium is only slightly miscible with aluminum in the liquid state and not miscible at all with aluminum in the solid state. The miscibility in the liquid state is as follows.

660°C	1220°F	0.06% Na
700°C	1292°F	0.10% Na
800°C	1472°F	0.13% Na

The presence of silicon, copper, or magnesium in the alloy seems to increase this miscibility to a small extent. The zone of immiscibility extends almost to 100 per cent sodium, where probably there is another zone of limited miscibility.

Sodium is used widely in the aluminum-silicon type of alloys to induce the modification (see Al-Si diagram). The amounts added are approximately 0.01 per cent. At present the use of sodium salts (usually fluorides) for modifying purposes is preferred. Sodium sometimes is used as a deoxidizer for aluminum alloys, but its effectiveness is questionable. For alloys containing magnesium, additions of sodium are decidedly detrimental; probably a MgNa compound is formed, which renders the alloys brittle and makes them unfit for working. Sodium in percentages up to 0.005 per cent commonly is present in commercial aluminum.

### **Al-Nd**

#### **Aluminum-Neodimium**

The only investigation of this system was done by Stillwell and Jukkola (299).

The only datum reported by them is the existence of a compound NdAl, which forms face-centered cubic crystals with a lattice parameter  $a = 3.73$  Å.

No aluminum alloy containing neodimium has ever been used commercially.

### **Al-Ni**

#### **Aluminum-Nickel**

The diagram (Fig. 30) is from data by Alexander and Vaughan (309), Bradley and Taylor (308), and Fink and Willey (306).

The solid solubility of nickel in aluminum is very low and ranges from 0.05 per cent at eutectic temperature ( $640^{\circ}\text{C}$ — $1184^{\circ}\text{F}$ ), to less than 0.01 per cent at  $500^{\circ}\text{C}$  ( $932^{\circ}\text{F}$ ). The first compound at the aluminum end is  $\text{NiAl}_3$ , rhombic with lattice parameters  $a = 6.5982$  Å,  $b = 7.3518$  Å,  $c = 4.8021$  Å. It contains 16 atoms in the unit cell in a peculiar type of close packing intermediate between face- and body-centered. Nickel atoms have 9 neighbors; aluminum atoms have 11 neighbors.  $\text{NiAl}_3$  forms a eutectic with Al at 5.7 per cent nickel,  $640^{\circ}\text{C}$  ( $1184^{\circ}\text{F}$ ). It forms primary crystals up to 29 per cent nickel; from there on it is formed at  $852^{\circ}\text{C}$  ( $1566^{\circ}\text{F}$ ) by peritectic reaction from  $\text{Ni}_2\text{Al}_3$ .  $\text{Ni}_2\text{Al}_3$  forms trigonal crystals. Several other phases are present with higher nickel concentrations, but the data about them are incomplete and uncertain and are not reported here.

Non-equilibrium conditions caused by fast cooling have little effect on aluminum-nickel alloys in the range reported. In alloys above 30 per cent nickel, the peritectic reaction  $\text{Ni}_2\text{Al}_3 + \text{liquid} \rightarrow \text{NiAl}_3$  is

sometimes incomplete. Alloys with lower nickel contents are not affected at all.

Nickel is one of the minor alloying elements for aluminum. Binary aluminum-nickel alloys were used at the beginning of the aluminum industry but did not show especially interesting properties. At present nickel is used mainly as an addition to alloys containing copper in

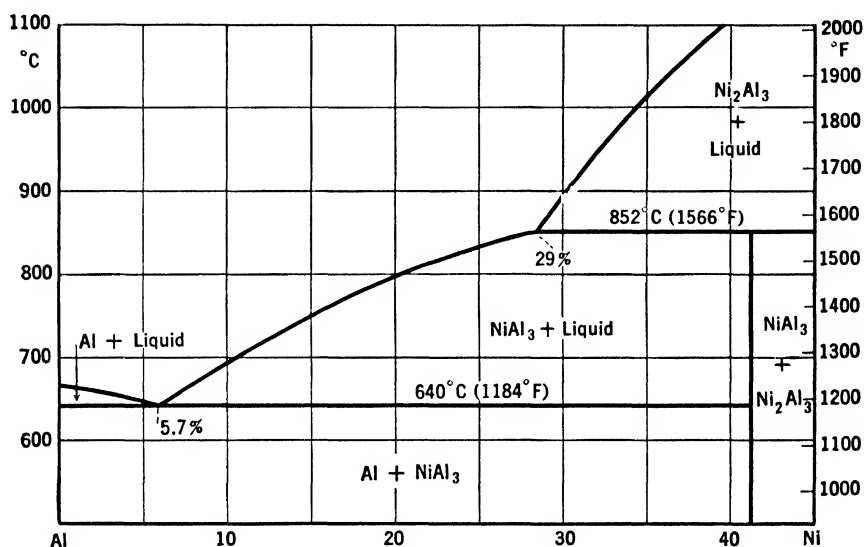


FIG. 30. System Al-Ni, aluminum end of the equilibrium diagram.

order to improve the mechanical properties at high temperatures. The ternary diagrams should be consulted for these alloys (see AlCuNi, AlFeNi, etc.).

## Al-Pb

### Aluminum-Lead

The diagram (Fig. 31) embodies the results of Kempf and Van Horn (317) and Campbell and Ashley (320).

Like bismuth and cadmium, lead does not form compounds with aluminum and is soluble in both the liquid and solid states to a limited extent. The solid solubility of lead in aluminum is about 0.20 per cent lead at the eutectic temperature 658.5°C (1217°F) and probably decreases with decreasing temperatures. The invariant point is at about 1.50 per cent lead, 658.5°C (1217°F). The miscibility in the liquid state from this point on increases to touch 15 per cent lead at about 1050°C (1922°F) and then goes on. The immiscibility zone almost

reaches the lead end, where there is another zone of limited miscibility.

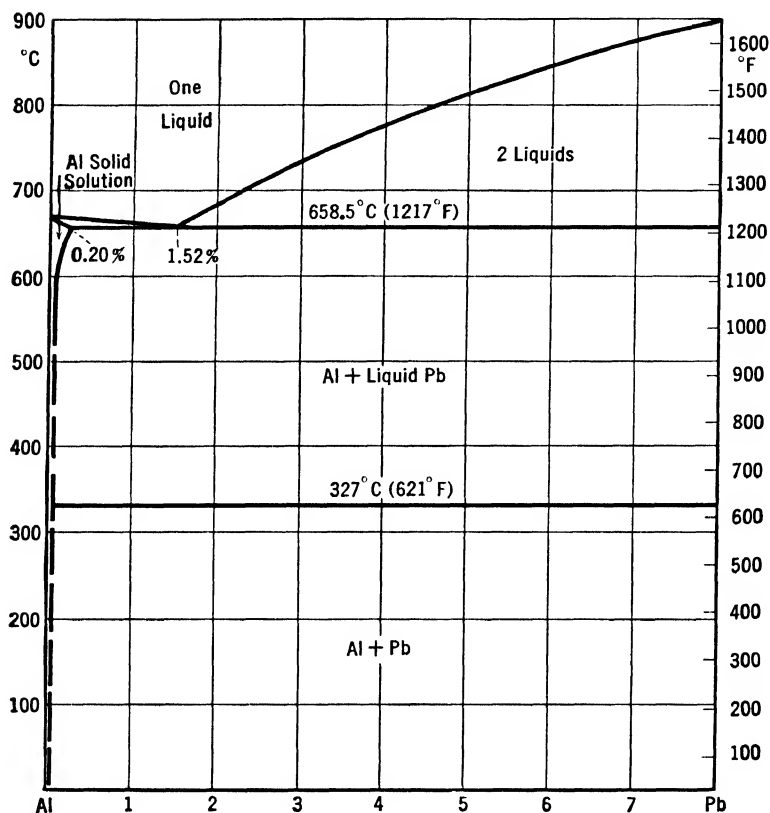


FIG. 31. System Al-Pb, aluminum end of the equilibrium diagram.

Together with bismuth, lead is added to aluminum alloys to improve the machinability. Small amounts of lead, up to 0.20 per cent, commonly are present in secondary alloys.

## Al-Pr

### Aluminum-Praseodymium

The only data available are those of Canneri (321).

Although no data about the solid solubility of praseodymium in aluminum are available, it is probably very small. At the aluminum end (Fig. 32) there is a eutectic at 14 per cent praseodymium, 658°C (1216°F), between Al and  $\alpha(\text{PrAl}_4)$ . As in the aluminum-cerium and aluminum-lanthanum alloys, two allotropic forms of  $\text{PrAl}_4$  exist:  $\alpha(\text{PrAl}_4)$  and  $\beta(\text{PrAl}_4)$ , transforming each into the other at 1018°C (1864°F).  $\alpha(\text{PrAl}_4)$  is stable below 1018°C (1864°F), whereas  $\beta(\text{PrAl}_4)$

is the phase stable above this temperature. Several other phases which are not reported here are present with higher praseodymium concentrations.

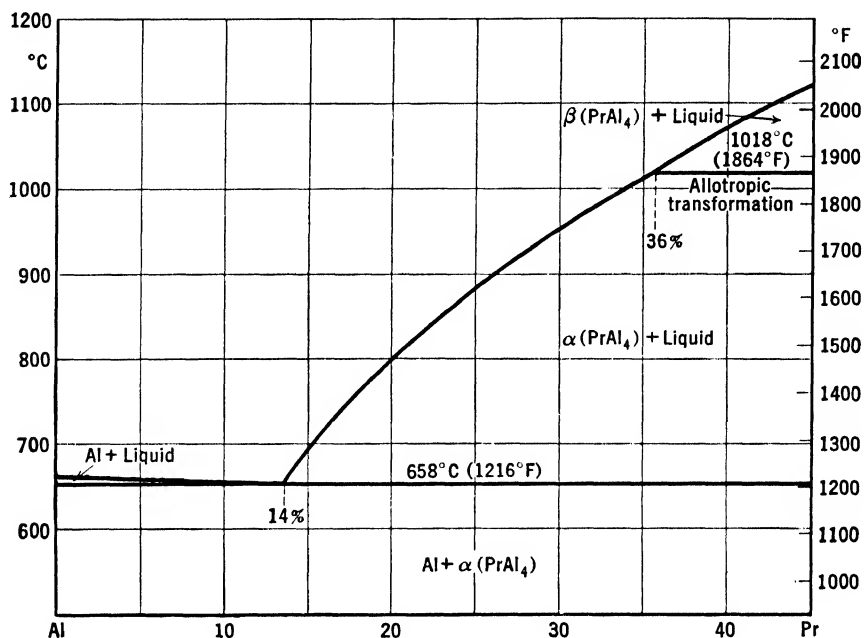


FIG. 32. System Al-Pr, aluminum end of the equilibrium diagram.

Additions of praseodymium to commercial aluminum alloys have never been investigated. From the equilibrium diagram it is to be expected that the improvements produced by additions of praseodymium will not be sufficient to warrant the use of such a rare and expensive metal in common practice.

## Al-Pt

### Aluminum-Platinum

Figure 33 is compiled from data by Chouriguine (324).

No data about the solid solubility of platinum in aluminum are available. The first compound at the aluminum end is PtAl<sub>6</sub>, which forms a eutectic Al-PtAl<sub>6</sub> at about 9 per cent platinum, 630°C (1166°F). PtAl<sub>6</sub> forms primary crystals up to about 40 per cent platinum; then it is formed at 760°C (1400°F) by peritectic reaction from PtAl<sub>3</sub>.

On account of its price, additions of platinum to commercial aluminum alloys have never been considered. Some alloys with high platinum content might be of practical interest, but to the author's knowledge they have not been investigated. In any event, they would be

outside the scope of this book because they are platinum alloys, rather than aluminum alloys.

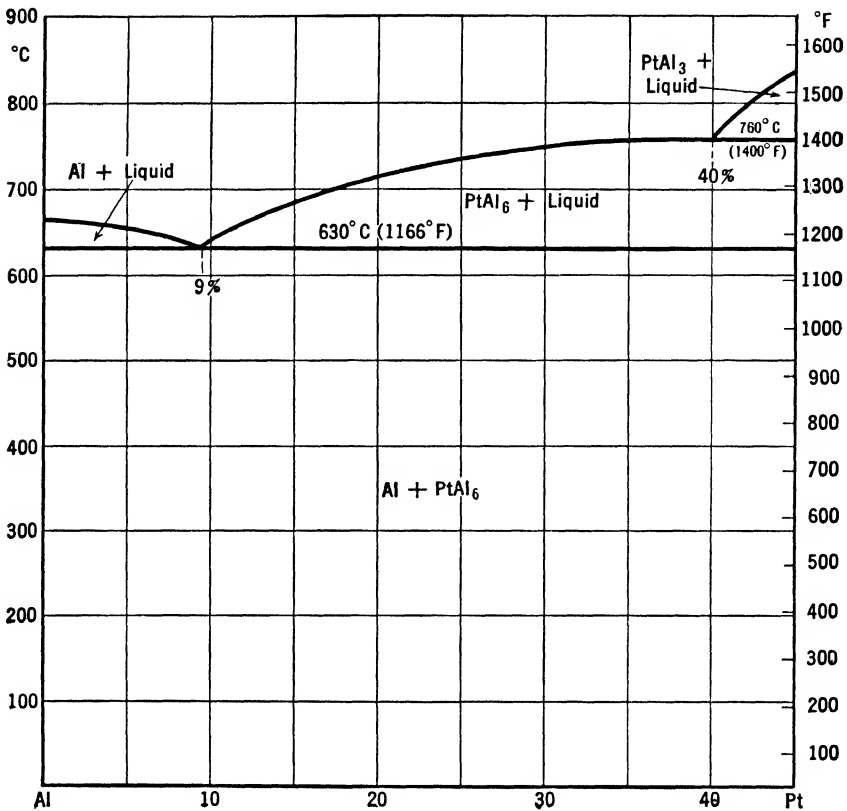


FIG. 33. System Al-Pt, aluminum end of the equilibrium diagram.

## Al-Rb

### Aluminum-Rubidium

The investigation of aluminum-rubidium alloys by Czochralski and Kakzynski (325) was concerned mostly with the modification of aluminum-silicon alloys.

From that investigation and some superficial investigations by the author it can be deduced that the aluminum-rubidium equilibrium diagram (Fig. 34) is analogous to the diagrams of aluminum-caesium, aluminum-potassium, aluminum-sodium. The miscibility in the liquid state is very limited; in the solid state no miscibility exists.

Rubidium can be used in aluminum-silicon alloys to induce modification. However, no particular reason exists to prefer it to sodium and,

since its price classifies it as a precious metal, its use commercially has never been considered.

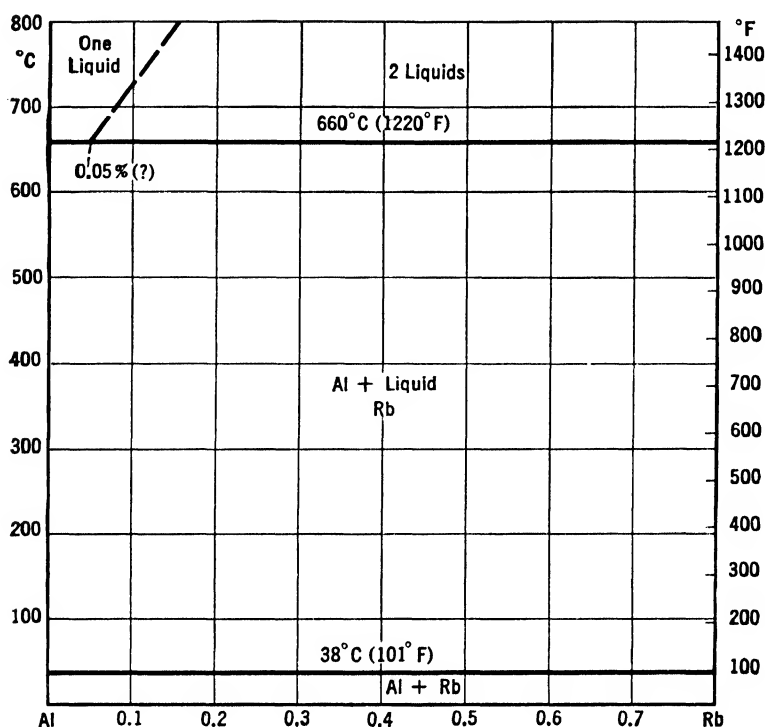


FIG. 34. System Al-Rb, aluminum end of the equilibrium diagram.

## Al-Sb

### Aluminum-Antimony

The equilibrium diagram (Fig. 35) is drawn from data by Guertler and Bergmann (339), Dix and colleagues (336), and Owen and Preston (335).

The solid solubility of antimony in aluminum is limited. It is less than 0.10 per cent antimony at the eutectic temperature 657°C (1215°F). Aluminum and antimony form a face-centered cubic compound SbAl. A eutectic Al-SbAl exists at about 1.1 per cent antimony—melting point 657°C (1215°F). Then the solidification temperature rises until at 81.6 per cent antimony it reaches 1050°C (1922°F), corresponding to the compound SbAl. From there on, the freezing point drops until at 100 per cent antimony it reaches 630°C (1166°F), for the eutectic Sb-SbAl practically corresponds to pure antimony.

Small additions of antimony to aluminum-magnesium alloys were



used at one time. It was then claimed that the formation of antimony oxychloride caused the good resistance to salt-water corrosion of these alloys, but it has since been proved that aluminum-magnesium alloys have good corrosion resistance even without antimony additions.

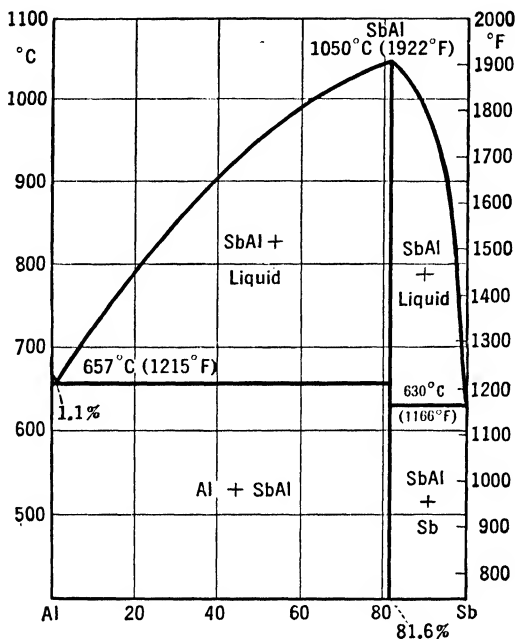


FIG. 35. System Al-Sb, equilibrium diagram.

Sometimes antimony is mentioned in patents covering aluminum alloys for pistons, but the reason is not clear, and the alloys containing antimony are not used commercially.

## Al-Se

### Aluminum-Selenium

The equilibrium diagram shown (Fig. 36) is from data by Chikashige and Aoki (340).

No data are reported about the solid solubility of selenium in aluminum. A compound, probably  $\text{Se}_4\text{Al}_3$  or perhaps  $\text{Se}_3\text{Al}_2$ , exists, forming a eutectic with Al at  $659^\circ\text{C}$  ( $1218^\circ\text{F}$ ) which contains only traces of selenium. The eutectic  $\text{Se}-\text{Se}_4\text{Al}_3$  melts at  $217^\circ\text{C}$  ( $423^\circ\text{F}$ ) and almost coincides with selenium.

Selenium as an alloying element for aluminum has never been used, and it seems doubtful that it ever will be because no special improvement can be expected by additions of selenium to aluminum alloys.

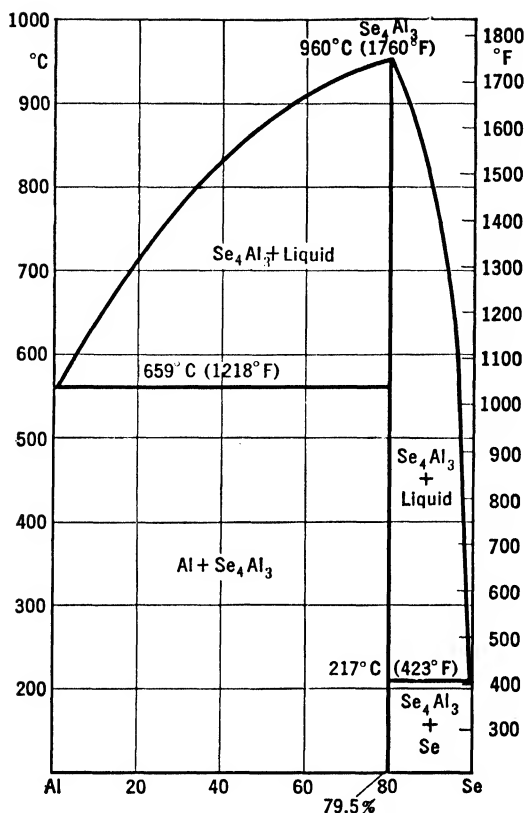


FIG. 36. System Al-Se, equilibrium diagram.

## Al-Si

### Aluminum-Silicon

The diagrams (Figs. 37 and 38) are from data by Gwyer and Phillips (358) and Dix and Heath (362).

Aluminum and silicon do not form any compound. There is a limited solid solubility of silicon in aluminum, as reported below.

577°C	1071°F	1.65% Si
550°C	1022°F	1.30% Si
500°C	932°F	0.80% Si
450°C	842°F	0.48% Si
400°C	752°F	0.29% Si
350°C	662°F	0.17% Si
300°C	572°F	0.10% Si
200°C	392°F	0.05% Si

The solid solubilities at different temperatures are reported in detail in Fig. 38. The constituents of the system are Al and Si, forming a eutectic at 11.7 per cent silicon, 577°C (1071°F). Aluminum is soluble

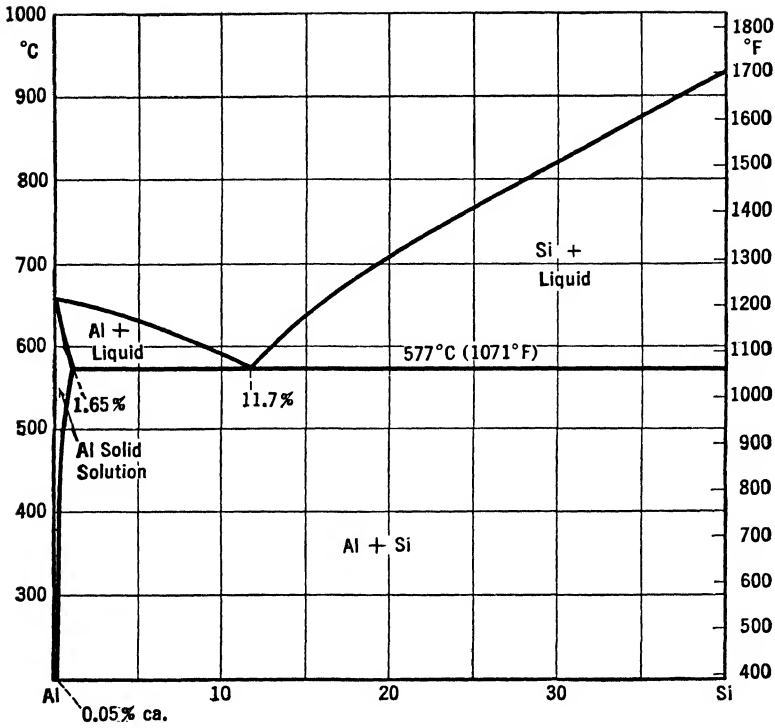


FIG. 37. System Al-Si, aluminum end of the equilibrium diagram.

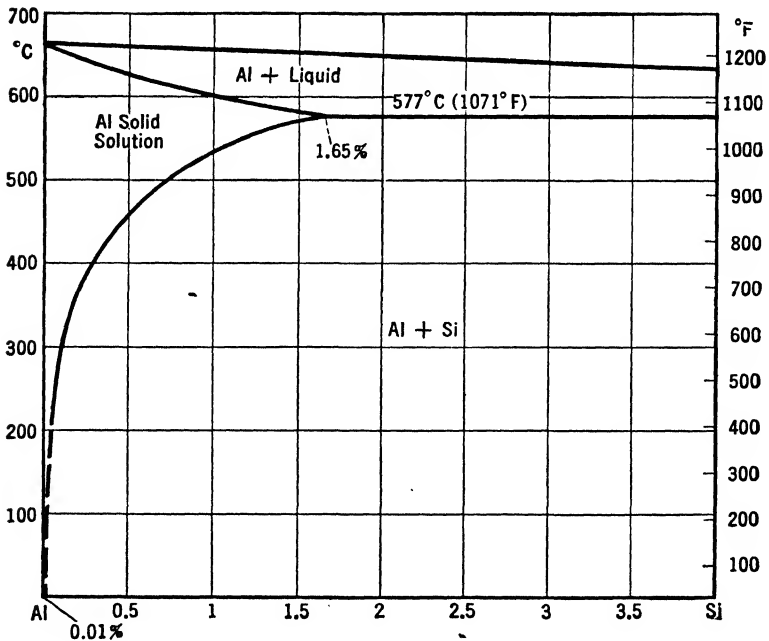


FIG. 38. System Al-Si, detail of the aluminum end of the equilibrium diagram, showing the solid solubility of silicon in aluminum.

in silicon to a certain extent, but this solubility has not been investigated very accurately.

In spite of its simplicity, the Al-Si equilibrium diagram has puzzled the investigators for a long time, and still is not thoroughly explained on account of the *modification* phenomenon. Of the many theories proposed as explanation, two are still considered: the ternary eutectic theory and the protector colloid theory. Briefly, they are as follows.

**Ternary eutectic.** The additions of sodium, potassium, etc., which are necessary to produce the modified structure, form with aluminum and silicon a ternary eutectic, which constitutes the refined structure of the modified alloys.

**Colloid protector.** In the liquid state aluminum and silicon are atomically dispersed. On solidification these atoms tend to coalesce to form the crystals which constitute the final structure in the solid state. If during this stage the alloy contains something (the modifying element) which tends to obstruct the coalescence, the final crystals must be smaller than when obstruction is absent.

As the existing experimental data fit both theories and there seems to be no means of establishing which of the two is correct, the problem has now lost its interest and research in this field has become almost negligible.

The effect of fast cooling on aluminum-silicon alloys is not very pronounced; the only differences it produces are a little more silicon in solid solution and smaller silicon crystals. The claim that modification can be induced by fast cooling alone has been proved inexact; it has been proved however that the amount of modifying agent necessary is smaller the faster the cooling. This can be caused by the fact that the faster the solidification the less time the modifying agent has to burn out.

Silicon is one of the most common alloying elements for aluminum. It is also one of the common impurities in aluminum, its minimum percentage being about 0.12 per cent in 99.7 per cent aluminum and, naturally, higher in lower-grade material. Because it combines with many of the other alloying elements, the ternary or quaternary diagrams should be consulted.

## Al-Sn

### Aluminum-Tin

The equilibrium diagram (Fig. 39) is from data by Gwyer (392), Crepaz (395), and Zamatorin (399).

Aluminum and tin do not form compounds; the Al-Sn eutectic is at

99 per cent tin, 229°C (444°F). The solid solubility of tin in aluminum is reported as ranging from 20 per cent at the eutectic temperature, 229°C (444°F), to 2 per cent at room temperature, but the data available are not completely reliable.

Aluminum-tin alloys were used in the early days of the aluminum industry, but later they disappeared from the commercial field.

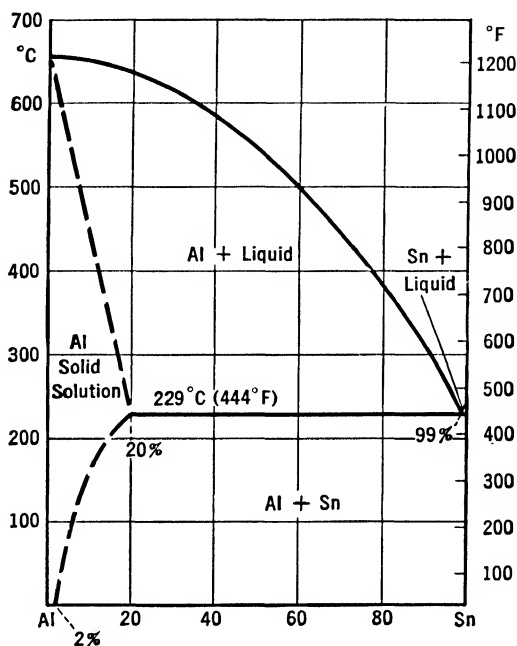


FIG. 39. System Al-Sn, equilibrium diagram.

Aluminum-copper alloys containing small additions of tin are still used sometimes. The present shortage of tin should make them disappear from the market, however, because they do not offer special advantages over the straight aluminum-copper alloys. Tin as an impurity commonly is present in low-grade secondary material in percentages up to 0.5.

## Al-Sr

### Aluminum-Strontium

Figure 40 has been constructed from data by Nowotny and Wesenberg (400), who are the only ones who have investigated aluminum-strontium alloys.

Strontium is not soluble in aluminum to any appreciable extent. The phase at the aluminum end of the diagram is  $\text{SrAl}_4$ , tetragonal body-centered, with lattice parameters  $a = 4.45 \text{ \AA}$ ,  $c = 11.05 \text{ \AA}$ . A

eutectic Al-SrAl<sub>4</sub> is formed at about 1 per cent strontium. The melting point is not reported. From theoretical considerations it can be deduced that it must be about 600°C (1112°F). The compound SrAl<sub>4</sub> at 700°C (1290°F) can take in solid solution about 2 per cent aluminum and 18 per cent strontium. Another constituent formed is SrAl<sub>2</sub>, cubic body-centered, with lattice parameter  $a = 15.8$  Å, and 116 atoms

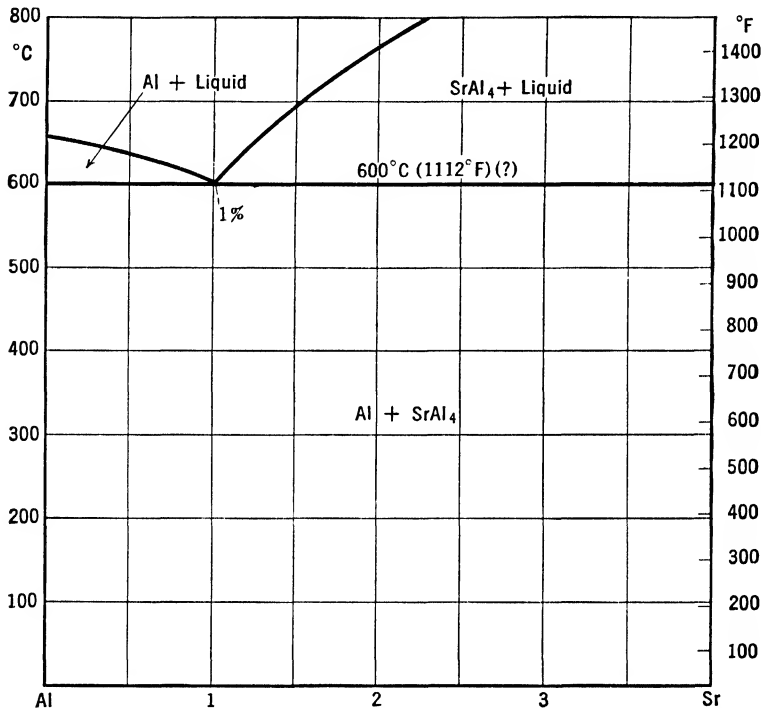


FIG. 40. System Al-Sr, aluminum end of the probable equilibrium diagram.

in the unit cell. It is unstable below 300°C (572°F) and decomposes in SrAl<sub>4</sub> and Sr. Only the aluminum end of the diagram is reported; the data about the rest are too limited to permit a diagram to be drawn.

No commercial aluminum-strontium alloys have ever been used, nor is it probable that they will be, because of the readiness with which strontium oxidizes as well as its high cost.

## Al-Ta

### Aluminum-Tantalum

The only datum available on this system is the existence of a compound TaAl<sub>3</sub>, reported by Brauer (403).

According to the report, TaAl<sub>3</sub> forms tetragonal crystals with lattice parameters  $a = 5.422$  Å,  $c = 8.536$  Å, and is isomorphous with TiAl<sub>3</sub> and CbAl<sub>3</sub>, forming a solid solution with the latter.

This system has only a theoretical interest because aluminum-tantalum alloys have never been commercially used, nor is it probable that they will be in the near future on account of the small amounts of tantalum produced.

## Al-Te

### Aluminum-Tellurium

Chikashige and Nose (405) have published an improbable equilibrium diagram, shown here as Fig. 41. Whitmore and Sisco (407),

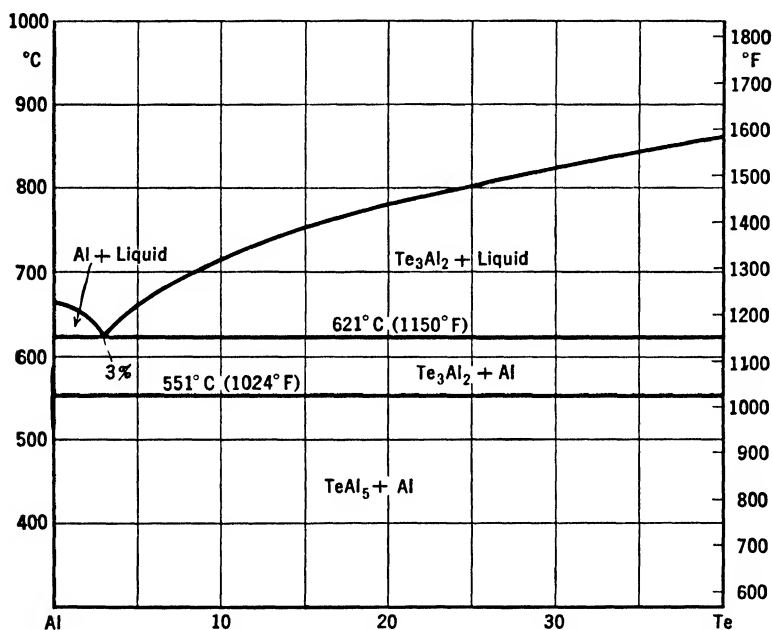


FIG. 41. System Al-Te, aluminum end of the equilibrium diagram.

however, report that aluminum and tellurium do not alloy and that the compound which is formed,  $\text{Te}_3\text{Al}_2$ , does not mix with aluminum but segregates at the surface.

No aluminum alloy containing tellurium has been investigated for commercial use. Since the investigation of Whitmore and Sisco is the most reliable, it is to be expected that commercial aluminum alloys will never contain tellurium.

## Al-Th

### Aluminum-Thorium

The equilibrium diagram shown as Fig. 42 is from data by von Leber (409), Brauer (411), and Grogan and Schofield (410).

The solid solubility of thorium in aluminum is negligible. Aluminum and thorium form several compounds; the one at the aluminum end is  $\text{ThAl}_3$ , which forms a eutectic with Al at 25.6 per cent thorium, melting at  $636^\circ\text{C}$  ( $1177^\circ\text{F}$ ).  $\text{ThAl}_3$  crystallizes in the hexagonal structure with lattice parameters  $a = 6.480 \text{ \AA}$ ,  $c = 4.601 \text{ \AA}$ , and 8 atoms in the unit cell. It forms primary crystals from the eutectic to about 42 per cent thorium; from there on it is formed by peritectic reaction at  $880^\circ\text{C}$

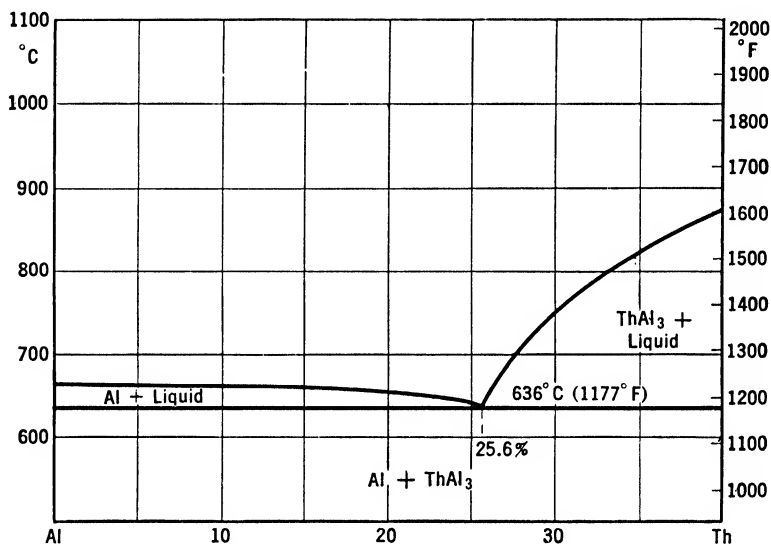


FIG. 42. System Al-Th, aluminum end of the equilibrium diagram.

( $1616^\circ\text{F}$ ) between the liquid and another phase richer in thorium whose composition is not known.

This diagram has only a theoretical interest because thorium is not used in commercial aluminum alloys.

## Al-Ti

### Aluminum-Titanium

The equilibrium diagrams (Figs. 43 and 44) are compiled from data by Fink, Van Horn, and Budge (419) and Manchot and von Leber (417).

The solid solubility of titanium in aluminum is about 0.28 per cent and probably decreases with decreasing temperatures. A compound  $\text{TiAl}_3$ , tetragonal, with lattice parameters  $a = 5.42 \text{ \AA}$ ,  $c = 8.57 \text{ \AA}$ , and 16 atoms in the unit cell, is present in the aluminum corner. A peritectic reaction,  $\text{Liquid} + \text{TiAl}_3 \rightarrow \text{Al (solid solution)}$ , takes place at  $665^\circ\text{C}$  ( $1229^\circ\text{F}$ ), 0.19 per cent titanium. Onward from this point, the line of the beginning of solidification rises steeply to reach  $1355^\circ\text{C}$



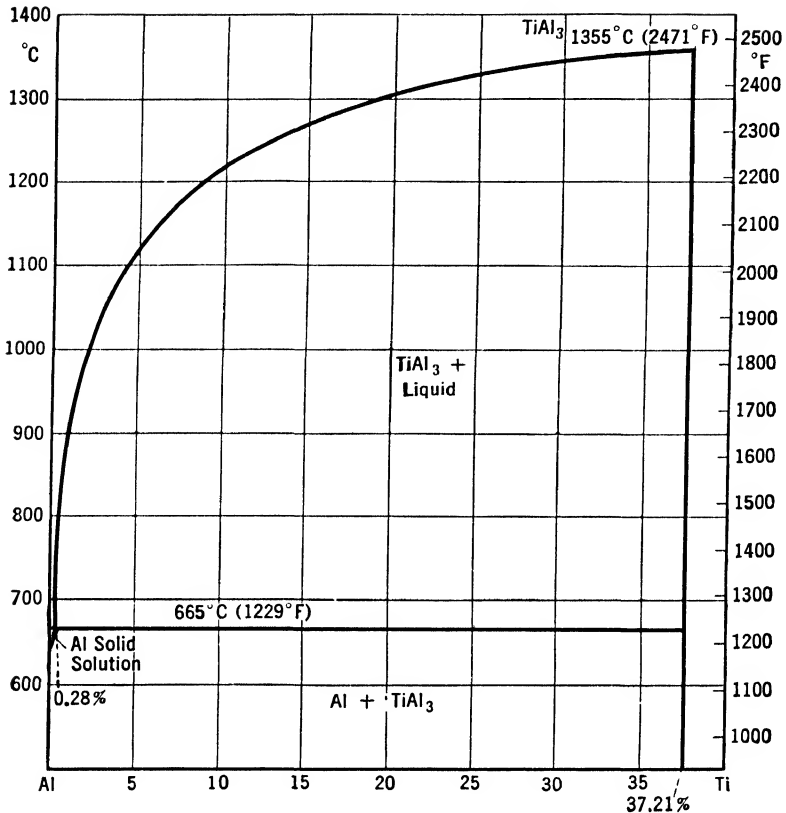


FIG. 43. System Al-Ti, aluminum end of the equilibrium diagram.

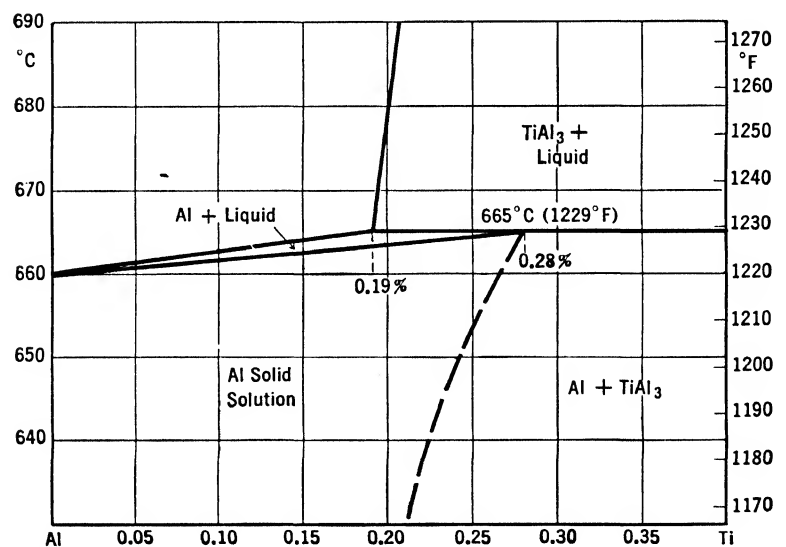


FIG. 44. System Al-Ti, detail of the aluminum end of the equilibrium diagram, showing the peritectic reaction.

(2471°F) at the compound  $\text{TiAl}_3$  (37.21 per cent titanium). The diagram has been investigated up to about  $\text{TiAl}_3$ ; from there on only scanty and doubtful data are available.

This diagram is important from the practical point of view, for titanium is the grain refiner most often used and is commonly added to commercial alloys in percentages as high as 0.20 per cent. The reasons for the grain-refining effect are not clear. Formerly it was supposed that  $\text{TiAl}_3$ , solidifying at high temperatures, acted as a crystallization nucleus. At present it is believed that the peritectic reaction is responsible for the grain refining, but the exact mechanism has been only vaguely surmised and has not yet been proved.

## Al-Tl

### Aluminum-Thallium

Doerincel (425), the only one who has investigated the aluminum-thallium alloys, reports complete immiscibility both in the liquid and solid state.

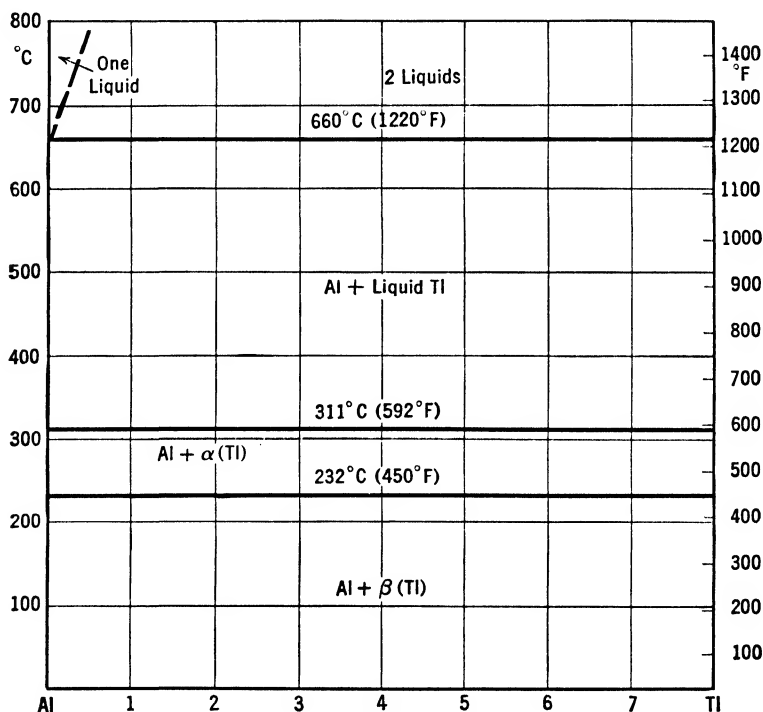


FIG. 45. System Al-Tl, aluminum end of the equilibrium diagram.

Probably, as with lead, cadmium, and bismuth, there are limited zones of miscibility in the liquid at both ends of the diagram (Fig. 45).

Thallium solidifies at 311°C (592°F) and undergoes an allotropic transformation at 232°C (450°F), changing from  $\alpha$  to  $\beta$ (Tl).

No commercial aluminum alloy containing thallium has been used, and in all probability never will be, because very little advantage is to be expected from the addition of thallium to aluminum alloys.

## Al-U

### Aluminum-Uranium

This system has only been investigated superficially.

Several intermetallic compounds are reported to exist, but the data about them are controversial and of no interest for the aluminum corner of the diagram, which has not been investigated at all.

No aluminum alloy containing uranium has ever been used and there are even very few patents on them. Unless aluminum-uranium alloys should be used as radio-active material their commercial future is certainly very limited.

## Al-V

### Aluminum-Vanadium

The only data available in the literature are on the existence of a compound  $VAI_3$ , reported by Czaco (429), and on the solid solubility determination of Roth (430).

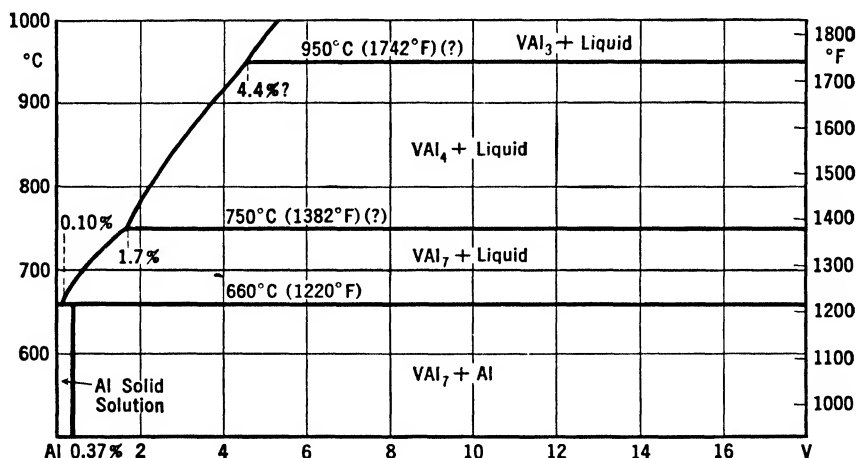


FIG. 46. System Al-V, aluminum end of the probable equilibrium diagram.

Investigations by the author point to the existence of a reaction by which a compound, probably  $VAI_7$ , combines with the liquid to form Al (solid solution).  $VAI_7$  is formed by peritectic reaction from another phase, probably  $VAI_4$ , which is also formed by peritectic reaction from  $VAI_3$ . These data are plotted in Fig. 46. The solid solubility of

vanadium in aluminum is 0.37 per cent at the eutectic temperature and does not seem to change with changes in temperature.

Vanadium is used to a slight extent as a grain refiner in aluminum alloys, especially in alloys of the aluminum-silicon type. No particular reason exists for its use in place of titanium; usually it is added for patent reasons. Vanadium is a minor impurity in aluminum. Its percentage ranges from traces hardly detectable even with a spectroscope to 0.02 per cent.

## Al-W

### Aluminum-Tungsten

Figure 47 is from data by Clark (433).

The solid solubility of tungsten in aluminum is between 1.5 and 1.8 per cent tungsten at 650°C (1202°F) and is reported constant with

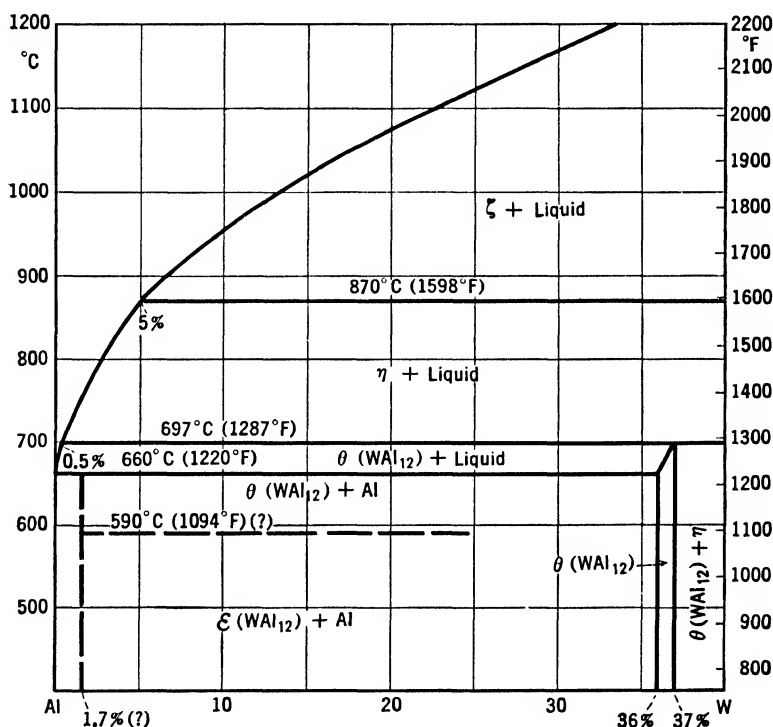


FIG. 47. System Al-W, aluminum end of the equilibrium diagram.

decreasing temperatures. An allotropic transformation, by which the phase  $\theta(\text{WAl}_{12})$  transforms into  $\epsilon(\text{WAl}_{12})$ , takes place in the solid at about 590°C (1094°F). The eutectic Al- $\theta(\text{WAl}_{12})$  almost coincides with Al. The phase  $\theta(\text{WAl}_{12})$  is formed at 697°C (1287°F) by peritectic

reaction from  $\eta = \text{W}_2\text{Al}_9$ , which is formed from the phase  $\xi$  (probably  $\text{WAl}_4$ ) by peritectic reaction at  $870^\circ\text{C}$  ( $1598^\circ\text{F}$ ).

At the present stage aluminum-tungsten alloys with high aluminum content have only a theoretical interest, for no commercial aluminum alloy containing tungsten is used. If the solid solubility in aluminum is exact, tungsten as an alloying element for aluminum may be worth investigating.

## Al-Y

### Aluminum-Yttrium

The only data available on this system are those reported by Kroll (434).

His paper deals almost exclusively with the mechanical properties; the only information that can be deduced is that yttrium and aluminum are miscible and probably form an intermediate phase.

Since the effects of yttrium on aluminum alloys, as reported by Kroll, are far from spectacular and since the same effects could probably be obtained by the use of much cheaper metals, it is not probable that alloys containing yttrium will enter the commercial field.

## Al-Zn

### Aluminum-Zinc

The equilibrium diagram shown as Fig. 48 is from data by Gayler and Sutherland (475) and Fink and Willey (473).

Zinc is soluble to a large extent in aluminum and its solid solubility at various temperatures is reported below.

382°C	720°F	84.0% Zn
275°C	527°F	77.7–31.6% Zn
256°C	482°F	22.3% Zn
225°C	437°F	16.1% Zn
200°C	392°F	12.6% Zn
175°C	347°F	9.5% Zn
150°C	302°F	7.0% Zn
125°C	257°F	5.4% Zn
20°C	68°F	2.0% Zn

No compound is formed between zinc and aluminum and there is a eutectic at  $382^\circ\text{C}$  ( $720^\circ\text{F}$ ) and 96 per cent zinc. A solubility gap exists between 31.6 and 77.7 per cent zinc at  $275^\circ\text{C}$  ( $527^\circ\text{F}$ ), narrowing with increasing temperatures until at  $353^\circ\text{C}$  ( $668^\circ\text{F}$ ) and 60 per cent zinc it disappears. In this field two phases—Al and AlB—are present which are two solid solutions of zinc in aluminum with different zinc contents.

Straight aluminum-zinc alloys occasionally were used at the beginning of the aluminum industry, but alloys also containing copper were soon substituted for them. Aluminum-copper-zinc alloys have been and are still used to some degree, and additions of zinc to alloys of the

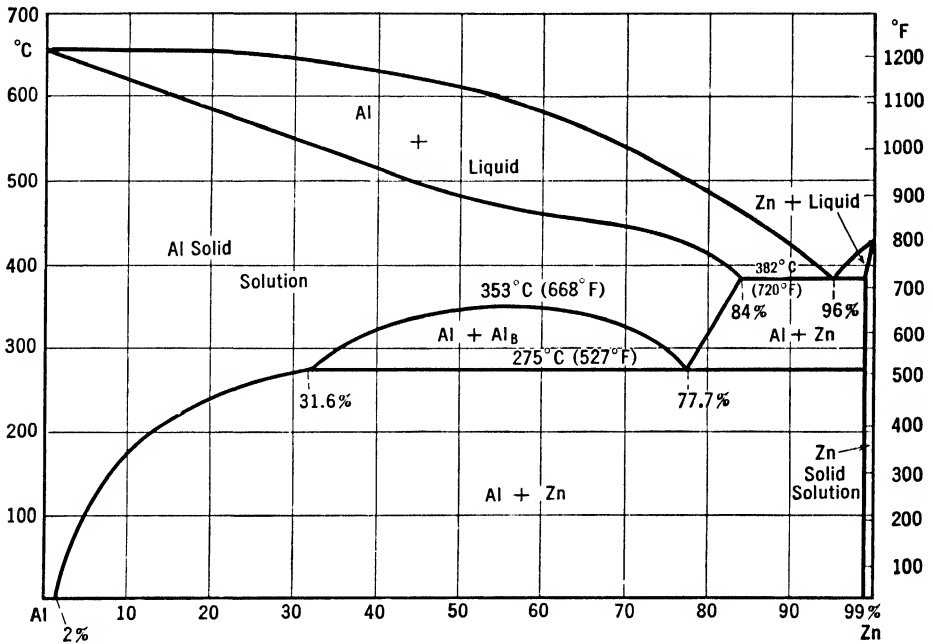


FIG. 48. System Al-Zn, equilibrium diagram.

aluminum-copper-nickel and duralumin type recently have been investigated. For all these alloys the ternary diagrams should be consulted to compensate for the lack of the quaternary diagrams.

## Al-Zr

### Aluminum-Zirconium

The equilibrium diagrams (Figs. 49 and 50) are from data by Fink and Willey (484) and Brauer (485).

The solid solubility of zirconium in aluminum is limited and from 0.28 per cent zirconium at 660.5°C (1221°F) decreases to 0.05 per cent zirconium at 500°C (932°F). A peritectic reaction takes place at 660.5°C (1221°F), from 0.11 per cent zirconium on, between the liquid and  $\text{ZrAl}_3$  to form Al(solid solution). The first compound at the aluminum end is  $\text{ZrAl}_3$ , which forms tetragonal crystals, with lattice parameters  $a = 4.00 \text{ \AA}$ ,  $c = 17.3 \text{ \AA}$ , and 16 atoms in the unit cell. The diagram has not been further investigated.

Zirconium has been used to a small extent as a grain refiner in aluminum alloys. As it does not offer any advantages over titanium, it is included in the composition primarily for patent reasons.

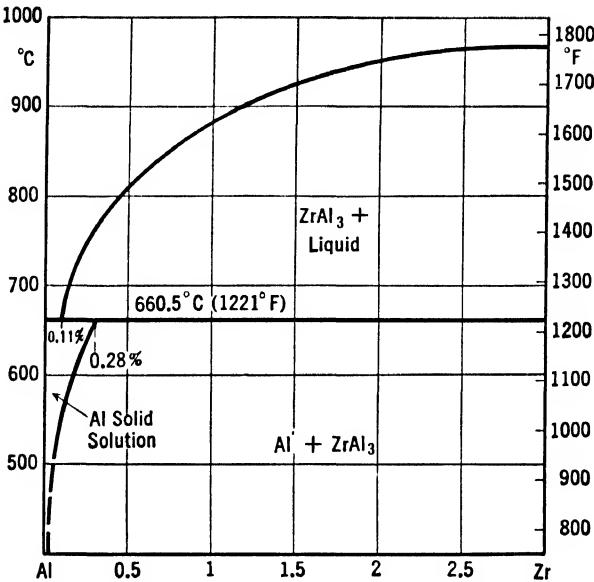


FIG. 49. System Al-Zr, aluminum end of the equilibrium diagram.

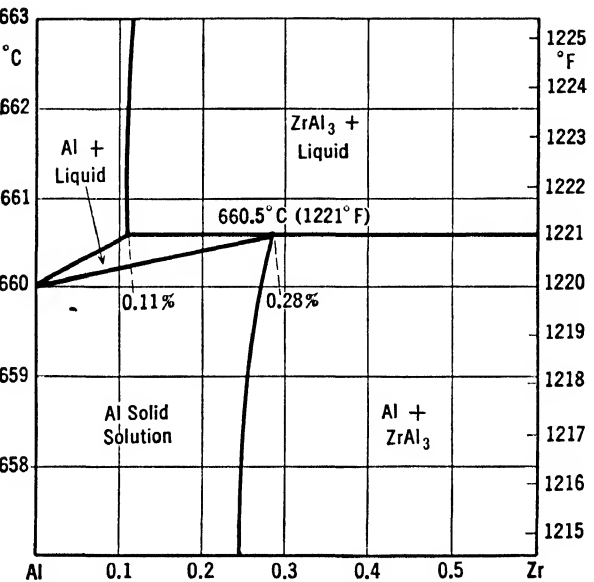


FIG. 50. System Al-Zr, detail of the aluminum end of the equilibrium diagram, showing the peritectic reaction.

## CHAPTER 2

### TERNARY DIAGRAMS

#### Al-Ag-Bi

#### Aluminum-Silver-Bismuth

This system was investigated by Wright (486).

No ternary constituent is formed, the immiscibility between bismuth and aluminum extends almost to the silver end of the diagram.

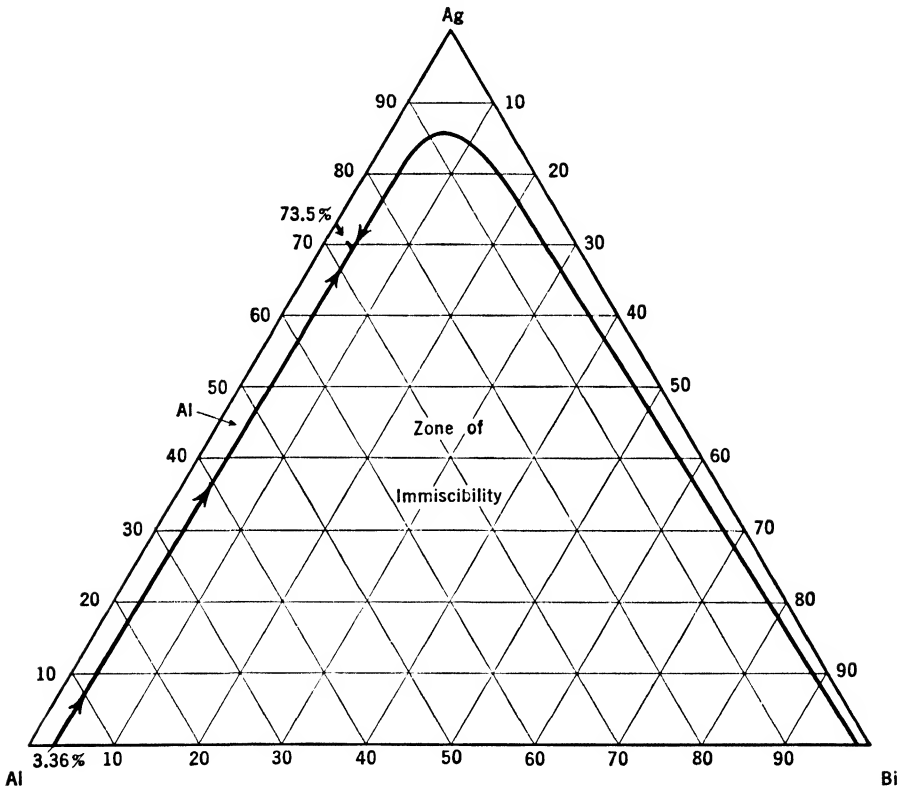


FIG. 51. System Al-Ag-Bi, surfaces of primary crystallization and limits of miscibility.

Figure 51 shows the surfaces of primary crystallization in the aluminum corner and the limits of miscibility at freezing temperature. In the



solid state the aluminum corner probably contains only the two phases Al and Bi because bismuth should not appreciably affect the solid solubility of silver in aluminum and because the solid solubility of bismuth should not be increased by silver.

This diagram has no practical interest, as is true for all diagrams on silver, because no commercial alloy contains silver.

### Al-Ag-Cu

#### Aluminum-Silver-Copper

This system has been investigated by Ueno (488) and Goto and Mishima (487), but the results of the latter are available only in Japanese.

According to Ueno, no ternary phase is formed in the aluminum corner, the phases present being Al,  $\text{CuAl}_2$ ,  $\beta(\text{AlAg})$ . A eutectic is formed by these phases at 32 per cent silver and 20 per cent copper. No data are available regarding the solid solubility of copper and silver in aluminum together. Probably, the respective solid solubilities are somewhat reduced.

This diagram has no practical importance because no commercial alloy contains silver.

### Al-Ag-Mg

#### Aluminum-Silver-Magnesium

The only investigation which covers the aluminum corner of this system was made by Otani (489). According to him, a ternary phase  $\text{AgMgAl}$  is formed at  $570^\circ\text{C}$  ( $1058^\circ\text{F}$ ) by the peritectic reaction:  $\text{Liquid} + \text{AgMg} = \text{AgMgAl}$ . Both magnesium and silver are soluble to a large extent in solid aluminum, although from Otani's data it appears that they reduce their respective solid solubilities. The solid solubilities at various temperatures of the compound  $\text{AgMgAl}$  in aluminum are reported below.

538°C	1000°F	14.00% AgMgAl
520°C	968°F	5.40% AgMgAl
500°C	932°F	4.40% AgMgAl
400°C	752°F	2.40% AgMgAl
300°C	572°F	0.40% AgMgAl

No further data are available.

This diagram has no practical importance; additions of silver to aluminum alloys have been investigated several times, but the properties of aluminum alloys containing silver are not promising enough to justify the high cost of such alloys.

## Al-Ag-Pb Aluminum-Silver-Lead

This system has been investigated by Wright (490) and lately by Campbell and colleagues (491).

Silver does not appreciably reduce the immiscibility of lead in aluminum. The miscibility increases slowly with silver additions

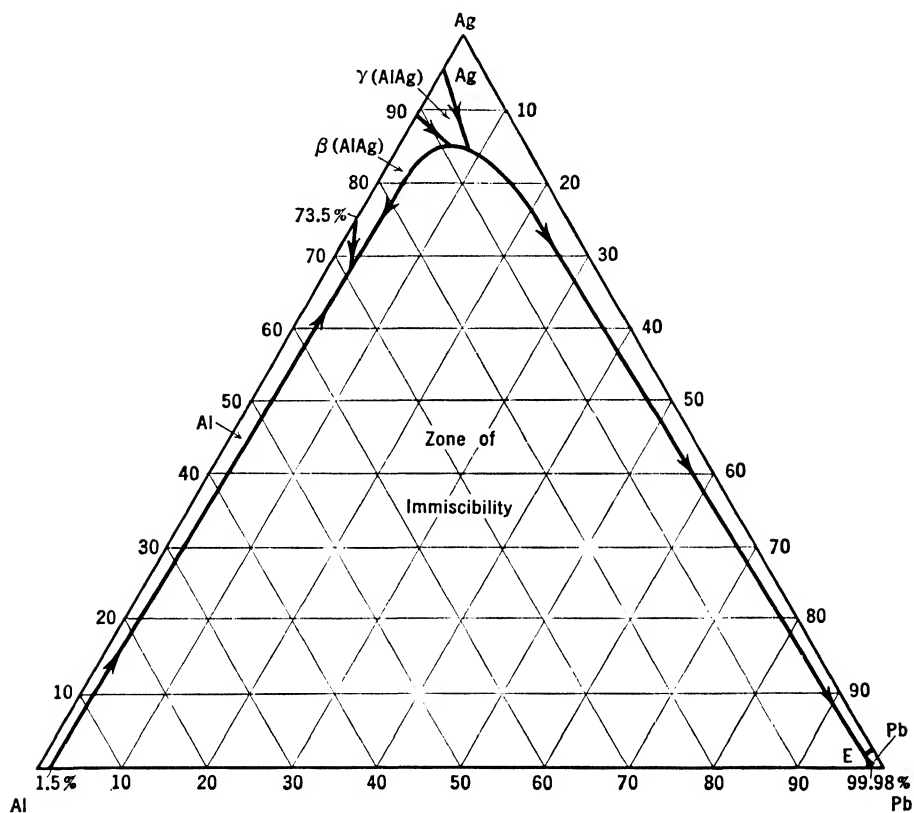


FIG. 52. System Al-Ag-Pb, surfaces of primary crystallization and limits of miscibility.

from about 1.5 per cent, in the binary alloys aluminum-lead, to a maximum of 4.7 per cent with a silver content of 85.5 per cent. A ternary eutectic  $E$  is formed at  $304^{\circ}\text{C}$  ( $579^{\circ}\text{F}$ ) and contains 2.30 per cent silver and less than 0.10 per cent aluminum. In the alloys rich in aluminum a line runs from the binary eutectic Al- $\beta$ (AlAg) (73.5% Ag,  $558^{\circ}\text{C}$ — $1036^{\circ}\text{F}$ ) toward the lead corner, striking the miscibility curve at 69 per cent silver, 1.73 per cent lead,  $548^{\circ}\text{C}$  ( $1018^{\circ}\text{F}$ ). The fields of primary crystallization are: Al,  $\beta$ (AlAg),  $\gamma$ (AlAg), Ag, and Pb,

distributed as in Fig. 52. In the solid state in the aluminum corner the phases Al,  $\beta(\text{AlAg})$ , and Pb should be present over all the field, due allowance being made for the solid solubility of silver in aluminum, which should not be appreciably affected by the presence of lead.

Since silver is not used as an addition in commercial aluminum alloys, this diagram at present is of only theoretical interest.

### **Al-Ag-Si**

#### **Aluminum-Silver-Silicon**

This system was investigated by Goto and Mishima (492); however, their original paper, in Japanese, has not been translated or abstracted in any European language.

From what can be gathered from the Japanese publication and from a superficial examination by the author, it seems that no ternary phase is formed; the constituents in the aluminum corner are Al, Si, and  $\beta(\text{AlAg})$  with the exception of the zone where silver is in solid solution and  $\beta(\text{AlAg})$  is not present.

### **Al-Ag-Zn**

#### **Aluminum-Silver-Zinc**

The only investigation of this system is by Ueno (493).

Both silver and zinc are soluble in aluminum to a large extent, and they do not seem to affect their respective solid solubilities. The aluminum corner, therefore, is very simple. Both the solidification surface and the solid at eutectic temperature will show only aluminum solid solution. At room temperature also the  $\beta(\text{AlAg})$  phase and Zn will be visible.

This system is unimportant because at present silver is not used as a commercial addition in aluminum alloys.

### **Al-Be-Mg**

#### **Aluminum-Beryllium-Magnesium**

The diagrams are from data by Masing and Dahl (495).

No ternary constituent is formed. The phases present in the aluminum corner are: Al,  $\text{Mg}_5\text{Al}_8$ , and Be. A eutectic  $E = \text{Al-Mg}_5\text{Al}_8\text{-Be}$  is formed at about 34 per cent magnesium and 0.5 per cent beryllium, with a melting point of about  $447^\circ\text{C}$  ( $837^\circ\text{F}$ ). The fields of primary crystallization and the distribution of the phases in the solid state are represented in Figs. 53 and 54. The solid solubility of beryllium is not

shown in Fig. 54, for even at eutectic temperature it is of the order of 0.003 per cent.

As with the binary aluminum-beryllium alloys the ternary alloys containing beryllium were investigated in the hope that additions of

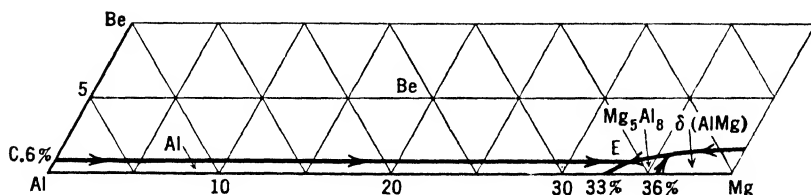


FIG. 53. System Al-Be-Mg, surfaces of primary crystallization in the aluminum corner of the equilibrium diagram.

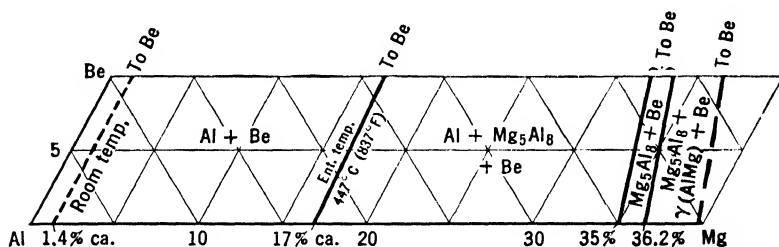


FIG. 54. System Al-Be-Mg, distribution of the phases in the solid in the aluminum corner of the equilibrium diagram.

beryllium to aluminum would produce useful alloys. The results, however, did not confirm the hopes, and no aluminum-beryllium-magnesium alloys are commercially used.

## Al-Be-Si

### Aluminum-Beryllium-Silicon

The equilibrium diagrams shown as Figs. 55 and 56 are from data by Kroll and colleagues (497) and Masing and Dahl (496).

No ternary compound is formed, the phases present being Al, Si, and Be. A ternary eutectic  $E = \text{Al-Be-Si}$  is formed at 0.30 per cent beryllium and 13.4 per cent silicon, with a melting point of  $575^{\circ}\text{C}$  ( $1067^{\circ}\text{F}$ ). Two eutectic lines run from the binary eutectic Al-Si, 11.7 per cent silicon at  $577^{\circ}\text{C}$  ( $1071^{\circ}\text{F}$ ), and Al-Be, 0.6 per cent beryllium at  $647^{\circ}\text{C}$  ( $1197^{\circ}\text{F}$ ), to the ternary eutectic, dividing the fields of primary crystallization of the three constituents. In the solid state the alloys contain a mixture of the three constituents, due allowance being made for the small zone where silicon is in solid solution in aluminum

and therefore invisible. The solid solubility of beryllium at eutectic and room temperature and the solid solubility of silicon at room temperature are not shown in Fig. 56 because they are too limited for an adequate representation.

This system was investigated in the hope that a binary phase similar to  $\text{Mg}_2\text{Si}$  would be formed, which would produce high mechanical

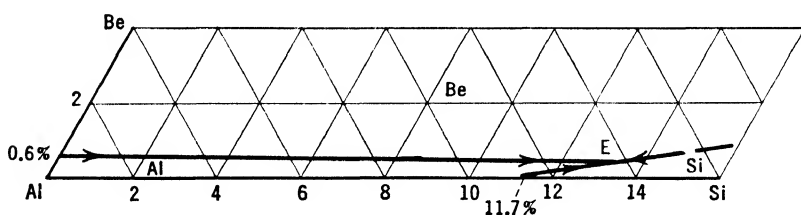


FIG. 55. System Al-Be-Si, surfaces of primary crystallization in the aluminum corner of the equilibrium diagram.

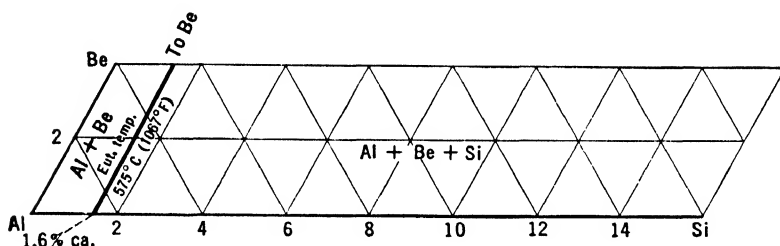


FIG. 56. System Al-Be-Si, distribution of the phases in the solid in the aluminum corner of the equilibrium diagram.

properties. As neither such a phase nor a ternary phase is formed, there is no reason whatsoever to expect properties from the ternary alloys much above those of the binary alloys, which are quite limited.

## Al-Bi-Sb

### Aluminum-Bismuth-Antimony

This system was investigated by Wright (498).

Figure 57 shows the surfaces of primary solidification in the extreme aluminum corner and the limits of miscibility at freezing temperature, according to Wright's data. No explanation is offered for the dent at about 10 per cent antimony, which seems rather improbable. In the solid state the phases Al,  $\text{SbAl}$ , and Bi should be present over all the field.

No practical application has been reported for alloys of this type, nor is it probable that they will be used.

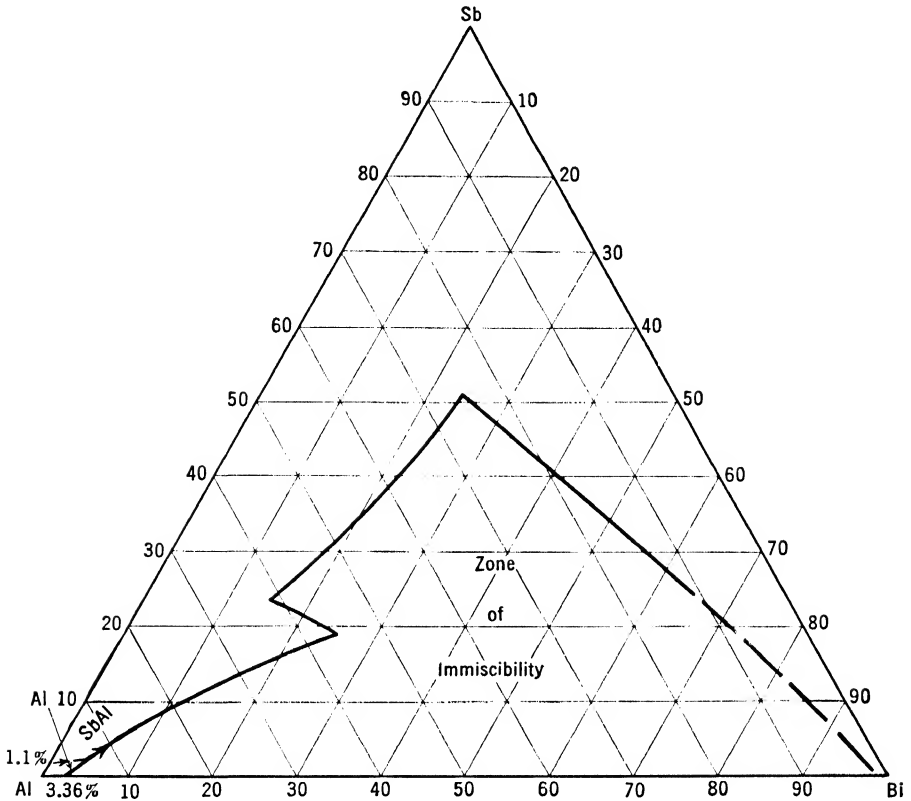


FIG. 57. System Al-Bi-Sb, surfaces of primary crystallization and limits of miscibility.

### Al-Bi-Sn Aluminum-Bismuth-Tin

This system was investigated by Wright (499).

Tin increases the miscibility of bismuth and aluminum as shown in the diagram (Fig. 58), which shows the miscibility at freezing temperature and the probable surfaces of primary crystallization. In the solid state the three phases Al, Bi, and Sn should be present in the aluminum corner, due allowance being made for the solid solubility of tin in aluminum, which should not be affected appreciably by bismuth.

These alloys have little practical importance because no high mechanical properties can be expected from them. They may find some applications as solders if their electrolytic potential is not so different from aluminum as to induce contact corrosion on it.



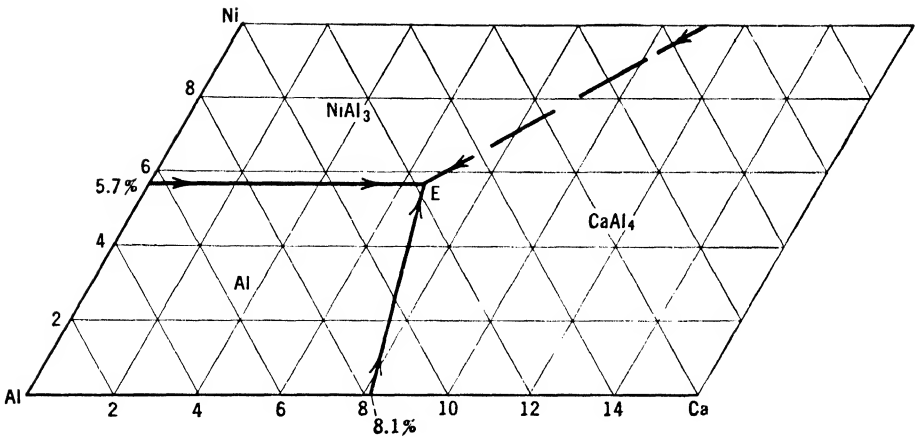


FIG. 59. System Al-Ca-Ni, surfaces of primary crystallization in the aluminum corner of the equilibrium diagram.

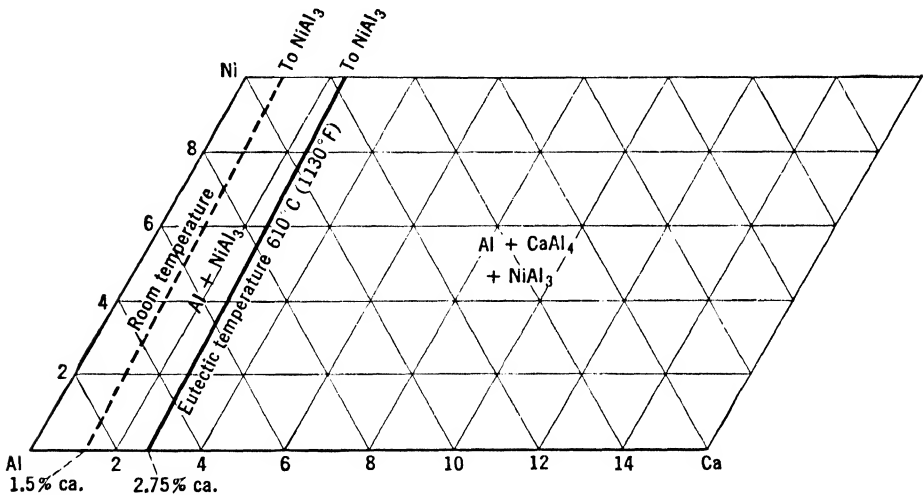


FIG. 60. System Al-Ca-Ni, distribution of the phases in the solid in the aluminum corner of the equilibrium diagram.

## Al-Ca-Si

### Aluminum-Calcium-Silicon

The equilibrium diagrams (Figs. 61 and 62) are from data by Doan (501), Grogan (502), and Shinoda (503).

No ternary phase is formed, the constituents being Al, Si,  $\text{CaAl}_4$ , and  $\text{CaSi}_2$ , which is formed preferentially to  $\text{CaAl}_4$ . Four zones of primary solidification are present and two ternary eutectics:  $E_1 = \text{Al-CaSi}_2\text{-Si}$ , containing 11.5 per cent silicon and 0.9 per cent calcium, with a melting point of  $576^\circ\text{C}$  ( $1069^\circ\text{F}$ );  $E_2 = \text{Al-CaSi}_2\text{-CaAl}_4$ , con-





without the need of prolonged annealing, which lowers the mechanical properties, aluminum wire could be used more generally for electrical conductors. However, in the meantime aluminum with lower and lower silicon contents has been produced and these alloys have never been widely used.

### Al-Cd-Mg

#### Aluminum-Cadmium-Magnesium

This system has been completely investigated several times, but, as all the investigations were based on magnesium-cadmium diagrams showing several intermetallic phases and on aluminum-magnesium diagrams showing only two phases, the data reported are rather

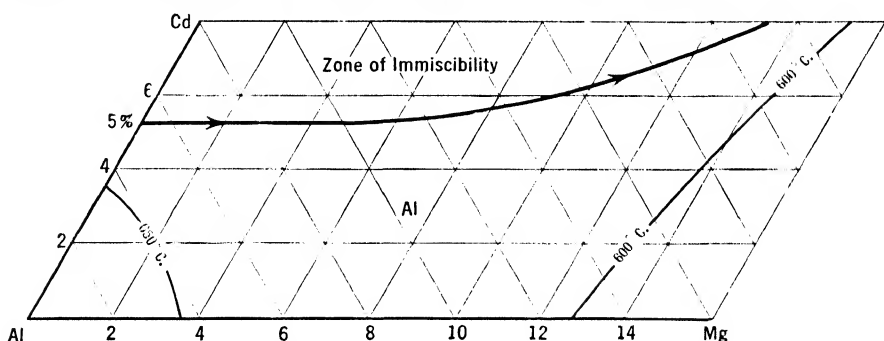


FIG. 63. System Al-Cd-Mg, surfaces of primary crystallization in the aluminum corner of the equilibrium diagram.

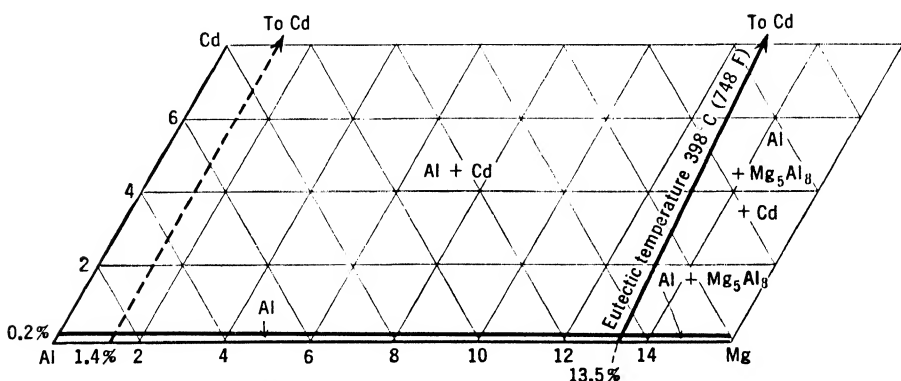


FIG. 64. System Al-Cd-Mg, distribution of the phases in the solid in the aluminum corner of the equilibrium diagram.

doubtful. However the data of Jaenecke (506) and Riederer (507) are reliable for the aluminum corner, therefore only this part of the diagram is shown in Figs. 63 and 64.

The immiscibility between cadmium and aluminum is decreased by additions of magnesium, probably through the formation of the solid

solution (MgCd). No ternary constituent is formed. A ternary eutectic, probably  $\text{Al-Mg}_5\text{Al}_8\text{-(MgCd)}$ , contains 52 per cent magnesium and 28 per cent cadmium and has a melting point of  $398^\circ\text{C}$  ( $748^\circ\text{F}$ ). Cadmium and magnesium do not seem to influence their respective solid solubilities. Figures 63 and 64 show the fields of primary solidification and the distribution of the phases in the solid. The solid solubility of cadmium is reported only at eutectic temperature, for at room temperature it is too small to be represented.

No aluminum-cadmium-magnesium alloy is used commercially. In the early days of the magnesium industry some magnesium alloys containing aluminum and cadmium were used, but now even they have been abandoned.

### Al-Cd-Sn

#### Aluminum-Cadmium-Tin

These alloys have been investigated by Wright (508).

No ternary phase is formed by aluminum, cadmium, and tin, and tin only slightly reduces the immiscibility of cadmium and aluminum.

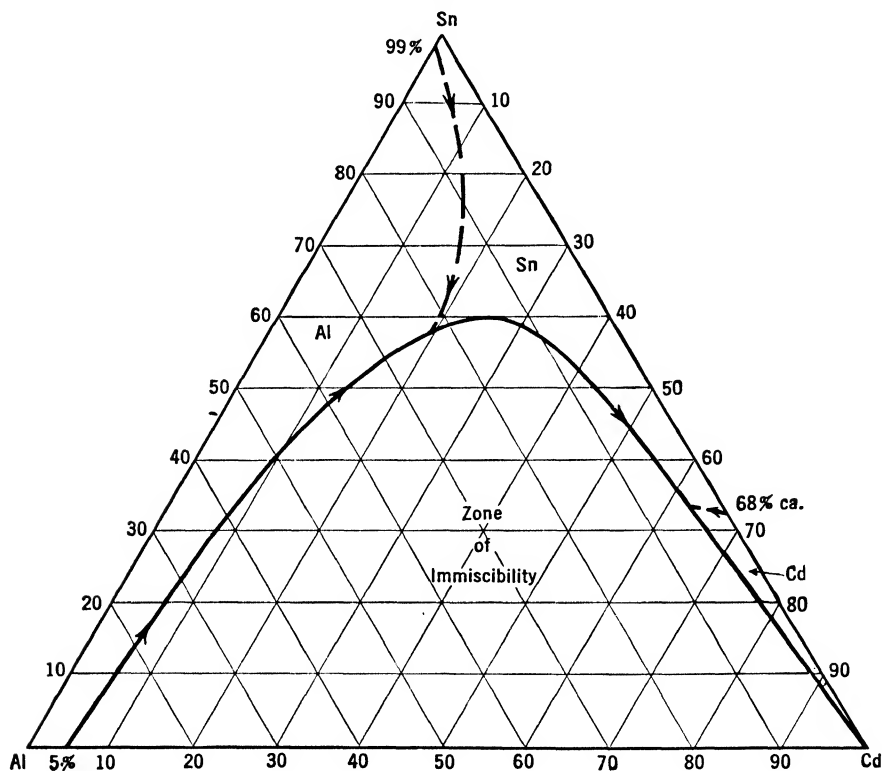


FIG. 65. System Al-Cd-Sn, surfaces of primary crystallization and limits of miscibility.

Figure 65 shows the limits of miscibility at freezing temperature and the probable surfaces of primary crystallization. In the solid state the three phases Al, Cd, Sn should be present over all the field, due allowance being made for the zones of solid solubility of tin and cadmium in aluminum.

No practical use for these alloys has been reported.

### Al-Cd-Zn

#### Aluminum-Cadmium-Zinc

The diagram shown as Fig. 66 is from data by Bugden (509).

No ternary phase is formed, the phases present being Al, Zn, and Cd. The gap of miscibility between aluminum and cadmium extends almost to the zinc corner. A ternary eutectic probably is formed very near the binary Cd-Zn [82.5 per cent cadmium, 266°C (511°F)] containing very little aluminum. Figure 66 shows the field of immiscibility and the fields of primary crystallization. No sufficient data on the distribution of the phases in the solid state are available; probably the

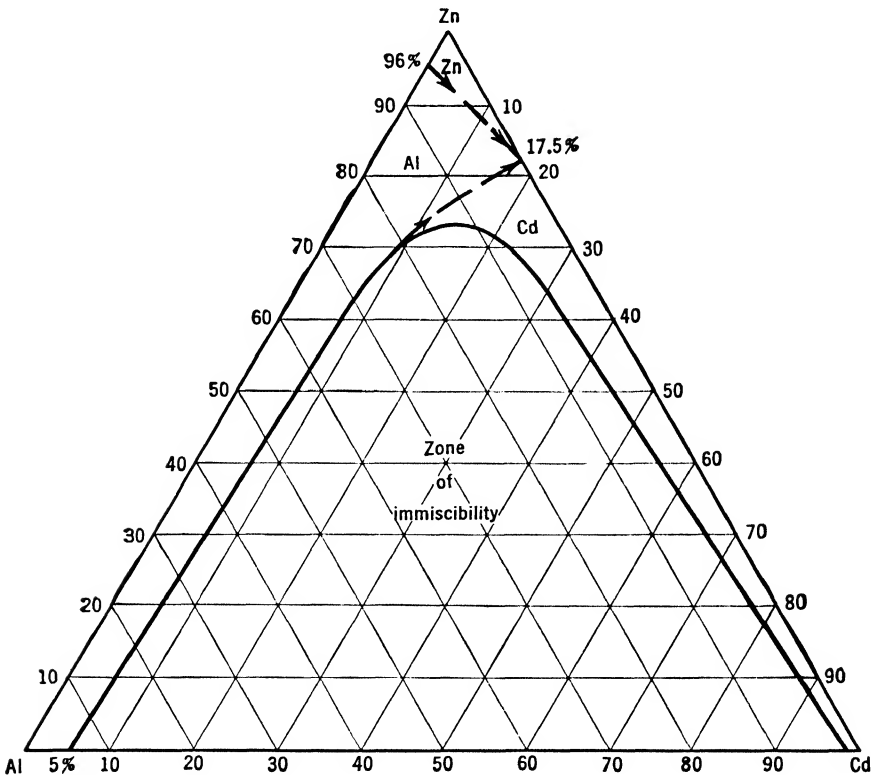


FIG. 66. System Al-Cd-Zn, surfaces of primary crystallization and miscibility at freezing temperature.

presence of cadmium does not affect the gap of miscibility between aluminum and zinc.

No aluminum alloy containing cadmium and zinc has found commercial use.

### **Al-Ce-Fe**

#### **Aluminum-Cerium-Iron**

The only investigations available on this system are those of Schulte (513) and of Meissner (512), which are rather sketchy and probably incorrect.

According to these authors, no ternary compound is formed and the addition of cerium to aluminum-iron alloys decomposes  $\text{FeAl}_3$  to form  $\text{CeFe}_6$  and Al. No data about solidification or eutectics are reported.

Since cerium sometimes is added to aluminum alloys, this diagram may have some interest for such alloys. The data reported, however, are not sufficient for any practical use and, if cerium should be used to a larger extent, this diagram would have to be investigated more thoroughly.

### **Al-Co-Cu**

#### **Aluminum-Cobalt-Copper**

No data about the aluminum corner of this system have been published.

Investigations by the author show the presence of at least one and probably two ternary phases, similar to the  $(\text{CuFe})\text{Al}_3$  and  $\text{Cu}_2\text{FeAl}_7$  phases in the Al-Cu-Fe diagram. Probably the diagram is similar to the Al-Cu-Fe diagram.

At present, cobalt is added only to alloys containing small amounts of copper. However, as additions of cobalt to aluminum-copper alloys could produce good properties, a thorough investigation of this diagram might reveal interesting data.

### **Al-Co-Fe**

#### **Aluminum-Cobalt-Iron**

The limited data published on this system refer to alloys rich in iron and cobalt and are of no interest for aluminum alloys; no data have been published on the aluminum corner.

Investigations by the author show that iron and cobalt form a ternary phase with aluminum, probably a series of solid solutions of  $\text{FeAl}_3$  and  $\text{Co}_2\text{Al}_9$  that extends across the whole field.

This diagram is important for alloys of the aluminum-silicon type which contain cobalt. Further investigations on the nature of the

ternary phase could be very useful for a better understanding of the effect of cobalt on the iron-bearing phases in aluminum alloys.

### Al-Co-Mg

#### Aluminum-Cobalt-Magnesium

No data on the aluminum corner of these alloys have been published.

Investigations by the author show that no ternary phase is formed, the constituents of the system being Al,  $\text{Co}_2\text{Al}_9$ , and  $\text{Mg}_5\text{Al}_8$ , which

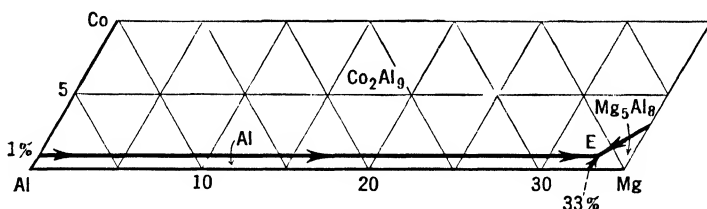


FIG. 67. System Al-Co-Mg, surfaces of primary crystallization in the aluminum corner of the equilibrium diagram.

form a ternary eutectic  $E$  at about 33 per cent magnesium, 0.5 per cent cobalt, with a melting point of about  $448^\circ\text{C}$  ( $838^\circ\text{F}$ ). In the solid state the three constituents are present over all the field, with the exception of the zone where magnesium is in solid solution and  $\text{Mg}_5\text{Al}_8$  cannot be seen. Cobalt does not appreciably affect the solid solubility of magnesium in aluminum. The solid solubility of cobalt is so small

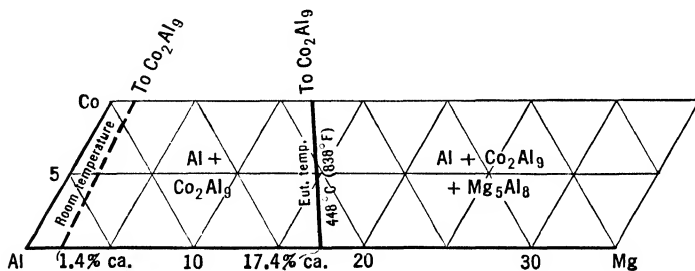


FIG. 68. System Al-Co-Mg, distribution of the phases in the solid in the aluminum corner of the equilibrium diagram.

that it can be considered practically non-existent. Figures 67 and 68 show the solidification surfaces and the distribution of the phases in the solid.

This diagram is of little interest from the practical point of view because no aluminum-magnesium alloy containing cobalt has ever been used.

### Al-Co-Si Aluminum-Cobalt-Silicon

No data have been published on the aluminum corner of this system.

Investigations by the author show that no ternary phase is formed and the constituents in the aluminum corner are Al,  $\text{Co}_2\text{Al}_9$ , and Si.

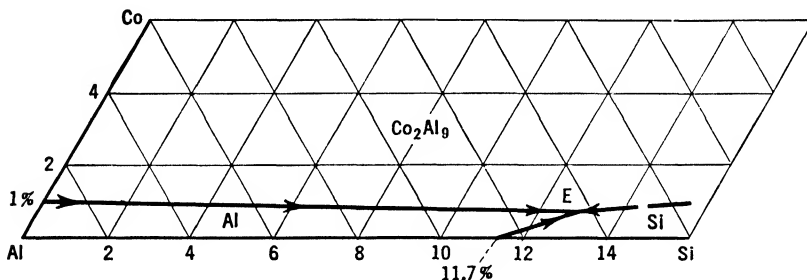


FIG. 69. System Al-Co-Si, surfaces of primary crystallization in the aluminum corner of the equilibrium diagram.

A ternary eutectic *E* is formed containing about 13 per cent silicon and 0.7 per cent cobalt, with a melting point of  $575^\circ\text{C}$  ( $1067^\circ\text{F}$ ). In the solid state the three phases are present together over all the field, due allowance being made for the solid solubility of silicon in aluminum, which is not appreciably affected by the presence of cobalt. The solid

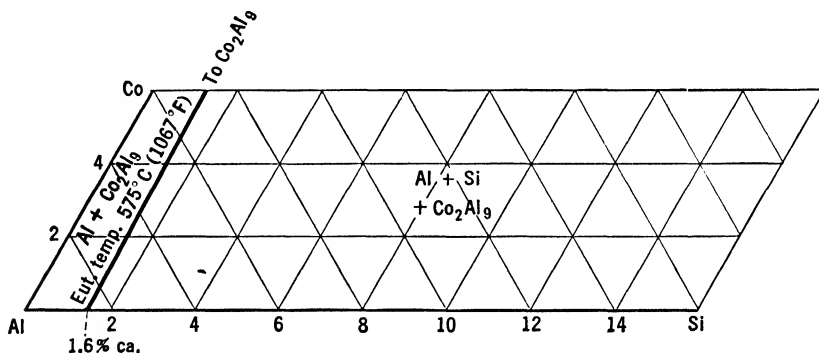


FIG. 70. System Al-Co-Si, distribution of the phases in the solid in the aluminum corner of the equilibrium diagram.

solubility of silicon is reported in the diagram only at eutectic temperature, since at room temperature it is too small to be adequately represented.

As in the Al-Co-Fe diagram, this diagram is important for aluminum-silicon alloys containing cobalt. The quaternary Al-Co-Fe-Si will be more interesting because commercial alloys always contain iron, but for practical applications the ternary diagrams give sufficient data.

## Al-Cr-Cu

## Aluminum-Chromium-Copper

The diagrams in Figs. 71 and 72 are plotted from data by Roentgen and Koch (514) and Knappwost and Nowotny (515).

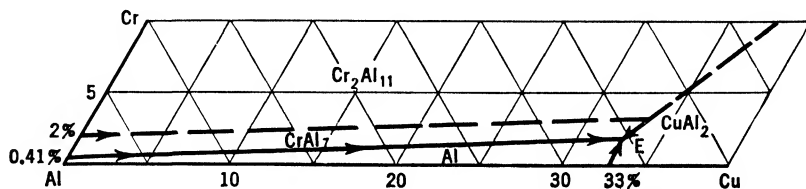


FIG. 71. System Al-Cr-Cu, surfaces of primary crystallization in the aluminum corner of the equilibrium diagram, according to Roentgen and Koch.

No ternary phase is formed in the aluminum corner, the phases present being Al,  $\text{CuAl}_2$ ,  $\text{CrAl}_7$ , and  $\text{Cr}_2\text{Al}_{11}$ . A ternary eutectic  $E = \text{Al-CuAl}_2\text{-CrAl}_7$  is formed at about 32 per cent copper, 1.5 per cent

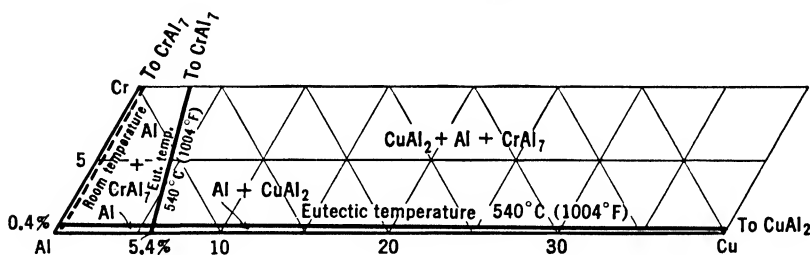


FIG. 72. System Al-Cr-Cu, distribution of the phases in the solid in the aluminum corner of the equilibrium diagram.

chromium, with a melting point of about  $540^\circ\text{C}$  ( $1004^\circ\text{F}$ ). Figure 72 shows the distribution of the phases in the solid. Chromium and copper do not affect appreciably their respective solid solubilities. The

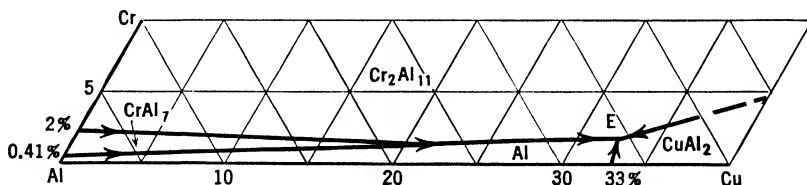


FIG. 73. System Al-Cr-Cu, surfaces of primary crystallization in the aluminum corner of the equilibrium diagram, according to the author.

solid solubility of chromium is shown in the diagram only at eutectic temperature because at room temperature it is practically zero.

Investigations by the author tend to show that the transformation  $\text{Cr}_2\text{Al}_{11} \rightarrow \text{CrAl}_7$  is hindered by the presence of copper so that, in



alloys with high copper content, the field of primary crystallization of  $\text{Cr}_2\text{Al}_{11}$  takes the place of the  $\text{CrAl}_7$  field. Accordingly, the ternary eutectic is  $\text{Al-CuAl}_2\text{-Cr}_2\text{Al}_{11}$ . The diagram shown as Fig. 73 embodies these data.

Chromium is not commonly added to alloys containing copper. In the rare instances when chromium and copper are present in the same alloy, this diagram is still unimportant because, in the presence of iron and silicon, chromium tends to combine with them to form ternary or quaternary phases.

## Al-Cr-Fe

### Aluminum-Chromium-Iron

The diagrams reported (Figs. 74 and 75) are from data by Taillandier (516) and the author.

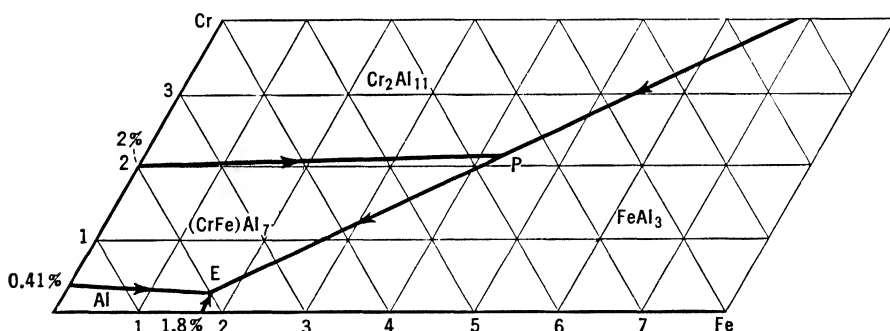


FIG. 74. System Al-Cr-Fe, surfaces of primary crystallization in the aluminum corner of the equilibrium diagram.

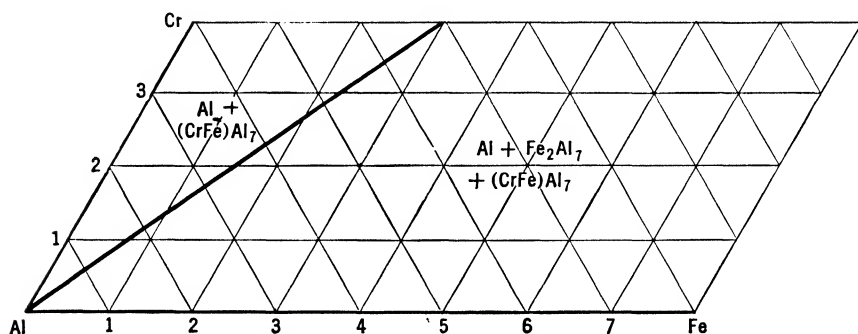


FIG. 75. System Al-Cr-Fe, distribution of the phases in the solid in the aluminum corner of the equilibrium diagram.

No ternary constituent is formed in the aluminum corner, and iron is soluble to a certain extent in  $\text{CrAl}_7$ , forming a phase with characteristics slightly different from straight  $\text{CrAl}_7$ . This phase will be

designated  $(\text{CrFe})\text{Al}_7$ . The phases in the aluminum corner are: Al,  $(\text{CrFe})\text{Al}_7$ ,  $\text{Cr}_2\text{Al}_{11}$ ,  $\text{Fe}_2\text{Al}_7$ , and  $\text{FeAl}_3$ . There are two singular points in the diagram: a peritectic  $P = \text{liquid} + \text{Cr}_2\text{Al}_{11} \rightarrow \text{CrAl}_7$  at about 4.2 per cent iron, 2.1 per cent chromium; and a eutectic  $E = \text{Al} - (\text{CrFe})\text{Al}_7 - \text{FeAl}_3$  at  $640^\circ\text{C}$  ( $1184^\circ\text{F}$ ), 1.7 per cent iron, 0.3 per cent chromium. Figures 74 and 75 show the fields of primary crystallization and the distribution of the phases in the solid state. No solid solubilities are reported in the diagram, for the presence of iron greatly reduces the solid solubility of chromium so that it becomes practically negligible even at eutectic temperature.

Non-equilibrium conditions produced by fast cooling have practically no effect on these alloys when the chromium and iron contents are not above 4 per cent each.

This system has some importance for commercial alloys. However, commercial alloys containing chromium usually contain silicon and magnesium as well, so that the ternary diagrams Al-Cr-Si and Al-Cr-Mg should also be consulted.

## Al-Cr-Mg

### Aluminum-Chromium-Magnesium

The partial diagrams (Figs. 76 and 77) are by Erdmann-Jesnitzer (517). According to him, aluminum, magnesium, and chromium form

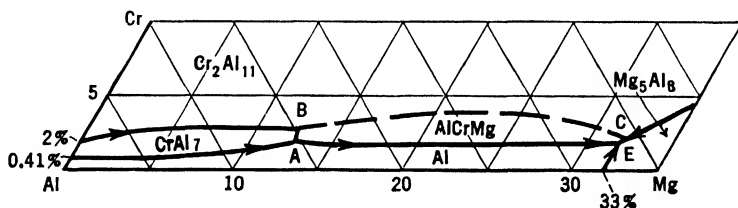


FIG. 76. System Al-Cr-Mg, surfaces of primary crystallization in the aluminum corner of the equilibrium diagram, according to Erdmann-Jesnitzer.

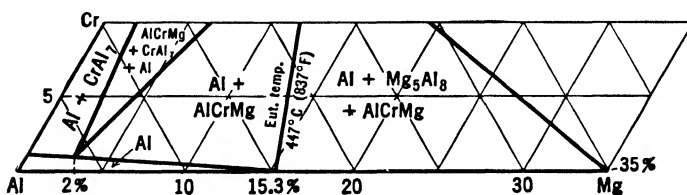


FIG. 77. System Al-Cr-Mg, distribution of the phases in the solid in the aluminum corner of the equilibrium diagram, according to Erdmann-Jesnitzer.

a ternary phase containing about 17 per cent chromium and 9 per cent magnesium, which is present in alloys containing more than 2 per cent

magnesium. There is a ternary eutectic:  $E = \text{Al}-\text{Mg}_5\text{Al}_8-\text{AlCrMg}$  at  $447^\circ\text{C}$  ( $837^\circ\text{F}$ ) containing 31.1 per cent magnesium and 1.7 per cent chromium. There are three other invariant points:  $A = \text{liquid} + \text{CrAl}_7 \rightarrow \text{AlCrMg}$ , Cr 1.7 per cent, Mg 12.8 per cent,  $632^\circ\text{C}$  ( $1170^\circ\text{F}$ );  $B$  with a composition Cr 2.3 per cent, Mg 12.6 per cent;  $C$  with an approximate composition Cr 2 per cent, Mg 32 per cent. The fields

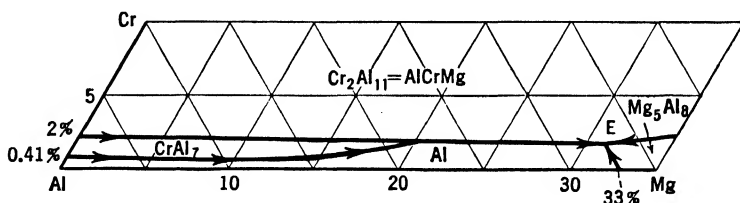


FIG. 78. System Al-Cr-Mg, surfaces of primary crystallization in the aluminum corner of the equilibrium diagram, according to the author.

of primary crystallization and the distribution of the phases in the solid are shown in Figs. 76 and 77.

Investigations by the author indicate somewhat different diagrams (Figs. 78 and 79). There is no real ternary constituent, the phases present in the aluminum corner being Al,  $\text{CrAl}_7$ ,  $\text{Mg}_5\text{Al}_8$ , and  $\text{Cr}_2\text{Al}_{11}$ , which can take a certain amount of magnesium in solid solution. The presence of magnesium reduces the field of primary crystallization of  $\text{CrAl}_7$  so that at about 20 per cent magnesium it disappears. The

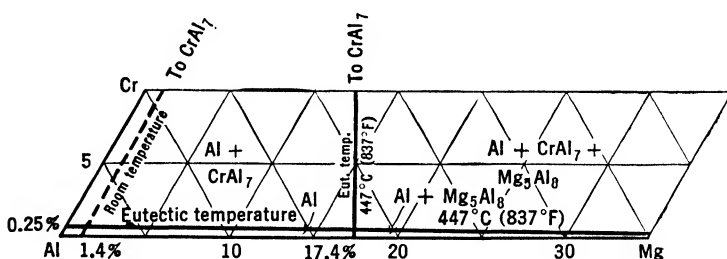


FIG. 79. System Al-Cr-Mg, distribution of the phases in the solid in the aluminum corner of the equilibrium diagram, according to the author.

ternary eutectic is  $\text{Al}-\text{Cr}_2\text{Al}_{11}-\text{Mg}_5\text{Al}_8$ . The solid solubility of chromium, from about 0.25 per cent in the binary aluminum-chromium alloys, is progressively reduced by additions of magnesium, so that at about 35 per cent magnesium (corresponding to the compound  $\text{Mg}_5\text{Al}_8$ ) no more chromium goes into solid solution. Similarly, the solid solubility of magnesium is reduced by additions of chromium, so that at 21.6 per cent chromium ( $\text{CrAl}_7$ ) is reduced to zero. The solid solubility of chromium is shown in the diagram (Fig. 79) only at eutectic tem-

perature because at room temperature it is too small to be represented.

Several alloys containing magnesium and chromium are in commercial use. However, this diagram can be used only in alloys with low silicon because, in the presence of silicon, magnesium forms  $\text{Mg}_2\text{Si}$  and chromium forms  $\alpha(\text{AlCrSi})$ , so that the ternary diagrams Al-Mg-Si and Al-Cr-Si must be consulted in those cases.

### Al-Cr-Ni

#### Aluminum-Chromium-Nickel

The only data available are those contained in a paper by Roentgen and Koch (519), which deals mostly with the mechanical properties.

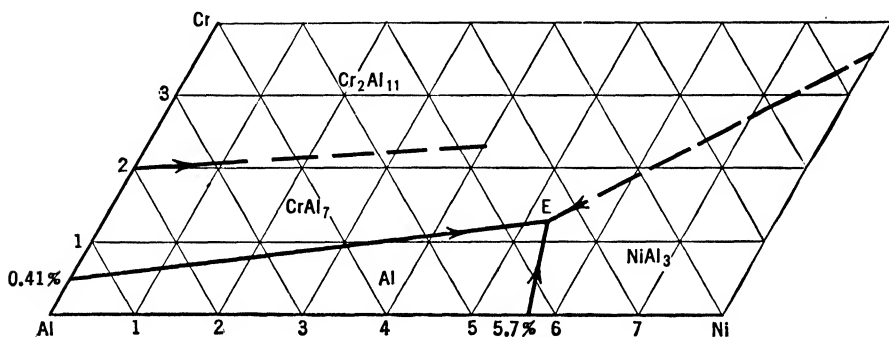


FIG. 80. System Al-Cr-Ni, surfaces of primary crystallization in the aluminum corner of the equilibrium diagram.

No ternary phase is formed, the phases present in the aluminum corner being Al,  $\text{NiAl}_3$ , and  $\text{CrAl}_7$ , which form a ternary eutectic  $E$ , containing about 1.3 per cent chromium and 5 to 6 per cent nickel.

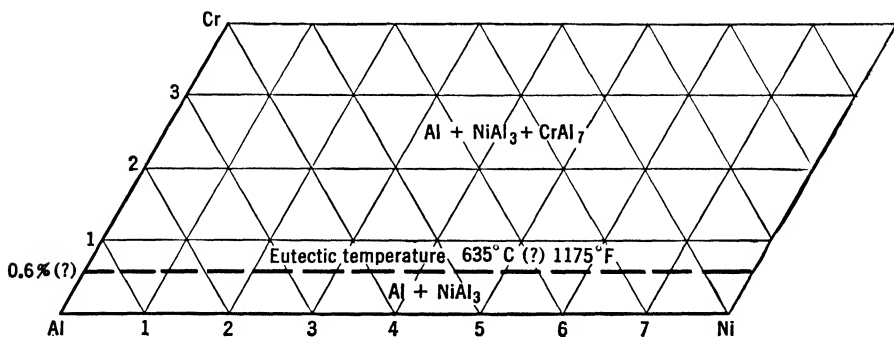


FIG. 81. System Al-Cr-Ni, distribution of the phases in the solid in the aluminum corner of the equilibrium diagram.

The fields of primary crystallization and the distribution of the phases in the solid are shown in Figs. 80 and 81. The solid solubility of

chromium at eutectic temperature is reported with a dashed line since the value is approximate. It is not reported at room temperature because it is so small that it can be considered zero.

Some alloys of the aluminum-copper-nickel type may contain small amounts of chromium. However, these diagrams are not very useful as the nickel tends to combine with the copper and the iron, and the chromium combines with the iron and the silicon.

## Al-Cr-Si

### Aluminum-Chromium-Silicon

The data published on this system are very limited.

Investigations by the author show the presence of two ternary phases. One of them,  $\alpha(\text{AlCrSi})$ , forms hexagonal crystals and tends

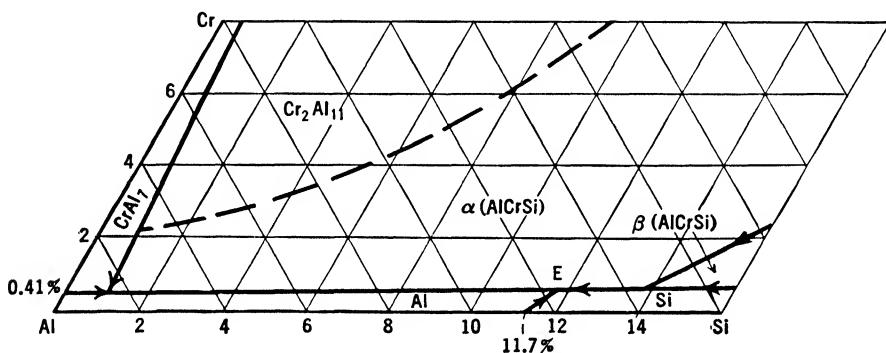


FIG. 82. System Al-Cr-Si, surfaces of primary crystallization in the aluminum corner of the equilibrium diagram.

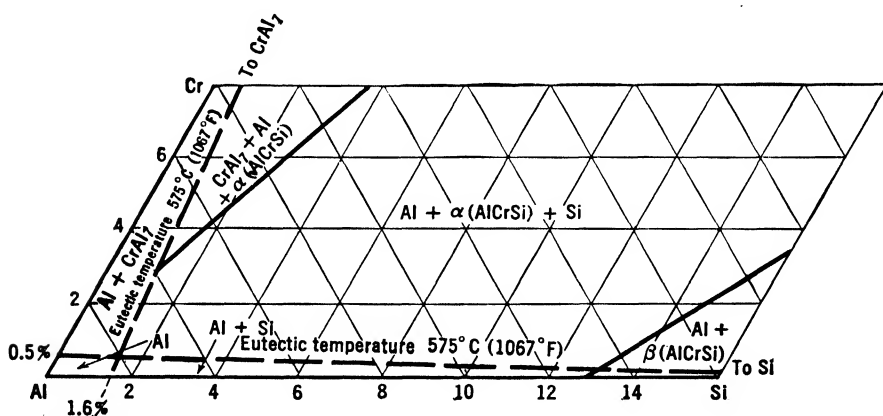


FIG. 83. System Al-Cr-Si, distribution of the phases in the solid in the aluminum corner of the equilibrium diagram.

to form a Chinese script pattern. The silicon content is low and its formula might be  $\text{CrSiAl}_6$ . The other phase  $\beta(\text{AlCrSi})$  probably forms

monoclinic crystals; it is formed only with high silicon contents; its formula should be approximately  $\text{CrSi}_2\text{Al}_4$ . A ternary eutectic  $E = \text{Al} - \alpha(\text{AlCrSi}) - \text{Si}$  is formed, containing about 12 per cent silicon and 0.5 per cent chromium, with a melting point of around  $575^\circ\text{C}$  ( $1067^\circ\text{F}$ ). The fields of primary crystallization and the distribution of the phases in the solid are illustrated in Figs. 82 and 83. The solid solubilities of chromium and silicon at eutectic temperature are shown by dashed lines because the values are only approximate; at room temperature they are so small that they are practically negligible.

This system may be useful for alloys of the  $\text{Mg}_2\text{Si}$  type, with chromium additions. For these alloys, however, the Al-Cr-Mg and Al-Mg-Si diagrams should also be consulted, for only silicon which is not otherwise combined tends to form AlCrSi phases. Additions of chromium to high-silicon alloys have been tried, but these alloys have never been used on a large scale because the  $\beta(\text{AlCrSi})$  phase which is formed tends to render the alloys brittle.

### Al-Cu-Fe

#### Aluminum-Copper-Iron

The partial equilibrium diagrams (Figs. 84 and 85) are from data by Bradley and Goldschmidt (528), Gwyer and colleagues (524), Brown and colleagues (529), and the author.

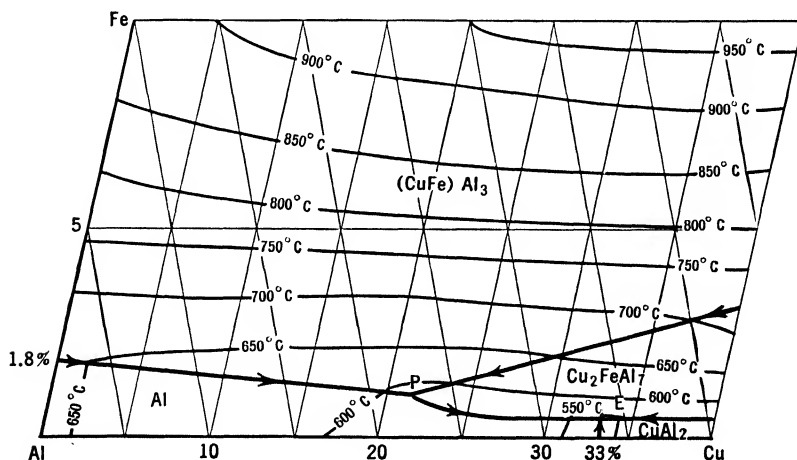


FIG. 84. System Al-Cu-Fe, surfaces of primary crystallization in the aluminum corner of the equilibrium diagram.

Aluminum, copper, and iron form several ternary phases, one of which,  $\text{Cu}_2\text{FeAl}_7$ , is present in the aluminum corner in equilibrium with Al. Another phase, pseudo-ternary, is formed by  $\text{FeAl}_3$  which

takes into solution up to about 15 per cent copper and assumes characteristics slightly different from  $\text{FeAl}_3$ ; this phase will be designated

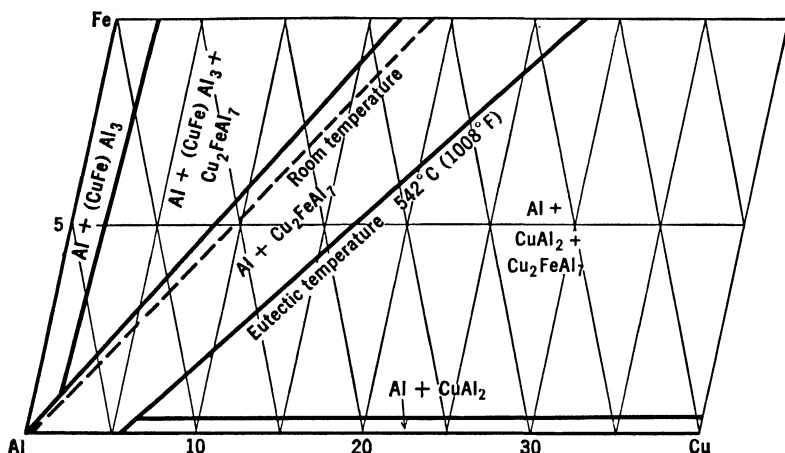


FIG. 85. System Al-Cu-Fe, distribution of the phases in the solid in the aluminum corner of the equilibrium diagram.

$(\text{CuFe})\text{Al}_3$ . There is a ternary eutectic  $E = \text{Al}-\text{CuAl}_2-\text{Cu}_2\text{FeAl}_7$  containing 32.5 per cent copper, 0.3 per cent iron, and melting at  $542^\circ\text{C}$  ( $1008^\circ\text{F}$ ). Another singular point  $P = \text{liquid} + \text{FeAl}_3 \rightarrow \text{Cu}_2\text{FeAl}_7$  is at 21.5 per cent copper, 1 per cent iron, and  $590^\circ\text{C}$  ( $1094^\circ\text{F}$ ). In

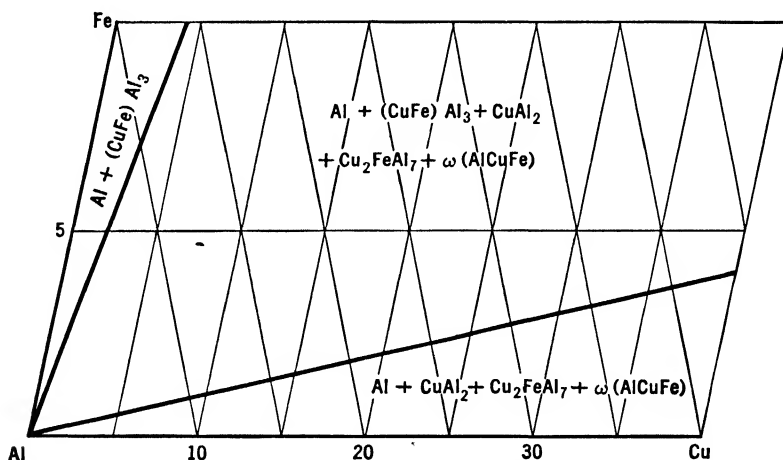


FIG. 86. System Al-Cu-Fe, distribution of the phases in the solid in the aluminum corner in non-equilibrium conditions.

the solid state the phases present in the aluminum corner are Al,  $\text{CuAl}_2$ ,  $(\text{CuFe})\text{Al}_3$ , and  $\text{Cu}_2\text{FeAl}_7$ . Iron is almost insoluble in aluminum and the solid solubility of copper changes with changes in temper-

ature. The shapes of the diagram in the solid state change accordingly. Consult Fig. 85 for the aluminum corner showing these changes.

In unstable conditions, especially when the cooling rate is high, another phase different from  $\text{Cu}_2\text{FeAl}_7$  can be found together with Al. This phase is unstable and tends to react with aluminum to form  $\text{Cu}_2\text{FeAl}_7$ . It is often detected in commercial alloys cast in permanent mold. Figure 86 shows the distribution of the phases in the solid in non-equilibrium conditions. Like all diagrams referring to non-equilibrium conditions, this one is only approximate.

These diagrams can be used for aluminum alloys containing copper. However, as aluminum alloys always contain silicon, in most cases the quaternary Al-Cu-Fe-Si should be consulted unless the silicon is otherwise combined. If the alloys contain magnesium, manganese, nickel, or chromium, these diagrams have no bearing because iron and, usually, copper tend to be combined differently.

### Al-Cu-Mg

#### Aluminum-Copper-Magnesium

Figures 87, 88, and 89 are from data by Nishimura (543) and Obinata and Mutuzaki (545).

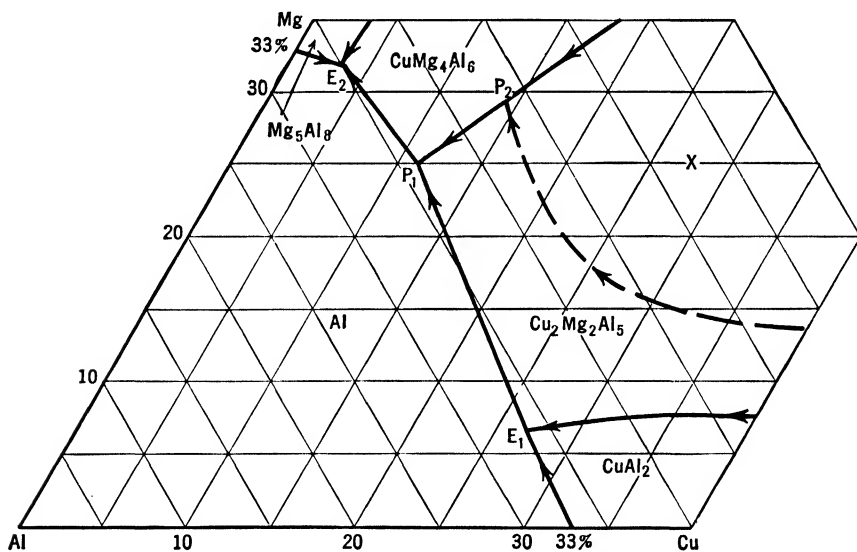


FIG. 87. System Al-Cu-Mg, surfaces of primary crystallization in the aluminum corner of the equilibrium diagram.

There are two ternary phases in the aluminum corner:  $\text{Cu}_2\text{Mg}_2\text{Al}_5$ , tetragonal, with lattice parameters  $a = 5.71 \text{ \AA}$ ,  $c = 7.94 \text{ \AA}$ , and 18



atoms in the unit cell;  $\text{CuMg}_4\text{Al}_6$ , cubic with lattice parameter  $a = 14.25 \text{ \AA}$ , and 161 atoms in the unit cell. The fields of primary crystallization are Al,  $\text{CuAl}_2$ ,  $\text{Mg}_5\text{Al}_8$ ,  $\text{Cu}_2\text{Mg}_2\text{Al}_5$ ,  $\text{CuMg}_4\text{Al}_6$ , and X, in which X is a phase richer in copper and magnesium of unknown composition. The two ternary eutectics are:

$$E_1 = \text{Al}-\text{CuAl}_2-\text{Cu}_2\text{Mg}_2\text{Al}_5; 26.8\% \text{ Cu}, 6.2\% \text{ Mg}, 500^\circ\text{C} (932^\circ\text{F}).$$

$$E_2 = \text{Al}-\text{Mg}_5\text{Al}_8-\text{CuMg}_4\text{Al}_6; 3\% \text{ Cu}, 32\% \text{ Mg}, 447^\circ\text{C} (837^\circ\text{F}).$$

The two peritectic points are:

$$P_1 = \text{liquid} + \text{Cu}_2\text{Mg}_2\text{Al}_5 \rightarrow \text{Al} + \text{CuMg}_4\text{Al}_6; 11\% \text{ Cu}, 25\% \text{ Mg}, 465^\circ\text{C} (869^\circ\text{F}).$$

$$P_2 = \text{liquid} + \text{X} \rightarrow \text{Cu}_2\text{Mg}_2\text{Al}_5 + \text{CuMg}_4\text{Al}_6; 14\% \text{ Cu}, 29.5\% \text{ Mg}, 525^\circ\text{C} (977^\circ\text{F}).$$

Figures 88 and 89 show the distribution of the phases in the solid state. Two solid solubilities at eutectic temperature are shown, corresponding to the two eutectic temperatures in the system. The solid solubilities at room temperature are shown with dotted lines, as usual.

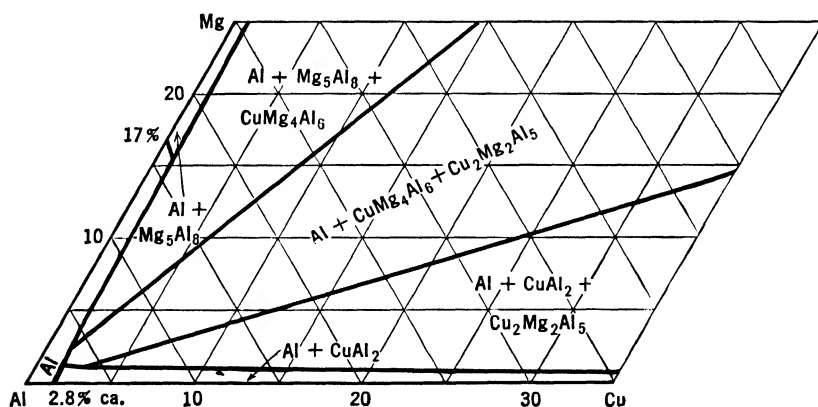


FIG. 88. System Al-Cu-Mg, distribution of the phases in the solid in the aluminum corner of the equilibrium diagram.

In non-equilibrium conditions alloys with high magnesium and copper contents show the presence of several unknown phases from which  $\text{Cu}_2\text{Mg}_2\text{Al}_5$  and  $\text{CuMg}_4\text{Al}_6$  are formed by peritectic reactions. At lower concentrations in the field of primary crystallization of Al, the non-equilibrium conditions produced by fast cooling affect only the amount of the constituents in solid solution.

Although many aluminum alloys contain copper and magnesium, these diagrams can be used in only a few cases, for the presence of

silicon changes the nature and distribution of the phases present. For this reason, these diagrams can be used only for alloys with very low silicon content; otherwise the quaternary Al-Cu-Mg-Si should be consulted.

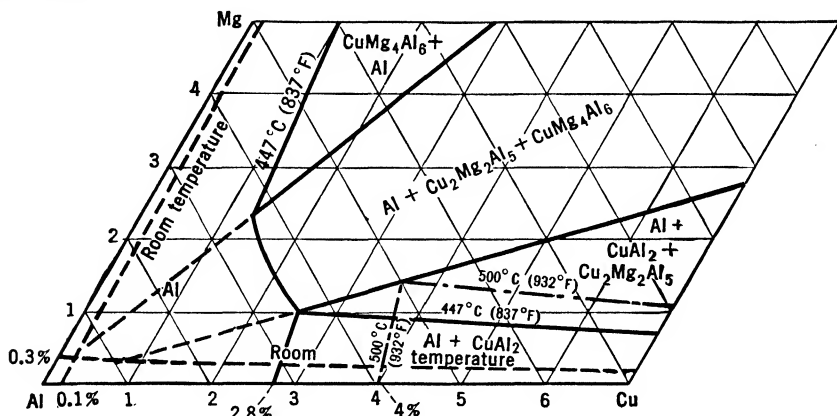


FIG. 89. System Al-Cu-Mg, detail of the distribution of the phases in the solid in the aluminum corner of the equilibrium diagram, showing the solid solubilities of the various phases.

## Al-Cu-Mn

## Aluminum-Copper-Manganese

The data available on this system are conflicting.

According to Petri (549), two ternary phases are present in the aluminum corner: *T*, rhombic with lattice parameters  $a = 7.69$  Å,  $b = 24.06$  Å,  $c = 12.48$  Å, containing 19 per cent copper and 24 per cent manganese; *Y*, rhombic with lattice parameters  $a = 14.79$  Å,  $b = 12.6$  Å,  $c = 12.43$  Å, containing 5.9 per cent copper and 32.5 per cent manganese. A ternary eutectic  $E = \text{Al}-T\text{-CuAl}_2$  has the composition: 31.5 per cent copper, 0.8 per cent manganese, and a melting point of 547°C (1017°F). Three invariant points are reported.

$$A = \text{liquid} + \text{MnAl}_6 \rightarrow \text{Al} + T; \text{Cu } 7\%, \text{Mn } 4\%, 628.5^\circ\text{C } (1164^\circ\text{F}).$$
$$B = \text{liquid} + \text{MnAl}_4 \rightarrow \text{MnAl}_6 + T; \text{ Cu } 8\%, \text{ Mn } 8\%, 700^\circ\text{C} \text{ (1292}^\circ\text{F)}.$$
$$C = \text{liquid} + \text{MnAl}_3 \rightarrow \text{MnAl}_4 + T; \text{Cu } 12\%, \text{Mn } 14\%.$$

The fields of primary solidification and the distribution of the phases in the solid at 500°C (932°F) are shown in Figs. 90 and 91. The compositions of the two points  $T_1$  and  $T_2$ , shown in Fig. 91, in the solid state are reported as:

$$T_1 = \text{Cu } 13\%, \text{ Mn } 24.9\%.$$
$$T_2 = \text{Cu } 15\%, \text{ Mn } 20\%.$$

Former investigations (547–548) do not agree with Petri's results, and investigations by the author confirm the older results. According

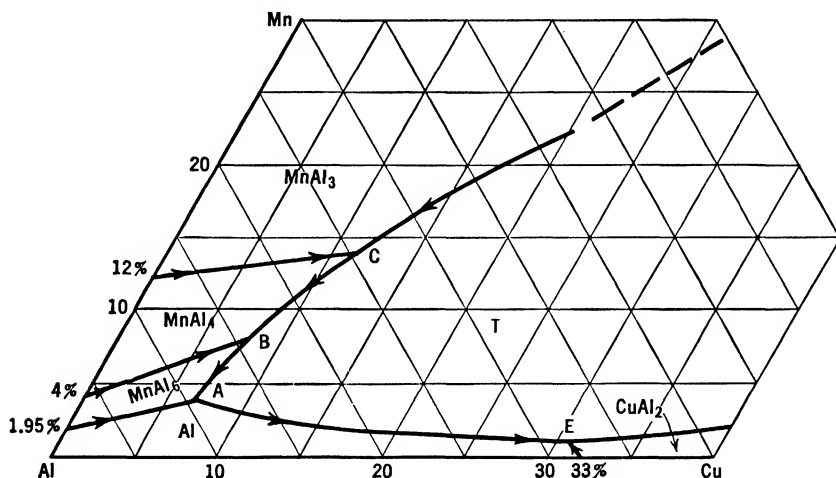


FIG. 90. System Al-Cu-Mn, surfaces of primary solidification in the aluminum corner of the equilibrium diagram, according to Petri.

to these older results, no real ternary phase is formed in the aluminum corner;  $\text{MnAl}_4$  can take some copper in solid solution; its field of crystallization is wide and increases with increasing copper contents

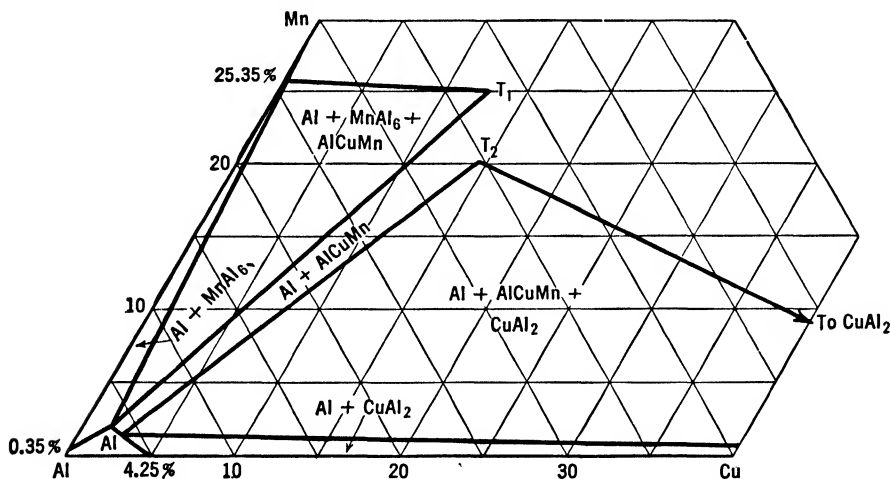


FIG. 91. System Al-Cu-Mn, distribution of the phases in the solid in the aluminum corner of the equilibrium diagram, according to Petri.

at the expense of  $\text{MnAl}_6$ , until the latter disappears, at about 20 per cent copper. The ternary eutectic is  $\text{Al}-(\text{CuMn})\text{Al}_4\text{-CuAl}_2$ , with the same composition and melting point as reported by Petri. In Figs. 92

and 93 the diagrams of the primary solidification surfaces and of the distribution of the phases in the solid state are shown. The solid solubility of manganese is reported only at eutectic temperature, for at room temperature it is too small to be represented.

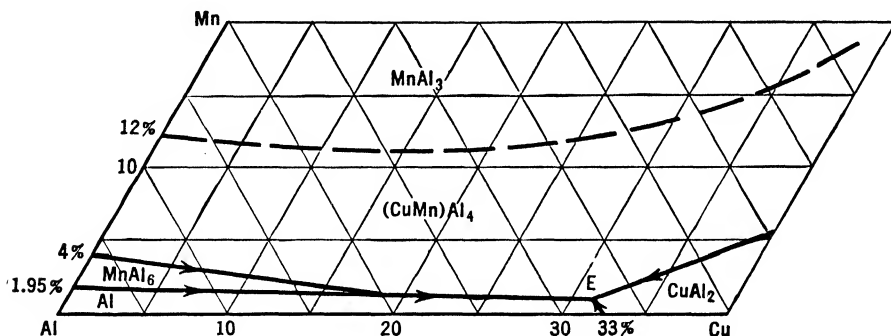


FIG. 92. System Al-Cu-Mn, surfaces of primary crystallization in the aluminum corner of the equilibrium diagram, according to the author.

Further investigations of these alloys are necessary before the diagram can be considered thoroughly established.

From a practical point of view, the discrepancies between the two diagrams reported are rather unimportant because the zone which is of interest for commercial alloys is the same in both diagrams. The

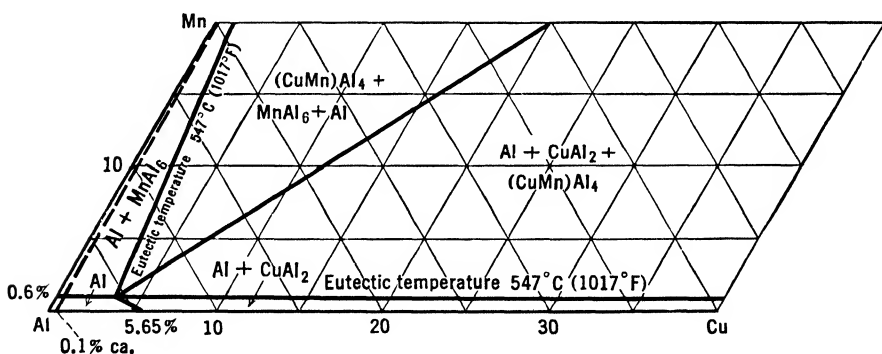


FIG. 93. System Al-Cu-Mn, distribution of the phases in the solid in the aluminum corner of the equilibrium diagram, according to the author.

importance of this system is further reduced by the fact that commercial alloys contain not only copper and manganese but also iron and silicon, and usually other elements too. In these alloys copper and manganese tend to combine with the other alloying elements rather than with each other.

**Al-Cu-Ni****Aluminum-Copper-Nickel**

The data available on this system are conflicting.

Rapp (561), who investigated the system by thermal, micro- and X-ray analyses, reports the presence of five ternary phases—*Z*, *T*, *Y*, *X*, *U*—of undetermined composition. A ternary eutectic  $E = \text{Al}-T\text{-CuAl}_2$ , containing 32.5 per cent copper, 0.9 per cent nickel, melts at  $546^\circ\text{C}$  ( $1015^\circ\text{F}$ ). Six invariant points are reported.

$A = \text{liquid} + \text{NiAl}_3 \rightarrow \text{Al} + Y$ ; Cu 16%, Ni 4%,  $599^\circ\text{C}$  ( $1110^\circ\text{F}$ ).

$B = \text{liquid} + Y \rightarrow \text{Al} + Z$ ; Cu 27%, Ni 2%,  $563^\circ\text{C}$  ( $1045^\circ\text{F}$ ).

$C = \text{liquid} + Z \rightarrow \text{Al} + T$ ; Cu 30%, Ni 1.5%,  $551^\circ\text{C}$  ( $1024^\circ\text{F}$ ).

$D = \text{liquid} + \text{Ni}_2\text{Al}_3 \rightarrow X + \text{NiAl}_3$ .

$F = \text{liquid} + X \rightarrow \text{NiAl}_3 + Y$ .

$G = \text{liquid} + U \rightarrow \text{CuAl}_2 + T$ .

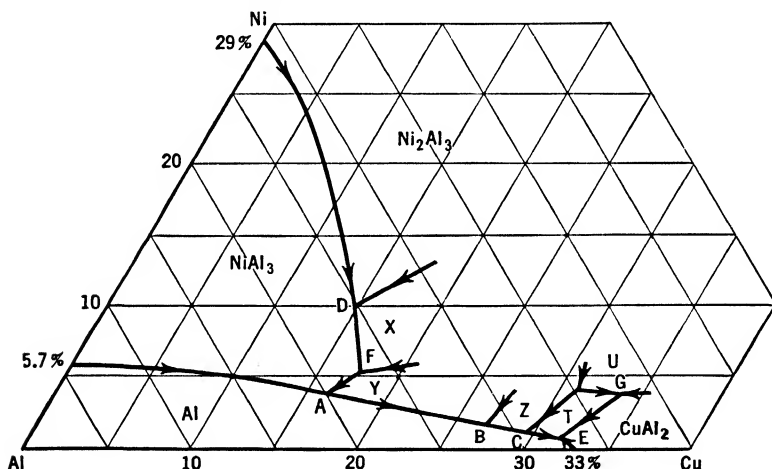


FIG. 94. System Al-Cu-Ni, surfaces of primary crystallization in the aluminum corner of the equilibrium diagram, according to Rapp.

Figure 94 shows the fields of primary crystallization according to Rapp.

Nishimura (556) and Bradley and Lipson (560), in agreement with the older investigators, find only one ternary phase. Figures 95 and 96 show the aluminum corner of the diagram according to their data. The ternary eutectic  $E = \text{Al}-\text{CuAl}_2\text{-AlCuNi}$  contains 32 per cent copper, 0.5 per cent nickel, and melts at  $540^\circ\text{C}$  ( $1004^\circ\text{F}$ ). Two singular points exist.

$P = \text{liquid} + \text{Ni}_2\text{Al}_3 \rightarrow \text{NiAl}_3 + \text{AlCuNi}$ ; Cu 23%, Ni 4%,  $600^\circ\text{C}$  ( $1112^\circ\text{F}$ ).

$Q = \text{liquid} + \text{NiAl}_3 \rightarrow \text{AlCuNi} + \text{Al}$ ;  $585^\circ\text{C}$  ( $1085^\circ\text{F}$ ).

The phases present in the solid are Al,  $\text{CuAl}_2$ ,  $\text{NiAl}_3$ ,  $\text{AlCuNi}$ , and  $\text{Ni}_2\text{Al}_3$ .  $\text{Ni}_2\text{Al}_3$  can have up to 50 per cent copper substituted for nickel and then corresponds to the formula  $\text{CuNiAl}_3$ .\* The ternary phase

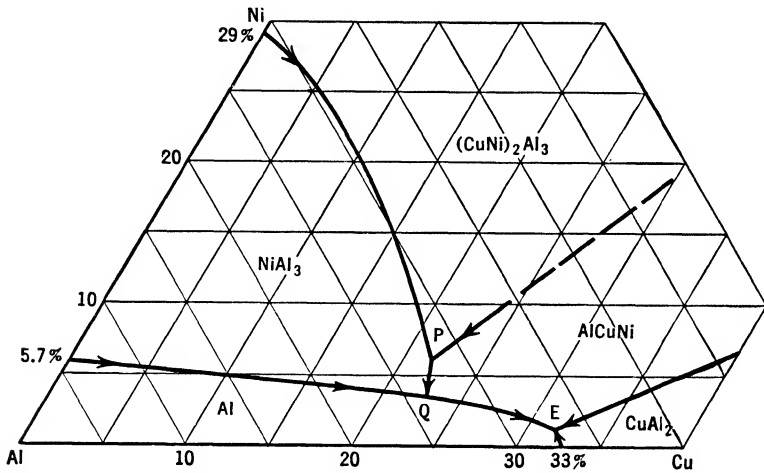


FIG. 95. System Al-Cu-Ni, surfaces of primary crystallization in the aluminum corner of the equilibrium diagram, according to Nishimura.

$\text{AlCuNi}$  has a composition corresponding approximately to the formula  $\text{Cu}_3\text{NiAl}_6$  and crystallizes in a deformed body-centered cubic lattice.

The disagreement on the data in this system is regrettable, since

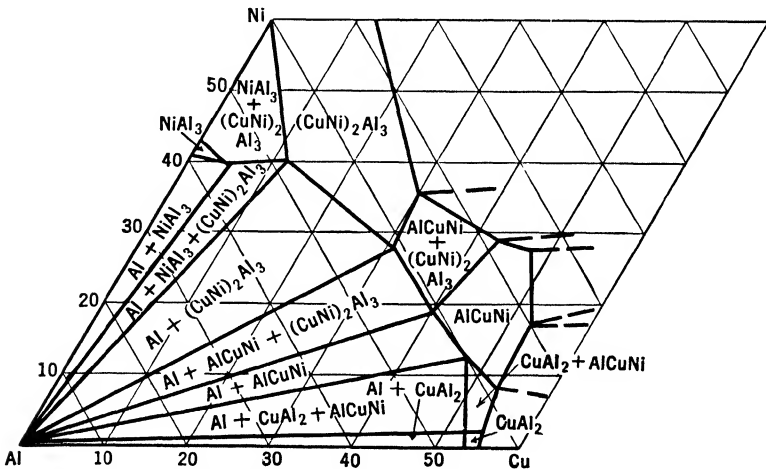


FIG. 96. System Al-Cu-Ni, distribution of the phases in the aluminum corner of the equilibrium diagram.

this diagram is necessary in order to understand alloys of the aluminum-copper-nickel group. Further investigations which could establish this diagram beyond doubt would be useful.

\* This phase will be indicated as  $(\text{CuNi})_2\text{Al}_3$ .

### Al-Cu-Pb Aluminum-Copper-Lead

This system has been investigated by Kempf and Van Horn (562) and Claus and Herrmann (563).

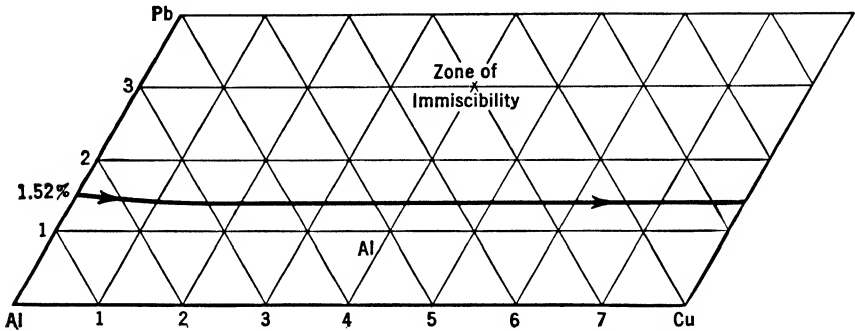


FIG. 97. System Al-Cu-Pb, surfaces of primary crystallization in the aluminum corner of the equilibrium diagram.

No ternary phases are formed, nor does copper affect the immiscibility of lead and aluminum to any great extent. The only effect of additions of copper to aluminum-lead alloys is probably a slight reduction of the miscibility. Lead, even in the molten state, does not appreciably affect the solid solubility of copper in aluminum. The fields of

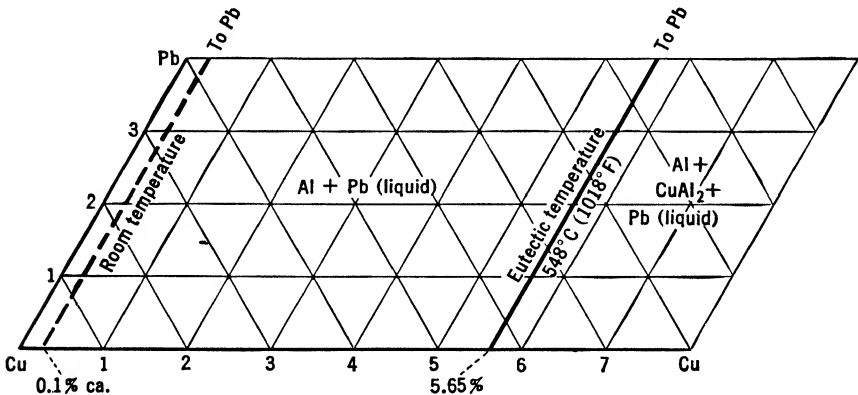


FIG. 98. System Al-Cu-Pb, distribution of the phases in the solid in the aluminum corner of the equilibrium diagram.

crystallization and the distribution of the phases in the solid are given in Figs. 97 and 98. The solid solubility of lead is not shown because even at eutectic temperature it is too small to be represented. It is to be noticed that lead at temperatures above 327°C (621°F) is molten. The phase reported in the diagram as Pb is therefore liquid lead.

Fast cooling affects the aluminum-copper-lead alloys in the aluminum corner in the same way as it affects the binary aluminum-copper; that is, the amount of copper in solid solution is increased.

This system is commercially important because alloys containing copper and lead, together with bismuth, are used to some extent.

### Al-Cu-Sb

#### Aluminum-Copper-Antimony

The equilibrium diagrams reported are drawn from data by Zamoto and Solaveva (565) and Matsukawa (564).

No ternary constituent is formed in the aluminum corner. The constituents are Al,  $\text{CuAl}_2$ , and  $\text{SbAl}$ , which form a ternary eutectic

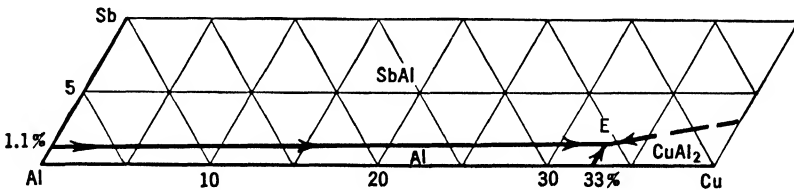


FIG. 99. System Al-Cu-Sb, surfaces of primary crystallization in the aluminum corner of the equilibrium diagram.

at 34.15 per cent copper, 1.5 per cent antimony,  $545^{\circ}\text{C}$  ( $1013^{\circ}\text{F}$ ). Antimony does not affect appreciably the solid solubility of copper in aluminum. The distribution of the phases in the aluminum corner are shown in Figs. 99 and 100. The solid solubility of antimony is not

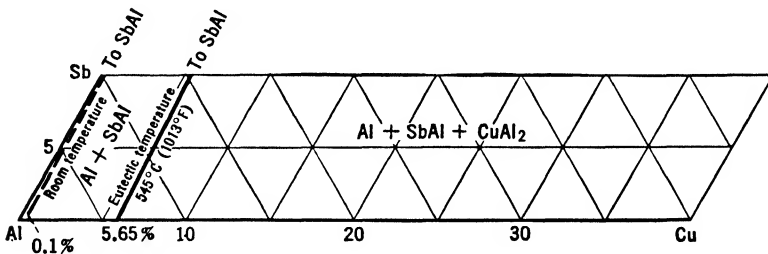


FIG. 100. System Al-Cu-Sb, distribution of the phases in the solid in the aluminum corner of the equilibrium diagram.

shown, for even at eutectic temperature it is so small that it cannot be represented.

No commercial alloy containing copper and antimony is actually used. This diagram, therefore, has little importance from a practical point of view.



**Al-Cu-Si****Aluminum-Copper-Silicon**

The equilibrium diagrams (Figs. 101 and 102) are from data by Gwyer and colleagues (570), Hisatsune (574), and Matsuyama (573).

No ternary constituent is formed in the aluminum corner, the phases present are Al, Si, and  $\text{CuAl}_2$ , which form a ternary eutectic *E*

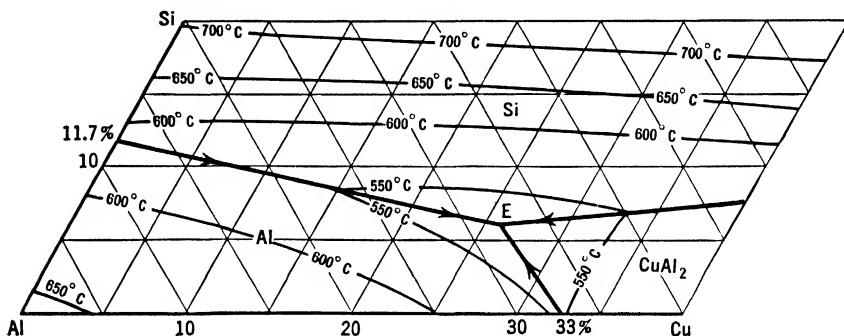


FIG. 101. System Al-Cu-Si, surfaces of primary crystallization in the aluminum corner of the equilibrium diagram.

at 525°C (977°F) containing about 6 per cent silicon and 26 to 27 per cent copper. The fields of primary crystallization and the distribution of the phases in the solid are reported in Figs. 101 and 102. The solid solubility of silicon at room temperature is so small that it cannot be represented adequately in the diagram; therefore it is not reported.

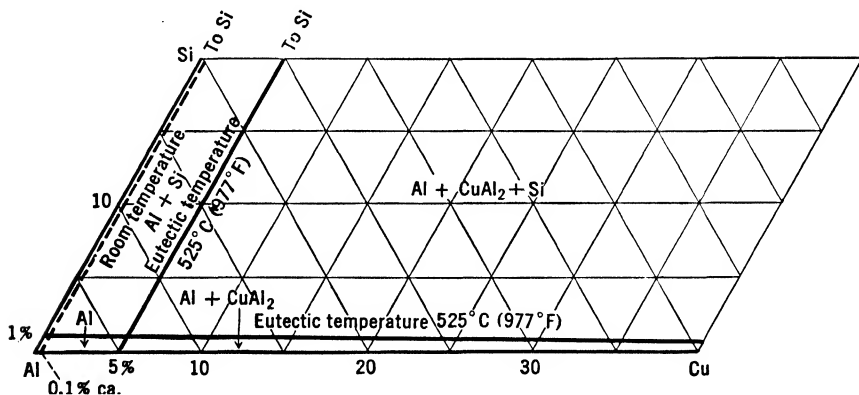


FIG. 102. System Al-Cu-Si, distribution of the phases in the solid in the aluminum corner of the equilibrium diagram.

In non-equilibrium conditions no appreciable differences are noted in these alloys, but sometimes the phases in the ternary eutectic form crystals so finely dispersed, that cannot be resolved even with high magnifications, and the eutectic has the aspect of a new phase.

Although many commercial alloys contain copper and silicon, this diagram has limited bearing on them, since the iron always present introduces new phases. The quaternary Al-Cu-Fe-Si should therefore be consulted for commercial alloys of the aluminum-copper type; whereas the quaternary Al-Cu-Mg-Si must be consulted for alloys which contain magnesium, as in these alloys both copper and silicon combine preferentially with magnesium rather than with iron.

### Al-Cu-Sn

#### Aluminum-Copper-Tin

Figures 103 and 104 are drawn from data by Zamotorin (578) and Edwards and Andrews (576).

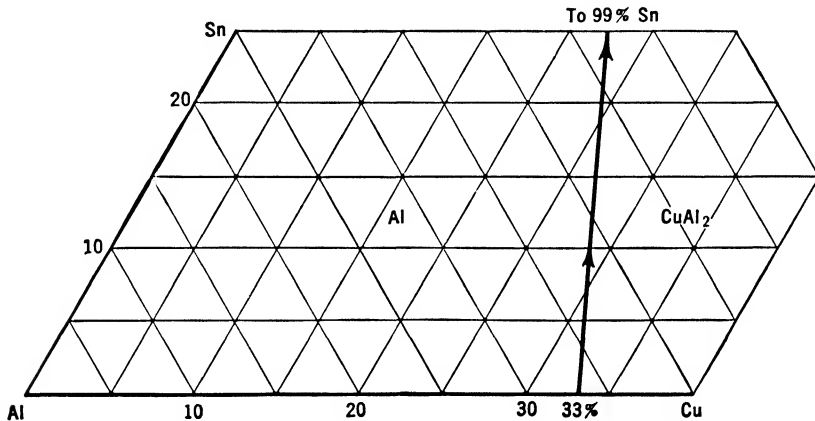


FIG. 103. System Al-Cu-Sn, surfaces of primary crystallization in the aluminum corner of the equilibrium diagram.

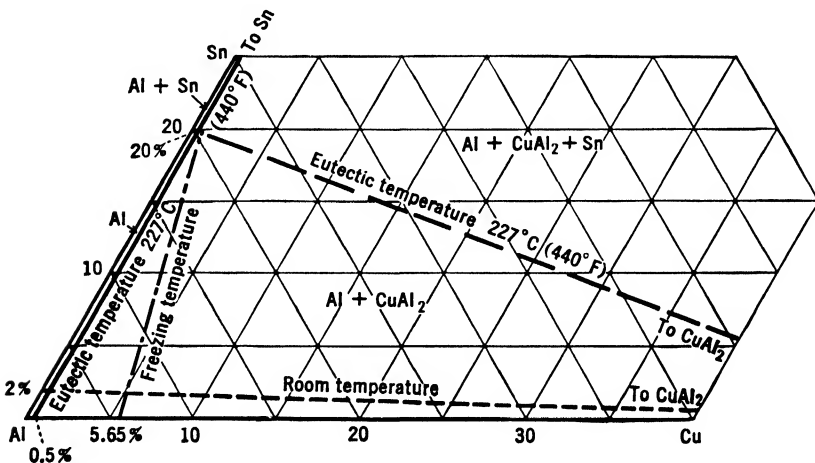


FIG. 104. System Al-Cu-Sn, distribution of the phases in the solid in the aluminum corner of the equilibrium diagram.

No ternary phase is formed; the phases present in the aluminum corner are  $\text{CuAl}_2$ , Sn, Al, forming a eutectic at the tin corner containing about 99 per cent tin, with a melting point of about  $227^\circ\text{C}$  ( $440^\circ\text{F}$ ). The solid solubility of copper at eutectic temperature is very low, as shown in Fig. 104, because the ternary eutectic  $\text{Al-CuAl}_2\text{-Sn}$  has a melting point of only  $227^\circ\text{C}$  ( $440^\circ\text{F}$ ). In the field of solid solubility of tin, where the lowest melting point is higher, more copper can go into solution; the dot-and-dash line shows the maximum solubility of copper in aluminum in the presence of tin.

As already mentioned in the discussion of the aluminum-tin diagram, alloys containing tin have almost disappeared from the market and this system has lost most of its practical use.

### Al-Cu-Ti

#### Aluminum-Copper-Titanium

Figures 105 and 106 are drawn from data by Nishimura and Kagiwada (580), corrected with data from the binary diagrams.

No ternary constituent is formed, the phases present in the aluminum corner being Al,  $\text{CuAl}_2$ ,  $\text{TiAl}_3$ . The peritectic line—Liquid +  $\text{TiAl}_3 \rightarrow \text{Al}$  (solid solution)—dividing the fields of primary solidification

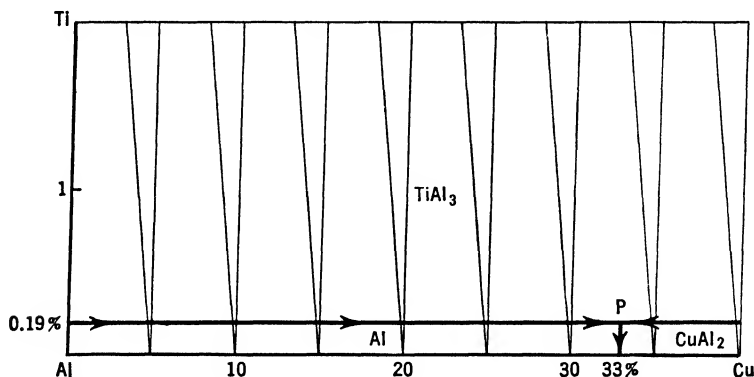


FIG. 105. System Al-Cu-Ti, surfaces of primary crystallization in the aluminum corner of the equilibrium diagram.

of Al and  $\text{TiAl}_3$ , runs at 0.19 per cent titanium, parallel to the Al-Cu axis. At about 33 per cent copper another line branches from it, sloping down to the Al- $\text{CuAl}_2$  eutectic and dividing the fields of primary crystallization of  $\text{CuAl}_2$  and Al. There is no evidence that copper or titanium affect the respective solid solubilities to an appreciable extent. The solid solubility of titanium at the temperature of the binary eutectic Al- $\text{CuAl}_2$  ( $548^\circ\text{C}$ — $1018^\circ\text{F}$ ) is depicted with a dashed

line, since the data available are not above doubt. No solid solubility at room temperature is reported because no data are available.

Titanium is quite frequently added to alloys of the aluminum-copper type; this diagram has therefore some practical interest, although the

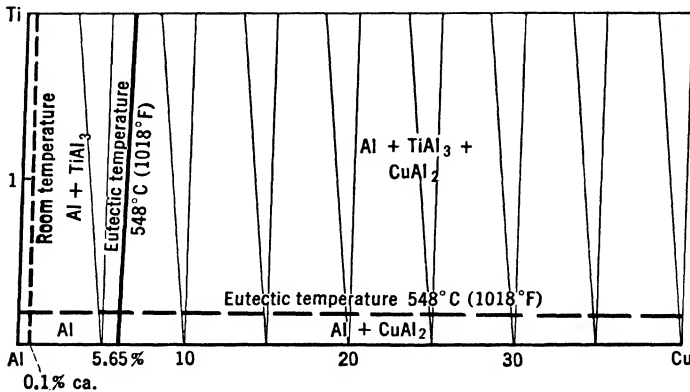


FIG. 106. System Al-Cu-Ti, distribution of the phases in the solid in the aluminum corner of the equilibrium diagram.

amounts of titanium added are commonly so small that they are in solid solution and do not form visible constituents.

### Al-Cu-W Aluminum-Copper-Tungsten

The only investigation of this system is by Whitmore and Sisco (581), which is quite superficial and concerned for the most part with the mechanical properties.

According to them, no ternary compound is formed; the constituents in the aluminum corner being Al, CuW, CuAl<sub>2</sub>. The probable presence of a eutectic Al-CuW is reported but no further data are given.

As has already been said in the aluminum-tungsten diagram, no commercial alloys containing tungsten are actually used; this diagram, therefore, is of only theoretical interest. If alloys of this type should be used, the phase reported as CuW should be investigated because it is probably a ternary phase containing aluminum also.

### Al-Cu-Zn Aluminum-Copper-Zinc

Figure 107 is plotted from data by Nishimura (586) and Hanson and Gayler (585).

No ternary phase is formed; the phases present in the aluminum corner are Al and CuAl<sub>2</sub>. Additions of zinc to aluminum-copper alloys

restrict the field of primary crystallization of  $\text{CuAl}_2$  until at 59 per cent zinc it disappears and is replaced by  $\text{CuAl}$ . No ternary eutectic is formed; three singular points are present.

$O = \text{liquid} + \text{CuAl}_2 \rightarrow \text{Al} + \text{CuAl}$ ; Cu 13%, Zn 59%, 450°C (842°F).

$P = \text{liquid} + \text{CuAl} \rightarrow \text{Al} + \text{CuZn}_4$ ; Cu 5.5%, Zn 84%, 400°C (752°F).

$Q = \text{liquid} + \text{CuZn}_4 \rightarrow \text{Al} + \text{Zn}$ ; Cu 1.5%, Zn 93%, 385°C (725°F).

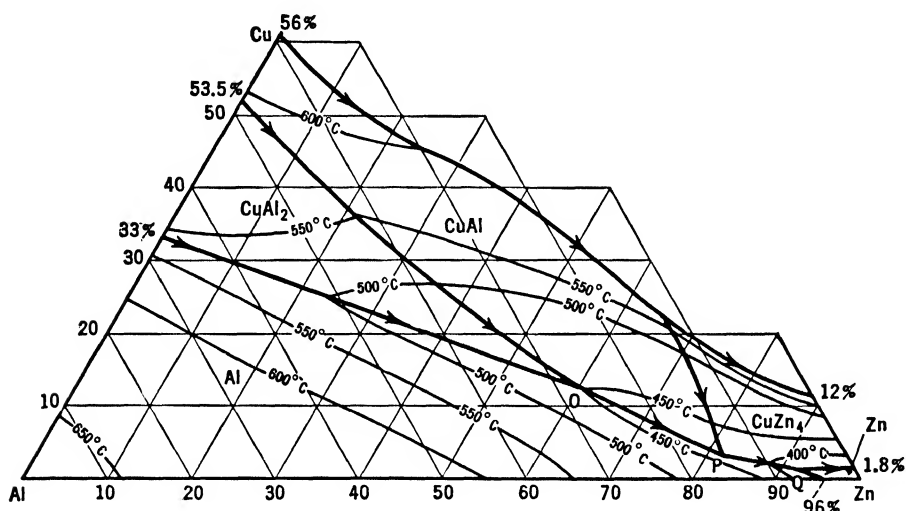


FIG. 107. System Al-Cu-Zn, surfaces of primary crystallization in the Al-Zn side of the equilibrium diagram.

Figure 107 illustrates the fields of primary solidification. In the solid state only the phase  $\text{CuAl}_2$  is present in the aluminum corner at eutectic temperature, since both copper and zinc probably do not affect appreciably their respective solid solubilities.

This diagram is important for alloys which contain copper and zinc; however, since at present the tendency is to add both zinc and magnesium, the ternary Al-Mg-Zn should also be consulted until the quaternary Al-Cu-Mg-Zn is available.

### Al-Fe-Mg

#### Aluminum-Iron-Magnesium

The equilibrium diagrams are from data by Barnick and Hanemann (589), Fuss (588), and Phillips (590).

No ternary phase is formed. The constituents in the aluminum corner are Al,  $\text{Mg}_5\text{Al}_8$ ,  $\text{FeAl}_3$ , or, in the solid,  $\text{Fe}_2\text{Al}_7$ . A ternary

eutectic  $E = \text{Al}-\text{FeAl}_3-\text{Mg}_5\text{Al}_8$  at  $445^\circ\text{C}$  ( $833^\circ\text{F}$ ), contains about 33 per cent magnesium and probably no more than 0.3 per cent iron. Iron

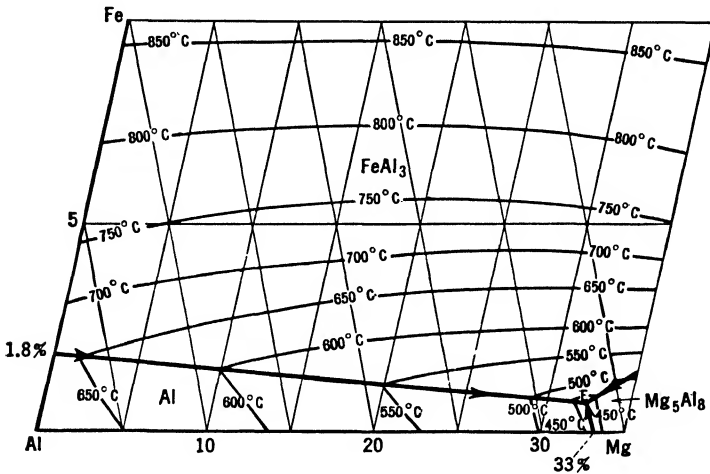


FIG. 108. System Al-Fe-Mg, surfaces of primary crystallization in the aluminum corner of the equilibrium diagram.

reduces the solid solubility of magnesium in aluminum to a considerable extent. In the absence of iron about 17 per cent magnesium is in solid solution at the eutectic temperature  $445^\circ\text{C}$  ( $833^\circ\text{F}$ ); whereas

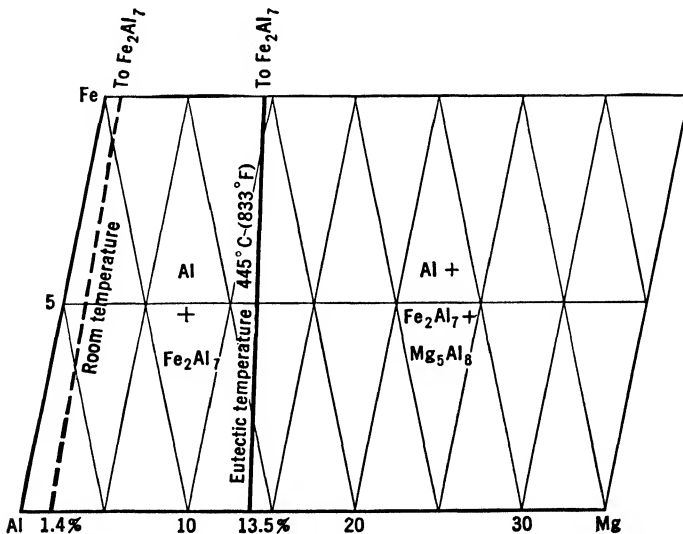


FIG. 109. System Al-Fe-Mg, distribution of the phases in the solid in the aluminum corner of the equilibrium diagram.

when iron is present the magnesium in solid solution is reduced to 13.5 per cent. In the solid state the three phases are present over all

the field, due exception being made for  $\text{Mg}_5\text{Al}_8$ , which in the zone of solid solubility of magnesium in aluminum is not visible.

In non-equilibrium conditions, such as may be encountered in commercial castings, Phillips reports no substantial deviations from equilibrium conditions, the only appreciable difference being, as usual, in the amount of magnesium retained in solution at low temperatures.

These diagrams are important for commercial aluminum-magnesium alloys which do not contain manganese or chromium. In the presence of sufficient manganese or chromium all the iron is combined with them and no  $\text{Fe}_2\text{Al}_7$  is then present.

## Al-Fe-Mn

### Aluminum-Iron-Manganese

The equilibrium diagrams (Figs. 110 and 111) are drawn from data by Degischer (591).

No ternary constituent is formed and the phases present in the aluminum corner are Al,  $\text{FeAl}_3$ ,  $\text{Fe}_2\text{Al}_7$ ,  $\text{MnAl}_4$ ,  $\text{MnAl}_6$ ,  $\text{MnAl}_3$ . Both

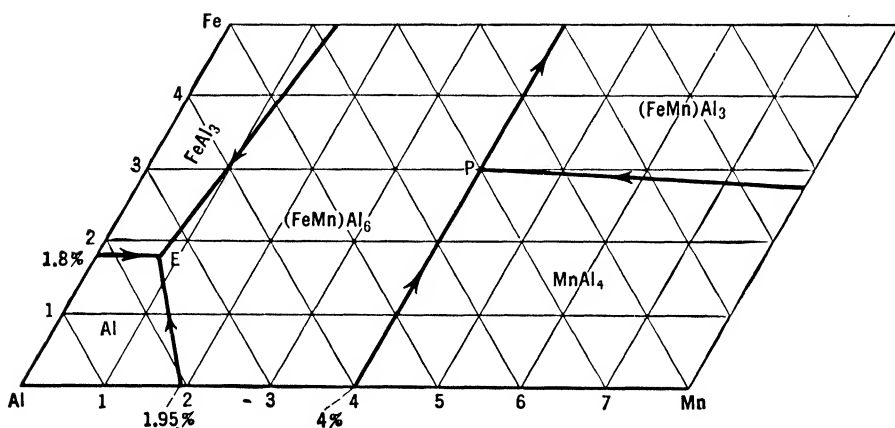


FIG. 110. System Al-Fe-Mn, surfaces of primary crystallization in the aluminum corner of the equilibrium diagram.

$\text{MnAl}_6$  and  $\text{MnAl}_3$  may take large amounts of iron in solid solution, forming phases somewhat different from the strictly binary phases from which they originate.\*

The primary solidification surfaces are Al,  $(\text{FeMn})\text{Al}_6$ ,  $\text{FeAl}_3$ ,  $\text{MnAl}_4$ ,  $(\text{FeMn})\text{Al}_3$ , distributed as in Fig. 110. There are two singular points: a eutectic  $E = \text{Al}-\text{FeAl}_3-(\text{FeMn})\text{Al}_6$  at 1.8 per cent iron, 0.7

\* These constituents will be called  $(\text{FeMn})\text{Al}_6$  and  $(\text{FeMn})\text{Al}_3$ .

per cent manganese, melting point  $654^{\circ}\text{C}$  ( $1209^{\circ}\text{F}$ ); and a peritectic  $P = \text{liquid} + \text{MnAl}_4 \rightarrow (\text{FeMn})\text{Al}_6 + (\text{FeMn})\text{Al}_3$  at about 3 per cent iron, 4 per cent manganese. The distribution of the phases in the solid state is shown in Fig. 111. Iron decreases the solid solubility of manganese in aluminum; at the eutectic temperature the solubility is about 0.3 per cent manganese instead of about 1.75 per cent manganese, as in alloys containing no iron. At room temperature it is practically zero.

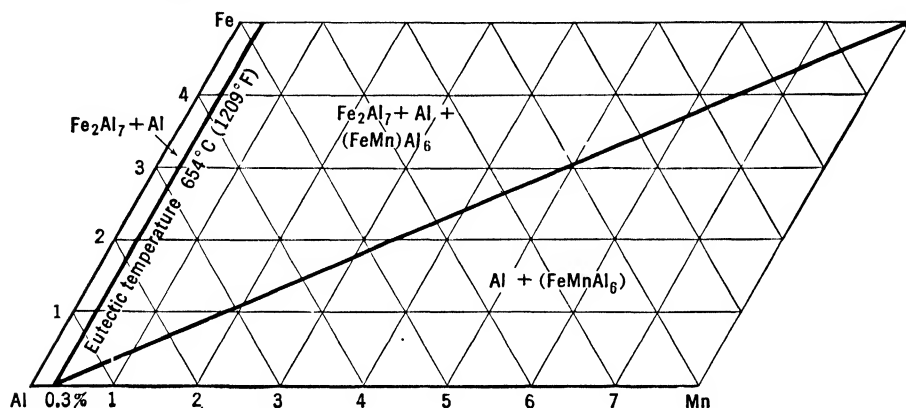


FIG. 111. System Al-Fe-Mn, distribution of the phases in the solid in the aluminum corner of the equilibrium diagram.

In non-equilibrium conditions such as are created by fast cooling, the peritectic reactions are seldom completed, as in the straight aluminum-manganese alloys, and this fact leads to the presence of more phases than are allowed by the phase rule. Alloys in the field of primary solidification of aluminum are only slightly affected and usually show equilibrium conditions even with fast cooling.

This system is rather important because it has a bearing on commercial alloys containing manganese and iron, where neither copper nor silicon is present or where they are otherwise combined. Aluminum-magnesium alloys containing manganese, aluminum-manganese alloys, and sometimes duralumins require the use of this diagram.

## Al-Fe-Ni

### Aluminum-Iron-Nickel

The diagrams are drawn from data by Bradley and Taylor (594), Fuss (593), Phillips (595), and the author.

A ternary phase is formed in the aluminum corner, which forms monoclinic crystals, isomorphous with  $\text{Co}_2\text{Al}_9$ . It has a composition corresponding to the formula  $\text{FeNiAl}_9$  and at high temperatures can



take nickel and aluminum in solution up to a composition corresponding to  $\text{FeNi}_2\text{Al}_{13}$ . The fields of primary solidification are Al,  $\text{FeAl}_3$ ,  $\text{NiAl}_3$ , and  $\text{FeNiAl}_9$  (Fig. 112). A eutectic  $E = \text{Al}-\text{FeNiAl}_9-\text{NiAl}_3$

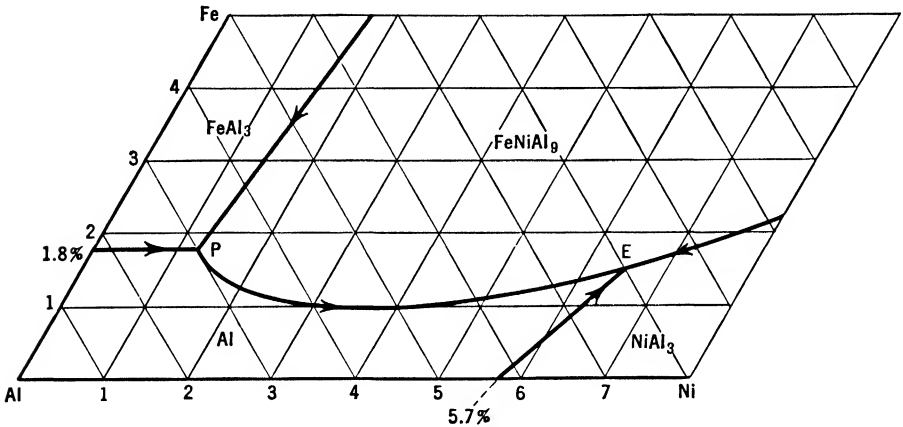


FIG. 112. System Al-Fe-Ni, surfaces of primary crystallization in the aluminum corner of the equilibrium diagram.

is formed at 6.5 per cent nickel, 1.5 per cent iron, with a melting point of  $638^\circ\text{C}$  ( $1180^\circ\text{F}$ ). A singular point  $P = \text{liquid} + \text{FeAl}_3 \rightarrow \text{FeNiAl}_9$  is at 1.2 per cent nickel, 1.8 per cent iron,  $649^\circ\text{C}$  ( $1200^\circ\text{F}$ ).

Non-equilibrium conditions caused by fast cooling affect only alloys in the field of primary solidification of  $\text{FeAl}_3$ . Especially with high

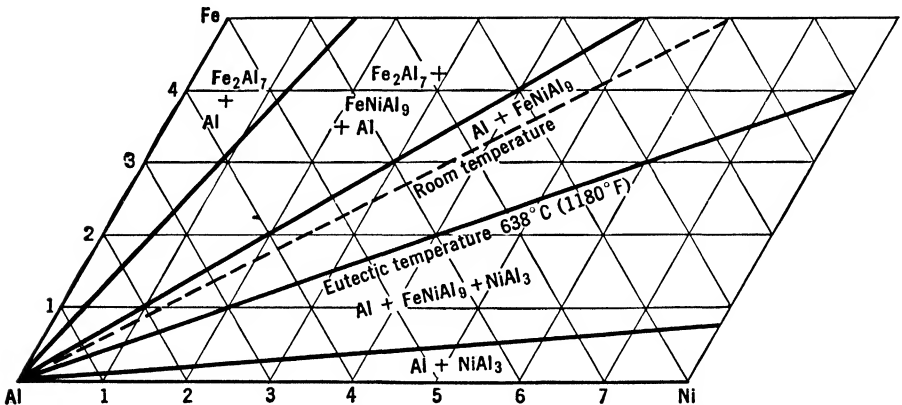


FIG. 113. System Al-Fe-Ni, distribution of the phases in the solid in the aluminum corner of the equilibrium diagram.

iron and nickel concentrations, the peritectic reaction leading to the formation of the ternary constituent sometimes is not completed, and  $\text{FeAl}_3$  can be seen surrounded by a sheath of  $\text{FeNiAl}_9$  together with  $\text{NiAl}_3$ . However, commercial alloys are outside the field thus affected.

This system has some importance for alloys of the aluminum-copper-nickel type. Although in these alloys iron and nickel usually are combined differently, sometimes with high iron content or in segregations, the ternary phase  $\text{FeNiAl}_9$  may be present.

## Al-Fe-Si

### Aluminum-Iron-Silicon

The equilibrium diagrams are compiled from data by Gwyer and Phillips (599-600), Dix (597), Fink and Van Horn (602), Jaeniche (605), and the author.

Three ternary phases are present in the field reported. Two of them are identified with Greek letters because they have been only tenta-

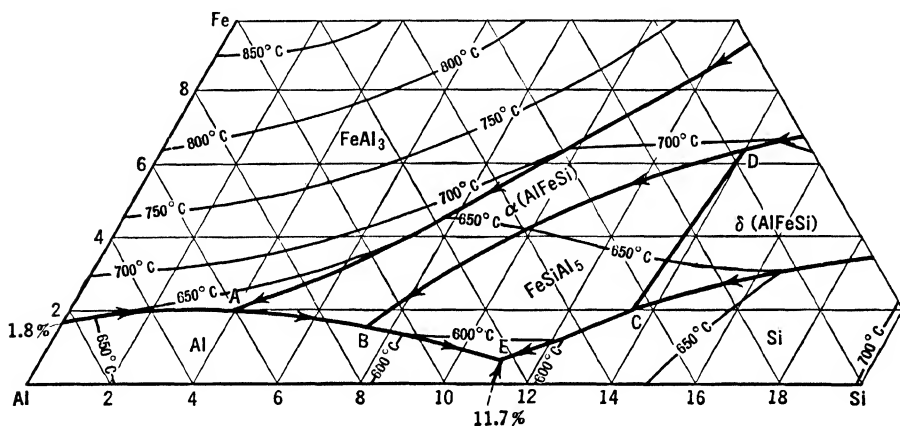


FIG. 114. System Al-Fe-Si, surfaces of primary crystallization in the aluminum corner of the equilibrium diagram.

tively identified with exact formulae:  $\alpha(\text{AlFeSi})$ , hexagonal, with a content of about 30 per cent iron and 8 per cent silicon, probably corresponding to the formula  $\text{Fe}_2\text{SiAl}_7$ ;  $\delta(\text{AlFeSi})$ , tetragonal, probably corresponding to the formula  $\text{FeSi}_2\text{Al}_4$ .  $\text{FeSiAl}_5$ , the third phase, is triclinic and contains 25.2 per cent iron and 13.4 per cent silicon. Another phase,  $\gamma(\text{AlFeSi})$ , rhombic, with a field of crystallization such that it can be identified with the formula  $\text{Fe}_2\text{SiAl}_3$ , sometimes reported in the literature, is present outside the field considered. It is mentioned here only because additions of copper and magnesium may bring its field near the range of commercial alloys. The diagram of primary crystallization is by Gwyer and Phillips. Although their investigations were conducted with non-equilibrium conditions in view, investigations by the author have proved that with small corrections they also represent equilibrium conditions. Five singular points exist in the field shown.

The eutectic  $E = \text{Al-Si-FeSiAl}_5$ ;  $577^\circ\text{C}$  ( $1071^\circ\text{F}$ ), 11.7% Si, 0.7% Fe, and four peritectic reactions:

$A = \text{liquid} + \text{FeAl}_3 \rightarrow \alpha(\text{AlFeSi})$ ;  $629^\circ\text{C}$  ( $1164^\circ\text{F}$ ), 4% Si, 2% Fe.

$B = \text{liquid} + \alpha(\text{AlFeSi}) \rightarrow \text{FeSiAl}_5$ ;  $611^\circ\text{C}$  ( $1132^\circ\text{F}$ ), 7.5% Si, 1.5% Fe.

$C = \text{liquid} + \delta(\text{AlFeSi}) \rightarrow \text{FeSiAl}_5$ ;  $595^\circ\text{C}$  ( $1103^\circ\text{F}$ ), 13.6% Si, 2% Fe.

$D = \text{liquid} + \alpha(\text{AlFeSi}) \rightarrow \delta(\text{AlFeSi}) + \text{FeSiAl}_5$ ;  $700^\circ\text{C}$  ( $1292^\circ\text{F}$ ), 14% Si, 6.5% Fe.

In equilibrium conditions the phases present in the solid are only Al,  $\text{Fe}_2\text{Al}_7$ ,  $\alpha(\text{AlFeSi})$ ,  $\text{FeSiAl}_5$ , and Si in the field considered, distributed

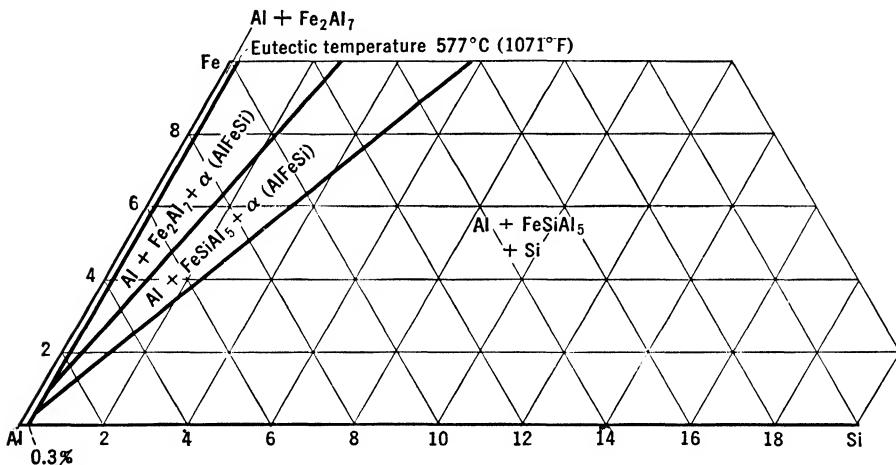


FIG. 115. System Al-Fe-Si, distribution of the phases in the solid in the aluminum corner of the equilibrium diagram.

as shown in Fig. 115. However, equilibrium conditions are seldom reached, owing to the slowness of the various peritectic reactions which take place. The presence of iron greatly reduces the solid solubility of silicon in aluminum. There is evidence that, when the iron is above 0.5 per cent, the solid solubility is about 0.3 per cent silicon at the eutectic temperature instead of 1.65 per cent as in the aluminum-silicon alloys.

In non-equilibrium conditions due to fast cooling, the peritectic reactions, for the most part, are only initiated and the fields of existence of the various phases overlap, so that  $\text{Fe}_2\text{Al}_7$  and Si, together with both  $\alpha(\text{AlFeSi})$  and  $\text{FeSiAl}_5$ , may be found in the same alloy. With silicon contents of about 15 per cent, commercial alloys usually contain the phase  $\delta(\text{AlFeSi})$  as well, associated with or sometimes partially

transformed into  $\text{FeSiAl}_5$ . No definite rule can be given for the distribution of the phases in commercial alloys. They are divided approximately as shown in Fig. 116, but the limits between the various fields are only approximate and represent average conditions.

This diagram is one of the most important ternary diagrams of aluminum alloys because iron and silicon are common impurities of

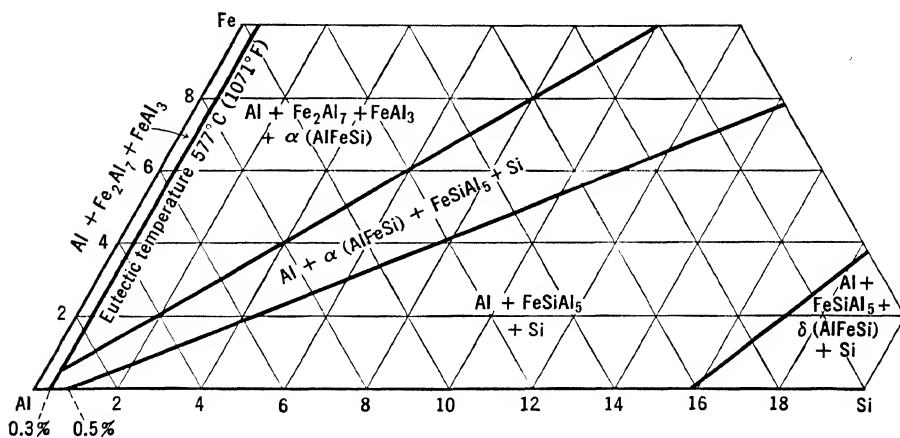


FIG. 116. System Al-Fe-Si, distribution of the phases in the solid in the aluminum corner in non-equilibrium conditions.

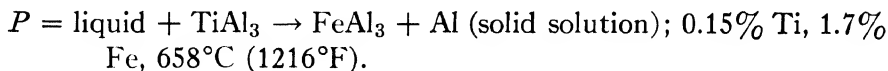
aluminum, and all commercial aluminum alloys contain appreciable percentages of both silicon and iron. Commercial aluminum and straight aluminum-silicon alloys are completely covered by this diagram, which also is of some importance for alloys containing copper. When manganese, cobalt, nickel, magnesium, chromium, or, to some extent, copper is present, this diagram has only a limited bearing on the alloys, for iron and silicon combine preferentially with them rather than together.

## Al-Fe-Ti

### Aluminum-Iron-Titanium

Figures 117 and 118 are from data by Nishimura and Matumoto (611).

No ternary phase is formed in the aluminum corner. The phases present are Al,  $\text{TiAl}_3$ ,  $\text{FeAl}_3$ , and in the solid  $\text{Fe}_2\text{Al}_7$ . Their fields of primary crystallization are shown in Fig. 117. The invariant point is



In the solid state (Fig. 118) the three phases, Al,  $\text{TiAl}_3$ ,  $\text{Fe}_2\text{Al}_7$ , are present over all the field, due exception being made for the zone where

titanium is in solid solution. This solid solubility at eutectic temperature is shown as a dotted line because the value has not been exactly determined. No solid solubility at room temperature is reported because no data are available.

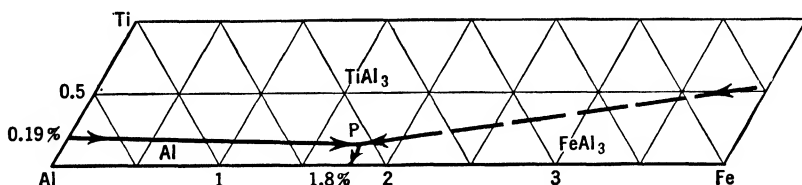


FIG. 117. System Al-Fe-Ti, surfaces of primary crystallization in the aluminum corner of the equilibrium diagram.

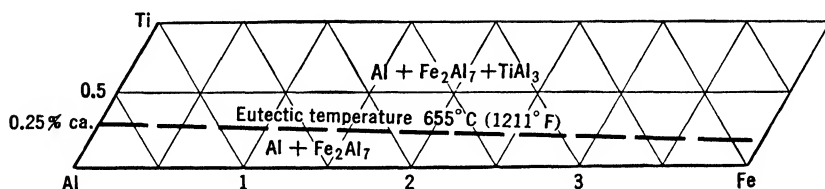


FIG. 118. System Al-Fe-Ti, distribution of the phases in the solid in the aluminum corner of the equilibrium diagram.

As reported for the Al-Cu-Ti diagram, the Al-Fe-Ti diagram may have some importance for commercial alloys since titanium is often used as a grain refiner.

## Al-Fe-Zn

### Aluminum-Iron-Zinc

This system has been investigated only by Fuss (612).

No ternary phase is formed, the phases present in the aluminum corner being  $\text{FeAl}_3$ , Zn, and Al, which form a eutectic at 94 per cent

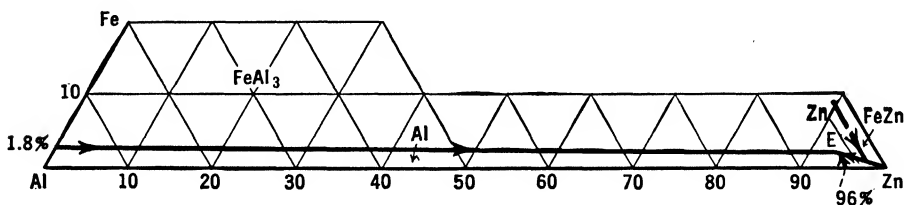


FIG. 119. System Al-Fe-Zn, surfaces of primary crystallization in the aluminum corner of the equilibrium diagram.

zinc, 1 per cent iron, with a melting point of about  $380^\circ\text{C}$  ( $716^\circ\text{F}$ ). The fields of primary solidification are shown in Fig. 119. Figure 120

shows the distribution of the phases in the solid state. The distribution of the phases is reported also at 275°C (527°F) (dot-and-dash line) in order to show the gap of miscibility which exists in these alloys, as in the binary aluminum-zinc alloys. By Al and Al<sub>B</sub> are indicated

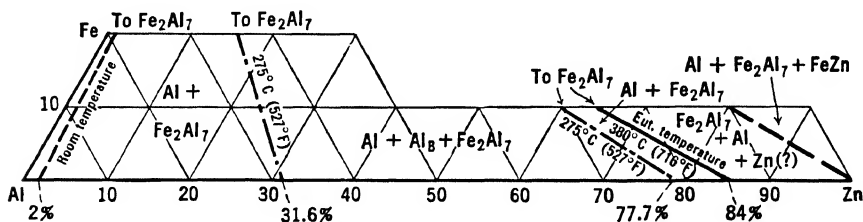


FIG. 120. System Al-Fe-Zn, distribution of the phases in the solid in the aluminum corner of the equilibrium diagram.

the two solid solutions of Zn in Al, as already reported in the Al-Zn diagram.

This diagram may have some practical interest for alloys containing zinc, although usually both iron and zinc are otherwise combined.

## Al-Ge-Mg

### Aluminum-Germanium-Magnesium

The only investigation of this system is by Kroll (613).

The presence of a compound  $\text{Mg}_2\text{Ge}$ , similar to  $\text{Mg}_2\text{Si}$ , is the only datum available. Probably the equilibrium diagram is similar to the Al-Mg-Si diagram.

No commercial aluminum-germanium-magnesium alloy has been used. The investigation of Kroll reveals that these alloys are similar to aluminum-magnesium-silicon alloys. As silicon is quite inexpensive, there seems to be little reason to substitute germanium for it when no special improvement is to be obtained.

## Al-Li-Si

## Aluminum-Lithium-Silicon

This system has been superficially investigated by Assmann (614).

The reported presence of a compound  $\text{Li}_3\text{Si}$ , responsive to heat treatment, is the only datum available.

Lithium has been used to a small extent as an alloying element in aluminum alloys. Its use, however, is at present probably very slight; so this diagram is of little practical importance.

**Al-Mg-Mn****Aluminum-Magnesium-Manganese**

The equilibrium diagrams have been drawn from data by Leemann (616) and the author.

No ternary compound is formed, and the phases which are primary are  $\text{MnAl}_4$ ,  $\text{MnAl}_6$ , Al, and  $\text{Mg}_5\text{Al}_8$ . A ternary eutectic Al-MnAl<sub>4</sub>- $\text{Mg}_5\text{Al}_8$  is formed at 26.4 per cent magnesium, 2.35 per cent man-

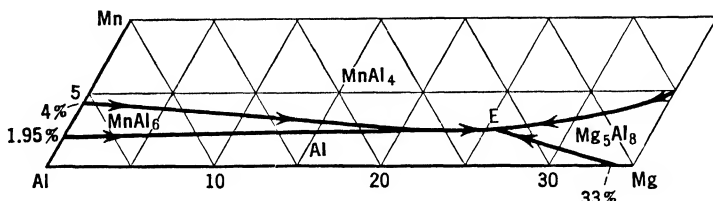


FIG. 121. System Al-Mg-Mn, surfaces of primary crystallization in the aluminum corner of the equilibrium diagram.

ganese, 437°C (819°F). Magnesium reduces the field of primary crystallization of  $\text{MnAl}_6$  until at about 22 per cent magnesium it disappears completely. In the solid state the phases present are  $\text{MnAl}_6$ ,  $\text{Mg}_5\text{Al}_8$ , and Al, distributed in the field as shown in Fig. 122. The solid solubility of magnesium in aluminum is reduced by manganese. From about 17 per cent magnesium at 437°C (819°F) for alloys without manganese, it drops gradually to zero, with a manganese content corresponding to  $\text{MnAl}_6$  (25 per cent manganese). Magnesium has

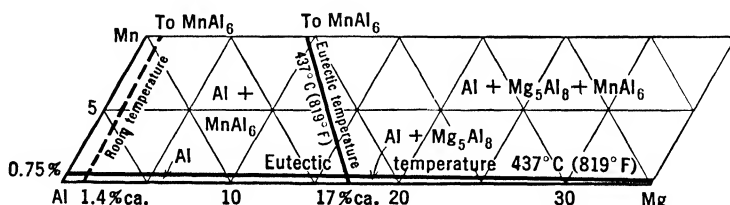


FIG. 122. System Al-Mg-Mn, distribution of the phases in the solid in the aluminum corner of the equilibrium diagram.

the same effect on the solid solubility of manganese. In Fig. 122 the solid solubility of manganese in aluminum is reported only at eutectic temperature, for at room temperature it is too small to be shown.

In non-equilibrium conditions the peritectic reactions in the manganese compounds are affected as in the Al-Mn diagram. The reactions leading to the formation of  $\text{MnAl}_6$  are seldom completed, and  $\text{MnAl}_4$  or  $\text{MnAl}_3$  is commonly present with manganese contents above

the eutectic. This system is of some importance for alloys of the aluminum-magnesium type which contain manganese. Because the silicon is in the form of  $\text{Mg}_2\text{Si}$ , it does not interfere with the manganese, and the only other element present is iron, which forms with manganese the pseudo-ternary phase  $(\text{FeMn})\text{Al}_6$ . By combining the diagrams Al-Fe-Mn, Al-Fe-Mg, and Al-Mg-Mn, it is therefore possible to have a good picture of these alloys. If the alloys do not contain enough magnesium for the formation of the phase  $\text{Mg}_5\text{Al}_8$ , this diagram has no bearing on them.

### Al-Mg-Ni

#### Aluminum-Magnesium-Nickel

This system has been investigated by Fuss (617) and the author.

No ternary phase is formed, the constituents being Al,  $\text{Mg}_5\text{Al}_8$ , and  $\text{NiAl}_3$ , forming a eutectic *E* at about 34 per cent magnesium and very

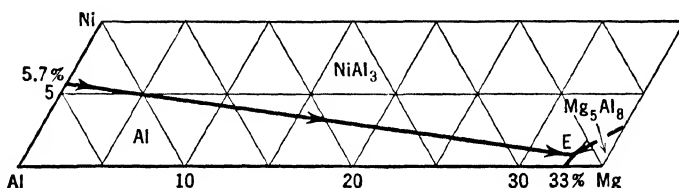


FIG. 123. System Al-Mg-Ni, surfaces of primary crystallization in the aluminum corner of the equilibrium diagram.

little nickel, with a melting point of  $447^\circ\text{C}$  ( $837^\circ\text{F}$ ). In the solid state the three phases are present together over all the field, with the exception of the zone where magnesium is in solid solution and  $\text{Mg}_5\text{Al}_8$

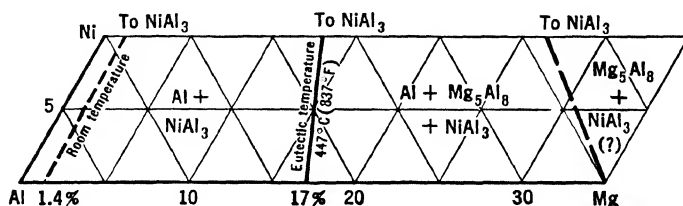


FIG. 124. System Al-Mg-Ni, distribution of the phases in the solid in the aluminum corner of the equilibrium diagram.

cannot be seen. Figures 123 and 124 show the fields of primary crystallization and the distribution of the phases in the solid.

No appreciable variations are caused by fast cooling, the only difference being the amount of magnesium in solid solution.



This system is of little importance from a practical point of view. No alloy containing only magnesium and nickel is commercially feasible, and a small amount of iron changes the structure of the alloys appreciably. When copper is present, or when the silicon is sufficient to absorb all the magnesium as  $\text{Mg}_2\text{Si}$ , this diagram becomes useless, for the phase  $\text{Mg}_5\text{Al}_8$  and also  $\text{NiAl}_3$  disappear to be replaced by more complex ternary or quaternary phases.

## Al-Mg-Pb

### Aluminum-Magnesium-Lead

This system has been investigated by Bauer (618).

Magnesium increases the miscibility of lead and aluminum in the liquid state. The miscibility, which at the freezing point is about 1.5

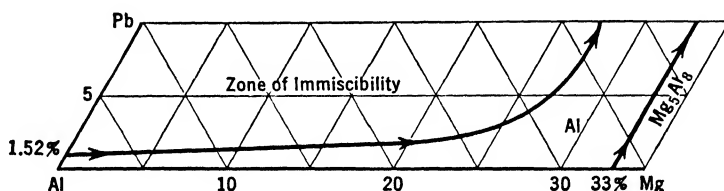


FIG. 125. System Al-Mg-Pb, surfaces of primary crystallization in the aluminum corner of the equilibrium diagram.

per cent lead with no magnesium, with 7 per cent magnesium is 2.5 per cent lead and reaches 3 per cent lead at 10 per cent magnesium. In the solid state the phases present are Al, Pb,  $\text{Mg}_2\text{Pb}$ , and  $\text{Mg}_5\text{Al}_8$ , distributed as in Fig. 126. No data are available about the effects of lead and magnesium in their respective solid solubilities, but the effects

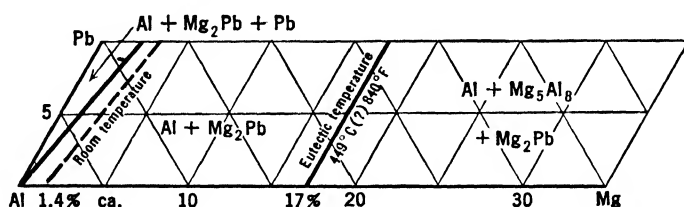


FIG. 126. System Al-Mg-Pb, distribution of the phases in the solid in the aluminum corner of the equilibrium diagram.

can be expected to be small. Figure 126 shows only the solid solubility of magnesium because the solid solubility of lead is so small that it cannot be adequately represented.

Experiments have been made recently with some alloys of the aluminum-silicon type containing magnesium and lead, but, even if

they should be used commercially, it is doubtful if this diagram will have practical importance, for probably magnesium will tend to combine with silicon rather than with lead.

### Al-Mg-Sb

#### Aluminum-Magnesium-Antimony

Figures 127 and 128 are from data by Loofs-Rassow (619) and Guertler and Bergmann (620).

No ternary constituent is formed. At the center of the diagram there is a gap of miscibility which covers a wide area and extends

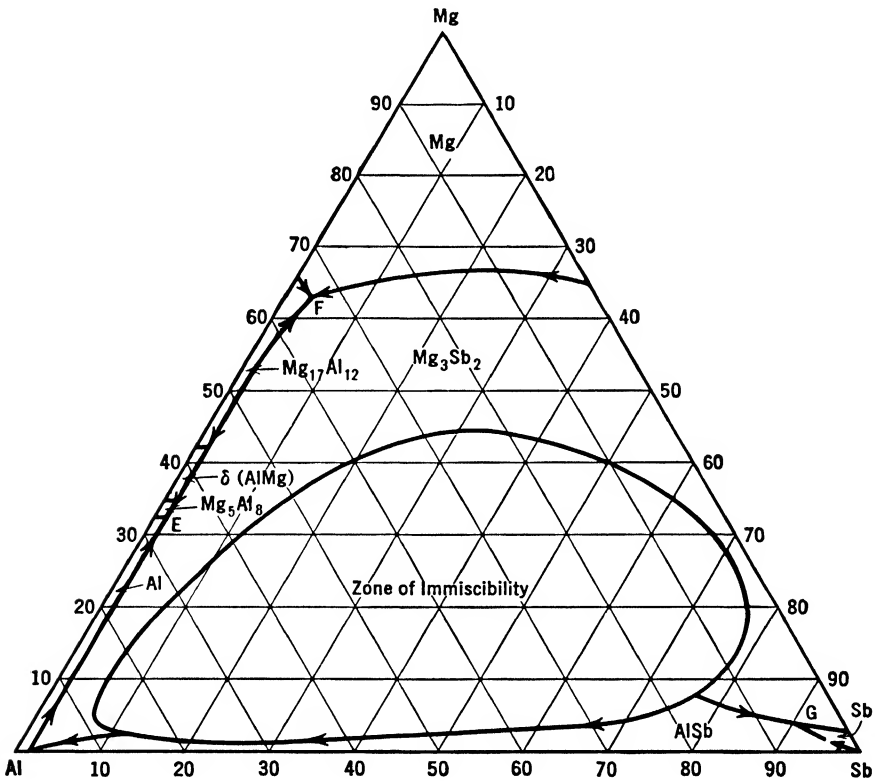


FIG. 127. System Al-Mg-Sb, surfaces of primary crystallization.

almost to the aluminum corner of the system. The phases present in the system are Al,  $\text{Mg}_5\text{Al}_8$ ,  $\gamma(\text{AlMg})$ ,  $\delta(\text{AlMg})$ ,  $\text{Mg}_{17}\text{Al}_{12}$ , Mg,  $\text{Mg}_3\text{Sb}_2$ , Sb, and SbAl. Three ternary eutectics are formed.

$E = \text{Al-Mg}_5\text{Al}_8\text{-Mg}_3\text{Sb}_2$ ;  $445^\circ\text{C}$  ( $833^\circ\text{F}$ ), Mg 33%, Sb 1% approx.

$F = \text{Mg}_{17}\text{Al}_{12}\text{-Mg-Mg}_3\text{Sb}_2$ ; Mg 65% approx., Sb 2% approx.

$G = \text{SbAl-Sb-Mg}_3\text{Sb}_2$ ; Mg 4% approx., Sb 92% approx.

The phases present in the solid are Al,  $\text{Mg}_5\text{Al}_8$ ,  $\gamma(\text{AlMg})$ ,  $\text{Mg}_{17}\text{Al}_{12}$ , Mg,  $\text{Mg}_3\text{Sb}_2$ , Sb, and  $\text{SbAl}$ , distributed as in Fig. 128. There is no evidence that antimony affects the solid solubility of magnesium in aluminum to any great extent. No data are available on the effect of magnesium on the solid solubility of antimony; for this reason only the solid solubility of magnesium is shown in the diagram.

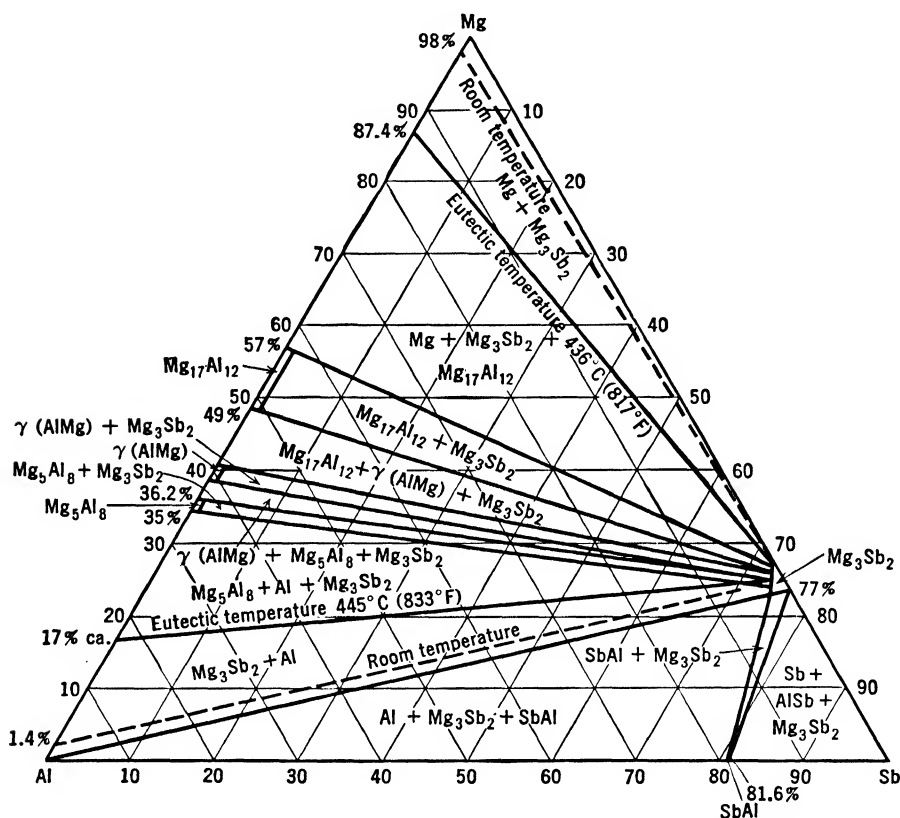


FIG. 128. System Al-Mg-Sb, distribution of the phases in the solid.

A few years ago alloys of the aluminum-magnesium type contained a small amount of antimony, which was supposed to impart good corrosion resistance to them. At present the antimony has disappeared from the composition and this system has lost its practical interest.

### Al-Mg-Si

#### Aluminum-Magnesium-Silicon

Figures 129, 130, and 131 are plotted from data by Losana (625), Hanson and Gayler (621), Dix, Keller, and Graham (626), Keller and Craighead (630), and Phillips (633).

No ternary compound is formed. The constituents in the aluminum corner are Al,  $\text{Mg}_2\text{Si}$ ,  $\text{Mg}_5\text{Al}_8$ , and Si, all of which have a field of pri-

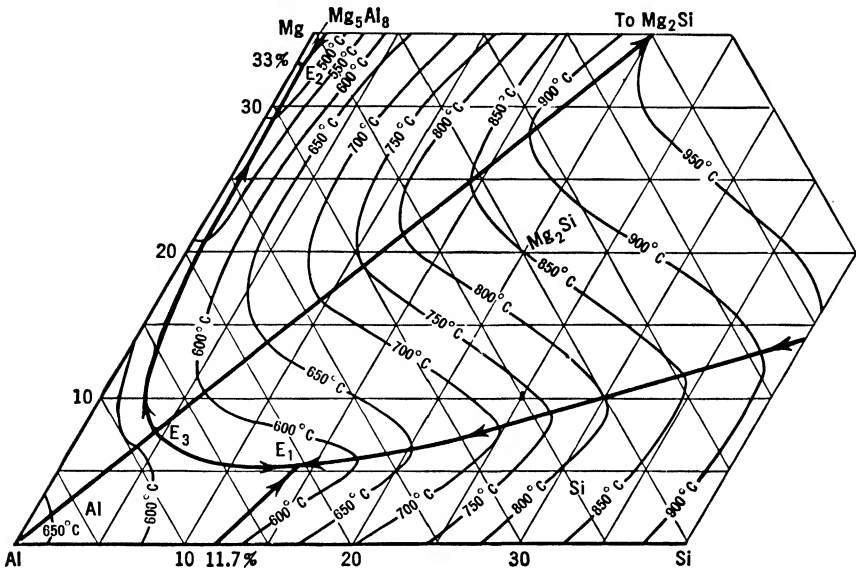


FIG. 129. System Al-Mg-Si, surfaces of primary crystallization in the aluminum corner of the equilibrium diagram.

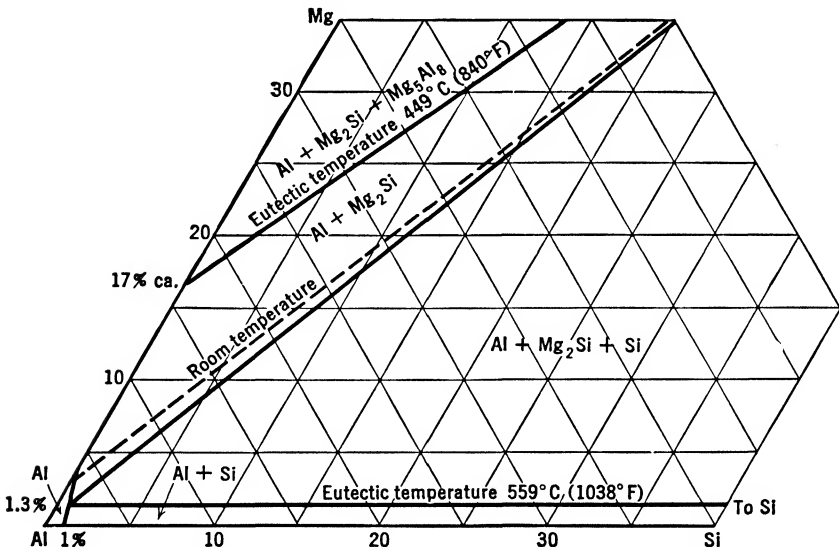


FIG. 130. System Al-Mg-Si, distribution of the phases in the solid in the aluminum corner of the equilibrium diagram.

mary crystallization as shown in Fig. 129. Two ternary eutectics are formed:  $E_1 = \text{Al}-\text{Mg}_2\text{Si}-\text{Si}$  at 14 per cent silicon, 5.5 per cent magnesium, melting point  $559^\circ\text{C}$  ( $1038^\circ\text{F}$ );  $E_2 = \text{Al}-\text{Mg}_2\text{Si}-\text{Mg}_5\text{Al}_8$ , almost

coincident with the binary  $\text{Al-Mg}_5\text{Al}_8$  both as to temperature and composition [33 per cent magnesium,  $449^\circ\text{C}$  ( $840^\circ\text{F}$ )]. The compound  $\text{Mg}_2\text{Si}$  forms a quasi-binary system with aluminum, with a eutectic  $E_3$  at 8.25 per cent magnesium, 4.75 per cent silicon, with a melting point of  $595^\circ\text{C}$  ( $1103^\circ\text{F}$ ).  $\text{Mg}_2\text{Si}$  is soluble to a certain extent in aluminum, and there are reports that it goes into solid solution as molecules rather than atoms. Figure 131 shows the section corresponding to the quasi-binary system  $\text{Al-Mg}_2\text{Si}$ . Silicon in excess does not appreciably affect

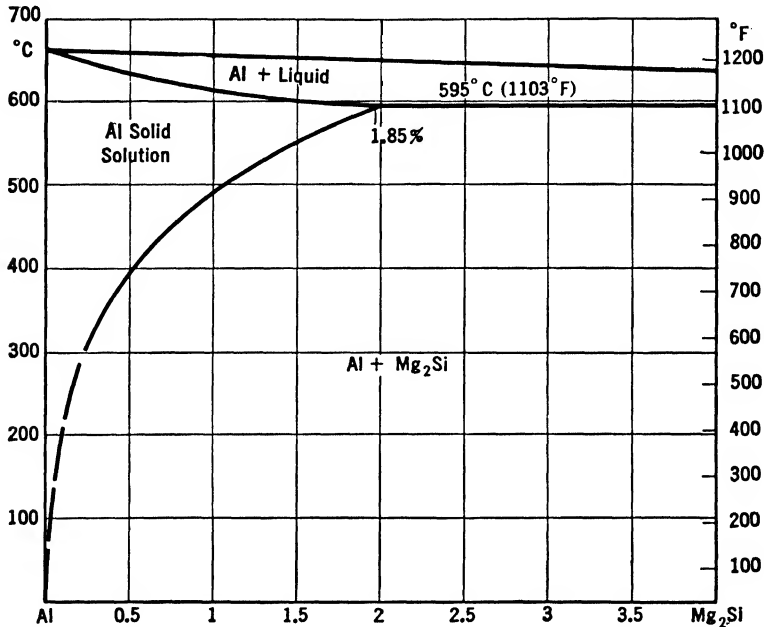


FIG. 131. System  $\text{Al-Mg-Si}$ , quasi-binary section  $\text{Al-Mg}_2\text{Si}$ , showing the solid solubility of  $\text{Mg}_2\text{Si}$  in aluminum.

the solid solubility of  $\text{Mg}_2\text{Si}$ . An excess of magnesium, on the other hand, reduces it to such an extent that, when the excess reaches 3 per cent magnesium, the solid solubility of  $\text{Mg}_2\text{Si}$  is reduced to zero at every temperature. Below are reported the solid solubilities at various temperatures with various magnesium excesses.

	MAGNESIUM EXCESS				
	0%	0.20%	0.40%	0.80%	1%
$595^\circ\text{C}$ ( $1103^\circ\text{F}$ )	1.85				
$535^\circ\text{C}$ ( $995^\circ\text{F}$ )	1.20	1.15	0.97	0.67	0.55
$500^\circ\text{C}$ ( $932^\circ\text{F}$ )	1.05	0.85	0.69	0.45	0.36
$400^\circ\text{C}$ ( $752^\circ\text{F}$ )	0.53	0.35	0.20	0	0
$300^\circ\text{C}$ ( $572^\circ\text{F}$ )	0.30	0.16	0.02	0	0
$200^\circ\text{C}$ ( $392^\circ\text{F}$ )	0.25	0.05	0	0	0

No great differences can be detected in alloys not in equilibrium conditions. Sometimes, probably on account of local segregations, in alloys containing the exact ratio  $\text{Mg} : \text{Si}$  (1.73) for the formation of  $\text{Mg}_2\text{Si}$ , some free Si or  $\text{Mg}_5\text{Al}_8$  can be detected.

This diagram is one of the most important equilibrium diagrams for aluminum alloys, for magnesium silicide is the hardening constituent of many commercial alloys. It should be consulted for every alloy containing magnesium and silicon, without copper. When copper is also present, the quaternary  $\text{Al-Cu-Mg-Si}$  should be used.

### Al-Mg-Zn

#### Aluminum-Magnesium-Zinc

The equilibrium diagrams (Figs. 132 to 134) are from data by Koester and colleagues (644), Riederer (645), Laves and colleagues (643), and Fink and Willey (647).

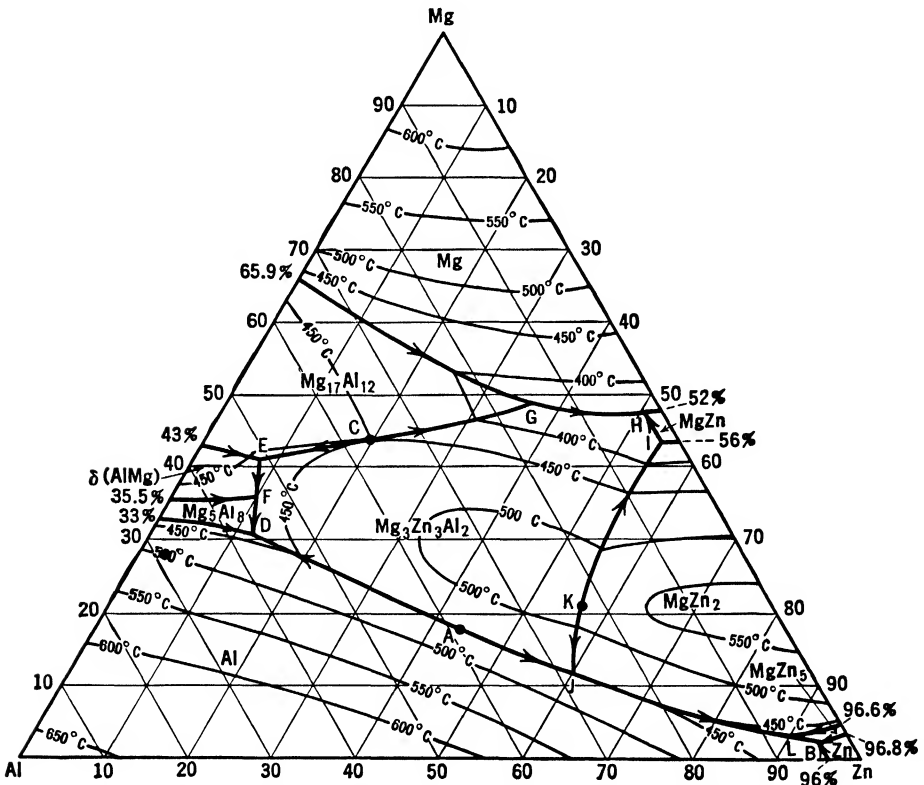


FIG. 132. System Al-Mg-Zn, surfaces of primary crystallization.

A ternary phase  $\text{Mg}_3\text{Zn}_3\text{Al}_2$  is formed, with a large field of existence, which at  $400^\circ\text{C}$  ( $752^\circ\text{F}$ ) extends from 23.7 per cent zinc and 31.7 per

cent magnesium to 40 per cent zinc and 32.5 per cent magnesium, decreasing with decreasing temperatures. This phase is cubic body-centered, with 161 atoms in the unit cell. The lattice parameter is 14.29 Å, increasing toward the extremities of the field to reach 14.71 Å at the end toward aluminum-magnesium and 14.60 Å at the end toward magnesium-zinc. The other phases in the system are Al, Mg, and Zn, and the binary  $\text{Mg}_5\text{Al}_8$ ,  $\gamma(\text{AlMg})$ ,  $\delta(\text{AlMg})$ ,  $\text{Mg}_{17}\text{Al}_{12}$ ,  $\text{MgZn}$ ,

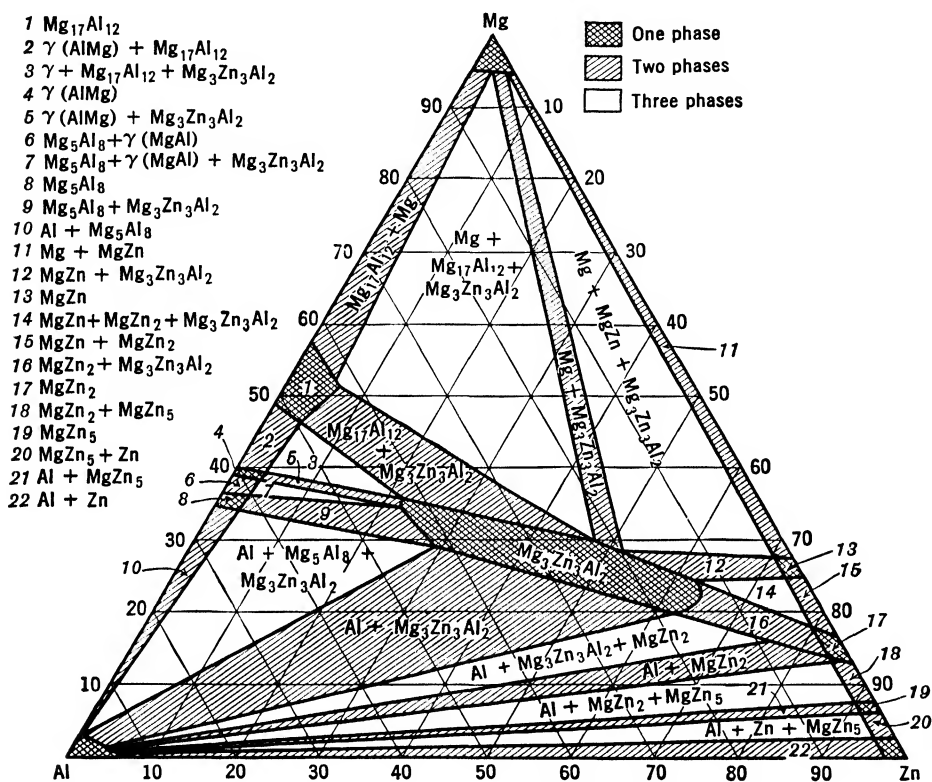


FIG. 133. System Al-Mg-Zn, distribution of the phases in the solid, at room temperature.

$\text{MgZn}_2$ ,  $\text{MgZn}_5$ . The fields of primary crystallization and the distribution of the phases in the solid are reported in Figs. 132 and 133. There are four eutectics in the system.

*A* = pseudo-binary Al- $\text{Mg}_3\text{Zn}_3\text{Al}_2$ ; 17% Mg, 44% Zn, 489°C (912°F).

*B* = Al- $\text{MgZn}_5$ -Zn; 2% Mg, 94% Zn, 350°C (662°F).

*C* = pseudo-binary  $\text{Mg}_{17}\text{Al}_{12}$ - $\text{Mg}_3\text{Zn}_3\text{Al}_2$ ; 44% Mg, 20% Zn, 450°C (842°F), where  $\text{Mg}_{17}\text{Al}_{12}$  contains 48% Mg and 11% Zn and  $\text{Mg}_3\text{Zn}_3\text{Al}_2$  contains 28% Mg and 50% Zn.

*D* = Al- $\text{Mg}_5\text{Al}_8$ - $\text{Mg}_3\text{Zn}_3\text{Al}_2$ ; 31% Mg, 12% Zn, 447°C (837°F).

There are nine other singular points: seven peritectic reactions and two transformations in the solid.

$E = \text{liquid} + \text{Mg}_{17}\text{Al}_{12} \rightarrow \delta(\text{AlMg}) + \text{Mg}_3\text{Zn}_3\text{Al}_2$ ; 41% Mg, 8% Zn, 449°C (840°F), where  $\text{Mg}_{17}\text{Al}_{12}$  contains 45% Mg, 5% Zn;  $\text{Mg}_3\text{Zn}_3\text{Al}_2$  contains 33% Mg, 23% Zn; and the liquid contains 39% Mg and 10% Zn.

$F = \text{liquid} + \delta(\text{AlMg}) \rightarrow \text{Mg}_5\text{Al}_8 + \text{Mg}_3\text{Zn}_3\text{Al}_2$ ; 36% Mg, 10% Zn, where  $\delta(\text{AlMg})$  contains 40% Mg, 5% Zn.

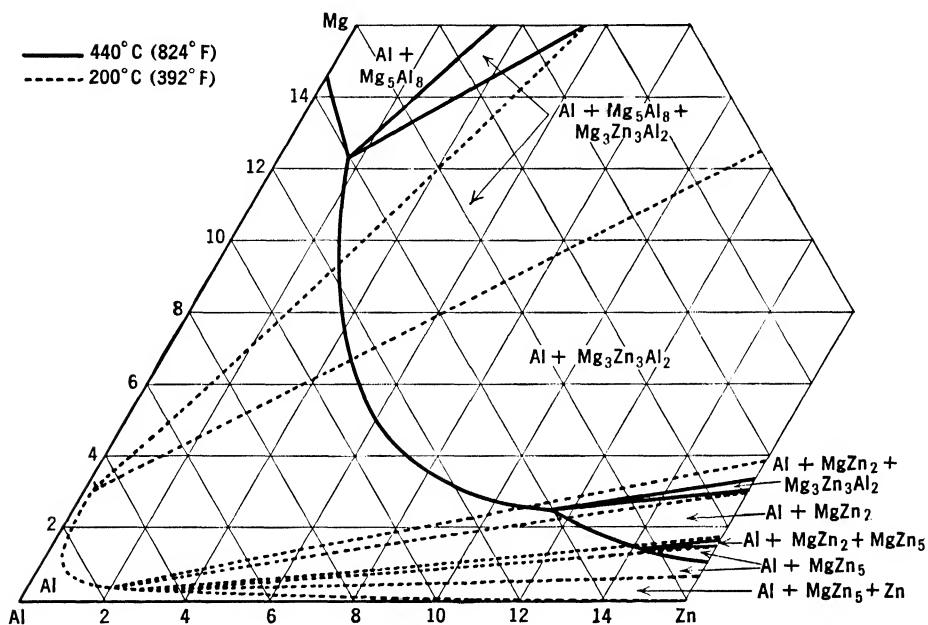


FIG. 134. System Al-Mg-Zn, detail of the aluminum corner of the equilibrium diagram, showing the solid solubilities of the various phases.

$G = \text{liquid} + \text{Mg}_{17}\text{Al}_{12} \rightarrow \text{Mg} + \text{Mg}_3\text{Zn}_3\text{Al}_2$ ; 9% Mg, 36% Zn, where the constituents have the composition: liquid = 49% Mg, 38% Zn;  $\text{Mg}_{17}\text{Al}_{12} = 49\%$  Mg, 12% Zn; Mg = 41% Mg, 55.5% Zn;  $\text{Mg}_3\text{Zn}_3\text{Al}_2 = 27\%$  Mg, 53% Zn.

$H = \text{liquid} + \text{Mg}_3\text{Zn}_3\text{Al}_2 \rightarrow \text{Mg} + \text{MgZn}$ ; 48% Mg, 50% Zn, where the constituents have the composition:  $\text{Mg}_3\text{Zn}_3\text{Al}_2 = 26.5\%$  Mg, 55% Zn; and both the liquid and MgZn do not contain any Al.

$I = \text{liquid} + \text{MgZn}_2 \rightarrow \text{MgZn} + \text{Mg}_3\text{Zn}_3\text{Al}_2$ ; 44% Mg, 54% Zn, 354°C (669°F).

$J = \text{liquid} + \text{Mg}_3\text{Zn}_3\text{Al}_2 \rightarrow \text{Al} + \text{MgZn}_2$ ; 12.5% Mg, 60% Zn, where the constituents have the composition: liquid = 11%



Mg, 71% Zn;  $\text{Mg}_3\text{Zn}_3\text{Al}_2 = 20\% \text{ Mg}, 64\% \text{ Zn}; \text{Al} = 4.5\% \text{ Mg}, 24.5\% \text{ Zn}; \text{MgZn}_2 = 15.5\% \text{ Mg}, 80.5\% \text{ Zn}.$

$K = \text{liquid} + \text{MgZn}_2 \rightarrow \text{Mg}_3\text{Zn}_3\text{Al}_2; 21\% \text{ Mg}, 56\% \text{ Zn}, 535^\circ\text{C} (995^\circ\text{F}),$  where  $\text{Mg}_3\text{Zn}_3\text{Al}_2$  contains 21% Mg, 66% Zn.

In the solid state:

$L = \text{Al}_B + \text{MgZn}_2 \rightarrow \text{Al} + \text{MgZn}_5; 325^\circ\text{C} (617^\circ\text{F}).$

$M = \text{Al}_B \rightarrow \text{Al} + \text{MgZn}_5 + \text{Zn}; 280^\circ\text{C} (536^\circ\text{F}).$

where  $\text{Al}_B$  and Al are the solid solutions of zinc in aluminum as reported for binary aluminum-zinc alloys.

Figure 134 gives the aluminum corner at  $440^\circ\text{C} (824^\circ\text{F})$  and  $200^\circ\text{C} (392^\circ\text{F})$  to show the solid solubilities of the various constituents.

Non-equilibrium conditions do not appreciably affect alloys in the aluminum corner, the only changes being, as usual, in the amount of constituents in solid solution.

This system is important for alloys of the aluminum-magnesium-zinc type, which are used to a certain extent. The magnesium corner is also important because it covers almost all the magnesium alloys in commercial use. The zinc corner has some importance too, although the additions of magnesium to zinc-aluminum alloys are usually so small that the alloys may be considered binary zinc-aluminum alloys.

## Al-Mn-Si

### Aluminum-Manganese-Silicon

Figures 135 and 136 are plotted from data by Bueckle (649).

Two ternary constituents are formed in the aluminum corner. One  $\alpha(\text{AlMnSi})$ , probably corresponding to the formula  $\text{Mn}_3\text{Si}_2\text{Al}_6$ ,

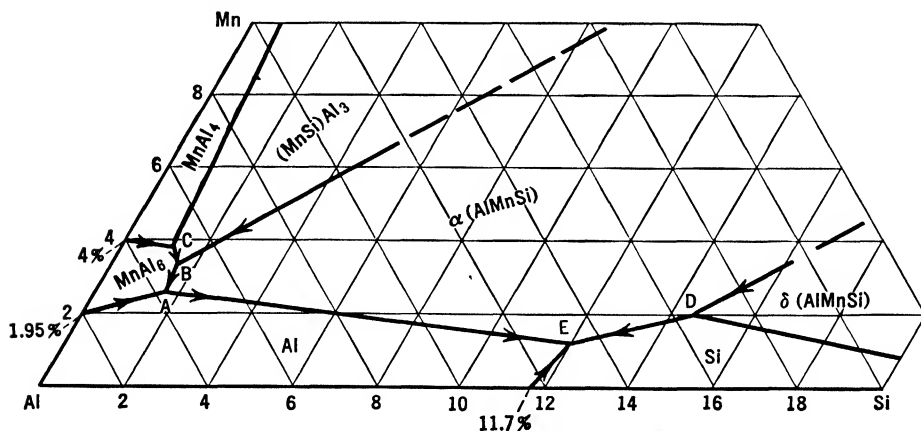


FIG. 135. System Al-Mn-Si, surfaces of primary crystallization in the aluminum corner of the equilibrium diagram.

hexagonal, contains 40 per cent manganese and 15 per cent silicon and may contain excesses of manganese and silicon in solid solution. The other  $\delta(\text{AlMnSi})$ , with a higher silicon and lower manganese content, tetragonal, begins to appear in alloys with a silicon content above 14 per cent and a manganese content above 1 per cent. A third phase, pseudo-ternary, is formed by the solid solution of silicon in  $\text{MnAl}_3$ , forming a phase closely related with the  $(\text{FeMn})\text{Al}_3$  of the Al-Fe-Mn system, and will be identified as  $(\text{MnSi})\text{Al}_3$ . The fields of

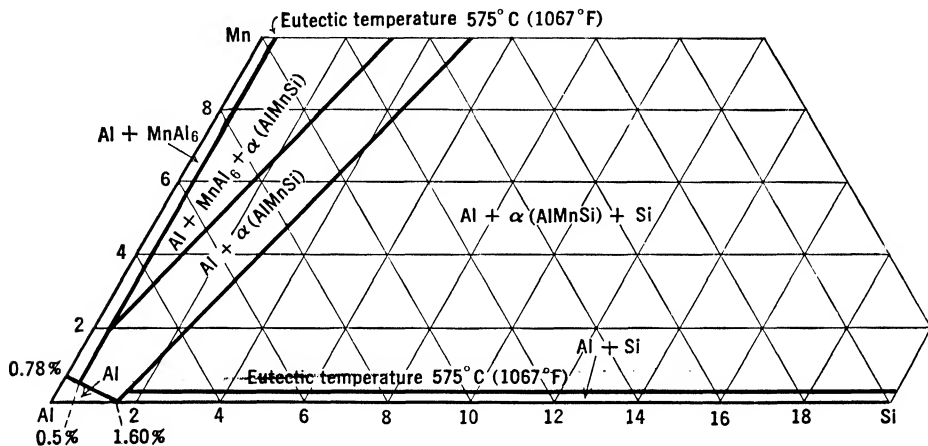


FIG. 136. System Al-Mn-Si, distribution of the phases in the solid in the aluminum corner of the equilibrium diagram.

primary crystallization are Al,  $\text{MnAl}_6$ ,  $\text{MnAl}_4$ ,  $(\text{MnSi})\text{Al}_3$ ,  $\alpha(\text{AlMnSi})$ ,  $\delta(\text{AlMnSi})$ , and Si, distributed as in Fig. 135. A ternary eutectic  $E = \text{Al}-\alpha(\text{AlMnSi})-\text{Si}$  is formed at 12 per cent silicon, 1.2 per cent manganese,  $575^\circ\text{C}$  ( $1067^\circ\text{F}$ ). Four peritectic reactions take place.

$A = \text{liquid} + \text{MnAl}_6 \rightarrow \alpha(\text{AlMnSi}); 1.7\% \text{ Si}, 2.6\% \text{ Mn}, 647^\circ\text{C}$  ( $1197^\circ\text{F}$ ).

$B = \text{liquid} + (\text{MnSi})\text{Al}_3 \rightarrow \text{MnAl}_6; 1.5\% \text{ Si}, 3.3\% \text{ Mn}, 690^\circ\text{C}$  ( $1274^\circ\text{F}$ ).

$C = \text{liquid} + \text{MnAl}_4 \rightarrow \text{MnAl}_6; 1.2\% \text{ Si}, 3.8\% \text{ Mn}, 710^\circ\text{C}$  ( $1310^\circ\text{F}$ ).

$D = \text{liquid} + \delta(\text{AlMnSi}) \rightarrow \alpha(\text{AlMnSi}); 15\% \text{ Si approx.}, 2\% \text{ Mn approx.}$

In equilibrium conditions the phases present in the solid state in the field reported are Al,  $\text{MnAl}_6$ ,  $\alpha(\text{AlMnSi})$ , and Si, distributed as in Fig. 136. The solid solubilities of manganese and silicon have been reported only at eutectic temperature, for at room temperature they are so small that they cannot be represented.

In non-equilibrium conditions caused by rapid cooling the peritectic reactions reported above are not usually completed and the phases  $\text{MnAl}_4$ ,  $(\text{MnSi})\text{Al}_3$ , and  $\delta(\text{AlMnSi})$  may also be present with low manganese and silicon concentrations. Only the alloys in the field of primary crystallization of aluminum reach equilibrium very easily and do not show foreign phases with rapid cooling.

This system is important for alloys of the aluminum-manganese type. As no important changes are produced by the presence of the amounts of iron that are encountered in commercial alloys, this diagram may also be used when iron is present.

### Al-Mn-Sn

#### Aluminum-Manganese-Tin

The only data available are those of Schueck (650), which have been corrected on the light of recent investigations of the binary diagrams involved.

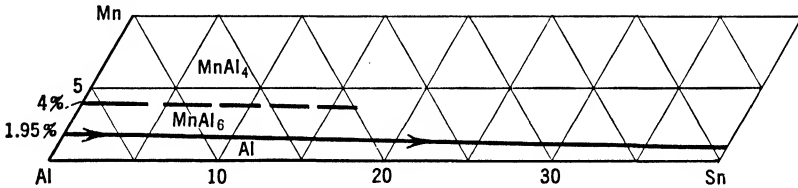


FIG. 137. System Al-Mn-Sn, surfaces of primary crystallization in the aluminum corner of the equilibrium diagram.

No ternary phase is formed, the constituents present in the aluminum corner being  $\text{MnAl}_4$ ,  $\text{MnAl}_6$ , Al, and Sn. A ternary eutectic Al-MnAl<sub>6</sub>-Sn is formed at 228°C (442°F), containing about 99.5 per cent tin and little manganese. A eutectic line runs from the binary eutectic

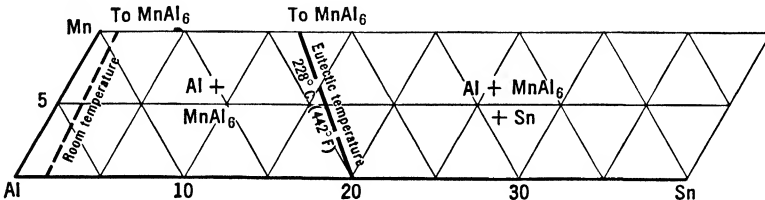


FIG. 138. System Al-Mn-Sn, distribution of the phases in the solid in the aluminum corner of the equilibrium diagram.

Al-MnAl<sub>6</sub> at 1.95 per cent manganese, to the ternary eutectic, dividing the fields of primary crystallization of  $\text{MnAl}_6$  and Al. Figure 137 shows the fields of primary crystallization. In the solid state (Fig. 138) the three constituents are present over all the field, due allowance being

made for the solid solubility of tin and manganese in aluminum, about which no data are available, besides those available in the binary diagrams. The solid solubility of tin in aluminum is therefore shown in the diagram with a dashed line; the solid solubility of manganese is so small even at eutectic temperature ( $228^{\circ}\text{C}$ — $442^{\circ}\text{F}$ ) that it cannot be represented.

No commercial alloy contains tin and manganese together; in fact, almost no commercial alloy contains tin. This system, therefore, is of little industrial interest.

### Al-Na-Si

#### Aluminum-Sodium-Silicon

The only data available on this diagram (Fig. 139) are those contained in a paper by Otani (651). According to him, a ternary eutectic  $E = \text{Al-Si-Na}$  is formed at 14 per cent silicon, 0.20 per cent sodium,

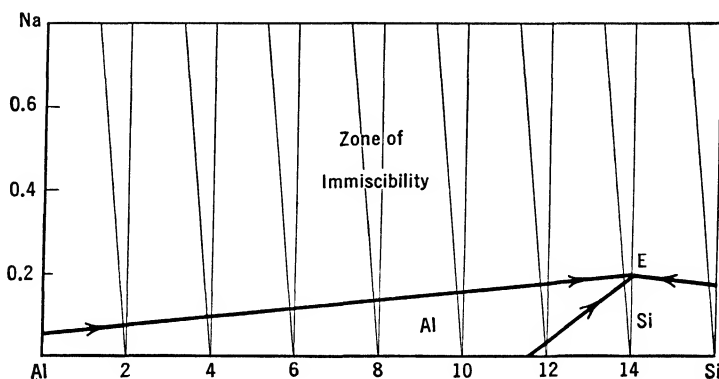


FIG. 139. System Al-Na-Si, surfaces of primary crystallization in the aluminum corner of the equilibrium diagram, according to Otani.

$573^{\circ}\text{C}$  ( $1063^{\circ}\text{F}$ ). This ternary eutectic is the modified eutectic Al-Si (see Al-Si diagram). Figure 139 shows the aluminum corner of Otani's diagram. If this diagram could be taken at its face value, the theory of the ternary eutectic could be considered substantiated, but, as the diagram has been drawn only to represent this theory, and not from additional experimental data, its existence does not substantiate the theory.

### Al-Ni-Si

#### Aluminum-Nickel-Silicon

The equilibrium diagrams (Figs. 140 and 141) are from data by Weisse (655) and Phillips (656).

No ternary compound is formed in the aluminum corner; the constituents are Al, Si, and  $\text{NiAl}_3$ , and they form a ternary eutectic *E* at about 11.00 per cent silicon, 5.0 per cent nickel,  $568^\circ\text{C}$  ( $1054^\circ\text{F}$ ).

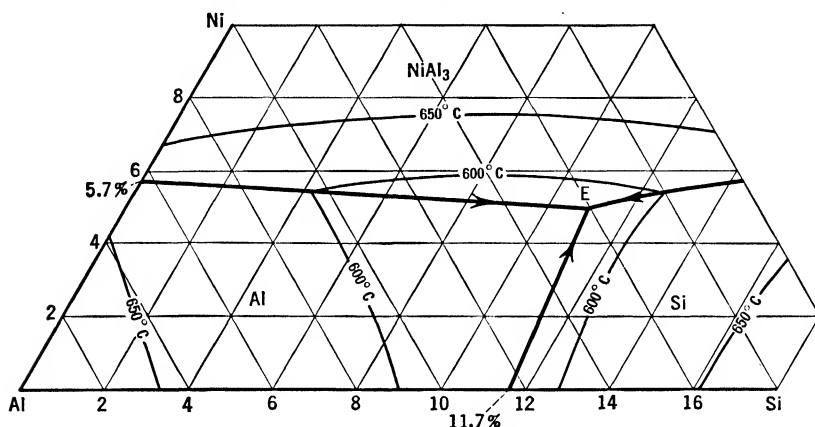


FIG. 140. System Al-Ni-Si, surfaces of primary crystallization in the aluminum corner of the equilibrium diagram.

Nickel decreases the solid solubility of silicon in aluminum. At  $520^\circ\text{C}$  ( $968^\circ\text{F}$ ) where, without nickel, the solid solubility is 0.90 per cent silicon, the presence of 10 per cent nickel reduces it to 0.70 per cent silicon and the presence of 20 per cent nickel reduces it to 0.40 per cent silicon. In the solid state the three phases are present together over all the

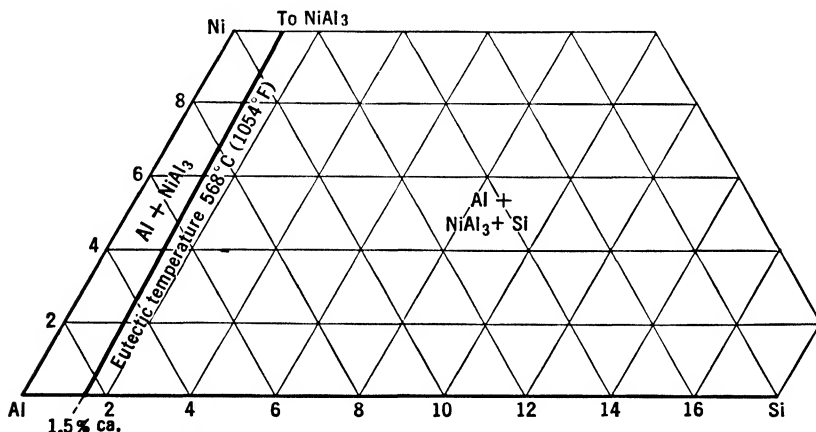


FIG. 141. System Al-Ni-Si, distribution of the phases in the solid in the aluminum corner of the equilibrium diagram.

field, due allowance being made for the solid solubility of silicon. In Fig. 141 the solid solubility of silicon is reported only at eutectic temperature, since at room temperature it is so small that it cannot be adequately shown.

In non-equilibrium conditions no appreciable difference from equilibrium structures can be noticed.

Commercial alloys contain copper and magnesium in addition to nickel and silicon. This diagram therefore has little bearing on commercial alloys, for both silicon and nickel tend to combine, respectively, with magnesium and copper.

## Al-Ni-Sn

### Aluminum-Nickel-Tin

The only data available are those of Kato (657).

No ternary phase is formed and the constituents in the aluminum corner are Al, Sn, and  $\text{NiAl}_3$ . The ternary eutectic is very near the

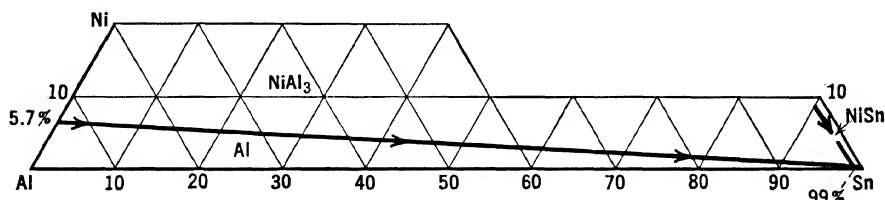


FIG. 142. System Al-Ni-Sn, surfaces of primary crystallization in the aluminum corner of the equilibrium diagram.

tin corner and has a melting point of  $227^{\circ}\text{C}$  ( $441^{\circ}\text{F}$ ). A eutectic line runs from the binary eutectic Al- $\text{NiAl}_3$  at 5.7 per cent nickel to the ternary eutectic, dividing the fields of crystallization of Al and  $\text{NiAl}_3$ . In the solid state the three phases are present over all the field, due allowance being made for the solid solubility of tin in aluminum. The

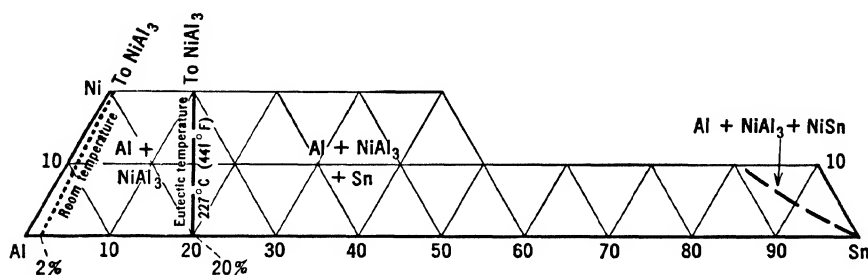


FIG. 143. System Al-Ni-Sn, distribution of the phases in the solid in the aluminum corner of the equilibrium diagram.

solid solubility of tin in aluminum is denoted by a dashed line because the data available are somewhat doubtful. Figures 142 and 143 show the fields of primary crystallization and the distribution of the phases in the solid.

No alloy containing tin and nickel is used commercially at present. This system, therefore, is of no importance from a practical point of view.

## Al-Ni-Zn

### Aluminum-Nickel-Zinc

These diagrams (Figs. 144 and 145) are from data by Fuss (658).

No ternary constituent is formed by aluminum, nickel, and zinc, the phases present in the aluminum corner being Al,  $\text{NiAl}_3$ , and Zn. A

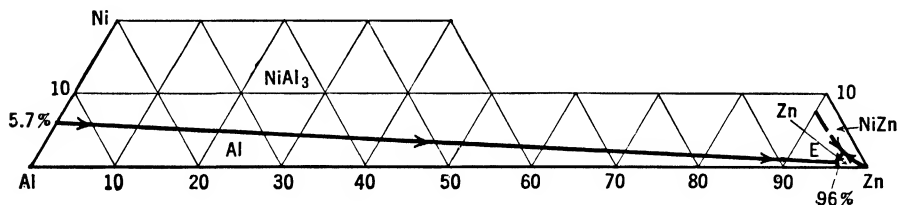


FIG. 144. System Al-Ni-Zn, surfaces of primary crystallization in the aluminum corner of the equilibrium diagram.

ternary eutectic  $E = \text{Al-NiAl}_3\text{-Zn}$  is formed near the zinc corner, containing about 96 per cent zinc and very little nickel, with a melting point of about  $380^\circ\text{C}$  ( $716^\circ\text{F}$ ). The presence of nickel does not affect the solid solubility of zinc in aluminum to any appreciable extent. The fields of primary solidification and the distribution of the phases in the solid are shown in Figs. 144 and 145. The distribution of the phases is shown also at  $275^\circ\text{C}$  ( $527^\circ\text{F}$ ), (dot-and-dash line), in order

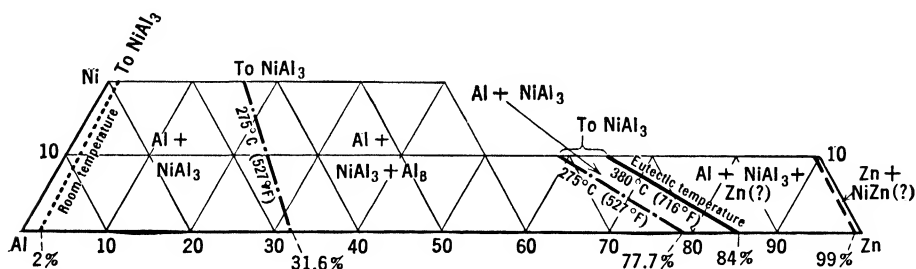


FIG. 145. System Al-Ni-Zn, distribution of the phases in the solid in the aluminum corner of the equilibrium diagram.

to show the gap of miscibility which exists in these alloys, as in the binary aluminum-zinc alloys.

Additions of zinc to alloys of the aluminum-copper-nickel type have been tried, it is claimed, with good results, and alloys of this type may be expected to enter the commercial field. This diagram, however, would still be of little importance, for both zinc and nickel would be combined differently.

**Al-Pb-Sb****Aluminum-Lead-Antimony**

This system has been investigated by Wright (659).

No ternary phase is formed by aluminum, lead, and antimony. The field of immiscibility between aluminum and lead is reduced by additions of antimony. Figure 146 shows the field of immiscibility at

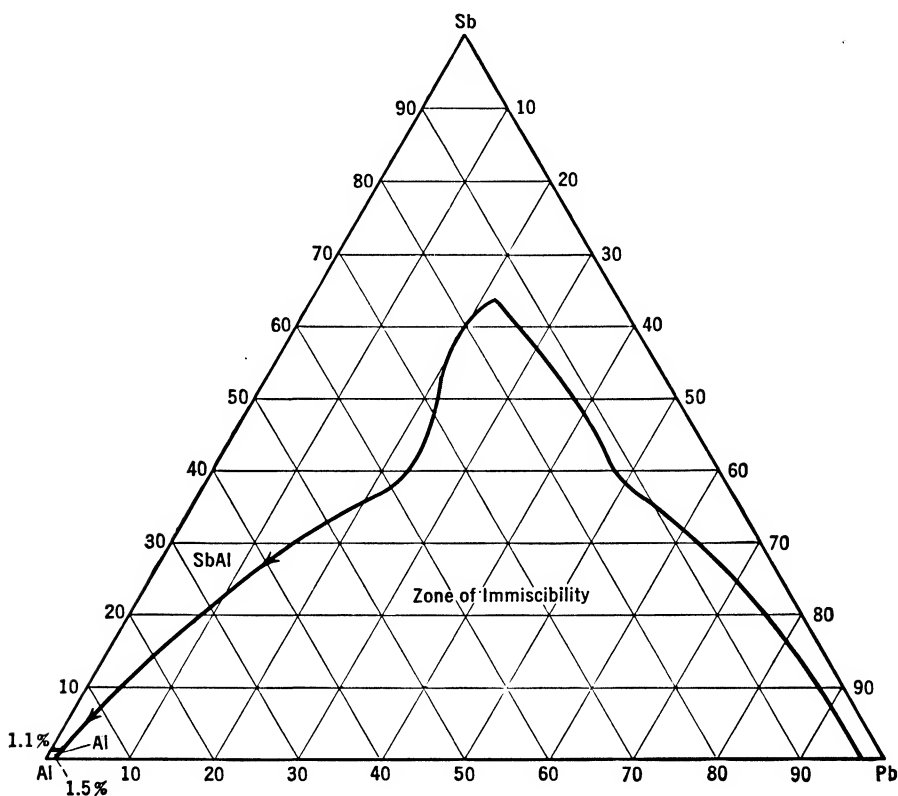


FIG. 146. System Al-Pb-Sb, miscibility at 880°C (1616°F).

freezing temperature and the probable surfaces of primary crystallization in the aluminum corner. In the solid state the phases present should be Al, SbAl, and Pb, distributed over all the field.

No practical application has been reported for these alloys.

**Al-Pb-Sn****Aluminum-Lead-Tin**

This diagram (Fig. 147) has been investigated by Wright (660).

No ternary phase is formed by aluminum, lead, and tin. Tin has very little effect on the field of immiscibility of lead and aluminum,



which almost reaches the tin corner. Figure 147 shows the field of immiscibility at freezing temperature and the probable surfaces of primary crystallization. In the solid the phases present should be Al, Pb, and Sn, distributed over all the field, due allowance being made for the solid solubilities of tin in aluminum and lead.

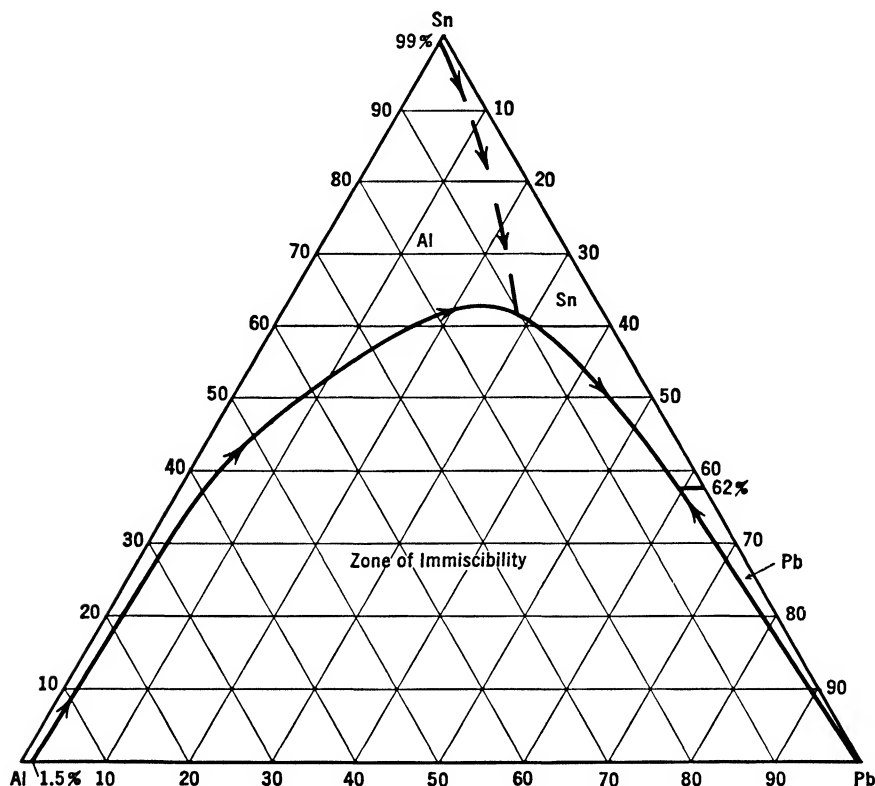


FIG. 147. System Al-Pb-Sn, miscibility at 800°C (1472°F).

No commercial alloy containing additions of lead and tin is now used, although most of the secondary material usually contains both lead and tin in amounts up to 0.5 per cent of each.

### Al-Sb-Si

#### Aluminum-Antimony-Silicon

This system has been investigated only by Matsukawa (661).

No ternary constituent is formed and the phases present in the aluminum corner are Al, Si, and SbAl. The ternary eutectic almost coincides with the binary Al-Si both as to composition (11.7 per cent silicon) and temperature (577°C—1071°F). The fields of primary crystallization are Al, Si, and SbAl; and the same three phases are

present over all the field in the solid state. No data about the solid solubility of silicon in aluminum in the presence of antimony are available; for this reason the solid solubility of silicon is indicated in the

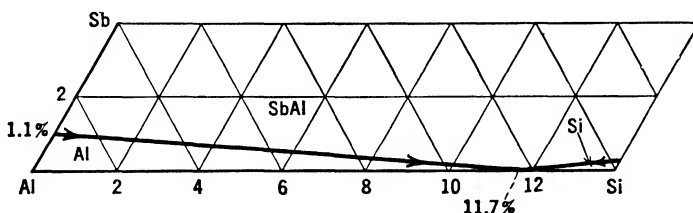


FIG. 148. System Al-Sb-Si, surfaces of primary crystallization in the aluminum corner of the equilibrium diagram.

diagram by a dashed line. Figures 148 and 149 show the primary crystallization surfaces and the distribution of the phases in the solid.

Some alloys with high silicon contents have been patented which may contain small amounts of antimony, but there is no evidence

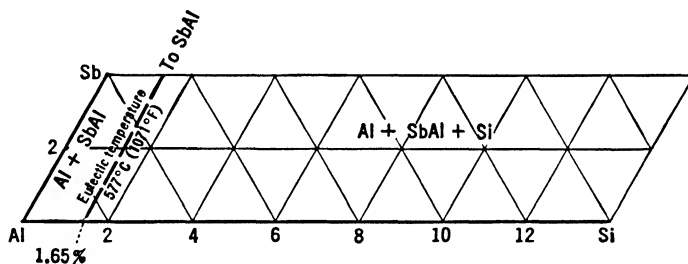


FIG. 149. System Al-Sb-Si, distribution of the phases in the solid in the aluminum corner of the equilibrium diagram.

that they are used in commercial practice. As no other alloys containing silicon and antimony are known, the importance of this system is limited.

## Al-Sb-Sn

### Aluminum-Antimony-Tin

The data on this diagram (Figs. 150 and 151) are by Fuss (662).

No ternary phase is formed; the phases present in the aluminum corner are Al, SbAl, and Sn. A ternary eutectic Al-SbAl-Sn is formed in the tin corner with a tin content of about 99 per cent and with a melting point of about 227°C (440°F). No data are available on the solid solubility of tin in aluminum in the presence of antimony; probably it is not affected to a great extent. The probable solid solubility

of tin in aluminum is shown with a dashed line in the diagram (Fig. 151). The fields of primary crystallization and the distribution of the phases in the solid are reported in Figs. 150 and 151.

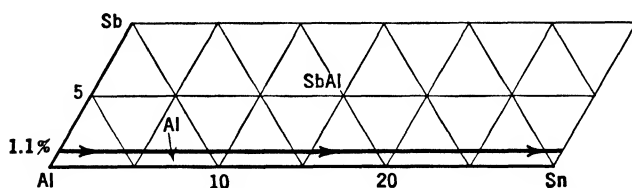


FIG. 150. System Al-Sb-Sn, surfaces of primary crystallization in the aluminum corner of the equilibrium diagram.

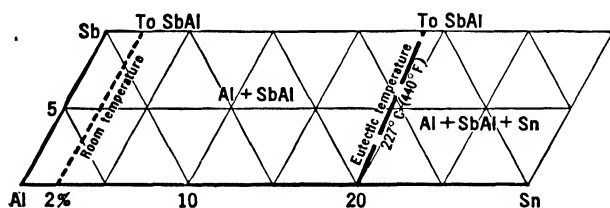


FIG. 151. System Al-Sb-Sn, distribution of the phases in the solid in the aluminum corner of the equilibrium diagram.

These alloys were investigated for soldering purposes, but with very little success, and never entered the commercial field.

## Al-Si-Sn

### Aluminum-Silicon-Tin

The only data available on this system are those reported by Matsukawa (663).

No ternary phase is formed; the constituents in the system are Al, Si, and Sn. A ternary eutectic is formed in the tin corner, almost

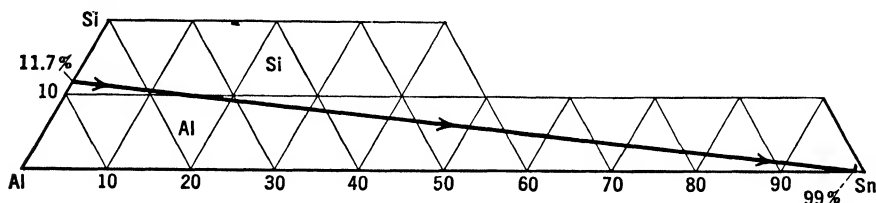


FIG. 152. System Al-Si-Sn, surfaces of primary crystallization in the aluminum corner of the equilibrium diagram.

coincident with the binary Al-Sn (99 per cent tin, 229°C—444°F) both as to composition and melting point. A eutectic line runs from the binary Al-Si (11.7 per cent silicon, 577°C—1071°F) to the ternary eutectic, dividing the fields of primary crystallization of aluminum and

silicon. Figures 152 and 153 show the fields of primary crystallization and the distribution of the phases in the solid. In the solid the three phases are present together over all the field, due allowance being made for the zone where tin is in solid solution. The solid solubility of tin is reported with a dashed line because it has not been established definitely. No solid solubility is reported for silicon, for at the eutectic

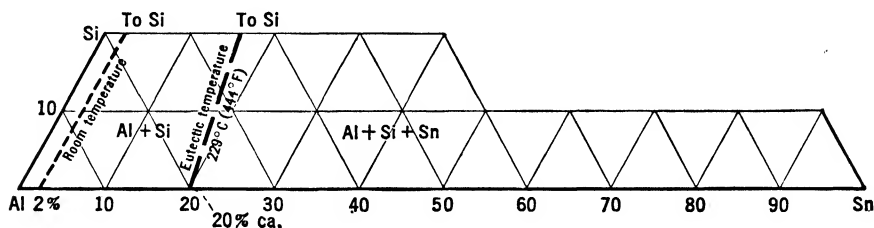


FIG. 153. System Al-Si-Sn, distribution of the phases in the solid in the aluminum corner of the equilibrium diagram.

temperature,  $229^{\circ}\text{C}$ — $444^{\circ}\text{F}$ , its solid solubility is so small that it cannot be represented.

Few alloys containing silicon and tin have been used in the past, and by now they have probably disappeared from the market completely.

### Al-Si-Th

#### Aluminum-Silicon-Thorium

This system was superficially investigated by Grogan and Schofield (664).

A compound  $\text{ThSi}_2$ , not responsive to heat treatment, is formed between thorium and silicon. No data are reported regarding solidification surfaces, eutectics, etc.

The same authors investigated the mechanical properties of the alloys, which are rather poor; therefore this diagram can be expected to remain unimportant, for it is improbable that aluminum-silicon-thorium alloys will find commercial applications.

### Al-Si-Zn

#### Aluminum-Silicon-Zinc

This diagram has been investigated by Sanders and Meissner (665) and Nishimura (667).

It can be deduced from their data that no ternary phase is formed, and the phases present are Al, Si, and Zn. A ternary eutectic  $E = \text{Al-Si-Zn}$  is formed at about 93 per cent zinc and 2 per cent silicon, with a melting point of about  $380^{\circ}\text{C}$  ( $716^{\circ}\text{F}$ ). The fields of primary crystallization are Al, Zn, and Si, distributed as shown in Fig. 154.

Figure 155 shows the distribution of the phases at eutectic temperature and at 275°C (527°F) (dot-and-dash line), in order to show the gap of miscibility of aluminum and zinc. No solid solubility is reported for

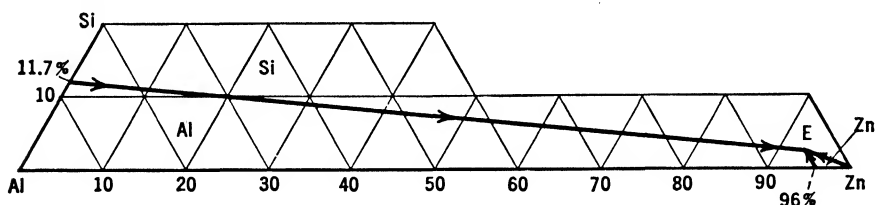


FIG. 154. System Al-Si-Zn, surfaces of primary crystallization in the aluminum corner of the equilibrium diagram.

silicon because the solubility even at eutectic temperature is so limited that it cannot be represented.

This system is of very little interest for commercial alloys. The alloys used at present do not contain only silicon and zinc but also

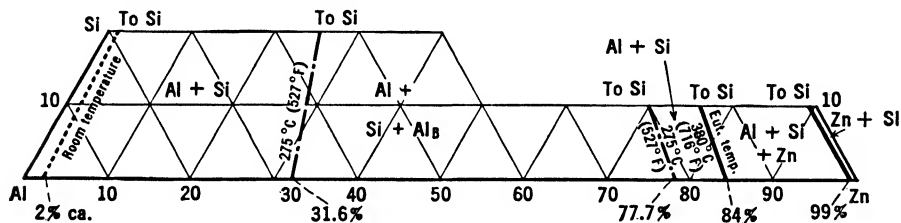


FIG. 155. System Al-Si-Zn, distribution of the phases in the aluminum corner of the equilibrium diagram.

appreciable amounts of magnesium and iron, among others, which tend to combine with silicon and zinc to form new phases.

## Al-Sn-Zn

### Aluminum-Tin-Zinc -

This system was investigated by Nishimura and Suzuki (670).

No ternary constituent is formed. The phases present are Al, Sn, and Zn. A ternary eutectic is formed, almost coincident with the binary Sn-Zn (9 per cent tin, 199°C—390°F). Aluminum forms primary crystals in most of the field and is almost the only constituent visible in the aluminum corner on account of the solid solubilities of zinc and tin in aluminum.

No commercial alloy containing appreciable amounts of tin and zinc is used. Secondary material may contain these two elements, but they are associated with so many other impurities that this system cannot be of any real use.

## CHAPTER 3

### QUATERNARY DIAGRAMS

#### **Al-Cu-Fe-Mn**

##### **Aluminum-Copper-Iron-Manganese**

The only datum available on this system is the presence of a quaternary phase of undetermined composition, reported by Keller and Wilcox (672).

Investigations by the author have confirmed the existence of a quaternary phase in alloys in non-equilibrium conditions but have proved that this phase does not exist in the stable state, where only ternary or binary phases can be detected. There is good evidence that the quaternary phase derives from the ternary unstable  $\omega(\text{AlCuFe})$  (see the Al-Cu-Fe diagram) by substitution of manganese for iron. No further data are available.

This diagram is important for alloys of the duralumin type, where the quaternary phase commonly is encountered in the cast structure. More investigations, both of equilibrium and non-equilibrium conditions, are necessary before the data may be of real use.

#### **Al-Cu-Fe-Si**

##### **Aluminum-Copper-Iron-Silicon**

The aluminum corner of this system has been thoroughly investigated by Gwyer and colleagues (673).

Although their whole investigation has been conducted with commercial casting conditions in view, successive investigations by the author show that the diagrams of primary crystallization surfaces, reported for metastable conditions, represent also equilibrium conditions, within limits of experimental error. The diagrams reported here (Figs. 156 to 167) reproduce some of the most important sections of this system. All the phases present in the quaternary diagram can be traced back to the ternary and binary diagrams involved; however, a pseudo-quaternary phase is formed by the phase  $\text{FeSiAl}_5$  and the phase  $\text{Cu}_2\text{FeAl}_7$ , which, being isomorphic, form a continuous series of solid solutions.\* The phases present in the aluminum corner are Al, Si,  $\text{FeAl}_3$ ,  $\text{CuAl}_2$ ,  $\alpha(\text{AlFeSi})$ ,  $\gamma(\text{AlFeSi})$ ,  $\delta(\text{AlFeSi})$ ,  $\text{AlCuFeSi}$ . In

\* This phase will be called  $\text{AlCuFeSi}$ .

addition to the singular points existing in the binary and ternary diagrams concerned, which in the quaternary alloys become, respectively, surfaces and lines, the following singular points exist in the quaternary—three peritectics:

$A = \text{liquid} + \text{FeAl}_3 \rightarrow \text{Al} + \alpha(\text{AlFeSi}) + \text{AlCuFeSi}; 20.5\% \text{ Cu}, 1.8\% \text{ Si}, 1.5\% \text{ Fe}, 590^\circ\text{C} (1094^\circ\text{F}).$

$B = \text{liquid} + \gamma(\text{AlFeSi}) \rightarrow \alpha(\text{AlFeSi}) + \delta(\text{AlFeSi}) + \text{Si}; 36.3\% \text{ Cu}, 11.3\% \text{ Si}, 4\% \text{ Fe}, 665^\circ\text{C} (1229^\circ\text{F}).$

$C = \text{liquid} + \delta(\text{AlFeSi}) \rightarrow \text{Si} + \text{AlCuFeSi} + \alpha(\text{AlFeSi}); 38\% \text{ Cu}, 6.6\% \text{ Si}, 2.5\% \text{ Fe}, 620^\circ\text{C} (1148^\circ\text{F}).$

One eutectic:

$E = \text{Al-CuAl}_2\text{-AlCuFeSi-Si}; 26\% \text{ Cu}, 6.5\% \text{ Si}, 0.5\% \text{ Fe}, 520^\circ\text{C} (968^\circ\text{F}).$

**Additions of iron to aluminum-copper-silicon.** Additions of iron to aluminum-copper-silicon alloys introduce the phase  $\text{AlCuFeSi}$ , which

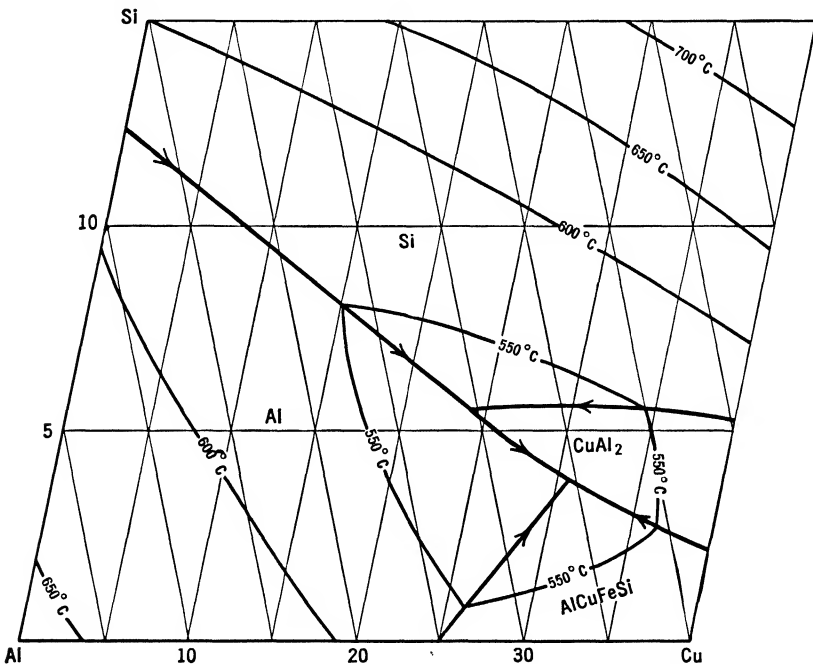


FIG. 156. System Al-Cu-Fe-Si, surfaces of primary crystallization in the aluminum corner of the equilibrium diagram, section at 0.5% Fe.

becomes primary immediately, invading the field of primary crystallization of  $\text{CuAl}_2$  until, at 1 per cent iron,  $\text{AlCuFeSi}$  is substituted for  $\text{CuAl}_2$  completely. At 1.5 per cent iron, the two phases  $\alpha(\text{AlFeSi})$

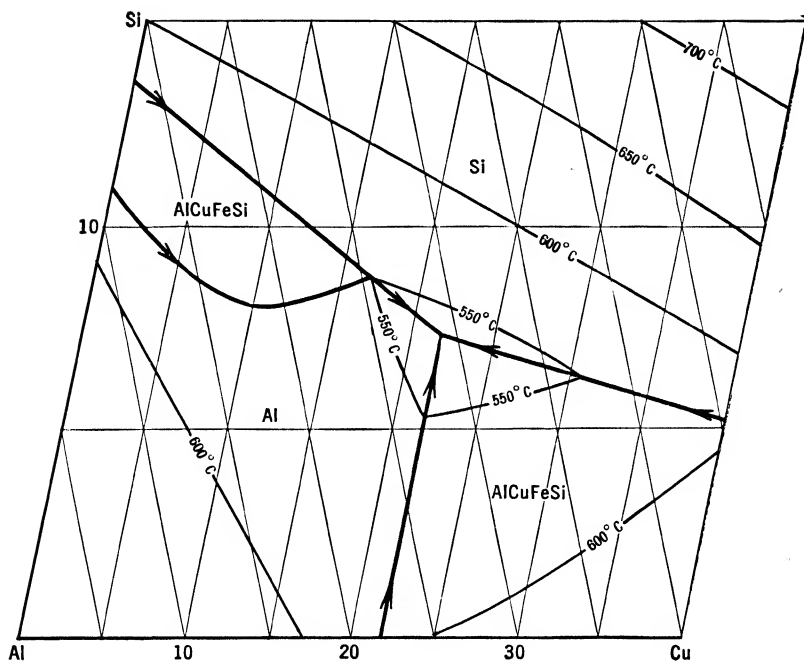


FIG. 157. System Al-Cu-Fe-Si, surfaces of primary crystallization in the aluminum corner of the equilibrium diagram, section at 1% Fe.

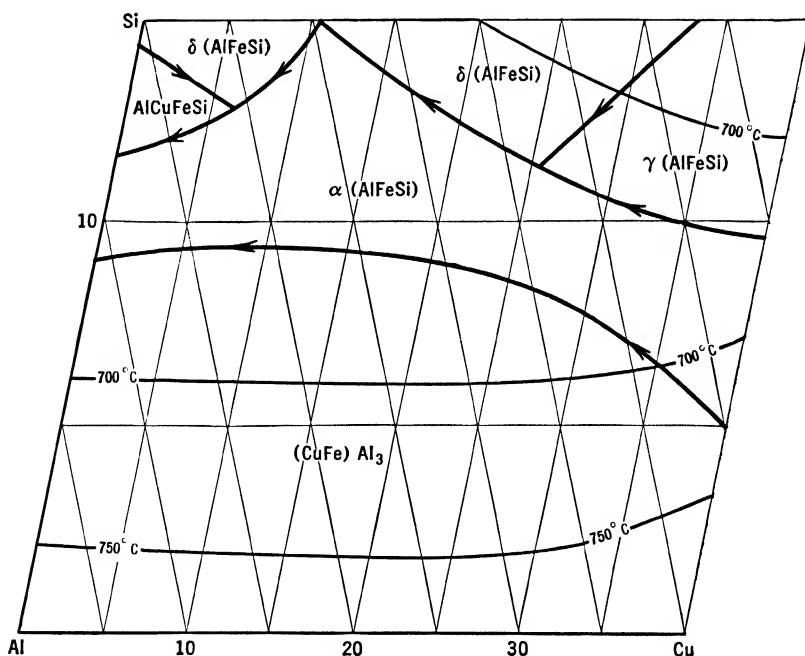


FIG. 158. System Al-Cu-Fe-Si, surfaces of primary crystallization in the aluminum corner of the equilibrium diagram, section at 5% Fe.



and  $\delta(\text{AlFeSi})$  become primary and, at 1.80 per cent iron,  $\text{FeAl}_3$  becomes primary in place of Al. At 3.5 per cent iron, the phase  $\gamma(\text{AlFeSi})$  appears as primary in the field covered by the diagrams (15 per cent silicon, 40 per cent copper). Further additions of iron increase the field of primary crystallization of  $\text{FeAl}_3$  and decrease the

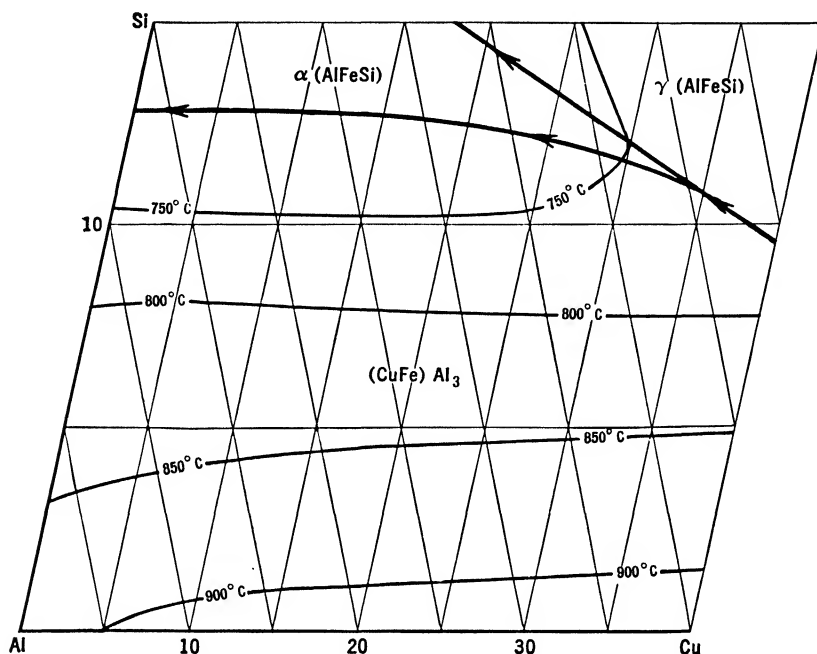


FIG. 159. System Al-Cu-Fe-Si, surfaces of primary crystallization in the aluminum corner of the equilibrium diagram, section at 10% Fe.

field of  $\text{AlCuFeSi}$  until, at 10 per cent iron,  $\text{FeAl}_3$  primary covers most of the field considered, with the fields of  $\alpha(\text{AlFeSi})$  and  $\gamma(\text{AlFeSi})$  at the border.

**Addition of silicon to aluminum-copper-iron.** Additions of silicon to aluminum-copper-iron alloys introduce the phase  $\alpha(\text{AlFeSi})$ , which becomes primary at 1 per cent silicon, taking place between the fields of  $\text{FeAl}_3$  and  $\text{AlCuFeSi}$ . At 6 per cent silicon,  $\text{CuAl}_2$  disappears as primary and its place is taken by Si. At 8 per cent silicon,  $\delta(\text{AlFeSi})$  becomes primary, invading the field of  $\text{AlCuFeSi}$ . At 8.5 per cent silicon,  $\gamma(\text{AlFeSi})$  enters the field considered (40 per cent copper, 10 per cent iron) and, at 12 per cent silicon, Al disappears as primary, its place being taken by Si. Further additions of silicon increase the fields of  $\alpha(\text{AlFeSi})$ ,  $\gamma(\text{AlFeSi})$ ,  $\delta(\text{AlFeSi})$ , and Si, at the expense of  $\text{FeAl}_3$  and  $\text{AlCuFeSi}$ , until at 15 per cent silicon they have disappeared from the field considered.

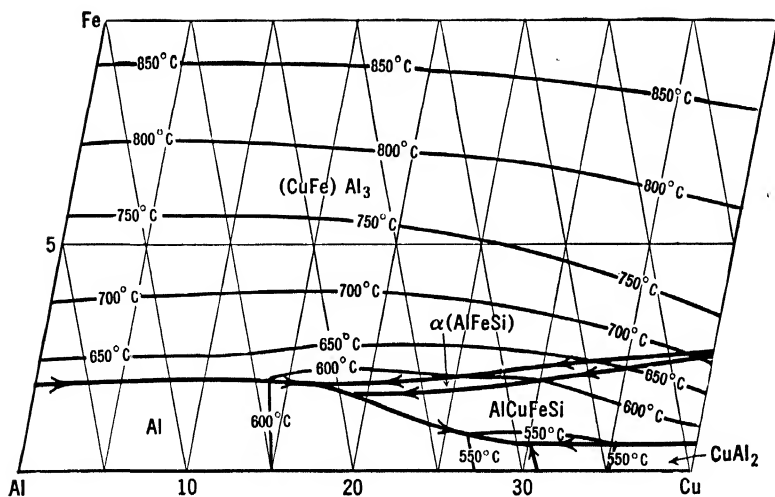


FIG. 160. System Al-Cu-Fe-Si, surfaces of primary crystallization in the aluminum corner of the equilibrium diagram, section at 2% Si.

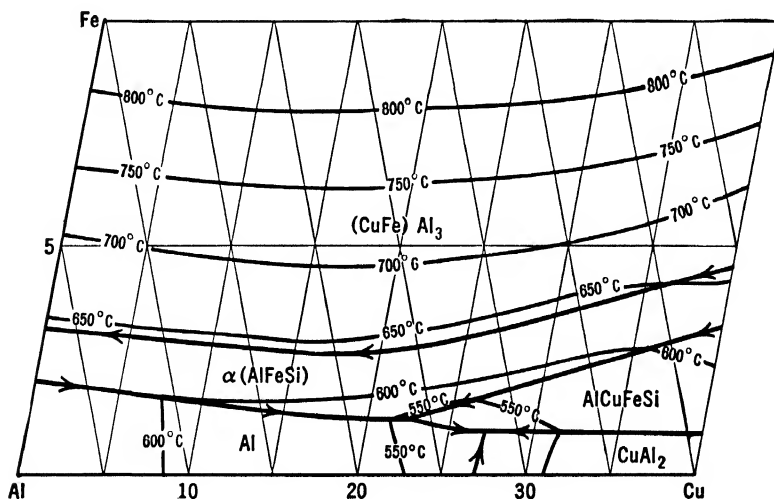


FIG. 161. System Al-Cu-Fe-Si, surfaces of primary crystallization in the aluminum corner of the equilibrium diagram, section at 5% Si.

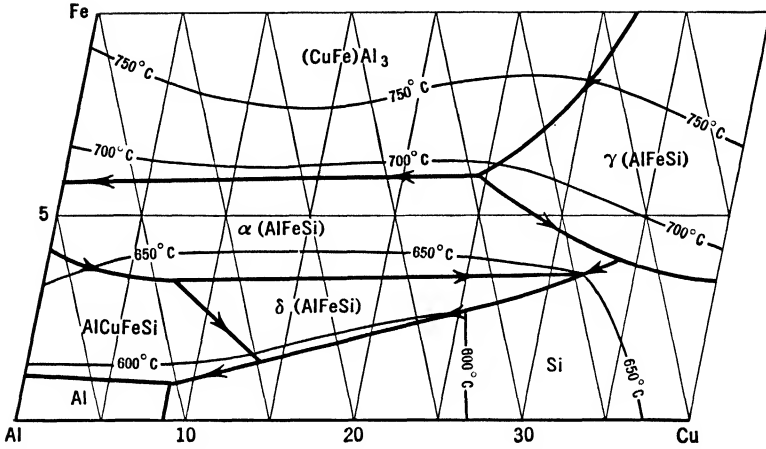


FIG. 162. System Al-Cu-Fe-Si, surfaces of primary crystallization in the aluminum corner of the equilibrium diagram, section at 10% Si.

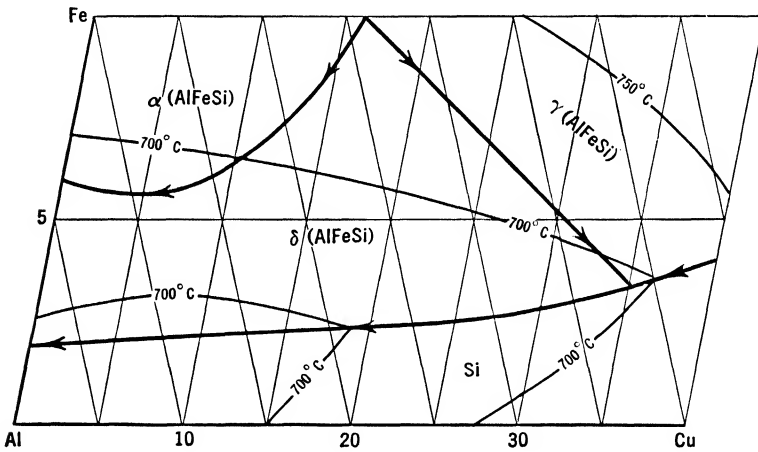


FIG. 163. System Al-Cu-Fe-Si, surfaces of primary crystallization in the aluminum corner of the equilibrium diagram, section at 15% Si.

**Additions of copper to aluminum-iron-silicon.** Additions of copper to aluminum-iron-silicon alloys change only the shape of the primary fields but do not bring any substantial change in the diagram. At 18 per cent copper,  $\gamma(\text{AlFeSi})$  enters the field considered (10 per cent iron, 15 per cent silicon). At 20 per cent copper, the field of  $\text{AlCuFeSi}$  is reduced to its minimum; then it starts moving toward the aluminum-iron axis until, at 25 per cent copper, it reaches it. At 33 per cent copper, Al disappears as primary and its place is taken by  $\text{CuAl}_2$ .

The data about the distribution of the phases in the solid state are limited and not sufficiently reliable to allow for the drawing of dia-

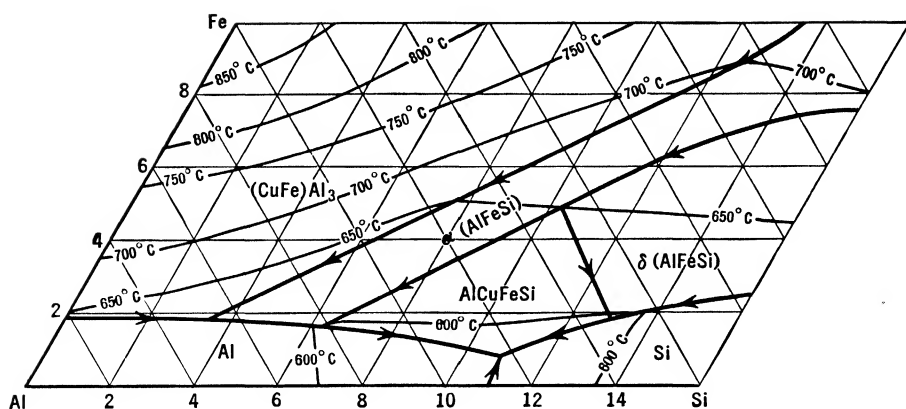


FIG. 164. System Al-Cu-Fe-Si, surfaces of primary crystallization in the aluminum corner of the equilibrium diagram, section at 5% Cu.

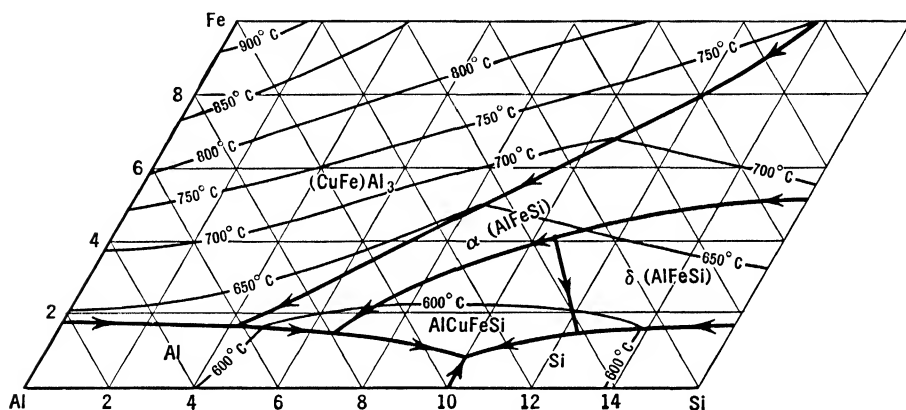


FIG. 165. System Al-Cu-Fe-Si, surfaces of primary crystallization in the aluminum corner of the equilibrium diagram, section at 10% Cu.

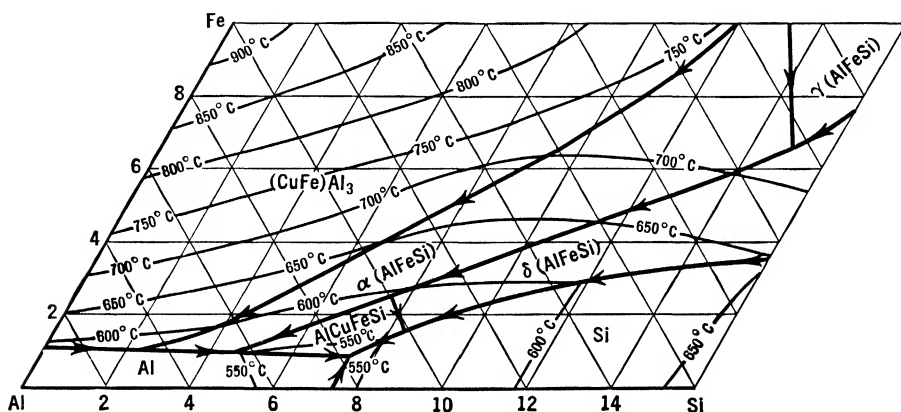


FIG. 166. System Al-Cu-Fe-Si, surfaces of primary crystallization in the aluminum corner of the equilibrium diagram, section at 20% Cu.

grams. The paper by Gwyer and colleagues gives sections for different copper contents but, in view of the method of casting used, they do not represent equilibrium conditions. No precautions were taken to

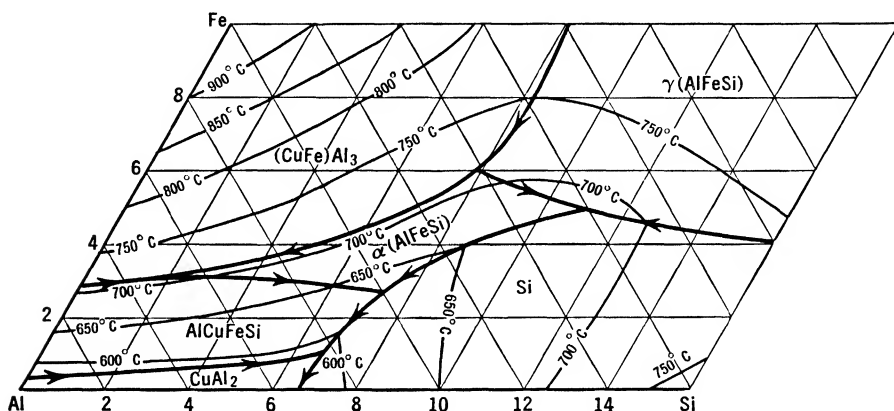


FIG. 167. System Al-Cu-Fe-Si, surfaces of primary crystallization in the aluminum corner of the equilibrium diagram, section at 40% Cu.

avoid local segregations and incomplete peritectic reactions; that accounts for the presence in the various fields of more phases than the phase rule would allow. Also, as a representation of commercial casting conditions, they are not true; for the unstable phase  $\omega(\text{AlCuFe})$

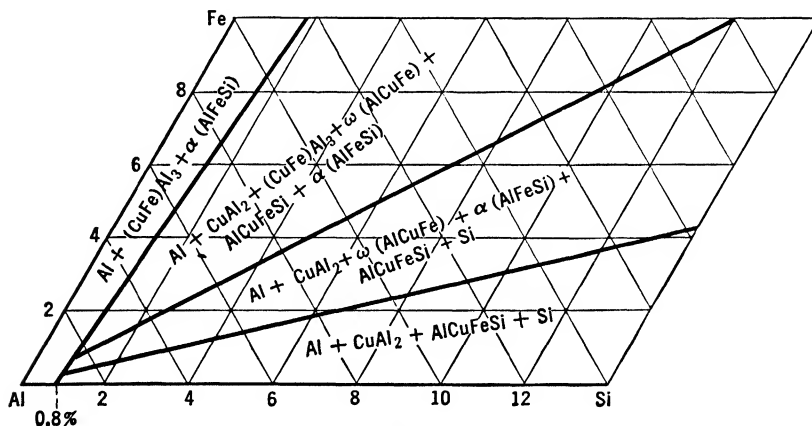


FIG. 168. System Al-Cu-Fe-Si, distribution of the phases in the solid in the aluminum corner in non-equilibrium conditions, section at 4% Cu.

(see the Al-Cu-Fe diagram) has been completely overlooked, although the author has sometimes encountered it in commercial castings. Shown in Figs. 168 and 169 are the sections for 4 per cent and 8 per cent copper, amended by data from Gayler (674) and the author to

represent commercial conditions. However, the diagrams reported are to be considered only approximate and indicative, as variations in the cooling rate have been proved to change the microstructure substantially.

Of all the phases present in the diagram only  $\text{CuAl}_2$  is soluble in aluminum to any appreciable extent, and there is evidence that the presence of other phases reduces its solid solubility only slightly.

This equilibrium diagram completely covers most of the alloys of the aluminum-copper type and can be valuable for alloys of the

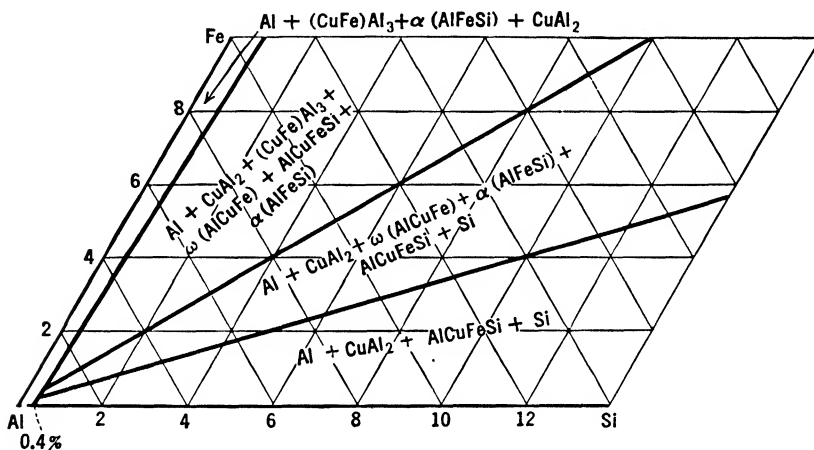


FIG. 169. System Al-Cu-Fe-Si, distribution of the phases in the solid in the aluminum corner in non-equilibrium conditions, section at 8% Cu.

aluminum-silicon, duralumin, and aluminum-copper-nickel types; it is, therefore, one of the most important diagrams and should always be consulted instead of the binary and the ternary diagrams for commercial alloys.

### Al-Cu-Mg-Ni

#### Aluminum-Copper-Magnesium-Nickel

This system has been partially explored by Bingham (675). However, the aluminum used for the investigations contained 0.13 per cent silicon, which distorted the results by the formation of the compound  $\text{Mg}_2\text{Si}$ . Moreover, the two phases  $\text{AlCuMg}$  were completely overlooked, although the author has detected  $\text{Cu}_2\text{Mg}_2\text{Al}_5$  in aluminum-copper-nickel alloys, even with magnesium contents as low as 0.5 per cent. For these reasons the diagrams in that paper are of very little value and are not reported here. From Bingham's investigations it can be deduced, however, that no quaternary phase is formed by additions

of magnesium to aluminum-copper-nickel alloys, which fact is also confirmed by the author's experience.

This system is of some interest for alloys of the aluminum-copper-nickel type. However, for these alloys the Al-Cu-Fe-Ni and Al-Cu-Mg-Si diagrams are more important.

### Al-Cu-Mg-Si

#### Aluminum-Copper-Magnesium-Silicon

The diagrams shown (Figs. 170 to 179) are mainly from data by the author, integrated by data from Dix and colleagues (677).

A quaternary phase, corresponding to the formula  $\text{CuMg}_5\text{Si}_4\text{Al}_4$ , or possibly  $\text{CuMg}_4\text{Si}_4\text{Al}_4$ , is present in alloys where the silicon content is higher than that required for the formation of  $\text{Mg}_2\text{Si}$ . This phase forms well-shaped hexagonal crystals when primary, elongated needles when eutectic. Its field of primary crystallization starts from the eutectic Al-CuAl<sub>2</sub>-Si, is inserted between the fields of primary crystallization of CuAl<sub>2</sub> and Si in the ternary Al-Cu-Si diagram, and extends to the eutectic Al-Mg<sub>2</sub>Si-Si in the Al-Mg-Si diagram, where it inserts itself between the fields of primary crystallization of  $\text{Mg}_2\text{Si}$  and Si. Outside this field, the quaternary is formed by peritectic reaction from  $\text{Mg}_2\text{Si}$  and the liquid. Besides the binary and ternary eutectics formed already in the binary and ternary alloys, two quaternary eutectics are formed.

Al-CuAl<sub>2</sub>-Mg<sub>2</sub>Si; 517°C (963°F), 28% Cu, 6% Mg, 3.5% Si.

Al-CuAl<sub>2</sub>-CuMg<sub>5</sub>Si<sub>4</sub>Al<sub>4</sub>-Si; 520°C approx. (968°F), 26% Cu, 2% Mg, 5% Si.

Figures 170 to 178 show the distribution of the phases in the solid state, at room temperature. The effect of the various phases on the solid solubility of the various elements is approximately as follows.

**Mg<sub>5</sub>Al<sub>8</sub>.** The solid solubility of copper is not affected to any great extent by it. Silicon in its presence is in the form of  $\text{Mg}_2\text{Si}$ , mostly insoluble, as in the ternary alloys aluminum-magnesium-silicon.

**CuMg<sub>4</sub>Al<sub>6</sub> and Cu<sub>2</sub>Mg<sub>2</sub>Al<sub>5</sub>.** Copper and silicon are affected in the same manner as with  $\text{Mg}_5\text{Al}_8$ . The solid solubility of magnesium is somewhat reduced by the presence of these two phases.

**Mg<sub>2</sub>Si.** The solid solubility of copper and silicon are only slightly reduced by  $\text{Mg}_2\text{Si}$ . Magnesium is not affected by it.

**CuAl<sub>2</sub>.** It does not affect appreciably the solid solubility of silicon. It cannot coexist with magnesium because it will form one of the two ternary AlCuMg phases.

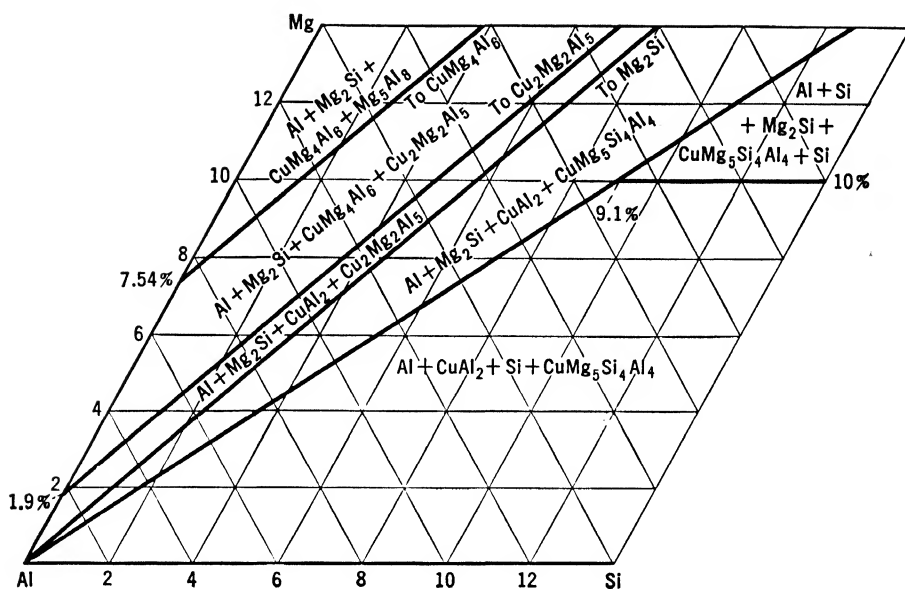


FIG. 170. System Al-Cu-Mg-Si, distribution of the phases in the solid in the aluminum corner of the equilibrium diagram, section at 5% Cu.

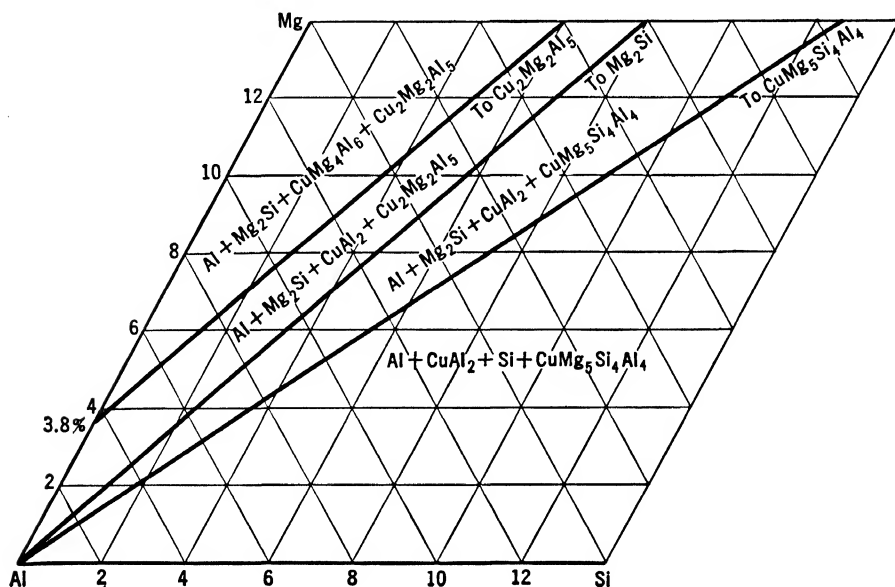


FIG. 171. System Al-Cu-Mg-Si, distribution of the phases in the solid in the aluminum corner of the equilibrium diagram, section at 10% Cu.



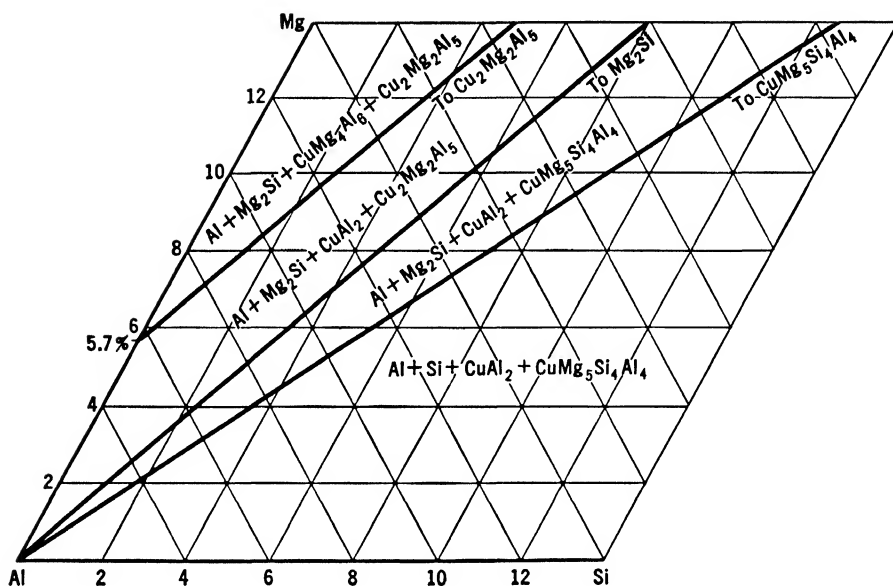


FIG. 172. System Al-Cu-Mg-Si, distribution of the phases in the solid in the aluminum corner of the equilibrium diagram, section at 15% Cu.

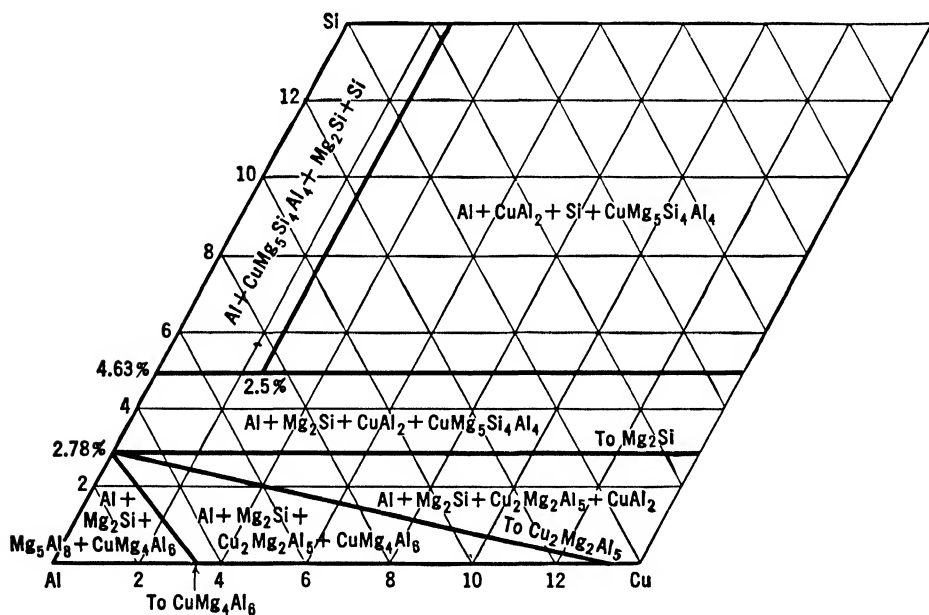


FIG. 173. System Al-Cu-Mg-Si, distribution of the phases in the solid in the aluminum corner of the equilibrium diagram, section at 5% Mg.

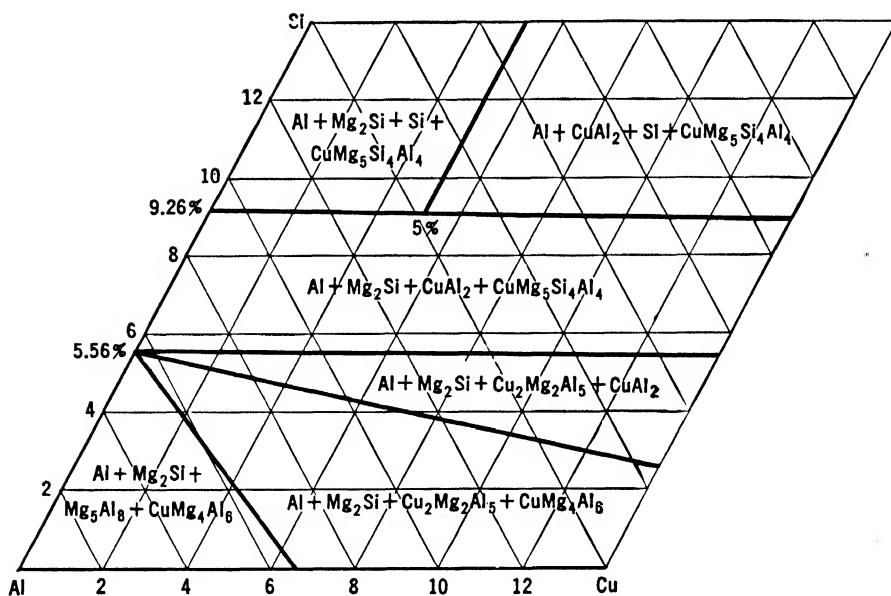


FIG. 174. System Al-Cu-Mg-Si, distribution of the phases in the solid in the aluminum corner of the equilibrium diagram, section at 10% Mg.

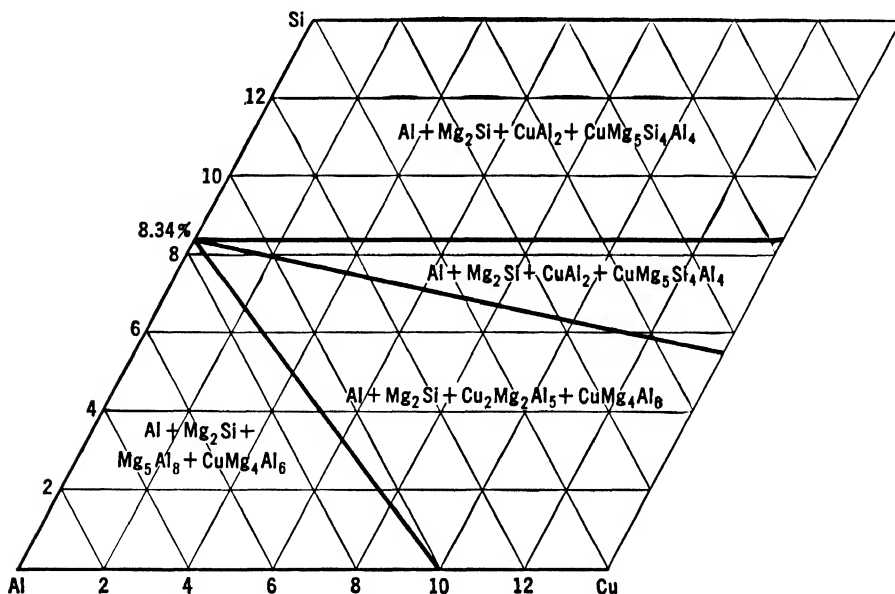


FIG. 175. System Al-Cu-Mg-Si, distribution of the phases in the solid in the aluminum corner of the equilibrium diagram, section at 15% Mg.

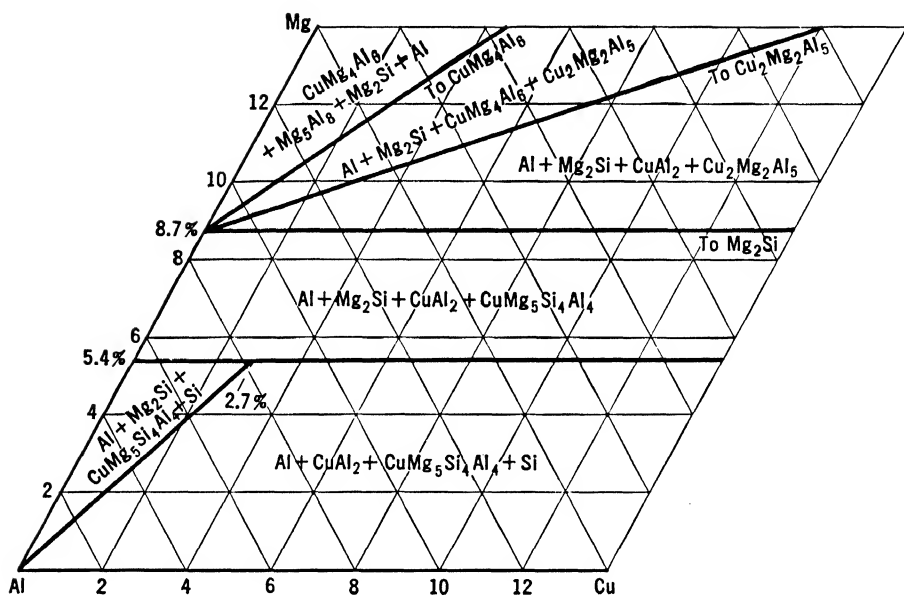


FIG. 176. System Al-Cu-Mg-Si, distribution of the phases in the solid in the aluminum corner of the equilibrium diagram, section at 5% Si.

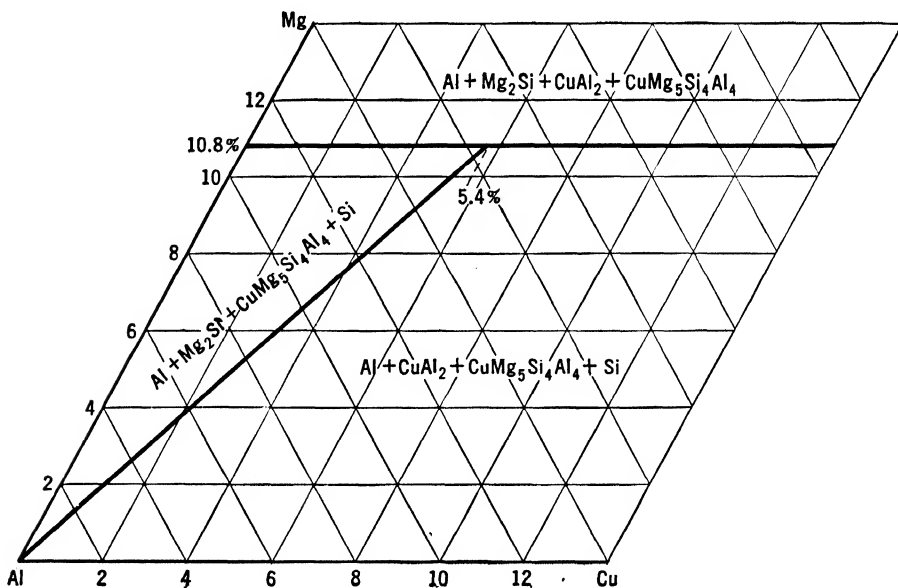


FIG. 177. System Al-Cu-Mg-Si, distribution of the phases in the solid in the aluminum corner of the equilibrium diagram, section at 10% Si.

**CuMg<sub>5</sub>Si<sub>4</sub>Al<sub>4</sub>.** It does not affect the solid solubility of copper and silicon to any great extent. It cannot coexist with magnesium, for in that case Mg<sub>2</sub>Si and CuAl<sub>2</sub> or an AlCuMg phase would be formed.

**Si.** It does not affect the solid solubility of copper to any extent. With magnesium it forms the compound Mg<sub>2</sub>Si, whose solid solubility is almost the same as in the ternary alloys aluminum-magnesium-silicon.

Figure 179 shows the distribution of the phases at 500°C (932°F) in the section at 4 per cent copper. Note that the copper content is

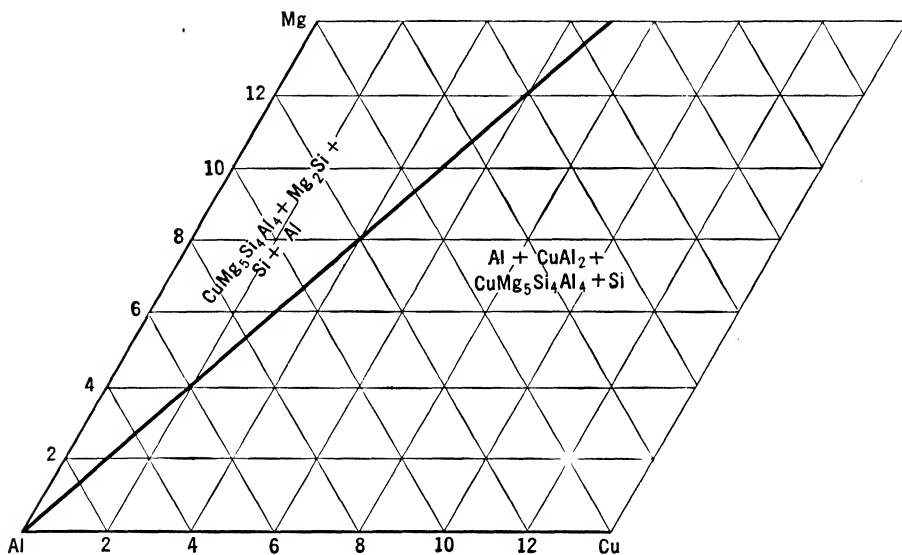


FIG. 178. System Al-Cu-Mg-Si, distribution of the phases in the solid in the aluminum corner of the equilibrium diagram, section at 15% Si.

below its maximum solubility at this temperature. All the copper, therefore, is in solid solution, even that which should be combined as the quaternary phase, leaving the less soluble constituents, namely, Mg and Si, out of solution. These constituents recombine to form new constituents which, in the absence of free copper, are Mg<sub>2</sub>Si and Si. For this reason, in the field of existence of the quaternary, only Mg<sub>2</sub>Si and Si are visible at this temperature with this copper concentration.

Non-equilibrium conditions caused by rapid cooling appreciably affect these alloys. Alloys, where the quaternary phase is present, are the most affected. The peritectic reaction Mg<sub>2</sub>Si + liquid → CuMg<sub>5</sub>Si<sub>4</sub>Al<sub>4</sub> is rather slow and with rapid cooling is not completed, yielding alloys where CuAl<sub>2</sub>, Mg<sub>2</sub>Si, and Si coexist together with the

quaternary. This condition can be detected even in alloys with copper, magnesium, and silicon contents of the commercial alloys. Also affected by rapid cooling are alloys containing the phases  $\text{Cu}_2\text{Mg}_2\text{Al}_5$  and  $\text{CuMg}_4\text{Al}_6$ , but only when the magnesium and copper contents surpass 20 per cent. Less affected are alloys in the  $\text{Mg}_2\text{Si}$  or high-silicon ranges.

This system is very important for an exact understanding of the age-hardening phenomena in commercial alloys, for the data from the

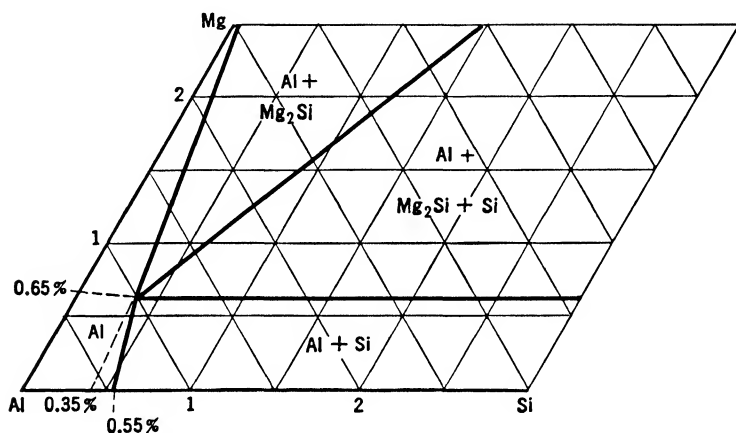


FIG. 179. System Al-Cu-Mg-Si, distribution of the phases in the solid in the aluminum corner of the equilibrium diagram, section at 4% Cu, detail showing the solid solubilities of the various phases at 500°C (932°F).

binary alloys can only give an approximate idea. Especially for duralumin and aluminum-copper-nickel alloys this diagram is very valuable and further investigations would be very useful.

### Al-Cu-Mg-Zn

#### Aluminum-Copper-Magnesium-Zinc

This system has been partially investigated by Laves, Loehberg, and Witte (679).

Their investigations deal mainly with the crystalline structure of the intermediate phases, and they report that  $\text{CuMg}_4\text{Al}_6$  and  $\text{Mg}_3\text{Zn}_3\text{Al}_2$  form a continuous series of solid solutions. No other data have been reported.

This diagram is important for alloys containing copper, magnesium, and zinc, which have been shown to possess some interesting properties. More thorough investigations, however, are necessary before these data are to be used.

**Al-Fe-Mg-Si****Aluminum-Iron-Magnesium-Silicon**

The only data available on this system are the report by Phillips (633) of the presence of a quaternary phase and the existence of a quaternary phase  $\text{FeMg}_3\text{Si}_8\text{Al}_8$  (680). Investigations by the author confirm the presence of a quaternary phase with a field of existence in the place of the phase  $\text{FeSiAl}_5$ , from which it is formed by peritectic reaction between  $\text{FeSiAl}_5$  and the liquid. This field of existence, however, does not coincide with the above reported formula. There is the possibility that the above formula refers to another quaternary constituent.

This diagram is very important for many alloys of the aluminum-silicon and the aluminum-magnesium type, among others, and further investigations of it will prove very valuable.

**Al-Fe-Mn-Si****Aluminum-Iron-Manganese-Silicon**

No investigation of these alloys is reported in the literature. Investigations by the author show that there is a range of miscibility of the following ternary phases.

$\alpha(\text{AlFeSi})$  with  $\alpha(\text{AlMnSi})$  to form  $\alpha(\text{AlFeMnSi})$ .

$\delta(\text{AlFeSi})$  with  $\delta(\text{AlMnSi})$  to form  $\delta(\text{AlFeMnSi})$ .

$(\text{FeMn})\text{Al}_3$  with  $(\text{MnSi})\text{Al}_3$  to form  $(\text{FeMnSi})\text{Al}_3$ .

In the solid,  $\alpha(\text{AlFeMnSi})$  is present in the aluminum corner over most of the field. There is evidence that besides forming primary crystals on a wide range of compositions it can also be formed by peritectic reaction from  $(\text{FeMn})\text{Al}_6$ .

This system is important for alloys of the aluminum-silicon and aluminum-magnesium type and especially for alloys of the aluminum-manganese and duralumin type. A thorough investigation to clear the points only superficially investigated by the author would be very useful.

**Al-Mg-Si-Zn****Aluminum-Magnesium-Silicon-Zinc**

This diagram has been investigated by Sanders and Meissner (681).

However, as their investigation is based on an aluminum-zinc diagram showing an intermetallic compound  $\text{AlZn}$ , and in the course of the investigation the ternary  $\text{Mg}_3\text{Zn}_3\text{Al}_2$  has been completely overlooked, their results are valueless and are not reported.

This diagram would be useful for alloys of the aluminum-magnesium-zinc type and for all the alloys containing zinc and magnesium, but further investigations are necessary before useful data can be obtained.

## *PART II*

### *POLISHING AND ETCHING*

#### CHAPTER 4

#### **MACRO-EXAMINATION**

By macro-examination is understood the examination of the macro-structure, or gross structure, as distinguished from micro-examination, which is understood to be the examination of the fine structure. According to this definition, any examination of the size, distribution, or orientation of the crystals is to be considered macro-examination; whereas the examination of the internal structure of the crystals is micro-examination. This distinction, although etymologically correct, does not correspond to the practical use, because many grain-size examinations require the use of the microscope and are therefore to be considered micro- rather than macro-examination. A differentiation that works better for practical purposes can be based on the enlargement used: all the examinations not requiring the use of enlargements above 10 diameters are macro-examinations; all those requiring higher magnifications are micro-examinations.

The simplest form of macro-examination is the inspection of a broken surface without any preparation or etching. Inclusions, both metallic and non-metallic, cracks, and large grain size can be detected in this examination, and to a certain extent also porosity and irregular crystallization. This method, which in the hands of an experienced metallurgist can give good results, should be limited, however, to a rough preliminary examination, and for more accurate examinations the surface should be prepared and etched. The preparation of the surface depends somewhat upon the problem at hand: if only porosity and cracks are to be investigated, the surface as cut by a saw will be satisfactory (Fig. 180); if a more accurate investigation of the grain structure is necessary, a better preparation of the surface is required.

The best method for the preparation of the surface is the machining in a lathe or in a milling machine because it is fast and, when properly

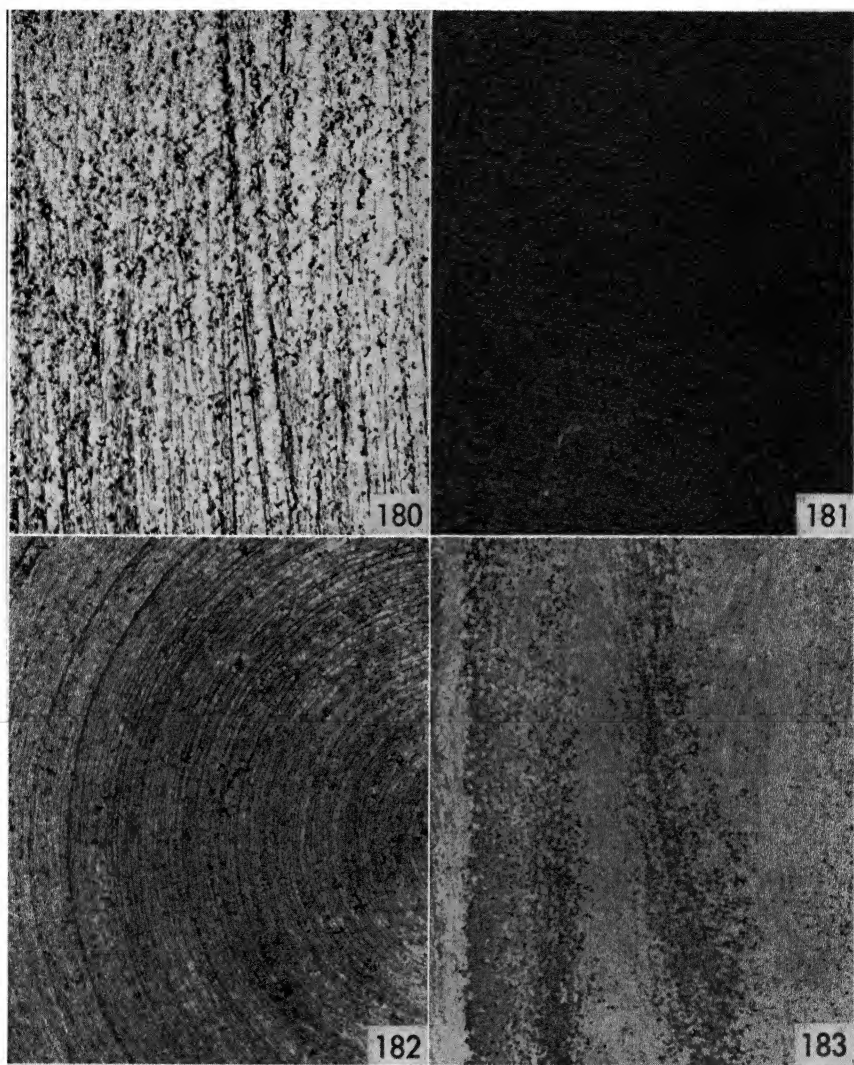


FIG. 180. Ingot, cut with saw, etched with NaOH on the sawed surface. The porosity (black spots) can be easily detected—Cu 4.25%, Fe 0.85%, Mn 0.24%, Si 1.25%—X 2.

FIG. 181. Ingot for extrusion, machined with too high feeding speed and dulled tool. Presence of ridges which mask the structure somewhat. Natural size, etched with 10% NaOH solution—Cu 4.05%, Fe 0.42%, Mg 1.05%, Mn 0.54%, Si 0.45%.

FIG. 182. Sand-cast, machined at low revolution speed and with dulled tool. Dragged material and ridges on the surface. Natural size, not etched—Cu 0.20%, Fe 0.94%, Mn 0.42%, Si 12.04%, Zn 0.25%.

FIG. 183. Forging, etched with 20% NaOH solution, washed with 50% HNO<sub>3</sub> and then re-etched with NaOH for a few seconds. Darker lines of copper segregations—X 3—Cu 4.48%, Fe 0.41%, Mg 0.36%, Mn 0.72%, Si 0.84%.



done, will give surfaces as good as any other method of preparation. By the use of sharp tools, a high revolution speed, slow feeding, and fine cut, almost anybody will be able to prepare a good surface. The most common defect produced by poor machining is shown in Fig. 181. When ridges like those shown are formed, the feeding speed and the thickness of the cut should be reduced. Eventually the tool may need resharpener. It is very poor practice to smooth down these ridges with a file or grinding paper, as some machinists do, since this practice tends to drag the metal and blur the structure.

Another defect produced by the use of dulled tools and too low revolution speed is shown in Fig. 182. The metal is dragged and deeply distorted so that even a protracted etching will not be able to eat away the distorted material, and the real structure will not be revealed. This defect can be corrected by higher rotation speeds and the use of sharper tools. In some cases carbide tools or diamonds may be useful. If they are not available, the surface can be improved by passing it over papers of decreasing grit size, as for the microscopic polishing. If the machining is done properly, the grain structure should be visible even before etching—sometimes very clearly; usually only faintly.

Some metallographers rather than use machining prepare the surface by grinding over papers of decreasing grit size, down to 3/0 or even 4/0. In most cases, however, there is no reason for this preparation. The surface may look better, but that will not have any effect after etching since the etching reagents will eat away the first layer of disturbed material. Besides, this method does not permit the preparation of large surfaces and requires an excessive time even if the grinding is limited to coarser papers. Under normal conditions a lathe or milling machine, if available, is preferable.

After the surface has been prepared, an accurate examination usually will reveal the presence of cracks and porosity. However, it is better to do the etching before drawing definite conclusions.

Several etching reagents are used. The most common are sodium hydroxide and hydrofluoric acid.

### **Sodium Hydroxide**

Solutions of NaOH in water, containing from 10 to 30 per cent NaOH, are commonly used, at temperatures ranging from 100° to 200°F (40° to 90°C). When the etching is done by immersion, the time ranges from 3 to 20 minutes, depending on the alloy, freshness of the solution, temperature of the bath, etc. When the etching is done by swabbing, as with pieces too big to be etched by immersion, the time

required increases. In alloys containing copper a dark coating is produced, more or less thick, the thickness depending on the amount of copper present in the alloy. Since the coating masks the structure, it must be removed. This is done by dissolving it with a solution of  $\text{HNO}_3$ , containing from 20 to 50 per cent acid. Of course, the specimen must be washed freely before and after this treatment.

In special cases it may be convenient, after the specimen has been etched and washed with  $\text{HNO}_3$  and water, to etch it again for a while (from a few seconds to a few minutes) and then wash it only with water. This second etching will reveal segregations of copper much better than the straight etching, for it will enhance the contrast. Figure 183 shows a section of a forging in which this method of etching reveals the presence of copper segregations, which remain in spite of the extrusion prior to forging and the forging itself. After this etching the specimen should be examined immediately, for on standing it tends to darken and loses its clearness.

### Hydrofluoric Acid

Another etching reagent commonly used is HF, diluted in water or alcohol. The water solutions are the most common and contain usually from 1 to 10 per cent acid. They are applied by swabbing rather than by immersion. The etching time ranges from 1 minute to 10 minutes.

Many modifications of this reagent have been proposed, most of which consist of the addition of HCl or  $\text{HNO}_3$  or both. Sometimes, as when pure aluminum is etched, they give better results than the straight HF solutions. They are applied by swabbing or by immersion, depending more than anything else on the size of the specimen, the laboratory facilities available, etc., since the method of application does not produce any difference on their effect. Listed below are some of the compositions suggested.

1. Flick's reagent (689)	3. HF conc.	5
HF conc.	$\text{HNO}_3$ conc.	10
HCl conc.	Water	85
Water	4. HF conc.	5
2. HF conc.	HCl conc.	20
HCl conc.	$\text{HNO}_3$ conc.	20
$\text{HNO}_3$ conc.	Water	55
Water		65

Several other compositions have been reported but they are similar to the ones above. There is no reason to list a few more, when their

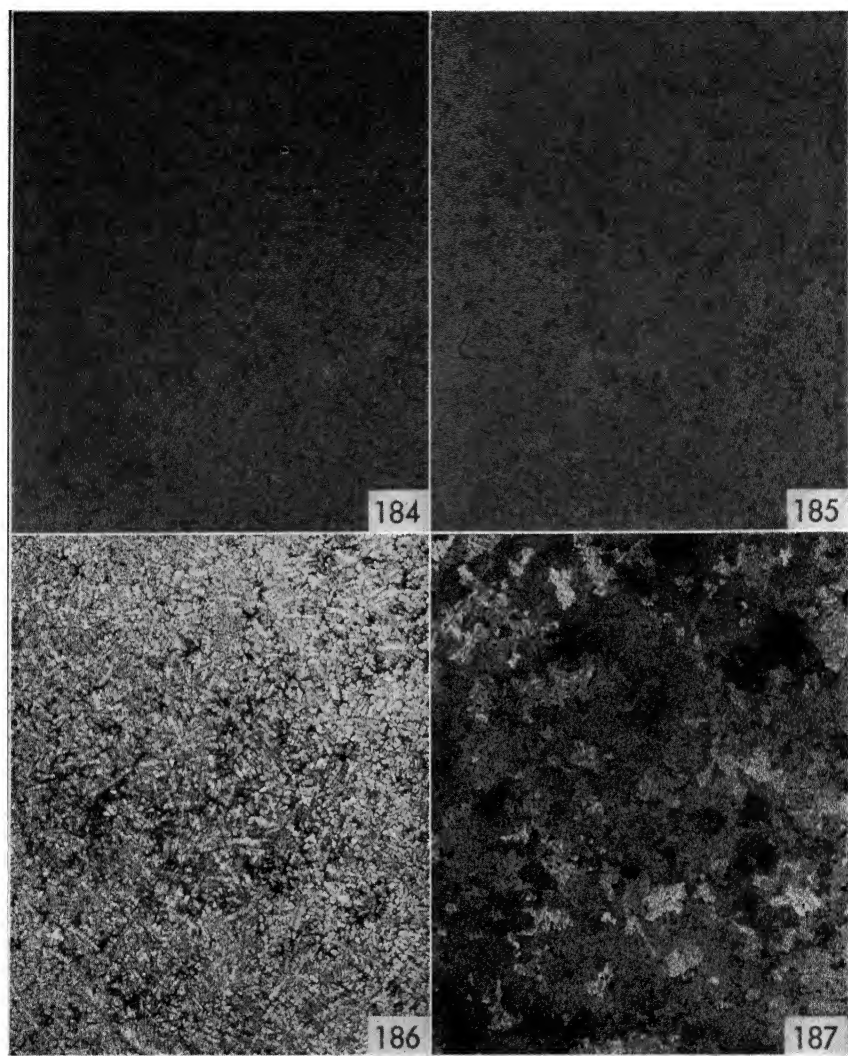


FIG. 184. Ingot, natural size, etched with 20% NaOH solution—Cu 2.24%, Fe 1.52%, Mg 0.76%, Ni 1.02%, Si 1.25%.

FIG. 185. Ingot, natural size, etched with 1% HF solution. Same material as in Fig. 184.

FIG. 186. Sand-cast, X 3, etched with 20% NaOH solution—Cu 0.12%, Fe 0.82%, Mn 0.24%, Si 12.10%. The etching has revealed perfectly the dendritic structure of the crystals but there is no contrast between the various grains. Dark spots due to porosity.

FIG. 187. Same specimen as in Fig. 186, X 3, etched with  $\text{CuCl}_2$ , then washed with 30%  $\text{HNO}_3$  solution. The grain size is clearly visible, slightly visible also the dendritic structure of the grains.

composition and effect are almost the same as that of the reagents listed.

Both NaOH and HF, with its modifications, act similarly in the majority of cases, and either can be used with no difference in the results. Figures 184 and 185 show two samples of the same alloy etched, respectively, with NaOH and HF. Although the grain size is slightly different, owing probably to different casting conditions, no difference can be detected on the effect of the etching reagent.

Some metallographers claim that HF will reveal more clearly segregations and microporosity. Others insist that pure aluminum cannot be etched with NaOH, but there is little ground for these claims. It seems doubtful, therefore, that the complications resulting from the use of HF, which attacks glass and most metals and must be handled in Bakelite, paraffin, or lead containers, are worth while.

### Copper Chloride Solutions

Aluminum-silicon alloys cannot be etched properly with any of the above reagents. A special reagent, proposed by Hume-Rothery (693), must be used. This consists of a 10 to 30 per cent solution of  $\text{CuCl}_2$  in water, sometimes containing a few drops of HF. The etching is done by immersion, and the black coating of copper which forms must be continuously removed by swabbing to allow an even attack over the whole surface. Figures 186 and 187 show an alloy of the aluminum-silicon type etched, respectively, with NaOH and  $\text{CuCl}_2$  solutions in order to show the effect of these reagents. As can be seen, the NaOH etch has revealed the dendritic structure inside the grains, but the grain boundaries only faintly; and has etched the various grains evenly so that there is no contrast. The  $\text{CuCl}_2$  solution instead has etched the different grains differently so that good contrast results.

The surface to be etched should be degreased before etching to avoid uneven attack. With NaOH solutions this cleaning is not necessary if proper care is taken to swab the surface at the beginning to insure that the solution comes in contact with all the surface. Uneven etching is one of the defects produced by defective technique, others are underetching and overetching. Underetching can easily be detected because the structure will hardly be visible; overetching is slightly more difficult to detect and requires some experience. Figures 188, 189, 190 show the same specimen, respectively, properly etched, somewhat overetched, and strongly overetched. In the properly etched sample the grain size is clearly visible notwithstanding a somewhat hurried preparation. In Fig. 189 the grain size is still visible, but the grain boundaries have been corroded and show as deep furrows.

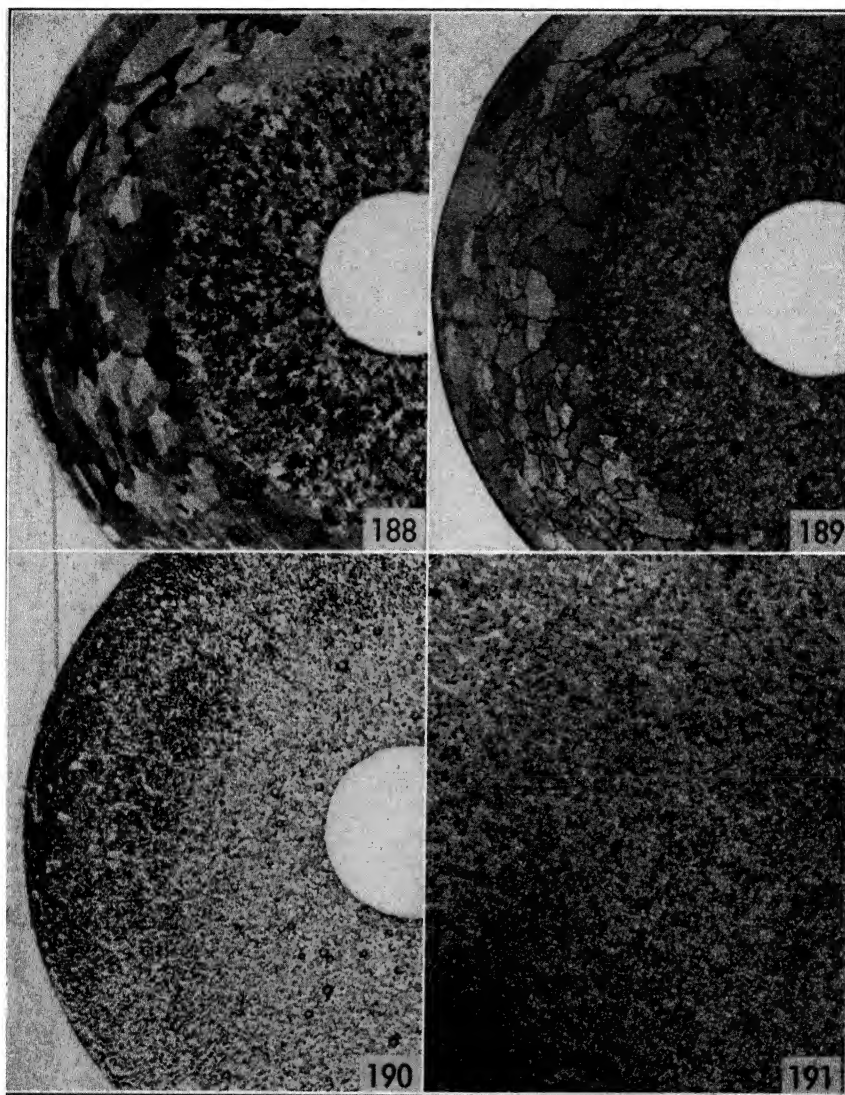


FIG. 188. Forging, X 3, etched with 20% NaOH solution. Proper etching, good contrast between the grains—Cu 4.48%, Fe 0.32%, Mg 0.38%, Mn 0.68%, Si 0.80%.

FIG. 189. Same specimen as in Fig. 188, overetched, X 3, etched with 20% NaOH solution. The grain boundaries are deeply etched, few etching pits appear.

FIG. 190. Same specimen as in Fig. 188, strongly overetched, X 3, etched with NaOH solution. The grain contrast has disappeared, few grain boundaries are still visible as deep grooves, few etching pits are present.

FIG. 191. Ingot, natural size, etched with 20% NaOH solution, overetched; the porosity (dark spots) is rounded and enlarged by the excessive etching, the grain contrast has disappeared—Cu 4.22%, Fe 0.45%, Si 0.84%, Zn 0.22%.

There are few etching pits visible. In Fig. 190 the surface is deeply corroded and there is no more contrast between the various grains.

Figure 191 shows another specimen cut from a porous ingot, over-etched. Here the general structure is not visible any more and the porosity holes, which normally have sharp borders, in this case are rounded and enlarged by the etching.

Macro-etching is commonly used to investigate the grain size of casts. For wrought products higher enlargements may be necessary because the grain size is much smaller. Sometimes, as in the sample shown in Fig. 192, macro-etching is useful also in the investigation of forgings. Improper forging technique has caused irregular recrystallization so that coarsely grained zones are intermixed with very finely grained zones.

Another use of macro-etching in connection with wrought products is the identification of the fiber direction or flow direction. The purpose is to determine if the movement of the metal takes place so as to produce grains elongated in the required direction. Figure 193 shows a forging where the direction of the fiber is not perfect, for it tends to go out at the bottom instead of flowing continuously from one end to the other. Figure 194 is another example of an extruded tubing, where the macro-etching, showing the fiber direction, reveals that the crack was already present before the last drawing, since the fiber around it is twisted. In all these illustrations it can be seen that the reagents act similarly and any one of them can be employed with no difference in the results.

Also in the investigation of porosity and cracks the various reagents act similarly. Figure 195 shows an ingot where hot-shortness cracks are clearly visible. Figure 196 shows another sample where porosity can hardly be detected although it is present, as it can be seen in Fig. 197, which shows the same specimen before etching. Figure 197, however, does not show all the porosity present in the specimen because the machining has masked it with dragged metal; special methods must be resorted to in order to show, in the photography, all the porosity existent in the specimen. Figure 198 shows the same specimen as in Figs. 196 and 197, after etching and successive treatment of the surface. This makes the grain contrast disappear so that the presence of black spots of porosity can be seen. Several methods can be used to obliterate the grain contrast: a fine grinding or a light machining can be used. Very good results however, as shown in Fig. 198, can be obtained by the use of an eraser.

Macro-etching is used for the detection of cracks. For this kind of work no preparation is necessary if the purpose of the examination is

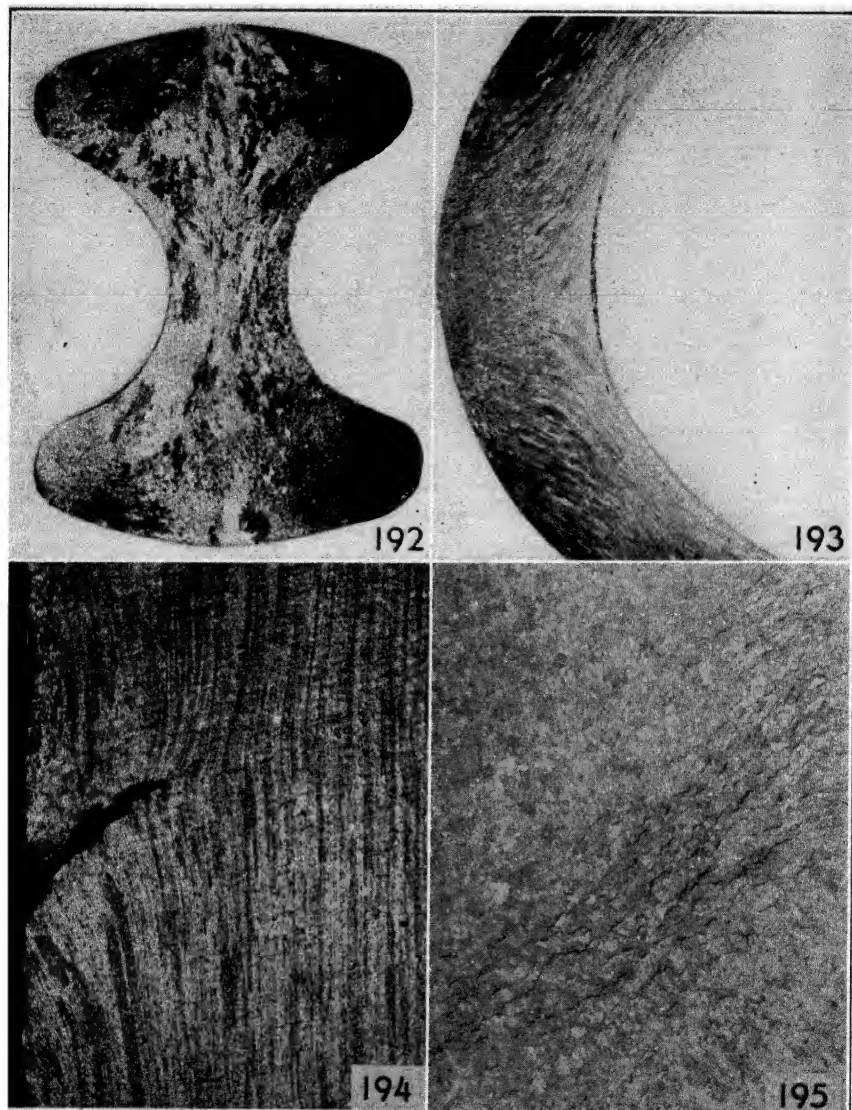


FIG. 192. Forging, X 3, etched with NaOH. Irregular crystallization caused by improper forging technique—Cu 4.20%, Fe 0.47%, Mg 0.54%, Mn 0.48%, Si 0.52%.

FIG. 193. Forging, natural size, etched with 1% HF solution, irregular flow of metal, causing the fiber to be cut at the bottom. Same alloy as in Fig. 192.

FIG. 194. Tubing, extruded and drawn, X 10, etched with acid mixture. The twisting of the fiber around the crack shows that the crack was present before the drawing—Cu 4.55%, Fe 0.41%, Mg 1.56%, Mn 0.57%, Si 0.22%.

FIG. 195. Ingot, X 2, etched with 20% NaOH solution. Hot-shortness cracks caused by uneven cooling(?)—Cu 4.27%, Fe 0.42%, Mg 1.65%, Mn 0.42%, Si 0.28%.



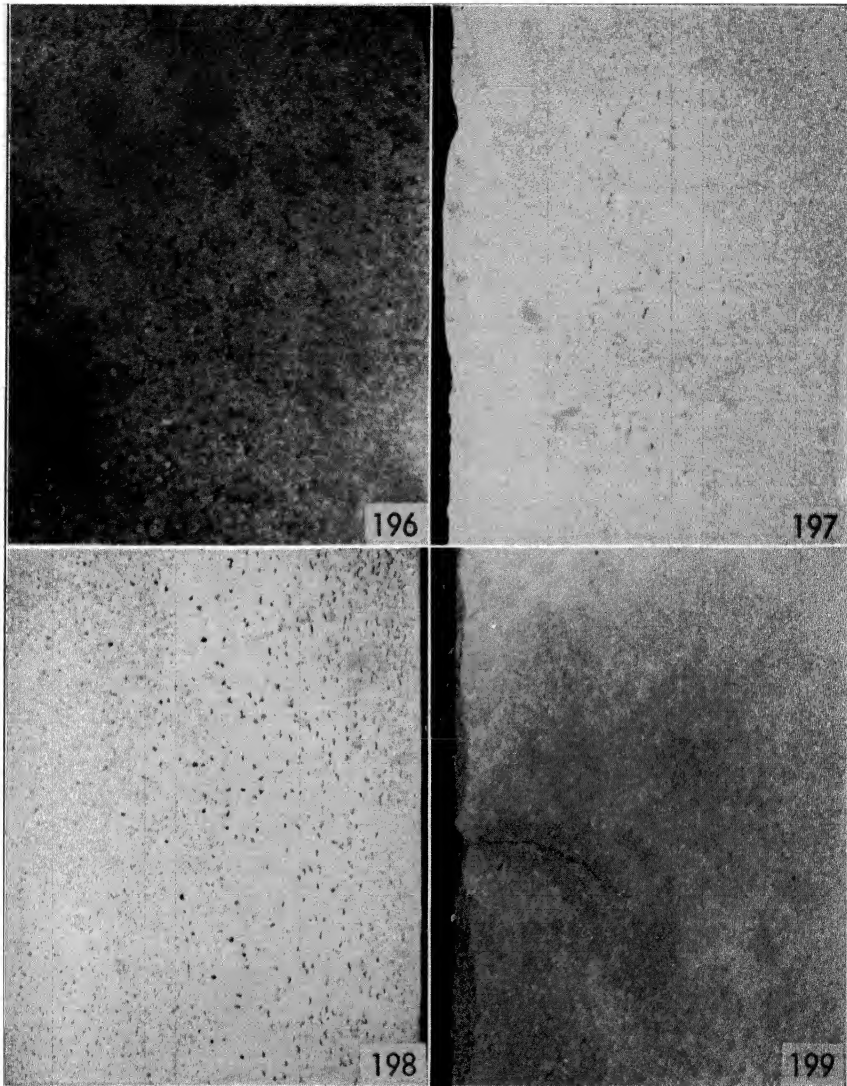


FIG. 196. Ingot, natural size, etched with 20% NaOH solution. The grain contrast caused by the etching masks the porosity present—Cu 4.22%, Fe 0.48%, Mg 0.54%, Mn 0.48%, Si 0.28%.

FIG. 197. Same specimen as in Fig. 196, natural size, not etched. Porosity slightly visible.

FIG. 198. Same specimen as in Fig. 196, natural size, etched with 20% NaOH solution and then cleaned with eraser. Porosity clearly visible.

FIG. 199. Water-cooled ingot, broken down, X 3, etched with 20% NaOH solution. Crack relieved by halo of seeped back water—Cu 4.38%, Fe 0.24%, Mg 1.52%, Mn 0.58%, Si 0.17%.



only the detection of the crack itself. If investigations of the causes are intended, the surface should be prepared carefully in order to study the path of the crack in relation to the structure of the surrounding material.

A common trouble in the examination of cracks is shown in Fig. 199. Although the specimen has been washed and dried carefully, some NaOH, entrapped in the crack, seeped back producing the darker halo around the crack. It is questionable, however, if this is a defect or an asset of the etching. It is true that photographs do not look well, but the halo has the advantage of showing unmistakably the presence of a crack and draws attention to it.

In fact, several methods of detection of cracks, flaws, etc., are based on this phenomenon. Among them is the bichromate etch, developed by Kraetsch and Schenk (692). This etch consists in dipping the piece to be examined in a 10 to 20 per cent solution of bichromate for a few minutes, then following with a rinse in running water to wash out the excess of bichromate. If there are flaws in the piece examined, after it has been standing some of the bichromate which penetrated into the flaws will seep back and underline the flaw with a yellow ring. A similar method, which uses a hot oil bath followed by sandblasting, is also useful in detecting superficial defects.

As can be seen from the examples above and from the few examples in Part IV, macro-etching is useful in a great variety of problems and should constitute the preliminary step in any investigation. Also as a means of control of production it can be used extensively, for in most cases the piece examined does not have to be destroyed but only to be washed very carefully.

## CHAPTER 5

### POLISHING

The preparation of samples for microscopic examination, commonly called polishing, includes three different groups of operations.

1. Choosing the specimen and preparing it for polishing.
2. Grinding to remove deep scratches.
3. Polishing proper, to produce a surface free from scratches and suitable for examination.

There is little to be said about choosing the sample; aluminum alloys do not differ from other alloys in this respect. A good macro-etching will be, in most cases, the best guide for the selection of the sample.

Whether the macro-etching is used or not in choosing the specimen for micro-examination, the most important factor in cutting a sample is to include the whole area to be examined and to obtain at the same time a specimen which is best fitted for the method of polishing to be used. Several methods of polishing are more or less in use; among them, the polishing by grinding on abrasive papers, followed by polishing with magnesia or alumina, is the most commonly used. Another method, which may be considered a short cut to the grinding method, is reported in some detail, since it is valuable for saving time in industrial work. Electrolytic polishing, although widely investigated with very promising results in the last few years, must still be considered in the experimental stage, and its use cannot be advised to routine metallurgists, who cannot afford to spend hours finding out by trial and error the best conditions for the polishing of a specimen.

#### Grinding Polishing

This is the most commonly used method for polishing metals and, as the reader is probably familiar with it, it will not be described in detail. Only the points in which the method for aluminum alloys differs from the general use will be mentioned.

The shape or size of the specimen to be polished is mostly a matter of personal taste: square, round, or rectangular specimens ranging from  $\frac{1}{4}$  to 1 inch are commonly used. The only precaution to observe is to keep the height of the specimen to a minimum because specimens

too high tend to rock. The edges and corners should be rounded to prevent catching in the papers or the cloths. The rounding, however, should not be too liberal because specimens with a wide radius tend to rock, making the polished surface convex rather than plane. When the specimen is small or irregular in shape so that it is difficult to hold firmly, it should be mounted.

A good mounting should have the following qualities.

The same hardness as the material mounted.

The same electrolytic potential as the material mounted, or else be electrolytically inert.

Ease of handling and should fill well around the specimen.

No requirement of high temperature or pressure for mounting.

Several methods of mounting are in use, the most common being:

Mounting in low-melting alloys.

Mounting in sulfur.

Mounting in Bakelite or other plastics.

Pack mounting.

None of these methods is perfect and each is defective in one or more respects.

Low-melting alloys are rather soft and they are less electro-negative than aluminum alloys, so that in etching and even in polishing, the specimen corrodes preferentially.

Sulfur is rather pasty and does not fill well, especially around intricate shapes; air tends to remain entrapped in the form of holes, which become filled with grinding material and make polishing free from scratches almost impossible. Besides, sulfur is softer than most aluminum alloys and, on grinding, it is abraded faster than the metal and the edges of the sample become rounded.

Bakelite is one of the best mountings, for it is electrically inert, fills well around any shape, and its hardness is almost the same as that of aluminum alloys. The only drawbacks are the high pressure and temperature required, but they are not so important since only in special cases, such as blisters or very brittle alloys, do they have any effect on the sample.

The other plastics, transparent or light colored, are slightly inferior to Bakelite because they have some tendency to crack.

Pack-mounting is the best method for the examination of sheet materials, or of the edges of specimens. It consists in bolting several pieces of sheet together. The practice of inserting soft material, usually pure copper, between sheets when pack-mounting should be

avoided because the presence of heterogeneous material tends to establish electro-corrosion, and the alloys will be corroded in preference to the copper. Besides, the softer material tends to abrade faster and the edges tend to become rounded.

For this reason, when examining clad material, dummy sheets of bare material should be inserted so that the width of the soft surface is reduced to a minimum. Pack-mounted samples are difficult to prepare properly, because, even when bolts are tightly screwed, the various sheets may slip, one on the other, and spoil the sample. For really accurate work, when the samples must be handled many times, the best method is to mount the whole pack in Bakelite so that any movement between the various pieces will be impeded.

Another drawback of pack-mounting is the fact that, when one is polishing or etching, water or etching reagents tend to seep between the various pieces and will seep back at the most inopportune moments. To avoid this, the whole specimen, heated to insure penetration, can be immersed in a bath of molten paraffin so that all cavities will be filled with it.

When the sample has been cut and finally mounted, the surface must be prepared for examination. A good way to prepare a flat surface, especially in soft alloys, is the use of a microtome. If this instrument is not available, a lathe can be used successfully in most cases if proper care is taken to center the tool. The use of a file or a grinding wheel, followed by grinding on a belt grinder will give good results if the filing is limited to the minimum necessary and the grinding on the belt is protracted until the whole specimen has a flat surface. When files or grinding wheels are used, they should be smeared with chalk, which helps to keep small particles from becoming embedded in the tool, and prevents deep scratches in the specimen.

When a flat surface, free of heavy scratches, has been obtained, the specimen is ready for fine grinding. Fine grinding is done by the use of papers of decreasing grit size. The grinding can be done by hand, holding the paper on a flat surface (a heavy glass plate or a mirror is particularly suitable) and by moving the sample; or the paper can be clamped or pasted in a rotating disc and the sample held against it. When the grinding is done on rotating discs, the speed of the discs should not exceed 400 to 500 rpm; otherwise too much dragging of the metal will result.

There are polishing machines on the market which permit the grinding of 3-5-7 specimens at the same time, but, even for laboratories which have a large number of samples to polish, these machines are not very efficient, for no appreciable saving in time can be accomplished.

Unless the alloy is very hard (200 Brinell or above), which rarely happens with aluminum alloys, some lubrication is required between the specimen and the paper. For hand grinding the use of a little wax dissolved in kerosene is preferred; for machine or automatic polishing, alcohol or acetone can replace the wax. If wax is used before one passes the specimen from one paper to the next, it is necessary to wash the specimen carefully in kerosene or alcohol, to clean every trace of wax from it, because the wax may contain some of the grit of the last paper. If alcohol or acetone is used on grinding, washing in water is sufficient for this purpose.

The grinding on each paper must be continued until all the scratches from the preceding one are gone. The best way to check this is to pass the specimen in the same direction on each paper, so as to have all the scratches parallel and to rotate the specimen  $90^\circ$  when changing to the next paper. With very soft material, like pure aluminum, it may be necessary to pass the specimen twice on the same paper. The first passage is intended to remove the scratches from the preceding paper; the second passage should remove the scratches from the first passage. This is necessary because the longer the specimen is passed on a paper, the deeper the scratches produced by it are likely to be. The second passage, with the specimen turned at  $90^\circ$  on the same paper, will produce scratches that are not so deep as the first.

The papers commonly used are five, ranging from 1 to 4/0. Many metallurgists prefer to omit the last as the abrasive, although fine is usually not uniform. If the grinding is done on a rotating disc, only three papers need to be used, the 1 or 0, followed by 2/0 and then 3/0, after which the sample is ready for polishing proper.

The real polishing usually is done in two steps—rough polishing and final polishing. The rough polishing is done on a cloth clamped in a rotating disc and wetted continuously with a suspension of abrasive in water. Several types of abrasives and cloths are used. Commonly broadcloth and Alundum 600 X are used with success. The speed of the rotating disc should be between 200 and 400 rpm. The amount of grinding material required is somewhat elastic. A suspension of 3 to 5 per cent in volume of Alundum gives good results.

Some pressure should be applied to the specimen to avoid too much relief of the hard constituents. On the other hand, too much pressure tends to drag the metal and produces heavy scratches which require long polishing afterward. The best pressure varies from alloy to alloy, and no definite rule can be given.

The disc on which the cloth is clamped is important. If the material is less electro-negative than the alloy to be polished, electro-corrosion

sets in and the specimen is badly attacked. For this reason discs of iron, copper, or nickel alloys should not be used. The discs for polishing aluminum alloys should be cast or machined out of aluminum alloys. Alloys containing 2 to 10 per cent magnesium are the best, as they are the most electro-negative of aluminum alloys. Good, too, are alloys containing manganese or magnesium silicide. From the standpoint of corrosion, pure aluminum is also good, but it is too soft and does not stand the inevitable bumps in handling.

If it is necessary to use discs of other metals, corrosion can be avoided to a certain extent by coating the disc with an insulating material so that there is no electrical contact between the disc and the specimen. Cellulose paints can be used for this purpose. However, it is very difficult to keep a film of paint absolutely continuous so as to avoid any contact whatever.

Rough polishing can be controlled by observation with the microscope. If the specimen is well polished, it should be possible to distinguish the structure of the alloy and, to a certain extent at least, the constituents. If the specimen is in this state, it is time to pass it to the final polishing disc, having previously carefully washed it to get rid of any particles of Alundum.

The speed of the final polishing disc should be about 200 rpm. With harder alloys, somewhat higher speeds can be used, but the best results are obtained with low speeds. For the material of the final polishing disc, the same precautions reported for the rough polishing disc apply. They are even more important because the time for final polishing is much longer and there will be no further polishing to correct a corrosive attack. As in rough polishing, several types of cloths are used. Kitten's-ear broadcloth or chamois skin are the most used and are probably the best; sometimes silk is used successfully.

Two polishing materials are commonly used: alumina and heavy magnesia. Either of them can give good results in skilled hands. Magnesia, however, yields much better results, especially with soft alloys. The alumina commonly used is the No. 3, which is the alumina for softer alloys. It is suspended in distilled water and is sprayed from a wash bottle toward the center of the disc during polishing so as to keep a constant stream of fresh alumina under the specimen. The amount of alumina to be used depends on several factors. Usually about 200 cc of the suspended solution should be sufficient to polish a sample.

Toward the end of the polishing, distilled water is substituted for the alumina, and the sample is passed for a few minutes more over the cloth.

With the use of alumina, the matrix of pure aluminum, which constitutes the mass of most alloys, tends to be rough and dragged. When really good samples are desired, magnesia should be used.

Figure 200 shows a sample polished with alumina, where the aluminum is dragged and shows small scratches.

The method of applying magnesia differs from that of applying alumina. Instead of suspending it in distilled water and spraying the

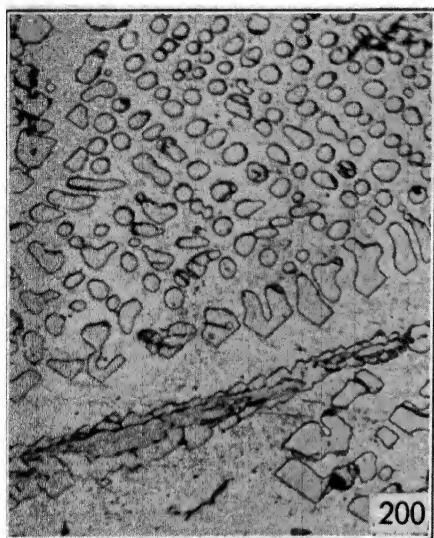


FIG. 200. Specimen polished with alumina. The Al matrix is rough and scratched.  $\text{MnAl}_6$  and  $\text{MnAl}_4$  are the constituents visible—Mn 8.40%, Fe 0.32%, Si 0.41%. Ingot, X 250, not etched.

mixture on the cloth, about a teaspoon of magnesia is smeared on the moistened cloth and distributed with a finger all over the surface to be used. Some more water is then added to facilitate the flow, and the disc is set in motion, the sample on it being kept without excessive pressure. The pressure used here is much less than in rough polishing; and, as in rough polishing, no definite rule can be given. The best amount of water, of magnesia, and of pressure must be found by trial and error.

When it is necessary to add some magnesia in the course of the polishing, a salt shaker can be used. By this means it is possible to distribute the magnesia on the surface of the cloth without stopping the polishing; water can be added with a wash bottle, and the moistness

of the cloth regulated so as to keep the best polishing conditions. The fact that this can be done without stopping is very helpful, because, with a little experience, it is possible to tell how the polishing is progressing from the feel of the pressure necessary to hold the specimen in place.

Too little pressure and too little water tend to drag the softer constituents and flatten the harder; too much water has the contrary effect and tends to corrode  $\text{Mg}_2\text{Si}$  and the  $\text{AlCuMg}$  constituents and to make  $\text{CuAl}_2$  reddish brown. Too long a period of polishing tends to round the softer constituents and to increase the relief of the harder too much. The polishing should be stopped as soon as no more scratches are visible. Sometimes there are heavy scratches in the

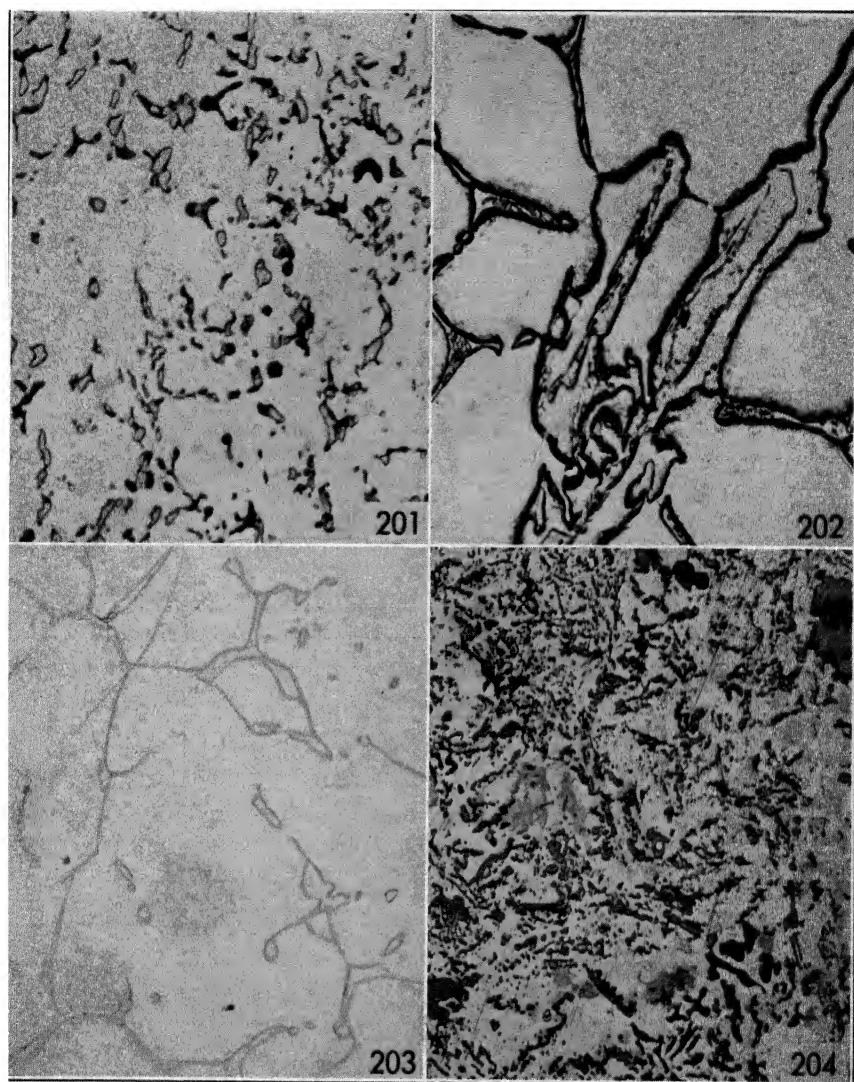


FIG. 201. Mg<sub>2</sub>Si black, AlCuFeNi light, both rounded by too much polishing—Cu 2.25%, Fe 1.25%, Mg 2.04%, Ni 1.02%, Si 1.23%. Cast in permanent mold, X 250, not etched.

FIG. 202. CuAl<sub>2</sub> and MnAl<sub>4</sub> (surrounded by AlCuMn) relieved and darkened by too much water in polishing—Cu 7.61%, Mn 3.97%. Sand-cast, X 250, not etched.

FIG. 203. Polished with too much pressure, the constituents are hardly visible—Cu 4.50%, Fe 0.55%, Mg 1.54%, Mn 0.66%, Si 0.24%. Ingot water-cooled, X 250, not etched.

FIG. 204. Specimen insufficiently polished. Si primary and eutectic gray, Mg<sub>2</sub>Si black, AlCuFeNi light—Cu 0.82%, Fe 0.51%, Mg 0.83%, Ni 2.26%, Si 13.96%. Cast in permanent mold, X 250, not etched.



sample, which would require long polishing to remove. If they affect the spot which is to be observed, the specimen should be brought back to the rough polishing. Otherwise, when the polishing of the rest of the sample is complete, they should be neglected.

Figure 201 shows a sample where too much polishing has rounded the constituents and corroded the  $Mg_2Si$  to a point where it has lost its typical form. Figure 202 shows a specimen where the use of too much water has relieved the constituents and darkened the  $CuAl_2$ . Figure 203 shows a sample where the use of too much pressure has flattened the constituents to a point where they are hardly visible. Figure 204 shows a specimen where the polishing was not protracted enough to remove the dragged material from the preceding rough polishing.

The use of magnesia requires several precautions, caused by its tendency to change to carbonate in the presence of the  $CO_2$  contained in the air and in the water. These precautions are:

Every evening the cloth should be taken off the disc and washed carefully, to get rid of all the magnesia imbedded in it, and then soaked overnight in distilled water, to which have been added a few drops of concentrated  $HCl$ . In the morning, before starting polishing, rinse the cloth thoroughly in order to wash out every trace of  $HCl$ , which otherwise would attack the specimens.

Only distilled or freshly boiled water should be used with magnesia. Once in a while (about every two weeks if the magnesia is kept in an open bottle, less often if kept in an airtight bottle), the magnesia should be calcined at about  $1650^{\circ}F$  ( $900^{\circ}C$ ), in order to decompose the carbonate formed. Then it should be passed through a sieve (120 X is about the right size), and the part that does not pass through should be ground and calcined again.

After one has been using magnesia for some time, it is possible to tell when it needs to be calcined. During polishing or even when smearing the magnesia on the cloth, hard particles can be felt.

With these precautions and a little care it should be possible for everyone to get fair results in most cases. The metallographer who is learning to polish aluminum alloys should not be discouraged by failures, for they are common, and even experienced metallographers occasionally have to repeat some polishings again and again.

### **Buffing Polishing**

Another method of polishing, which does not give as good results as the one reported above, but which has many advantages in regard

to speed, is polishing by means of a buffing wheel. This polishing has these advantages: it is very fast, gives good results even with soft alloys, requires very little training before good results can be obtained, and permits the examination of bigger samples, as even samples 2 to 3 square inches can be polished easily. On the other hand, the surface obtained is not perfect, and the sample will always contain deep scratches. It is almost impossible to keep the sample plane, and a deep layer of distorted material masks the constituents somewhat. Figures 205 and 206 show the same alloy polished by the usual method and by the buffing wheel. Figures 207 and 208 show samples tested in a corrosive solution, where the buffing polishing reveals the presence and absence of intergranular corrosion perfectly.

As the above examples show, this method cannot be used in every case. It has its limitations, but in many cases where only a superficial examination is required, the method is satisfactory. Polishing by this method can be improved by passing the specimen (very carefully washed beforehand) on a magnesia wheel. The results, then, may be compared to those obtained by the conventional method. Many of the photo-micrographs in this book are of specimens polished by buffing with subsequent magnesia polishing.

Etching, too, will improve the surface aspect, especially etching with HF and NaOH, which tend to dissolve the disturbed layer. Figures 209 and 210 show two alloys where the etching has improved the polishing so that the scratched layer is hardly visible.

This method is very simple: the specimen, where a plane for polishing has been prepared with a file, a grinding wheel, or better still a lathe, is held against a buffing wheel, deeply coated with paste. The speed of the wheel is not critical. Speeds from 2000 to 3000 rpm with the use of discs 6 to 10 inches in diameter give good results. Several types of buffing pastes are in the market. Pastes containing alumina as a grinding agent are the best; if successive polishing with magnesia is used, also pastes containing Alundum can be used. The paste should be soft and have a low melting point in order to act as a lubricant and avoid excessive dragging of the surface. Discs of unbleached muslin, completely stitched, are the best but require some breaking in. This breaking in can be speeded up by cutting the stitching for about one-fourth of an inch from the edge; after three or four specimens have been polished, the disc is ready for use. The surface to be polished does not need to be very smooth. Even surfaces with scratches 1/100 inch deep can be polished successfully. The specimen should be held with pliers or tongs, for high pressure against the wheel is necessary and the sample becomes so hot that it cannot be held with bare hands.

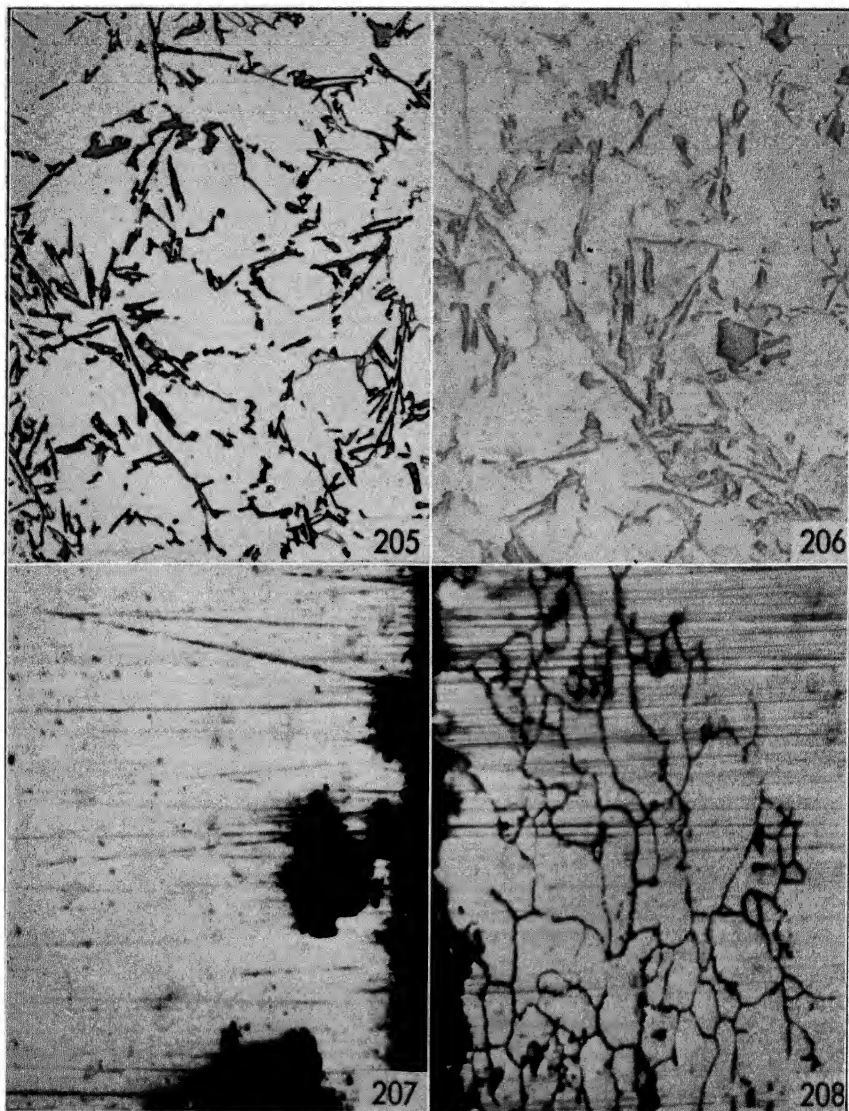


FIG. 205. Polished with magnesia, Si gray, AlCoFe light—Si 8.80%, Mg 0.46%, Co 0.44%, Fe 0.45%. Cast in permanent mold, X 250, not etched.

FIG. 206. Same specimen as in Fig. 205, polished by buffing.

FIG. 207. Specimen polished by buffing, which reveals clearly pitting corrosion—Cu 4.57%, Fe 0.35%, Mg 1.27%, Mn 0.56%, Si 0.24%. Sheet heat-treated, tested in corrosive solution, X 250, not etched.

FIG. 208. Specimen polished by buffing, which reveals the presence of intergranular corrosion. Same alloy as in Fig. 207 heat-treated and tested as the above specimen, X 250, not etched.

When a smooth surface has been obtained, the pressure must be greatly reduced, until the surface becomes highly brilliant and mirror-like. At this stage the specimen is ready for washing before microscopic examination. Wash carefully, especially if the specimen is intended for further polishing. The polishing paste is greasy and must be dissolved. Alcohol, acetone, or carbon tetrachloride can be used for washing; even gasoline, or any liquid that will dissolve grease, can be

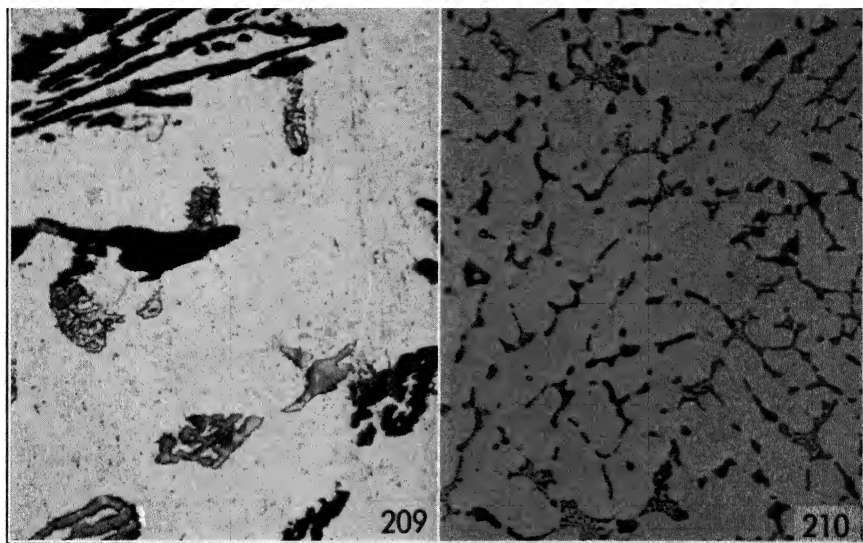


FIG. 209. Polished by buffing and etched with HF. Dark AlCuFeNi, light Si—Si 4.91%, Cu 0.25%, Fe 0.72%, Ni 0.56%. Sand-cast, X 250.

FIG. 210. Polished by buffing, etched with  $\text{Fe}(\text{NO}_3)_3$  and  $\text{H}_2\text{SO}_4$ . Both  $\alpha(\text{AlFeSi})$  and  $\text{CuAl}_2$  blackened—Cu 10.10%, Fe 1.25%, Mg 0.33%, Si 0.62%. Cast in permanent mold, X 250.

used. The polished surface should be gently swabbed with cotton that has been immersed in the detergent liquid. The cotton should be moved in the same direction as the polishing in order not to produce cross scratching when washing.

If the sample has been prepared with a file or a grinding wheel, the polishing should be done perpendicularly to the direction of the scratches in order to check when they have disappeared, as in normal polishing. The polishing should always be in the same direction until these scratches have completely disappeared.

When the sample is ready for light-pressure polishing, it may sometimes be convenient to turn it at  $90^\circ$  and polish it again with high pressure in the cross direction so as to take off the scratches from the

preceding polishing. This practice is especially recommended when the preparation of the sample has been rather rough and long polishing is necessary to make the specimen smooth.

If the sample is not completely sound in that pinhole porosity is present, grease and thread from the polishing wheel tend to remain in the holes, causing a drift of grease that tends to smear the surface. In this event, it may be expedient to keep turning the sample during polishing so as to avoid formation of drifts or *comet tails*. The same inconvenience is experienced sometimes when the surface to be polished is very rough and contains scratches of varying depths. Then, obviously, a better preparation of the surface or a prolonged polishing will overcome the difficulty.

When examined under the microscope, specimens should be turned around the beam of light until the direction on which the scratches are least visible is found.

### Electrolytic Polishing

A sample for electrolytic polishing is prepared, until the grinding is finished, in the same way as a sample for ordinary polishing. At this stage the sample, already ground and ready for the rough polishing, is made the positive pole of an electrolytic cell containing a special solution, and current is passed through it; in about 15 minutes the specimen should be ready for examination even with very high magnifications.

The most detailed description of the technique has been published by Jacquet (706). The solution recommended is as follows.

785 cc Acetic anhydride  
215 cc Perchloric acid density 1.48

This solution should be prepared by pouring the acetic anhydride into the perchloric acid, under continuous cooling because of the danger of explosion involved. For the same reason no organic matter should ever be immersed in this solution; therefore, samples mounted in Bakelite or other plastics cannot be electrolyzed. The sample is immersed vertically in the solution, about  $\frac{1}{2}$  to 1 inch from the cathode, which should be made of a plate of aluminum. The cell should be water cooled. A direct current of 50 to 100 volts should be passed through for about 15 minutes. The temperature of the solution should be kept below 120°F (50°C); the amperage should be 0.2 to 0.3 ampere per square inch for pure aluminum. For alloys a lower amperage should be used.

More recently, Keller (710) suggested the use of fluoboric acid to replace the acetic anhydride-perchloric acid solution. Excellent micrographs accompany Keller's paper. Unfortunately, no concentrations, amperages, etc., are reported. Several other papers (see Bibliography) have been published on this matter, some of them reporting original work, but no further details are available.

The author has experimented upon both solutions for either pure aluminum or for aluminum alloys. Although mostly unsuccessful, these experiments showed that the temperature of the bath, the voltage, the current density, the time, the distance between electrodes, the size and flatness of both electrodes must be closely controlled if duplication of results is to be obtained. The nature and state of the alloy are also major factors; variations in the composition, the casting technique, and especially the heat treatment change the optimum conditions.

At the present stage this method does not seem practical for commercial work unless some way of determining the specific conditions for the polishing of each alloy can be worked out.

## CHAPTER 6

### ETCHING

Many etching reagents have been used for aluminum alloys. Unfortunately, data about their effect on the several constituents are scanty and unreliable, for most of the metallographers have completely ignored the ternary and quaternary phases and have limited their observations to the binary constituents, and have often reported as  $\text{FeAl}_3$  or  $\text{CuAl}_2$  ternary constituents, which have a form similar to that of the binaries.

Almost the only exception is in the work by Keller and Wilcox (685), which, although now somewhat outdated, is still widely used and copied.

In the following pages the etching reagents used for aluminum alloys will be described, with details as full as possible about their use.

Two types of etching reagents can be distinguished.

Those which do not etch the aluminum matrix at all, but etch only some of the constituents, and whose use is limited to the identification of constituents.

Those which, besides etching some constituents, produce a differential discoloration on differently oriented crystals, permitting the identification of the crystals themselves.

Below is a short description of each reagent, including the concentration, time, temperature, and method of use.

#### **Nitric Acid**

Water solutions containing 1 to 25 per cent  $\text{HNO}_3$  have been used. The one most often recommended for general work is the 25 per cent solution, whose reactions with the constituents in aluminum alloys are tabulated in Chapter 7. Etching with this solution is done by immersion for 40 seconds in the solution, heated to  $160^\circ\text{F}$  ( $70^\circ\text{C}$ ), followed by rinsing in cold running water. Weaker solutions require a longer time for etching and, when cold, give somewhat different results, but their reactions with the constituents in aluminum alloys have not been thoroughly investigated. Solutions in alcohol, containing 1 to 10 per cent  $\text{HNO}_3$ , with an etching time of 1 to 5 minutes, have

been suggested (712), but they do not seem to offer any advantage over water solutions.

### Ferric Nitrate

Solutions of ferric nitrate, in either water or alcohol, sometimes with the addition of a few drops of hydrofluoric acid, can be used advantageously for the etching of aluminum alloys. The best of these solutions is the 25 per cent solution in water, used by swabbing for 30 to 40 seconds, followed by rinsing in water. Its reactions with the aluminum constituents are tabulated in Chapter 7. As for nitric acid, alcoholic solutions are sometimes suggested (720), but there seems to be no reason to prefer them to water solutions.

Ferric nitrate is a useful reagent for checking the results of solution treatments. Only some hardening constituents, namely,  $\text{CuAl}_2$ ,  $\text{Mg}_2\text{Si}$ ,  $\text{Cu}_2\text{Mg}_2\text{Al}_5$ , are etched by it, so that it is possible to detect how effective the solution treatment has been by the amount of blackened constituents seen. Sometimes, if the sample is slightly greasy or the swabbing too delicate, the etching is not complete and the hardening constituents are only outlined by a black border (Fig. 211).



FIG. 211.  $\text{CuAl}_2$  etched only at the borders, needles of  $\text{AlCuFeSi-Cu}$  7.12%, Fe 0.63%, Si 0.76%. Sand-cast, X 1000, etched with  $\text{Fe}(\text{NO}_3)_3$ .

### Ferrous Sulfate

Ferrous sulfate in water solutions containing 5 to 10 per cent of the salt has been suggested (713) as a good etchant for aluminum alloys. The etching time ranges from 40 seconds to 3 minutes, depending on the concentration of the solution. Little information is available on its reactions with the constituents in aluminum alloys. However, it seems to act in a manner similar to ferric nitrate.

### Sulfuric Acid

The most common is the 20 per cent solution, used by immersion. The etching temperature is  $160^\circ\text{F}$  ( $70^\circ\text{C}$ ); the etching time, 30 sec-



onds. Its reactions with the aluminum constituents are tabulated in Chapter 7. This reagent is particularly useful for the identification of the iron constituents because  $\text{FeAl}_3$ ,  $\text{Fe}_2\text{Al}_7$ ,  $\alpha(\text{AlFeSi})$ ,  $\alpha(\text{AlFeMnSi})$ ,  $\text{AlCuFeMn}$ , and  $\text{AlCuFeSi}$  are etched by it. Different concentrations and different times have also been used, but no important differences are noted.

### Picric Acid

This reagent is very seldom used for aluminum alloys. The 4 per cent water solution is sometimes mentioned (715). The etching time ranges from 10 to 20 minutes. Very little is known about its reactions with the aluminum constituents.

### Chromic Acid

Chromic acid solutions, containing from 5 to 20 per cent acid, sometimes have been used for alloys containing magnesium (711). The etching time ranges from 5 to 20 seconds, depending upon the concentration.

### Ferrocyanide Solutions

Ferrocyanide solutions can be used for the detection of constituents containing iron due to the formation of iron ferrocyanides which are colored deep blue (16). One of the best solutions contains:

$\text{HNO}_3$ conc.	10 drops
$\text{HF}$ 28%	10 drops
$\text{K}_4\text{Fe}(\text{CN})_6$ 10% solution	10 drops
$\text{H}_2\text{O}_2$ 30% solution	5 cc
$\text{H}_2\text{O}$	100 cc

This solution must be mixed immediately before it is used, directly from stock solutions. The etching time is 20 seconds to 1 minute, and all the constituents containing iron are colored from light to deep blue, depending on the amount of iron.

### Phosphoric Acid

Phosphoric acid solutions ranging from 5 to 10 per cent are used sometimes for alloys containing magnesium because phosphoric acid gives a good even etching on  $\text{Mg}_5\text{Al}_8$  (724). The etching time ranges from 10 to 30 seconds.

### Ammonium Persulfate

Water solutions containing approximately 2 per cent ammonium persulfate are sometimes used for etching aluminum alloys (711). The etching time is 1 to 2 minutes, by immersion. Very little is known about the reactions of the constituents of the aluminum alloys with this reagent.

### Sodium Hydroxide

Sodium hydroxide is one of the reagents most often used for etching aluminum, and a great variety of concentrations and etching temperatures is suggested. The concentrations commonly used for identifying constituents are the 1 and 10 per cent: the 1 per cent cold, with an etching time of 10 seconds by swabbing (685); the 10 per cent at 160°F (70°C), with an etching time of 5 seconds by immersion. The 1 per cent solution is rather weak and does not give very even results; the 10 per cent solution is much better. Its reactions with the aluminum constituents are tabulated in Chapter 7.

For grain size the 10 and 20 per cent solutions, boiling, give very good results, especially if followed by rinsing with nitric acid. The etching time varies with the alloy, ranging usually from 5 to 20 seconds. Several additions to the sodium hydroxide have been proposed, among them a water solution containing:

NaOH	2 grams
Na <sub>2</sub> CO <sub>3</sub>	4 grams
H <sub>2</sub> O	94 cc

Its use by immersion at room temperature for 60 seconds is suggested for pure aluminum. For wrought alloys of the aluminum-manganese type the addition of 0.5 per cent sodium silicate to the 10 per cent sodium hydroxide solution, to be used boiling, is recommended. Recently Keller and Bossert (730) suggested a solution containing:

NaOH	1 gram
Na <sub>2</sub> CO <sub>3</sub>	1 gram

Solution containing:

0.5% ZnCl <sub>2</sub> and 0.5% SnCl <sub>2</sub>	4 cc
H <sub>2</sub> O	94 cc

This solution has been shown to give very good results in determining the grain size, even in annealed or cold-worked duralumin. The etching is done by immersion, for 3 to 5 minutes, followed by a quick rinse in water, then in nitric acid and then in water again. This reagent

cannot be kept but must be prepared at the moment of use. A stock solution, containing 0.5 per cent of zinc chloride, 0.5 per cent of stannous chloride, with some metallic tin at the bottom, can be used advantageously.

### Hydrofluoric Acid

Water solutions, containing from 0.5 to 3 per cent hydrofluoric acid, are commonly used. The weaker solutions sometimes are used during polishing to dissolve the disturbed layer, then the sample is further polished. For the identification of constituents the 0.5 per cent solution is most often used. The etching time is 15 seconds by swabbing, at room temperature; its reactions with the aluminum constituents are tabulated in Chapter 7.

For grain identification the solution containing 1 per cent hydrofluoric acid is preferred; it is used by swabbing for 30 seconds to 2 minutes. However, much better results are obtained with solutions which also contain hydrochloric acid and nitric acid.

Several additions have been proposed to these etching reagents, among them the best-known compositions are:

A.	HF	10%
	HCl	15%
	H <sub>2</sub> O	75%

This is used by immersion, 20 to 30 seconds, followed by nitric acid rinse. It was suggested by Flick (716).

B.	HF	20%
	HNO <sub>3</sub>	20%
	Glycerin	60%

This is used by heating the specimen in boiling water and immersing it without drying in the reagent for a few seconds. It was suggested by Vilella (717).

C.	HF 30%	10 drops
	HNO <sub>3</sub> conc.	10 drops
	H <sub>2</sub> O	100 cc

This is used by swabbing or immersion for from 15 to 40 seconds. It was suggested by Panseri (16).

D.	HF	1 %
	HNO <sub>3</sub>	2.5%
	HCl	1.5%
	H <sub>2</sub> O	95%

This is used by swabbing or immersion for 10 to 30 seconds. It was suggested by Dix and Keller (719). This reagent, commonly known as acid mixture, is one of the best for grain-size identification in micro-examinations. It is also used for the identification of constituents, and its reactions with the aluminum constituents are shown in Chapter 7. A modification of this reagent, proposed by Keller (723), contains:

Sodium fluoride	0.5 gram
HNO <sub>3</sub> conc.	1 cc
HCl	2 cc
Water	97 cc

Its use in conjunction with a nitric acid etch is suggested for the detection of precipitate in age hardening. For this purpose the recommended practice is as follows: immerse the specimen in a 25 per cent nitric acid solution at 160°F (70°C) for 1 minute; wash in running water and immerse for about 1 minute in the above solution; wash in running water and dry.

It is not possible to say which of the reagents listed above is the best in any given case; the choice of reagent will be determined by the problem at hand. For the identification of constituents the best way to proceed is to examine the specimen before etching and, on the basis of the composition and of the form of the constituents, make a tentative list of the constituents which are probably present. With this list in mind the etching is greatly facilitated and with a little experience it is possible to limit the probable constituents to only a few, and generally a single etching will reveal the structure completely.

Figure 212 shows an alloy where the examination prior to etching revealed the presence of Cu<sub>2</sub>Mg<sub>2</sub>Al<sub>5</sub>, CuAl<sub>2</sub>, Mg<sub>2</sub>Si, and another constituent which, on the basis of the composition, was identified as  $\alpha$ (AlFeSi) or as  $\omega$ (AlCuFe). An etching of sulfuric acid (Fig. 213) revealed the presence of  $\alpha$ (AlFeSi) and confirmed the identification of CuAl<sub>2</sub> and Cu<sub>2</sub>Mg<sub>2</sub>Al<sub>5</sub>. Figure 214 shows a duralumin. The examination without etching revealed the presence of Mg<sub>2</sub>Si, Cu<sub>2</sub>Mg<sub>2</sub>Al<sub>5</sub> and of one or perhaps two other phases. The etching with sulfuric acid (Fig. 215) permits the identification of one of the constituents as AlCuFeMn, whereas the other, not etched, can be identified as CuAl<sub>2</sub> by its form and color.

Sometimes, especially when dealing with new alloys or with a specimen of unknown composition, one etching may not be sufficient and several reagents may be necessary. In this case it may be expedient to mark a certain spot in the specimen in which the suspected constituents are all present and to examine it after etching. If the sample is polished

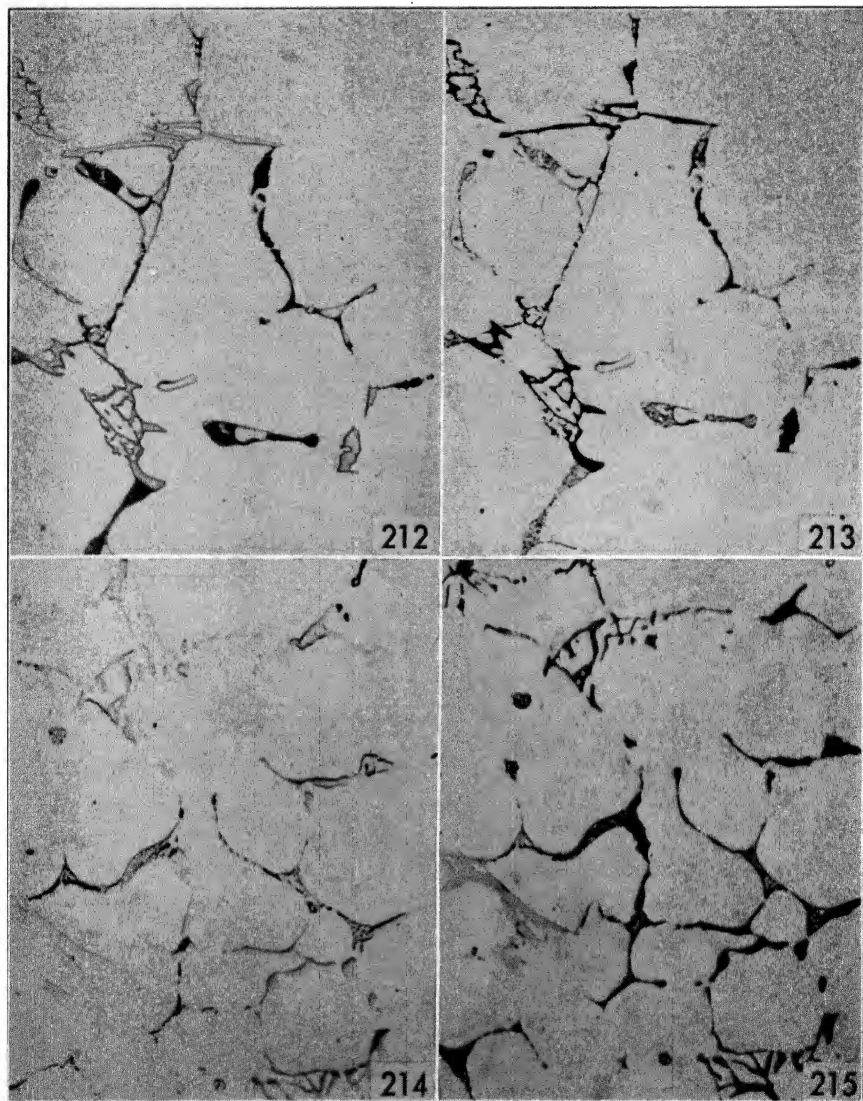


FIG. 212.  $\text{Mg}_2\text{Si}$  black,  $\text{Cu}_2\text{Mg}_2\text{Al}_5$  dark,  $\text{CuAl}_2$  light, fourth constituent not identified—Cu 3.86%, Fe 0.50%, Mg 1.50%, Si 0.32%. Sand-cast, X 250, not etched.

FIG. 213. Same as in Fig. 212. Etched with  $\text{H}_2\text{SO}_4$ , which has blackened the fourth constituent, permitting its identification as  $\alpha(\text{AlFeSi})$ .

FIG. 214.  $\text{Mg}_2\text{Si}$  black,  $\text{Cu}_2\text{Mg}_2\text{Al}_5$  dark brown as eutectic  $\text{Al}-\text{Cu}_2\text{Mg}_2\text{Al}_5-\text{CuAl}_2$ , other constituents not identified—Cu 4.20%, Fe 0.58%, Si 0.39%, Mg 1.65%, Mn 0.65%. Ingot water-cooled, X 250, not etched.

FIG. 215. Same as Fig. 214. Etched with  $\text{H}_2\text{SO}_4$  which has colored dark blue (black in figure)  $\text{AlCuFeMn}$ , leaving  $\text{CuAl}_2$  not etched and permitting their identification.

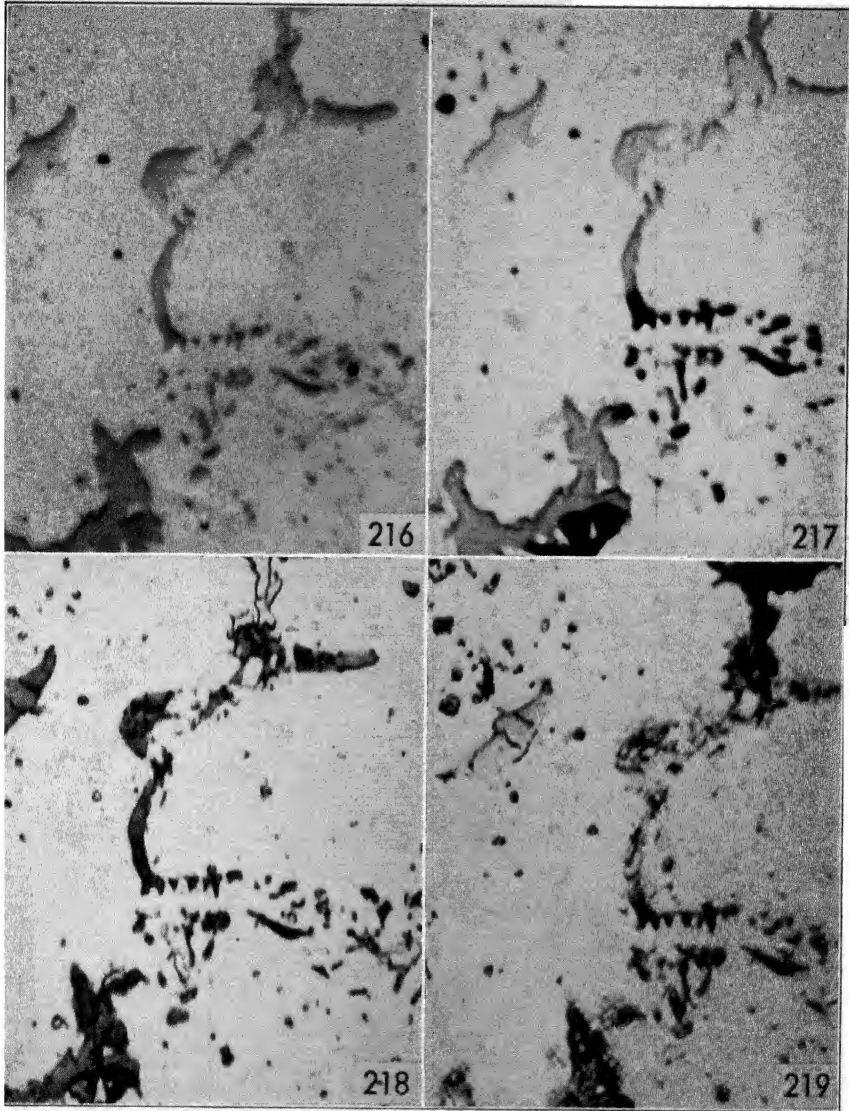


FIG. 216. Black  $\text{CuAl}_2$ , other constituents not identified—Cu 3.06%, Fe 1.54%, Mg 0.58%, Ni 0.57%, Si 0.69%. Cast in permanent mold and heat-treated, X 1000, etched  $\text{Fe}(\text{NO}_3)_3$ .

FIG. 217. Same as Fig. 216. Subsequently etched with  $\text{H}_2\text{SO}_4$  which has blackened  $\alpha(\text{AlFeSi})$ .

FIG. 218. Same as Fig. 216. Subsequently etched with HF which has colored dark brown (dark gray in the figure)  $\text{AlCuFeNi}$ .

FIG. 219. Same as Fig. 216. Subsequently etched with  $\text{HNO}_3$  which has colored dark brown (black in figure)  $\text{AlCuNi}$ .

after each etching until the effects of the etching have completely disappeared, no doubt will arise concerning the effects of the etching. This method, however, has the disadvantage of requiring a considerable time, and sometimes successive polishings wear a constituent down before it has been possible to identify it. In many cases it is possible to etch with different etching reagents in succession without polishing and to examine the progressive effect of each etching. Great care should be taken, however, to wash the sample thoroughly after each etching and this method should not be relied upon blindly, for occasionally etching reagents will act differently upon samples that have been previously etched.

Figures 216, 217, 218, and 219 show the same spot in a heat-treated alloy, etched successively with ferric nitrate, sulfuric acid, hydrofluoric acid, and nitric acid. The identification of the constituents by this method is fairly complete, in spite of the complexity of the alloy. Ferric nitrate has blackened only a few small spots, which may be any one of the following constituents:  $\text{CuAl}_2$ ,  $\text{Cu}_2\text{Mg}_2\text{Al}_5$ ,  $\text{Mg}_2\text{Si}$ . On account of the fact that, prior to etching, no black spots were visible,  $\text{Cu}_2\text{Mg}_2\text{Al}_5$  and  $\text{Mg}_2\text{Si}$  can be ruled out, leaving only  $\text{CuAl}_2$  as possible. The etching with sulfuric acid has blackened another constituent. Only  $\text{FeAl}_3$  and  $\alpha(\text{AlFeSi})$  of all the constituents blackened by sulfuric acid can be present, and the latter is most probable, since the first can be ruled out by the consideration that  $\text{FeAl}_3$  in the presence of copper would form some of the  $\text{AlCuFe}$  constituents. The constituent colored dark brown by hydrofluoric acid could be any one of the following:  $\text{NiAl}_3$ ,  $\text{FeNiAl}_9$ ,  $(\text{CuFe})\text{Al}_3$ ,  $\text{AlCuFeNi}$ .  $(\text{CuFe})\text{Al}_3$ ,  $\text{NiAl}_3$ , and  $\text{FeNiAl}_9$  can be excluded because of the form, leaving only  $\text{AlCuFeNi}$  as possible. The last etching with nitric acid confirms the presence of  $\text{AlCuNi}$ .

In summation, the following constituents have been identified:  $\text{CuAl}_2$ ,  $\alpha(\text{AlFeSi})$ ,  $\text{AlCuFeNi}$ , and  $\text{AlCuNi}$ . The results of this analysis should be confirmed by other etching reagents. This is especially necessary with wrought alloys, where the form cannot be a criterion of identification.

The few examples reported give an idea of how to attempt the identification in certain cases, but no definite rule can be given, for the number of constituents is too large to permit a fixed routine for all alloys.

## CHAPTER 7

### CONSTITUENTS

Although the alloying elements usually added to aluminum and the common impurities are only six, with some seven or eight others only occasionally present, the complete list of the constituents that they are known to form, in the percentages in which they are present in commercial aluminum alloys, includes more than 40 constituents, and there may be others not yet identified.

The known constituents, which range from simple metallic elements, which do not form compounds with aluminum, to complex little-known quaternary phases, are listed below and will be illustrated in detail in the following pages.

Bi, Pb, Si.

$\text{Co}_2\text{Al}_9$ ,  $\text{CrAl}_7$ ,  $\text{CuAl}_2$ ,  $\text{FeAl}_3$ ,  $\text{Fe}_2\text{Al}_7$ ,  $\text{Mg}_5\text{Al}_8$ ,  $\text{MnAl}_6$ ,  $\text{MnAl}_4$ ,  $\text{NiAl}_3$ ,  $\text{TiAl}_3$ ,  $\text{Mg}_2\text{Si}$ ,  $\text{MgZn}_2$ ,  $\text{MgZn}_5$ .

$\text{AlCoFe}$ ,  $(\text{CrFe})\text{Al}_7$ ,  $\text{AlCrMg}$ ,  $\alpha(\text{AlCrSi})$ ,  $\beta(\text{AlCrSi})$ ,  $(\text{CuFe})\text{Al}_3$ ,  $\text{Cu}_2\text{FeAl}_7$ ,  $\omega(\text{AlCuFe})$ ,  $\text{Cu}_2\text{Mg}_2\text{Al}_5$ ,  $\text{CuMg}_4\text{Al}_6$ ,  $\text{AlCuMn}$ ,  $(\text{CuNi})_2\text{-Al}_3$ ,  $\text{AlCuNi}$ ,  $(\text{FeMn})\text{Al}_6$ ,  $\text{FeNiAl}_9$ ,  $\alpha(\text{AlFeSi})$ ,  $\text{FeSiAl}_5$ ,  $\delta(\text{AlFeSi})$ ,  $\text{Mg}_3\text{Zu}_3\text{Al}_2$ ,  $\alpha(\text{AlMnSi})$ ,  $\delta(\text{AlMnSi})$ .

$\text{AlCrFeSi}$ ,  $\text{AlCuFeMn}$ ,  $\text{AlCuFeNi}$ ,  $\text{AlCuFeSi}$ ,  $\text{CuMg}_5\text{Si}_4\text{Al}_4$ ,  $\text{AlFeMgSi}$ ,  $\alpha(\text{AlFeMnSi})$ ,  $\delta(\text{AlFeMnSi})$ .

Great care has been taken to illustrate every constituent in the form in which it is most likely to appear in commercial alloys, since most of the identification can be done by means of the form of the constituent. Where differences in the cooling rate or in concentrations make it appear in more than one typical form, photo-micrographs of each form have been supplied. No particular care has been taken to show each constituent alone, as in practice it would be commonly found accompanied by others. The reactions of these constituents to several etching reagents have been tabulated, as a further help to identification. A table of the reactions has been preferred to photo-micrographs because it is impossible to render the colors in most of their true shades by photographic means.



## Bi and Pb

Both Bi and Pb in aluminum alloys appear from light gray to black, depending on the amount of polishing which the specimens have received. The longer the polishing time, the more the soft Bi and Pb are removed. The deeper, therefore, become the holes formed and the darker the color of the spot where Bi and Pb were. Both Bi and Pb are present as small globules within the grains, if they have been formed by precipitation from the solution, or as segregations at the grain boundaries, where they were the last to solidify. When they are at the grain boundaries and deeply polished or etched, it is sometimes almost impossible to distinguish them from porosity.

Figure 220 shows a small globule of Bi formed by precipitation. Figure 221 shows Pb segregated at the grain boundaries.

## Si

Si may be present as primary crystals in alloys with silicon above 11 per cent, as eutectic Al-Si, modified or not modified, and as isolated crystals in complex alloys. Figure 222 shows a primary crystal of Si in the midst of modified eutectic. Figure 223 shows a few crystals of Si in a copper alloy. More examples will be found in Part III.

Si crystals are much harder than Al and tend to stand in relief during polishing. This fact, together with their typical slate color and their form, permit easy identification and it is seldom necessary to resort to etching to identify particles of Si.

## Co<sub>2</sub>Al<sub>9</sub>

When cobalt is added to pure aluminum, the constituent formed is Co<sub>2</sub>Al<sub>9</sub> (Fig. 224). In commercial alloys, which contain iron, this constituent is seldom present since the constituent AlCoFe is preferentially formed. Co<sub>2</sub>Al<sub>9</sub> is rather soft and of a very light violet color. For this reason an accurate polishing or etching is necessary to detect it.

## CrAl<sub>7</sub>

Aluminum and chromium form the constituent CrAl<sub>7</sub>, which is shown in Fig. 225 in its primary and eutectic forms. In alloys containing more than 2 per cent chromium, Cr<sub>2</sub>Al<sub>11</sub> may also be present in its typical form of hexagonal crystals. In commercial alloys, CrAl<sub>7</sub> and Cr<sub>2</sub>Al<sub>11</sub> are present only in the master alloys, since chromium combines first with iron and silicon to form AlCrFeSi. Both CrAl<sub>7</sub> and Cr<sub>2</sub>Al<sub>11</sub> are harder than Al, especially CrAl<sub>7</sub>, and they stand in relief in aluminum alloys.

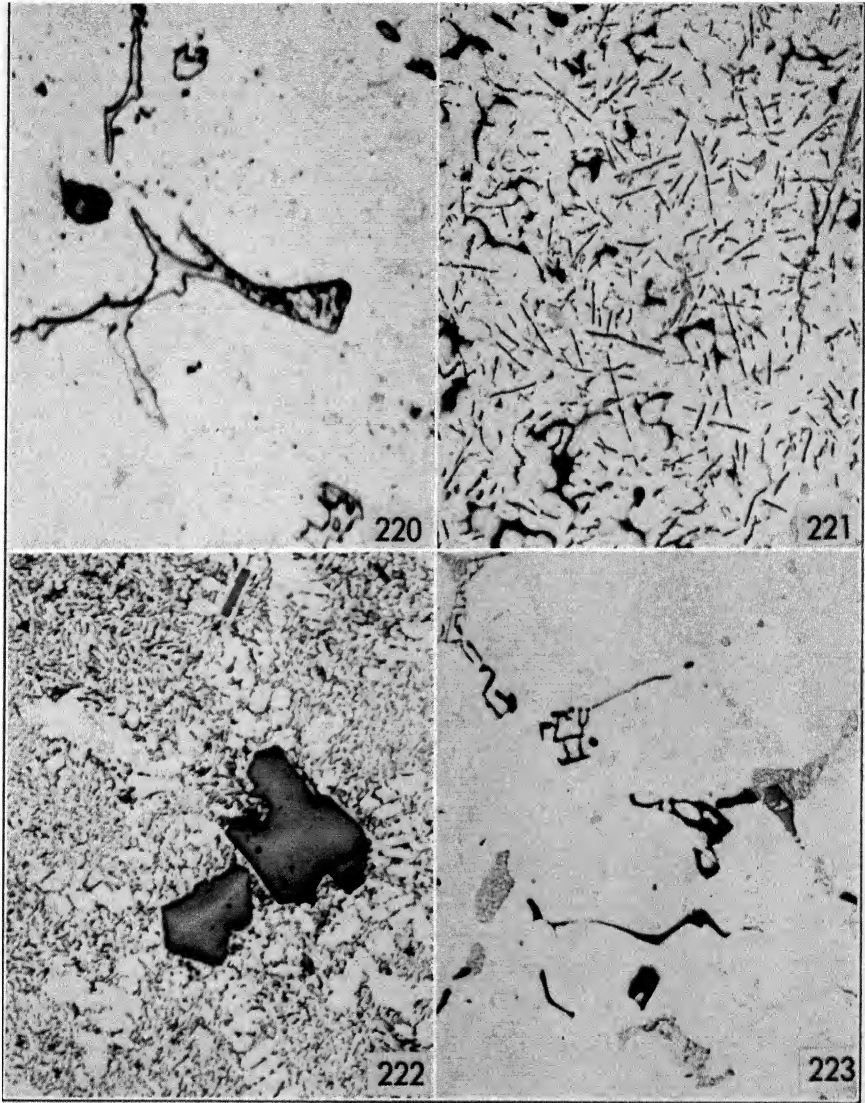


FIG. 220. Globule of Bi dark, CuAl<sub>2</sub> light. Cast in permanent mold—Bi 0.42%, Cu 5.12%, Fe 0.41%, Si 0.30%—X 1000, not etched.

FIG. 221. Pb segregated at the grain boundaries, needles of Cu<sub>2</sub>FeAl<sub>7</sub> (?). Ingot—Cu 2.33%, Fe 2.15%, Pb 1.52%, Si 0.50%—X 75, not etched.

FIG. 222. Primary crystal of Si in a background of modified eutectic Al-Si. Ingot—Si 12.80%, Fe 0.54%—X 250, not etched.

FIG. 223. Si present as isolated crystal (gray) and as eutectic Al-CuAl<sub>2</sub>-Si, black etched α(AlFeSi). Sand-cast—Cu 1.30%, Fe 1.19%, Si 0.76%, X 250, etched with H<sub>2</sub>SO<sub>4</sub>.

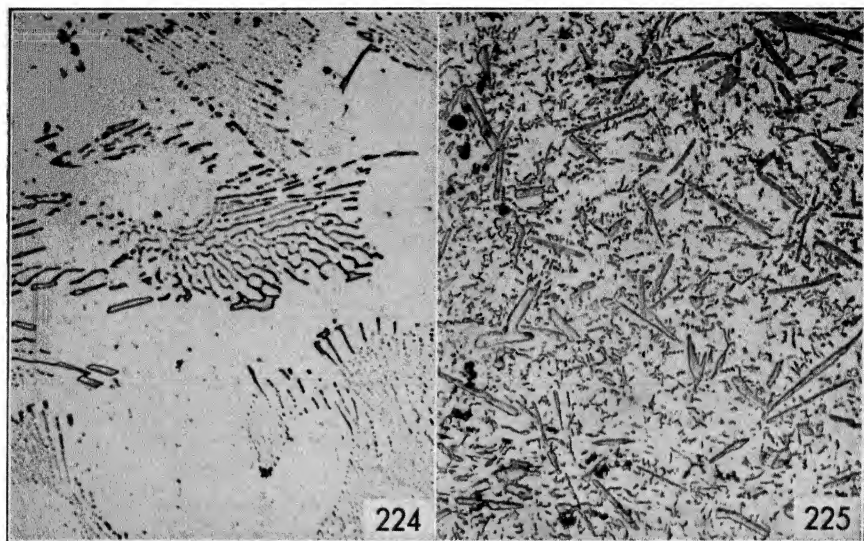


FIG. 224.  $\text{Co}_2\text{Al}_9$  as eutectic  $\text{Al-Co}_2\text{Al}_9$ . Sand-cast—Co 0.85%, Fe 0.17%, Si 0.12%, X 250, not etched.

FIG. 225. Needles of primary  $\text{CrAl}_7$  in a background of eutectic  $\text{Al-CrAl}_7$ . Black spots of oxide (?) at the grain boundaries—Cr 1.75%, Fe 0.13%, Si 0.12%. Cast in permanent mold, X 250, not etched.

## **$\text{CuAl}_2$**

$\text{CuAl}_2$  is one of the most common constituents of aluminum alloys. It is always present as eutectic  $\text{Al-CuAl}_2$  or as complex eutectics, for there is no commercial alloy where the copper content is above the eutectic percentage. Its form is somewhat influenced by the cooling rate. In slowly cooled alloys it forms a lacelike network at the grain boundaries (Fig. 226). In chilled alloys it appears more as globules inside the grains and as lines at the grain boundaries (Fig. 227). When  $\text{CuAl}_2$  is formed by precipitation from a supersaturated solid solution, it does not assume any of these typical structures but appears as small points and needles, sometimes in a Widmanstaetten pattern (Fig. 228).

By annealing after cold working, the points and needles tend to coagulate and form small globules similar to those formed by chilling, and it is in this form that they are usually present in wrought alloys (Fig. 229). Although  $\text{CuAl}_2$  is harder than aluminum, it does not acquire much relief with proper polishing. If too much pressure is exerted, it may even be so flattened as to be almost invisible. The color of  $\text{CuAl}_2$  in well-polished specimens is a pale pink, brilliant. With too much polishing it turns to a light reddish brown.

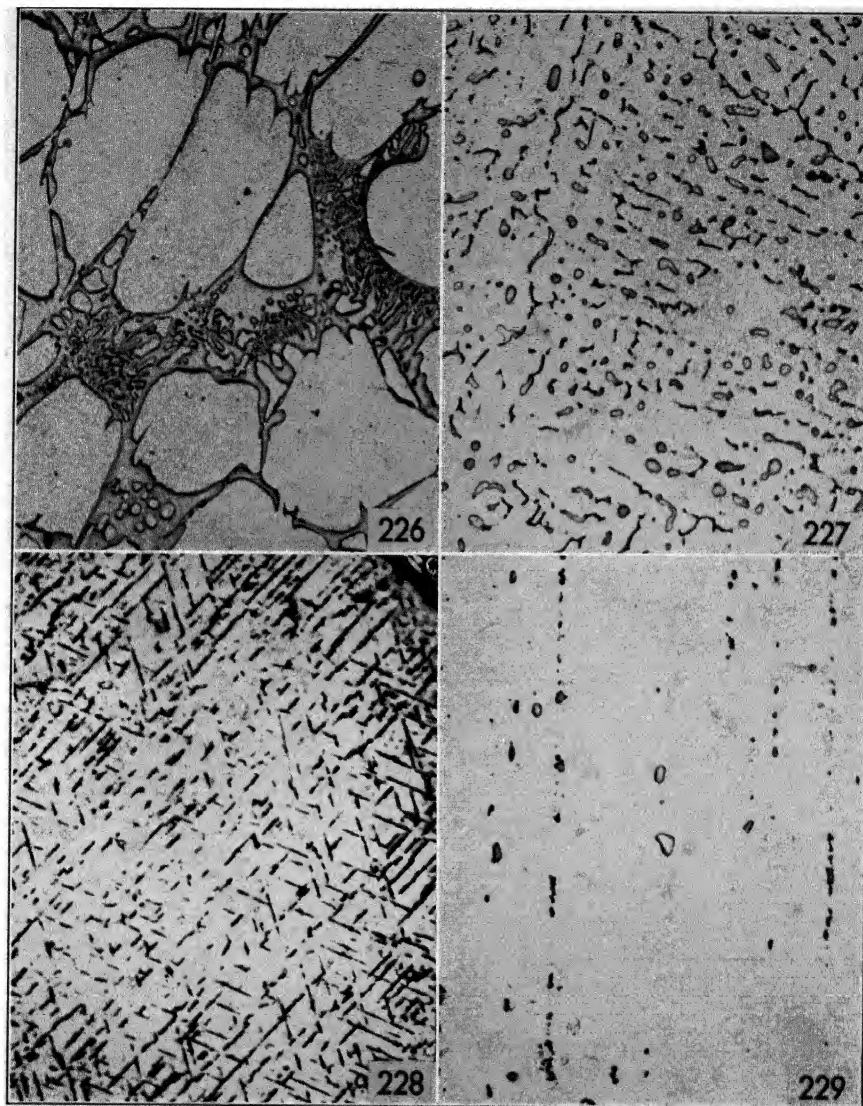


FIG. 226. Network of  $\text{CuAl}_2$ , needles of  $\text{AlCuFeSi}$  embedded in  $\text{CuAl}_2$  and hardly visible. Sand-cast—Cu 13.20%, Fe 0.57%, Si 0.56%—X 250, not etched.

FIG. 227.  $\text{CuAl}_2$  as globules and lines at the grain boundaries. Cast in permanent mold—Cu 6.39%, Fe 0.15%, Si 0.12%—X 250, not etched.

FIG. 228.  $\text{CuAl}_2$  reprecipitated from a solid solution in a Widmanstaetten pattern. Furnace-cooled—Cu 6.40%, Fe 0.39%, Si 0.66%—X 250, not etched.

FIG. 229. Few small particles of  $\text{CuAl}_2$  (light) still undissolved after rolling and heat treatment; small points of Mn constituents—Cu 4.09%, Fe 0.31%, Si 0.59%, Mg 0.58%, Mn 0.56%—X 250, not etched.

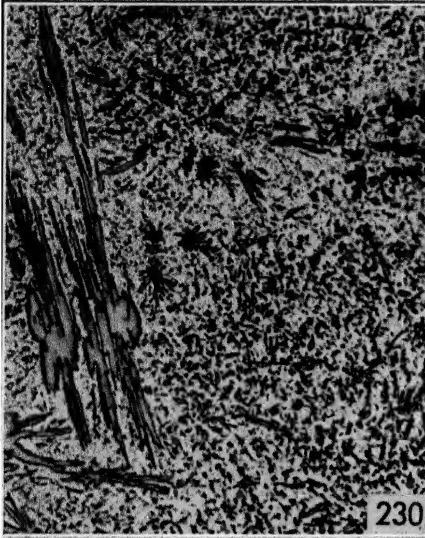


FIG. 230. Primary crystals of  $\text{FeAl}_3$  in their typical form of star-shaped clusters. Cast in permanent mold—Fe 10.6%, Si 0.45%—X 75, not etched.

FIG. 231. Primary crystals of  $\text{Fe}_2\text{Al}_7$  in a background of eutectic Al- $\text{Fe}_2\text{Al}_7$ . Same alloy as in Fig. 230, slowly solidified in the furnace, X 20, not etched.

FIG. 232. Needles of  $\text{Fe}_2\text{Al}_7$ . Sand-cast—Fe 1.02%, Si 0.01%—X 250, not etched.

### **FeAl<sub>3</sub> and Fe<sub>2</sub>Al<sub>7</sub>**

Additions of iron to aluminum form two constituents whose composition corresponds to the above formulae. As already reported in Part I, their distinction is not yet clear, and there is need for further investigation.

As far as the common etching reagents are concerned, the two constituents have the same etching characteristics, so that the distinction between them must be based on form alone. This is usually easy in hyper-eutectic alloys, where the two constituents are primary, but when only a few particles of the constituents are visible, it is almost impossible to distinguish between them. Figures 230 and 231 show, respectively, FeAl<sub>3</sub> and Fe<sub>2</sub>Al<sub>7</sub>.

The distinction between the two constituents has only a theoretical interest, for they are not commonly encountered in commercial alloys, where iron is combined in complex constituents. When FeAl<sub>3</sub> or Fe<sub>2</sub>Al<sub>7</sub> is present, its presence is caused by heavy local segregations, and it does not make much difference if the segregation is of FeAl<sub>3</sub> or Fe<sub>2</sub>Al<sub>7</sub>. Figure 232 shows the form of the iron constituent, probably Fe<sub>2</sub>Al<sub>7</sub>, when iron is below eutectic concentration.

The iron constituents are much harder than aluminum, and, when primary, they stand on relief. They have a purplish-gray color which distinguishes them from some other constituents, but, as this color is common to many complex constituents, etching must be resorted to for an exact identification.

### **Mg<sub>5</sub>Al<sub>8</sub>**

This phase is present only in alloys with high magnesium content, as the magnesium in aluminum alloys combines first with silicon to form the compound Mg<sub>2</sub>Si and then with copper if the latter is present. Moreover, the solid solubility of magnesium in aluminum is quite high.

Mg<sub>5</sub>Al<sub>8</sub> is affected by the cooling rate in the same way as CuAl<sub>2</sub>. Figure 233 shows the globular form produced by rapid chilling. Figure 234 shows the netlike form produced by slow cooling.

Mg<sub>5</sub>Al<sub>8</sub> is rather soft, and accurate polishing is required for its detection. When slightly overpolished, as often happens, its color ranges from ivory to pale yellow. If the polishing is protracted for a long time, Mg<sub>5</sub>Al<sub>8</sub> is eaten out, and in the presence of other constituents accurate focusing is not possible.

Mg<sub>5</sub>Al<sub>8</sub> does not usually require etching for its identification, for most of the phases with which it may be associated in commercial alloys are much darker and have characteristic forms.



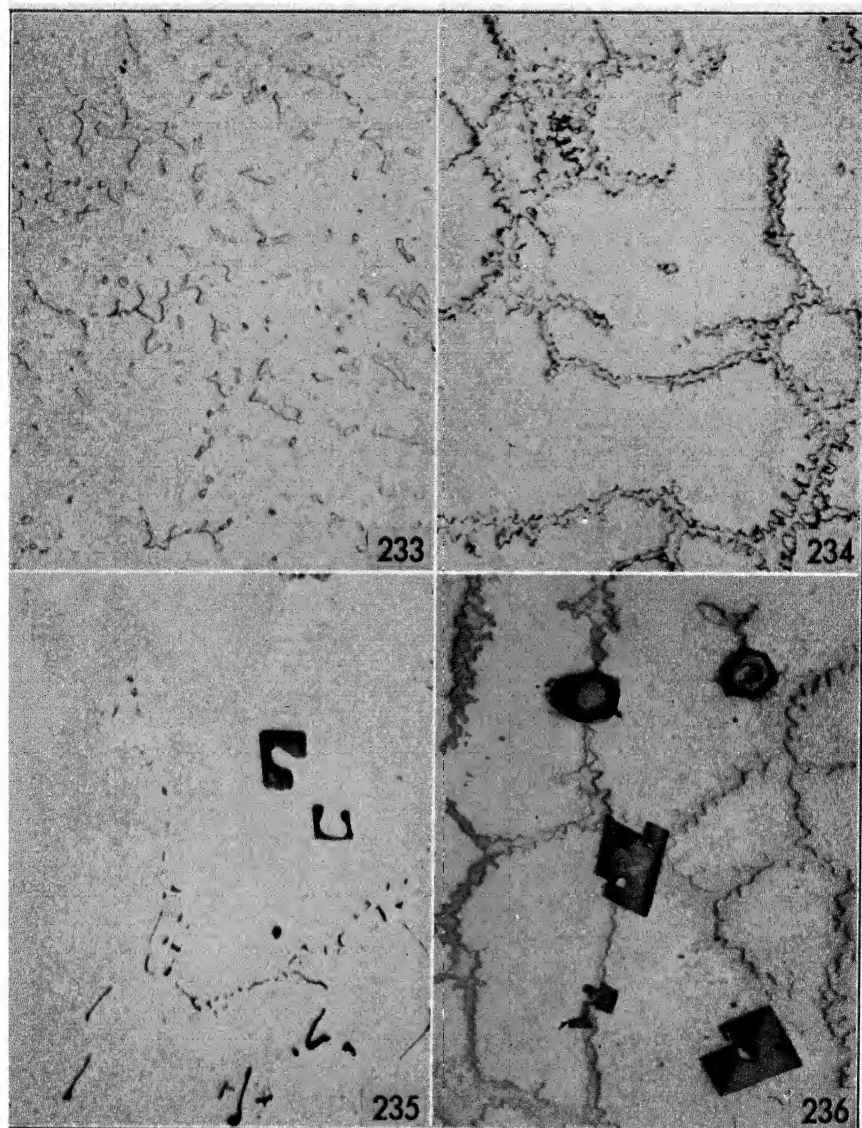


FIG. 233. Globules of  $Mg_5Al_8$  in the typical form when chilled, black points of  $Mg_2Si$  (?). Cast in permanent mold—Mg 8.12%, Si 0.02%—X 250, not etched.

FIG. 234.  $Mg_5Al_8$  as a network at the grain boundaries, black spots of  $Mg_2Si$ . Sand-cast—Mg 12.52%, Si 0.04%—X 250, not etched.

FIG. 235.  $MnAl_6$  as primary crystals and as eutectic Al- $MnAl_6$ . Sand-cast—Mn 1.48%, Fe 0.01%, Si 0.01%—X 250, not etched.

FIG. 236. Primary crystals of hexagonal  $MnAl_4$ ,  $MnAl_6$  tetragonal, network of  $Mg_5Al_8$ . Sand-cast—Mg 11.71%, Mn 2.45%—X 250, not etched.

### **MnAl<sub>6</sub> and MnAl<sub>4</sub>**

Additions of manganese to pure aluminum form these constituents. In commercial alloys, where iron and silicon are present, these phases are uncommon. When manganese is below the eutectic concentration, MnAl<sub>6</sub> is formed, and it is almost impossible to distinguish it from several other phases, as its form ranges from needles and globules, when formed by reprecipitation from a solid solution, to a Chinese script (Fig. 235).

Fortunately for the metallographer, MnAl<sub>6</sub>, also at low concentrations of manganese, tends to form primary crystals, assuming the typical form of incomplete tetragonal crystals. With large concentrations of manganese or high magnesium, the constituent MnAl<sub>4</sub> can also be present. Figure 236 shows a slowly cooled alloy where two crystals of MnAl<sub>4</sub> are present in their characteristic form of hollow hexagonal crystals, together with several crystals of MnAl<sub>6</sub>. As can be seen, MnAl<sub>4</sub> is harder than MnAl<sub>6</sub> and therefore more relieved. MnAl<sub>6</sub> is rather soft and requires careful polishing. Its color is light gray.

### **NiAl<sub>3</sub>**

There are usually no primary crystals of NiAl<sub>3</sub> present in commercial alloys, for the nickel content is always below the eutectic. NiAl<sub>3</sub> is easily identified when present in certain amounts, for it has the tendency to form eutectic colonies (Fig. 237). In the identification of separate particles, their droplike form may help, but etching is usually necessary to make their identification certain. When not etched, NiAl<sub>3</sub> is of a gray-yellowish color, which is common to many other constituents.

### **TiAl<sub>3</sub>**

The amounts of titanium added to commercial aluminum alloys usually are so small that particles of TiAl<sub>3</sub> are very seldom detected. Figure 238 shows the typical form of TiAl<sub>3</sub> with slow cooling. With rapid chilling TiAl<sub>3</sub> appears in the form of small globules, which may be confused with anything, including polishing defects.

### **Mg<sub>2</sub>Si**

Mg<sub>2</sub>Si is one of the few real compounds in a chemical sense that are formed by alloying elements in aluminum alloys. It is quite common in aluminum alloys and is probably the most easily identified. Primary crystals of Mg<sub>2</sub>Si like those shown in Fig. 239 are seldom found in commercial alloys, where Mg<sub>2</sub>Si appears in its typical form of Chinese



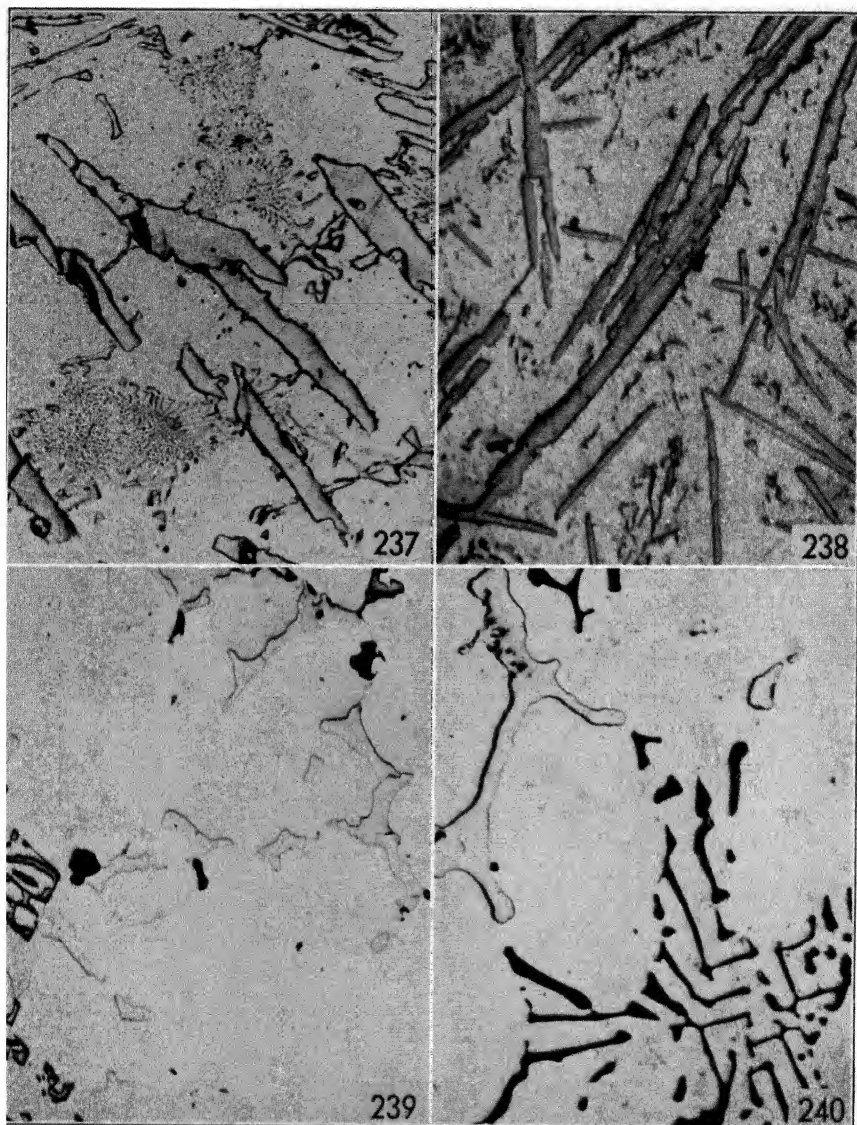


FIG. 237. Colonies of  $\text{NiAl}_3$ , large crystals of  $\text{FeNiAl}_9$ . Sand-cast—Ni 5.20%, Fe 4.20%, Si 0.27%—X 250, not etched.

FIG. 238. Typical crystals of  $\text{TiAl}_3$ . Ingot—Ti 4.37%, Fe 0.55%, Si 0.29%—X 250, not etched.

FIG. 239. Primary crystals of  $\text{Mg}_2\text{Si}$  (black),  $\text{Mg}_5\text{Al}_8$  light, gray  $\text{NiAl}_3$  or  $\text{AlFeMgNi}$  (?). Sand-cast—Mg 7.30%, Si 0.18%, Ni 1.19%, Fe 0.37%—X 250, not etched.

FIG. 240.  $\text{Mg}_2\text{Si}$  black,  $\text{Mg}_5\text{Al}_8$  light relieved. Sand-cast—Mg 9.50%, Si 1.91%, Fe 0.01%—X 250, not etched.

script (Fig. 240).  $\text{Mg}_2\text{Si}$  is slate gray, slightly darker than Si, but it is easily attacked by water so that in most cases it is colored from bright blue to black. Prolonged polishing and excessive water tend to erode it to the point where it is at a lower level than the other constituents and exact focusing is not possible.

### **$\text{MgZn}_2$ and $\text{MgZn}_5$**

These constituents are formed in alloys with very high zinc and magnesium. Only in heavy segregations can they be detected in commercial alloys, as the amount of zinc required for their appearance is higher than the amount usually present. Their form is the same as that of  $\text{Mg}_5\text{Al}_8$ , namely, globules or network at the grain boundaries, depending on the rate of cooling. When they are associated with  $\text{Mg}_5\text{Al}_8$  or  $\text{Mg}_3\text{Zn}_3\text{Al}_2$ , as often happens, etching must be resorted to for their identification, since the form and aspect is the same for them all.

### **$\text{AlCoFe}$**

This constituent is commonly present in alloys containing cobalt. It is probably a solid solution of iron in  $\text{Co}_2\text{Al}_9$ , as its crystal habit is the same as  $\text{Co}_2\text{Al}_9$ , and only its etching characteristics are slightly different (Fig. 241). Its normal color is a pale violet and it is not usually relieved from the aluminum. For this reason it is sometimes quite difficult to detect it in the midst of aluminum. Its etching characteristics are not constant and range from those of pure  $\text{Co}_2\text{Al}_9$  to those reported in the table; this would confirm the solid solution of iron in  $\text{Co}_2\text{Al}_9$ , where variable amounts of iron in solution would account for the variation in etching characteristics.

### **$(\text{CrFe})\text{Al}_7$**

The crystal form and the crystal habit of this constituent do not differ from those of  $\text{CrAl}_7$ , as it is only a solid solution of iron in  $\text{CrAl}_7$ . The etching characteristics are slightly different. Figure 242 shows an alloy where primary crystals of  $\text{Cr}_2\text{Al}_{11}$  and  $(\text{CrFe})\text{Al}_7$  are present together with the eutectic  $\text{Al}-(\text{CrFe})\text{Al}_7\text{-FeAl}_3$ .

### **$\text{AlCrMg}$**

This constituent, whose composition is not known exactly, may be present in alloys containing chromium and more than 2 per cent magnesium. Figure 243 shows it in the eutectic and primary forms. Its form and color are similar to that of  $\text{Mg}_5\text{Al}_8$ , but it is much harder and tends to be relieved by the polishing.

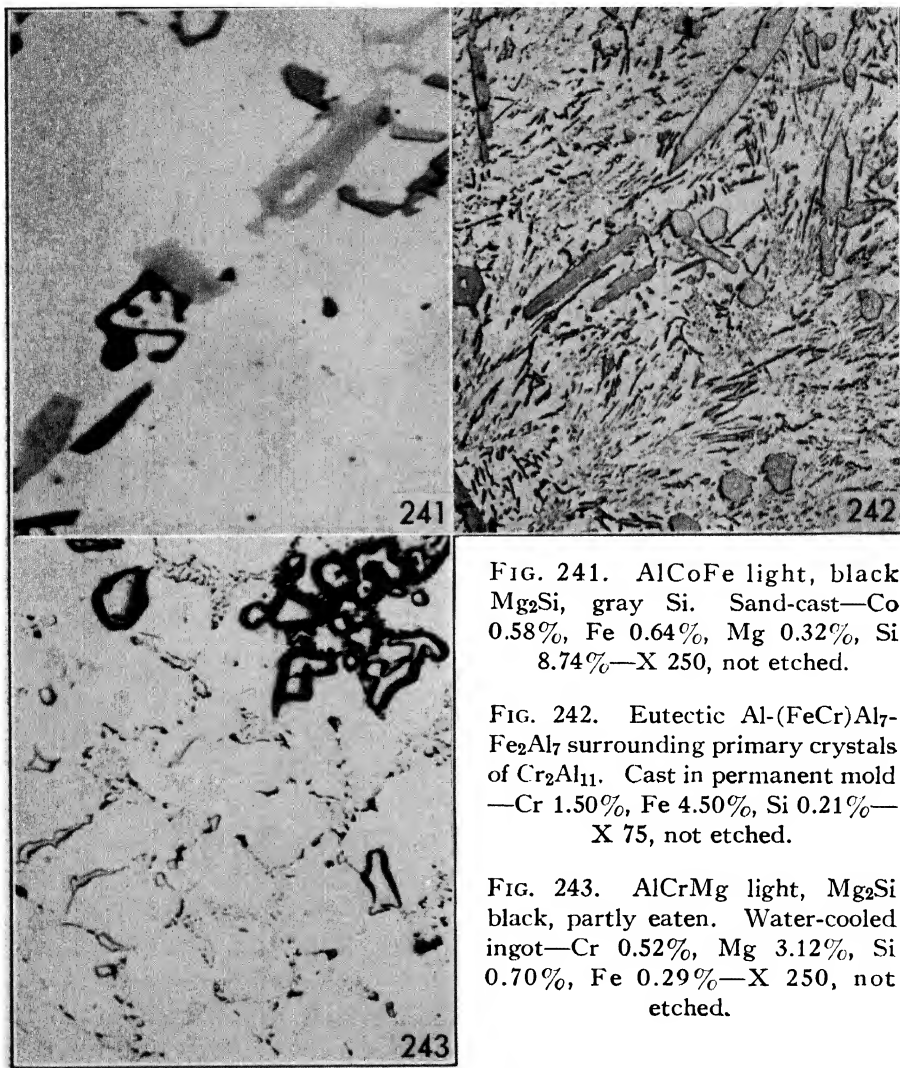


FIG. 241. AlCoFe light, black  $Mg_2Si$ , gray Si. Sand-cast—Co 0.58%, Fe 0.64%, Mg 0.32%, Si 8.74%—X 250, not etched.

FIG. 242. Eutectic Al-(FeCr)Al<sub>7</sub>-Fe<sub>2</sub>Al<sub>7</sub> surrounding primary crystals of Cr<sub>2</sub>Al<sub>11</sub>. Cast in permanent mold—Cr 1.50%, Fe 4.50%, Si 0.21%—X 75, not etched.

FIG. 243. AlCrMg light,  $Mg_2Si$  black, partly eaten. Water-cooled ingot—Cr 0.52%, Mg 3.12%, Si 0.70%, Fe 0.29%—X 250, not etched.

**$\alpha(\text{AlCrSi})$** 

At least two phases are formed by chromium and silicon in aluminum alloys. The one usually present with low amounts of chromium and silicon is  $\alpha(\text{AlCrSi})$ , usually in the eutectic form as Chinese script (Fig. 244). This phase, however, is seldom present in commercial alloys because  $\text{AlCrFeSi}$  is preferentially formed.

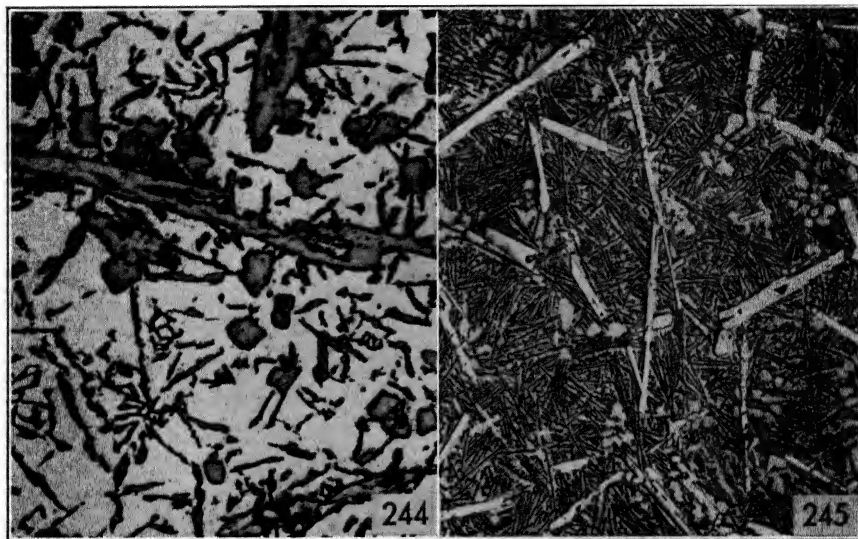


FIG. 244.  $\alpha(\text{AlCrSi})$  as Chinese script, blackened, Si and  $\beta(\text{AlCrSi})$  needles and points not etched. Ingot—Cr 2.50%, Si 20.60%, Fe 0.25%—X 75, etched with  $\text{H}_2\text{SO}_4$ .

FIG. 245. Light crystals of  $\beta(\text{AlCrSi})$  in a background of eutectic Al-Si. Furnace-cooled—Cr 1.20%, Si 14.5%, Fe 0.17%—X 10, not etched.

 **$\beta(\text{AlCrSi})$** 

This phase is formed with high silicon concentrations. It is needle-form and quite resistant to etching reagents. When it is present, fusion with carbonates must be resorted to for chemical analysis, for it does not dissolve in any acid or acid mixture and with difficulty in sodium hydroxide solutions. Figure 245 shows several well-formed crystals of  $\beta(\text{AlCrSi})$  in the midst of eutectic Al-Si. The crystals are very hard and of a brilliant silvery color and are not darkened appreciably by any etching reagent.

 **$(\text{CuFe})\text{Al}_3$** 

This phase, sometimes identified as  $\alpha(\text{CuFe})$ , is a solid solution of copper in  $\text{FeAl}_3$ . Its form approaches that of undercooled  $\text{FeAl}_3$  but

its etching characteristics are somewhat different, as is to be expected (Fig. 246). This phase is often present in alloys of the aluminum-copper-nickel group with high iron content, where it cannot easily be distinguished from  $\text{NiAl}_3$ , as their etching characteristics are the same and their form only slightly different.

### **$\text{Cu}_2\text{FeAl}_7$**

This phase, usually identified as  $\beta(\text{CuFe})$ , has a tendency to form primary crystals also with low concentrations of copper and iron, in the form of long thin needles (Fig. 247). The presence of manganese, nickel, chromium, or cobalt in the alloy hinders the formation of  $\text{Cu}_2\text{FeAl}_7$ . It has almost the same color of  $\text{CuAl}_2$  in which it is commonly imbedded and requires etching for its detection. When silicon is not combined otherwise, this phase is substituted by the quaternary  $\text{AlCuFeSi}$ . For this reason  $\text{Cu}_2\text{FeAl}_7$  is only occasionally present in commercial alloys.

### **$\omega(\text{AlCuFe})$**

This is an unstable phase, formed sometimes by fast cooling. Its characteristic form is shown in Fig. 248. As already reported in Part I, when dealing with the equilibrium diagram aluminum-copper-iron, this phase tends to transform into  $\text{Cu}_2\text{FeAl}_7$ . For this reason it is sometimes possible to find this phase cored, with a central part having the etching characteristics of  $\omega(\text{AlCuFe})$  and an outside sheath, sometimes only partial, having the etching characteristics of  $\text{Cu}_2\text{FeAl}_7$  (Fig. 249).

### **$\text{Cu}_2\text{Mg}_2\text{Al}_5$**

This phase is usually present in alloys containing copper and magnesium, when the silicon is insufficient to saturate all the magnesium to form  $\text{Mg}_2\text{Si}$ ; and constitutes the main hardening agent of several alloys.  $\text{Cu}_2\text{Mg}_2\text{Al}_5$  is readily attacked and, depending on the amount of water used in polishing, its color ranges from light brown to black in the unetched specimen. As for  $\text{CuAl}_2$  and  $\text{Mg}_5\text{Al}_8$ , the cooling rate influences its form and changes it from globules, when fast chilled, to a network, when slow cooled. Figure 250 shows the globules, of different colors, as they often appear in commercial alloys. Figure 251 shows  $\text{Cu}_2\text{Mg}_2\text{Al}_5$  associated with  $\text{CuAl}_2$  as eutectic  $\text{Al-Cu}_2\text{Mg}_2\text{Al}_5\text{-CuAl}_2$ .

This structure is reported because it is common in commercial alloys, and in most cases the eutectic is difficult to resolve.  $\text{Cu}_2\text{Mg}_2\text{Al}_5$  can be identified easily by polishing, for it is the only one that becomes

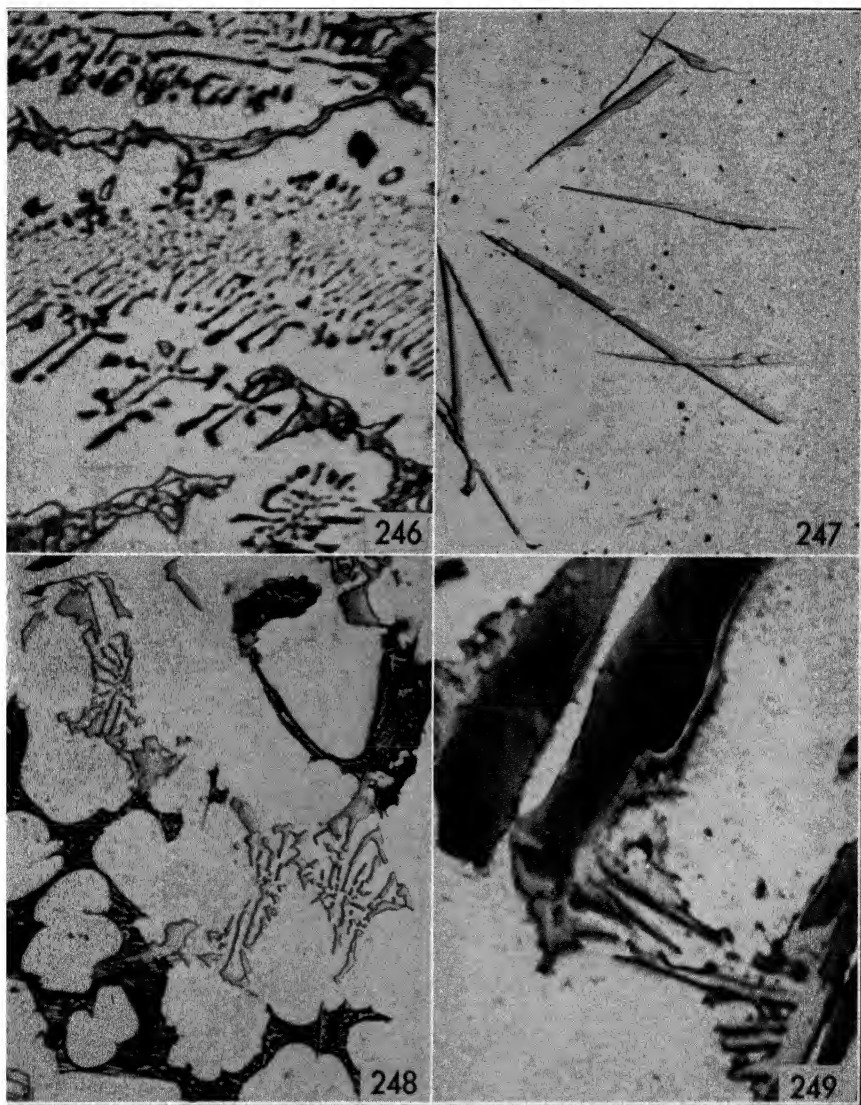


FIG. 246.  $(\text{FeCu})\text{Al}_3$  dark, light network of  $\text{CuAl}_2$  with some needles of  $\text{Cu}_2\text{FeAl}_7$  embedded in it and partly visible. Cast in permanent mold—Cu 8.14%, Fe 5.52%, Si 0.35%—X 1000, etched with HF.

FIG. 247. Needles of  $\text{Cu}_2\text{FeAl}_7$ . Sand-cast—Cu 4.16%, Fe 1.12%, Si 0.01%—X 250, not etched.

FIG. 248. Light  $\omega(\text{AlCuFe})$ , black etched  $\text{CuAl}_2$ , some  $\text{Cu}_2\text{FeAl}_7$  needles embedded in  $\text{CuAl}_2$  and partly visible. Sand-cast—Cu 7.94%, Fe 1.10%, Si 0.01%—X 250, etched with  $\text{Fe}(\text{NO}_3)_3$ .

FIG. 249.  $\omega(\text{AlCuFe})$  dark, partially surrounded by a sheath of  $\text{Cu}_2\text{FeAl}_7$ , which forms needles. Sand-cast. Same alloy as in Fig. 248, X 1000, etched with HF.

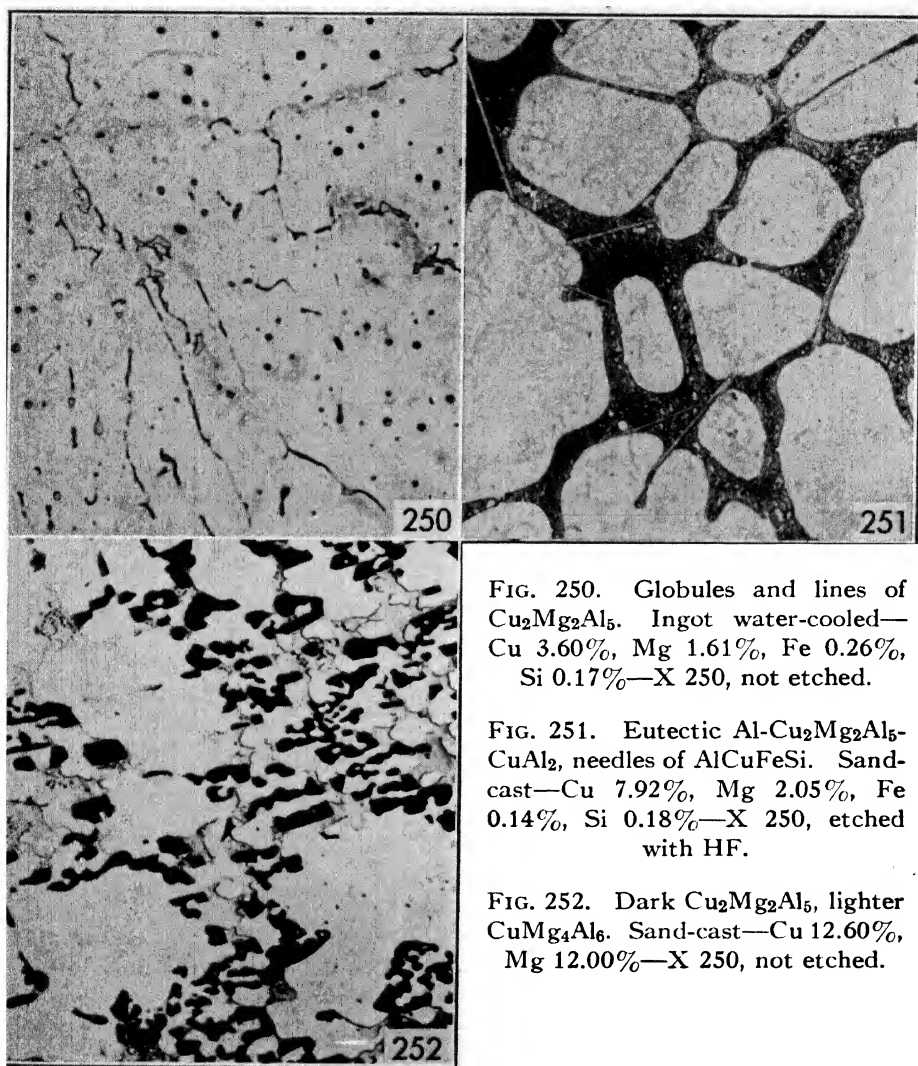


FIG. 250. Globules and lines of  $\text{Cu}_2\text{Mg}_2\text{Al}_5$ . Ingot water-cooled—Cu 3.60%, Mg 1.61%, Fe 0.26%, Si 0.17%—X 250, not etched.

FIG. 251. Eutectic Al- $\text{Cu}_2\text{Mg}_2\text{Al}_5$ - $\text{CuAl}_2$ , needles of AlCuFeSi. Sand-cast—Cu 7.92%, Mg 2.05%, Fe 0.14%, Si 0.18%—X 250, etched with HF.

FIG. 252. Dark  $\text{Cu}_2\text{Mg}_2\text{Al}_5$ , lighter  $\text{CuMg}_4\text{Al}_6$ . Sand-cast—Cu 12.60%, Mg 12.00%—X 250, not etched.



brown. If its presence is expected, the specimen should be examined after polishing as dry as possible, and then it should be polished further with increasing amounts of water, and should be examined from time to time until the brown coloration can be detected. As the only other constituent attacked by water is  $\text{Mg}_2\text{Si}$ , which has a characteristic form, the identification of  $\text{Cu}_2\text{Mg}_2\text{Al}_5$  by this method should not offer difficulties.

### **$\text{CuMg}_4\text{Al}_6$**

This phase is present in alloys where the ratio  $\text{Cu} : \text{Mg}$  is lower than 2.65, but there is no commercial alloy of this nature. However, as it might be present in local segregations or in exceptional cases where copper is present in magnesium alloys, it is reported here.  $\text{CuMg}_4\text{Al}_6$  is very similar to  $\text{Cu}_2\text{Mg}_2\text{Al}_5$ , both as to form and etching characteristics, the only difference being that in polishing it does not darken as much as  $\text{Cu}_2\text{Mg}_2\text{Al}_5$ .

If the two constituents are present together as in Fig. 252, it is very easy to distinguish between them. Otherwise a distinction between the two is mostly conjecture.

### **$\text{AlCuMn}$**

Little is known about the nature of this phase. According to the latest equilibrium diagram it is decidedly a ternary constituent, but there is evidence that it may be only a solid solution of copper in  $\text{MnAl}_4$ . It is very seldom encountered in commercial alloys, where manganese and copper tend to combine, respectively, with iron and silicon or magnesium.

Figure 253 shows this phase in the etched state. It is usually present as eutectic  $\text{Al}-\text{AlCuMn}-\text{CuAl}_2$ , as shown in Fig. 254. With high cooling speeds, this eutectic appears as a continuous constituent, with etching characteristics common to  $\text{CuAl}_2$  and  $\text{AlCuMn}$ .

### **$(\text{CuNi})_2\text{Al}_3$**

This phase is a solid solution of copper in  $\text{Ni}_2\text{Al}_3$ . It is usually present in alloys which have a nickel content equal or higher than the copper content and has somewhat variable characteristics, depending on the copper content. Figure 255 shows its typical form. It can be distinguished from  $\text{AlCuNi}$  only by its form, since there is no substantial difference in the etching characteristics.

### **$\text{AlCuNi}$**

According to the last equilibrium diagram, at least three  $\text{AlCuNi}$  compounds can be in equilibrium with aluminum. However, this is



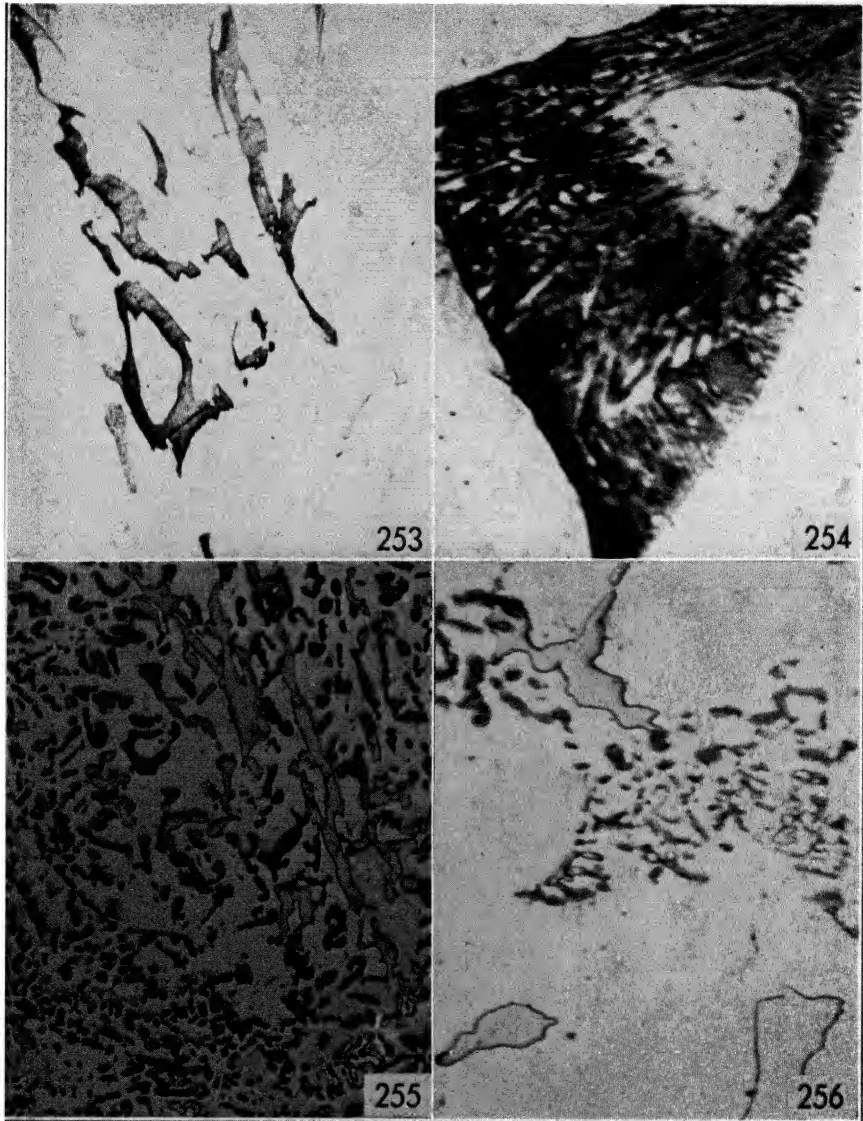


FIG. 253.  $\text{AlCuMn}$  dark,  $\text{CuAl}_2$  light. Cast in permanent mold—Cu 2.64%, Mn 2.70%—X 500, etched with HF.

FIG. 254. Eutectic  $\text{Al-AlCuMn-CuAl}_2$ . Sand-cast, same alloy as in Fig. 253, X 1000, etched with HF.

FIG. 255.  $(\text{CuNi})_2\text{Al}_3$  light,  $\text{Mg}_2\text{Si}$  black, Si gray. Cast in permanent mold—Cu 0.82%, Fe 0.51%, Mg 0.83%, Ni 2.26%, Si 14.20%—X 250, not etched.

FIG. 256.  $\text{AlCuNi}$  light,  $\text{AlCuFeNi}$  dark. Cast in permanent mold—Cu 3.07%, Fe 1.35%, Mg 0.50%, Ni 0.54%, Si 0.54%—X 1000, etched with NaOH.

not confirmed by other investigations, and by microscopic examination only one phase can be detected. Figure 256 shows this phase in its typical form. Its color is rather dark. This fact, together with its typical form and its resistance to etching reagents, facilitates its identification.

### **(FeMn)Al<sub>6</sub>**

This constituent is a solid solution of iron in MnAl<sub>6</sub>. For this reason, although the etching characteristics are somewhat different, its form and crystal habit are exactly the same as for MnAl<sub>6</sub>. As in all solid solutions where the content of the dissolved element is variable, the etching characteristics are not sharply defined and vary continuously from the pure constituent to the saturated solution, whose reactions are reported in the table. This constituent commonly is present in commercial alloys, where the silicon is otherwise combined. In the presence of free silicon the quaternary phase  $\alpha(\text{AlFeMnSi})$  is preferentially formed. Figure 257 shows (FeMn)Al<sub>6</sub> in a chilled alloy, in the eutectic form. The primary crystals are exactly the same as MnAl<sub>6</sub>.

### **FeNiAl<sub>9</sub>**

This phase is formed in alloys containing iron and nickel, and is usually present in the eutectic form (Fig. 258). Its etching characteristics are very similar to NiAl<sub>3</sub> and (CuFe)Al<sub>3</sub>. The only difference is that, when etched with sodium hydroxide 10 per cent for 5 seconds at 160°F, NiAl<sub>3</sub> and (CuFe)Al<sub>3</sub> are etched dark brown, whereas FeNiAl<sub>9</sub> is etched light brown.

### **$\alpha(\text{AlFeSi})$**

Although this is one of the most common phases in aluminum alloys and was discovered as early as 1919, its exact composition is still unknown. It is formed in alloys where the iron content is higher than the silicon content and is usually present in the eutectic form as Chinese script, under which name it is sometimes described. Figure 259 shows the Chinese script form; Fig. 260 shows several primary crystals.

It is commonly found in alloys of the aluminum-copper type and sometimes in alloys of the aluminum-copper-nickel type. In the presence of manganese it is replaced by  $\alpha(\text{AlFeMnSi})$ . With high silicon content, as in all the aluminum-silicon type alloys, it is never present, for the phase formed then is FeSiAl<sub>5</sub>. The presence of copper and zinc seems to favor its formation, even in the presence of free silicon.

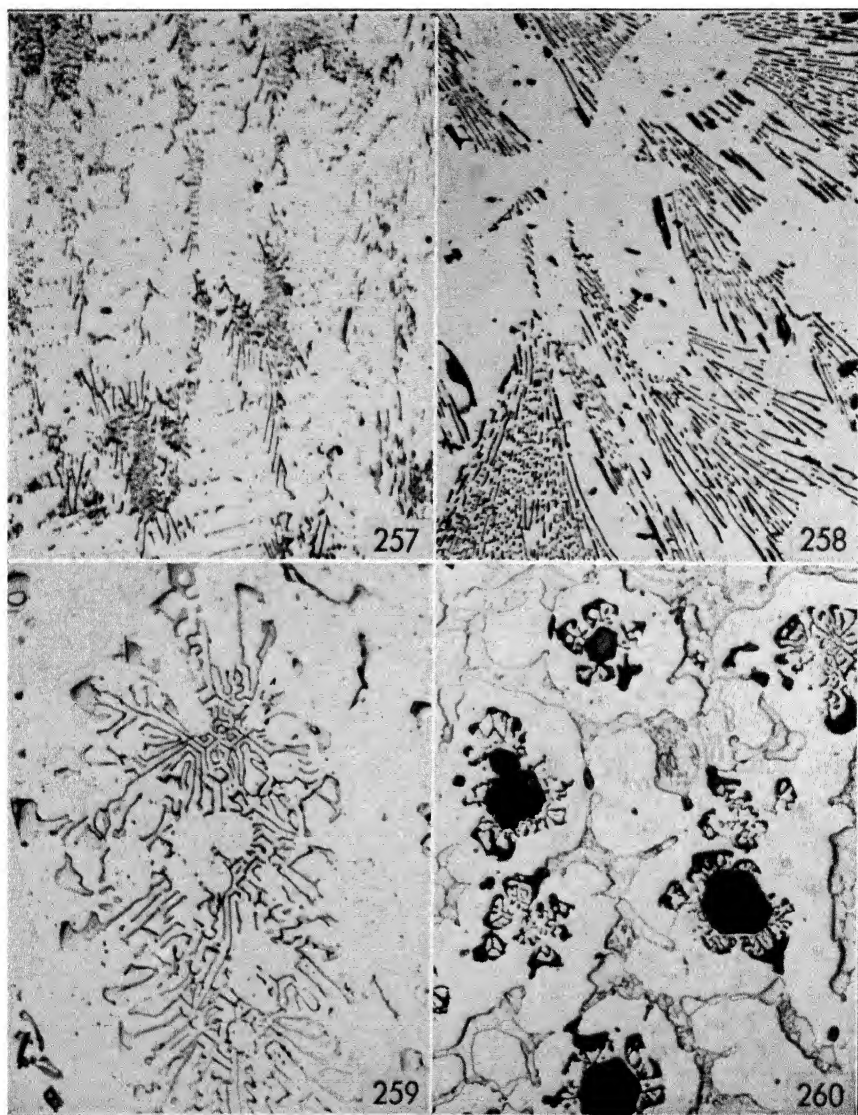


FIG. 257.  $(\text{FeMn})\text{Al}_6$  in its typical form when chilled. Cast in permanent mold—Fe 1.03%, Mn 1.01%, Si 0.01%—X 250, not etched.

FIG. 258. Needles of  $\text{FeNiAl}_9$  in their typical grouping. Sand-cast—Fe 3.02%, Ni 2.04%, Si 0.12%—X 250, etched with HF.

FIG. 259.  $\alpha(\text{AlFeSi})$  as typical Chinese script. Cast in permanent mold—Fe 1.94%, Si 0.89%—X 250, not etched.

FIG. 260. Primary crystals of  $\alpha(\text{AlFeSi})$  hexagonal, surrounded by  $\alpha(\text{AlFeSi})$  as Chinese script,  $\text{CuAl}_2$  and Si as eutectic  $\text{Al-CuAl}_2\text{-Si}$ . Sand-cast—Fe 3.55%, Si 2.28%, Cu 10.31%—X 75, etched with HF.

**FeSiAl<sub>5</sub>**

This phase, usually known as  $\beta(\text{FeSi})$ , is present in alloys where silicon is predominant. It crystallizes in the form of long thin plates, which in a section appear as thin needles. In aluminum-silicon alloys, when present in the eutectic  $\text{Al-FeSiAl}_5\text{-Si}$ , it can hardly be detected because it forms needles exactly like silicon except for a lighter color, which in thin needles can hardly be distinguished. When it forms primary crystals, the needles are much longer and the light color can be recognized much better, so that their identification is much easier. The higher the iron content, the longer and wider the needles. Figure 261 shows small primary needles in the midst of eutectic  $\text{Al-Si}$ ; Fig. 262 shows several long needles in another silicon alloy with higher iron. This phase is usually associated with silicon. In the presence of copper the quaternary phase  $\text{AlCuFeSi}$  is formed. Manganese, chromium, cobalt, magnesium, and nickel hinder its formation, for they tend to form other ternary or quaternary constituents with iron and silicon.

 **$\delta(\text{AlFeSi})$** 

This phase can be found only in alloys with a silicon content of above 14 per cent, and it is not stable until silicon percentages of about 25 per cent are reached. Between these limits it tends to transform to  $\text{FeSiAl}_5$  by peritectic reaction. Figure 263 illustrates a typical crystal of  $\delta(\text{AlFeSi})$  in the midst of  $\text{Si}$ . Nearby can be seen another crystal in an advanced state of transformation to  $\text{FeSiAl}_5$ .  $\delta(\text{AlFeSi})$  is very light and hard and is only slightly darkened by some etching reagents.

 **$\text{Mg}_3\text{Zn}_3\text{Al}_2$** 

This phase is formed, over a wide range of compositions, in alloys containing magnesium and zinc. It is seldom detected in commercial alloys since the amount of zinc required for its appearance in commercial alloys is far above the amounts usually present in them. Its form and color are the same as those of  $\text{Mg}_5\text{Al}_8$ ,  $\text{MgZn}_2$ , and  $\text{MgZn}_5$ . Etching must be resorted to for their identification. Its etching characteristics are reported in the table.

 **$\alpha(\text{AlMnSi})$** 

This phase is formed when manganese and silicon are present in aluminum alloys in the absence of iron (Fig. 264). At high concentrations of manganese and silicon it may be present in the form of primary crystals, such as those shown in Fig. 265, associated with primary sili-

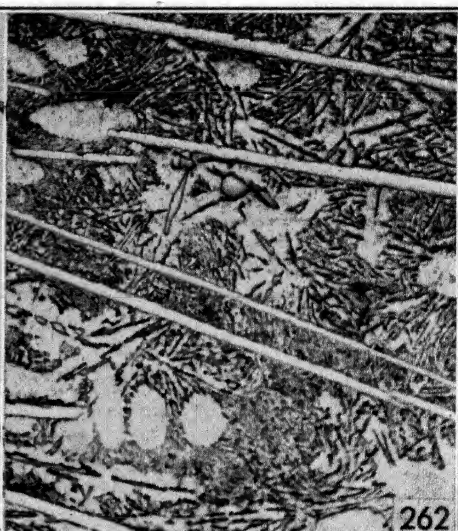
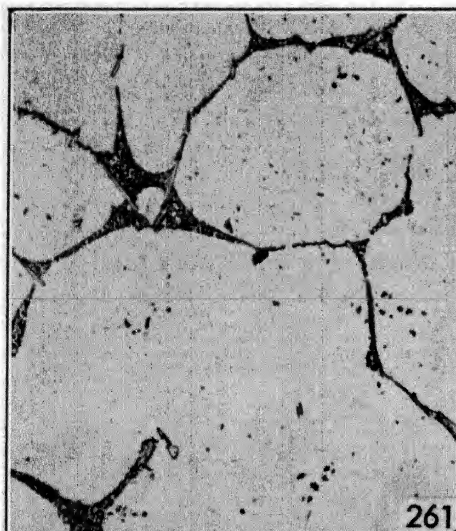


FIG. 261. Needles of  $\text{FeSiAl}_5$  in the eutectic Al-Si. Sand-cast—Fe 0.93%, Si 1.91%—X 250, not etched.

FIG. 262. Long needles of primary  $\text{FeSiAl}_5$  on a background of eutectic Al-Si. Sand-cast—Fe 2.94%, Si 11.34%—X 250, not etched.

FIG. 263. Light crystal of  $\delta(\text{AlFeSi})$  in its typical form, near by another crystal mostly transformed to  $\text{FeSiAl}_5$  and blackened by the etching. In the background primary and eutectic Si. Sand-cast—Fe 3.32%, Si 16.38%—X 75, etched with HF.

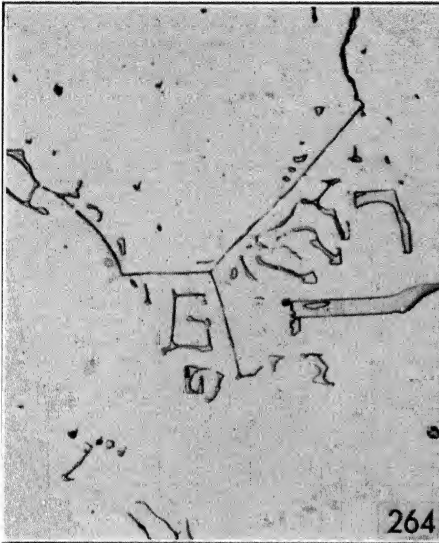


FIG. 264. Typical form of  $\alpha(\text{AlMnSi})$ . Sand-cast—Mn 1.35%, Si 0.53%, Fe 0.01%—X 250, not etched.

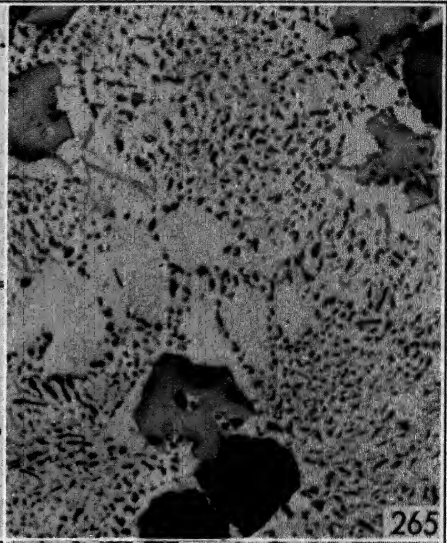


FIG. 265. Primary crystals of  $\alpha(\text{AlMnSi})$  light, Si crystals dark. Sand-cast, heat-treated—Mn 1.65%, Si 12.98%, Fe 0.01%—X 250, not etched.

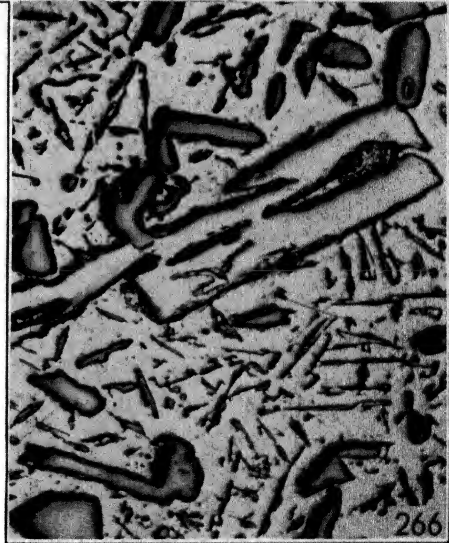


FIG. 266. Crystal of  $\delta(\text{AlMnSi})$  light, surrounded by primary and eutectic Si. Sand-cast—Mn 2.25%, Si 17.70%, Fe 0.01%—X 75, not etched.

con crystals. When iron is present in the alloy, the quaternary phase  $\alpha(\text{AlFeMnSi})$  is formed, which can hardly be distinguished from  $\alpha(\text{AlMnSi})$ .  $\alpha(\text{AlMnSi})$  is light in color and is not attacked by most of the usual etching reagents.

### $\delta(\text{AlMnSi})$

This phase is similar to the  $\delta(\text{AlFeSi})$  illustrated above, and there is no appreciable difference in form or etching characteristics between the two. Figure 266 shows a typical crystal of  $\delta(\text{AlMnSi})$  in the midst of silicon.  $\delta(\text{AlMnSi})$  is light, hard, and has the tendency to stand in relief on polishing.

### $\text{AlCrFeSi}$

When chromium and silicon are present together with iron in aluminum alloys, this phase is formed. It is probably a solid solution of iron in  $\alpha(\text{AlCrSi})$ . Its form does not differ very much from that of the constituents from which it is formed. Figure 267 shows it in the primary and eutectic form in a silicon alloy. Its etching characteristics are somewhat variable and range from those of  $\alpha(\text{AlCrSi})$  to those reported in the table.

### $\text{AlCuFeMn}$

This phase usually is present in alloys of the duralumin type when chilled. With slow cooling it does not form since it is an unstable phase. It probably derives from the unstable  $\omega(\text{AlCuFe})$  in which manganese is substituted for some iron. Its typical form is shown in Fig. 268. It is very hard to distinguish from  $\alpha(\text{AlFeMnSi})$  because the typical form is almost the same.  $\alpha(\text{AlFeMnSi})$  tends to be more elongated, especially when it contains high silicon, and the etching characteristics differ very little. The only difference is that sulfuric acid attacks  $\text{AlCuFeMn}$  brown to blue, whereas  $\alpha(\text{AlFeMnSi})$  is attacked black.

### $\text{AlCuFeNi}$

This phase is commonly present in the alloys of the  $\text{AlCuNi}$  type when chilled. It is unstable and with slow cooling does not form at all. Very little is known about its composition, but it is probably a solid solution of nickel in  $(\text{CuFe})\text{Al}_3$ , in which copper and nickel are present in limited amounts. Usually it is present in the form of globules or small needles (Fig. 269).



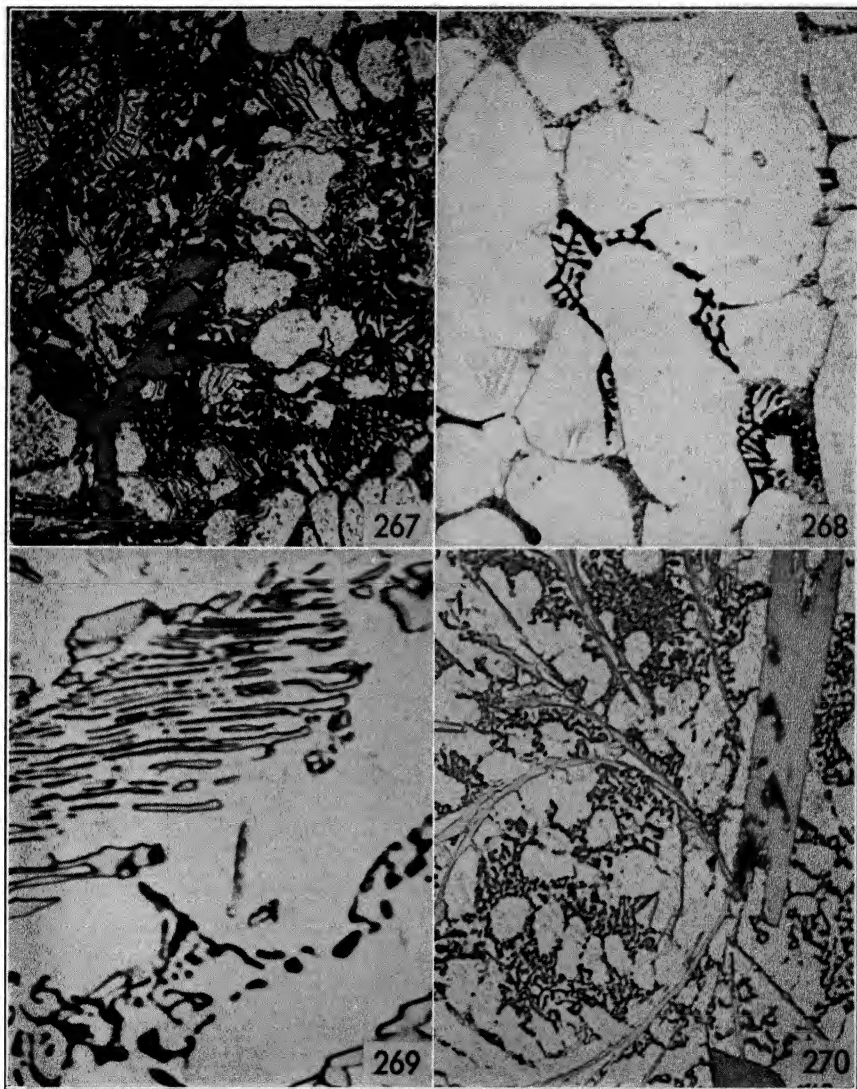


FIG. 267. Primary crystals of  $\text{AlCrFeSi}$  partly etched, eutectic crystals in the form of Chinese script in the midst of the  $\text{Al-Si}$  eutectic. Cast in permanent mold— $\text{Cr}$  0.58%,  $\text{Fe}$  1.70%,  $\text{Si}$  18.89%— $\times 250$ , etched with  $\text{HF}$ .

FIG. 268.  $\text{AlCuFeMn}$  black etched, in the midst of eutectic  $\text{Al-CuAl}_2\text{-Mg}_2\text{Si}$  (?). Segregation in water-cooled ingot— $\text{Cu}$  6.45%,  $\text{Fe}$  0.86%,  $\text{Si}$  0.69%,  $\text{Mn}$  0.54%,  $\text{Mg}$  1.13%— $\times 500$ , etched with  $\text{H}_2\text{SO}_4$ .

FIG. 269.  $\text{AlCuFeNi}$  light, black  $\text{Mg}_2\text{Si}$ . Ingot water-cooled— $\text{Cu}$  2.22%,  $\text{Fe}$  1.12%,  $\text{Mg}$  2.14%,  $\text{Ni}$  1.05%,  $\text{Si}$  1.17%— $\times 1000$ , not etched.

FIG. 270. Needles of  $\text{AlCuFeSi}$ , light crystal of primary  $\delta(\text{AlFeSi})$ , primary and eutectic  $\text{Si}$ . Cast in permanent mold— $\text{Cu}$  1.15%,  $\text{Fe}$  1.03%,  $\text{Si}$  19.66%— $\times 250$ , not etched.



**AlCuFeSi**

This phase is formed by a mixture of  $\text{FeSiAl}_5$  and  $\text{Cu}_2\text{FeAl}_7$  which, being isomorphic, crystallize together. Its form is the same as that of the two phases from which it derives, namely, long thin needles which tend to be curved. The etching characteristics are slightly different. Figure 270 illustrates it in a complex silicon alloy, together with a crystal of  $\delta(\text{AlFeSi})$ .

**CuMg<sub>5</sub>Si<sub>4</sub>Al<sub>4</sub>**

This quaternary phase is present in alloys where the Mg : Si ratio is below 1.73, that is, where there is more silicon than necessary for the formation of  $\text{Mg}_2\text{Si}$ . It is never present as primary crystals in commercial alloys. Owing to the high solid solubility of its components, usually it is not visible. In many commercial alloys it is formed by peritectic reaction from  $\text{Mg}_2\text{Si}$ . For this reason sometimes it is found in the form of a sheath around  $\text{Mg}_2\text{Si}$ , as in the specimen shown in Fig. 272.

Figure 271 shows its typical form of needles. Its color is slightly darker than  $\text{CuAl}_2$  and lighter than Si, with which it is commonly associated.

**AlFeMgSi**

This phase is formed by peritectic reaction from  $\text{FeSiAl}_5$ . Little is known about its field of existence or its presence in commercial alloys. Figure 273 shows it in its typical form of Chinese script. It is very light and tends to have a watery appearance. It is not darkened by any of the common etching reagents.

 **$\alpha(\text{AlFeMnSi})$  and  $\delta(\text{AlFeMnSi})$** 

These two phases have exactly the same form as the corresponding phases in the aluminum-manganese-silicon and aluminum-iron-silicon alloys, for they are mixed crystals of the two. The etching characteristics of  $\alpha(\text{AlFeMnSi})$  (Fig. 274) are slightly different.  $\delta(\text{AlFeMnSi})$  is not etched by any reagent, as are the two ternary phases.

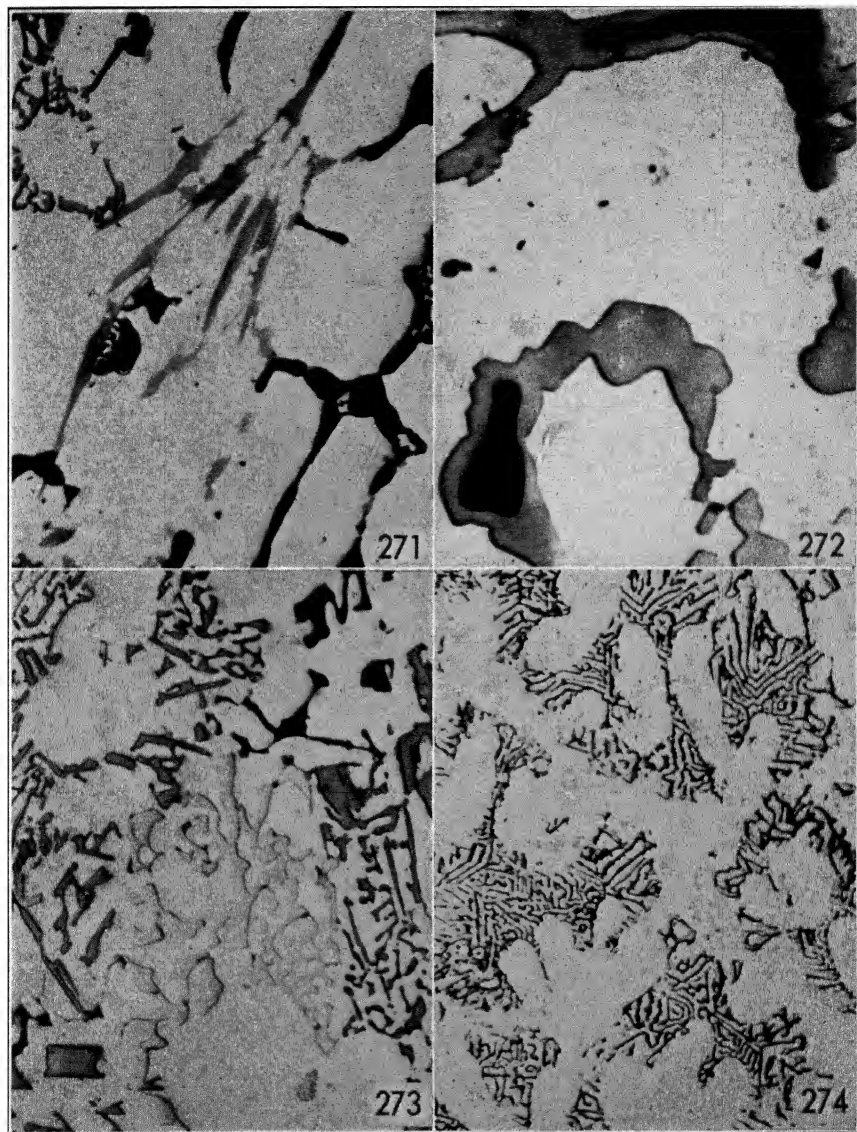


FIG. 271. Needles of  $\text{CuMg}_5\text{Si}_4\text{Al}_4$ , black  $\text{CuAl}_2$ , gray relieved Si. Sand-cast—Cu 10.24%, Mg 2.40%, Si 4.05%, Fe 0.01%—X 250, etched with  $\text{Fe}(\text{NO}_3)_3$ .

FIG. 272. Core of  $\text{Mg}_2\text{Si}$  (black), surrounded by  $\text{CuMg}_5\text{Si}_4\text{Al}_4$  formed by peritectic reaction. Sand-cast—Cu 2.77%, Mg 6.00%, Si 6.66%—X 1000, not etched.

FIG. 273.  $\text{AlFeMgSi}$  light, gray Si, black  $\text{Mg}_2\text{Si}$ . Ingot—Fe 0.72%, Mg 6.79%, Si 5.96%—X 250, not etched.

FIG. 274.  $\alpha(\text{AlFeMnSi})$  in its Chinese script form. Cast in permanent mold—Fe 1.77%, Mn 0.79%, Si 1.00%—X 500, not etched.

ETCHING CHARACTERISTICS OF CONSTITUENTS IN ALUMINUM ALLOYS

Constituent	Not Etched	$\text{Fe}(\text{NO}_3)_3$ , 25%, 30 Sec, by Swabbing	$\text{H}_2\text{SO}_4$ , 20%, 160°F, 30 Sec, by Immersion	$\text{HNO}_3$ , 25%, 160°F, 40 Sec, by Immersion	$\text{HF}$ , 0.5%, 15 Sec, by Swabbing	$\text{NaOH}$ , 10%, 160°F, 5 Sec, by Immersion	Acid Mixture, 0.5% $\text{HF}$ , 1.5% $\text{HCl}$ , 2.5% $\text{HNO}_3$ , 15 Sec, by Immersion
Bi	Gray to black	Black	Black	Black	Black	Black	Black
Pb	Gray to black	Black	Black	Black	Black	Black	Black
Si	Slate-gray	Unattacked	Unattacked	Unattacked	Lighter	Unattacked	Unattacked
$\text{Co}_2\text{Al}_9$	Pale violet	Unattacked	Unattacked	Unattacked	Light brown	Light brown	Light brown
$\text{CrAl}_7$	Gray	Unattacked	Unattacked	Unattacked	Unattacked	Light brown to blue	Unattacked
$\text{CuAl}_2$	Pale pink	Dark brown to black	Lighter	Black	Unattacked	Light to dark brown	Unattacked
$\text{FeAl}_3$ and $\text{Fe}_2\text{Al}_7$	Purplish-gray	Unattacked	Black	Unattacked	Light to dark brown	Dark brown	Slightly darkened
$\text{Mg}_2\text{Al}_3$	Pale ivory	Unattacked	Black	Unattacked	Unattacked	Light to dark brown	Black
$\text{MnAl}_6$	Pale blue	Unattacked	Unattacked	Unattacked	Slightly darkened	Brown to blue	Unattacked
$\text{NiAl}_3$	Yellowish-gray	Unattacked	Unattacked	Unattacked	Brown to blue	Dark brown to blue	Brown to black
$\text{TiAl}_3$	Gray	Unattacked	Unattacked	Unattacked	Darkened	Light brown	Darkened
$\text{Mg}_2\text{Si}$	From blue-gray to blue or black	Black	Black	Black	Dark brown, eaten	Brown	Black
$\text{MgZn}_2$ and $\text{MgZn}_5$	Light gray	Black, eaten	Black, eaten	Black, eaten	Brown	Unattacked	Black, eaten
$\text{AlCoFe}$	Pale violet	Unattacked	Unattacked	Unattacked	Dark brown to black	Brown	Dark brown to black
$(\text{CrFe})\text{Al}_7$	Gray	Unattacked	Unattacked	Unattacked	Light brown	Dark brown to black	Light brown
$\text{AlCrMg}$	Pale gray-yellow	Unattacked	Unattacked	Unattacked	Light brown	Light brown	Light brown

$\alpha(\text{AlCrSi})$	Gray	Unattacked	Unattacked	Unattacked	Unattacked	Light brown	Light brown	Light brown
$\beta(\text{AlCrSi})$	Light gray	Unattacked	Unattacked	Unattacked	Unattacked	Unattacked	Unattacked	Unattacked
$(\text{CuFe})\text{Al}_3$	Light yellowish gray	Unattacked	Unattacked	Unattacked	Unattacked	Brown	Dark brown to blue	Black
$\text{Cu}_2\text{FeAl}_7$	Light gray	Unattacked	Unattacked	Unattacked	Unattacked	Unattacked	Light brown	Light brown
$\omega(\text{AlCuFe})$	Gray	Unattacked	Light brown	Unattacked	Unattacked	Light brown	Unattacked	Brown
$\text{Cu}_2\text{Mg}_2\text{Al}_5$	From pale brown to black	Black	Black	Black	Black	Black	Black	Black
$\text{CuMg}_4\text{Al}_6$	From pale to dark brown	Black	Black	Black	Black	Black	Black	Black
$\text{AlCuMn}$	Brown gray	Unattacked	Unattacked	Unattacked	Unattacked	Brown to blue	Light brown	Black
$(\text{CuNi})_2\text{Al}_3$	Gray	Unattacked	Unattacked	Unattacked	Unattacked	Light brown	Light brown	Brown to black
$\text{AlCuNi}$	Gray	Unattacked	Unattacked	Unattacked	Unattacked	Unattacked	Unattacked	Unattacked
$(\text{FeMn})\text{Al}_6$	Gray	Unattacked	Unattacked	Unattacked	Unattacked	Brown to blue	Brown to blue	Darkened
$\text{FeNiAl}_9$	Gray	Unattacked	Unattacked	Unattacked	Unattacked	Dark brown to blue	Light brown	Dark brown to blue
$\alpha(\text{AlFeSi})$	Gray violet	Unattacked	Black	Unattacked	Unattacked	Light brown	Dark brown	Brown
$\text{FeSiAl}_5$	Light gray	Unattacked	Unattacked	Unattacked	Unattacked	Unattacked	Light brown	Dark brown
$\delta(\text{AlFeSi})$	Very light gray	Unattacked	Unattacked	Unattacked	Unattacked	Light brown	Unattacked	Light brown
$\text{Mg}_2\text{Zn}_2\text{Al}_2$	Light gray	Brown to black	Black	Black	Black	Brown to black	Unattacked	Black
$\alpha(\text{AlMnSi})$	Gray	Unattacked	Light brown	Unattacked	Unattacked	Light brown	Unattacked	Light brown
$\delta(\text{AlMnSi})$	Light gray	Unattacked	Unattacked	Unattacked	Unattacked	Slightly darkened	Slightly darkened	Slightly darkened
$\text{AlCrFeSi}$	Gray	Unattacked	Black	Unattacked	Unattacked	Light brown	Light brown	Light brown
$\text{AlCuFeMn}$	Gray	Unattacked	Brown to blue	Unattacked	Unattacked	Dark brown to blue	Unattacked	Dark brown to blue
$\text{AlCuFeNi}$	Light brown-gray	Unattacked	Unattacked	Unattacked	Unattacked	Brown to blue	Brown to blue	Brown to blue
$\text{AlCuFeSi}$	Light gray	Unattacked	Light brown to black	Unattacked	Unattacked	Dark brown	Light brown	Dark brown
$\text{CuMg}_5\text{Si}_4\text{Al}_4$	Gray	Unattacked	Unattacked	Unattacked	Unattacked	Dark brown to black	Unattacked	Black
$\text{AlFeMgSi}$	Very light gray-blue	Unattacked	Unattacked	Unattacked	Unattacked	Unattacked	Unattacked	Unattacked
$\alpha(\text{AlFeMnSi})$	Gray	Unattacked	Black	Unattacked	Unattacked	Dark brown	Dark brown	Light brown
$\delta(\text{AlFeMnSi})$	Light gray	Unattacked	Unattacked	Unattacked	Unattacked	Light brown	Light brown	Light brown

# PART III

## COMMERCIAL ALLOYS

### CHAPTER 8

#### MASTER ALLOYS

By the terms *master alloys*, *rich alloys*, *hardeners*, etc., are meant all those alloys which are prepared as intermediate compositions in order to facilitate the addition of alloying elements to aluminum. They are used generally to add the elements which do not easily dissolve in aluminum, like manganese, nickel, and cobalt; but there are cases in which they are prepared to assure the addition of the correct amount (usually small) without difficulty.

As a rule, the master alloys are binary, and more than one is used to add several constituents. Sometimes, however, ternary or complex alloys are used when the amount of production warrants the greater difficulties involved in their preparation.

With the exception of metals with low melting points, like magnesium, tin, and zinc, most elements are added to aluminum through hardeners, and the most common of them are:

Aluminum-copper	50%, 33% Cu
Aluminum-silicon	30%, 20%, 13% Si
Aluminum-manganese	10%, 5% Mn
Aluminum-nickel	20%, 10% Ni
Aluminum-cobalt	10%, 5% Co
Aluminum-chromium	5%, 2% Cr
Aluminum-iron	10%, 5% Fe
Aluminum-titanium	5%, 1% Ti
Aluminum-vanadium	5%, 2.5% V

Aluminum-magnesium 30% Mg and 10% Mg are also used at times to add small amounts of magnesium while avoiding the losses through oxidation, which might change the composition.

Among the ternary alloys most commonly used are:

Aluminum-copper-manganese	20-30% Cu, 5-10% Mn
Aluminum-nickel-silicon	20-30% Ni, 5-10% Si
Aluminum-silicon-cobalt	20-30% Si, 2- 5% Co
Aluminum-copper-iron	20-30% Cu, 5-10% Fe

Several other master alloys have been used from time to time, among them aluminum-copper-nickel for the preparation of aluminum-copper-nickel alloys and aluminum-magnesium-silicon for the preparation of magnesium-silicide type alloys.

The micro-examination of master alloys is unimportant. The identification of the constituents in them is of little value since, in remelting, new constituents may be formed. Even the presence of inclusions, porosity, or shrinkage cavities has no definite meaning because a certain amount of oxide in the master alloys that require high temperatures for their preparation is almost unavoidable and does not affect the properties of the final alloy, especially if the amount of master alloy added is small and the final alloy is properly fluxed prior to pouring.

The detection of heavy segregation is of some importance, although microscopic examination is not the best method of detecting it. Segregation within an ingot has almost no importance, whereas differences in composition between different ingots are almost unavoidable and may reach unsuspected proportions. If the microscope is used to detect segregation, several samples from different ingots should be examined in succession.

Also, microscopic examination can be useful as a rapid means of determining the approximate composition of a master alloy within limits sufficiently precise for most applications. An experienced metallographer can tell within 1 per cent the composition of a 33 per cent copper or a 13 per cent silicon alloy and, once trained on the job, can distinguish the approximate composition of most of the master alloys.

### **Aluminum-Copper Master Alloys**

Two aluminum-copper alloys commonly are used: the 50 per cent copper and the 33 per cent copper. The main constituent in the microstructure in both cases is  $\text{CuAl}_2$ , mostly as primary crystals in the 50 per cent copper, as eutectic  $\text{Al-CuAl}_2$  in the 33 per cent copper. Figure 275 shows the structure of the 50 per cent copper alloy. The primary crystals of  $\text{CuAl}_2$  are tetragonal and are embedded in a matrix of eutectic  $\text{Al-CuAl}_2$ . The usual impurities are iron and silicon. Most times they cannot be seen because they are probably dispersed in the eutectic or are in solid solution in  $\text{CuAl}_2$ .

### **Aluminum-Silicon Master Alloys**

Three aluminum-silicon alloys are in common use: the 13 per cent, the 20 per cent, and the 30 per cent. Figure 276 shows the microstructure of a 30 per cent silicon alloy. The constituents are primary

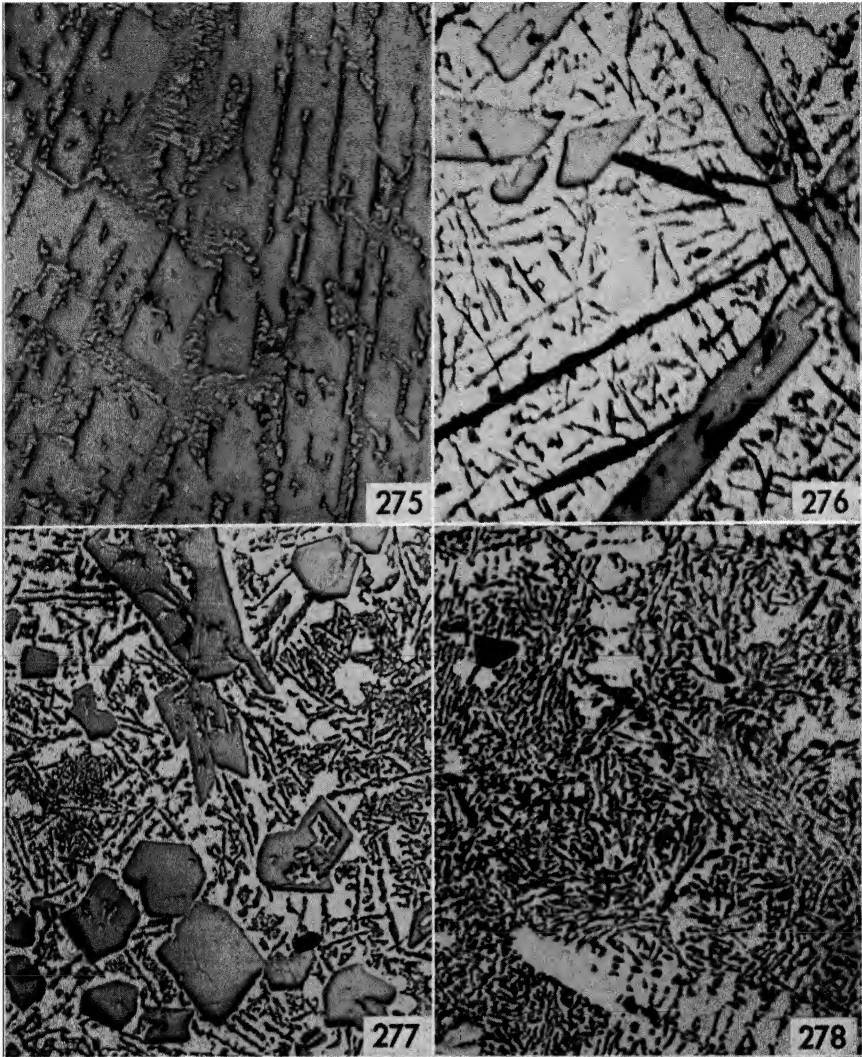


FIG. 275. Ingot—Cu 49.80%, Fe 0.61%, Si 0.39%. Primary crystals of  $\text{CuAl}_2$  in a background of eutectic  $\text{Al-CuAl}_2$ , X 75, not etched.

FIG. 276. Ingot—Si 30.21%, Fe 0.84%, Cu 0.12%. Si primary and eutectic, dark-etched needles of  $\text{FeSiAl}_5$ , X 75, etched with HF.

FIG. 277. Ingot—Si 19.87%, Fe 0.46%. Si primary and eutectic partly modified, X 75, not etched.

FIG. 278. Ingot—Si 13.10%, Fe 0.37%. Si primary and eutectic partly modified, some primary Al, X 75, not etched.

and eutectic Si and, in the form of long needles,  $\text{FeSiAl}_5$ . Figure 277 shows a 20 per cent silicon alloy. The structure is almost the same, but of course the amount of primary Si is less and the crystals tend to be less elongated. The 13 per cent alloy is eutectic; Fig. 278 shows a sample of it. On account of local segregations primary Si and primary Al appear together with the eutectic partly modified. Owing to the use of fluxes containing sodium or potassium salts, these alloys sometimes show the modified structure.

### **Aluminum-Manganese Master Alloys**

The most often used aluminum-manganese alloys are the 5 per cent and the 10 per cent. No higher percentages are common, for the addition of manganese to aluminum raises the melting point of the alloys and their preparation becomes difficult.

Figure 279 shows a 10 per cent manganese alloy. There are needles which were originally  $\text{MnAl}_3$ , transformed to  $\text{MnAl}_4$  and partially to  $\text{MnAl}_6$ . Primary  $\text{MnAl}_6$  forms the typical pattern at the bottom of the figure.

### **Aluminum-Nickel Master Alloys**

The most commonly used aluminum-nickel alloys contain 10 per cent or 20 per cent nominal nickel. Figure 280 shows the 10 per cent nickel alloy; primary and eutectic  $\text{NiAl}_3$  are the constituents visible. Occasionally the phase  $\text{FeNiAl}_9$  is present. Usually, however, the iron is in solid solution in  $\text{NiAl}_3$  and cannot be seen. Silicon is probably in solid solution in the aluminum or in the  $\text{NiAl}_3$  or dispersed in the eutectic.

### **Aluminum-Cobalt Master Alloys**

The cobalt master alloy commonly used has a nominal content of 5 per cent cobalt. The 10 per cent cobalt alloy is used very seldom because of the high temperatures necessary for its production. Figure 281 shows the 5 per cent cobalt alloy, where  $\text{Co}_2\text{Al}_9$  and Al are the constituents visible.

### **Aluminum-Chromium Master Alloys**

The chromium master alloys commonly used contain 5 or 2.5 per cent chromium. Figure 282 shows the 5 per cent chromium alloy. The primary crystals, mostly hexagonal, are  $\text{Cr}_2\text{Al}_{11}$ , probably partly transformed to  $\text{CrAl}_7$ . The needle-form crystals are primary  $\text{CrAl}_7$ ; the small points are probably a  $\text{AlCrSi}$  compound.



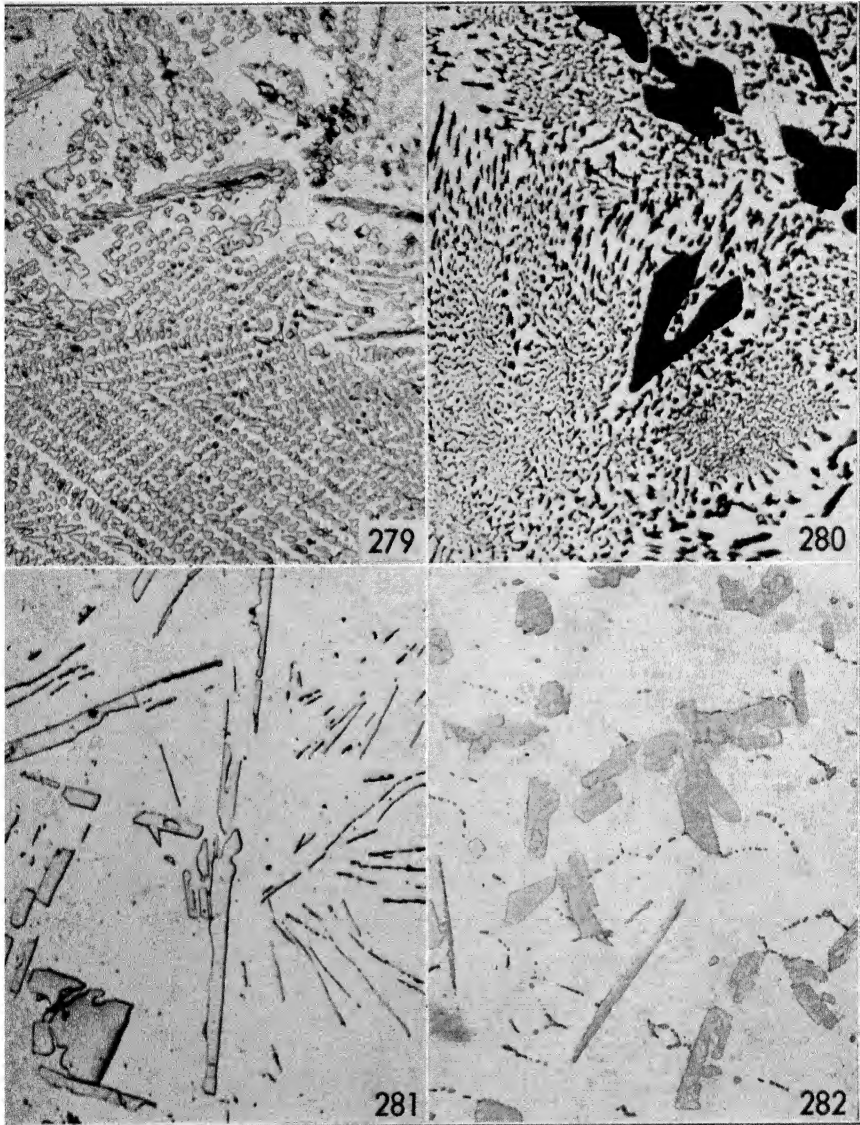


FIG. 279. Ingot—Mn 9.84%, Fe 0.32%, Si 0.31%. Needles of  $\text{MnAl}_3$ , transformed to  $\text{MnAl}_4$  and partially to  $\text{MnAl}_6$ , typical pattern of chilled  $\text{MnAl}_6$ , X 75, not etched.

FIG. 280. Ingot—Ni 9.95%, Fe 0.47%, Si 0.31%.  $\text{NiAl}_3$  primary and eutectic, X 250, etched with HF.

FIG. 281. Ingot—Co 4.94%, Fe 0.56%, Si 0.32%.  $\text{Co}_2\text{Al}_9$  primary and eutectic, X 250, not etched.

FIG. 282. Ingot—Cr 5.17%, Fe 0.81%, Si 0.51%. Crystals of  $\text{Cr}_2\text{Al}_{11}$  hexagonal, needles of  $\text{CrAl}_7$ , points of  $\alpha(\text{AlCrFeSi})(?)$ , X 75, not etched.

### Aluminum-Iron Master Alloys

The alloys used in the rare cases when it is necessary to raise the iron content of aluminum are the 10 per cent iron and the 5 per cent iron. Figure 283 shows the 10 per cent iron alloy. The primary crystals are probably  $\text{FeAl}_3$  and the eutectic crystals  $\text{Fe}_2\text{Al}_7$ , however the identification of the two iron constituents is rather doubtful.

### Aluminum-Titanium Master Alloys

Titanium is the most commonly used grain refiner. Master alloys usually contain low amounts of titanium, mostly because of the very high temperatures involved in their preparation. Figure 284 shows the 5 per cent titanium alloy, which is the highest percentage alloy used for adding titanium to aluminum.

### Aluminum-Vanadium Master Alloys

Another grain refiner sometimes used is vanadium. It is added in the form of a 5 per cent or 2.5 per cent hardener; the 2.5 per cent is preferred because it dissolves better in aluminum. Figure 285 shows the structure of a 2.5 per cent alloy. Three AlV constituents are visible, transforming peritectically one to the other.

### Aluminum-Magnesium Master Alloys

Aluminum-magnesium master alloys are not in common use, for pure magnesium usually is added to the final alloy just before pouring. In special cases when it is necessary to add a small amount (0.10 to 0.30 per cent magnesium), which must be closely controlled, they are employed. For example, this is done when scrap of magnesium-bearing alloy is remelted in small charges and it is necessary to add the amount of magnesium which is lost during remelting and fluxing without overshooting the right amount. Two magnesium hardeners are used in this connection: a 30 per cent and 10 per cent magnesium. Figure 286 shows the structure of the 30 per cent magnesium alloy. The dark mass is  $\text{Mg}_5\text{Al}_8$ , the white crystals are Al, the black crystals are primary  $\text{Mg}_2\text{Si}$ , and the points and needles are  $\text{Fe}_2\text{Al}_7$ . The 10 per cent magnesium alloy contains the same constituents although, naturally, in different proportions.

### Aluminum-Copper-Manganese Master Alloys

Master alloys of aluminum-copper-manganese are common in European practice for the preparation of duralumin. The alloys are prepared by dissolving the commercial 25/75 manganese-copper in molten

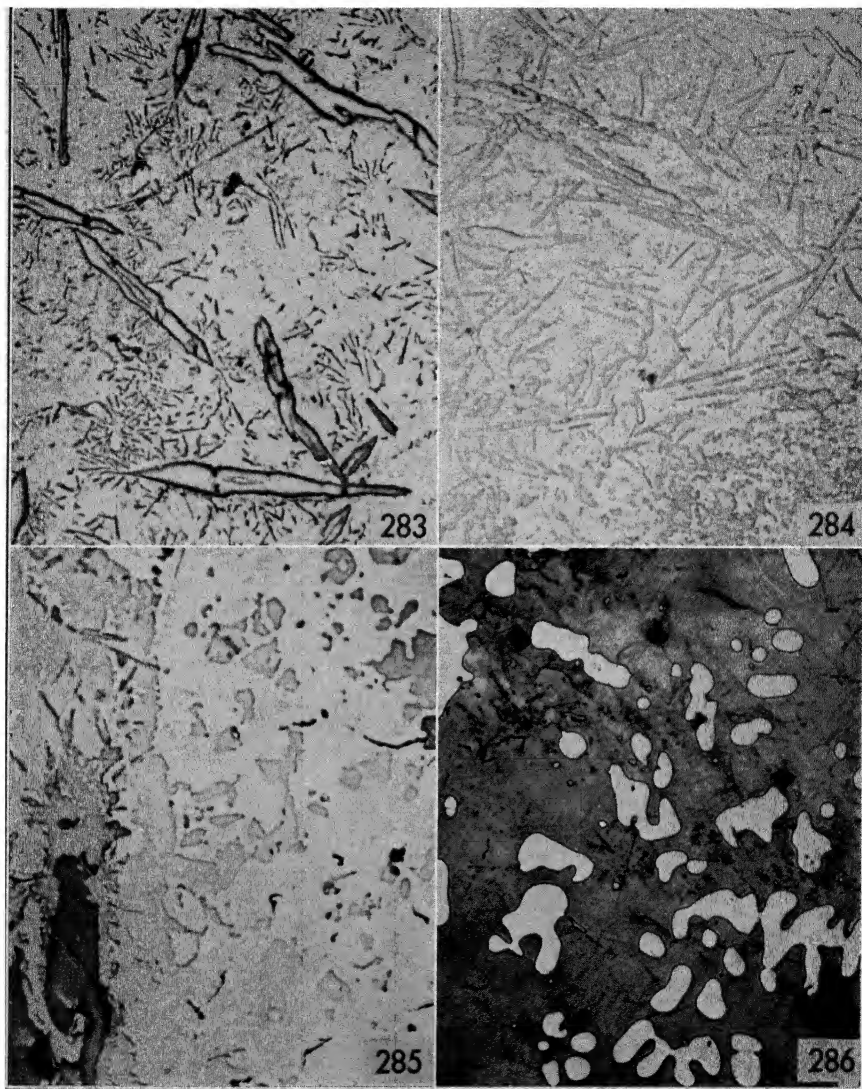


FIG. 283. Ingot—Fe 9.84%, Si 0.28%. Primary crystals of  $\text{FeAl}_3$  (?) and eutectic  $\text{Al-Fe}_2\text{Al}_7$ , X 75, not etched.

FIG. 284. Ingot—Ti 4.57%, Fe 0.55%, Si 0.29%. Primary crystals of  $\text{TiAl}_3$ , small crystals of  $\text{FeSiAl}_5$  or of a  $\text{SiTi}$  constituent, X 75, not etched.

FIG. 285. Ingot—V 2.40%, Fe 0.48%, Si 0.41%. Crystals of  $\text{VAl}_3$  (?) dark gray, surrounded by  $\text{VAl}_4$  (?), surrounded by  $\text{VAl}_7$  (?) light, dark points of  $(\text{AlFeSi})$ , X 75, not etched.

FIG. 286. Ingot—Mg 30.50%, Fe 0.56%, Si 0.47%. Primary  $\text{Mg}_2\text{Si}$  black, Al white, small needles and points of  $\text{FeAl}_3$ , gray background of  $\text{Mg}_5\text{Al}_8$ , X 75, etched with  $\text{Fe}(\text{NO}_3)_3$ .

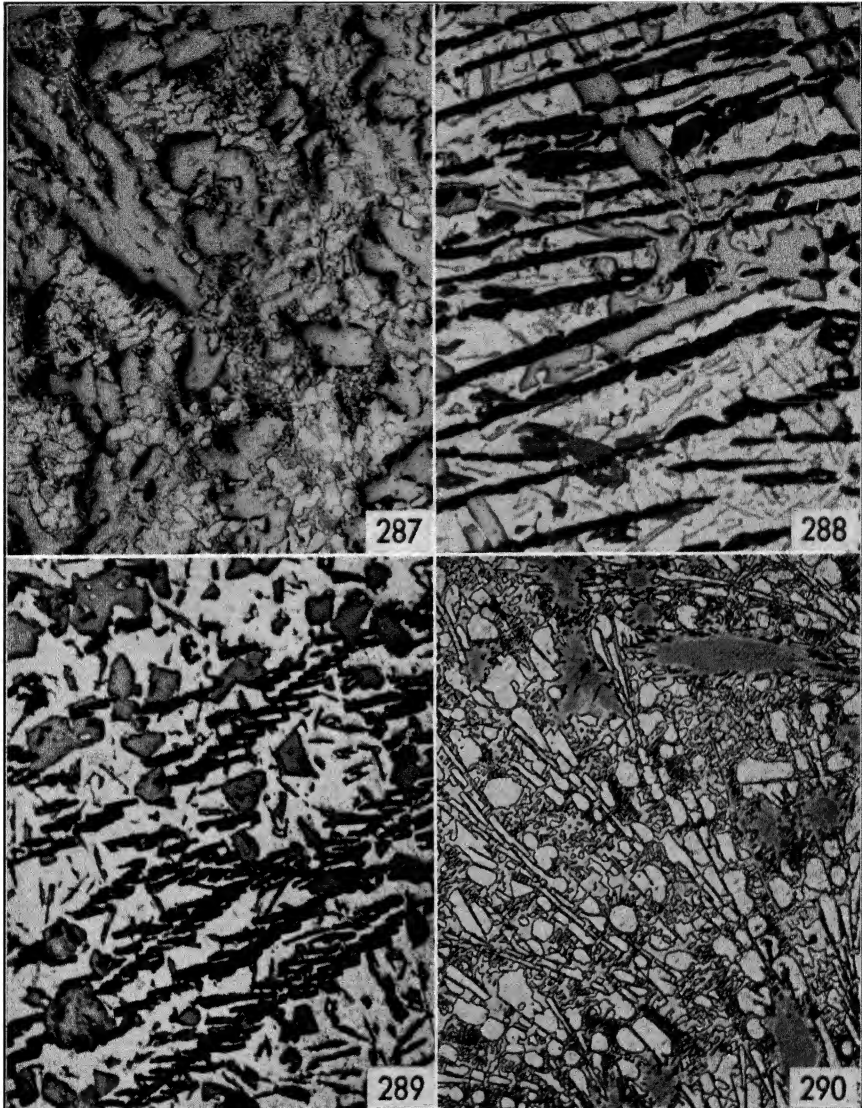


FIG. 287. Ingot—Cu 20.80%, Mn 8.01%, Fe 0.57%, Si 0.32%. Primary crystals of AlCuMn in a background of eutectic Al-CuAl<sub>2</sub>-AlCuMn, X 75, not etched.

FIG. 288. Ingot—Si 16.46%, Ni 13.06%, Fe 0.70%. Dark NiAl<sub>3</sub>, light Si, X 75, etched with HF.

FIG. 289. Ingot—Si 18.82%, Co 4.52%, Fe 0.48%. Black Co<sub>2</sub>Al<sub>9</sub>, light Si, X 75, etched with HF.

FIG. 290. Ingot—Cu 24.30%, Fe 5.02%, Si 0.34%. Crystals of FeAl<sub>3</sub> partially transformed to Cu<sub>2</sub>FeAl<sub>7</sub> needle form, on a background of CuAl<sub>2</sub>, X 75, etched with HF.

aluminum. The copper and manganese contents of these alloys usually range between 15 and 30 per cent copper and 5 to 10 per cent manganese. Sometimes a 30/70 or even a 40/60 manganese-copper alloy is used, in which case the master alloys will have a nominal composition somewhat different from the one reported. Figure 287 shows a 20 per cent copper, 8 per cent manganese alloy, in which the constituents visible are primary AlCuMn, in a background of eutectic Al-CuAl<sub>2</sub>-AlCuMn.

#### **Aluminum-Nickel-Silicon and Aluminum-Cobalt-Silicon Master Alloys**

These alloys usually are employed for the addition of nickel and cobalt to alloys with silicon contents of 18 to 25 per cent. They are used mainly to avoid excessive dilution of the master aluminum-silicon by additions of aluminum. The alloys most frequently used contain 15 to 25 per cent silicon and about 10 per cent nickel or 5 per cent cobalt. Figures 288 and 289 show, respectively, an aluminum-nickel-silicon alloy and an aluminum-cobalt-silicon alloy. The constituents are Si, primary and eutectic in both cases, accompanied by NiAl<sub>3</sub> or Co<sub>2</sub>Al<sub>9</sub> (dark etched).

#### **Aluminum-Copper-Iron Master Alloys**

These alloys are used sometimes for the preparation of alloys of the aluminum-copper-nickel type with high iron content. As the copper content in them is usually about 2 or 3 per cent and it is necessary to add 0.5 to 1 per cent iron, the most commonly used alloys contain from 20 to 30 per cent copper and from 5 to 10 per cent iron. Figure 290 shows a 25 per cent copper, 5 per cent iron aluminum-copper-iron alloy, where CuAl<sub>2</sub>, Cu<sub>2</sub>FeAl<sub>7</sub>, and FeAl<sub>3</sub>, surrounded by a sheath of Cu<sub>2</sub>FeAl<sub>7</sub>, are visible.

## CHAPTER 9

### ALUMINUM-COPPER ALLOYS

These alloys, which were the first to be used to any great extent at the beginning of the aluminum industry, are still favorably regarded as casting alloys, in spite of their many weaknesses, partly on account of their all-around fair properties, partly on account of the large backlog of scrap existing in the market, which makes it difficult for the users to shift to another alloy economically.

Five main groups of these alloys can be distinguished.

1. Alloys with a copper content of 10 per cent and more.
2. Alloys with a copper content of 6 to 8 per cent.
3. Alloys with a copper content of 4 to 6 per cent.
4. Alloys containing copper and silicon.
5. Alloys containing copper and zinc.

Alloys with intermediate compositions have been used from time to time and probably are still in use, but there are sufficient differences among the five groups to justify the above division.

#### Aluminum-Copper Alloys with 10 or More Per Cent Copper

The composition of these alloys usually has the following range.

Cu	9 -14%
Fe	0.5-1.5%
Si	0.5-4%
Mg	0 -0.5%

Also, an alloy containing about 14 per cent copper and up to 7 per cent silicon is used to a certain extent. Manganese and nickel sometimes are added in percentages up to 1.5 per cent. Zinc, tin, and lead may be present as impurities in percentages up to 0.5 per cent each, in low-grade secondary material. Sometimes grain refiners like titanium, chromium, vanadium, and molybdenum are added in amounts up to 0.30 per cent.

The microstructure of these alloys is simple; copper is partly in solid solution, usually about 3 to 3.5 per cent in permanent mold castings, and 2 to 2.5 per cent in sand castings, the remaining copper forms

$\text{CuAl}_2$  in a hypo-eutectic network. Iron combines with silicon to form  $\alpha(\text{AlFeSi})$  or  $\text{AlCuFeSi}$ , depending on the ratio  $\text{Fe} : \text{Si}$  in the alloy. The critical ratio is about 1 ( $\text{Fe} = \text{Si}$ ). Usually with such a ratio both  $\alpha(\text{AlFeSi})$  and  $\text{AlCuFeSi}$  are present, although the cooling speed has some influence and may shift the equilibrium in one direction or the other. High speeds of solidification usually produce  $\alpha(\text{AlFeSi})$ ; low speeds,  $\text{AlCuFeSi}$ . With higher ratio ( $\text{Fe}$  lower than  $\text{Si}$ )  $\text{AlCuFeSi}$  is predominant, usually associated with free  $\text{Si}$ .

The presence of magnesium, tin, and zinc in the amounts reported has no effect on the microstructure; even with slow freezing they are in solid solution and not visible, nor do they seem to influence the  $\text{AlFeSi}$  compounds.

Nickel, if present, combines with copper to form  $\text{AlCuFeNi}$ , reducing slightly the amount of  $\text{CuAl}_2$  present. Manganese combines with iron and silicon to form the quaternary  $\alpha(\text{AlFeMnSi})$  even with the  $\text{Fe} : \text{Si}$  ratio favorable to the formation of  $\text{AlCuFeSi}$ .

Titanium, vanadium, molybdenum, and chromium, if added, are present in amounts of the order of 0.05 to 0.20 per cent and are visible only with heavy segregation. Little is known of their effect on the constituents but in the amounts mentioned above their effect cannot be expected to be appreciable.

Figures 291 and 292 show the structure of two alloys of this type, cast in permanent mold, containing, respectively,  $\text{AlCuFeSi}$  and  $\alpha(\text{AlFeSi})$ . Figure 293 shows another sand-cast alloy, and Fig. 294 shows a specimen of the same alloy taken from the crown of a piston after several hundred hours of service. Worthy of note is the reprecipitation of  $\text{CuAl}_2$  caused by the high temperature ( $550^\circ$  to  $650^\circ\text{F}$ — $300^\circ$  to  $350^\circ\text{C}$ ) reached in service.

The eutectics normally present in these alloys are:

$\text{Al-CuAl}_2\text{-AlCuFeSi-Si}$ ;  $968^\circ\text{F}$  ( $520^\circ\text{C}$ ),  $\text{Cu}$  26%,  $\text{Fe}$  0.5%,  $\text{Si}$  6.5%.

$\text{Al-CuAl}_2\text{-Si}$ ;  $977^\circ\text{F}$  ( $525^\circ\text{C}$ ),  $\text{Cu}$  26%,  $\text{Si}$  6%.

$\text{Al-CuAl}_2$ ;  $1018^\circ\text{F}$  ( $548^\circ\text{C}$ ),  $\text{Cu}$  33%.

The temperature for correct heat treatment is limited by the eutectic  $\text{Al-CuAl}_2\text{-AlCuFeSi-Si}$  and must be below  $968^\circ\text{F}$  ( $520^\circ\text{C}$ ). The other elements reported as occasionally present do not affect the eutectics to any appreciable degree, if kept within the limits reported.

The usual heat-treatment practice for these alloys is: soaking at  $900^\circ$  to  $950^\circ\text{F}$  ( $480^\circ$  to  $510^\circ\text{C}$ ) for 4 to 12 hours, followed by quenching in water and artificial aging at  $300^\circ$  to  $400^\circ\text{F}$  ( $150^\circ$  to  $200^\circ\text{C}$ ) for 4 to 12 hours. Sometimes for castings in permanent mold, the soaking and the quenching are omitted and the castings are artificially aged



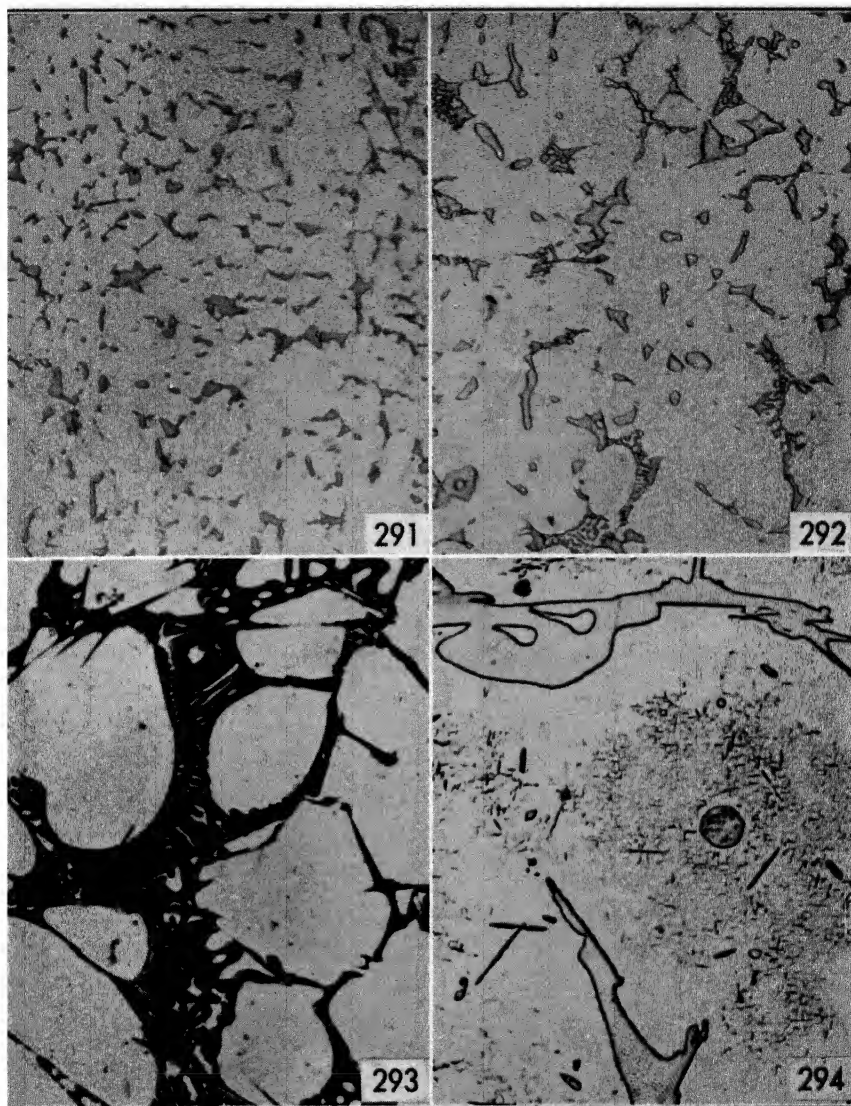


FIG. 291. Cast in permanent mold—Cu 9.88%, Fe 1.50%, Mg 0.45%, Si 0.77%. Globules of  $\text{CuAl}_2$ , needles of  $\text{AlCuFeSi}$  embedded in it and only partly visible, X 250, not etched.

FIG. 292. Same alloy as in Fig. 291, cast in permanent mold. Globules of  $\text{CuAl}_2$  and  $\alpha(\text{AlFeSi})$  as Chinese script, X 250, not etched.

FIG. 293. Sand-cast—Cu 13.20%, Fe 0.57%, Si 0.56%. Network of  $\text{CuAl}_2$  black etched, needles of  $\text{AlCuFeSi}$  embedded in it, X 250, etched with  $\text{Fe}(\text{NO}_3)_3$ .

FIG. 294. Same alloy as in Fig. 293. Crown of a Diesel piston, sand-cast and heat-treated, after several hundred hours of service. Network of  $\text{CuAl}_2$ , points and globules of reprecipitated  $\text{CuAl}_2$ , X 500, not etched.



only, relying on the fast cooling caused by the metallic mold for solution. After aging, the mechanical properties, on the average, are lower than for soaked material and much less uniform.

Natural aging sometimes is employed for castings other than pistons. Annealing at 570° to 650°F (300° to 350°C) for 3 to 4 hours is employed for uses where dimensional stability is the most important factor.

The castability of these alloys is good, especially with alloys containing high silicon, which, however, have the lowest mechanical properties. Machinability is good, especially in the heat-treated condition. The mechanical properties to be expected from these alloys in different conditions are reported in the table.

	YIELD STRENGTH 0.2%; PSI	TENSILE STRENGTH PSI	ELONGA- TION % ON 2 IN.	BRINELL HARDNESS 500/10/30
Sand-cast	15,000-20,000	20,000-25,000	1 -3	60-100
Sand-cast heat-treated	20,000-30,000	30,000-35,000	0 -1	90-130
Permanent-mold cast	18,000-25,000	25,000-30,000	0.5-2	70-110
Permanent mold heat-treated	25,000-35,000	35,000-45,000	0 -1	100-140

Corrosion resistance is not particularly good, as is true of all alloys containing copper.

The main use for these alloys is for cast pistons, for the mechanical properties at high temperature compare favorably with those of other aluminum alloys. Their main drawback for this use is their high-expansion coefficient which, combined with permanent growth, requires large tolerances between cylinder and piston. The permanent growth is the increase of volume caused by the reprecipitation of  $\text{CuAl}_2$  from solid solution, which is produced by the temperatures to which the piston is subjected in service.

### Aluminum-Copper Alloys with 6 to 8 Per Cent Copper

The ranges for the usual compositions of these alloys are:

Cu	6 -8%
Fe	0.3-1.5%
Sn	0 -1%
Si	0.3-4%
Zn	0 -2.5%

Secondary material usually is employed to produce these alloys. For this reason manganese, nickel, chromium, lead, and other elements are common impurities. Magnesium is considered a very dangerous impurity because it tends to liquate on the outside of the casting as  $\text{Mg}_2\text{Si}$ ,

and imparts a blue discoloration which mars the appearance of the surface. The content of magnesium usually is prescribed below 0.10 per cent, although no reliable method of analysis has been agreed upon for its determination.

Sometimes titanium, vanadium, molybdenum, chromium, and even columbium are intentionally added as grain refiners, in percentages below 0.30 per cent.

The microstructure of these alloys is analogous to that of the 10 per cent copper alloys. The constituents present are:  $\text{CuAl}_2$ ,  $\alpha(\text{AlFeSi})$ , or  $\text{AlCuFeSi}$ , and sometimes Si; Zn and Sn are in solid solution and do not appear as separate constituents. The presence of impurities and heat treatment have the same effect on these alloys as in the 10 per cent copper alloys.

The eutectics normally present in these alloys are:

$\text{Al-CuAl}_2\text{-AlCuFeSi-Si}$ ; 968°F (520°C), Cu 26%, Fe 0.5%, Si 6.5%.

$\text{Al-CuAl}_2\text{-Si}$ ; 977°F (525°C), Cu 26%, Si 6%.

$\text{Al-CuAl}_2$ ; 1018°F (548°C), Cu 33%.

Figure 295 shows a sand-cast alloy where  $\text{CuAl}_2$  light,  $\alpha(\text{AlFeSi})$  black, and the eutectic  $\text{Al-CuAl}_2\text{-Si}$  are present. Figure 296 shows another alloy where, the silicon content being much higher than the iron content,  $\text{AlCuFeSi}$  and Si are present together with  $\text{CuAl}_2$ . Figures 297 and 298 show a third alloy, where both  $\alpha(\text{AlFeSi})$  and  $\text{AlCuFeSi}$  are present together with Si as eutectic  $\text{Al-CuAl}_2\text{-AlCuFeSi-Si}$ .

As for the 10 per cent alloys, the maximum safe temperature for heat treatment is below 968°F (520°C) and the practice is the same. However, heat treatment is seldom used in connection with these alloys because the improvement obtained through it does not warrant the cost.

The castability of these alloys is good, especially for alloys with high silicon. Machinability is good although not so good as for the 10 per cent copper alloys, owing to the lack of heat treatment and the higher silicon contents. The mechanical properties to be expected from these alloys are given in the table.

	YIELD STRENGTH 0.2%; PSI	TENSILE STRENGTH PSI	ELONGA- TION % ON 2 IN.	BRINELL HARDNESS 500/10/30
Sand-cast	10,000-15,000	18,000-25,000	0.5-2	65-75
Permanent-mold cast	18,000-25,000	22,000-30,000	0.5-2	70-80
Die-cast	20,000-25,000	30,000-35,000	0.5-2	70-80

Corrosion resistance is not particularly good and is slightly poorer than that of the 10 per cent copper alloys.

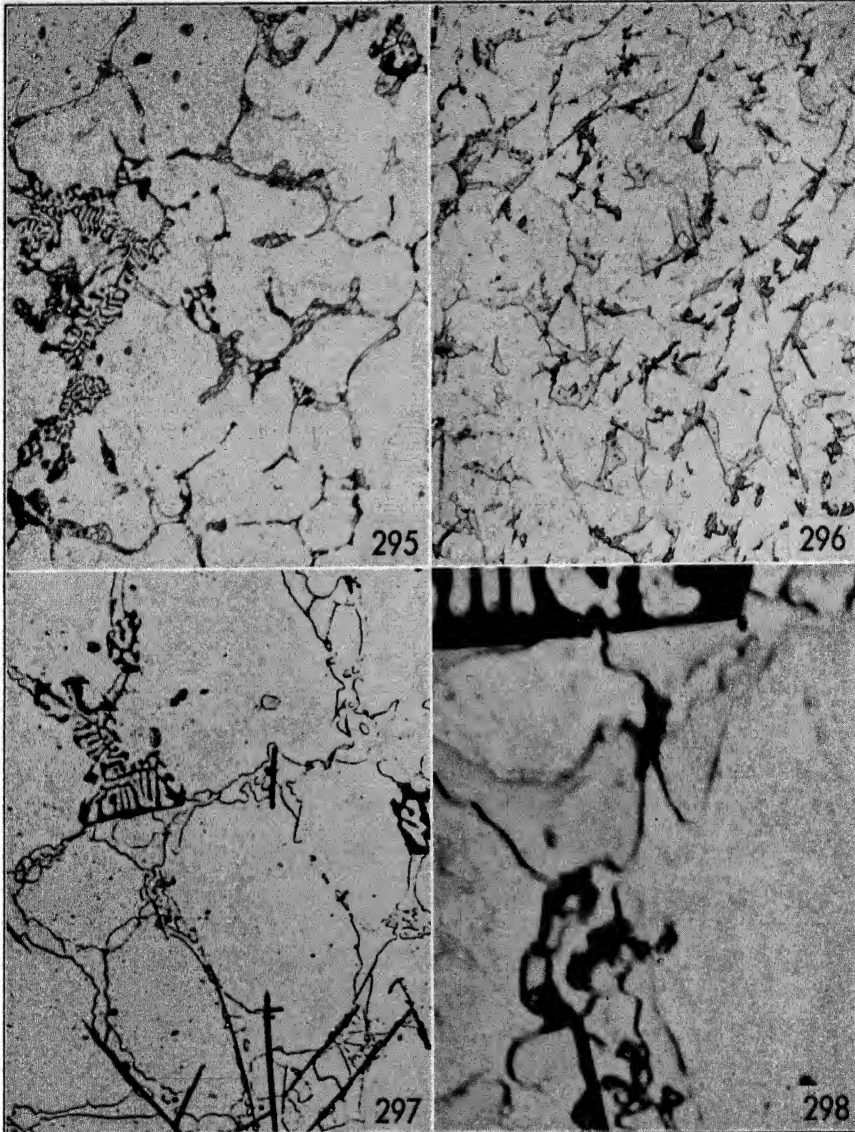


FIG. 295. Ingot—Cu 7.00%, Fe 1.25%, Si 2.03%, Zn 1.85%. Black  $\alpha(\text{AlFeSi})$ , gray Si, light  $\text{CuAl}_2$ , X 250, etched with  $\text{H}_2\text{SO}_4$ .

FIG. 296. Cast in permanent mold—Cu 6.80%, Fe 1.15%, Si 3.71%, Zn 1.75%.  $\text{CuAl}_2$  light, Si gray, needles of  $\text{AlCuFeSi}$ , X 250, etched with HF.

FIG. 297. Sand-cast—Cu 8.84%, Fe 1.18%, Si 1.72%. Light  $\text{CuAl}_2$ , black  $\text{AlCuFeSi}$  needle form, black as Chinese script  $\alpha(\text{AlFeSi})$ , X 250, etched with  $\text{H}_2\text{SO}_4$ .

FIG. 298. Enlargement of Fig. 297 to show the presence of the eutectic  $\text{Al-AlCuFeSi-CuAl}_2\text{-Si}$ , X 1000, etched with  $\text{H}_2\text{SO}_4$ .

These alloys constitute the bulk of the American production of castings and are generally known as No. 12 alloy. They are used extensively for all purposes and there is no casting which at one time or another has not been produced with these alloys. Their good castability, ease of handling, and the wide tolerances permissible in composition make them favorites, especially with small foundries which are not equipped to handle more complex alloys. However, in the last few years, especially in Europe, these alloys have been losing ground in favor of newer alloys, which have better mechanical properties.

### Aluminum-Copper Alloys with 4 to 6 Per Cent Copper

The composition of these alloys ranges within the following limits.

Cu	4 -6%
Fe	0.3-1.5%
Si	0.3-3%
Sn	0 -2%
Zn	0 -4%

Quite often grain refiners are added to these alloys, especially in European practice where titanium is the favorite. One variety of these alloys contains lead and bismuth in amounts of about 0.5 per cent each. These elements, which are somewhat difficult to alloy with aluminum, owing to their limited range of miscibility with liquid aluminum, are added to improve the machinability and produce a free machining material.

Lead and bismuth, being insoluble in solid aluminum, during solidification separate as small inclusions dispersed through the mass. During machining, every time one of these inclusions is hit by the tool, the chip is broken and the tool is freed. Moreover, lead and bismuth, being soft metals with low melting points, act as lubricant between the metal and the tool to a certain extent, thus reducing the wear of the tool.

The microstructure of straight aluminum-copper alloys is quite simple.  $\text{CuAl}_2$ ,  $\alpha(\text{AlFeSi})$ , and/or  $\text{AlCuFeSi}$  and Si are the constituents. The same constituents are present in alloys containing lead and bismuth. In addition, another constituent is present, probably a PbBi compound, insoluble in aluminum.

Figure 299 shows an alloy of this type containing  $\text{CuAl}_2$  and  $\alpha(\text{AlFeSi})$ . Figure 300 shows another alloy containing  $\text{CuAl}_2$  and

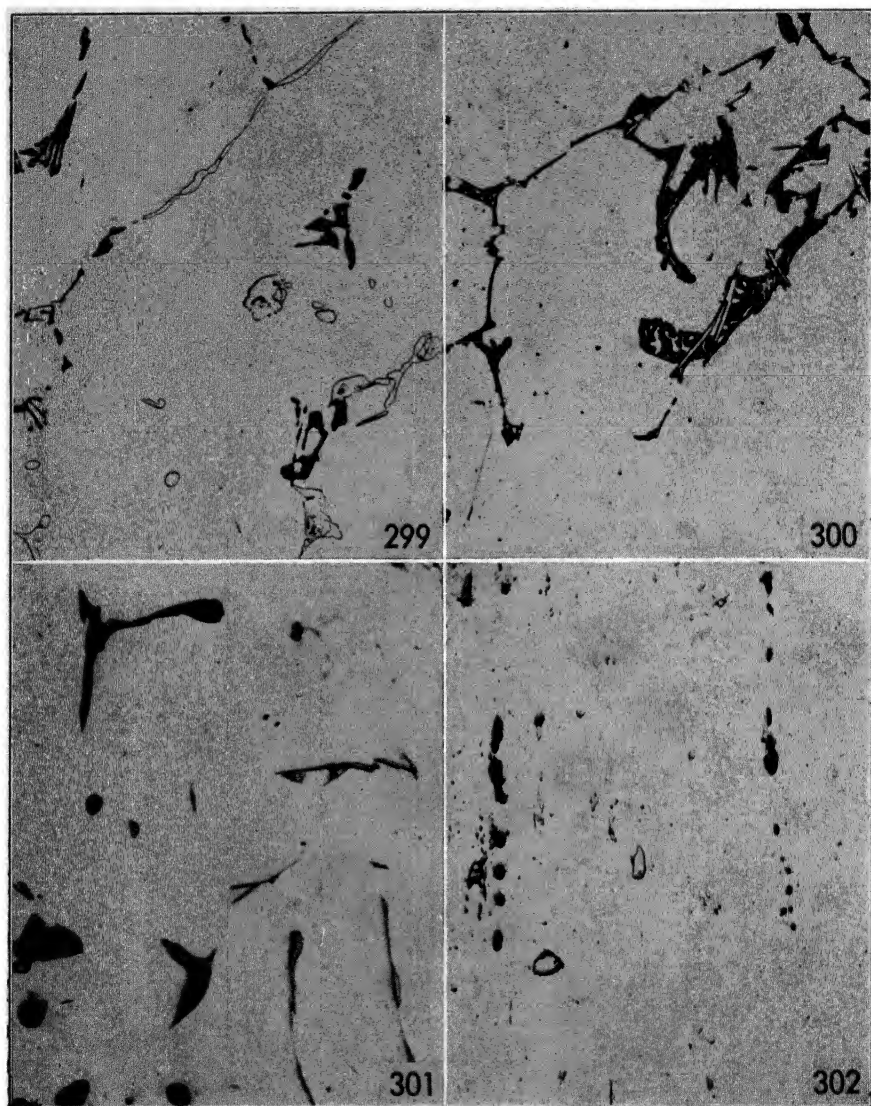


FIG. 299. Sand-cast—Cu 4.26%, Fe 0.56%, Si 0.29%. Light  $\text{CuAl}_2$ , black  $\alpha(\text{AlFeSi})$ , X 250, etched with  $\text{H}_2\text{SO}_4$ .

FIG. 300. Sand-cast—Cu 4.64%, Fe 0.50%, Si 0.67%. Black  $\text{CuAl}_2$ , light needles of  $\text{AlCuFeSi}$ , X 250, etched with  $\text{HNO}_3$ .

FIG. 301. Water-cooled ingot—Cu 5.29%, Bi 0.41%, Pb 0.37%, Fe 0.29%, Si 0.35%. Black globules of the BiPb constituent (?), gray  $\text{CuAl}_2$ , containing needles of  $\text{AlCuFeSi}$ , X 250, not etched.

FIG. 302. Same alloy as in Fig. 301, extruded and heat-treated. Black the BiPb constituent, globules of  $\text{CuAl}_2$  or a FeSi constituent, X 250, not etched.

AlCuFeSi. Figure 301 shows the structure of an ingot for extrusion of the lead-bismuth-bearing alloy. Pb and Bi are black and CuAl<sub>2</sub> contains a few partly visible needles of AlCuFeSi. Figure 302 shows the same alloy extruded and heat-treated: the Pb and Bi have been elongated in the direction of extrusion; a few small particles, probably of CuAl<sub>2</sub>, remain out of solution.

The eutectics which may be present in these alloys are:

Al-CuAl<sub>2</sub>-AlCuFeSi-Si; 968°F (520°C), Cu 26%, Fe 0.5%, Si 6.5%.

Al-CuAl<sub>2</sub>-Si; 977°F (525°C), Cu 26%, Si 6%.

Al-CuAl<sub>2</sub>; 1018°F (548°C), Cu 33%.

In alloys containing tin, the binary eutectic

Al-Sn; 444°F (229°C), Sn 99%

or the ternary

Al-CuAl<sub>2</sub>-Sn; 440°F (227°C), about Sn 99%, Cu 0.5%

may be present on account of segregation.

In alloys containing lead and bismuth the lowest melting point is about 250°F (125°C); therefore, during hot working and heat treatment lead and bismuth are in the molten state. However, on melting, bismuth shrinks and lead dilates. This fact, together with the fact that aluminum is not soluble to any appreciable extent in lead or bismuth, makes their melting harmless. The melting takes place with practically no change in volume, and no deterioration of the surrounding alloy takes place.

Alloys containing appreciable amounts of tin and zinc are not heat-treated as a rule. For alloys with silicon above 0.7 per cent, the heat-treating practice is as follows: soak at 930° to 950°F (500° to 510°C) for 6 to 12 hours followed by quenching in hot water. Alloys to be wrought usually have a low silicon content, and the eutectics Al-CuAl<sub>2</sub>-AlCuFeSi-Si and Al-CuAl<sub>2</sub>-Si are not formed for lack of silicon. The lowest melting eutectic in this case is Al-CuAl<sub>2</sub>. For alloys where the silicon content is below 0.7 per cent the heat treatment can be carried on at higher temperatures and the usual practice is to soak at 970° to 1000°F (520° to 540°C) and follow by quenching and artificial aging.

For the development of their best properties these alloys require artificial aging. This is carried on at 300° to 400°F (150° to 200°C)

for 4 to 12 hours. The properties obtained with these alloys are reported in the table.

	YIELD STRENGTH 0.2%; PSI	TENSILE STRENGTH PSI	ELONGA- TION % ON 2 IN.	BRINELL HARDNESS 500/10/30
Sand-cast	10,000–15,000	18,000–24,000	4–10	60– 80
Sand-cast heat-treated	15,000–25,000	30,000–40,000	5–10	80–100
Permanent-mold cast	12,000–18,000	22,000–27,000	5–10	70– 90
Permanent mold heat- treated	27,000–35,000	35,000–45,000	3–10	75–120
Wrought quenched	30,000–40,000	50,000–55,000	12–20	90–120
Wrought aged	35,000–45,000	55,000–60,000	10–15	100–130

The castability of these alloys is rather poor, owing to the low fluidity and the high-shrinkage coefficient. The tin- and zinc-bearing alloys are an exception, for they have good fluidity, although they have a tendency to be hot-short. The formability is good if the precautions for strong aluminum alloys are observed, with the exception of the tin-bearing alloys, which, owing to the presence of the low-melting eutectics containing tin, can be wrought only at temperatures below 440°F (227°C). Machinability is rather poor, especially in the cast and annealed condition but better in the heat-treated condition. Lead- and bismuth-bearing alloys are an exception because their machinability is better than that of any other aluminum alloy. The corrosion resistance is not particularly good, as for all copper-bearing alloys. In the aged state they are susceptible to intergranular corrosion.

The straight aluminum-copper alloys have lost most of their importance, both as casting and working alloys, although they are still used for small castings in sand where high properties are obtained by heat treatment. Alloys containing tin and zinc are still widely used for the casting of intricate shapes which require a good surface such as patterns. Alloys containing lead and bismuth have a wide field of application on account of their excellent machinability. Produced usually in extruded or rolled bars, they are used as free-machining screw stock.

### Aluminum-Copper-Silicon Alloys

The range of composition of these alloys is wide and covers:

Cu	2–6%
Si	3–6%
Fe	up to 1%

The microstructure of these alloys is rather simple. The constituents usually present are:  $\text{CuAl}_2$ , Si, and  $\text{AlCuFeSi}$  or  $\text{FeSiAl}_5$ .

Figure 303 shows an alloy where  $\text{CuAl}_2$  and  $\text{AlCuFeSi}$  are present. Figure 304 shows an alloy of the same type, cast in permanent mold, where the eutectic  $\text{Al-CuAl}_2\text{-AlCuFeSi-Si}$  is so finely dispersed that it is not resolved at the magnification used.

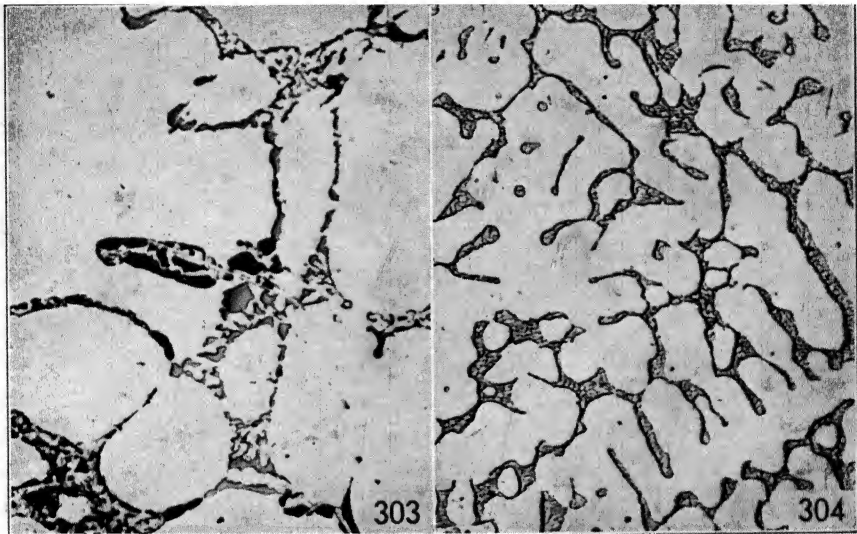


FIG. 303. Sand-cast—Cu 5.30%, Si 3.40%, Fe 0.40%. Black  $\text{CuAl}_2$ , gray Si, light needles of  $\text{AlCuFeSi}$ , X 250, etched with  $\text{Fe}(\text{NO}_3)_3$ .

FIG. 304. Cast in permanent mold—Cu 4.20%, Si 3.50%, Fe 0.25%.  $\text{CuAl}_2$ , Si, and  $\text{AlCuFeSi}$  as eutectics  $\text{Al-AlCuFeSi-CuAl}_2\text{-Si}$  and  $\text{Al-CuAl}_2\text{-Si}$ , only partially resolved by the enlargement used, X 250, not etched.

The eutectics present in these alloys are:

$\text{Al-CuAl}_2\text{-AlCuFeSi-Si}$ ;  $968^\circ\text{F}$  ( $520^\circ\text{C}$ ), Cu 26%, Si 6.5%, Fe 0.5%.

$\text{Al-CuAl}_2\text{-Si}$ ;  $977^\circ\text{F}$  ( $525^\circ\text{C}$ ), Cu 26%, Si 6%.

$\text{Al-CuAl}_2$ ;  $1018^\circ\text{F}$  ( $548^\circ\text{C}$ ), Cu 33%.

$\text{Al-Si}$ ;  $1071^\circ\text{F}$  ( $577^\circ\text{C}$ ), Si 11.7%.

No heat treatment is used for these alloys.

The castability of these alloys is excellent: they retain the fluidity and low-shrinkage coefficient of the silicon alloys, but, by the addition of copper, they lose the tendency to have shrinkage pinholes, characteristic of the straight aluminum-silicon alloys. These alloys have probably the best castability of all the aluminum alloys and for this reason they are used extensively in the die-casting industry. The machinability is not so good and is decidedly inferior to the straight aluminum-copper alloys and probably also to the aluminum-silicon



alloys of the same silicon content. The usual mechanical properties of these alloys are:

	YIELD STRENGTH 0.2%; PSI	TENSILE STRENGTH PSI	ELONGA- TION % ON 2 IN.	BRINELL HARDNESS 500/10/30
Sand-cast	12,000-16,000	20,000-25,000	1-3	55-70
Permanent-mold cast	15,000-19,000	25,000-35,000	1-5	60-75
Die-cast	14,000-20,000	30,000-35,000	1-3	60-75

The corrosion resistance is fair and only slightly less than that of alloys with the same copper content. The finished aspect is good, although alloys with high silicon content tend to be a dull dark gray like straight aluminum-silicon alloys.

The weldability is excellent on account of the high fluidity in the molten state, caused by low-melting eutectics containing silicon.

Owing to their excellent castability and good mechanical properties, these alloys are widely used for mass production of small parts, cast in permanent mold or die-cast, especially for pipes and fittings which must stand high pressures in service. Together with the 8 per cent copper and the 5 per cent silicon alloys, from the mixing of which they derive, these alloys make up the largest part of the material in use for the production of castings for all-round purposes. They are used in preference to the other two for small castings, destined for airplane production, on account of their somewhat superior mechanical properties.

### Aluminum-Copper-Zinc Alloys

The chemical analyses of these alloys range between:

Cu	1- 4%
Fe	up to 1.5%
Mn	0- 1%
Ni	0- 1%
Si	up to 3%
Zn	4-15%

Sometimes magnesium is also added in amounts up to 0.5 per cent.

The microstructure of these alloys is rather simple. Zinc and magnesium are in solid solution and do not form visible constituents. Copper, iron, and silicon form  $\text{CuAl}_2$ ,  $\alpha(\text{AlFeSi})$ , and less often  $\text{AlCuFeSi}$ , as probably the presence of zinc in solid solution displaces the equilibrium from  $\text{AlCuFeSi}$  to  $\alpha(\text{AlFeSi})$ . Manganese, if present,

forms  $\alpha(\text{AlFeMnSi})$ . Nickel combines with copper and sometimes with iron to form  $\text{AlCuNi}$  or  $\text{AlCuFeNi}$ .

Figure 305 illustrates an alloy of this type, sand-cast, in which the constituents visible are  $\alpha(\text{AlFeSi})$ ,  $\text{CuAl}_2$ , and Si, as eutectic  $\text{Al-CuAl}_2\text{-Si}$ . Figure 306 shows another alloy of this type, where, on account of a segregation of iron and silicon, a primary crystal of  $\alpha(\text{AlFeSi})$  is present, together with  $\alpha(\text{AlFeSi})$  as Chinese script, with some  $\text{CuAl}_2$  and Si.

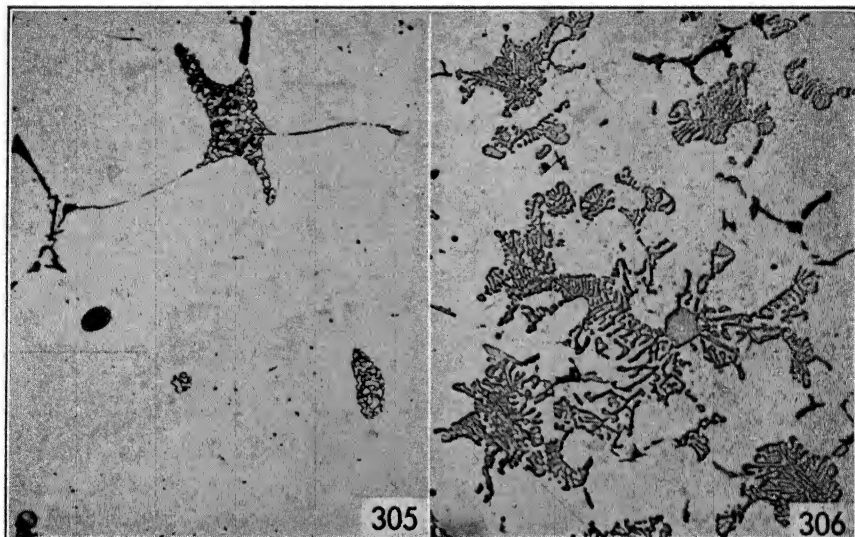


FIG. 305. Sand-cast—Cu 3.62%, Fe 0.49%, Si 0.87%, Zn 12.20%. Black  $\alpha(\text{AlFeSi})$ ,  $\text{CuAl}_2$  and Si as eutectic  $\text{Al-CuAl}_2\text{-Si}$ , X 250, etched with  $\text{H}_2\text{SO}_4$ .

FIG. 306. Cast in permanent mold—Cu 2.90%, Si 2.80%, Fe 1.25%, Zn 10.90%. Black  $\text{CuAl}_2$ , primary crystal of  $\alpha(\text{AlFeSi})$ , surrounded by  $\alpha(\text{AlFeSi})$  in the form of Chinese script, dark gray Si, X 250, etched with  $\text{Fe}(\text{NO}_3)_3$ .

The eutectics present in these alloys are the same as in zinc-free alloys, namely:

$\text{Al-CuAl}_2\text{-AlCuFeSi-Si}$ ; 968°F (520°C), Cu 26%, Si 6.5%, Fe 0.5%.

$\text{Al-CuAl-Si}$ ; 977°F (525°C), Cu 26%, Si 6%.

$\text{Al-CuAl}_2$ ; 1018°F (548°C), Cu 33%.

However, their melting points are lowered some 10° to 40°F (5° to 20°C) by the presence of zinc in solid solution in aluminum.

These alloys are heat-treated only when magnesium is present. The heat-treatment practice is to soak at 870° to 895°F (465° to 480°C) and to quench; then to follow by natural aging.

The mechanical properties of these alloys are shown in the accompanying table.

	YIELD STRENGTH 0.2%; PSI	TENSILE STRENGTH PSI	ELONGA- TION % ON 2 IN.	BRINELL HARDNESS 500/10/30
Sand-cast	10,000-20,000	20,000-26,000	2-4	50-70
Sand-cast heat-treated	25,000-35,000	30,000-40,000	0-2	100-120
Permanent-mold cast	12,000-22,000	23,000-28,000	1-3	60-80
Permanent-mold heat-treated	30,000-40,000	35,000-45,000	0-2	100-120

Although the castability is good and these alloys fill the molds well, when low in iron, copper, and silicon they are hot-short and cannot

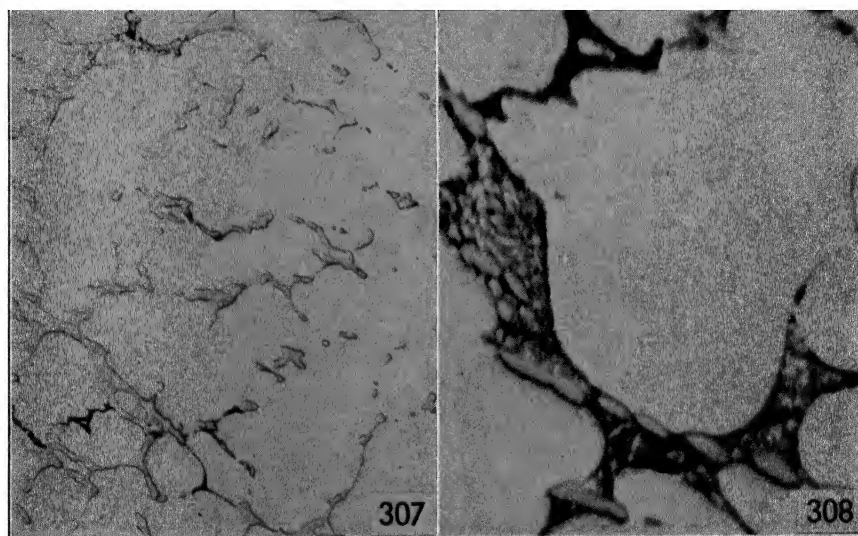


FIG. 307. Ingot water-cooled—Cu 2.30%, Fe 0.41%, Mg 2.82%, Ni 0.87%, Si 0.21%, Zn 5.24%. Black  $Mg_2Si$ , other constituents unidentifiable, X 250, not etched.

FIG. 308. Enlargement of Fig. 307. Black  $Mg_2Si$ , complex eutectic unidentified, globules of an unknown constituent, X 1000, etched with HF.

be cast in permanent mold. However, with higher iron, copper, and silicon contents, this defect almost completely disappears. Corrosion resistance is very poor and these alloys are susceptible to intergranular corrosion and also to a certain extent to stress corrosion.

The uses of these alloys are few and are limited to unimportant parts where cheapness of production is the most important factor.

Recently some alloys of this type have appeared on the market in the wrought form. The mechanical properties claimed for them are

higher than those of any other aluminum alloy, and may surpass 100,000 psi, but the alloys seem to be very sensitive to intergranular and stress corrosion.

The microstructure of these alloys is complex and has not as yet been resolved.

Figures 307 and 308 show an alloy of this type.  $\text{Mg}_2\text{Si}$ , black, can be identified very easily. A complex eutectic, probably containing  $\text{CuAl}_2$ , Al, and  $\text{Cu}_2\text{Mg}_2\text{Al}_5$  or  $\text{Mg}_3\text{Zn}_3\text{Al}_2$  (or possibly a quaternary compound  $\text{AlCuMgZn}$ ) is also present. The globular constituent cannot be identified and may be formed by the combination of Fe, Ni, Mg, and Zn.

The eutectics present in these alloys have not been identified, the lowest-melting eutectic is at about 850°F (455°C) and should contain  $\text{Mg}_3\text{Zn}_3\text{Al}_2$  or the quaternary phase.

No data have been published about the heat treatment of these alloys. Probably the practice is to soak at 820° to 840°F (440° to 450°C) and follow by rapid quenching and artificial aging, at about 300°F (150°C).

## CHAPTER 10

### ALUMINUM-SILICON ALLOYS

Although the effect of additions of silicon to aluminum was investigated by St. Claire-Deville as early as 1856, aluminum-silicon alloys were not widely used until 1920, when Pacz discovered the possibility of improving their mechanical properties through modification. The modified alloys, which have a tensile strength and an elongation up to 50 per cent higher than the non-modified alloys, were favorably received, especially in Germany, where the 12 per cent silicon alloy, known as silumin, is one of the alloys most often used in castings.

Several other alloys are in use. They have been divided into three groups, which correspond to somewhat different compositions and consequently to different properties and applications. They are:

1. Straight aluminum-silicon alloys.
2. Aluminum-silicon alloys containing magnesium.
3. Aluminum-silicon alloys containing copper, manganese, nickel, magnesium, etc.

#### **Straight Aluminum-Silicon Alloys**

These alloys contain only aluminum and silicon, except for the usual impurities found in aluminum, namely, iron and occasionally titanium and copper. The silicon content is variable. European practice has centered around eutectic alloys containing 12 to 13 per cent silicon, which are used in the modified state, while American practice prefers the 5 per cent alloys without modification. At present there is a tendency for the two practices to meet halfway, and alloys with a silicon content of about 8 to 10 per cent are being used more and more, both in the modified and unmodified states. This is caused by the fact that alloys of eutectic composition have a tendency to contain shrinkage pinholes because of their small interval of solidification, which is only some 20 to 30 degrees wide; whereas alloys with a low silicon content have poorer mechanical properties and a somewhat higher shrinkage coefficient.

The microstructure of these alloys is very simple. Al, Si, and  $\text{FeSiAl}_5$  are the only constituents present. When the iron content is below

0.7 per cent,  $\text{FeSiAl}_5$  is hardly detectable, since it is present as a fine eutectic  $\text{Al-Si-FeSiAl}_5$  and its form and etching characteristics differ only slightly from Si.

Figure 309 shows a 5 per cent alloy cast in permanent mold. Figure 310 shows a 13 per cent alloy cast in permanent mold in the unmodified state. Figure 311 shows an alloy of the same composition in the modified state. In each case  $\text{FeSiAl}_5$  can only be distinguished from Si particles with difficulty. Figure 312 shows a 5 per cent silicon alloy, where the iron content is above 0.7 per cent, and therefore  $\text{FeSiAl}_5$  is present as long primary needles, which make the alloy very brittle and practically useless.

Only two eutectics are present in these alloys.

$\text{Al-FeSiAl}_5\text{-Si}$ ;  $1067^\circ\text{F}$  ( $575^\circ\text{C}$ ), Si 11.7%, Fe 0.7%.

$\text{Al-Si}$ ;  $1071^\circ\text{F}$  ( $577^\circ\text{C}$ ), Si 11.7%.

These alloys are never heat-treated because the improvement in the mechanical properties produced by dissolving Si is very little.

The castability of these alloys is excellent; the fluidity in the molten state is high, and the shrinkage on solidification is very low. All this permits very good castings, even of complicated shapes with adjacent thin and thick sections. The machinability is rather poor, as the hard particles of Si, embedded in a soft matrix of Al, tend to be dragged, spoiling the surface and wearing out the tools. The mechanical properties are rather poor as reported below.

	YIELD STRENGTH 0.2%; PSI	TENSILE STRENGTH PSI	ELONGA- TION % ON 2 IN.	BRINELL HARDNESS 500/10/30
Sand-cast	9,000-14,000	17,000-25,000	3- 8	40-60
Permanent-mold cast	10,000-15,000	20,000-28,000	3-10	40-65
Die-cast	10,000-15,000	25,000-32,000	1- 5	50-70

Corrosion resistance is very good and these alloys were used as corrosion resistant for some time, before the introduction of the more resistant magnesium-bearing alloys. The appearance of the surface is not good, the alloys are a dull gray and machining does not improve the surface aspect. The weldability is very good. Sometimes these alloys are used as welding material for the joining of other alloys.

General castings, especially complicated shapes and pressure-tight parts, are often produced with these alloys. They are preferred to the 8 per cent copper and the copper-silicon alloys when corrosion is an important factor, and there are cases in which they have been used for ornamental purposes.

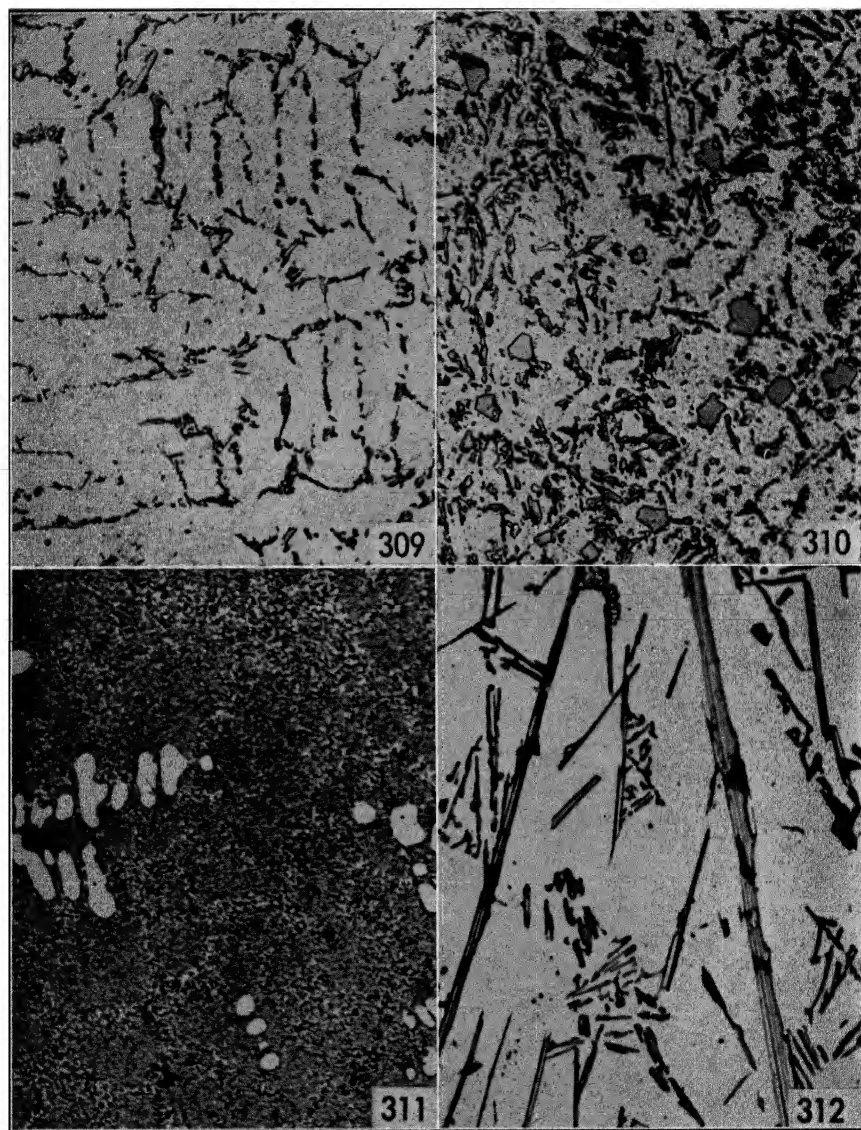


FIG. 309. Cast in permanent mold—Si 5.64%, Fe 0.52%, Cu 0.12%, Zn 0.20%. Crystals of Si, a few hardly visible needles of  $\text{FeSiAl}_5$  lighter, X 250, not etched.

FIG. 310. Cast in permanent mold—Si 12.17%, Fe 0.42%. Si as primary crystals and as eutectic Al-Si, X 250, not etched.

FIG. 311. Cast in permanent mold, modified—Si 12.90%, Fe 0.56%. Primary crystals of Al (white) on a background of modified eutectic Al-Si, X 250, not etched.

FIG. 312. Sand-cast—Si 5.80%, Fe 1.80%. Long needles of  $\text{FeSiAl}_5$  light, Si crystals slightly darker, X 250, not etched.

**Aluminum-Silicon Alloys Containing Magnesium**

The usual composition of these alloys ranges between:

Si	5 -13%
Fe	up to 0.7%
Mg	0.2- 0.7%
Mn or Co	0 - 0.6%

Manganese and cobalt sometimes are added to alloys with a high iron content to avoid the formation of  $\text{FeSiAl}_5$ . Sometimes nickel also is added in amounts up to 0.8 per cent.

The constituents normally present in these alloys are Al, Si,  $\text{FeSiAl}_5$ , and  $\text{Mg}_2\text{Si}$  in alloys without cobalt or manganese. In alloys containing manganese,  $\alpha(\text{AlFeMnSi})$  is substituted for  $\text{FeSiAl}_5$ ; in alloys containing cobalt,  $\text{AlFeCo}$  is substituted for  $\text{FeSiAl}_5$ . When nickel is present, it usually forms  $\text{NiAl}_3$ , seldom  $\text{FeNiAl}_9$ .  $\text{AlFeMgSi}$  may be present occasionally in these alloys, although a magnesium content above 1 per cent is required for its formation. In alloys with a magnesium content of about 0.3 per cent,  $\text{Mg}_2\text{Si}$  usually is not visible since all the Mg is in solid solution.

In alloys containing only magnesium the eutectics present are:

Al- $\text{Mg}_2\text{Si}$ -Si; 1038°F (559°C), Si 14%, Mg 5.5%.

Al- $\text{FeSiAl}_5$ -Si; 1067°F (575°C), Si 11.7%, Fe 0.7%.

Al-Si; 1071°F (577°C), Si 11.7%.

In alloys containing manganese are present also the eutectics:

Al- $\alpha(\text{AlFeMnSi})$ - $\text{Mg}_2\text{Si}$ -Si; 1000°F (537°C), Si 13% approx., Mg 5% approx., Fe + Mn 1% approx.

Al- $\alpha(\text{AlFeMnSi})$ -Si; 1058°F (570°C), Si 12% approx., Fe + Mn 1% approx.

In alloys containing cobalt are present also the eutectics:

Al- $\text{Mg}_2\text{Si}$ - $\text{AlCoFe}$ -Si; 1000°F (537°C), Si 12% approx., Mg 5% approx., Co + Fe 1% approx.

Al- $\text{AlCoFe}$ -Si; 1058°F (570°C), Si 13% approx., Co + Fe 1% approx.

The phase  $\text{AlFeMgSi}$  is present only in segregations and there is no evidence that it forms eutectics with the other phases. If any eutectic is formed, its melting point must be only a few degrees below those reported above. The same is true for  $\text{NiAl}_3$ , which does not form any eutectic besides the ternary:

Al- $\text{NiAl}_3$ -Si; 1054°F (568°C), Si 11%, Ni 5%.



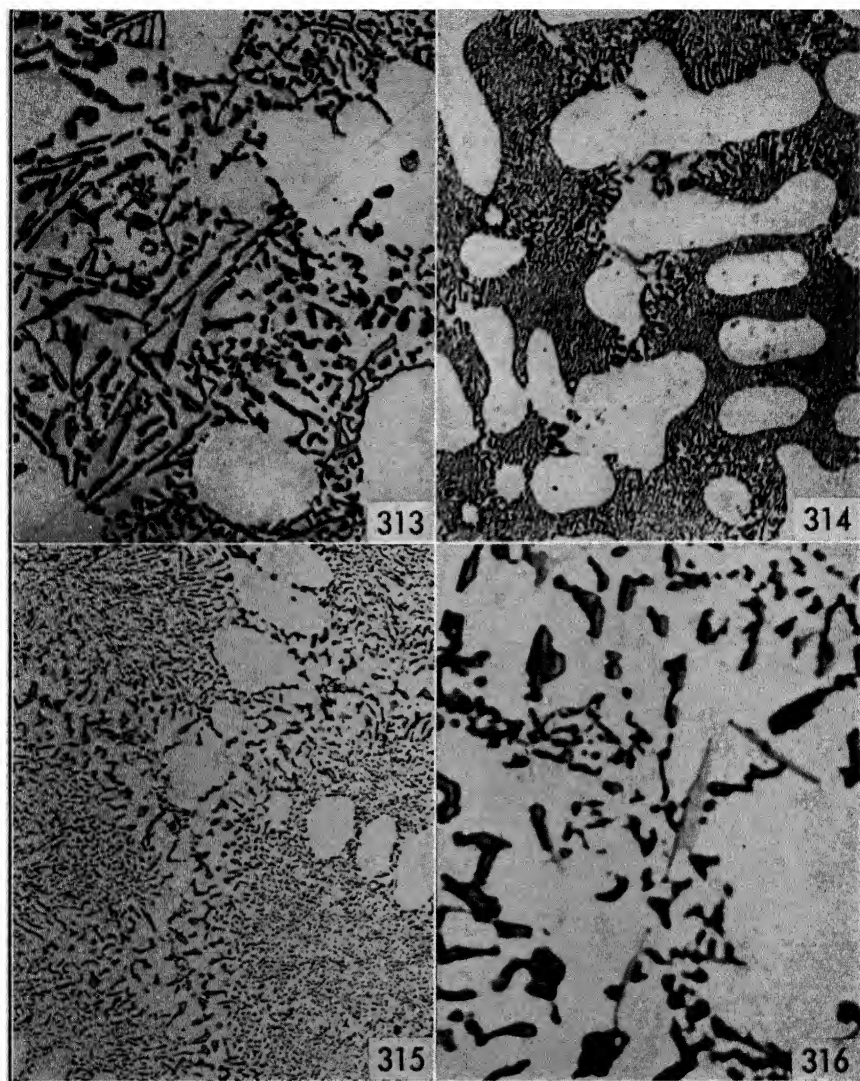


FIG. 313. Sand-cast—Si 8.25%, Fe 0.70%, Mg 0.28%, Mn 0.58%. Si dark gray,  $\alpha(\text{AlFeMnSi})$  light, X 250, not etched.

FIG. 314. Cast in permanent mold, modified—Si 9.10%, Fe 0.56%, Mg 0.40%, Co 0.61%. Light crystals of AlCoFe, primary crystals of Al, white, modified eutectic Al-Si, X 250, not etched.

FIG. 315. Cast in permanent mold, modified—Si 12.74%, Fe 0.61%, Mg 0.69%, Mn 0.48%. Small black points at the grain boundaries  $\text{Mg}_2\text{Si}$ , light crystals of  $\alpha(\text{AlFeMnSi})$ , gray Si, X 250, not etched.

FIG. 316. Enlargement of Fig. 315, to show the eutectic Al- $\alpha(\text{AlFeMnSi})$ - $\text{Mg}_2\text{Si}$ -Si at the grain boundaries. Si gray,  $\text{Mg}_2\text{Si}$  black small points,  $\alpha(\text{AlFeMnSi})$  light, X 1000, not etched.

Figure 313 shows an alloy containing manganese, sand-cast, in the unmodified state. The constituents visible are Si and  $\alpha(\text{AlFeMnSi})$ .  $\text{Mg}_2\text{Si}$  is not visible owing to the low magnesium content. Figure 314 shows an alloy of the same type, containing cobalt instead of manganese, in the modified state. Si is in the modified form. A few particles of  $\text{AlFeCo}$  are visible at the grain boundaries. Here, too,  $\text{Mg}_2\text{Si}$  is invisible.

Figures 315 and 316 show another alloy, of higher silicon and magnesium content, where  $\text{Mg}_2\text{Si}$  can be seen in the form of eutectic  $\text{Mg}_2\text{Si}-\alpha(\text{AlFeMnSi})-\text{Si}-\text{Al}$  at the grain boundaries.

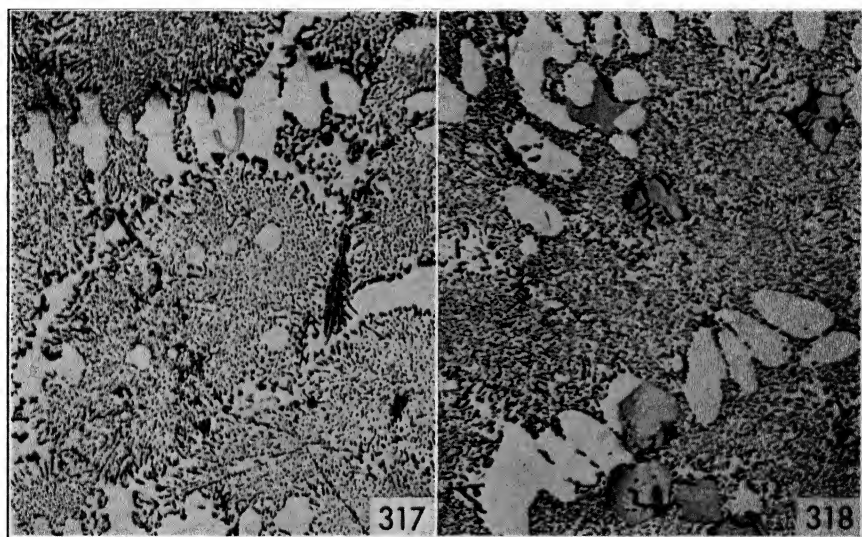


FIG 317. Cast in permanent mold, modified—Si 13.00%, Fe 0.78%, Mg 0.56%, Mn 0.57%. Light crystals of  $\text{AlFeMgSi}$ , gray Si, needles partly visible of  $\text{FeSiAl}_3$ , and ladder-like crystal of  $\alpha(\text{AlFeMnSi})$ , X 250, not etched.

FIG. 318. Cast in permanent mold, modified—Si 12.90%, Fe 0.87%, Mg 0.42%, Mn 0.75%. Primary crystals of  $\alpha(\text{AlFeMnSi})$  on a background of modified eutectic  $\text{Al-Si}$ , X 250, not etched.

Figure 317 shows an alloy of the same type, where  $\text{AlFeMgSi}$  is present. Figure 318 shows an alloy in which, on account of the high iron and manganese contents,  $\alpha(\text{AlFeMnSi})$  is primary in the form of hexagonal crystals.

The heat-treatment practice for alloys containing manganese or cobalt is somewhat different from that for alloys containing only magnesium and silicon. For the first types the soaking temperature must not surpass  $1000^\circ\text{F}$  ( $537^\circ\text{C}$ ) and usually ranges between  $950^\circ$  and  $985^\circ\text{F}$  ( $510^\circ$  and  $530^\circ\text{C}$ ); whereas the second type can safely be heated

up to 1038°F (559°C), and the soaking temperatures used are between 980° and 1020°F (530° and 550°C). In both cases the quenching may be done in either cold or hot water and the castings may be naturally aged or artificially aged at 280° to 330°F (140° to 160°C), for from 4 to 12 hours.

The mechanical properties are reported below:

	YIELD STRENGTH 0.2%; PSI	TENSILE STRENGTH PSI	ELONGA- TION % ON 2 IN.	BRINELL HARDNESS 500/10/30
Sand-cast	10,000–15,000	20,000–25,000	3– 8	50– 70
Sand-cast heat-treated	15,000–20,000	28,000–35,000	3–10	60– 90
Permanent-mold cast	15,000–20,000	25,000–30,000	3–10	60– 80
Permanent-mold heat-treated	15,000–22,000	30,000–40,000	2–10	70–100

As for the straight aluminum-silicon alloys, the castability is very good; the possibility of improving the mechanical properties by heat treatment makes these alloys the best for the casting of complicated shapes, requiring high mechanical properties. The machinability is quite good in the heat-treated state; the corrosion resistance is good, as is the weldability.

These alloys find a minor use in America, but are widely used in Europe. They are especially used for airplane construction, their employment ranging from supercharger housings to wheels for airplanes. Complicated shapes requiring pressure tightness are also cast from these alloys and heat-treated to acquire high mechanical properties.

### **Aluminum-Silicon Alloys Containing Copper, Magnesium, Etc.**

Several types of these alloys are in use, with compositions ranging between:

Si	5 – 30%
Fe	up to 1.5%
Mg	0 – 1%
Cu	0.4– 3%
Ni	0 – 3%
Mn	0 – 1.5%
Co	0 – 1.5%
Cr	0 – 0.5%

Grain refiners, such as titanium, vanadium, and molybdenum, are added sometimes, and alloys with additions of antimony, zinc, tin, and lead of the order of 0.1 to 0.4 per cent have been used.

The microstructure of these alloys is rather complex and cannot be completely resolved in most cases. Silicon is present as eutectic Al-Si or, in alloys with silicon contents above 12 per cent, as primary crystals; magnesium usually forms  $\text{Mg}_2\text{Si}$ , but may form  $\text{CuMg}_5\text{Si}_4\text{Al}_4$  or the  $\text{AlFeMgSi}$  phase. Copper and nickel usually combine to form one of the  $\text{AlCuNi}$  phases. Manganese combines with silicon and iron to form  $\alpha(\text{AlFeMnSi})$  or  $\delta(\text{AlFeMnSi})$ ; cobalt probably combines with iron; chromium and silicon form one of the  $\text{AlCrSi}$  phases, usually  $\beta(\text{AlCrSi})$ . When more than one of the following, manganese, nickel, chromium, cobalt, is added, the structure becomes practically irresolvable at the present state of knowledge. Si and  $\text{Mg}_2\text{Si}$  have characteristic colors and shapes and can easily be distinguished; the other constituents cannot be positively identified.

Little is known about the eutectics present in these alloys. It has been established that the eutectic with the lowest melting point melts at about 1000°F (537°C), but, except for the eutectics:

Al- $\text{Mg}_2\text{Si}$ -Si; 1038°F (559°C), Si 14%, Mg 5.5%.

Al-Si; 1071°F (577°C), Si 11.7%.

no other eutectics have been identified with certainty.

Figure 319 illustrates one of the simplest alloys of this type. Figure 320 shows another alloy containing copper, manganese, and nickel, where  $\alpha(\text{AlFeMnSi})$ ,  $\text{AlCuNi}$ ,  $(\text{CuNi})_2\text{Al}_3$ , and Si can be identified. Figure 321 shows another alloy of this type. Figure 322 shows an alloy commonly employed in the United States, containing Si mostly modified,  $\text{Mg}_2\text{Si}$ , and an  $\text{AlCuNi}$  constituent. Figure 323 shows an alloy containing higher silicon and iron, with additions of manganese: here are Si,  $\text{Mg}_2\text{Si}$ ,  $\alpha(\text{AlFeMnSi})$ , or  $\alpha(\text{AlMnSi})$  interspersed with Si,  $\delta(\text{AlFeMnSi})$  primary, and  $\text{AlCuFeNi}$ . The alloy in Fig. 324 is beyond explanation; Si and  $\text{Mg}_2\text{Si}$  are easily recognized, and two or three more constituents which contain cobalt, copper, iron, nickel, and manganese. Figure 325 illustrates the effect of a high iron content on the microstructure, as was reported for the other silicon alloys. The long needles of  $\text{AlCuFeSi}$ , which form in this case, make the alloy very brittle and practically useless. Additions of manganese prevent the formation of  $\text{AlCuFeSi}$  through the formation of  $\alpha$  and  $\delta(\text{AlFeMnSi})$ , as shown in Fig. 323. Figure 326 illustrates the effect of cobalt. Although the constituents cannot be identified with certainty, there is evidence that cobalt absorbs at least part of the iron to form  $\text{AlCoFe}$ .

The heat treatment of these alloys is usually: soaking for 2 to 6 hours at 950° to 985°F (510° to 530°C) and quenching, followed by artificial

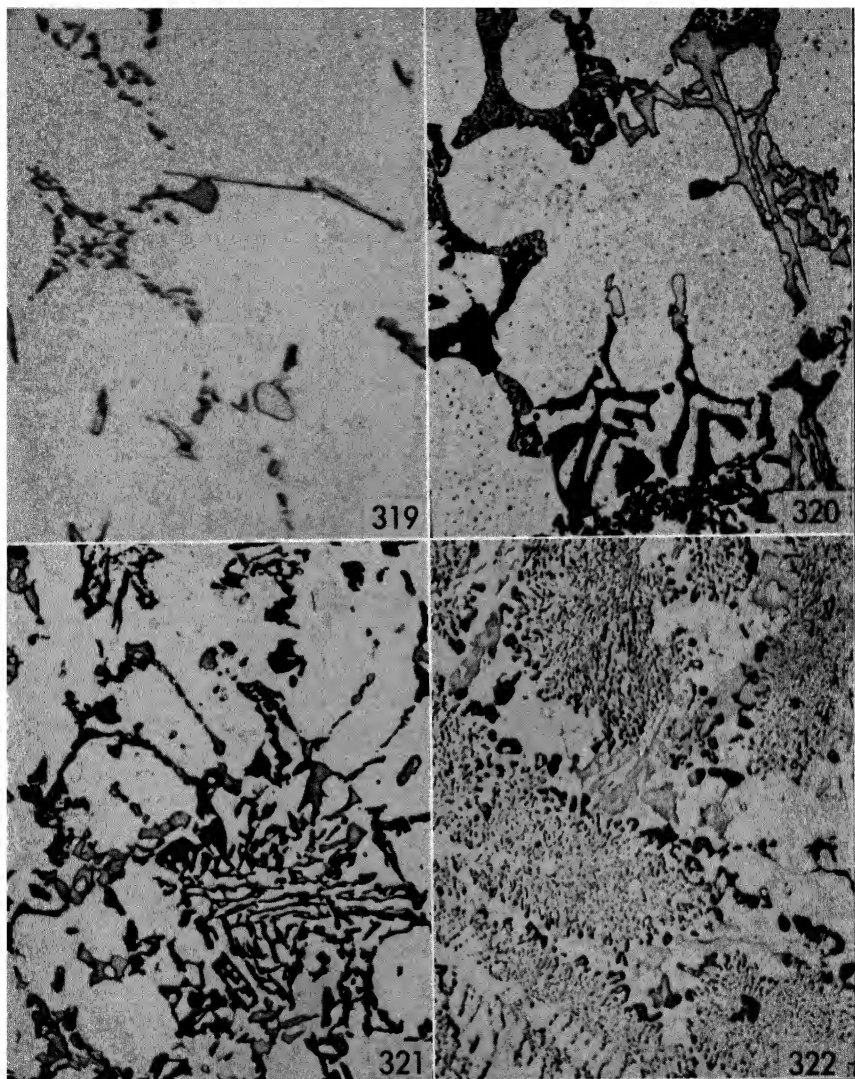


FIG. 319. Cast in permanent mold—Si 5.10%, Fe 0.62%, Cu 0.89%, Mg 0.37%. Gray points of Si, needles of  $\text{FeSiAl}_5$  or  $\text{AlCuFeSi}$ , light globule of  $\text{CuAl}_2$ , X 1000, not etched.

FIG. 320. Sand-cast—Si 5.05%, Cu 1.26%, Fe 0.75%, Mn 0.45%, Ni 0.78%, Mg 0.35%. Dark points of Si, dark Chinese script  $\alpha(\text{AlFeMnSi})$ , gray  $\text{AlCuNi}$ , and lighter  $(\text{CuNi})_2\text{Al}_3$ . The reprecipitated constituent (small points in the Al matrix) probably  $\text{CuMg}_5\text{Si}_4\text{Al}_4$ , X 250, etched with HF.

FIG. 321. Cast in permanent mold—Si 8.99%, Mg 0.92%, Cu 2.70%, Ni 0.91%, Fe 0.60%.  $\text{Mg}_2\text{Si}$  black, Si dark,  $\text{AlCuNi}$  or  $\text{AlCuFeNi}$  light, X 250, not etched.

FIG. 322. Cast in permanent mold—Si 13.96%, Fe 0.51%, Cu 0.82%, Mg 0.83%, Ni 2.26%. Black  $\text{Mg}_2\text{Si}$ , gray Si, light  $\text{AlCuNi}$  or  $\text{AlCuFeNi}$ , X 250, not etched.

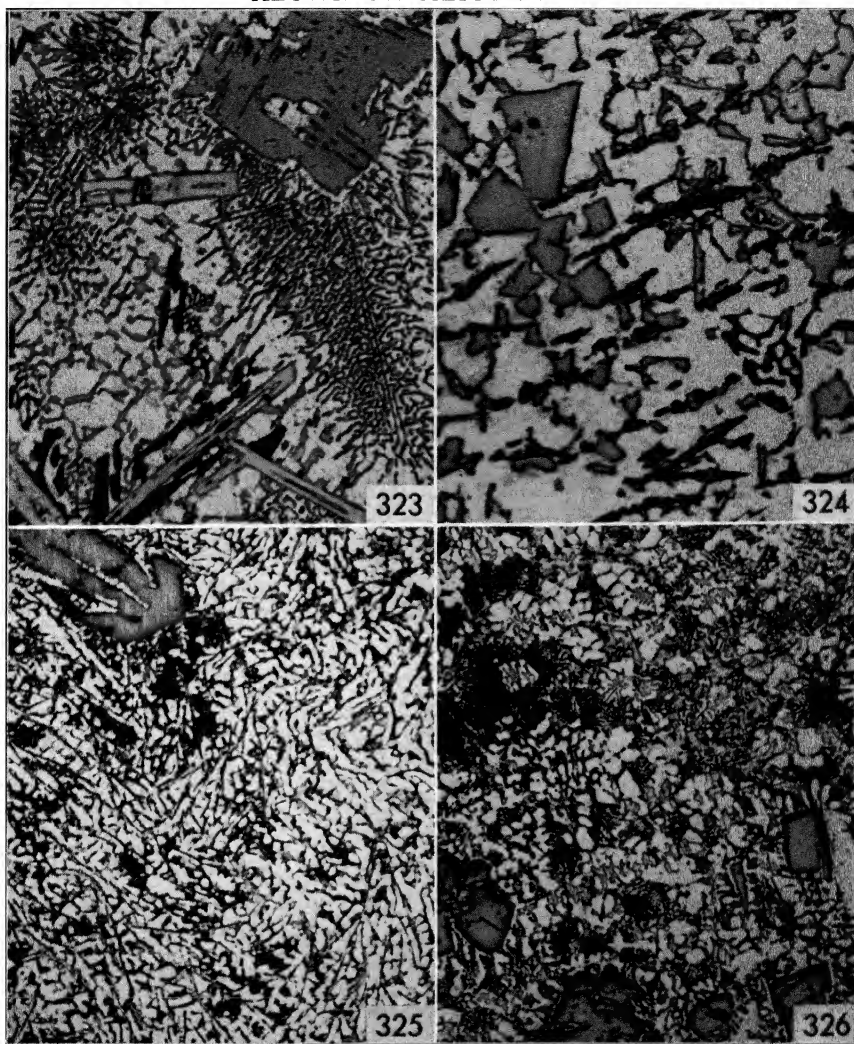


FIG. 323. Cast in permanent mold—Si 18.89%, Fe 1.15%, Cu 1.05%, Mg 0.76%, Mn 0.57%, Ni 2.13%. Si primary and eutectic gray, light crystals of  $\delta(\text{AlFeMnSi})$ , black  $\text{Mg}_2\text{Si}$  and  $\text{AlCuFeNi}$ ,  $\alpha(\text{AlFeMnSi})$  interspersed in the eutectic Al-Si, X 250, etched with HF.

FIG. 324. Cast in permanent mold—Cu 1.82%, Si 21.53%, Fe 0.77%, Mg 0.53%, Mn 0.57%, Ni 1.72%, Co 1.58%. Black  $\text{Mg}_2\text{Si}$ , gray Si, dark gray  $\text{AlCuFeNi}$  (?) light  $\text{AlCuNi}$  (?), X 500, etched with HF.

FIG. 325. Cast in permanent mold—Cu 1.05%, Fe 1.15%, Si 19.46%, Mg 0.79%, Ni 2.35%. Needles of  $\text{AlCuFeSi}$  in a background of eutectic Al-Si with  $\text{AlCuNi}$  interspersed in it. Some primary crystals of Si, X 75, not etched.

FIG. 326. Cast in permanent mold—Cu 1.03%, Fe 1.13%, Si 19.52%, Ni 2.05%, Mg 0.63%, Co 0.45%. The addition of Co has transformed the long needles of  $\text{AlCuFeSi}$  shown above in a grape-like constituent, probably a complex  $\text{AlCoCuFe}$ , X 75, not etched.

aging from 300° to 400°F (150° to 200°C). The high aging temperature is used for the heat treatment of pistons, where the aging must not be done much below the service temperature of 550° to 650°F (300° to 350°C).

The mechanical properties of these alloys are reported in the accompanying table.

	YIELD STRENGTH 0.2%; PSI	TENSILE STRENGTH PSI	ELONGA- TION % ON 2 IN.	BRINELL HARDNESS 500/10/30
Sand-cast	10,000-15,000	20,000-30,000	1- 5	60- 80
Sand-cast heat-treated	15,000-25,000	25,000-35,000	0- 5	80-120
Permanent-mold cast	12,000-20,000	20,000-30,000	1- 5	60- 90
Permanent-mold heat- treated	20,000-30,000	30,000-40,000	0- 4	90-150
Die-cast	15,000-25,000	25,000-35,000	0- 3	70-100
Wrought heat-treated	40,000-50,000	50,000-60,000	3-10	100-130

The castability is good for alloys with silicon below 15 per cent. Alloys with high silicon content are difficult to handle because of the high melting point and wide freezing range of the alloy. The high melting point requires high temperatures of the molten metal, with the consequent evils of oxidation and gas absorption; the wide interval of solidification favors segregation. The machinability ranges from fair to very poor, depending on the heat treatment and the silicon content. Grinding, or the use of diamonds, is resorted to for high-silicon alloys when a good finish is required. The corrosion resistance, weldability, and appearance depend somewhat on the silicon content. With high silicon, they are not particularly good but, considering the use of these alloys, which is mostly for pistons, this fact is unimportant.

The low-silicon alloys are used for general casting, especially for complicated shapes, where good mechanical properties are required. The high-silicon alloys are used for parts subject to high temperatures, mostly for pistons. An alloy of this type, which has a silicon content of about 13 per cent, is sometimes employed for forged pistons. Two special properties make these alloys particularly fitted for this purpose: they have a very low expansion coefficient and very good frictional properties. The low-expansion coefficient permits a closer fit between piston and cylinder than would be possible with any other aluminum alloy, and the good frictional properties, due to the hard silicon particles, permit longer use of these pistons, making them, in the end, more economical than pistons of other alloys less expensive to produce.



## CHAPTER 11

### CORROSION-RESISTANT ALLOYS

The alloys of this group are not closely related to each other as those of the other groups are, but they will be discussed together, partly for ease of description, partly because they have the property of very good corrosion resistance in common. Four main groups of alloys can be distinguished.

1. Commercial aluminum.
2. Aluminum-magnesium and aluminum-magnesium-zinc alloys.
3. Aluminum-magnesium-silicide alloys.
4. Aluminum-manganese alloys.

#### Commercial Aluminum

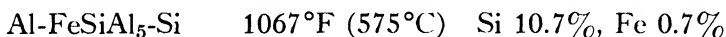
Aluminum is produced in several grades, ranging from 99.998 per cent to 98 per cent. Commercial grades, however, do not reach such high purity and the best grade on the market is 99.7 per cent. The main impurities found in aluminum are iron and silicon; copper, titanium, vanadium, are less important, both as to frequency and as to percentages present. Sometimes gallium, zirconium, and manganese are found in amounts below 0.01 per cent. That refers to primary aluminum, which is the aluminum produced from the ore. Secondary aluminum, namely aluminum produced by remelting scrap, may contain anything, depending upon the source of the scrap. Iron or silicon may predominate according to the source of the ore. The usual product contains more iron than silicon, although aluminum produced from minerals other than bauxite tends to be higher in silicon. Primary aluminum usually ranges between 99 per cent and 99.7 per cent. The best secondary aluminum seldom reaches a grade of 99.5 per cent and is commonly marketed as 98/99 per cent.

The microstructure of primary aluminum is simple,  $\text{Fe}_2\text{Al}_7$ ,  $\alpha(\text{AlFeSi})$ , and  $\text{FeSiAl}_5$  being the common constituents. Free Si is present less often. The slight amounts of copper, titanium, vanadium, etc., present in amounts below 0.05 per cent are probably in solid solution, although there is some evidence that the last, under special conditions, may form compounds with silicon, insoluble in aluminum. Not much can be said of the constituents present in secondary aluminum, owing



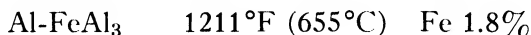
to the variety of analyses possible. Most of the constituents formed in aluminum alloys may be present, but usually they are in such limited amounts that positive identification is impossible in most cases.

In primary aluminum the ternary eutectic



is seldom present.

More commonly the following eutectic is present.



The same eutectics, as well as a score of others, formed by the impurities, usually are present in secondary aluminum.

Figures 327 and 328 show the structure of two samples of primary aluminum, grades 99.5 per cent and 99 per cent, respectively. In both cases  $\alpha(\text{AlFeSi})$  is present. In Fig. 328 a needle of  $\text{Fe}_2\text{Al}_7$  can also be detected. Figure 329 shows a sample of secondary aluminum, grade 98 per cent, where fast cooling has made the constituents practically unidentifiable.

Pure aluminum is not heat-treated, and the only operation carried out is annealing, to produce recrystallization after cold work. The highest temperature which can be used safely for aluminum is below  $1050^\circ\text{F}$  ( $565^\circ\text{C}$ ). In usual practice temperatures above  $1000^\circ\text{F}$  ( $537^\circ\text{C}$ ) are seldom reached.

The castability of commercial aluminum is rather poor on account of the small amount of eutectics. In the rare cases in which it is employed for castings, special precautions have to be taken to insure proper feeding of every part of the casting. Aluminum is hot- and cold-worked readily, but it requires intermediate annealings if the deformation surpasses 80 to 90 per cent. The machinability is poor on account of the softness of the material; weldability is rather good. The mechanical properties in the cast and wrought state are given below.

	YIELD STRENGTH 0.2%; PSI	TENSILE STRENGTH PSI	ELONGA- TION % ON 2 IN.	BRINELL HARDNESS 500/10/30
Cast	4,000- 8,000	8,000-12,000	20-40	20-25
Wrought soft	4,000- 7,000	10,000-15,000	35-45	20-25
Wrought half hard	12,000-16,000	15,000-18,000	10-20	30-35
Wrought hard	20,000-25,000	25,000-30,000	5-15	40-50

The data refer to aluminum of 99 per cent grade. Higher grades have lower yield and tensile strength and higher elongation. The corrosion resistance is very good, especially with material of high purity.

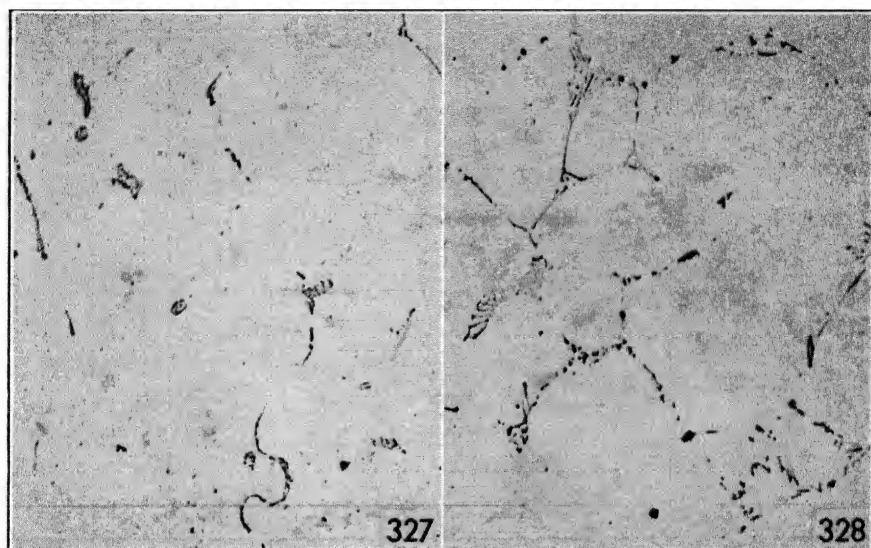
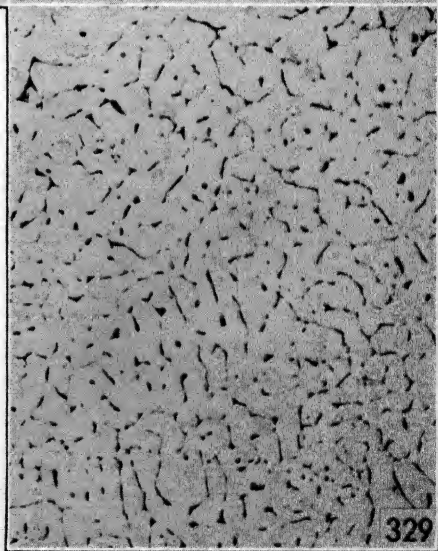


FIG. 327. Ingot of aluminum 99.5% —Fe 0.24%, Si 0.18%.  $\alpha(\text{AlFeSi})$  is the only constituent visible, X 250, not etched.

FIG. 328. Ingot of aluminum 99% —Fe 0.53%, Si 0.22%.  $\alpha(\text{AlFeSi})$  as Chinese script, few needles of  $\text{Fe}_2\text{Al}_7$  (or  $\text{FeAl}_3$ ?), X 250, etched with  $\text{H}_2\text{SO}_4$ .

FIG. 329. Secondary aluminum 98/99 grade, cast in permanent mold —Cu 0.15%, Fe 0.55%, Si 0.75%, Mn 0.08%, Cr 0.02%, Mg 0.03%, Ni tr., Pb 0.11%, Sn 0.05%, Zn 0.07%. Network of unidentifiable constituents, X 250, not etched.



Pure aluminum is used for castings in the chemical industry, where corrosion resistance is the most important factor, superseding all other considerations of mechanical properties and cost; otherwise alloys are preferred. Foil, sheet, rod, tubing, and extruded shapes are currently produced of pure aluminum, and these products are formed into thousands of parts, the whole list of which would cover at least half of all the metallic articles produced.

### Aluminum-Magnesium and Aluminum-Magnesium-Zinc Alloys

The main alloying elements of these alloys are magnesium and sometimes zinc, with small additions of manganese or chromium. The first alloy of this type to be used contained a certain amount of antimony (0.15 to 0.50 per cent), which was supposed to impart good corrosion resistance. Later experiments showed that the antimony had practically no effect, and it was eliminated from the composition. More recently zinc has been added to some of these alloys, and the range used at present is:

Mg	2 - 12%
Zn	0 - 3%
Mn or Cr	0.1- 1%

Silicon and especially iron, which are present as impurities, should be as low as possible in order to insure the best corrosion resistance. One variety of these alloys used for casting purposes, however, contains additions of silicon up to 1 per cent, to increase fluidity in the molten state. Grain refiners, usually titanium, may be added to these alloys. Some alloys with nickel up to 0.7 per cent have been used, but the reason for this addition is not clear.

The microstructure of these alloys is simple. Most of the magnesium and zinc, when present, are in solid solution, the excess forming  $Mg_5Al_8$  or, depending on the percentages of magnesium and zinc present,  $Mg_3Zn_3Al_2$  or  $MgZn_2$  or  $MgZn_5$ . Silicon combines to form  $Mg_2Si$ , mostly insoluble on account of the excess of magnesium present. Iron combines with manganese or chromium, dissolving in the compounds  $MnAl_6$  and  $CrAl_7$ ; sometimes, when manganese or chromium are low, it may be present as  $Fe_2Al_7$ .

The eutectics present in these alloys are:

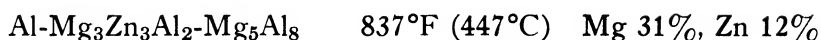
Al- $Mg_5Al_8$ -(FeMn) $Al_6$ ; 817°F (436°C), Mg 26.4%, Mn + Fe 2% approx.

Al- $Mg_5Al_8$ - $Fe_2Al_7$ ; 833°F (445°C), Mg 33%, Fe 0.3%.

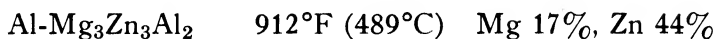
Al- $Mg_5Al_8$ - $Mg_2Si$ ; 840°F (449°C), Mg 33%, Si 0.1% approx.

Al- $Mg_5Al_8$ ; 840°F (449°C), Mg 33%.

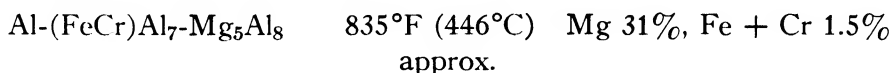
In alloys containing also zinc, the eutectic



or the quasi-binary,



are very seldom present in heavily segregated material, since zinc is normally in solid solution. In alloys containing chromium the eutectic  $\text{Al-Mg}_5\text{Al}_8\text{-(FeMn)Al}_6$  is substituted by



When magnesium or zinc are in solid solution these eutectics are not present and the lowest melting eutectic is probably the quasi-binary,

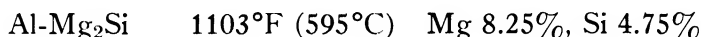


Figure 330 shows a sample of the oldest alloy containing antimony. The antimony, however, is probably in solid solution and cannot be seen. Figure 331 shows an alloy containing manganese, with high magnesium content. Figure 332 shows another alloy containing manganese with a lower magnesium content. In the alloy in Fig. 331 magnesium is only partly in solid solution and  $\text{Mg}_5\text{Al}_8$  can be seen. In the second, cast in permanent mold, almost all the magnesium is in solid solution and  $\text{Mg}_5\text{Al}_8$  can hardly be detected. The alloys with high magnesium content can be heat-treated successfully. The improvement in properties obtainable by heat treatment in the others is limited and is caused more by homogenization of the solid solution than by solution of undissolved constituents. Figure 333 shows an alloy of the same type with high silicon. Figures 334 and 335 show the same alloy, containing chromium, respectively cast in cold mold and extruded. The few particles of  $\text{Mg}_5\text{Al}_8$ , hardly detectable in the as-cast specimen, have completely disappeared in the extruded sample, through solution of the magnesium, caused by the solution treatment prior to extrusion. Figure 336 shows an alloy, cast in permanent mold, which contains zinc. Figure 337 shows another alloy, containing zinc, extruded. In both cases zinc is in solid solution and no difference from zinc-free alloys can be detected.

Heat treatment is not often used in connection with these alloys. Most of the magnesium and zinc are in solid solution already, and little improvement can be expected from heat treatment. Only with magnesium above 8 per cent will heat treatment have appreciable effects on the mechanical properties. The heat-treatment practice is

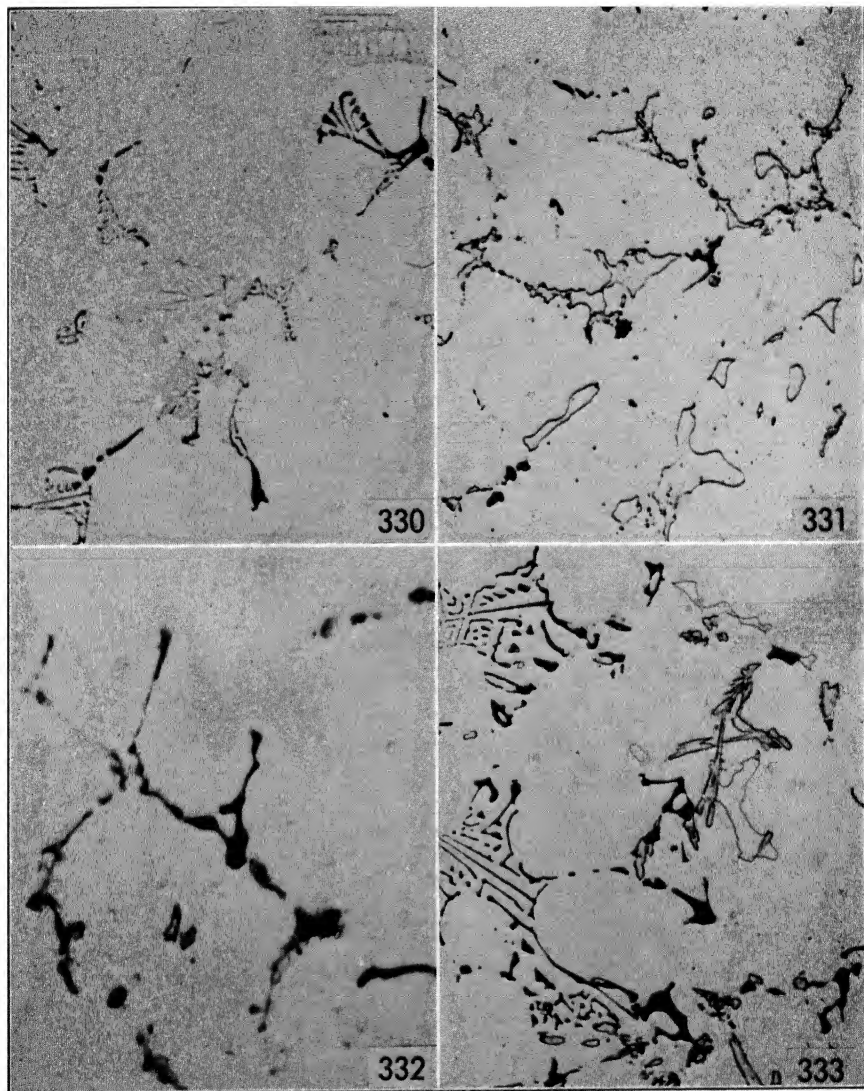


FIG. 330. Sand-cast—Mg 2.33%, Mn 1.02%, Fe 0.33%, Si 0.42%, Sb 0.19%.  $Mg_2Si$  black,  $(FeMn)Al_6$  light, Sb in solid solution, not visible, X 250, not etched.

FIG. 331. Sand-cast—Mg 11.90%, Fe 0.30%, Si 0.22%, Mn 0.23%. Black  $Mg_2Si$ , light  $Mg_5Al_8$ , a few globules of Fe and Mn constituents are embedded in  $Mg_5Al_8$  and hardly visible, X 250, not etched.

FIG. 332. Cast in permanent mold—Mg 7.0%, Si 0.33%, Fe 0.42%, Mn 0.20%. Dark  $Mg_2Si$ , Fe and Mn constituents light relieved, few globules of  $Mg_5Al_8$  relieved and darkened by the etching, X 1000, etched with HF.

FIG. 333. Sand-cast—Mg 7.20%, Si 1.02%, Fe 0.47%, Mn 0.12%, Ti 0.09%.  $Mg_2Si$  black,  $Mg_5Al_8$  light,  $(FeMn)Al_6$  and  $Fe_2Al_7$  gray, X 250, not etched.

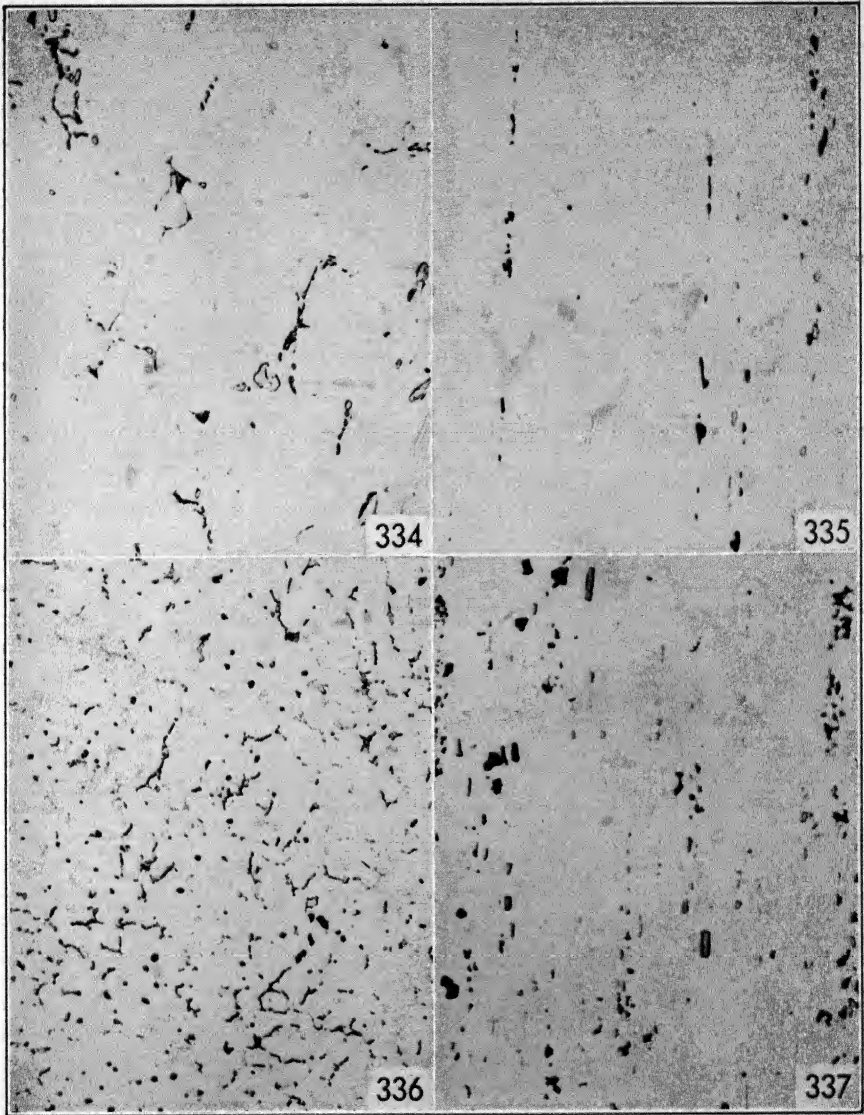


FIG. 334. Ingot cast in cold mold—Mg 4.25%, Fe 0.35%, Si 0.27%, Cr 0.22%.  $Mg_2Si$  black,  $Mg_5Al_8$  light,  $(FeCr)Al_7$  hardly visible, X 250, not etched.

FIG. 335. Same ingot as in Fig. 334, after extrusion.  $Mg_2Si$  black and  $(FeCr)Al_7$  are the only constituents visible;  $Mg_5Al_8$ , dissolved, is not visible. X 250, not etched.

FIG. 336. Cast in permanent mold—Mg 2.23%, Zn 1.25%, Fe 0.14%, Si 0.19%.  $Mg_2Si$  black, light  $Mg_5Al_8$  or a  $MgZn$  constituent, X 250, not etched.

FIG. 337. Extruded rod—Mg 4.52%, Zn 0.81%, Fe 0.65%, Si 0.81%, Mn 0.31%.  $Mg_2Si$  black, gray Mn and Fe constituents, light, hardly visible, a few globules of  $Mg_5Al_8$  or of a  $MgZn$  constituent, X 250, not etched.

as follows: 12 to 24 hours soaking at 790° to 815°F (420° to 435°C) and eventually quenching in water, followed by natural or artificial aging at 300° to 350°F (150° to 180°C) for 10 to 20 hours. The long soaking is required by the slowness of diffusion in these alloys. For the same reason quenching in water is unnecessary. These alloys require protective atmosphere during heat treatment to avoid high-temperature deterioration. German practice uses sulfur dioxide as protective atmosphere successfully, although sulfur is reported to cause high-temperature deterioration in duralumin.

The castability is not particularly good, and these alloys need careful handling to avoid the oxidation of magnesium. For this reason the high magnesium alloys are commonly melted under protective fluxes. Up to 8 per cent magnesium these alloys are rolled or extruded without much difficulty, although great care must be taken in the amount of reduction for every pass on rolling. The machinability is good, especially with high magnesium contents; the weldability is poor. The mechanical properties are reported in the table below.

	YIELD STRENGTH 0.2%; PSI	TENSILE STRENGTH PSI	ELONGA- TION % ON 2 IN.	BRINELL HARDNESS 500/10/30
Sand-cast	15,000-20,000	20,000-30,000	5-10	50- 70
Sand-cast heat-treated	20,000-30,000	40,000-50,000	5-15	70- 80
Permanent-mold cast	20,000-30,000	35,000-50,000	5-15	60- 80
Permanent-mold heat-treated	30,000-40,000	40,000-55,000	5-15	70- 90
Wrought soft	15,000-25,000	25,000-35,000	20-30	40- 60
Wrought hard	30,000-40,000	40,000-50,000	5-10	80-100
Wrought heat-treated	35,000-45,000	50,000-70,000	15-25	80-100

The properties in the heat-treated state refer to alloys with magnesium contents above 6 per cent or with zinc, those under wrought soft and wrought hard refer to alloys with magnesium contents below 5 per cent. The corrosion resistance of these alloys is very good, especially to salt water. However, wrought alloys containing magnesium above 6 per cent and cast alloys with magnesium above 10 per cent, or those containing zinc, are susceptible to stress corrosion and forfeit their main use, which is as corrosion-resistant alloys. Within these limits the probability of stress corrosion is very remote and can be considered practically non-existent.

These alloys, with the exception of those containing zinc or high silicon, are very white and take a good polish. This fact, together with good corrosion resistance, makes them appropriate for ornamental purposes. They also are frequently used for parts subject to marine

atmosphere, and in Germany these alloys have been extensively used to replace parts of naval brass.

### Aluminum-Magnesium-Silicide Alloys

The usual composition of these alloys ranges within:

Mg	0.5–2%
Si	0.5–3%
Mn or Cr	0.2–1.5%
Cu	up to 0.4%
Fe	up to 0.7%

Grain refiners are usually added to these alloys for casting. The alloys of higher silicon content are limited to casting purposes, for silicon improves the fluidity in the molten state.

The constituents present in these alloys are  $Mg_2Si$ , Si, and sometimes  $FeSiAl_5$ , coupled with  $\alpha(AlFeMnSi)$ ,  $\alpha(AlMnSi)$ , or  $(FeMn)Al_6$  in alloys containing manganese;  $\alpha(AlCrFeSi)$  and  $(FeCr)Al_7$  in alloys containing chromium.  $Mg_5Al_8$  should never be present in these alloys. The ratio of magnesium to silicon should be well above 1.73. That is, it should be on the silicon side of  $Mg_2Si$ , for an excess of silicon has practically no effect on the properties, whereas an excess of magnesium reduces the solid solubility of  $Mg_2Si$ .

The eutectics which have been identified in these alloys are:

Al- $Mg_2Si$ -Si; 1038°F (559°C), Si 14%, Mg 5.5%.

Al- $FeSiAl_5$ -Si; 1067°F (575°C), Si 11.7%, Fe 0.7%.

Al-Si; 1071°F (577°C), Si 11.7%.

Al- $Mg_2Si$ ; 1103°F (595°C), Si 4.75%, Mg 8.25%.

Alloys with manganese additions may contain:

Al- $Mg_2Si$ - $\alpha(AlFeMnSi)$ -Si; 1000°F (537°C), Si 13%, Mg 5%, Fe + Mn 1% approx.

Al- $\alpha(AlFeMnSi)$ -Si; 1058°F (570°C), Si 12%, Fe + Mn 1% approx.

There is no evidence that eutectics similar to those mentioned above are formed in alloys containing chromium. It seems that the phases containing chromium form quasi-binary eutectics with aluminum, having melting points well above 1100°F (600°C).

Figure 338 shows an alloy containing manganese, sand-cast. The visible constituents are  $\alpha(AlFeMnSi)$  and Si. Figure 339 shows an alloy containing chromium cast in water-cooled mold for rolling. The visible constituents are  $Mg_2Si$  and a hard-relieved chromium constituent, probably containing some silicon in addition to the iron.



These alloys are used mostly in the heat-treated condition. The practice is: soaking at 960° to 995°F (515° to 535°C) and quenching, eventually followed by artificial aging at about 300°F (150°C) for 8 to 20 hours. Artificial aging is usually omitted for castings, as the elongation drops too much for most purposes.

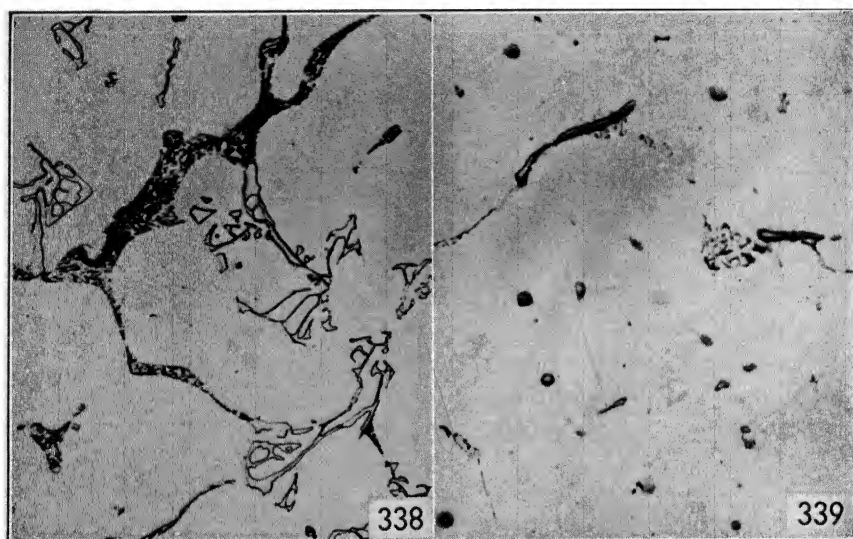


FIG. 338. Sand-cast—Si 2.12%, Mg 0.45%, Mn 0.81%, Fe 0.40%, Ti 0.12%.  $\alpha$ (AlFeMnSi) light, with its typical elongated form when it contains high silicon. Si as eutectic Al-Si, X 250, not etched.

FIG. 339. Ingot water-cooled—Mg 1.32%, Si 0.75%, Cr 0.22%, Fe 0.27%.  $Mg_2Si$  black, globules of a Cr constituent, probably containing the Fe and some Si, X 250, not etched.

The mechanical properties of these alloys are reported in the table below.

	YIELD STRENGTH 0.2%; PSI	TENSILE STRENGTH PSI	ELONGA- TION % ON 2 IN.	BRINELL HARDNESS 500/10/30
Sand-cast	15,000–20,000	20,000–30,000	1– 5	60– 80
Sand-cast heat-treated	20,000–35,000	30,000–40,000	1– 5	80–110
Permanent-mold cast	20,000–25,000	25,000–35,000	2– 5	70– 90
Permanent-mold heat-treated	30,000–38,000	35,000–45,000	1– 4	80–120
Wrought annealed	5,000–10,000	15,000–20,000	25–35	50– 80
Wrought heat-treated nat. aged	20,000–25,000	30,000–40,000	20–40	60– 80
Wrought heat-treated art. aged	30,000–40,000	40,000–60,000	5–15	80–110

The castability is good in alloys with a high silicon content, and the machinability quite good, especially in the aged condition. The formability is good in the annealed and quenched state, and as the natural aging is practically negligible, the alloys sometimes are produced in the quenched state for further forming, after which artificial aging produces the high mechanical properties. The corrosion resistance is very good, especially for wrought alloys, where the silicon content is lower than in casting alloys.

Although for castings there is a tendency to substitute for these alloys magnesium alloys, which do not require heat treatment to reach their maximum properties, in the field of wrought alloys this group is preeminent for those uses where good corrosion resistance and high mechanical properties are necessary.

### Aluminum-Manganese Alloys

The usual composition range of these alloys is

Mn	1-2.5%
Fe + Si	less than 1%

The microstructure of these alloys is very simple:  $\alpha(\text{AlFeMnSi})$ , with variable amounts of iron and silicon, is the main phase present, sometimes with  $(\text{FeMn})\text{Al}_6$  or  $\alpha(\text{AlMnSi})$ .

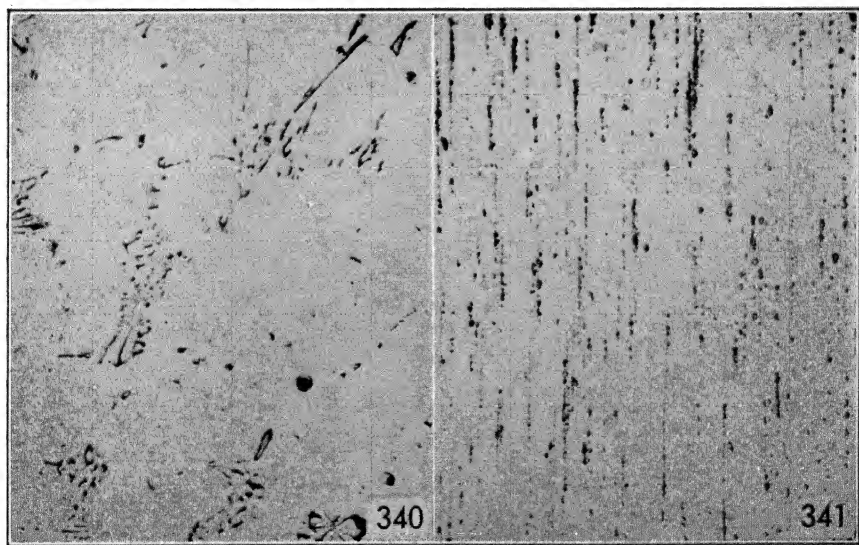


FIG. 340. Ingot cast in cold mold—Mn 1.17%, Fe 0.49%, Si 0.32%.  $\alpha(\text{AlFeMnSi})$  as Chinese script, X 250, etched with HF.

FIG. 341. Same material as in Fig. 340, rolled to sheet, X 250, not etched. Few particles of  $\alpha(\text{AlFeMnSi})$  (?) rounded and elongated by the rolling are visible.

Little is known about the eutectics present in these alloys, but their melting point has been established as above 1100°F (600°C) and is probably about 1150°F (620°C).

Figure 340 illustrates an alloy of this type, where only  $\alpha(\text{AlFeMnSi})$  can be seen. Figure 341 shows the same alloy in the form of sheet.

No heat treatment is ever used for these alloys; solution treatment before rolling is usually carried out at 950°F (510°C). These alloys have a tendency to grain growth and attention must be paid to the factors governing it, and especially to the rate of heating during intermediate annealing.

The castability is poor, on account of the narrow range of solidification, and these alloys are therefore seldom used for castings. The alloys can be hot- and cold-worked almost as easily as pure aluminum. Machinability is rather poor and little better than that of pure aluminum.

The mechanical properties are reported in the table below.

	YIELD STRENGTH 0.2%; PSI	TENSILE STRENGTH PSI	ELONGA- TION % ON 2 IN.	BRINELL HARDNESS 500/10/30
Cast	5,000–10,000	10,000–15,000	15–30	25–30
Wrought soft	3,000– 8,000	14,000–18,000	30–40	25–30
Wrought half hard	15,000–20,000	20,000–25,000	8–16	35–45
Wrought hard	20,000–30,000	25,000–35,000	4–10	50–60

Corrosion resistance is very good and sometimes is reported as better than pure aluminum. The weldability is good.

The main use of these alloys is for products where resistance to corrosion and ease of fabrication must be coupled with mechanical properties somewhat higher than those of pure aluminum. Their largest field of use is in kitchen utensils. They are also used for ornamental parts

## CHAPTER 12

### DURALUMIN

Under the name *dural*, *duralumin*, *superdural*, etc., are meant all the alloys whose composition ranges between:

Cu	3–5%
Fe	below 0.8%
Mg	0.3–2%
Mn	0.3–1.5%
Si	0.2–1.5%

Although the usual specifications divide these alloys for the most part according to their mechanical properties, from the metallographic point of view the grouping is better done according to their hardening constituents. Depending on the Mg : Si ratio, which almost entirely governs the microstructure, three groups can be distinguished.

1. Mg : Si > 1.73; hardening constituent  $\text{Mg}_2\text{Cu}_2\text{Al}_5$  with or without  $\text{CuAl}_2$ .
2. Mg : Si = 1.73; hardening constituents  $\text{Mg}_2\text{Si}$  and  $\text{CuAl}_2$ .
3. Mg : Si < 1.73; hardening constituents  $\text{CuMg}_5\text{Si}_4\text{Al}_4$  and  $\text{CuAl}_2$ .

Differences in the hardening constituents call for differences in the heat treatment, and especially in the age hardening, as the first and third group reach the best all-round properties through natural aging, whereas the second group requires artificial aging to reach its maximum.

The general properties are not appreciably affected by the Mg : Si ratio, but rather by the magnesium content. They are given here for all three groups, to avoid unnecessary repetition.

Castability is poor. The alloys have high shrinkage and a tendency to segregation. They require careful handling in the foundry and at the mills, especially when magnesium surpasses 1 per cent. Machinability is good in the hardened state, less good in the annealed state.

The mechanical properties are shown in the table, with the understanding that the properties in the heat-treated state refer to the first

and third group naturally aged and to the second group artificially aged.

	YIELD STRENGTH 0.2%; PSI	TENSILE STRENGTH PSI	ELONGA- TION % ON 2 IN.	BRINELL HARDNESS 500/10/30
Annealed	10,000–15,000	20,000–30,000	15–25	40– 60
Heat-treated	30,000–50,000	50,000–75,000	10–25	100–130
Heat-treated and cold- rolled	60,000–80,000	70,000–90,000	2–10	150–170

The corrosion resistance is rather poor and these alloys are susceptible to intergranular corrosion, especially with high copper, in the artificially aged state. The low corrosion resistance, which makes the alloy unfit for many uses, is corrected largely by cladding, with a sacrifice of about 10 per cent in the mechanical properties.

The uses of duralumins, bare and clad, are many, especially in the field of transportation, where they constitute the most-used aluminum alloys for airplanes.

### Alloys with Hardening Constituent $\text{Cu}_2\text{Mg}_2\text{Al}_5$

For the formation of this constituent the Mg : Si ratio must be above 1.73; that means that there must be more magnesium in the alloy than the amount necessary for the formation of  $\text{Mg}_2\text{Si}$ . If this is true, the excess of magnesium combines with copper to form  $\text{Cu}_2\text{Mg}_2\text{Al}_5$ . If there is more copper than the amount necessary to form this compound,  $\text{CuAl}_2$  will be present; if less,  $\text{CuMg}_4\text{Al}_6$  will be present. The Cu : Mg ratio required for the formation of  $\text{Cu}_2\text{Mg}_2\text{Al}_5$  alone is 2.65 (that means that the copper content must be 2.65 times the magnesium content), where the magnesium considered in the proportion is not the total magnesium but only that in excess of the compound  $\text{Mg}_2\text{Si}$ . The real ratio must therefore be:

$$= \frac{\% \text{ Cu}}{\% \text{ Mg} - 1.73\% \text{ Si}} = 2.65$$

If the ratio is higher than 2.65, as in most alloys,  $\text{CuAl}_2$  will be present, usually forming the eutectic  $\text{Al-Cu}_2\text{Mg}_2\text{Al}_5\text{-CuAl}_2$ .

In equilibrium conditions the manganese combines with aluminum and iron to form  $(\text{FeMn})\text{Al}_6$ ; with fast cooling the phase  $\text{AlCuFeMn}$  is usually present. In special conditions the compound  $\text{Cu}_2\text{FeAl}_7$  may be present and sometimes the  $\text{AlCuMn}$  phase, further complicating the identification of the constituents formed by manganese and iron.

Figure 342 shows an alloy where the ratio Cu : Mg is

$$\frac{3.22\text{Cu}}{1.16\text{Mg} - (1.73 \times 0.18\text{Si})} = 3.78$$

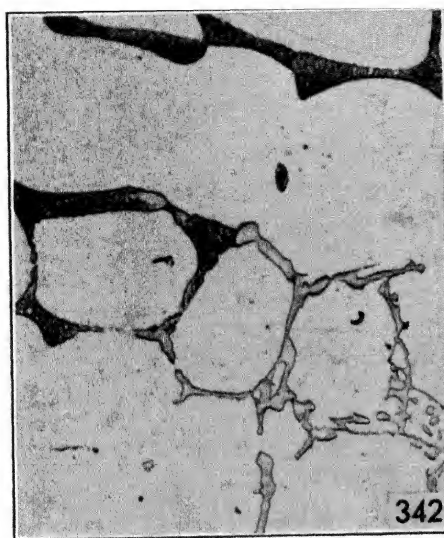


FIG. 342. Ingot water-cooled—Cu 3.22%, Mg 1.16%, Mn 0.65%, Si 0.18%, Fe 0.42%. Dark eutectic  $\text{Al-CuAl}_2\text{-Cu}_2\text{Mg}_2\text{Al}_5$ ,  $(\text{FeMn})\text{Al}_6$ (?) light. Some  $\text{CuAl}_2$  as eutectic  $\text{Al-CuAl}_2$  is visible, X 250, not etched.

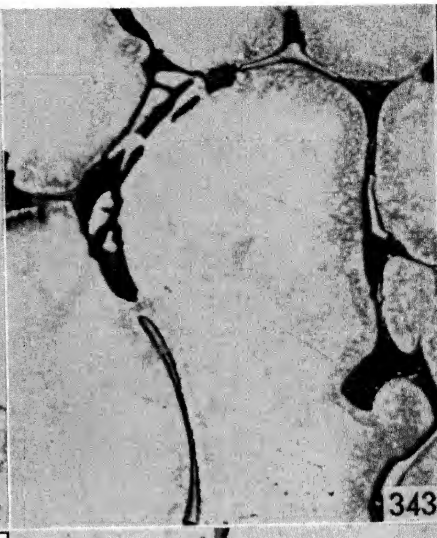


FIG. 343. Ingot water-cooled—Cu 4.58%, Mg 1.54%, Si 0.24%, Fe 0.55%, Mn 0.66%.  $\text{CuAl}_2$  light, eutectic  $\text{Al-CuAl}_2\text{-Cu}_2\text{Mg}_2\text{Al}_5$  dark,  $\text{AlCuFeMn}$  or  $\alpha(\text{AlFeMnSi})$  dark etched; the etching reveals coring in the Al crystals, X 250, etched with HF.



FIG. 344. Extruded shape, heat-treated—Cu 4.54%, Mg 1.52%, Si 0.16%, Fe 0.27%, Mn 0.56%.  $\text{CuAl}_2$  light,  $\text{Cu}_2\text{Mg}_2\text{Al}_5$  gray,  $(\text{FeMn})\text{Al}_6$  relieved, X 250, not etched.

and  $\text{CuAl}_2$  and  $\text{Cu}_2\text{Mg}_2\text{Al}_5$  are present as eutectic  $\text{Al-CuAl}_2\text{-Cu}_2\text{Mg}_2\text{Al}_5$ , together with a slight excess of  $\text{CuAl}_2$  and a manganese constituent, probably  $(\text{FeMn})\text{Al}_6$ . Figure 343 shows another alloy, widely employed in the United States. Figure 344 shows the same alloy extruded and heat-treated. Visible are  $\text{CuAl}_2$ , light;  $(\text{FeMn})\text{Al}_6$ , in relief; and  $\text{Cu}_2\text{Mg}_2\text{Al}_5$ , small gray particles, showing that the heat treatment was not sufficient to dissolve  $\text{CuAl}_2$  and  $\text{Cu}_2\text{Mg}_2\text{Al}_5$  completely, probably because they were present in an amount above the solid solubility limit at the heat treatment temperature.

The eutectics present in these alloys are:

$\text{Al-CuAl}_2\text{-Cu}_2\text{Mg}_2\text{Al}_5$ ; 932°F (500°C), Cu 26.8%, Mg 6.2%.

$\text{Al-CuAl}_2\text{-Mg}_2\text{Si}$ ; 965°F (517°C), Cu 28%, Mg 6%, Si 3.5%.

$\text{Al-CuAl}_2$ ; 1018°F (548°C), Cu 33%.

The manganese and iron compounds do not enter eutectics formed by copper and magnesium compounds, but form quasi-binary eutectics with aluminum, with melting points of about 1150°F (620°C).

The heat treatment of these alloys must be conducted below 932°F (500°C), and the usual practice is to soak at 900° to 925°F (480° to 495°C) for from 30 minutes to 4 hours, depending on the thickness of the material, and to follow with quenching in cold water. These alloys are seldom artificially aged. The slight gains obtained in the yield strength and in the tensile strength do not compensate for the increase in susceptibility to intergranular corrosion. Natural aging is complete in about 7 days; however, even a day after quenching the properties have reached about 90 per cent of their maximum.

### **Alloys with Hardening Constituents $\text{CuAl}_2$ and $\text{Mg}_2\text{Si}$**

Alloys of this group have a Mg : Si ratio around 1.73; that is, all the magnesium and silicon are combined to form  $\text{Mg}_2\text{Si}$ . Naturally, most of the alloys of this group will contain a slight excess of magnesium or silicon for it is almost impossible to have the exact ratio. Although these excesses have no importance from the point of view of the mechanical properties, they must not be overlooked because they may introduce small amounts of new phases producing new eutectics. For instance, an excess of 0.07 to 0.10 per cent magnesium may cause the formation of  $\text{Cu}_2\text{Mg}_2\text{Al}_5$  and introduce enough eutectic  $\text{Al-CuAl}_2\text{-Cu}_2\text{Mg}_2\text{Al}_5$  to ruin the alloy when heat-treated above 932°F (500°C). Alloys with a Mg : Si ratio below 1.73 sometimes fall into this group, when the manganese content is in excess of the amount necessary for the formation of  $(\text{FeMn})\text{Al}_6$  and the constituents



FIG. 345. Ingot water-cooled—Cu 3.70%, Mg 0.71%, Si 0.41%, Mn 0.62%, Fe 0.43%.  $Mg_2Si$  black,  $CuAl_2$  light,  $(FeMn)Al_6$  gray in its typical form of tetragonal crystals, X 250, not etched.

FIG. 346. Same specimen as in Fig. 345. Presence of the eutectic  $Al-CuAl_2-Mg_2Si$ , together with an excess of  $CuAl_2$  light, and some  $(FeMn)Al_6$  dark, X 1000, etched with HF.

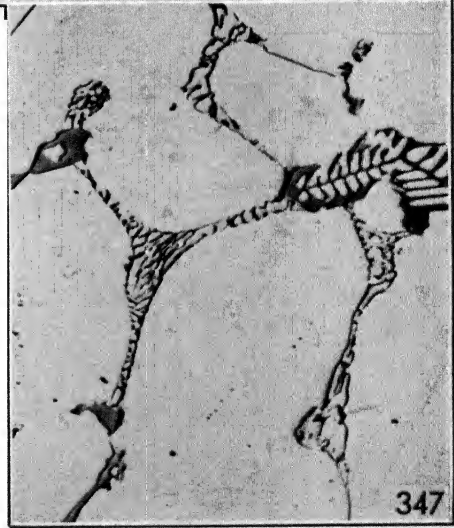


FIG. 347. Ingot water-cooled—Cu 4.26%, Mg 1.50%, Si 1.03%, Mn 0.61%, Fe 0.34%.  $\alpha(AlFeMnSi)$  gray etched,  $Mg_2Si$  black, and  $CuAl_2$  light, mostly as eutectic  $Al-CuAl_2-Mg_2Si$ , X 250, etched with HF.



$\alpha(\text{AlMnSi})$  or  $\alpha(\text{AlFeMnSi})$  are formed, reducing the effective silicon content.

Figures 345 and 346 show an alloy where the magnesium and silicon contents are exactly in the amount required for the formation of  $\text{Mg}_2\text{Si}$  and where  $(\text{FeMn})\text{Al}_6$ ,  $\text{CuAl}_2$ , and  $\text{Mg}_2\text{Si}$ , are the constituents present, the last two as eutectic  $\text{Al-CuAl}_2\text{-Mg}_2\text{Si}$ . Figure 347 shows an alloy containing a slight excess of silicon (1.03 per cent instead of 0.95 per cent) over the exact ratio. The manganese content is a little higher than required for the formation of  $(\text{FeMn})\text{Al}_6$ . The excess silicon combines, therefore, with iron and manganese to form  $\alpha(\text{AlFeMnSi})$ .

The eutectics present in these alloys are:

$\text{Al-CuAl}_2\text{-Mg}_2\text{Si}$ ; 965°F (517°C), Cu 28%, Mg 6%, Si 3.5%.

$\text{Al-CuAl}_2$ ; 1018°F (548°C), Cu 33%.

As for the other groups, there is evidence that the manganese compounds do not enter the eutectics formed by magnesium and copper but form eutectics with aluminum, mostly quasi-binary, with melting points well above 1100°F (600°C). When there is an excess of magnesium the following eutectic may be present.

$\text{Al-CuAl}_2\text{-Cu}_2\text{Mg}_2\text{Al}_5$  932°F (500°C) Cu 26.8%, Mg 6.2%

The heat treatment of these alloys is limited by the eutectic  $\text{Al-CuAl}_2\text{-Mg}_2\text{Si}$  with a melting point of about 965°F (517°C). The usual practice is to soak at 930° to 950°F (500° to 510°C) and to quench in cold water, artificially age at 250° to 300°F (120° to 150°C) for 8 to 12 hours. Artificial aging will develop the maximum properties; when naturally aged these alloys will have mechanical properties from 30 to 50 per cent lower than those in the table. Alloys of this group with a magnesium excess should be avoided, for the presence of the compound  $\text{Cu}_2\text{Mg}_2\text{Al}_5$  limits the maximum soaking temperature to 925°F (493°C) and they do not develop their maximum properties at this temperature. It is much better to have a silicon excess with high manganese, for then the eutectics formed have about the same melting point as those in alloys with the exact Mg : Si ratio, and there is no need to reduce the soaking temperature.

### **Alloys with Hardening Constituents $\text{CuMg}_5\text{Si}_4\text{Al}_4$ and $\text{CuAl}_2$**

The Mg : Si ratio in this group must be below 1.73 and should be precisely 1.08. When this is the ratio, copper, magnesium, and silicon are combined to form the quaternary compound  $\text{CuMg}_5\text{Si}_4\text{Al}_4$  and the excess of copper is present as  $\text{CuAl}_2$ . If the ratio is above 1.08, some

$\text{Mg}_2\text{Si}$  is present; if below, there is an excess of silicon which will combine with the manganese and eventually the iron to form  $\alpha(\text{AlMnSi})$  or  $\alpha(\text{AlFeMnSi})$ . Figure 348 shows an alloy of this type where the excess of silicon,  $1.03 - (0.94/1.08) = 0.16$  per cent, is combined with manganese to form the quaternary phase  $\alpha(\text{AlFeMnSi})$ . The other constituents are  $\text{CuAl}_2$  and  $\text{CuMg}_5\text{Si}_4\text{Al}_4$ . Figure 349 shows another alloy after rolling and heat treatment. The quaternary and most of the  $\text{CuAl}_2$  went into solid solution. The constituents visible

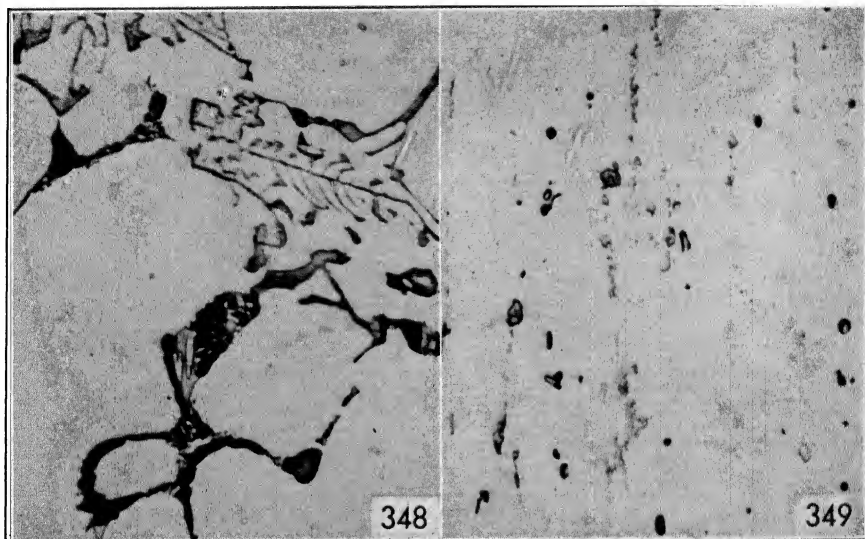


FIG. 348. Ingot water-cooled—Cu 4.44%, Fe 0.56%, Si 1.03%, Mg 0.94%, Mn 0.65%. Black  $\text{CuAl}_2$ , light globules and needles of  $\text{CuMg}_5\text{Si}_4\text{Al}_4$ ,  $\alpha(\text{AlFeMnSi})$  in its typical form when it contains high silicon, X 250, etched with  $\text{Fe}(\text{NO}_3)_3$ .

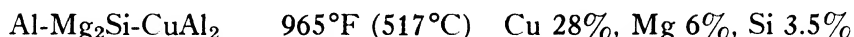
FIG. 349. Rolled rod, heat-treated—Cu 4.05%, Fe 0.50%, Si 0.55%, Mg 0.61%, Mn 0.48%.  $\text{CuAl}_2$  black etched, Mn constituents light, X 250, etched with  $\text{Fe}(\text{NO}_3)_3$ .

are manganese compounds and a few particles of  $\text{CuAl}_2$  which did not go into the solid solution.

The eutectics present in these alloys are:



and the eutectics formed by the manganese compounds, which are mostly quasi-binary and have melting points above  $1100^\circ\text{F}$  ( $600^\circ\text{C}$ ). Sometimes small amounts of the eutectic



are present if the silicon available is insufficient to form the quaternary.

The proper heat treatment of these alloys should be: soak at 950° to 970°F (510° to 520°C) and quench in cold water; but it is commonly conducted at temperatures between 940° and 960°F (505° and 515°C), probably because, when heavy segregations are present, it may be possible that some  $\text{Mg}_2\text{Si}$  is present, forming the eutectic  $\text{Al-CuAl}_2\text{-Mg}_2\text{Si}$ , which melts at 965°F (517°C).

These alloys are not commonly artificially aged, for little improvement is obtained this way. Natural aging is influenced by the amount of constituents present and may be complete in 3 to 4 days for alloys with higher percentages of magnesium but may require even 15 to 20 days for alloys with lower magnesium percentages.

## CHAPTER 13

### ALUMINUM-COPPER-NICKEL ALLOYS

Under the heading Aluminum-Copper-Nickel Alloys several alloys, containing copper and nickel together with magnesium, sometimes with additions of iron and silicon, will be reviewed. These alloys are used widely in Europe and especially in England, where they originated. Their high mechanical properties in the cast and heat-treated state, and the fact that they also maintain high properties at temperatures above room temperature, make them particularly fit for the production of castings and forgings subjected to high temperature. Some similarity exists between these alloys and duralumin and sometimes alloys of this group are called duralumins. The similarity is in the hardening constituents, which produce the high properties in these alloys. However, a division of these alloys along lines similar to these of the duralumins is not possible because these alloys are not so definite, and alloys containing more than one hardening constituent are in common use. Two groups can be distinguished, depending on the iron content.

1. Iron as an impurity.
2. Iron between 1 and 1.5 per cent.

#### Alloys with Low Iron

The main type of this group is the so-called *Y alloy*. The composition of this group ranges between:

Cu	3-5%
Ni	1-2.5%
Mg	0.5-2%
Fe	up to 0.7%
Si	up to 0.7%

The microstructure of these alloys is greatly affected by the rate of cooling. Depending on it, the copper remains in solid solution or combines with iron and nickel. This affects the mechanical properties because, if the copper is in solid solution, it takes part in the aging

and strengthens the alloy; if it is combined, its strengthening effect is largely lost. For this reason sand-cast alloys have mechanical properties which are 30 to 40 per cent lower than alloys cast in permanent mold, although no wide difference can be detected in the grain size or distribution of the constituents.

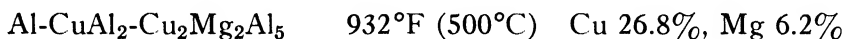
The magnesium in the alloy first combines with all the silicon present to form  $\text{Mg}_2\text{Si}$ . The remaining magnesium combines with copper to form  $\text{Cu}_2\text{Mg}_2\text{Al}_5$ .

With fast cooling iron and nickel form a constituent different from  $\text{FeNiAl}_9$  and which probably contains little copper. In this case most of the free copper (that is, the copper which is not combined with magnesium) remains in solid solution and takes part subsequently in the age hardening.

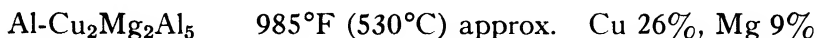
With low cooling rates the copper combines with iron and nickel to form an  $\text{AlCuNi}$  and an  $\text{AlCuFe}$  phase, which have a high copper content so that most of the free copper is combined in insoluble constituents and does not participate in the heat treatment.

Figure 350 illustrates a sand-cast alloy where  $\text{Mg}_2\text{Si}$ ,  $\text{AlCuNi}$ , and an  $\text{AlCuFe}$  phase (probably  $(\text{CuFe})\text{Al}_3$ ) are present. Figure 351 illustrates a point in another alloy, where a segregation of  $\omega(\text{AlCuFe})$  is present together with small amounts of  $\text{AlCuNi}$ . Figure 352 shows an alloy cast in a semi-permanent mold which has low mechanical properties.  $\text{Mg}_2\text{Si}$  and small amounts of  $\text{Cu}_2\text{Mg}_2\text{Al}_5$  are associated with  $\text{AlCuNi}$  and probably  $(\text{CuFe})\text{Al}_3$ . The same alloy cast in permanent mold is shown in Fig. 353. This sample had extremely high mechanical properties (tensile strength of 63,000 psi after heat treatment). The constituents visible after heat treatment are the quaternary  $\text{AlCuFeNi}$  and some  $\text{AlCuNi}$ , showing that most of the copper was in solid solution.

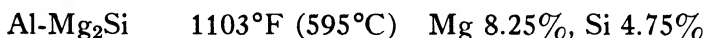
Little is known about the eutectics present in these alloys. The eutectic



is present so seldom in heavy segregations and in alloys with very high copper and low nickel that, from a practical point of view, it may be stated that it is not present in commercial production. The lowest melting eutectic is probably the quasi-binary



in alloys with low silicon. In alloys with higher silicon the eutectic



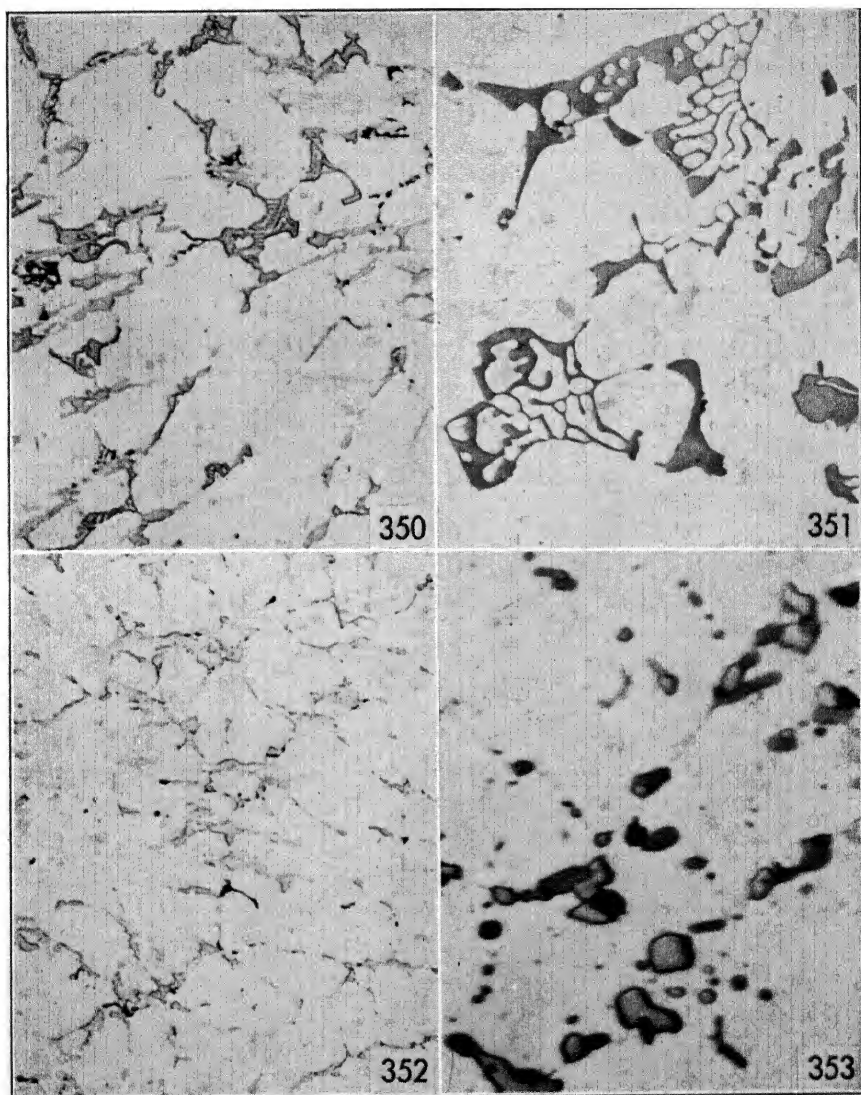


FIG. 350. Sand-cast—Cu 3.90%, Fe 0.38%, Mg 1.47%, Ni 2.08%, Si 0.42%.  $Mg_2Si$  black, AlCuNi dark gray, an AlCuFe constituent light, X 250, not etched.

FIG. 351. Sand-cast—Cu 4.05%, Fe 0.72%, Si 0.44%, Mg 1.55%, Ni 2.12%. Segregation of an Fe containing phase, probably  $\omega(AlCuFe)$  gray, small crystal of AlCuNi lighter, X 250, etched with HF.

FIG. 352. Cast in semi-permanent mold—Cu 3.96%, Fe 0.40%, Si 0.42%, Mg 1.55%, Ni 2.16%. Black  $Mg_2Si$ , AlCuNi relieved, an Fe constituent light not relieved, X 250, not etched.

FIG. 353. Same alloy as in Fig. 352 cast in permanent mold and heat-treated. Black  $Mg_2Si$ , dark-etched AlCuFeNi, light AlCuNi, X 1000, etched with HF.

should be the lowest melting, since no eutectic  $\text{Al-Mg}_2\text{Si-Cu}_2\text{Mg}_2\text{Al}_5$  is formed, and the eutectics formed by the constituents containing iron or nickel have melting points above  $1100^\circ\text{F}$  ( $600^\circ\text{C}$ ).

The heat-treatment practice for both cast and wrought products of these alloys is as follows: soak at  $960^\circ$  to  $980^\circ\text{F}$  ( $515^\circ$  to  $527^\circ\text{C}$ ) and quench; follow with artificial aging at  $320^\circ$  to  $390^\circ\text{F}$  ( $160^\circ$  to  $200^\circ\text{C}$ ) for 8 to 10 hours.

The mechanical properties in the cast and wrought state are given in the table below.

	YIELD STRENGTH 0.2%; PSI	TENSILE STRENGTH PSI	ELONGA- TION % ON 2 IN.	BRINELL HARDNESS 500/10/30
Sand-cast	15,000-20,000	25,000-30,000	1- 4	75- 90
Sand-cast heat-treated	25,000-30,000	30,000-40,000	0- 2	95-120
Permanent-mold cast	18,000-25,000	30,000-40,000	1- 3	85-110
Permanent-mold heat-treated	35,000-45,000	45,000-60,000	0- 2	100-150
Wrought heat-treated	35,000-50,000	55,000-65,000	5-20	100-150

In the molten state these alloys have a great tendency to absorb gases, especially water vapors; melting in reverberatory furnaces should be avoided as much as possible. The high magnesium and nickel content give them a high-shrinkage coefficient. Additions of silicon reduce it somewhat and increase the fluidity so that even complicated shapes can be cast with proper care. The working of these alloys requires the same precautions as any strong aluminum alloy. Particular care must be taken in casting the billets for forming because the alloys have a great tendency to segregation and large grain size.

The machinability is good, especially in the heat-treated state. The corrosion resistance is not very good. After aging, especially artificial aging, there is a tendency to intergranular corrosion.

These alloys are used mainly when good mechanical properties at low and at elevated temperatures are the most important consideration. Pistons and especially cylinder heads for airplane engines are cast or forged from these alloys.

### Alloys with High Iron

Several alloys are included in this group and the analyses range thus:

Cu	1-3.5%
Fe	1-1.5%
Mg	0.5-2.5%
Ni	0.5-1.5%
Si	0.5-2.5%

Occasionally titanium, chromium, molybdenum, and even columbium and cerium have been added to these alloys in amounts up to 0.25 per cent, but their effect, if any, is as grain refiners, and they will not affect the properties of the alloys to any great extent.

The microconstituents of these alloys are similar to those of the first group, and the rate of solidification has a similar effect. The alloying elements, within the limits reported above, combine as follows in commercial casting.

**Magnesium** forms first  $Mg_2Si$ . If there is still free silicon and copper—that is, copper and silicon not combined with iron and nickel—the quaternary  $CuMg_5Si_4Al_4$  is formed. Sometimes  $Cu_2Mg_2Al_5$  may be formed if the silicon present is insufficient to combine with all the magnesium to form  $Mg_2Si$ .

**Copper** with quick solidification combines partly with iron and nickel to form the quaternary  $AlCuFeNi$ . The rest remains in solid solution during solidification and reprecipitates later as  $CuAl_2$  or reacts with magnesium and silicon to form  $CuMg_5Si_4Al_4$  if magnesium and silicon are available. With slow solidification copper combines with iron and nickel to form one of the  $AlCuNi$  phases and one or more of the three  $AlCuFe$  phases. If some copper is left uncombined, it forms  $CuAl_2$  or, in the presence of magnesium alone,  $Cu_2Mg_2Al_5$  and, in the presence of magnesium and enough silicon,  $CuMg_5Si_4Al_4$ .

**Silicon** first of all forms  $Mg_2Si$ . If some silicon remains uncombined it may form  $\alpha(AlFeSi)$  if not all the iron is combined with copper or nickel. Otherwise it reacts with copper and  $Mg_2Si$  to form  $CuMg_5Si_4Al_4$ , or, in the absence of available copper, it may remain as free Si.

**Iron** with high cooling speeds forms  $AlCuFeNi$ ; if there is an excess of silicon, it reacts with it to form  $\alpha(AlFeSi)$ . With slow cooling, iron forms one of the three  $AlCuFe$  phases, or it may combine with nickel to form  $FeNiAl_9$ . If there is some silicon not combined as  $Mg_2Si$ , it forms  $\alpha(AlFeSi)$ . In some rare cases iron may be present as  $Fe_2Al_7$ .

**Nickel** with high solidification speeds forms the  $AlCuFeNi$  phase or sometimes  $FeNiAl_9$ . If there is an excess of nickel it may be in the form of  $NiAl_3$ . With slow solidification it forms one or more of the  $AlCuNi$  phases and sometimes it may be present as  $NiAl_3$ .

The following examples will illustrate these constituents. Figure 354 shows an alloy sand-cast, where  $Mg_2Si$  is associated with  $AlCuNi$  and  $(CuFe)Al_3$ . Figure 355 shows one of the rare cases where  $Cu_2Mg_2Al_5$  is present, together with  $Mg_2Si$ . Figure 356 shows a segregated spot in a water-cooled ingot, where a large amount of



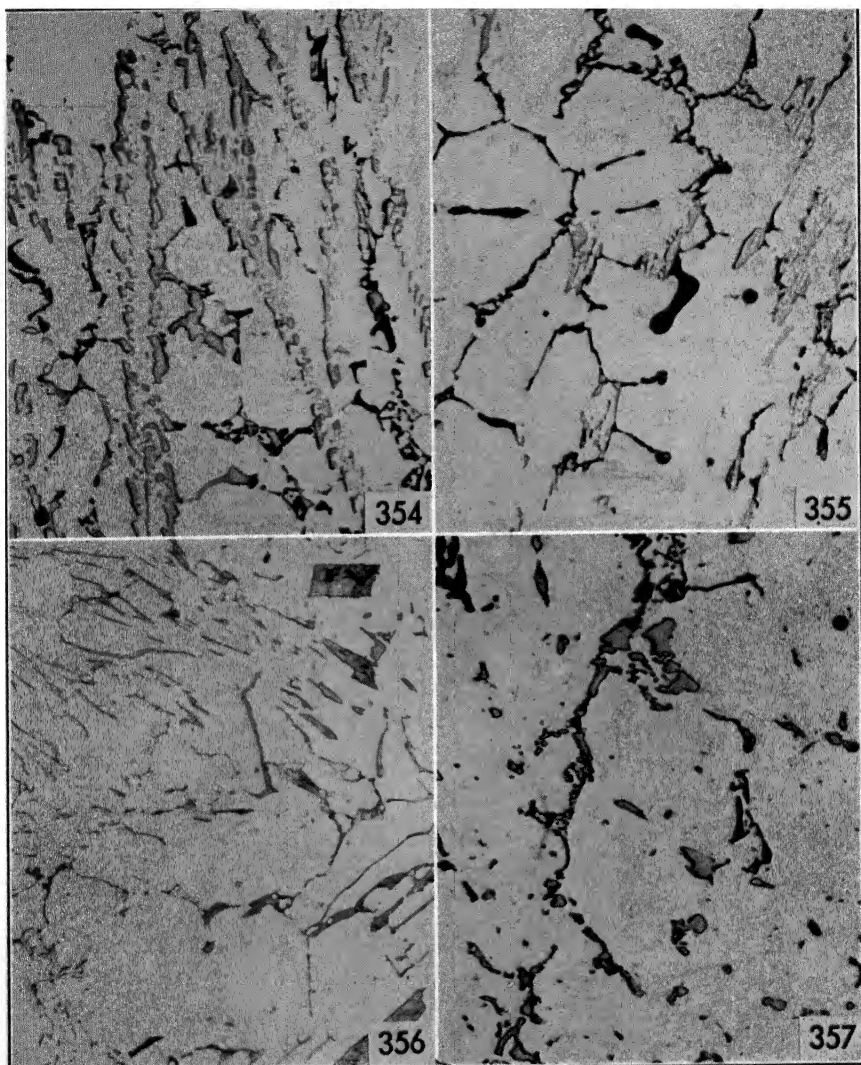


FIG. 354. Sand-cast—Cu 2.31%, Fe 1.12%, Si 1.22%, Mg 1.54%, Ni 1.15%.  $Mg_2Si$  black,  $AlCuNi$  relieved,  $(CuFe)Al_3$  lighter not relieved, X 250, not etched.

FIG. 355. Sand-cast—Cu 2.30%, Fe 1.05%, Si 0.87%, Mg 2.19%, Ni 1.24%.  $Mg_2Si$  black and  $Cu_2Mg_2Al_5$  (globules), light  $AlCuFeNi$  and  $AlCuNi$ , X 250, etched with  $Fe(NO_3)_3$ .

FIG. 356. Ingot water-cooled, segregated—Cu 2.30%, Ni 1.20%, Fe 1.12%, Si 0.52%, Mg 0.88%. Primary crystals of  $FeNiAl_3$ , some other constituent containing Fe and Cu in the background, X 250, not etched.

FIG. 357. Same alloy as in Fig. 356. Ingot water-cooled. Normal structure,  $Mg_2Si$  black,  $AlCuFeNi$  light, X 250, not etched.

$\text{FeNiAl}_9$  is present together with some  $\text{AlCuFe}$ . Figure 357 shows the normal structure of a water-cooled ingot of the same alloy. Figure 358 shows the presence of  $\omega(\text{AlCuFe})$  and of the eutectic  $\text{Al-CuAl}_2\text{-Mg}_2\text{Si}$ . Figure 359 shows another alloy, cast in permanent mold, where  $\alpha(\text{AlFeSi})$ ,  $\text{NiAl}_3$ ,  $\text{AlCuNi}$  and some free Si are present. Figure 360 shows an alloy where  $\text{AlCuNi}$  and  $(\text{FeCu})\text{Al}_3$  are the only constituents visible, as Mg and Si and some Cu are in solid solution. Figure 361 shows another alloy cast in permanent mold where  $\alpha(\text{AlFeSi})$ ,  $\text{AlCuFeNi}$ , and  $\text{AlCuNi}$  are visible.

The examples given above show some of the more common structures encountered in these alloys, but a complete illustration of them is impossible, for each specimen is different from the next, even in the same casting.

Very little is known about the eutectics in these alloys; the lowest-melting eutectic

$\text{Al-CuAl}_2\text{-Mg}_2\text{Si}$      $965^\circ\text{F}$  ( $517^\circ\text{C}$ )    Cu 28%, Mg 6%, Si 3.5%

is almost never present. The quasi-binary

$\text{Al-Cu}_2\text{Mg}_2\text{Al}_5$      $985^\circ\text{F}$  ( $530^\circ\text{C}$ )    Cu 26%, Mg 9%

also very seldom present, has the next lowest melting point. The eutectics commonly present are the quasi-binary

$\text{Al-Mg}_2\text{Si}$      $1103^\circ\text{F}$  ( $595^\circ\text{C}$ )    Mg 8.25%, Si 4.75%

and the eutectics formed by constituents containing iron and nickel associated with copper and silicon, whose melting points are above  $1100^\circ\text{F}$  ( $600^\circ\text{C}$ ).

The heat-treatment practice is somewhat different for the various alloys, as the alloys containing sufficient amounts of quaternary  $\text{CuMg}_5\text{Si}_4\text{Al}_4$  attain good average properties with natural aging, whereas the alloys containing  $\text{Mg}_2\text{Si}$  as the main hardening agent require artificial aging to develop their higher properties. The heat-treatment practice is as follows: soak at  $970^\circ$  to  $1000^\circ\text{F}$  ( $520^\circ$  to  $540^\circ\text{C}$ ) and follow with quenching; if necessary follow with artificial aging at  $300^\circ$  to  $390^\circ\text{F}$  ( $150^\circ$  to  $200^\circ\text{C}$ ) for 6 to 12 hours.

The mechanical properties of these alloys are as follows.

	YIELD STRENGTH 0.2%; Psi	TENSILE STRENGTH Psi	ELONGA- TION % ON 2 IN.	BRINELL HARDNESS 500/10/30
Sand-cast	9,000-15,000	15,000-25,000	1- 5	70- 90
Sand-cast heat-treated	20,000-30,000	30,000-45,000	0- 2	80-120
Permanent-mold cast	20,000-25,000	30,000-40,000	1- 3	70- 90
Permanent-mold cast heat-treated	20,000-40,000	35,000-50,000	0- 3	80-150
Wrought heat-treated	35,000-50,000	40,000-60,000	5-20	100-150

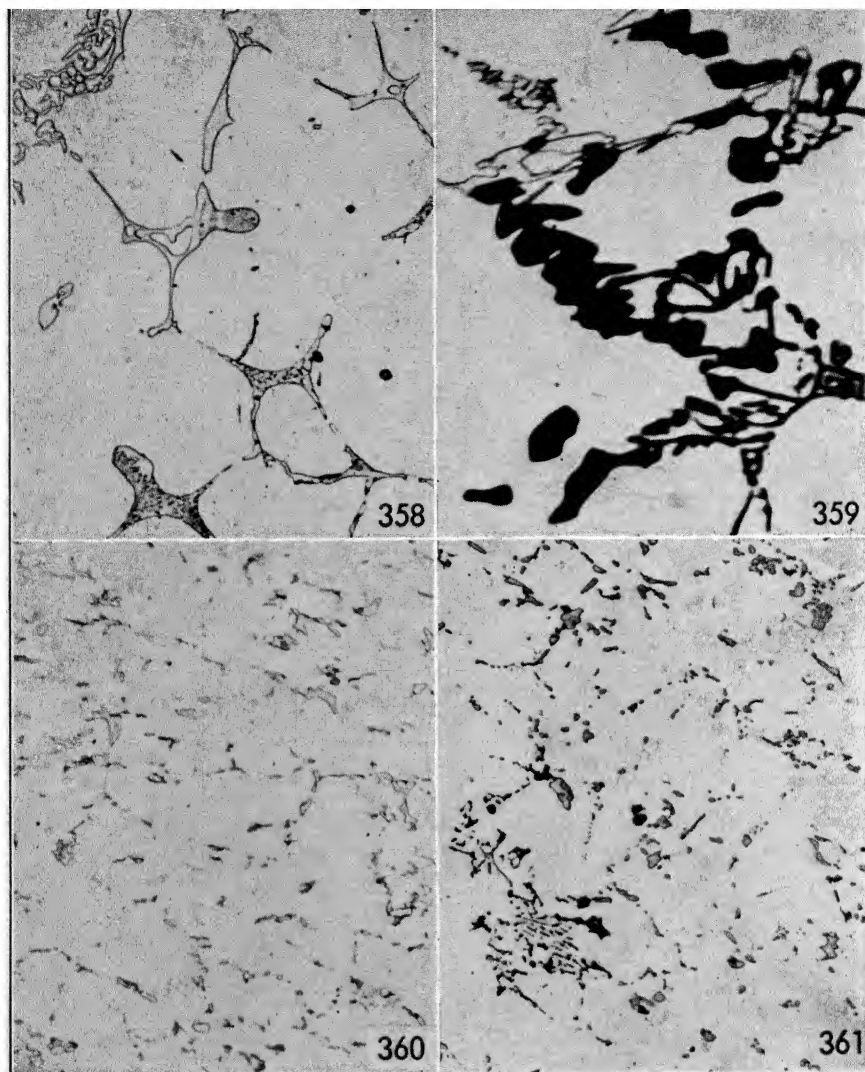


FIG. 358. Sand-cast—Cu 3.36%, Fe 1.33%, Si 0.63%, Mg 0.92%, Ni 0.72%. Eutectic Al-CuAl<sub>2</sub>-Mg<sub>2</sub>Si and  $\omega$ (AlCuFe), X 250, not etched.

FIG. 359. Cast in permanent mold—Cu 1.50%, Fe 1.62%, Mg 0.57%, Si 2.05%, Ni 0.86%. Black Chinese script  $\alpha$ (AlFeSi), dark NiAl<sub>3</sub>, gray points of Si, light AlCuNi, X 1000, etched with H<sub>2</sub>SO<sub>4</sub> and NaOH.

FIG. 360. Cast in permanent mold—Cu 3.06%, Fe 1.42%, Mg 0.57%, Si 0.69%, Ni 0.56%. Light relieved AlCuNi, dark points of (FeCu)Al<sub>3</sub>, X 250, etched with NaOH.

FIG. 361. Cast in permanent mold—Cu 2.15%, Fe 1.52%, Mg 0.60%, Si 0.72%, Ni 0.65%. Black  $\alpha$ (AlFeSi), dark AlCuNi, light AlCuFeNi, X 250, etched with H<sub>2</sub>SO<sub>4</sub>.

The castability of these alloys is rather good, but especially alloys with high magnesium contents require careful handling to avoid oxidation of the magnesium. These alloys can be wrought, if the proper precautions for strong aluminum alloys are observed, similarly to the alloys of the low-iron group. The machinability is good, especially for alloys with high magnesium and silicon contents in the heat-treated state. Corrosion resistance is not particularly good and alloys in the upper copper range are subject to intergranular corrosion.

These alloys are used widely for pistons and parts requiring good mechanical properties at high temperatures. They also find use, in the heat-treated state, for castings and forgings where high mechanical properties are necessary.

*PART IV*  
*EFFECT OF FABRICATING ON*  
*THE MICROSTRUCTURE*

CHAPTER 14

**MELTING, FLUXING, POURING, CASTING**

The first three operations, when properly performed, will not affect the microstructure of the resulting alloy in the least. However, when one or more of them is carelessly executed, the defects introduced may extend until they decidedly affect the subsequent fabrications and the final properties of the alloy.

The most important defects arising from improper technique in melting, fluxing, and pouring are gas or oxide inclusions. Loss of certain alloying elements through burning or segregations may also be caused by improper melting or pouring techniques, but they affect the chemical composition mainly, and therefore chemical analysis will reveal them more accurately than microscopic examination. The term gas inclusions is misleading, as many gases are not entrapped in aluminum in the gaseous state, but rather in the solid state, forming with aluminum hydrides, nitrides, carbides, etc., whose shape and appearance usually cannot be distinguished from that of the oxide. A distinction between solid and gaseous inclusions is also hindered by the effect of polishing operations. Brittle constituents, as most solid inclusions are, are easily broken in the first stages of polishing, and the polishing agents tend to fill their place.

Gas inclusions are cavities filled with gas. In polishing they become filled with the polishing agent, in the same way as the cavities left by broken solid inclusions. At the end of the polishing only a cavity is left, filled with dirt, with the edges more or less dragged, depending on the skill of the polisher. A direct distinction between solid and gaseous inclusions is therefore impossible. Sometimes the distribution, form and size of the defects may help in the identification. Solid inclusions tend to have jagged edges, are distributed at random within the grains

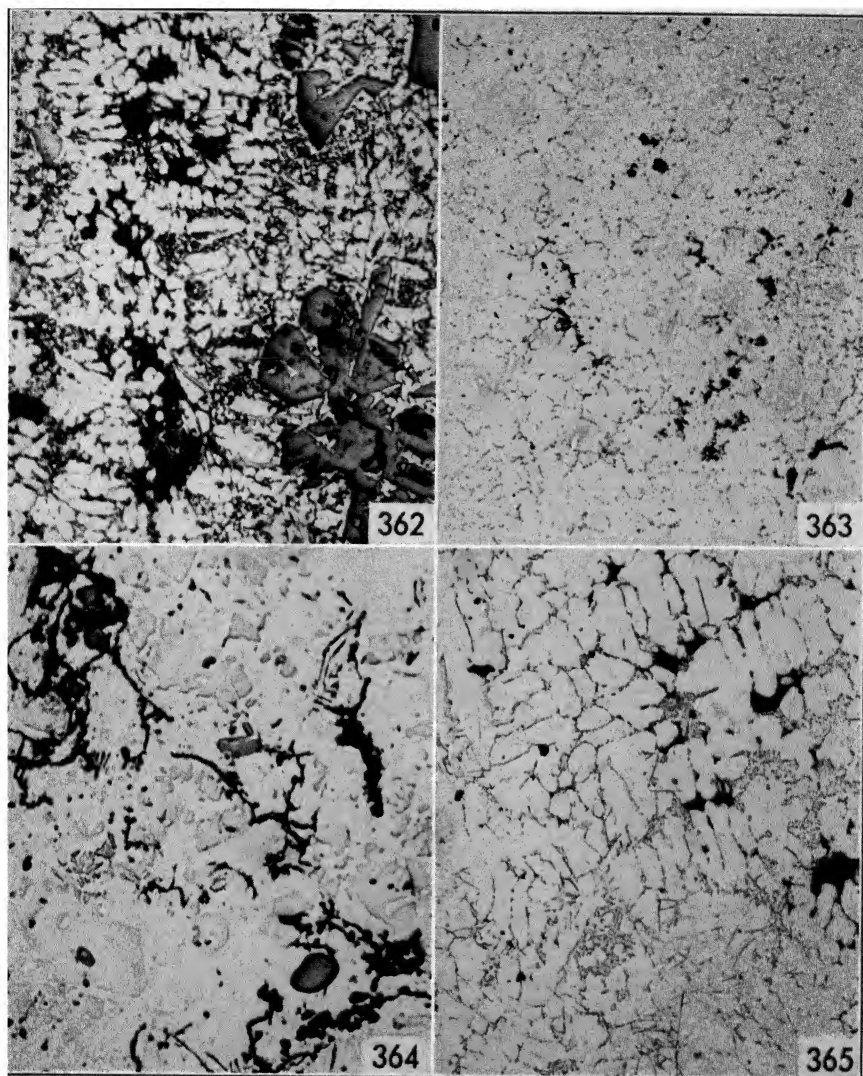


FIG. 362. Black inclusions of oxide, crystals of primary Si, needles of  $\text{FeSiAl}_5$  mixed with eutectic Al-Si. Cast in permanent mold—Si 20.45%, Cu 1.05%, Fe 1.14%, Mg 1.09%, Ni 2.35%, X 75, etched with NaOH.

FIG. 363. Inclusions of oxide (probably MgO) black in a network of  $\text{Mg}_2\text{Si}$  and  $(\text{FeMn})\text{Al}_6$ —Mg 4.23%, Fe 0.50%, Si 0.18%, Cu 0.19%, Mn 0.16%. Cast in permanent mold, X 75, not etched.

FIG. 364. Oxide inclusions (probably some V oxide) in an AlV master alloy; three AlV constituents of decreasing darkness. Ingot—V 2.42%, Si 0.42%, Fe 0.56%, X 75, not etched.

FIG. 365. Inclusions of oxide in a network of  $\text{CuAl}_2$ , with  $\alpha(\text{AlFeSi})$  and  $\text{AlCuFeSi}$  interspersed—Cu 6.80%, Fe 1.15%, Si 3.71%, Zn 1.87%, Sn 0.35%—X 75, not etched.

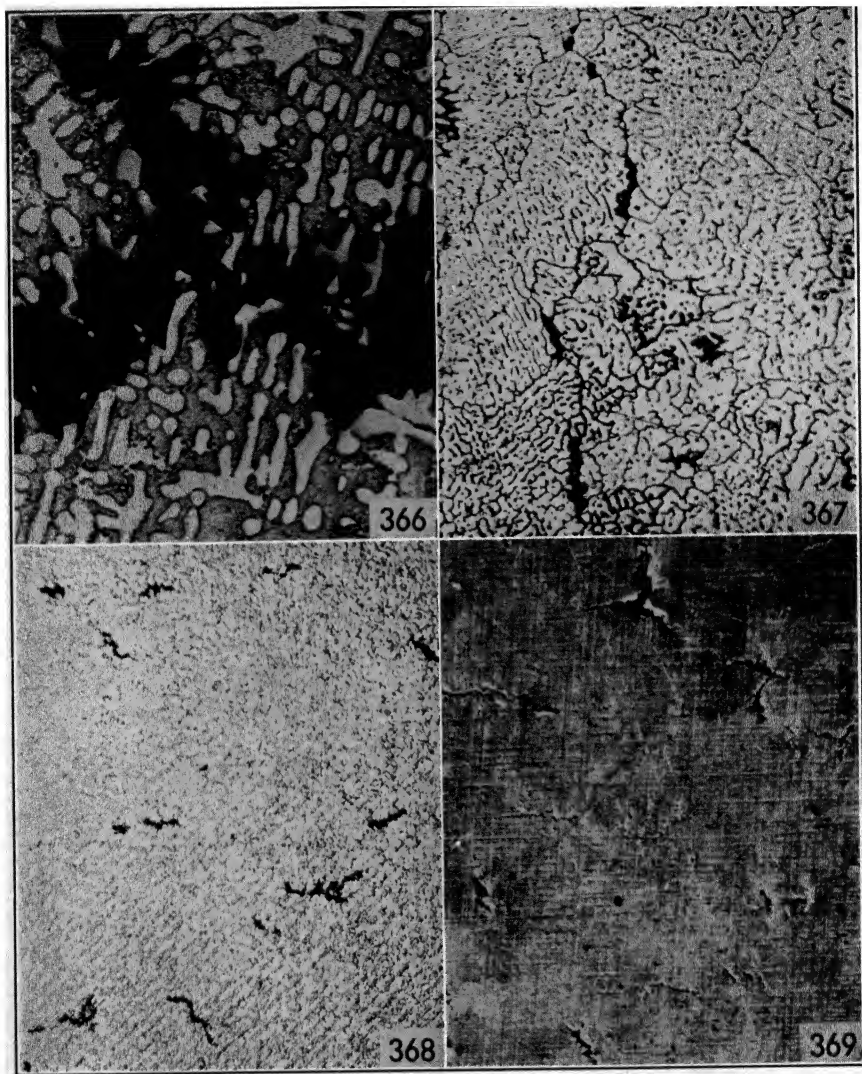


FIG. 366. Oxide or gas inclusions at the grain boundaries. White primary crystals of Al in a background of Al-Si eutectic. Cast in permanent mold—Si 9.10%, Fe 0.56%, Mg 0.40%, Co 0.61%, X 75, not etched.

FIG. 367. Gas or oxide inclusions at the grain boundaries. Ingot water-cooled—Cu 4.02%, Fe 0.51%, Si 0.29%, Mg 0.71%, Mn 0.54%—X 30, etched with acid mixture.

FIG. 368. Oxide inclusions in a water-cooled ingot—Cu 4.51%, Fe 0.42%, Si 0.21%, Mg 1.49%, Mn 0.55%—X 10, not etched.

FIG. 369. Same ingot as in Fig. 368 after rolling to sheet. Surface cracks caused by oxide inclusions, X 10, not etched.

and usually have varied sizes; whereas gaseous inclusions are concentrated at the grain boundaries, tend to be round, and the variation of size among them is very limited. However, that is only approximately true; there is no steadfast rule. To complicate the matter further, shrinkage cavities also tend to be at the grain boundaries, sometimes rounded. Eutectic melting and high-temperature deterioration may have the appearance of inclusions. Examples of these defects will be seen later. Figures 362 to 365 show inclusions, which are probably produced by oxides or the like, respectively in a 20 per cent silicon, 4 per cent magnesium, vanadium master alloy, and a 7 per cent copper alloy. Figures 366 and 367 show inclusions, probably gaseous, respectively in a 10 per cent silicon alloy and a duralumin.

Inclusions affect the workability of the alloy in the sense that they produce small cracks, which in further fabrications become slivers. Figure 368 shows oxide inclusions in a large ingot for rolling. Figure 369 shows the surface of another part of the ingot after partial rolling, where the defects have been opened up in the direction of rolling to form cracks. Inclusions may also be caused by reactions between the molten metal and the mold during pouring. This type of defect, however, can be detected, in the rare cases when it appears, because it tends to be limited to the surface of the casting instead of being evenly distributed through the mass of the metal.

An operation, which may be considered as a special fluxing, is the modification of the aluminum-silicon alloys. The theoretical aspect has been dealt with in Part I, and in Part III are several examples of modified and unmodified alloys, so that there is no need to show the effect of this operation on the microstructure. For this reason only the defects which may be produced by improper technique will be considered here. Two main defects can arise: the incomplete modification and the overmodification. The names are self-explanatory. Figure 370 shows an alloy where unmodified crystals of silicon are surrounded by zones of modified alloy. Figures 371, 372, and 373 show overmodification. The structure of Fig. 371 is typical of alloys which have been overmodified by metallic sodium. The structure of Figs. 372 and 373 is typical of alloys overmodified by the use of alkaline salts.

Casting is the most important operation in fabricating aluminum alloys, as it is the first step in aluminum production. Therefore, defects in the casting will influence all further fabrications as well as the final properties of the product. There are two types of casting: the casting which gives the piece in its final form, due allowance being made for machining and finishing; the casting which is intended to supply the alloy in a form suitable for further forming (rolling, extrusion, forging,



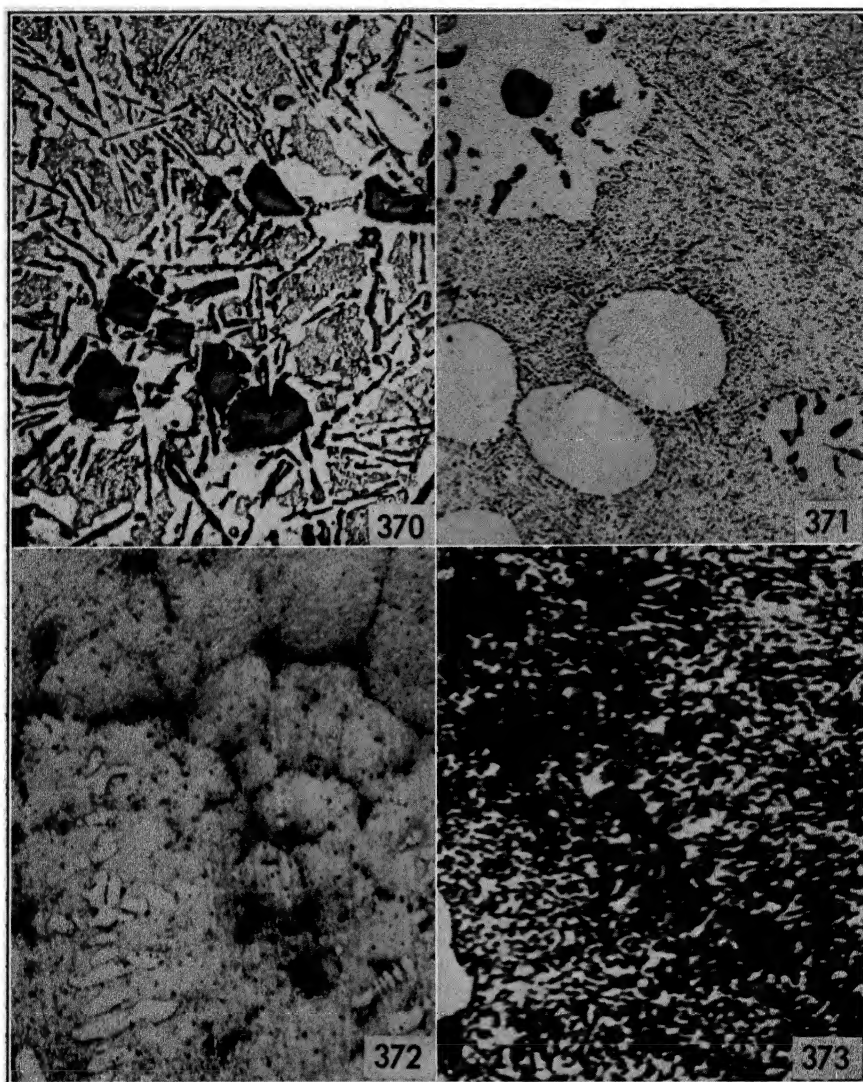


FIG. 370. Sand-cast, modified with sodium salts. Incomplete modification, probably caused by too long interval between modification and pouring. Primary crystals of Si, eutectic Al-Si partly modified—Si 13.10%, Fe 0.53%—X 250, not etched.

FIG. 371. Sand-cast, modified with metallic sodium. Globules of Si (?) inside the crystals of primary Al—Si 12.10%, Fe 0.48%—X 250, not etched.

FIG. 372. Cast in permanent mold, modified with sodium salts. Network at the grain boundaries, probably of salts, attacked by water in polishing—Si 12.50%, Fe 0.38%—X 75, not etched.

FIG. 373. Detail of Fig. 372, showing rounded particles which constitute the network, X 1000, not etched.

etc.). The first type of casting generally is classified according to the type of mold used, the three main types being sand, permanent mold, and die casting. The second type is usually called ingot or billet casting and can be divided in two types: cold-mold casting and continuous casting, depending on the method of casting used.

### **Sand, Permanent Mold, Die Casting**

Aluminum alloys are cast by all the three methods. The selection of the method to be used generally is based more on economic than on technical factors. No definite rule exists for the results of the different methods. Broadly it may be stated that sand-cast alloys have a slower cooling rate, whereas die-cast alloys have a faster cooling rate. Yet no sharp difference exists, and the cooling rate ranges from dry sand castings to die castings, through the gradual steps of green sand, semi-permanent mold, hot mold, cold mold. Also to be kept in mind is the effect of chills, which, if extensively used, may produce sand castings with a structure approximating permanent mold castings. Moreover, the rate of cooling influences the various alloys differently, being rather unimportant on alloys approximating eutectic compositions and becoming the most important factor for alloys of the aluminum-copper-nickel type.

The examples given in the following pages, together with the few in Part III, are intended to give an idea of the variations in structure which may be caused by the different methods of casting. Figures 374, 375, and 376 show a 7 per cent copper alloy which has been, respectively, sand, permanent mold, and die cast. Some difference in the grain size and distribution of the constituents exists between sand and permanent-mold cast; no difference between permanent mold and die cast is visible, as the die-cast sample is taken from the outside and does not show the inclusions, which are almost unavoidable, and must be considered an integral part of the structure in the center of die-cast material.

Figures 377 and 378 show a modified 13 per cent silicon alloy, sand- and permanent-mold cast. Besides a slight difference in the size of the primary crystals of aluminum, which may be occasional, no other difference can be detected.

Figures 379 and 380 show a 5 per cent silicon alloy, sand and permanent-mold cast. There is a difference in the distribution of the eutectic network, which in the permanent-mold casting is more finely distributed, being at the grain boundaries, and there is probably a slight difference in the amount of Si visible, as in the permanent-mold casting more is dissolved and therefore not visible.

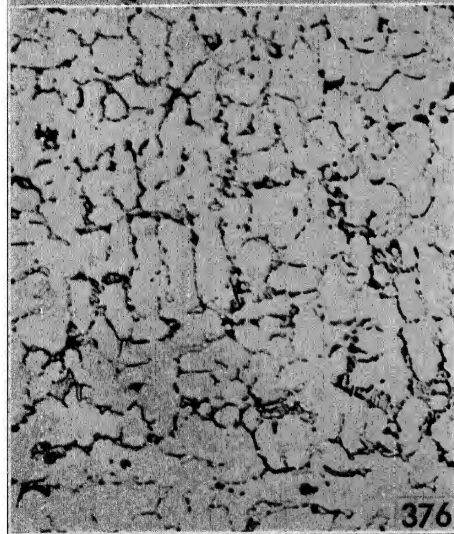
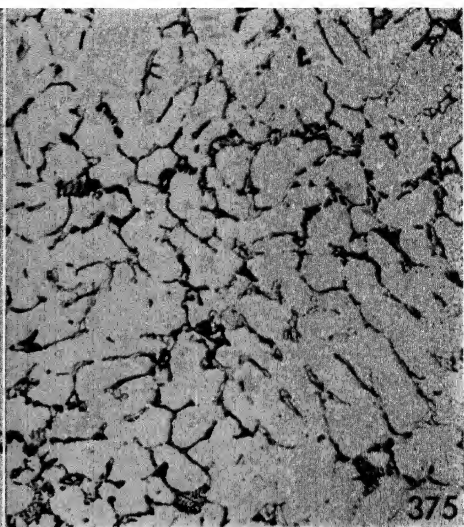
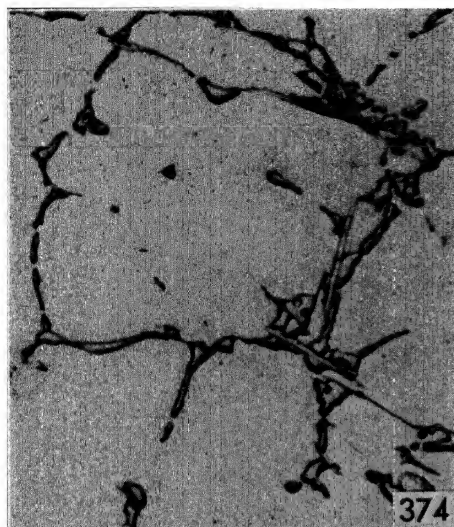


FIG. 374. Sand-cast—Cu 7.12%, Fe 0.64%, Si 0.76%. Needles of AlCuFeSi on a network of eutectic Al-CuAl<sub>2</sub>, X 250, etched with Fe(NO<sub>3</sub>)<sub>3</sub>.

FIG. 375. Same alloy as in Fig. 374 cast in permanent mold.  $\alpha$ (AlFeSi) on a network of eutectic Al-CuAl<sub>2</sub>, X 250, etched with H<sub>2</sub>SO<sub>4</sub>.

FIG. 376. Same alloy as in Fig. 374, die cast. Same constituents as in Fig. 375, X 250, etched with H<sub>2</sub>SO<sub>4</sub>.

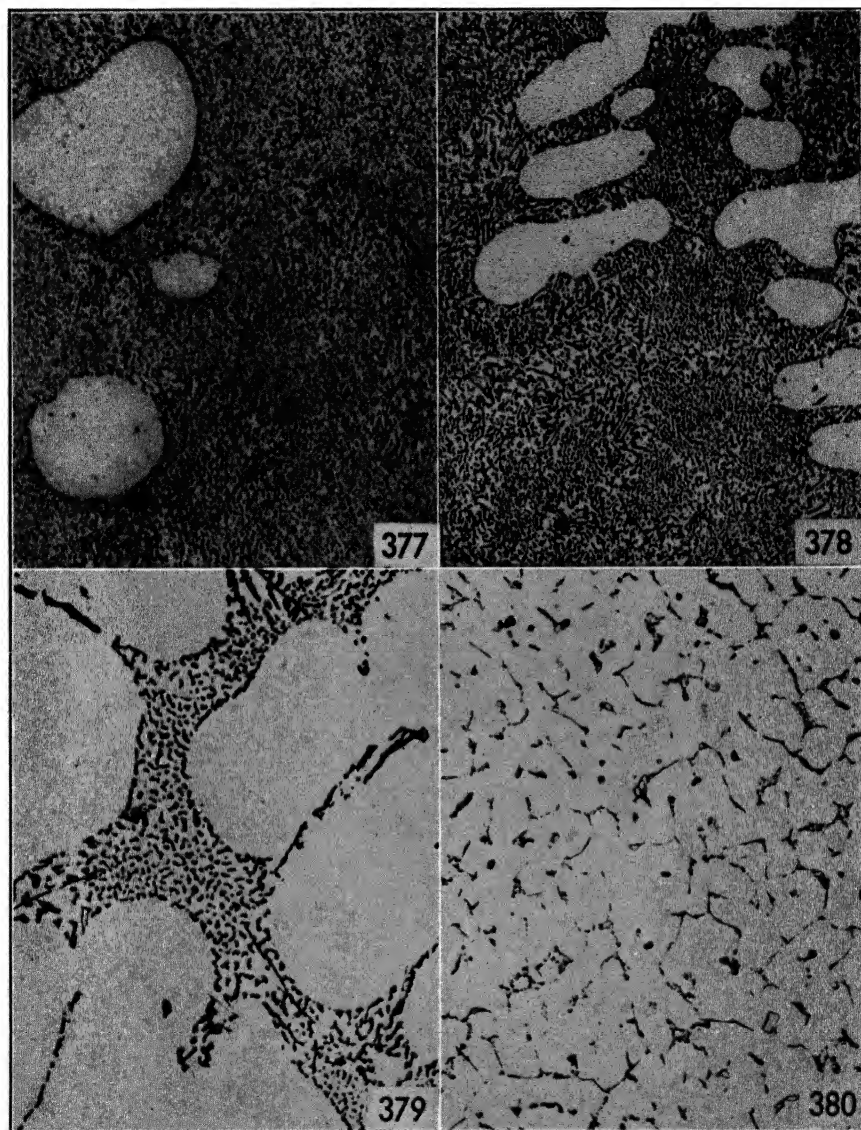


FIG. 377. Cast in sand—Si 12.90%, Fe 0.56%. Primary crystals of Al on a background of modified eutectic Al-Si, X 250, not etched.

FIG. 378. Same alloy as in Fig. 377. Cast in permanent mold. Same constituents as in Fig. 377, X 250, not etched.

FIG. 379. Sand-cast—Si 5.10%, Fe 0.62%, Cu 0.89%, Mg 0.32%. Needles of FeSiAl<sub>5</sub> on network of eutectic Al-Si, X 250, not etched.

FIG. 380. Same alloy as in Fig. 379. Cast in permanent mold. Same constituents as in Fig. 379, X 250, not etched.

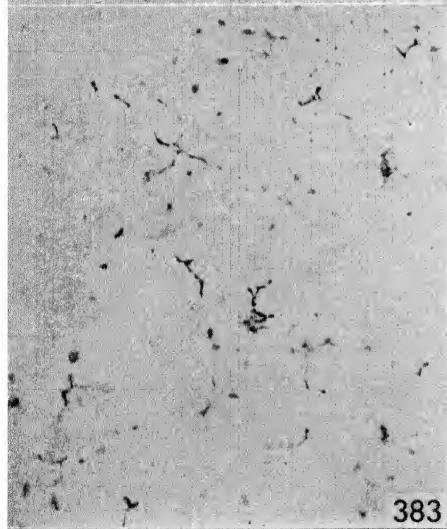
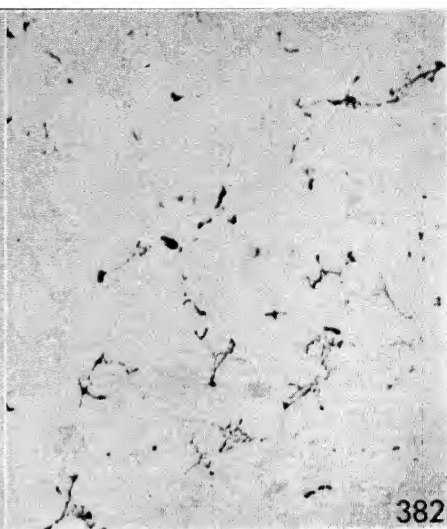
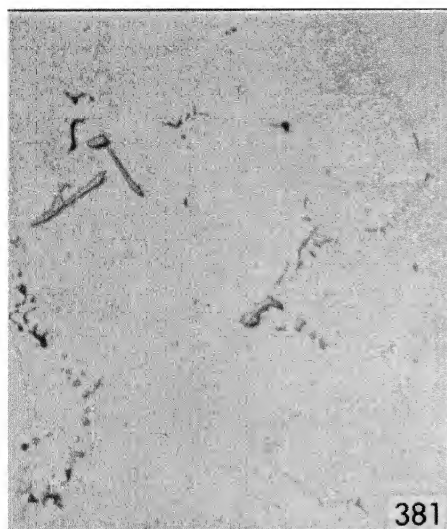


FIG. 381. Sand-cast—Mg 6.02%, Si 0.30%, Fe 0.35%, Mn 0.18%.  $Mg_2Si$  black,  $(FeMn)Al_6$  gray relieved,  $Mg_5Al_8$  light, X 250, not etched.

FIG. 382. Same alloy as in Fig. 381. Cast in permanent mold. Only  $Mg_2Si$  and few round crystals of  $(FeMn)Al_6$  are visible, X 250, not etched.

FIG. 383. Same alloy as in Fig. 381. Die cast. Same constituents as in Fig. 382, X 250, not etched.

Figures 381, 382, and 383 show a 6 per cent magnesium alloy, respectively, sand, permanent mold, and die cast. The usual difference in grain size between sand and permanent mold is present, and the sand-cast sample shows some  $Mg_5Al_8$  (light) in addition to  $Mg_2Si$  and  $(FeMn)Al_6$ , which alone are present in the permanent-mold and die-cast samples. The die-cast sample shows a finer grain, as it is taken near the skin.

Figures 384 and 385 show an aluminum-copper-nickel alloy, sand- and permanent-mold cast. In this case the difference is not only in the

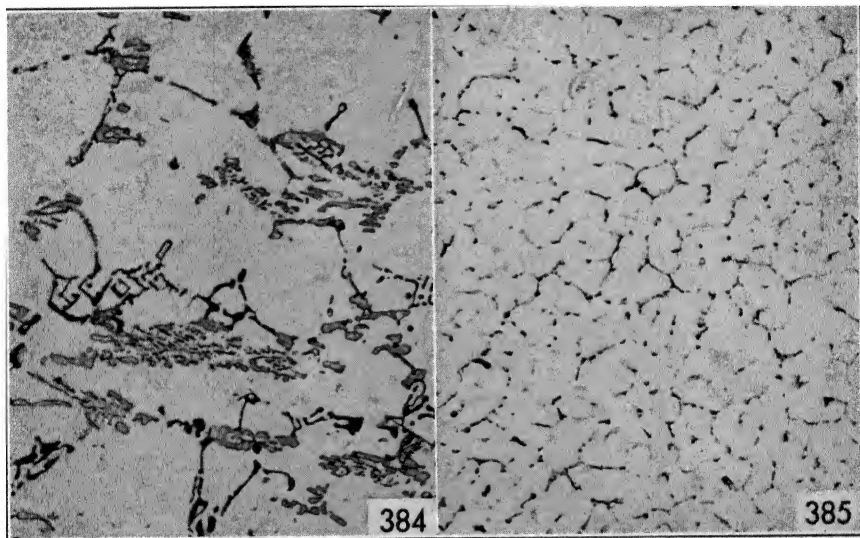


FIG. 384. Sand-cast—Cu 2.24%, Fe 1.25%, Si 1.12%, Mg 2.04%, Ni 1.12%.  $Mg_2Si$  black,  $AlCuFeNi$  light, X 250, not etched.

FIG. 385. Same alloy as in Fig. 384. Cast in permanent mold. Same constituents as in Fig. 384, X 250, not etched.

grain size but especially in the distribution of the constituents, which is completely different.

The defects arising from casting are:

Segregation.

Shrinkage cracks and pinholes.

In addition, inclusions sometimes are considered casting defects although, with the exception of those resulting from reactions between the metal and the mold, they are better considered as melting, pouring, and fluxing defects.

**Segregation.** It is impossible to draw a definite line between what is normal structure and what is segregation. In aluminum alloys the



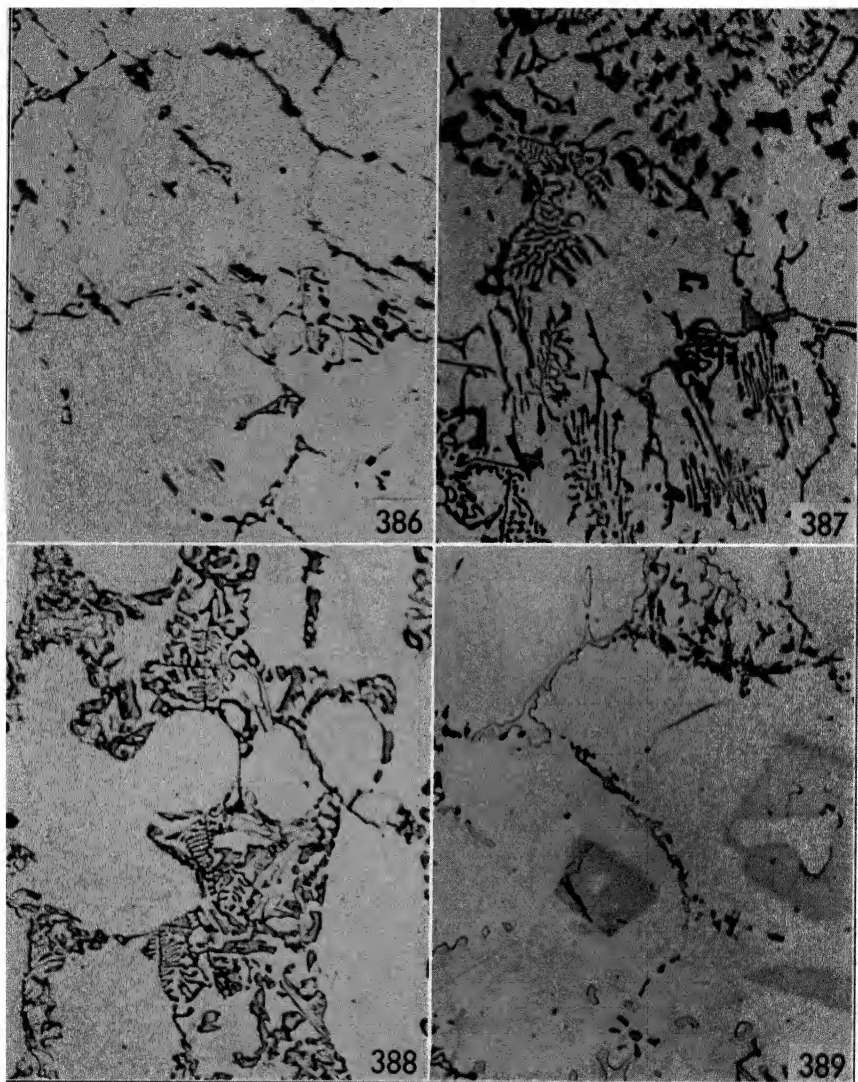


FIG. 386. Normal structure of a sand-cast alloy containing Cu 2.21%, Fe 1.34%, Si 1.07%, Mg 2.19%, Ni 1.24%. Black  $Mg_2Si$ , gray AlCuFeNi, light AlCuNi, X 250, etched with NaOH.

FIG. 387. Same alloy as in Fig. 386. Segregation of AlCuFeNi gray, black  $Mg_2Si$ , light AlCuNi. Sand-cast, X 250, etched with NaOH.

FIG. 388. Segregation of eutectic Al- $Mg_2Si$ -AlCoFe-Si. Sand-cast—Si 8.50%, Fe 0.70%, Mg 0.65%, Co 0.71%—X 250, not etched.

FIG. 389. Presence of abnormal constituent (AlFeMgSi) due to segregation. Water-cooled ingot—Mg 7.02%, Fe 0.58%, Si 0.41%, Mn 0.13%. Black  $Mg_2Si$ , dark needles of  $Fe_2Al_7$ , large light crystals of AlFeMgSi, small crystals of  $Mg_5Al_8$ , X 250, not etched.

constituents are normally *segregated* at the grain boundaries, and it requires considerable experience and confidence to affirm in any one case whether a certain concentration of constituents is to be considered as a segregation or not.

Figures 386 and 387 represent a case where, by comparing the structures in two different castings, segregation can be detected without doubt. The constituents are the same, namely,  $Mg_2Si$  (black),  $AlCuNi$  (light), and  $AlCuFeNi$  (gray), but the large amount of constituents present in Fig. 387 is abnormal. Figure 388 represents a

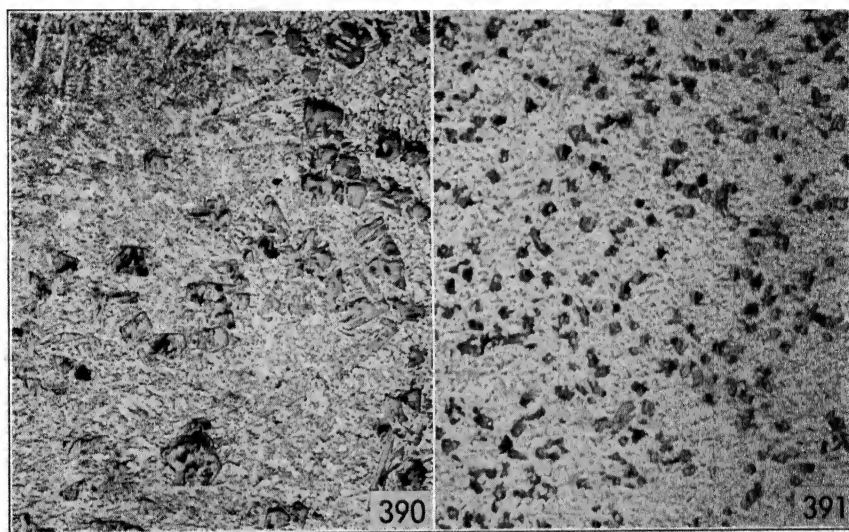


FIG. 390. Somewhat irregular distribution of the primary crystals of Si on a background of eutectic Al-Si and dendrites of primary Al. Cast in permanent mold—Si 20.17%, Fe 0.55%, Cu 1.02%, Mg 0.59%, Ni 1.97%—X 20, not etched.

FIG. 391. Same alloy as in Fig. 390. Abnormally regular distribution of the primary Si crystals. Same constituents as in Fig. 390, X 20, not etched.

doubtful case. There is a heavy concentration of eutectic  $Al-AlCoFe-Mg_2Si-Si$ , but, even by comparing it with other points of the casting, it is not possible to tell how abnormal it is.

Figure 389 shows an example of segregation where no doubt can exist. The alloy shown is a 7 per cent magnesium alloy, where the normal constituents are  $Mg_2Si$ ,  $Mg_5Al_8$ , and  $(FeMn)Al_6$ , together with some  $Fe_2Al_7$ . In the sample shown, in addition to these constituents, owing to a local segregation of silicon, two primary crystals of  $AlFeMgSi$  are also present. Figures 390 and 391 show another doubtful case: the distribution of the primary Si in Fig. 391, compared with that of Fig. 390, leads to the diagnosis of a segregation in the sample in



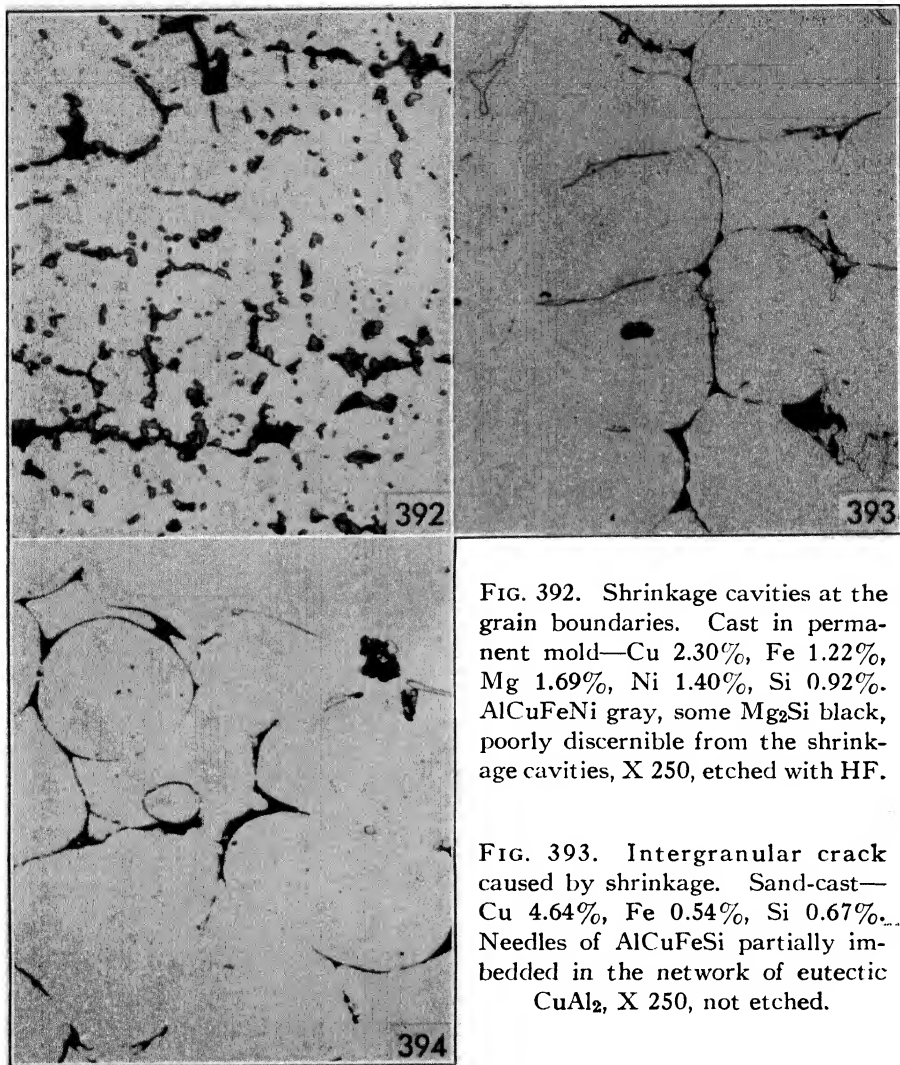


Fig. 390. However, the structure in Fig. 390 is perfectly normal and is the very regular structure in Fig. 391 which is abnormal, as special conditions are required for its formation.

**Shrinkage.** Shrinkage can produce either pinhole porosity or cracks, depending on the alloy. Alloys with a wide range of solidification tend to show pinhole porosity. Alloys of the solid solution or eutectic type, which solidify over a narrow range of temperature, cracks. Figures 392 and 393 show, respectively, pinhole porosity and a crack caused by shrinkage in two different alloys—one with a wide range of solidification, the other of the solid-solution type (4 per cent copper). The identification of the defects in this case is not difficult. In the majority of cases, however, it is almost impossible because shrinkage defects cannot be distinguished from gas or oxide inclusions. Figure 394, for instance, represents a structure very similar to that in Fig. 393, although it has been caused by oxide formed during pouring.

### Ingot Casting—Cold-Mold Casting

Cold-mold casting in modern practice is limited to common alloys (commercial aluminum, aluminum-manganese and aluminum-magnesium alloys), where segregations have relatively no importance. It is rapidly being discarded in favor of water cooling with strong alloys (duralumin,  $Mg_2Si$  type, aluminum-copper-nickel type of alloys), where segregation is an important factor, both in the fabrication and final properties.

In this method a thick mold, usually of cast iron or brass, sometimes of graphite, is filled with molten metal. The cooling is produced by dispersion of the heat through the mold. The ingot shrinks during freezing, and molten metal must be fed at the top to compensate for the shrinkage.

The structure resulting from this method of casting is rather poor. The rate of cooling is slow, and large grain size, accompanied by heavy segregation, is produced. In spite of the feeding from the top, small shrinkage cavities commonly are present throughout the ingot.

Casting in cold mold is not a particularly delicate operation and the defects arising from improper technique are not very important. Besides oxide inclusions, which have already been considered, the most common defects encountered are:

Excessive grain orientation.

Excessive grain size.

Excessive segregation.

It is difficult, however, to determine when these structures must be considered as defects, since a certain amount of them is inherent in the

casting process and cannot be avoided. The composition of the alloy is an important factor in the crystallization. A columnar grain or grain size absolutely out of the ordinary for an alloy may be perfectly normal for another alloy. Moreover, these defects are not very important, as successive fabrications break down the structure and homogenize the alloy.

### **Ingot Casting—Water Cooling**

Water cooling is preferred for complex alloys on account of the rapid cooling which may be obtained throughout the mass, yielding a compact and homogeneous structure. Several types of molds are in use for this type of casting, but the principle of cooling is the same for all of them.

Substantially, the method consists in pouring the metal into a thin mold of steel, brass, or aluminum, water-cooled on the outside, so that the freezing of the metal is very rapid. The mold in this process has no real cooling effect but is present only to give form to the molten metal and to avoid the contact of water with it. In many of the modern molds, as soon as a shell of frozen metal is formed, water is brought to act directly on the metal without the protection of the mold.

To insure proper feeding and cooling, the metal is cooled by strata. When the bottom is completely frozen and approaches room temperature, the top is still molten and feeds all the small cavities which have been formed by shrinkage. This is accomplished differently in different molds: some of them are built so that the metal can be poured at the same rate at which it freezes; some of them have heaters in the top, which keep the metal molten until the freezing moment has arrived.

The cooling is so rapid that the metal is not only frozen rapidly, avoiding segregations, but is in reality quenched from the molten state.

Figure 395 shows the macrostructure of an ingot properly cooled. Figure 396 shows the microstructure of the sample near the edge of the ingot, where the quenching effect is particularly noticeable. Figure 397 shows the sample from the center.

Casting with water cooling is a very delicate process, and small deviations from the correct practice may completely change the structure. The main defects are:

Segregation.

Inverse segregation.

Columnar grain and large grain size.

Cracking and twinning.

Porosity.

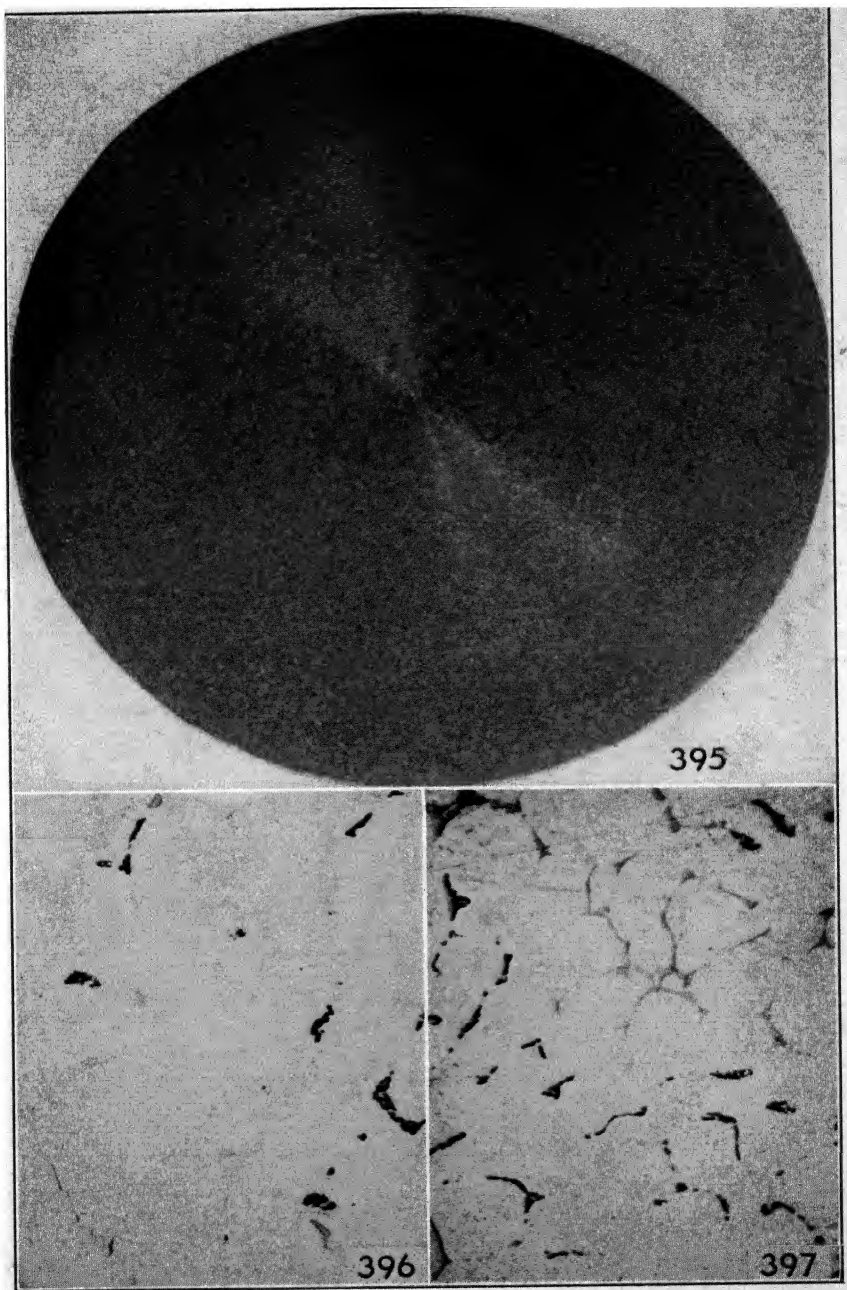


FIG. 395. Normal structure of a water-cooled ingot—Cu 4.52%, Fe 0.44%, Si 0.32%, Mg 1.50%, Mn 0.52%. Natural size, etched with 20% NaOH solution.

FIG. 396. Sample from the edge of Fig. 395. Structure of material quenched by fast cooling.  $\text{Cu}_2\text{Mg}_2\text{Al}_5$  black, Mn compounds light, X 250, not etched.

FIG. 397. Sample from the center of Fig. 395. Regular structure of properly cooled ingot. Same constituents as in Fig. 396, X 250, not etched.

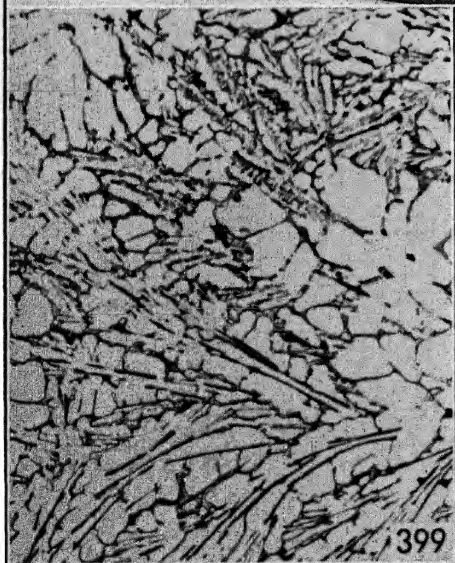
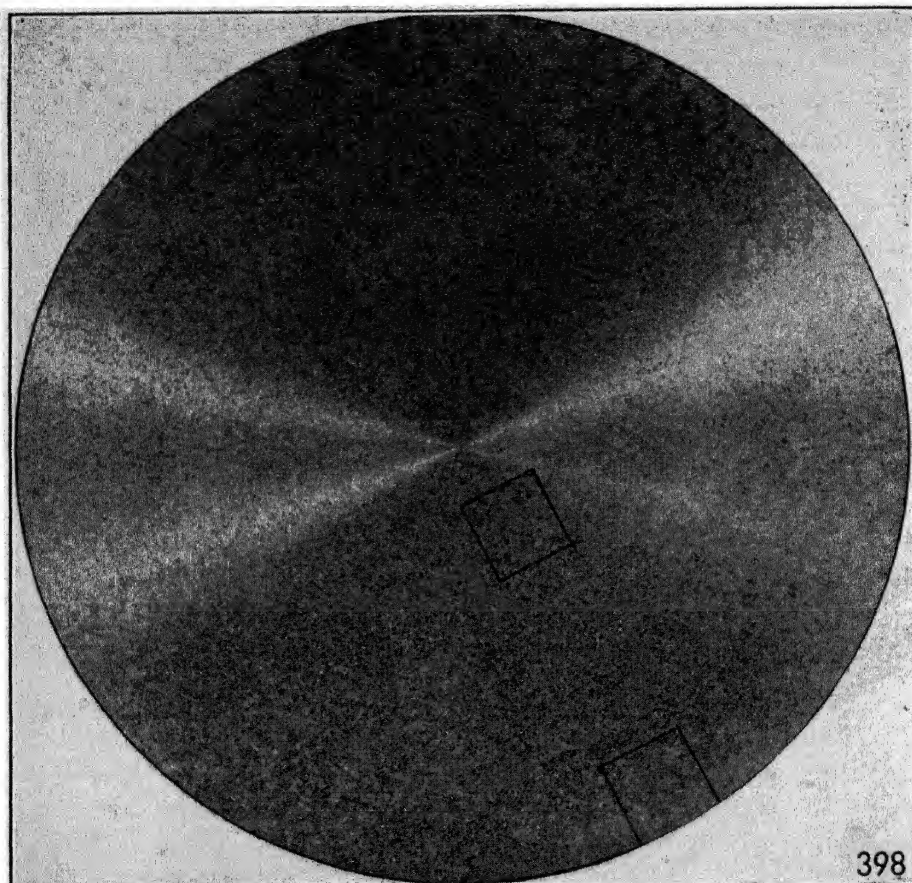


FIG. 398. Macrostructure of segregated ingot water-cooled—Cu 4.12%, Fe 0.62%, Si 0.61%, Mg 1.26%, Ni 2.04%. Natural size, etched with a 20% NaOH solution.

FIG. 399. Sample from center of Fig. 377. Dendritic crystals of Al in a background of eutectic Al-FeNiAl<sub>9</sub>-CuAl<sub>2</sub>-Mg<sub>2</sub>Si-X75, etched with HF.

As for cold-mold casting, a certain amount of these defects, with the exception of cracking, is usually considered unavoidable. However, in water-cooling casting, contrary to cold-mold casting, with close control of all the factors involved, it is possible to produce ingots which do not show any of these defects.

**Segregation.** Figure 398 shows the macrostructure of a completely segregated ingot. Figure 399 shows the microstructure of the sample from the center. Figures 400 and 401 show the partially segregated structure in duralumin. With due allowance made for the difference in composition, it can be seen that the two structures are basically the same, namely, crystals of Al surrounded by large masses of eutectics.

Segregation usually is produced by a low rate of cooling, the causes for which may be several and cannot be examined here in detail.

Although ingots showing segregation require long preheating before working and sometimes offer difficulties in the subsequent fabrications, segregation within certain limits is not to be considered a major defect, for the working is done mostly in order to homogenize the structure, and with sufficient working segregation should disappear.

Figure 402 shows an alloy extruded for forging stock. A segregation of manganese compounds is visible, probably on account of the low (3/1) reduction rate. However, a segregation of this size is practically negligible, as it does not affect the properties of the alloy to any appreciable extent.

**Inverse segregation.** This method of casting favors inverse segregation, especially when the cooling is managed so as to induce fast chilling at the beginning, after which the rate of cooling is reduced. The real causes of inverse segregation, commonly called *liquation*, are still not precisely known. It is established that inverse segregation is produced by an internal pressure, inside the partly solidified metal, which pushes the molten part outward, it being more or less of eutectic composition. The reasons for the pressure are not definitely ascertained, and are reported in different ways—as evolution of gases during solidification or shrinkage of the outside shell.

Figure 403 shows the macrostructure of an ingot in which there has been heavy liquation. Three zones can be distinguished. The first two zones are (1) the outside zone, made up of the liquated material (dark), and (2) the center zone, which in reality is the first to solidify and where the black lines running at the grain boundaries are made up of the eutectics migrating outward. When this zone was solidified, the rate of cooling decreased sharply, probably because the contact between mold and metal ended. This gave origin to the third zone, from which started the migration of eutectics. Figure 404 shows the

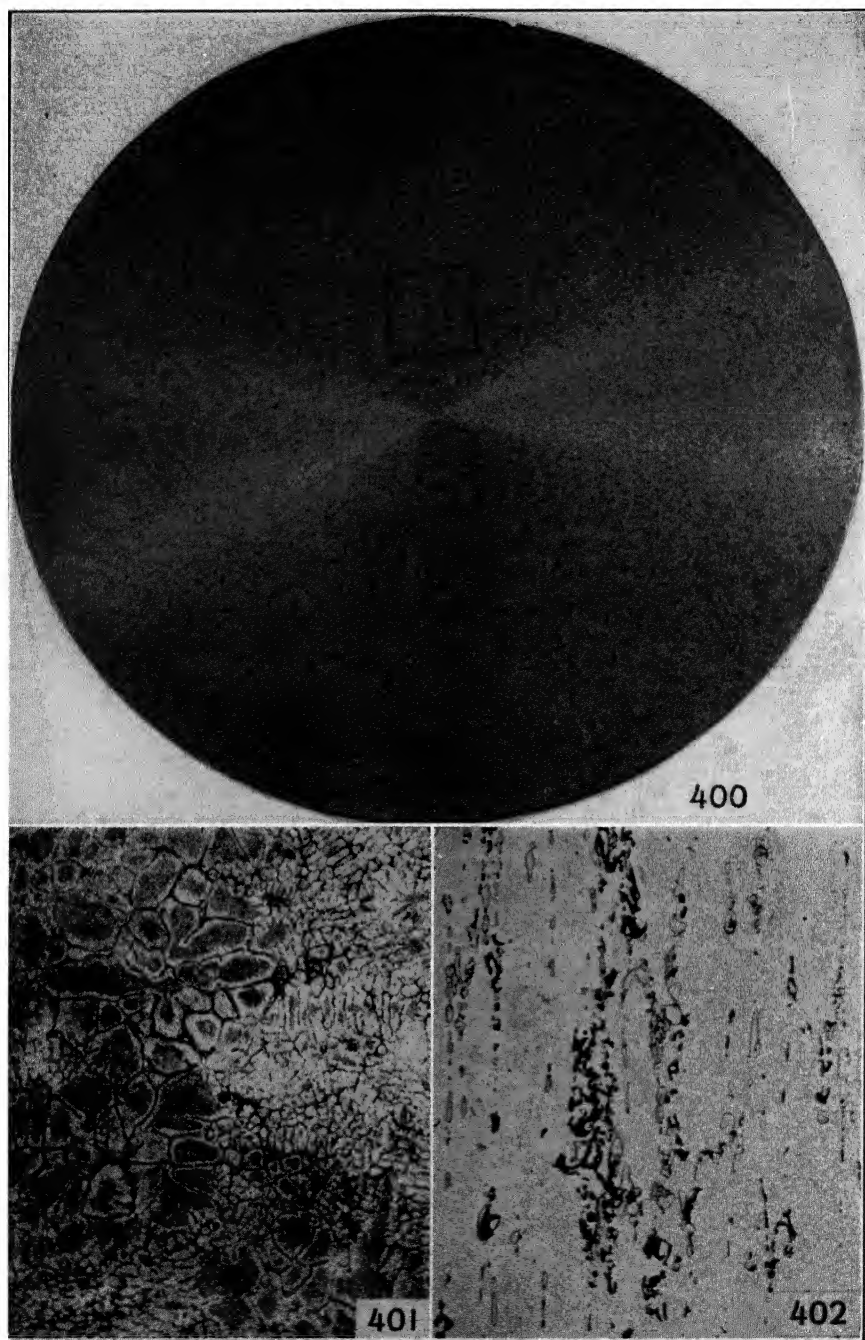


FIG. 400. Macrostructure of partially segregated ingot, water-cooled—Cu 4.50%, Fe 0.42%, Si 0.23%, Mg 1.56%, Mn 0.55%. Natural size, etched with a 20% NaOH solution.

FIG. 401. Sample from Fig. 400. The enlargement reveals that the black points in the macro are primary crystals of Al in a background of eutectics, X 30, etched with acid mixture.

FIG. 402. Segregation persisting after extrusion—Cu 4.26%, Fe 0.51%, Si 0.83%, Mg 1.75%, Mn 0.62%.  $Mg_2Si$  and Mn compounds dark,  $CuAl_2$  light, X 250, etched with  $H_2SO_4$ .



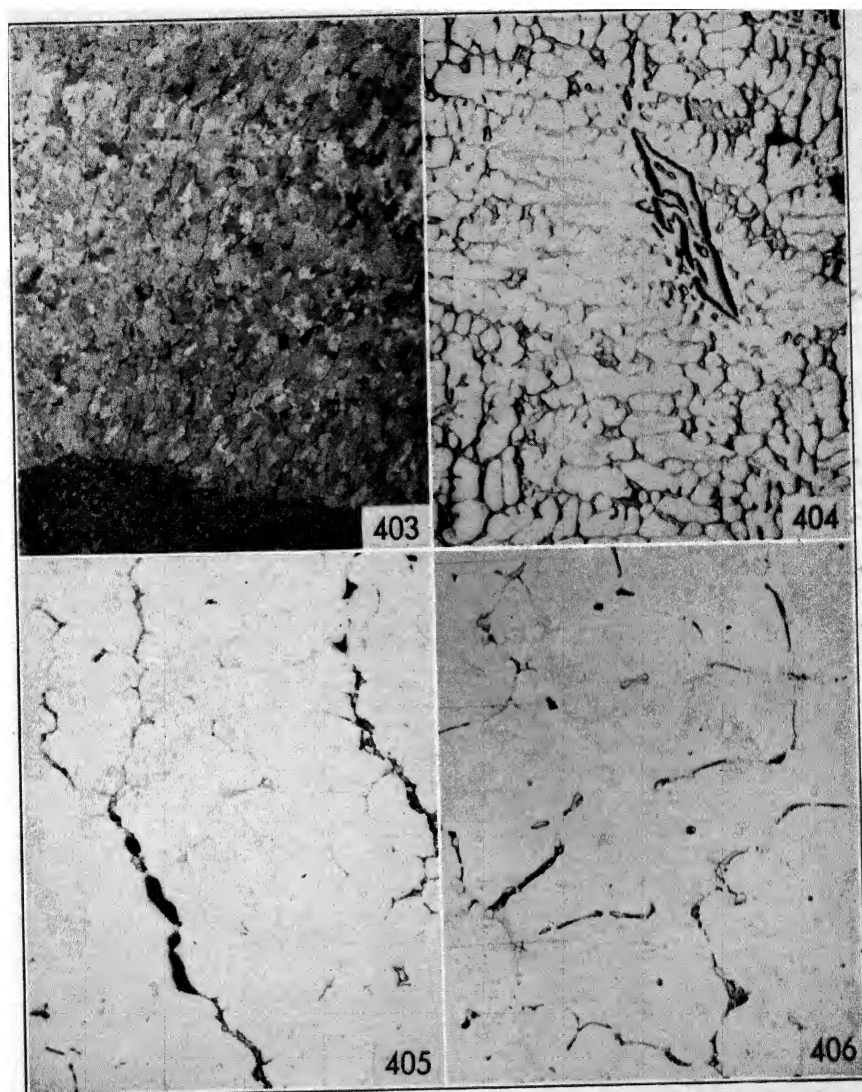


FIG. 403. Inverse segregation in water-cooled ingot. Outside (bottom) zone of segregation, central zone crossed by lines of migrating eutectics, third zone (top) of normal structure—Cu 4.35%, Fe 0.45%, Si 0.28%, Mg 1.50%, Mn 0.52%, X 3, etched with a 20% NaOH solution.

FIG. 404. Sample from outside zone of Fig. 403. Large crystal of  $(\text{FeMn})\text{Al}_6$  on a background of eutectics. Composition of this zone: Cu 10.21%, Fe 0.89%, Si 0.69%, Mn 0.44%, Mg 1.13%—X 75, not etched.

FIG. 405. Central zone in Fig. 403. Lines of eutectics at the grain boundaries, containing gas inclusions or shrinkage cavities, X 75, not etched.

FIG. 406. Third zone in Fig. 403. Normal structure. Black  $\text{Cu}_2\text{Mg}_2\text{Al}_5$  and  $\text{Mg}_2\text{Si}$ , light  $\text{CuAl}_2$  and Mn compounds, X 75, not etched.



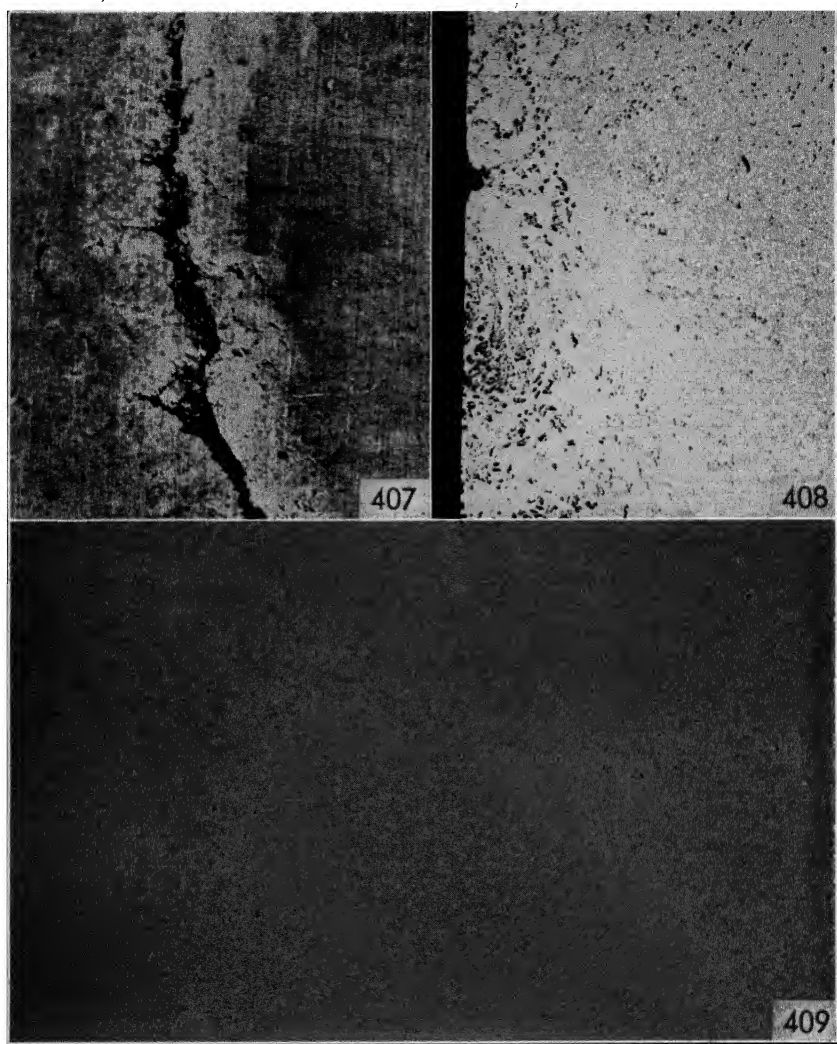


FIG. 407. Crack caused by segregation in a water-cooled ingot, broken down, scalped, and rolled again—Cu 4.50%, Fe 0.38%, Mg 1.52%, Si 0.26%, Mn 0.53%—X 10, not etched.

FIG. 408. Section through the crack in Fig. 407. Segregation of Mn compounds around the crack, X 30, not etched.

FIG. 409. Large grain size, columnar grain, and twinning in a water-cooled ingot—Cu 4.72%, Fe 0.55%, Si 0.54%, Mg 1.67%, Mn 0.53%. One-third natural size, etched with a 20% NaOH solution.

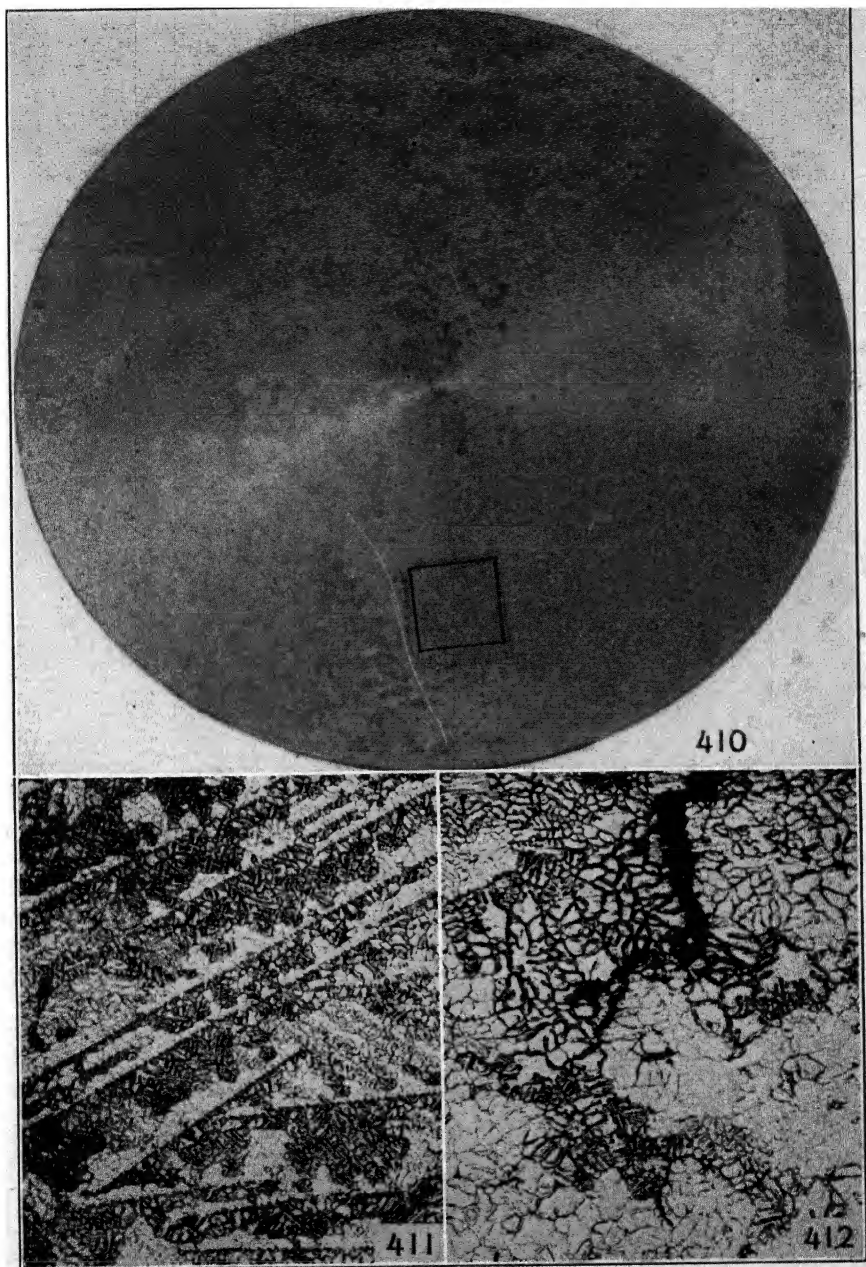


FIG. 410. Twinning in a water-cooled ingot—Cu 4.15%, Si 0.52%, Fe 0.45%, Mg 0.64%, Mn 0.53%. Natural size, etched with a 20% NaOH solution.

FIG. 411. Sample from Fig. 410. Twinned crystals white and dark, depending on the orientation, X 30, etched with acid mixture.

FIG. 412. Intergranular crack formed in the hot-shortness range. Water-cooled ingot—Cu 3.97%, Fe 0.47%, Si 0.52%, Mg 0.62%, Mn 0.53%—X 30, etched with acid mixture.

microstructure of the liquated zone, where a primary crystal of  $(\text{FeMn})\text{Al}_6$  is prominent in a network of eutectics; Fig. 405 shows the second zone with two lines of eutectics running at the grain boundaries. Figure 406 shows the third zone where the structure is more or less normal.

Inverse segregation is an obstacle during fabrication, especially rolling. Ingots which show inverse segregation need to be scalped.

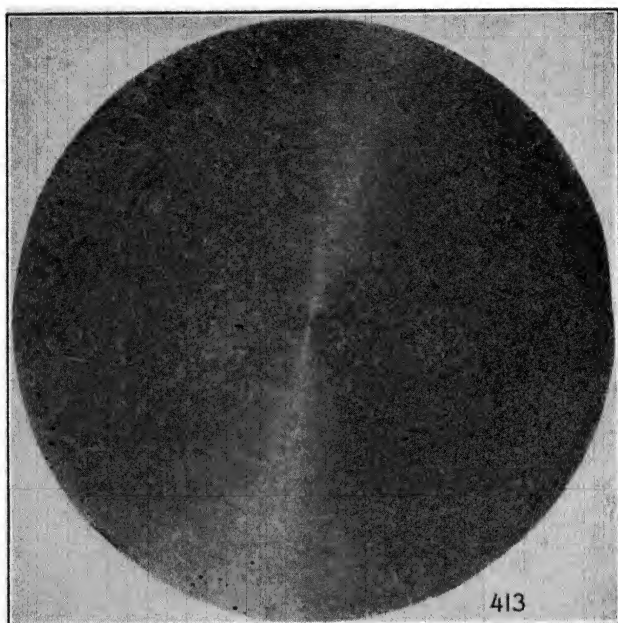


FIG. 413. Porosity caused by leakage of water in the mold of a water-cooled ingot—Cu 2.23%, Fe 1.12%, Si 1.05%, Mg 1.58%, Ni 1.14%. One-half natural size, etched with a 20% NaOH solution.

Sometimes the scalping is carried out after partial rolling. This rolling is termed *breaking down*, for it is intended to break down the cast structure. When the liquation is particularly heavy, the scalping may not be sufficient to eliminate the defective zone completely and, in further rolling, cracks appear, as the one depicted in Fig. 407, and make the ingot useless. Figure 408 shows the section through the crack, in which a heavy segregation of manganese constituents is clearly visible.

**Columnar grain and large grain size.** Unless exceptionally pronounced, these defects can be considered unimportant and without appreciable effect on the final structure and properties of the material. Figure 409 shows a section of an ingot, where both these defects are

present. Macro-etching should be used to investigate these defects, as with many of the defects in casting, because micro-examination does not permit the large areas which are necessary in these cases to be examined.

**Cracking and twinning.** Both defects arise from uneven cooling, which sets up stresses within the ingot. When the stresses arise in metal in the hot-short range, the billet splits at the grain boundaries. Figure 412 shows the end of a crack of this kind, which is decidedly intergranular. Sometimes the stresses do not exceed the breaking point of the alloy. Deformation takes place and twinning arises. Figures 410 and 411 illustrate the macro- and microstructure of a twinned billet.

**Porosity.** In addition to the porosity caused by improper melting, fluxing, and pouring, porosity in these ingots may be caused by the contact of water with molten metal. As with porosity caused by reaction between the metal and the mold, porosity from this source usually is limited to an outside layer of the cast.

Figure 413 shows the typical macrostructure of an ingot, where water seeped through the mold at an early stage of solidification. The black points represent the bubbles of steam entrapped in the metal.

## CHAPTER 15

### WORKING

The working of aluminum alloys, regardless of the method employed, has the main effect of breaking down the cast structure, which consists of soft crystals surrounded by a brittle network of constituents, into a more homogeneous structure, where the insoluble constituents are dispersed as inclusions in the mass. An accessory effect is to reduce the grain size and to facilitate the diffusion of soluble constituents. The process may be gradual, as in rolling or forging, where it is accomplished in many passes, or all at one time, as in extrusion. Work may be hot or cold. Generally, however, both are applied in the order mentioned.

From the metallographic point of view, drawing, stretching, straightening, and to a certain extent cold rolling, are to be considered finishing operations since their effect on the microstructure is usually negligible. The deformation produced by these operations is only a small fraction of the total and these operations are applied more in regard to surface or dimensional conditions than in regard to the properties.

Also from the metallographic point of view, the differences due to the various methods of working, both cold and hot, are small and limited mainly to the grain structure, without any appreciable effect on the microconstituents.

Figures 414 and 415 illustrate the same alloy rolled and extruded. No real difference can be detected between the two structures. Figures 416 and 417 show, respectively, an aluminum-copper-nickel alloy and a magnesium-silicide alloy. These figures, together with the few examples shown in Part III, illustrate the effect of working on the microstructure of various alloys.

Slight differences exist between the grain structures of material that was rolled, extruded, or forged. In extruded products, where the deformation is done all at one time and no intermediate recrystallization takes place, as in rolling, between different passes, the resulting grain structure tends to be more elongated in the direction of working. Figures 418 and 419 show the same alloy heat treated after extrusion and after rolling; a difference in elongation of the grains is clearly visible. However the two examples above are extreme cases; the whole

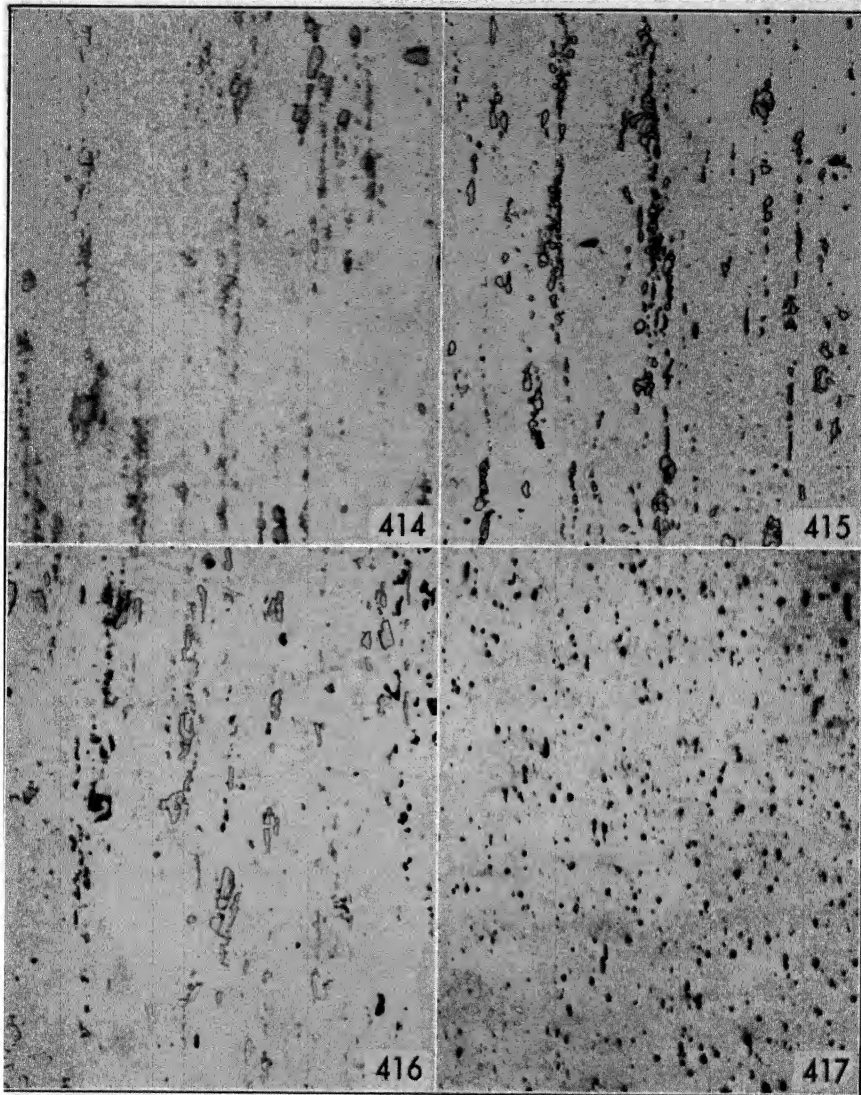


FIG. 414. Rod rolled to 2-in. diameter—Cu 4.07%, Si 0.29%, Fe 0.56%, Mg 0.58%, Mn 0.54%. Mn compounds and  $\text{CuAl}_2$  are the visible constituents, X 250, not etched.

FIG. 415. Same alloy as in Fig. 414, rod extruded to 2-in. diameter. Same structure and constituents as in Fig. 414, X 250, not etched.

FIG. 416. Extruded bar—Cu 2.28%, Fe 1.18%, Si 1.13%, Mg 2.31%, Ni 1.12%.  $\text{Mg}_2\text{Si}$  black and  $\text{AlCuFeNi}$  light, X 250, not etched.

FIG. 417. Rolled sheet—Mg 1.30%, Fe 0.35%, Si 0.73%, Cr 0.31%.  $\text{Mg}_2\text{Si}$ , black, is the only constituent visible, the Fe and Cr constituents dispersed in the mass are unrecognizable, X 250, not etched.

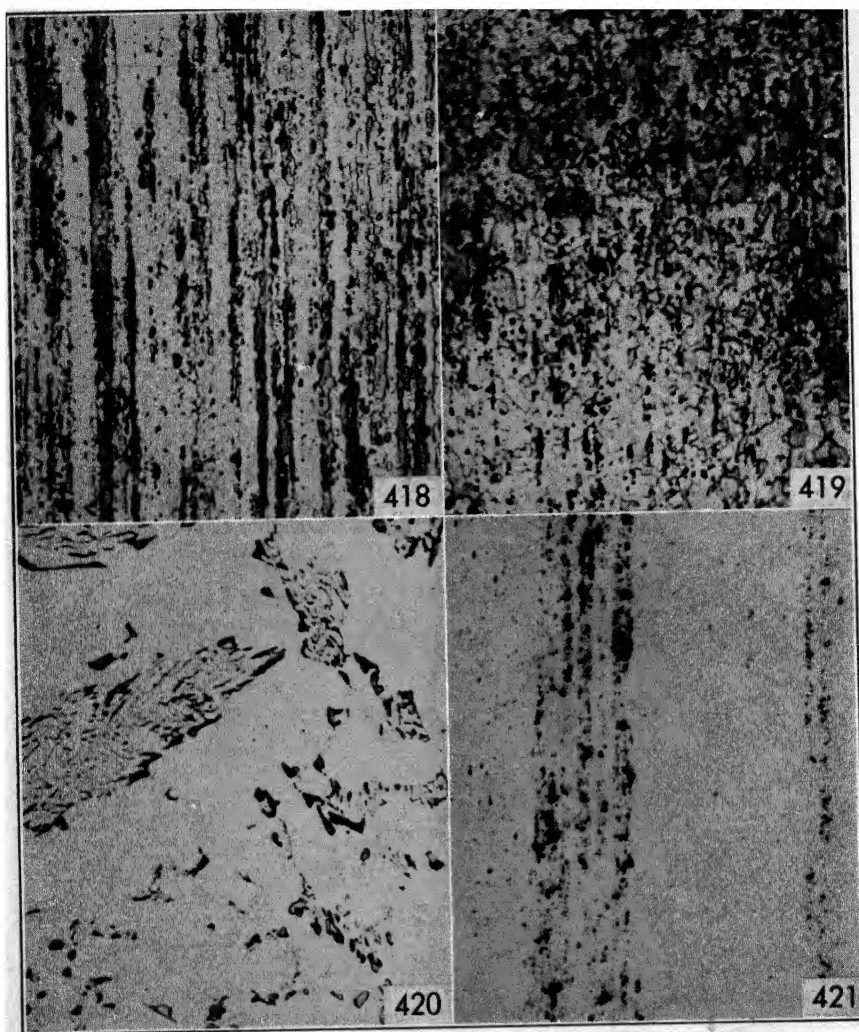


FIG. 418. Elongated grain structure in extruded rod—Cu 3.92%, Fe 0.46%, Mg 0.59%, Mn 0.54%, Si 0.48%. X 75, etched with acid mixture.

FIG. 419. Equiaxed grain structure in rolled sheet. Same alloy as in Fig. 418, X 75, etched with acid mixture.

FIG. 420. Forged from cast stock. Constituents only slightly deformed by forging—Cu 3.02%, Fe 1.43%, Mg 0.62%, Ni 0.58%, Si 0.55%—X 250, etched with  $H_2SO_4$ .

FIG. 421. Extruded bar, oxidized skin entrapped in extruding—Cu 4.05%, Fe 0.52%, Mg 0.64%, Mn 0.56%, Si 0.55%—X 75, not etched.





FIG. 422. Irregular grain size in extruded rod—Cu 4.07%, Fe 0.43%, Mg 0.59%, Mn 0.48%, Si 0.52%. Natural size, etched with 20% NaOH solution.



FIG. 423. Enlargement of section in Fig. 422 to show large grains, X 30, etched with acid mixture

FIG. 424. Transverse section of sample in Fig. 423. The small-grained zone corresponds to the two large grains in the other section, the large grain corresponds to finely grained material, X 30, etched with acid mixture.



range of intermediate structures can be produced indifferently by both methods.

Forgings usually show a more equiaxed structure, but this is to be ascribed, more than anything else, to the fact that forging is employed to obtain deformation in all directions so that the material is elongated in all dimensions.

The tendency now is to produce forgings from extruded stock. It is therefore possible to detect in forgings a very elongated grain, due to extrusion, in spots where the deformation from forging was very limited. In forging from cast stock it is often possible to detect the cast structure partially deformed. In some spots, like the one shown in Fig. 420, the deformation can hardly be seen. A point like that must be considered defective, however, as the main purpose of using forgings instead of castings has been defeated by a poor die design.

Defects due to improper working are mostly dimensional or surface defects, like buckles, scratches, pits, and handling marks. Splitting, cracking, checking, and slivering, which are commercial names for various grades of the same defect, are usually ascribed to working because they show during working. However, in most cases they are due to improper handling prior to work. They are treated in Chapters 14 and 16.

A defect which is due mainly to extrusion is the oxide inclusions shown in Fig. 421. These inclusions, which are found only at the end of extruded material, are caused by the oxidized skin at the end of the billet which is extruded into the end of the shape.

Another irregularity of structure, which, however, should not be considered detrimental except in special cases, is illustrated in Fig. 422. The material was cold-drawn after extrusion, and the outside finely grained ring must be ascribed to the recrystallization induced by cold working. The central part seems to show very coarse grain size. A more accurate examination, however, shows that what appears as enormous grains in the transverse section (Fig. 423) in the longitudinal section (Fig. 424) shows as an aggregate of small crystals having one of the axes strictly parallel. Thus, when the plane perpendicular to that axis is etched, they react all in the same way, and no difference can be detected.

## CHAPTER 16

### HEAT TREATMENT

Under this heading will be considered not only the solution treatment, which is the one commonly understood as heat treatment, but all the following operations, which are properly to be considered as heat treatments.

Annealing.

Solution treatment for hot work or for homogenization, whether followed by quenching or not.

Artificial aging.

No real distinction exists between the first two operations. Annealing usually is carried on at a lower temperature, but in many cases high-temperature annealing may be necessary or economical, and much commercial annealing, from the metallographic point of view, can be considered as a poorly executed solution treatment followed by air quenching.

Under the heading *Annealing*, therefore, will be considered the heat treatments for the following purposes.

To relieve strains.

To induce recrystallization.

To precipitate dissolved constituents.

Under the heading *Solution Treatment* will be considered heating to cause diffusion of soluble constituents and homogenization of the alloy, whether or not followed by quenching, depending on the further use of the material.

The third type of treatment, *Artificial Aging*, is self-explanatory and does not need definition. Cast and wrought structures will be considered together since, from a metallographic point of view, no difference exists in the operations. Data about temperatures and practices of these operations have been given in Part III, in connection with the various alloys. Here the subject will be limited to variations in the microstructure caused by heat treatment.

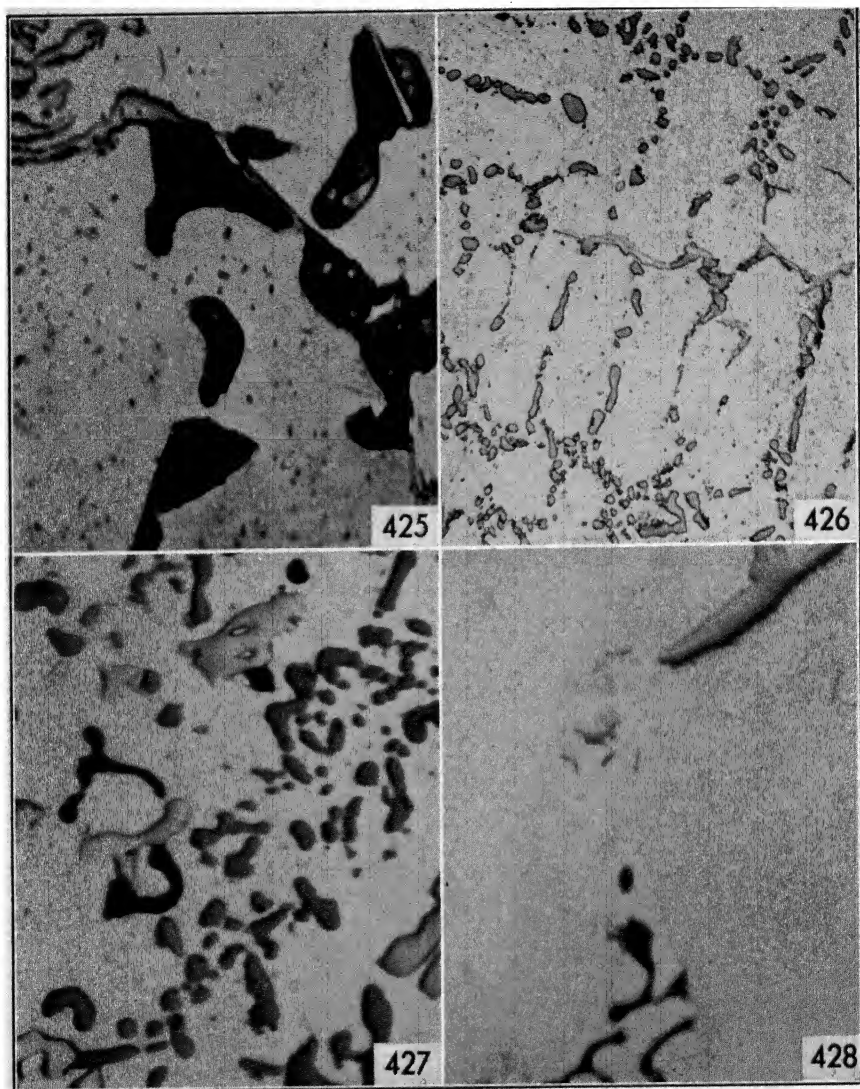


FIG. 425. Cast in permanent mold, annealed for 12 hours at 840°F (450°C). Fine precipitate of  $\text{CuAl}_2$ ,  $\alpha(\text{AlFeSi})$  and  $\text{AlCuFeSi}$  light,  $\text{CuAl}_2$  black—Cu 9.88%, Fe 1.45%, Mg 0.46%, Si 0.76%—X 1000, etched with  $\text{Fe}(\text{NO}_3)_3$ .

FIG. 426. Sand-cast, annealed 6 h 700°F (370°C). Si rounded by annealing, light needles of  $\text{FeSiAl}_5$ —Cu 0.20%, Fe 0.46%, Si 5.56%—X 250, not etched.

FIG. 427. Cast in permanent mold, annealed 4 h 700°F (370°C). All the constituents are rounded by the annealing.  $\text{Mg}_2\text{Si}$  black, Si gray,  $\text{AlCuFeNi}$  light—Cu 0.82%, Fe 0.54%, Mg 0.81%, Ni 2.25%, Si 14.30%—X 1000, not etched.

FIG. 428. Sand-cast, annealed 4 h 600°F (315°C). The constituents are not affected by the heat treatment.  $\text{Mg}_2\text{Si}$  black, needle of  $\text{Fe}_2\text{Al}_7$ , and small particles of  $\text{Mg}_5\text{Al}_8$ —Mg 5.02%, Fe 0.35%, Si 0.30%, Mn 0.18%—X 1000, not etched.

## Annealing

Annealing is carried on either above or below the recrystallization temperature of the alloy. When below this temperature, it is usually called *stabilization*, as its main purpose is to stabilize the material from internal stresses caused by previous cold work without destroying the effect of cold work on the mechanical properties. Stabilization, when properly conducted, does not affect the microstructure of the material to any extent and cannot be detected by microscopic means, except in

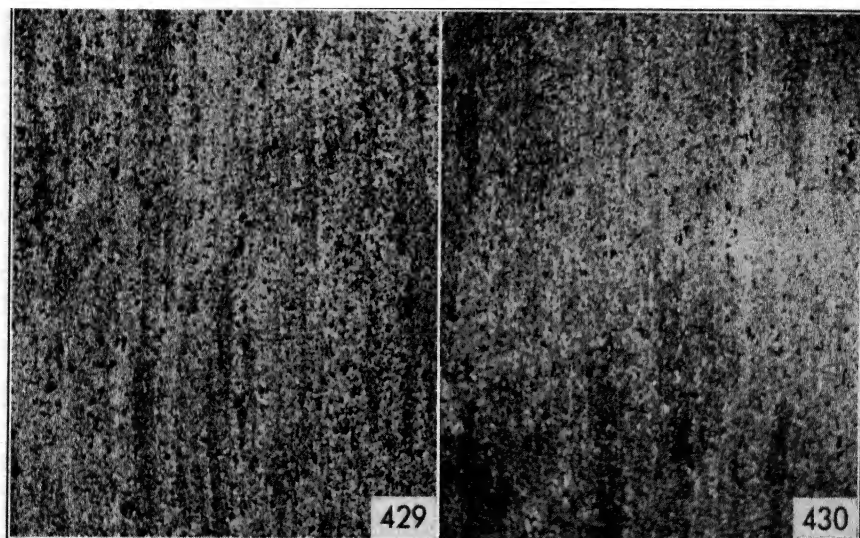


FIG. 429. Sheet cold rolled to 0.040 in., typical grain structure of cold-rolled material—Cu 4.53%, Fe 0.36%, Mg 1.53%, Mn 0.56%, Si 0.25%—X 75, etched with acid mixture.

FIG. 430. Same sheet as in Fig. 429 after annealing for 2 hours 700°F (370°C), typical grain structure of annealed material, X 75, etched with acid mixture.

special cases, such as when it has been improperly done and recrystallization or precipitation has taken place.

The effect of annealing is different for the various alloys and is also influenced by previous treatments to which the material has been subjected; important factors are also temperature and time of annealing.

The following examples will illustrate the effect of annealing on several alloys. Figure 425 shows a 10 per cent copper alloy cast in permanent mold, annealed for a long time at 840°F (450°C) and slowly cooled. The only noticeable effects of this drastic annealing are a slight rounding of the constituents and the reprecipitation of some  $\text{CuAl}_2$  which was previously in solid solution.

Figures 426 and 427 show, respectively, a 5 per cent and a 15 per cent silicon alloy. In both cases the only variation caused by annealing is a rounding of the constituents. Figure 428 shows a 5 per cent magnesium alloy where the annealing has not caused any appreciable change in the shape or distribution of the constituents.

As can be seen from the preceding examples, annealing has very little effect on the cast structures. In wrought structures the effect is even less; the constituents are already rounded by the working, and the effect of annealing is limited to reprecipitation of solubilized constituents.

It may also be noted that the grain structure does not seem to change even when recrystallization takes place, for most of the alloys cannot be etched properly in the cold-worked or annealed state and the grain boundaries are only detected with great difficulty. Figures 429 and 430 show the same alloy after cold working and after annealing. Although recrystallization has taken place, the etching does not reveal appreciable differences and the grain boundaries are hardly discernible in either condition.

### Solution Treatment

The effect of solution treatment on the microstructure is more pronounced than that of annealing, especially in alloys approaching the composition of the saturated solid solution, as with many wrought alloys. In castings, solution treatment is almost always followed by quenching in water, to retain the solid solution in the supersaturated condition. Material intended for further fabrication is usually air-quenched if it is not worked immediately after the solution treatment.

Figures 431, 432, 433, and 434 illustrate the heat-treated structure in different alloys. Figures 435 and 436 show the variations produced by heat treatment in a silicon alloy.

Figure 437 illustrates an alloy for working after preheating to effect solution, followed by air cooling, which has allowed some of the dissolved constituents to reprecipitate. Figure 438 shows an alloy of the same type, reheated after a partial working, which has elongated the cast structure without breaking it completely.

Figures 439 and 440, together with the examples reported in Part III, show the structure of wrought alloys after solution treatment followed by quenching.

Figures 441 and 442 show the same alloy in sheet form before and after heat treatment. The small round particles of  $\text{Cu}_2\text{Mg}_2\text{Al}_5$  (small gray) and  $\text{CuAl}_2$  (light) have completely disappeared. Only the man-

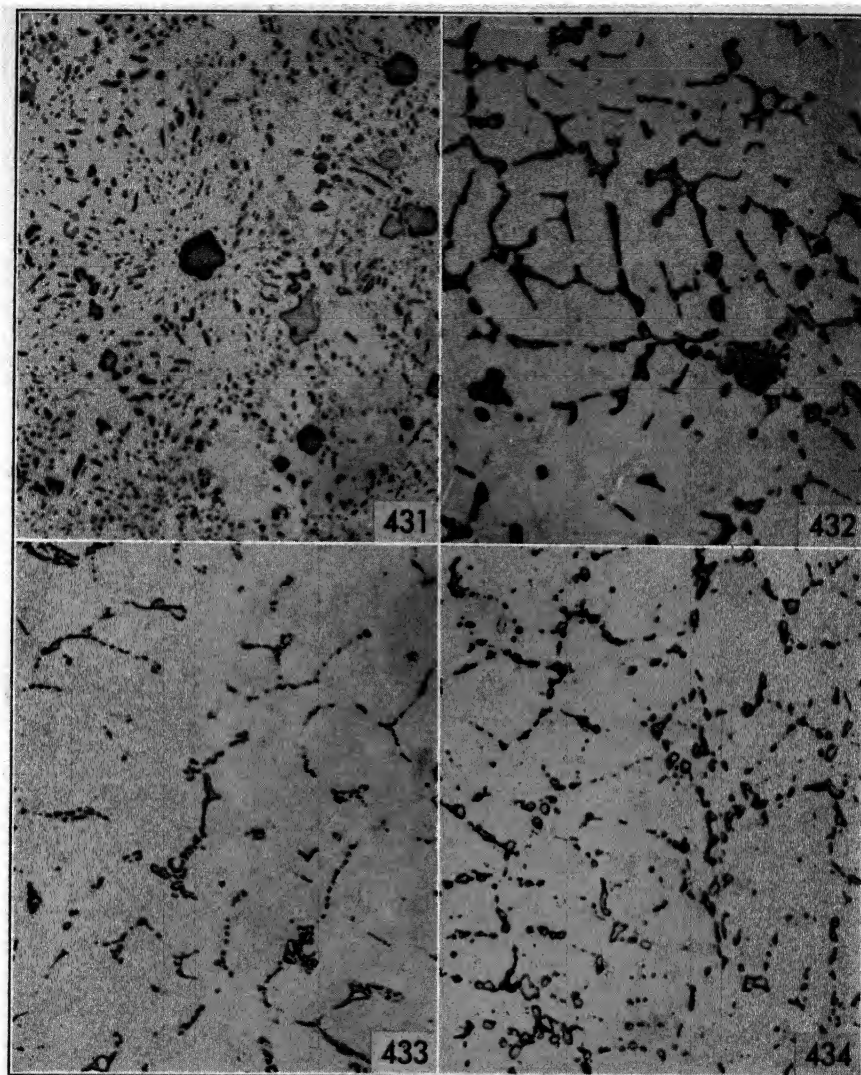


FIG. 431. Sand-cast, solution treated and quenched. The eutectic Si is rounded and partly dissolved by the heat treatment, primary crystals of Si and  $\alpha(\text{AlFeMnSi})$  (light) not affected—Si 13.12%, Fe 0.55%, Mg 0.49%, Mn 0.65%—X 250, not etched.

FIG. 432. Cast in permanent mold, solution treated and quenched.  $\text{CuAl}_2$  gray rounded by heat treatment,  $\alpha(\text{AlFeSi})$  black not affected—Cu 10.10%, Fe 1.20%, Mg 0.33%, Si 0.62%—X 250, etched with  $\text{H}_2\text{SO}_4$ .

FIG. 433. Cast in permanent mold, solution treated and quenched. Si (small points) rounded and partly dissolved by heat treatment,  $\alpha(\text{AlFeMnSi})$  not affected—Fe 0.40%, Mg 0.50%, Mn 0.72%, Si 2.18%—X 250, not etched.

FIG. 434. Cast in permanent mold, solution treated and quenched.  $\text{AlCuNi}$  and  $\text{AlCuFeNi}$  rounded by the heat treatment, other constituents dissolved and not visible—Cu 4.16%, Fe 0.35%, Mg 1.36%, Ni 1.91%, Si 0.27%—X 250, not etched.

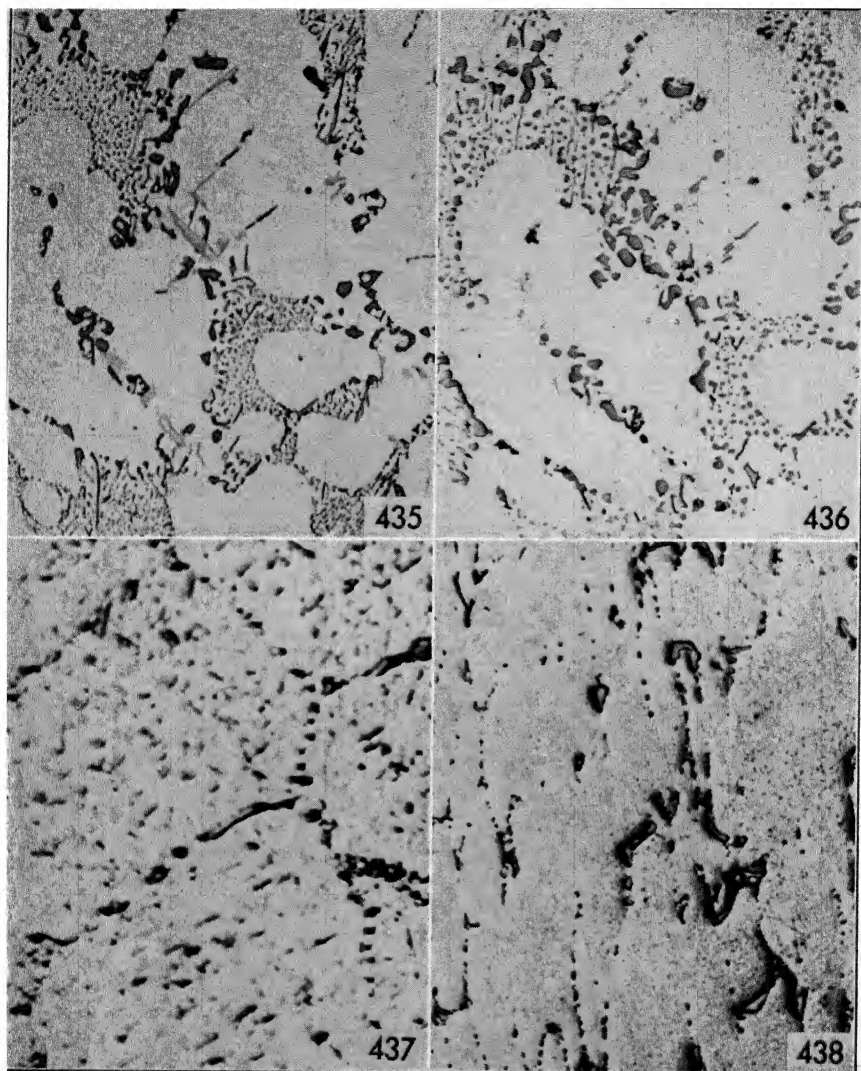


FIG. 435. Sand-cast alloy, as cast—Co 0.58%, Fe 0.54%, Mg 0.37%, Si 8.74%. Gray Si, black Mg<sub>2</sub>Si, light AlCoFe, X 250, not etched.

FIG. 436. Same spot as in Fig. 435 after solution treatment. Mg<sub>2</sub>Si partly dissolved, Si rounded, AlCoFe eaten out in the polishing, X 250, not etched.

FIG. 437. Water-cooled ingot preheated 24 hours at 920°F (497°C). Most of the constituents went in solution, leaving Mg<sub>2</sub>Si black and some CuAl<sub>2</sub> light. The air quenching permitted the reprecipitation of soluble constituents—Cu 4.53%, Fe 0.42%, Mg 1.52%, Mn 0.48%, Si 0.24%—X 1000, not etched.

FIG. 438. Water-cooled ingot rolled from 6 in. to 2 in. and preheated for further rolling. The rolling has deformed the cast structure without breaking it completely; the constituents visible are mostly Mn constituents. Cu 4.35%, Fe 0.38%, Mg 1.62%, Mn 0.56%, Si 0.23%—X 250, not etched.



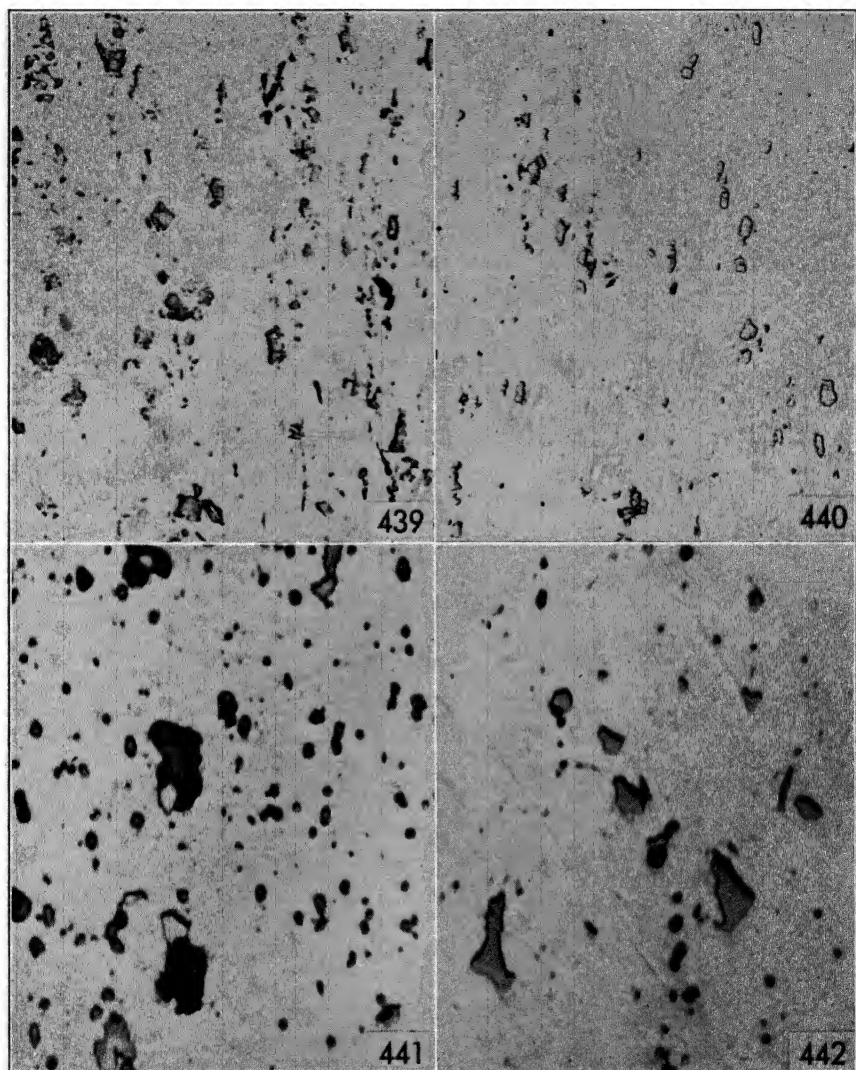


FIG. 439. Extruded, solution treated and quenched. Black  $\text{Mg}_2\text{Si}$ ,  $\text{AlCuNi}$  in relief,  $\text{AlCuFeNi}$  light, slightly affected by the heat treatment—Cu 4.01%, Fe 0.57%, Mg 1.49%, Ni 2.12%, Si 0.49%—X 250, not etched.

FIG. 440. Extruded, solution treated and quenched. Only constituents still visible are Mn compounds and some  $\text{Mg}_2\text{Si}$  (black). Cu 3.40%, Fe 0.58%, Si 0.89%, Mg 1.67%, Mn 0.65%—X 250, not etched.

FIG. 441. Sheet as cold rolled.  $\text{Mg}_2\text{Si}$  black,  $\text{Cu}_2\text{Mg}_2\text{Al}_5$  dark gray, Mn compounds light gray,  $\text{CuAl}_2$  light. Cu 4.62%, Fe 0.21%, Mg 1.67%, Mn 0.42%, Si 0.18%—X 1000, not etched.

FIG. 442. Same sheet as in Fig. 441 after solution treatment and quenching.  $\text{Cu}_2\text{Mg}_2\text{Al}_5$  and  $\text{CuAl}_2$  completely dissolved, Mn compounds and  $\text{Mg}_2\text{Si}$  still visible, X 1000, not etched.



ganese compound (large gray) and  $\text{Mg}_2\text{Si}$  (black) did not go into solution.

### Artificial Aging

Discordant claims have been made on the detectability of age hardening with the microscope. Most investigators now agree that precipitation cannot be detected until after the maximum aging has been reached and overaging has already begun. Reprecipitation at the grain boundaries is probably discernible when the aging peak is reached, but that is true only for alloys of high purity, where there are no insoluble constituents at the grain boundaries to confuse the results.

As age hardening can be detected and followed very easily by hardness measurements, among other methods, it seems needless to investigate it with the microscope, which is a less accurate means for this purpose. For this reason no examples are given.

### Defective Treatments

The most common defects arising from improper heat treatment are:

Incomplete solution.

Eutectic melting.

High-temperature deterioration.

Blistering.

**Incomplete solution.** Incomplete solution, except in extreme cases, is rather hard to detect and requires a good knowledge of the alloy under examination. Equilibrium diagrams are of little use and give only general indications because they deal with the solid solubilities in binary or ternary alloys without the presence of impurities or other soluble constituents, which may affect the solution to a large extent.

Figure 443 shows an example. Although the  $\text{Mg}_2\text{Si}$  content (0.95 per cent) of the alloy is within the limit of solid solubility (1 per cent) at the heat-treatment temperature  $915^\circ\text{F}$  ( $490^\circ\text{C}$ ), a large amount of  $\text{Mg}_2\text{Si}$  undissolved is present because  $\text{Cu}_2\text{Mg}_2\text{Al}_5$  and probably also  $\text{CuAl}_2$  and the manganese compounds reduce the solid solubility of  $\text{Mg}_2\text{Si}$ .

Figure 444 is another example of incomplete solution. Here segregation is probably the main reason, and the treatment must be considered insufficient only because it did not overcome the segregation, although the same treatment may be proper or even excessive for a better casting.

Usually the best way to distinguish between the two types of defective treatment is to repeat the treatment, possibly at higher tempera-

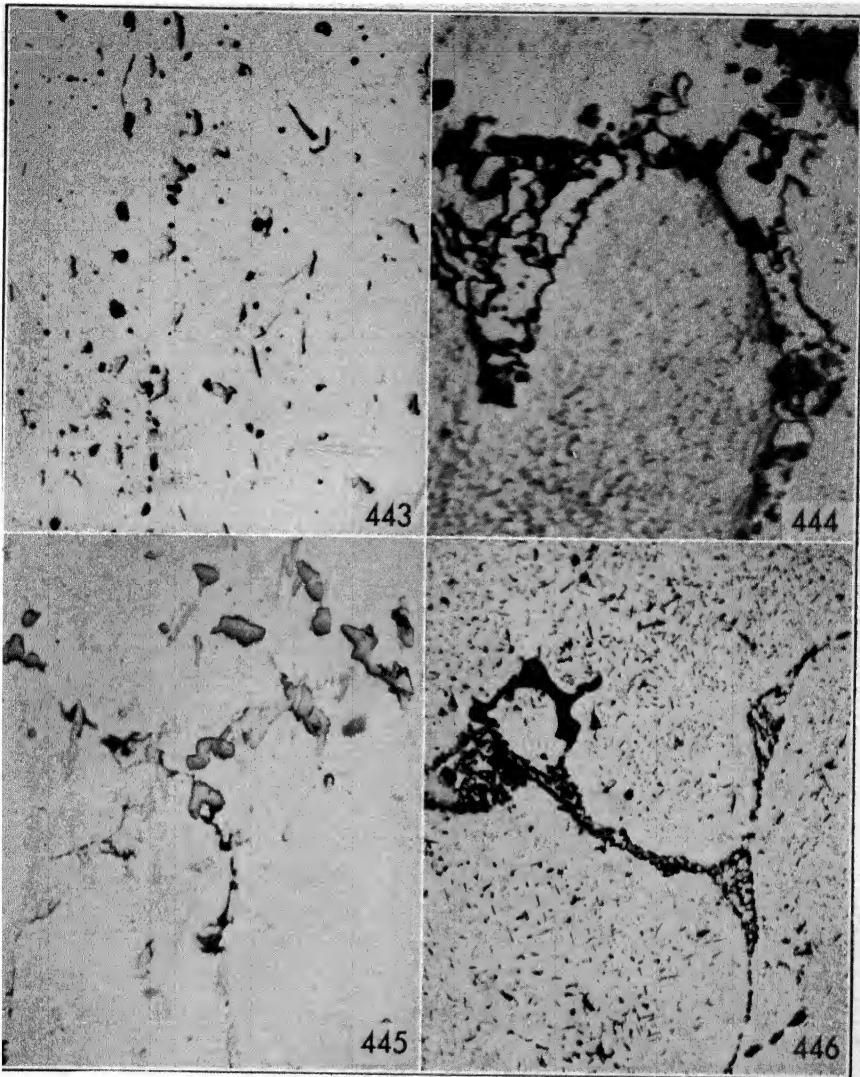


FIG. 443. Sheet solution treated and quenched. Black  $\text{Mg}_2\text{Si}$ , not dissolved, Mn compounds light. Cu 4.32%, Fe 0.32%, Mg 0.60%, Mn 0.56%, Si 0.35%—X 250, not etched.

FIG. 444. Billet preheated 12 hours at 920°F (495°C). Incompletely dissolved constituents,  $\text{Mg}_2\text{Si}$  black,  $\text{Cu}_2\text{Mg}_2\text{Al}_5$  gray,  $\text{CuAl}_2$  light. Cu 4.35%, Fe 0.38%, Mg 1.61%, Mn 0.43%, Si 0.25%—X 1000, not etched.

FIG. 445. Sand-cast, heated to 1040°F (560°C). Eutectic melting which produced cracks,  $\text{AlCuNi}$  (in relief) and  $\text{AlCuFeNi}$  (light) rounded. Cu 3.70%, Fe 0.40%, Mg 1.55%, Ni 2.14%, Si 0.42%—X 250, not etched.

FIG. 446. Ingot water-cooled preheated to 950°F (510°C). Eutectic melting, the eutectics  $\text{Al-Cu}_2\text{Mg}_2\text{Al}_5\text{-CuAl}_2$  and  $\text{Al-Mg}_2\text{Si-CuAl}_2$  partly resolved, a reprecipitated constituent (probably  $\text{Cu}_2\text{Mg}_2\text{Al}_5$ ) in the Al matrix. Cu 4.56%, Fe 0.35%, Mg 1.43%, Mn 0.46%, Si 0.32%—X 500, not etched.

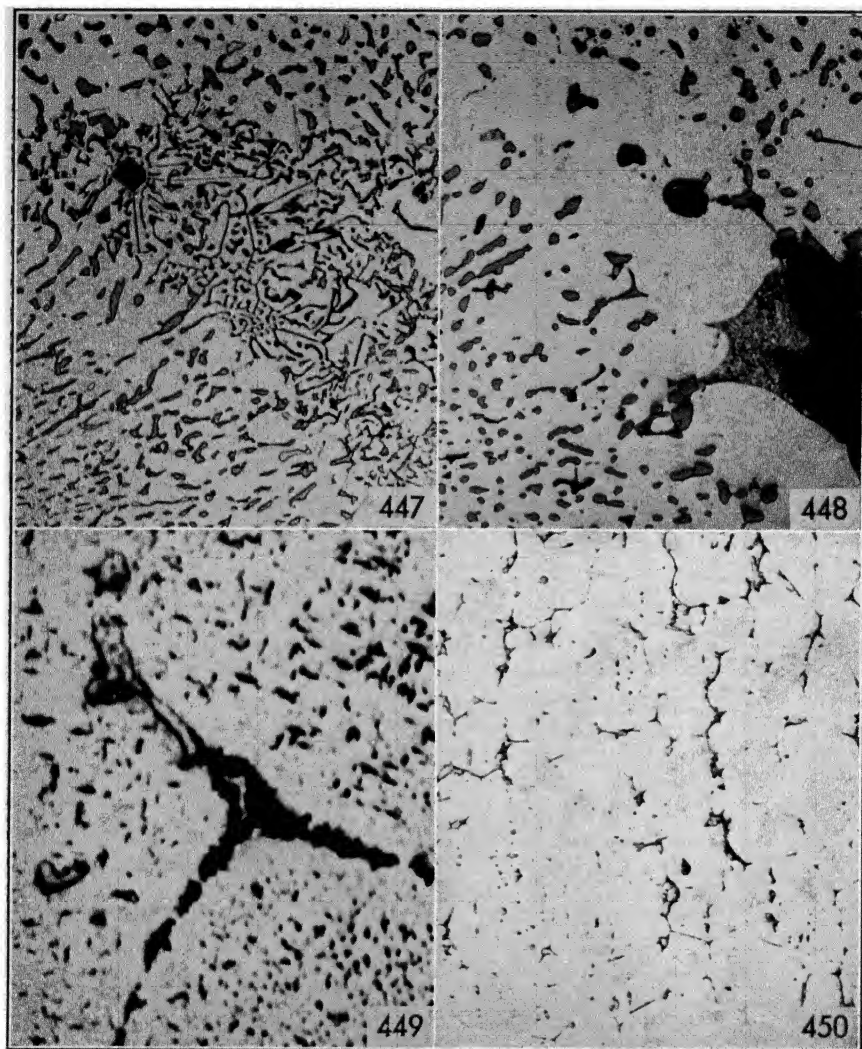


FIG. 447. Cast in permanent mold, as cast. Segregation of eutectic Al-Mg<sub>2</sub>Si black, Si gray, α(AlFeMnSi) light at the grain boundaries. Fe 0.57%, Mg 0.76%, Mn 0.56%, Si 13.10%—X 250, not etched.

FIG. 448. Same spot as in Fig. 447 after solution treatment above 1000°F (540°C) and quenching. The eutectic melted and collected in a spot where the quenching solidified it so finely dispersed that it cannot be resolved, Si particles rounded by the heat treatment, X 250, not etched.

FIG. 449. Ingot water-cooled, preheated above 935°F (500°C). Intergranular crack caused by eutectic melting or gas inclusions (?). Different orientation of the precipitate in the three grains. Cu 4.62%, Fe 0.34%, Mg 1.43%, Mn 0.52%, Si 0.29%—X 1000, not etched.

FIG. 450. Extruded bar solution treated at 1000°F (537°C). Intergranular cracks caused by eutectic melting. Cu 4.58%, Fe 0.55%, Mg 1.74%, Mn 0.66%, Si 0.24%—X 75, not etched.

ture. If no change takes place, especially in the mechanical properties, the treatment is correct and the insoluble constituents must be considered in excess from the solid solubility. If the solution progresses, the first treatment itself was improper. In this event, as almost always, the microscope alone cannot give the answer but can be of value as a means for confirming data from other sources.

**Eutectic melting.** Eutectic melting, especially in the advanced stages, is easily detected with the microscope because the expansion of the eutectic which melts usually creates intergranular cracks.

Figures 445 and 446 show eutectic melting in cast material. Figures 447 and 448 show the transformation caused by eutectic melting, followed by quenching, in a 13 per cent silicon alloy. When heat treatment is continued after eutectic melting, the constituents of the eutectic may tend to go in solid solution and disappear. Then it is difficult to diagnose eutectic melting, for there remains only the crack to identify the spot where melting took place. In addition to the fact that the crack may be covered by dragging of metal during polishing, most often the crack cannot be distinguished from a gas inclusion. Figure 449 shows one of these doubtful cases.

Figures 450, 451, and 452 illustrate eutectic melting in wrought products. Figures 453 and 454 show the longitudinal and transverse section of a special alloy for rivets, where eutectic melting has reached large proportions. In Figs. 455 and 456 the eutectic point has just been reached so that no cracks have formed, and the molten eutectic requires high magnification to be detected. Cases like the last two are very difficult to diagnose and, even when spots like those shown have been detected, the possibility that they may be due to high-temperature deterioration must not be overlooked. Figure 457 illustrates high-temperature deterioration which has been identified through examination of other parts of the material, as the spot depicted is not clearly distinguishable from eutectic melting. Figure 458 shows both eutectic melting and high-temperature deterioration present together.

**High-temperature deterioration.** Very little is known about the mechanism of formation of high-temperature deterioration or oxidation. It is established beyond doubt that water vapor in the furnace atmosphere is one of the most important causes. How it diffuses through the metal and how it reacts is yet to be demonstrated. As for eutectic melting, extreme cases can easily be identified, but when the amount of deterioration is small, it is seldom possible to make an exact identification.

Figures 459, 460, and 461 illustrate cases of severe deterioration where no doubt can exist. Figure 462 is not so easily identifiable and may even represent oxide inclusions from casting.

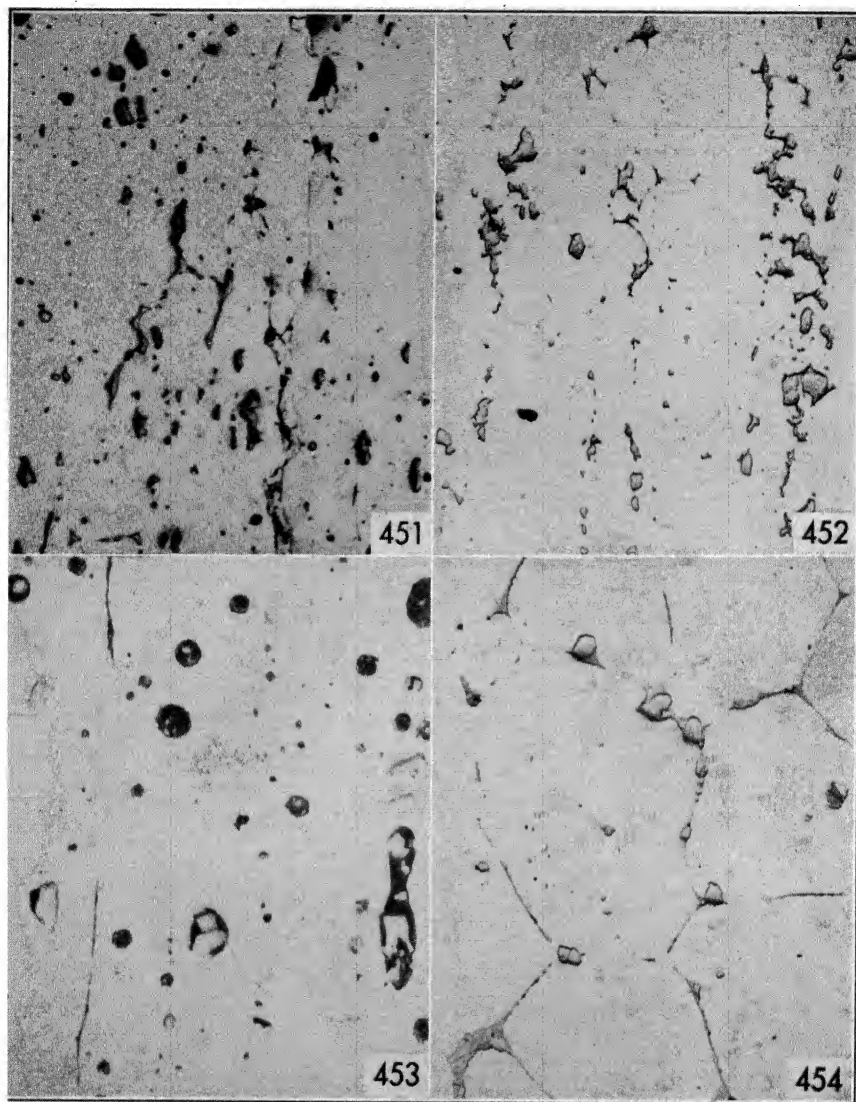


FIG. 451. Sheet overheated in heat treatment. Intergranular cracks and rounding of constituents caused by overheating. Cu 4.38%, Fe 0.35%, Mg 1.35%, Mn 0.47%, Si 0.36%—X 250, not etched.

FIG. 452. Extruded rod, solution treated at 1000°F (540°C). Small intergranular cracks caused by a limited amount of eutectic melting. Cu 3.22%, Fe 0.54%, Mg 1.05%, Si 0.28%, Mn 0.46%—X 250, not etched.

FIG. 453. Extruded rod, solution treated at 950°F (510°C). Rounded constituents, globules of eutectics and intergranular cracks caused by overheating. Cu 3.88%, Fe 0.44%, Mg 2.43%, Mn 0.45%, Si 0.45%—X 250, not etched.

FIG. 454. Transverse section of Fig. 453, X 250, not etched.

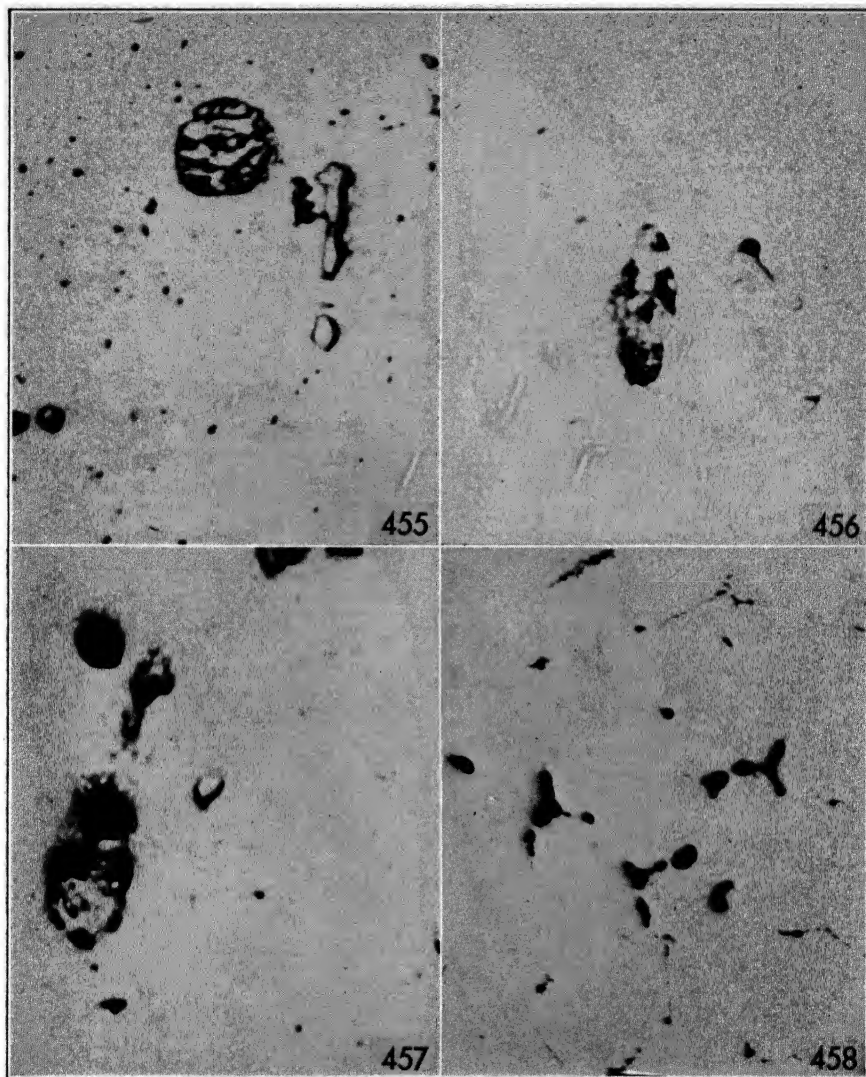


FIG. 455. Sheet solution treated above 935°F (500°C). Globule of eutectic Al-Cu<sub>2</sub>Mg<sub>2</sub>Al<sub>5</sub>-CuAl<sub>2</sub> molten and resolidified, nearby a Mn constituent. Cu 4.35%, Fe 0.32%, Mg 1.62%, Mn 0.56%, Si 0.28%—X 1000, not etched.

FIG. 456. Rolled rod, solution treated above 970°F (520°C). Globule of eutectic Al-Cu<sub>2</sub>Mg<sub>2</sub>Al<sub>5</sub>-CuAl<sub>2</sub> molten and resolidified. Cu 4.06%, Fe 0.53%, Mg 0.68%, Mn 0.56%, Si 0.24%—X 1000, not etched.

FIG. 457. Sheet solution treated. High-temperature deterioration—Cu 4.34%, Fe 0.42%, Mg 1.35%, Mn 0.56%, Si 0.23%—X 1000, not etched.

FIG. 458. Water-cooled ingot, preheated at 900°F (480°C). Eutectic melting or high-temperature deterioration? Probably both—Cu 0.04%, Fe 0.31%, Mg 2.53%, Si 0.19%, Cr 0.25%—X 250, not etched.



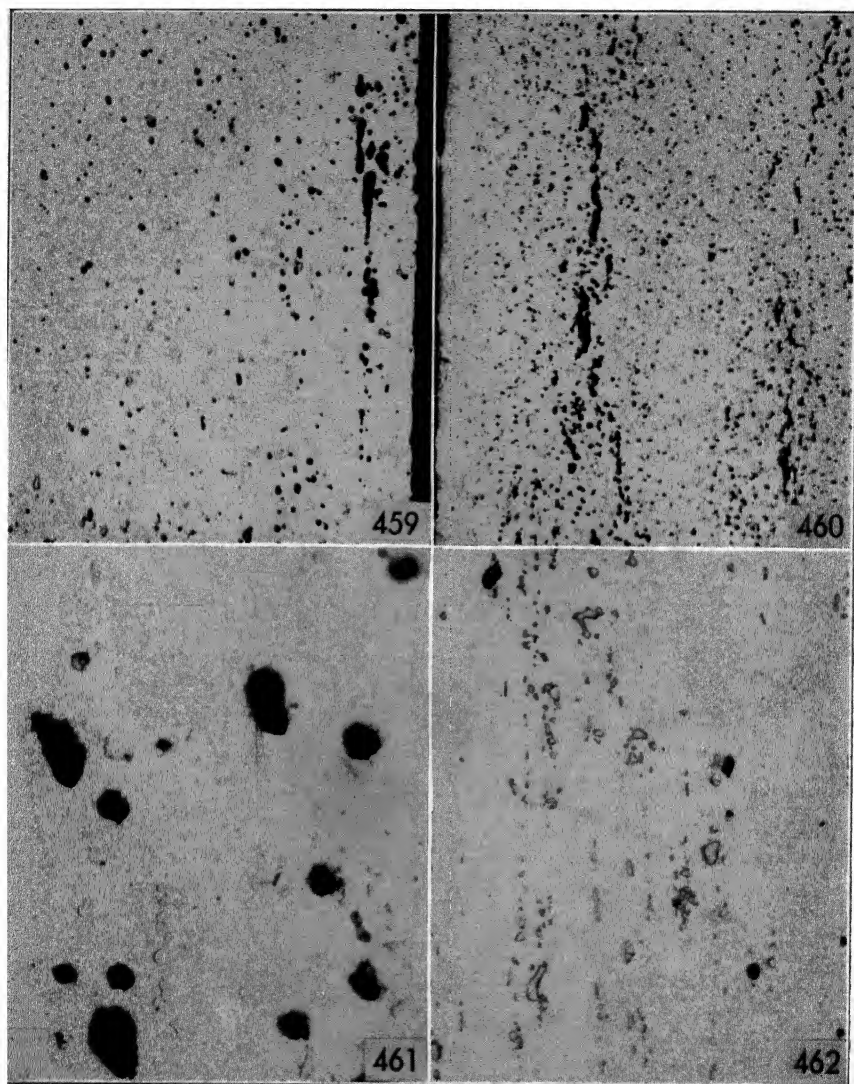


FIG. 459. Sheet solution treated several times. Black spots of high-temperature deterioration concentrated at the edge. Cu 4.52%, Fe 0.34%, Mg 1.25%, Mn 0.47%, Si 0.39%—X 75, not etched.

FIG. 460. Alclad sheet solution treated many times. Severe case of high-temperature deterioration with formation of blisters. Cu 4.45%, Fe 0.33%, Mg 1.32%, Mn 0.47%, Si 0.25%—X 30, not etched.

FIG. 461. Enlargement of Fig. 460. Black spots of deteriorated constituents (probably  $\text{Cu}_2\text{Mg}_2\text{Al}_5$ ), Mn constituents not oxidized, light, X 1000, not etched.

FIG. 462. Extruded rod solution treated. Black spots of oxide or high-temperature deterioration? Mn constituents and  $\text{CuAl}_2$  light. Cu 4.01%, Fe 0.54%, Mg 0.62%, Mn 0.54%, Si 0.62%—X 250, not etched.

**Blistering.** Blistering usually accompanies eutectic melting and high-temperature deterioration, and in these cases it can be attributed to these defects. It is also commonly encountered in clad material, where blisters form between the cladding and the base metal, as will be shown under the heading *Cladding*. However, there are some cases

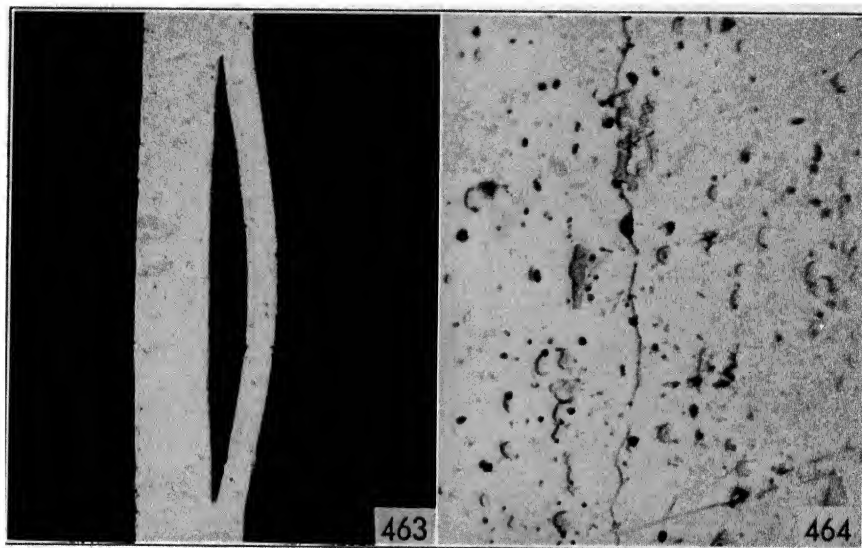


FIG. 463. Sheet annealed. Blister of unknown origin. Cu 4.32%, Fe 0.39%, Mg 1.64%, Mn 0.52%, Si 0.28%—X 30, not etched.

FIG. 464. Sheet annealed. Section through a blister without detectable cause. Cu 4.24%, Fe 0.35%, Mg 1.34%, Mn 0.57%, Si 0.45%—X 250, not etched.

where blisters are found in material which is otherwise perfectly sound. The explanation of this is still hypothetical.

Figures 463 and 464 show two cases of this kind for which no explanation can be offered. The most probable hypothesis seems to be that, during heating, gases entrapped in the metal expand rapidly, forming gas pockets in the metal. But how the gases became concentrated in points instead of diffusing is beyond explanation.



## CHAPTER 17

### CORROSION AND PROTECTION

This chapter will deal with the effects of corrosion on aluminum alloys and with means of protection. Only one method of protection will be described in detail—cladding—since it is the only one which involves metallurgical operations. Anodic oxidation, electroplating, painting, etc., will not be described because they do not affect the structure of the metal protected and must be considered only as finishing operations, like buffing, polishing, etc., which are beyond the scope of this book.

#### Corrosion

There are two main types of corrosion usually found in aluminum alloys: pitting corrosion and intergranular corrosion. The difference between the two is that pitting corrosion attacks all parts of the surface indifferently, whereas intergranular corrosion attacks the grain boundaries and works its way inside the material in parts which from the surface appear to be intact. The reasons and the conditions for the formation of one type or the other have been deeply investigated, but the exact causes are not actually known in all details and cannot be reported here.

Figures 465 and 466 show the two types of corrosion in wrought material. Figure 467 shows a mixed case where the intergranular corrosion started at the bottom of a corrosion pit. Figure 468 shows intergranular corrosion in a sand-cast alloy. Figures 469, 470, and 471 show the progress of intergranular corrosion in a 7 per cent magnesium alloy, subjected for increasing periods of time to an accelerated corrosion test. Figure 472 shows pitting corrosion in a manganese alloy subjected to accelerated corrosion test.

#### Protection

**Cladding.** This process of protection consists in the rolling together of two sheets of a highly corrosion resistant material with the material

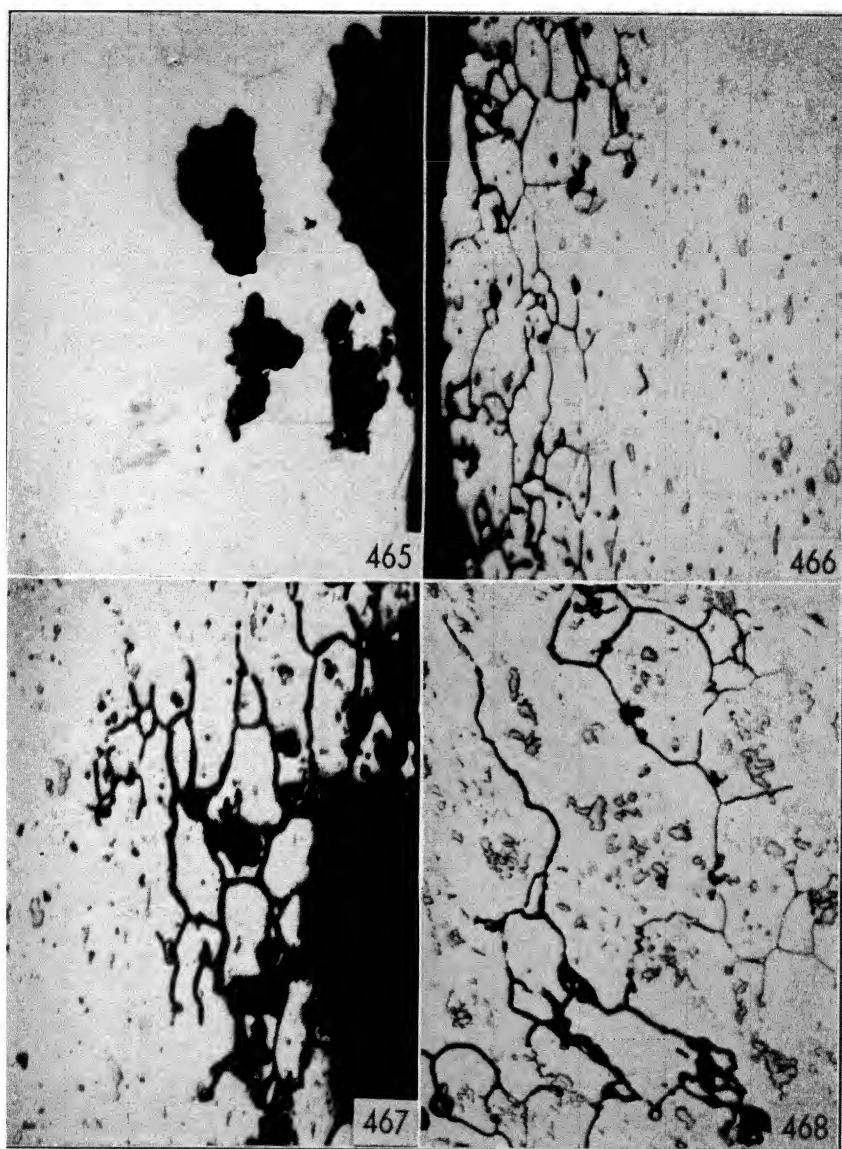


FIG. 465. Sheet solution treated and quenched. Pitting corrosion—Cu 4.54%, Fe 0.37%, Mg 1.45%, Mn 0.53%, Si 0.24%—X 250, not etched.

FIG. 466. Same material as in Fig. 465. Intergranular corrosion, X 250, not etched.

FIG. 467. Same material as in Fig. 465. Intergranular corrosion, starting from the bottom of a corrosion pit, X 250, not etched.

FIG. 468. Sand-cast, solution treated and quenched. Intergranular corrosion—Cu 2.97%, Fe 1.45%, Mg 0.67%, Ni 0.54%, Si 0.72%—X 250, not etched.

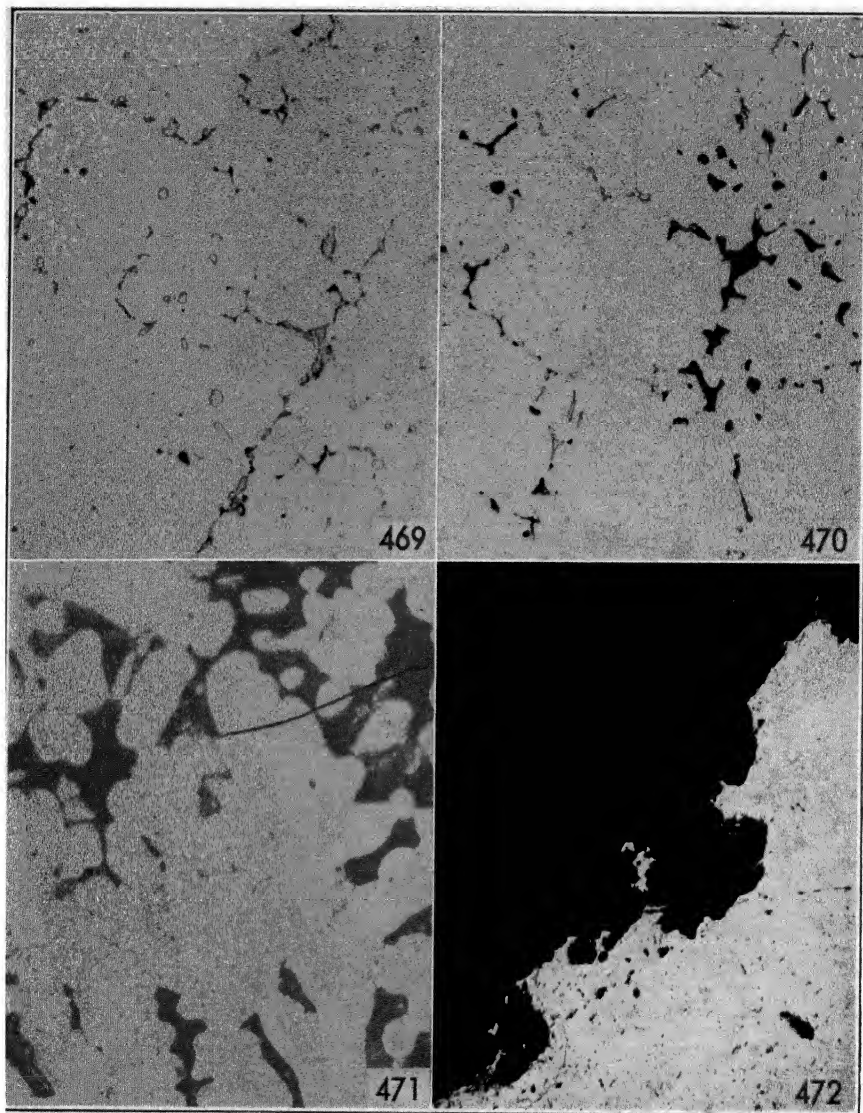


FIG. 469. Sand-cast, tested for three months in salt spray. Beginning of intergranular corrosion hardly detectable from  $\text{Mg}_2\text{Si}$ . Fe 0.23%, Mg 7.10%, Mn 0.15%, Si 0.18%—X 250, not etched.

FIG. 470. Same material as in Fig. 469 after six months in salt spray. Intergranular corrosion is easily detected at the grain boundaries, X 250, not etched.

FIG. 471. Same material as in Fig. 469 after 12 months in salt spray. Heavy corrosion has taken place, X 250, not etched.

FIG. 472. Sheet tested in corroding solution. Pitting corrosion—Fe 0.57%, Mn 1.24%, Si 0.33%—X 75, not etched.

to be protected, one for each side. During hot rolling the oxide film which covers the surfaces is broken so that unoxidized material is contacted, and under the effect of the heat and the pressure the different materials become welded together, forming only one sheet with a core of strong alloy and two outside layers of protective material.

Figure 473 shows an alloy of the duralumin type, hot-rolled, clad with pure aluminum. The bond between the two metals is already formed and no line of division can be detected between the two metals. Figure 474 shows the same alloy, cold-rolled from 0.320 inch to 0.080 inch. Figure 475 shows it finished to the gauge 0.040 inch, solution-treated and etched to reveal the grain size. Figure 476 is an enlargement of Fig. 475, showing in detail the bond zone. It can be seen that recrystallization has taken place across the bond, so that new crystals of pure aluminum and alloy dovetail together. Crystals are present also in the cladding, but the etching used reveals grain structures only in alloys containing copper. This fact is useful in examination of claddings because it reveals the extent to which the copper has diffused into the cladding and permits a fairly accurate measurement of the thickness of the protective layer. Figure 477 shows the same alloy clad with a  $\text{Mg}_2\text{Si}$ -type alloy instead of pure aluminum. The alloy is in the hot-rolled condition, as is the specimen in Fig. 473. The only difference existing between the two is the structure of the cladding, which in the last specimen shows a large amount of  $\text{Mg}_2\text{Si}$  particles not dissolved. In Fig. 478 is the same alloy, cold-rolled to 0.040 inch and etched to show the grain structure. Figure 479 shows the same alloy after heat treatment. All the  $\text{CuAl}_2$  and  $\text{Cu}_2\text{Mg}_2\text{Al}_5$  in the base metal went in solid solution, but because of the low heat-treatment temperature (not above  $930^\circ\text{F}$ — $500^\circ\text{C}$ ) required by the base metal, most of the  $\text{Mg}_2\text{Si}$  in the cladding did not go in solid solution.

The main defects arising from defective practice in cladding are:

Blisters between cladding and base metal.

Excessive diffusion of copper in the cladding.

Several other defects like rolled-in material, scratches, are production rather than metallographic problems and do not belong here.

Figure 480 shows an alloy clad with a  $\text{Mg}_2\text{Si}$ -type alloy after hot rolling. Probably on account of insufficient cleaning of the two surfaces which must weld in hot rolling, no bond was formed in the spot examined. When a spot like the one shown is heat-treated, the air entrapped in it will expand and form a blister. Figures 481 and 482 show an alloy, clad with pure aluminum, which has been held too long at solution-treatment temperature. The copper of the base metal

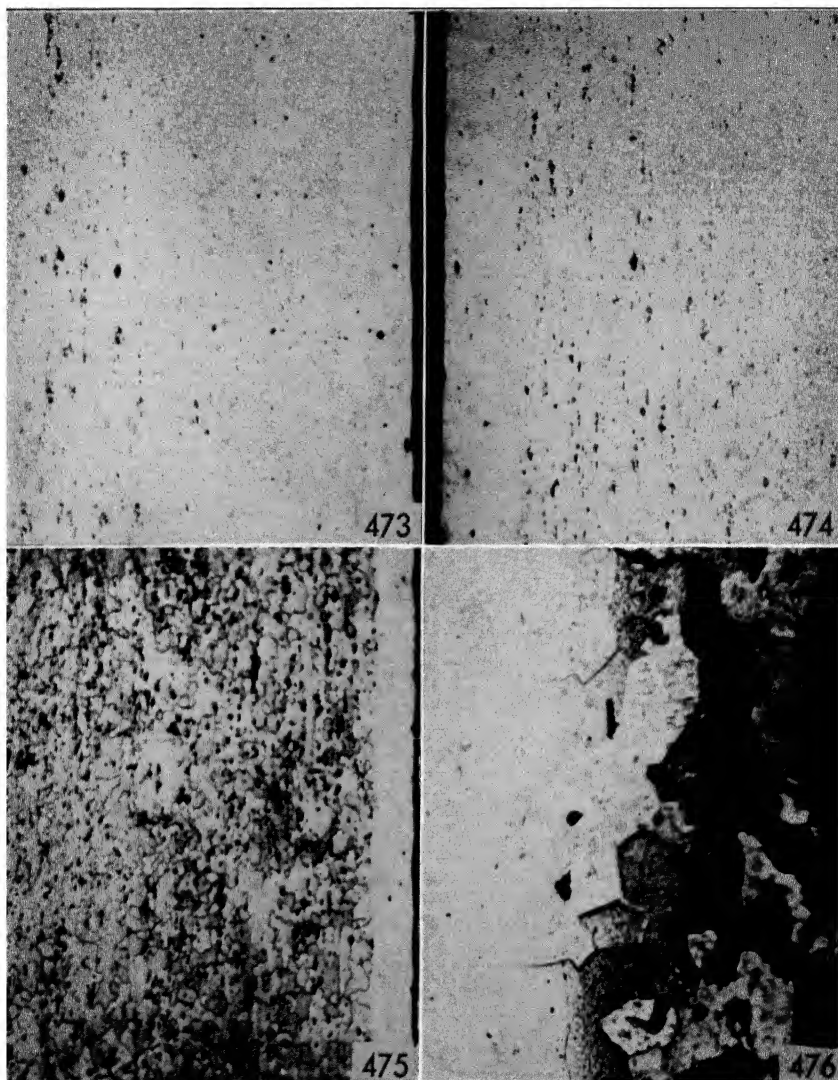


FIG. 473. Clad ingot hot rolled from 6 in. to 0.320 in. Perfect bonding of the two sheets. Base metal: Cu 4.47%, Fe 0.34%, Mg 1.72%, Mn 0.53%, Si 0.23%. Cladding: Al 99.7%. X 75, not etched.

FIG. 474. Same material as in Fig. 473 after cold rolling from 0.320 in. to 0.080 in., X 75, not etched.

FIG. 475. Same material as in Fig. 473 cold rolled to 0.040 in. and solution treated. In the base metal the grains have been etched and are visible, not in the cladding, X 75, etched with acid mixture.

FIG. 476. Enlargement of the bond zone in Fig. 475. Some diffusion of copper has taken place from the base metal to the cladding, cementing them together. X 500, etched with acid mixture.



FIG. 477. Ingot clad with a  $Mg_2Si$  alloy, hot and cold rolled from 6 in. to 0.160 in. In the cladding  $Mg_2Si$  highly dispersed, in the base metal Mn compounds and  $CuAl_2$ . Perfect bond. Base metal: Cu 4.56%, Fe 0.35%, Mg 1.67%, Si 0.23%, Mn 0.45%. Cladding: Cr 0.25%, Fe 0.29%, Mg 1.32%, Si 0.68%. X 75, not etched.

FIG. 478. Same material as in Fig. 477, cold rolled to 0.040 in., X 75, not etched.

FIG. 479. Same material as Fig. 477, heat treated. Most of the  $Mg_2Si$  in the cladding still undissolved, Mn compounds light. X 250 not etched.

FIG. 480. Same material as in Fig. 477, hot rolled from 6 in. to 0.320 in. Bond between base metal and cladding missing, X 75, not etched.

(also magnesium, silicon, manganese, and even iron diffuse, but to a much more limited extent) has diffused far into the cladding, reducing greatly its protective effect.

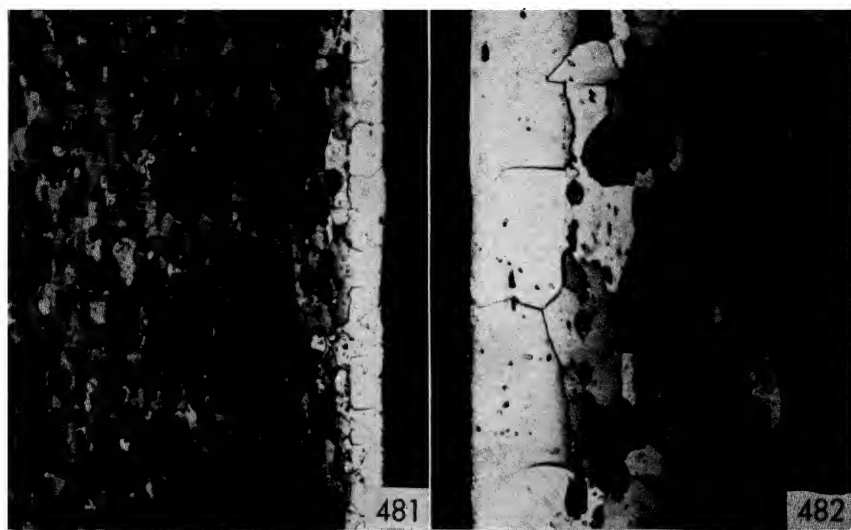


FIG. 481. Clad sheet, 0.032 in. gauge; held too long at solution treatment temperature. The etching, showing the grain boundaries also in the cladding, reveals that copper from the base metal has diffused into it. Base metal: Cu 4.72%, Fe 0.32%, Mg 1.62%, Si 0.22%, Mn 0.45%. Cladding: Al 99.7%. X 75, etched with acid mixture.

FIG. 482. Enlargement of Fig. 481 to show diffusion in cladding. X 250, etched with acid mixture.

## BIBLIOGRAPHY

### General

1. C. A. Tissier, *Guide pratique de la recherche, de l'extraction et de la fabrication de l'aluminium et des métaux alcalines*, Paris, 1858.
2. H. St. Claire-Deville, *De l'aluminium*, Paris, 1859.
3. Lejal, *L'aluminium*, Paris, 1864.
4. H. C. H. Carpenter and C. A. Edwards, *8th Report Alloy Res. Comm. Inst. Mech. Engrs.*, 1907.
5. U. S. Bureau of Standards, *Circ.* 76, 1919.
6. C. Grard, *L'aluminium et ses alliages*, Paris, 1920.
7. W. Rosenhain, S. L. Archbutt, and D. Hanson, *11th Report Alloy Res. Comm. Inst. Mech. Engrs.*, 1921.
8. R. J. Anderson, *The Metallurgy of Aluminum and Aluminum Alloys*, H. C. Baird & Co., New York, 1925.
9. M. G. Corson, *Aluminium*, Chapman & Hall, London, 1926.
10. U. S. Bureau of Standards, *Circ.* 346, 1927.
11. Lecouvre and R. Cazaud, *Recherches métallographiques de l'aluminium*, Blondel la Rougerie, Paris, 1928.
12. P. Melchior, *Aluminium*, V. D. I. Verlag, Berlin, 1929.
13. J. D. Edwards, F. C. Frary, Z. Jeffries, *The Aluminum Industry*, McGraw-Hill, New York, 1930.
14. N. F. Bugden, *Aluminium and Its Alloys*, Sir Isaac Pitman & Sons, Ltd., London, 1933.
15. R. J. Anderson, *Secondary Aluminum*, Chapman & Hall, London, 1933.
16. C. Panseri, *La fonderia d'alluminio*, U. Hoepli, Milano, 1934.
17. A. von Zeerleder, *Technologie des Aluminiums und seiner Legierungen*, Akad. Verlags Ges. m.b.H., Leipzig, 1935.
- 17b. *The same*, translated by A. J. Field, Nordmann Publ. Co., London, 1936.
18. Aluminium Zentrale G.m.b.H., *Aluminium Taschenbuch*, Berlin, 1937.
19. D. B. Hobbs, *Aluminium, Its History, Metallurgy and Uses*, Bruce Co., Milwaukee, Wis., 1938.
20. American Society of Metals, *Metals Handbook*, 1939.
21. L. Guillet, *Les métaux légers et leur alliages*, Dunod Frères, Paris, 1940.
22. C. Panseri, *L'alluminio e le sue leghe*, U. Hoepli, Milano, 1941.

## PART I

### General

23. K. Bornemann, *Binaren Metalllegierungen*, V. Knapp, Halle, Germany, 1909.
24. V. Fuss, *Metallographie des Aluminiums und seiner Legierungen*, Julius Springer, Berlin, 1934.
- 24b. *The same*, translated by R. J. Anderson, Sherwood Press, Inc., Cleveland, Ohio, 1936.
25. M. Hansen, *Der Aufbau der Zweistofflegierungen*, Julius Springer, Berlin, 1936.
26. E. Jaenecke, *Kurzgefasstes Handbuch aller Legierungen*, O. Spanner, Leipzig, 1937.



**Al-Ag**

27. C. R. A. Wright, *Proc. Roy. Soc. (London)*, **52**, 24 (1892).
28. H. Gautier, *Compt. rend.*, **123**, 109 (1896).
29. C. T. Heycock and F. H. Neville, *Phil. Tr. Roy. Soc. (London)*, **A189**, 69 (1897).
30. G. I. Petrenko, *Z. anorg. Chem.*, **46**, 49 (1905).
31. N. A. Pushin, *Zhur. Fiz. Khim.*, **39**, 528 (1907).
32. W. Brownieski, *Compt. rend.*, **150**, 1754 (1910).
33. B. Beckmann, *Z. Metallkunde*, **6**, 246 (1914).
34. M. Goto and T. Mishima, *Nippon Kogyo Kwaishi*, [474] **40**, 702 (1924).
35. M. Tazaki, *Kinzoku-no-Kenkyu*, **4**, 34 (1927).
36. W. Kroll, *Metall u. Erz*, **23**, 555 (1926).
37. G. Sachs and M. Hansen, *Z. Metallkunde*, **20**, 151 (1928).
38. A. F. Westgren and A. J. Bradley, *Phil. Mag.*, [7] **6**, 280 (1928).
39. M. Hansen, *Z. Metallkunde*, **20**, 217 (1928).
40. E. Crepaz, *Atti III Congr. Naz. Chimica Pura Appl.*, Firenze, 1930, p. 371.
41. T. P. Hoar and R. K. Rowntree, *J. Inst. Metals*, **45**, 119 (1931).
42. F. E. Tischenko, *Z. Obshchey Khim.*, **3**, 549 (1933).
43. N. Ageew and D. Shoyket, *J. Inst. Metals*, **52**, 119 (1933).
44. W. Hume-Rothery, *J. Inst. Metals*, **52**, 127 (1933).
45. C. S. Barrett, *Metals and Alloys*, **4**, 63 (1933).
46. E. R. Jette and F. Foote, *Metals and Alloys*, **4**, 78 (1933).
47. S. Kokubo, *Sci. Rep. Tôhoku Univ.*, **33**, 45 (1934).
48. F. E. Tischenko and I. K. Lukash, *Zhur. Fiz. Khim.*, **9**, 440, 605 (1937).
49. C. R. Barrett, A. H. Geisler, and R. F. Mehl, *Trans. A.I.M.E.*, **143**, 134 (1941).

**Al-As**

50. C. Winkler, *Jahrb. prakt. Chemie*, **91**, 206 (1864).
51. G. A. Mansuri, *J. Chem. Soc.*, [2] **121**, 2272 (1922).
52. M. Goto, *Kinzoku-no-Kenkyu*, **4**, 34 (1927).
53. G. Natta and L. Passerini, *Gazz. chim. ital.*, **58**, 458 (1928).

**Al-Au**

54. W. C. Roberts-Austen, *Proc. Roy. Soc. (London)*, **50**, 367 (1891/92).
55. C. T. Heycock and F. H. Neville, *Phil. Tr. Roy. Soc. (London)*, **194**, 201 (1900).
56. K. Bornemann, *Metall u. Erz*, **7**, 572 (1910).
57. C. T. Heycock and F. H. Neville, *Phil. Tr. Roy. Soc. (London)*, **214**, 267 (1914).
58. O. Eisenhut and E. Kaupp, *Z. Electrochem.*, **37**, 472 (1931).
59. C. D. West and A. W. Peterson, *Z. Krist.*, **88A**, 93 (1934).
60. A. S. Coffinberry and R. Hultgren, *Trans. A.I.M.E.*, **128**, 249 (1938).

**Al-B**

61. H. Giebelhausen, *Z. anorg. Chem.*, **91**, p. 262 (1915).
62. W. Guertler, *Metallographie*, Bd. 1, Teil 2, Heft 2, p. 760, Berlin: Gebr. Borntraeger, 1917.
63. P. Haenni, *Compt. rend.*, **181**, p. 864 (1925).
64. W. Hofmann and W. Jaeniche, *Z. Metallkunde*, **28**, p. 1 (1936).
65. F. Halla and R. Weil, *Naturwissenschaften*, **27**, p. 96 (1939).

**Al-Ba**

66. E. Alberti, *Z. Metallkunde*, **26**, p. 6 (1934).
67. E. Alberti and K. R. Andress, *Z. Metallkunde*, **27**, p. 126 (1935).

**Al-Be**

68. G. Oosterheld, *Z. anorg. Chem.*, **97**, 9 (1916).
69. *Nat. Phys. Lab. Rep.*, 1925, p. 205.
70. W. Kroll, *Metall u. Erz*, **23**, 616 (1926).
71. P. Hidnert and W. T. Sweeney, *U. S. Bureau of Standards, Sci. Pap.* 565, 1927.
72. R. S. Archer and W. L. Fink, *Proc. A.I.M.E.*, **78**, 616 (1928).
73. G. Masing and O. Dahl, *Wiss. Veroeff. Siemens-Konz.*, **1**, 249 (1929).
74. M. Haas and D. Uno, *Z. Metallkunde*, **22**, 277 (1930).
75. E. S. Makarov and L. Tarschisch, *Zhur. Fiz. Khim.*, [9] **3**, 350 (1937).
76. L. Losana, *Alluminio*, **9**, 8 (1940).
77. V. I. Mikheeva, *Izvest. Akad. Nauk U.S.S.R.*, **5**, 775 (1940).
78. C. B. Sawyer, *Metals and Alloys*, **12**, 37 (1941).

**Al-Bi**

79. C. T. Heycock and F. H. Neville, *J. Chem. Soc.*, **61**, 893 (1892).
80. C. R. A. Wright, *J. Soc. Chem. Ind.*, **11**, 492 (1892).
81. C. R. A. Wright, *J. Soc. Chem. Ind.*, **13**, 1014 (1894).
82. W. Campbell and J. A. Mathews, *J. Am. Chem. Soc.*, **24**, 255 (1902).
83. H. Pécheux, *Compt. rend.*, **138**, 1501 (1904).
84. H. Pécheux, *Compt. rend.*, **143**, 397 (1906).
85. A. G. C. Gwyer, *Z. anorg. Chem.*, **49**, 316 (1906).
86. W. Brownieski, *Ann. chim. phys.*, **25**, 66 (1912).
87. M. Hansen and B. Blumenthal, *Metallwirtschaft*, **10**, 925 (1931).
88. L. W. Kempf and K. R. Van Horn, *Trans. A.I.M.E.*, **133**, 81 (1939).

**Al-Ca**

89. K. Arndt, *Ber. deut. chem. Ges.*, **38**, 1972 (1905).
90. L. Stockem, *Metall u. Erz*, **3**, 149 (1906).
91. L. Donsky, *Z. anorg. Chem.*, **57**, 201 (1908).
92. J. M. Breckenridge, *Trans. Am. Electrochem. Soc.*, **17**, 367 (1910).
93. R. Kremann, H. Wostall, and H. Schoepper, *Z. Metallkunde*, **14**, 5 (1922).
94. J. D. Grogan, *Tech. Rep. Adv. Com. Aero.*, **2**, 425 (1922).
95. J. D. Edwards and C. S. Taylor, *Trans. Am. Electrochem. Soc.*, **50**, 391 (1926).
96. G. Doan, *Z. Metallkunde*, **18**, 350 (1926).
97. G. Bozza and C. Sonnino, *Gazz. chim. ind. appl.*, **58**, 443 (1928).
98. K. Matsuyama, *Sci. Rep. Tôhoku Univ.*, **17**, 783 (1928).
99. H. Nowotny and A. Mohrnheim, *Z. Krist.*, **100**, 540 (1939).
100. H. Nowotny, A. Mohrnheim, and E. Wormnes, *Z. Metallkunde*, **32**, 39 (1940).

**Al-Cb**

101. L. Maurignac, *Compt. rend.*, **66**, 180 (1868).
102. W. Von Bolton, *Z. Electrochem.*, **13**, 146 (1907).
103. S. Von Olshausen, *Z. Krist.*, **61**, 475 (1925).
104. G. Brauer, *Naturwissenschaften*, **26**, 43, 710 (1938).

**Al-Cd**

105. C. T. Heycock and F. H. Neville, *J. Chem. Soc.*, **61**, 911 (1892).
106. C. R. A. Wright, *Proc. Roy. Soc. (London)*, **55**, 130 (1894).
107. W. Campbell and J. A. Mathews, *J. Am. Chem. Soc.*, **24**, 255 (1902).
108. A. G. C. Gwyer, *Z. anorg. Chem.*, **57**, 149 (1908).
109. M. Hansen and B. Blumenthal, *Metallwirtschaft*, **10**, 925 (1931); **11**, 671 (1932).

## Al-Ce

- 110. W. Muthmann and H. Beck, *Liebigs Ann.*, **331**, 47 (1904).
- 111. O. Barth, *Metall u. Erz*, **9**, 274 (1912).
- 112. R. Vogel, *Z. anorg. Chem.*, **75**, 41 (1912).
- 113. J. Schulte, *Metall u. Erz*, **18**, 236 (1921).
- 114. K. L. Meissner, *Metall u. Erz*, **21**, 41 (1924).
- 115. M. Biltz and H. Pieper, *Z. anorg. Chem.*, **134**, 13 (1924).
- 116. M. Bosshard, *Alluminio*, **3**, 205 (1934).
- 117. H. J. Wallbaum, *Z. Krist.*, **103**, 147 (1940).

## Al-Co

- 118. O. Brunck, *Ber. deut. chem. Ges.*, **34**, 2734 (1901).
- 119. L. Guillet, *Génie civil*, **41**, 169 (1902).
- 120. A. G. C. Gwyer, *Z. anorg. Chem.*, **57**, 140 (1908).
- 121. S. Daniels, *Ind. Eng. Chem.*, **18**, 686 (1926).
- 122. T. Arada, *Suiyokwai-Shi*, **5**, 13 (1926).
- 123. H. Masumoto, *Sci. Rep. Tôhoku Univ.*, **15**, 449 (1926).
- 124. W. Ekmann, *Z. physik. Chem.*, **B12**, 57 (1930).
- 125. W. Hashimoto, *Kinzoku-no-Kenkyu*, **9**, 65 (1932).
- 126. W. L. Fink and H. R. Freche, *Trans. A.I.M.E.*, **99**, 141 (1932).
- 127. A. J. Bradley and C. S. Cheng, *Z. Krist.*, **99**, 480 (1938).
- 128. A. J. Bradley and G. C. Seager, *J. Inst. Metals*, **64**, 81 (1939).

## Al-Cr

- 129. L. Guillet, *Génie civil*, **41**, 391 (1902).
- 130. G. Hindricks, *Z. anorg. Chem.*, **59**, 430 (1908).
- 131. E. Jaenecke, *Z. Electrochem.*, **23**, 53 (1917).
- 132. M. R. Whitmore and F. T. Sisco, *Ind. Eng. Chem.*, **17**, 956 (1925).
- 133. A. J. Bradley and A. F. Ollard, *Nature*, **117**, 122 (1926).
- 134. M. Goto and G. Dogane, *Nippon Kogyo Kwaishi*, [512] **43**, 931 (1927).
- 135. K. Honda, *Trans. World Eng. Congr. Tokio*, 1929, p. 658.
- 136. W. L. Fink and H. R. Freche, *Trans. A.I.M.E.*, **104**, 325 (1933).
- 137. P. Roentgen and W. Koch, *Z. Metallkunde*, **25**, 184 (1933).
- 138. S. Hori, *Sumitomu Kinzoku Kôgyô Kenkyu Hokoku*, [5] **2**, 351 (1935).
- 139. A. J. Bradley and S. S. Lu, *J. Inst. Metals*, **60**, 319 (1937).
- 140. W. Koch and Winterhagen, *Metallwirtschaft*, **17**, 1159 (1938).
- 141. W. Hofmann and R. W. Herzer, *Metallwirtschaft*, **19**, 141 (1940).
- 142. A. Knappwost and H. Nowotny, *Z. Metallkunde*, **33**, 153 (1941).

## Al-Cs

- 143. J. Czochralski and J. Kakzynski, *Wiadamosci Inst. Metallurgii i Metaloznawstwa*, [1] **4**, 18 (1934).

## Al-Cu

- 144. H. Le Chatelier, *Compt. rend.*, **120**, 836 (1895).
- 145. C. T. Heycock and F. H. Neville, *Phil. Tr. Roy. Soc. (London)*, **A189**, 69 (1897).
- 146. L. Guillet, *Bull. Soc. Encour. Ind. Nat.*, **101**, 236 (1902).
- 147. W. Campbell and J. A. Mathews, *J. Am. Chem. Soc.*, **24**, 264 (1902); W. Campbell, *J. Am. Chem. Soc.*, **26**, 1290 (1904).
- 148. L. Guillet, *Rev. Met.*, **2**, 567 (1905).
- 149. B. A. Curry, *J. Phys. Chem.*, **11**, 425 (1907).

150. H. C. H. Carpenter and C. A. Edwards, *Proc. Inst. Mech. Eng. (London)*, **72**, 57 (1907).
151. A. G. C. Gwyer, *Z. anorg. Chem.*, **57**, 114 (1908).
152. W. Brownieski, *Ann. chim. phys.*, **25**, 86 (1912).
153. V. Jares, *Z. Metallkunde*, **10**, 2 (1919).
154. B. Otani and T. Hemmi, *Kōgyō Kwagaku Kwai*, **24**, 1353 (1921).
155. P. D. Merica, R. G. Waltenberg, and V. H. Scott, *Trans. A.I.M.E.*, **67**, 9 (1921).
156. J. L. Haughton and K. E. Bingham, *J. Inst. Metals*, **29**, 80 (1923).
157. K. Becker and F. Ebert, *Z. Physik*, **16**, 165 (1923).
158. E. A. Owen and G. D. Preston, *J. Inst. Metals*, **30**, 6 (1923).
159. E. R. Jette, G. Phragmen, and A. F. Westgren, *J. Inst. Metals*, **31**, 193 (1924).
160. M. Tazaki, *Kinzoku-no-Kenkyu*, **2**, 490 (1925).
161. G. Masing and W. Koch, *Wiss. Veroeff. Siemens-Konz.*, **4**, 109 (1925).
162. E. H. Dix and H. H. Richardson, *Trans. A.I.M.E.*, **73**, 560 (1926).
163. A. Von Zeerleder and M. Bosshard, *Z. Metallkunde*, **19**, 462 (1927).
164. H. Nishimura, *Mem. Coll. Eng. Kyoto Imp. Univ.*, **5**, 64 (1927).
165. J. B. Friauf, *J. Am. Chem. Soc.*, **49**, 3107 (1927).
166. W. Rosenhain, *J. Inst. Metals*, **40**, 299 (1928).
167. G. D. Preston, *Phil. Mag.*, **7**, **12**, 980 (1931).
168. D. Stockdale, *J. Inst. Metals*, **52**, 111 (1933).
169. A. J. Bradley and P. Jones, *J. Inst. Metals*, **51**, 131 (1933).
170. E. Schmid and G. Siebel, *Z. Physik*, **85**, 36 (1933).
171. W. Stenzel and J. Weerts, *Metallwirtschaft*, **12**, 353 (1933).
172. G. Phragmen, *J. Inst. Metals*, **52**, 117 (1933).
173. A. Phillips and R. M. Brick, *J. Franklin Inst.*, **215**, 557 (1933).
174. A. Vivanti, *Alluminio*, **3**, 268 (1934).
175. H. Kawai, *Nippon Kwagaku Kwaishi*, **55**, 1002 (1934).
176. D. Uno and Y. Murakami, *Kōgyō Kwagaku Zasshi*, **37**, 176 (1934).
177. C. Hisatsune, *Mem. Coll. Eng. Kyoto Imp. Univ.*, [2] **8**, 74 (1934).
178. G. Wassermann and J. Weerts, *Metallwirtschaft*, **14**, 605 (1935).
179. H. Auer, *Z. Metallkunde*, **28**, 164 (1936).
180. H. Lay, *Z. Metallkunde*, **28**, 376 (1936).
181. G. D. Preston, *Proc. Roy. Soc. (London)*, **A931**, [167] 526 (1938).
182. W. Brownieski, S. Jelnicki, and M. Skwara, *Compt. rend.*, **207**, 233 (1938).
183. M. I. Zaharova, *Izvest. Inst. Fiz. Khim. Anal.*, **10**, 113 (1938).
184. G. S. Rushbrooke, *Proc. Phys. Soc.*, **52**, 701 (1940).
185. R. H. Brown, W. L. Fink, and M. S. Hunter, *Trans. A.I.M.E.*, **143**, 115 (1941).

#### Al-Fe

186. W. C. Roberts-Austen, *Proc. Inst. Mech. Eng. (London)*, 1895, p. 245.
187. O. Brunck, *Ber. deut. chem. Ges.*, **34**, 2733 (1901).
188. L. Guillet, *Compt. rend.*, **134**, 236 (1902).
189. A. G. C. Gwyer, *Z. anorg. Chem.*, **57**, 126 (1908).
190. N. S. Kurnakow, G. Urasow, and A. Grigoriew, *Z. anorg. Chem.*, **125**, 207 (1922).
191. W. Rosenhain, S. L. Archbutt, and D. Hanson, *Proc. Inst. Mech. Eng. (London)*, 1921, p. 211.
192. E. H. Dix, *Proc. Am. Soc. Testing Materials*, [2] **25**, 120 (1925).
193. G. Masing and O. Dahl, *Z. anorg. Chem.*, **154**, 189 (1926).
194. A. G. C. Gwyer and H. W. L. Phillips, *J. Inst. Metals*, **36**, 299 (1926).

- 194b. A. G. C. Gwyer and H. W. L. Phillips, *J. Inst. Metals*, **38**, 29 (1927).  
195. M. Isawa and Y. Murakami, *Kinzoku-no-Kenkyu*, [12] **4**, 467 (1927).  
196. F. Wever and A. Mueller, *Mitt. Kaiser-Wilhelm Inst. Eisenforsch. Düsseldorf*, **11**, 220 (1928).  
197. N. W. Ageew and I. O. Vher, *J. Inst. Metals*, **44**, 84 (1930).  
198. A. Osawa, *Sci. Rep. Tôhoku Univ.*, [22] **1**, 803 (1933).  
199. E. Bachemetew, *Z. Krist.*, **88**, 575 (1934).  
200. A. J. Bradley and A. Taylor, *Proc. Roy. Soc. (London)*, **A166**, 353 (1938); *J. Inst. Metals*, **66**, 53 (1940).  
201. A. Roth, *Z. Metallkunde*, **31**, 299 (1939).  
202. P. Weiss and W. Klemm, *Z. anorg. Chem.*, **245**, 288 (1940).  
203. E. Orosco and H. B. Orosco, *Min. Trab. Ind. Comm. Inst. Nac. Tech.*, 1940.

#### Al-Ga

204. Lecoq de Boisbaudran, *Compt. rend.*, **86**, 1240 (1878).  
205. W. Kroll, *Metallwirtschaft*, **11**, 436 (1932).  
206. N. A. Pushin and V. Stajic, *Z. anorg. Chem.*, **216**, 26 (1933).  
207. E. Jenckel, *Z. Metallkunde*, **26**, 249 (1934).  
208. N. A. Pushin and O. D. Micic, *Z. anorg. Chem.*, **234**, 233 (1937).

#### Al-Ge

209. W. Kroll, *Metall u. Erz.*, **23**, 682 (1926).  
210. H. Stoehr and W. Klemm, *Z. anorg. Chem.*, **241**, 305 (1939).

#### Al-Hg

211. R. Kremann and A. Mueller, *Z. Metallkunde*, **12**, 289 (1920).  
212. J. Fogh, *K. Danske Videnskab. Selskab, Math.-fys. Medd.*, **3**, 15 (1921).  
213. A. Smits and C. J. De Gruyter, *Proc. Roy. Acad. Sci. (Amsterdam)*, **23**, 966 (1921).  
214. H. Gerding, *Z. Electrochem.*, **31**, 304 (1925).  
215. C. J. De Gruyter, *Rec. trav. chim.*, **44**, 945 (1925).  
216. A. Mueller, *Z. Electrochem.*, **35**, 240 (1929).  
217. H. Gerding, *Z. physik. Chem.*, **A151**, 195 (1930).

#### Al-K

218. D. P. Smith, *Z. anorg. Chem.*, **56**, 112 (1908).

#### Al-La

219. W. Muthmann and H. Beck, *Liebigs Ann.*, **331**, 46 (1904).  
220. G. Canneri, *Met. ital.*, **24**, 3 (1932).  
221. A. Rossi, *Atti Lincei, Classe sci. fis. mat. nat.*, **17**, 182 (1933).  
222. F. Weibke and W. Schmidt, *Z. Electrochem.*, **46**, 357 (1940).

#### Al-Li

223. P. Assmann, *Z. Metallkunde*, **18**, 51 (1926).  
224. A. Mueller, *Z. Metallkunde*, **18**, 231 (1926).  
225. S. Pastorello, *Gazz. chim. ital.*, **61**, 47 (1931).  
226. S. Bernadziekiewicz and W. Brownieski, *Prace Zakladu Metallurgicznego*, **3**, 102 (1933).  
227. G. Komowski and A. Maximow, *Z. Krist.*, **92**, 275 (1935).  
228. E. Zintl and G. Woltersdorf, *Z. Electrochem.*, **41**, 876 (1935).  
229. G. Grube, L. Mohr, and W. Breuning, *Z. Electrochem.*, **41**, 880 (1935).

230. H. Vosskuehler, *Metallwirtschaft*, **16**, 907 (1937).  
231. F. I. Shamray and P. J. Saldau, *Izvest. Akad. Nauk U.S.S.R.*, **3**, 631 (1937).

**Al-Mg**

232. O. Boudouard, *Compt. rend.*, **132**, 1325 (1901); **133**, 1003 (1901).  
233. G. Grube, *Z. anorg. Chem.*, **45**, 225 (1905).  
234. A. Wilm, *Metall u. Erz.*, **8**, 225 (1911).  
235. W. Brownieski, *Compt. rend.*, **152**, 85 (1911).  
236. H. Schirmeister, *Metall u. Erz.*, **11**, 522 (1911).  
237. R. Vogel, *Z. anorg. Chem.*, **107**, 267 (1919).  
238. P. D. Merica, R. G. Waltenberg, and J. R. Freeman, *U. S. Bur. Standards Sci. Paper*, 337, 1919.  
239. D. Hanson and M. L. V. Gayler, *J. Inst. Metals*, **24**, 201 (1920).  
240. B. Otani, *Kōgyō Kwagaku Kwai*, **25**, 36 (1922).  
241. K. Becker and F. Ebert, *Z. Physik*, **16**, 166 (1923).  
242. E. A. Owen and G. D. Preston, *Proc. Phys. Soc. (London)*, **36**, 25 (1923).  
243. R. F. Mehl, *Trans. Am. Electrochem. Soc.*, **46**, 164 (1924).  
244. G. Urasow, *Izvest. Inst. Fiz. Khim. Anal.*, **2**, 480 (1924).  
245. T. Halstead and D. P. Smith, *Trans. Am. Electrochem. Soc.*, **49**, 291 (1926).  
246. R. S. Archer, *Trans. Am. Soc. Metals*, **10**, 728 (1926).  
247. K. L. Meissner, *J. Inst. Metals*, **38**, 201 (1927).  
248. A. Von Zeerleder and M. Bosshard, *Z. Metallkunde*, **19**, 463 (1927).  
249. Z. Nishima, *Sci. Rep. Tōhoku Univ.*, **18**, 388 (1929).  
250. E. H. Dix and F. Keller, *Trans. A.I.M.E.*, **83**, 351 (1929).  
251. K. Miyazaki, *Kinzoku-no-Kenkyu*, **6**, 124 (1929).  
252. E. Schmid and G. Siebel, *Z. Metallkunde*, **23**, 202 (1931).  
253. M. Kawakami, *Kinzoku-no-Kenkyu*, **10**, 532 (1933).  
254. E. Schmid and G. Siebel, *Z. Physik*, **85**, 37 (1933).  
255. F. Laves, K. Loehberg, and P. Rahlfs, *Nachr. Ges. Wiss. Göttingen*, 1934, p. 67.  
256. P. J. Saldau and L. N. Sergeev, *Metallurg*, **4**, 67 (1934).  
257. E. Schmid and H. Seliger, *Mitt. Mat. Sonderheft*, **23**, 52 (1934).  
258. R. M. Brick, A. Phillips, and A. J. Smith, *Trans. A.I.M.E.*, **117**, 102 (1935).  
259. S. Kishino, *Kōgyō Kwagaku Zasshi*, **38**, 3 (1935).  
260. W. Koester and W. Dullenkopf, *Z. Metallkunde*, **28**, 309 (1936).  
261. K. Riederer, *Z. Metallkunde*, **28**, 312 (1936).  
262. P. Lacombe and G. Chaudron, *Compt. rend.*, **202**, 1790 (1936).  
263. M. Kawakami, *Sci. Rep. Tōhoku Univ.*, 1936, **Honda**, p. 727.  
264. N. S. Kurnakow and V. I. Mikheeva, *Izvest. Akad. Nauk U.S.S.R.*, **2**, 259 (1937).  
265. I. I. Kornilov, *Doklady Akad. Nauk U.S.S.R.*, [N.S. 21] **4**, 172 (1938).  
266. W. Hume-Rothery and G. V. Raynor, *J. Inst. Metals*, **62**, 201 (1938).  
267. F. Laves and K. Moeller, *Z. Metallkunde*, **30**, 232 (1938).  
268. M. I. Zaharova, *Izvest. Inst. Fiz. Khim. Anal.*, **10**, 113 (1938).  
269. G. Siebel and H. Vosskuehler, *Z. Metallkunde*, **31**, 359 (1939).  
270. N. S. Kurnakow and V. I. Mikheeva, *Izvest. Inst. Fiz. Khim. Anal.*, **13**, 201 (1940).

**Al-Mn**

271. F. Woehler and F. Michel, *Liebigs Ann.*, **115**, 104 (1860).  
272. O. Brunck, *Ber. deut. chem. Ges.*, **34**, 2735 (1901).  
273. L. Guillet, *Compt. rend.*, **134**, 237 (1902).

274. G. Hindricks, *Z. anorg. Chem.*, **59**, 44 (1908).  
275. W. Rosenhain and F. C. A. H. Lantsberry, *Proc. Inst. Mech. Eng. (London)*, **74**, 252 (1910).  
276. W. Brownieski, *Ann. chim. phys.*, **25**, 103 (1912).  
277. M. Goto and T. Mishima, *Nippon Kogyo Kwaishi*, [447] **41**, 1 (1925).  
278. S. Daniels, *Ind. Eng. Chem.*, **18**, 125 (1926).  
279. E. H. Dix and W. D. Keith, *Proc. A.I.M.E.*, 1927, p. 315.  
280. T. Ishiware, *Kinzoku-no-Kenkyu*, **3**, 13 (1926).  
281. E. Person, *Z. Physik*, **57**, 115 (1929).  
282. E. Von Rassow, *Aluminium*, **1**, 187 (1929).  
283. A. F. Westgren, *Z. Metallkunde*, **22**, 372 (1930).  
284. T. Ishiware, *Sci. Rep. Tôhoku Univ.*, **19**, 500 (1930).  
285. W. Ekmann, *Z. physik. Chem.*, **12B**, 57 (1931).  
286. A. J. Bradley and P. Jones, *Phil. Mag.*, [7], **12**, 1137 (1931).  
287. M. Bosshard, *Alluminio*, **1**, 361 (1932).  
288. E. H. Dix, W. L. Fink, and L. A. Willey, *Trans. A.I.M.E.*, **104**, 335 (1933).  
289. W. Hofmann, *Aluminium*, **20**, 865 (1938).

#### Al-Mo

290. F. Woehler and F. Michel, *Liebigs Ann.*, **115**, 103 (1860).  
291. L. Guillet, *Compt. rend.*, **132**, 1322 (1901); **133**, 291 (1901).  
292. H. Reimann, *Z. Metallkunde*, **14**, 119, 195 (1922).  
293. P. Roentgen and W. Koch, *Z. Metallkunde*, **25**, 184 (1933).  
294. W. Koch and F. V. Nothing, *Aluminium*, **17**, 535 (1935).  
295. K. Yamaguchi and K. Simizu, *Nippon Kinzoku Gakkai Shi*, [11] **4**, 390 (1940).

#### Al-Na

296. C. T. Heycock and F. H. Neville, *J. Chem. Soc.*, **55**, 668 (1889).  
297. C. H. Mathewson, *Z. anorg. Chem.*, **48**, 192 (1906).  
298. E. Scheuer, *Z. Metallkunde*, **27**, 83 (1935).

#### Al-Nd

299. C. W. Stillwell and E. E. Jukkola, *J. Am. Chem. Soc.*, **56**, 56 (1934).

#### Al-Ni

300. C. A. Tissier, *Guide pratique de la recherche, de l'extraction et de la fabrication de l'aluminium et des métaux alcalines*, Paris, 1858.  
301. F. Woehler and F. Michel, *Liebigs Ann.*, **115**, 102 (1860).  
302. O. Brunck, *Ber. deut. chem. Ges.*, **34**, 2734 (1901).  
303. A. G. C. Gwyer, *Z. anorg. Chem.*, **57**, 133 (1908).  
304. K. Honda, *Ann. phys.*, **32**, 1015 (1910).  
305. K. Becker and F. Ebert, *Z. Physik*, **16**, 166 (1923).  
306. W. L. Fink and L. A. Willey, *Trans. A.I.M.E.*, **111**, 293 (1934).  
307. E. Soenchen, *Metallwirtschaft*, **13**, 893 (1934).  
308. A. J. Bradley and A. Taylor, *Phil. Mag.*, [6] **23**, 1049 (1937).  
309. W. O. Alexander and N. B. Vaughan, *J. Inst. Metals*, **61**, 247 (1937).  
310. H. W. L. Phillips, *J. Inst. Metals*, 1942, p. 27.

#### Al-Pb

311. C. T. Heycock and F. H. Neville, *J. Chem. Soc.*, **61**, 888 (1892).  
312. C. R. A. Wright, *J. Chem. Soc.*, **11**, 492 (1892); **13**, 1014 (1894).

313. H. Pécheux, *Compt. rend.*, **138**, 1042 (1904); **143**, 397 (1906).  
314. A. G. C. Gwyer, *Z. anorg. Chem.*, **57**, 147 (1908).  
315. M. Hansen and B. Blumenthal, *Metallwirtschaft*, **10**, 925 (1931).  
316. W. Claus, *Aluminium*, **18**, 544 (1936).  
317. L. W. Kempf and K. R. Van Horn, *Trans. A.I.M.E.*, **133**, 81 (1939).  
318. W. Claus and I. Herrmann, *Metallwirtschaft*, **18**, 957 (1939).  
319. H. Bauer, *Alum. Archiv*, 1939, p. 24.  
320. A. N. Campbell and R. W. Ashley, *Can. J. Res.*, **B18**, 9, 281 (1940).

**Al-Pr**

321. G. Canneri, *Alluminio*, **2**, 87 (1933).

**Al-Pt**

322. O. Brunck, *Ber. deut. chem. Ges.*, **34**, 2735 (1901).  
323. W. Campbell and J. A. Mathews, *J. Am. Chem. Soc.*, **24**, 253 (1902).  
324. Chouriguine, *Compt. rend.*, **155**, 156 (1912).

**Al-Rb**

325. J. Czochralski and J. Kakzynski, *Wiadomości Inst. Metallurgii i Metaloznawstwa*, [1] **4**, 18 (1937).

**Al-Sb**

326. C. R. A. Wright, *J. Soc. Chem. Ind.*, **11**, 493 (1892).  
327. D. A. Roche, *Mon. Sci.*, [7] **4**, 269 (1893).  
328. H. Gautier, *Bull. Soc. Encour. Ind. Nat.*, **1**, 1313 (1896).  
329. E. Van Aubel, *Compt. rend.*, **132**, 1266 (1901).  
330. J. A. Mathews, *J. Franklin Inst.*, **153**, 121 (1902).  
331. G. Tammann, *Z. anorg. Chem.*, **48**, 53 (1906).  
332. K. Honda and T. Sone, *Sci. Rep. Tôhoku Univ.*, **2**, 7 (1913).  
333. G. Urasow, *Z. Fiz. Khim.*, **51**, 461 (1919).  
334. F. Sauerwald, *Z. Metallkunde*, **14**, 458 (1922).  
335. E. A. Owen and G. D. Preston, *Proc. Phys. Soc. (London)*, **36**, 345 (1924).  
336. E. H. Dix, F. Keller, and L. A. Willey, *Trans. A.I.M.E.*, **93**, 396 (1931).  
337. E. Loofs-Rassow, *Aluminium*, **3**, 20 (1931).  
338. J. Weszelka, *Kgl. Ung. Palatin Joseph Univ. Tech. Wirtschaftwiss. Sopron*, 1931, p. 193.  
339. W. Guertler and A. Bergmann, *Z. Metallkunde*, **25**, 82 (1933).

**Al-Se**

340. M. Chikashige and T. Aoki, *Mem. Coll. Eng. Kyoto Imp. Univ.*, **2**, 249 (1917).  
341. L. Moser and E. Doktor, *Z. anorg. Chem.*, **118**, 285 (1921).

**Al-Si**

342. H. St. Claire-Deville, *Compt. rend.*, **42**, 49 (1856).  
343. E. Vigouroux, *Compt. rend.*, **123**, 115, 1905 (1896); **141**, 951 (1896).  
344. O. Hoenigschmidt, *Compt. rend.*, **142**, 157 (1906).  
345. W. Fraenkel, *Z. anorg. Chem.*, **58**, 154 (1908).  
346. R. Frilley, *Rev. Met.*, **8**, 518 (1911).  
347. J. Czochralski, *Z. angew. Chem.*, [1] **26**, 503 (1913).  
348. C. E. Roberts, *J. Chem. Soc.*, [2] **105**, 1383 (1914).



349. E. Curran, *Chem. Met. Eng.*, **27**, 360 (1922).  
350. J. D. Edwards, *Chem. Met. Eng.*, **27**, 654 (1922).  
351. L. Guillet, *Rev. Met.*, **19**, 303 (1922).  
352. E. von Rassow, *Z. Metallkunde*, **15**, 106 (1923).  
353. J. D. Edwards, *Chem. Met. Eng.*, **28**, 167 (1923).  
354. L. Guillet, *Compt. rend.*, **158**, 2081 (1924).  
355. N. Parravano and A. Scortecchi, *Atti Congr. Naz. Chim. Ind.*, 1924, p. 291.  
356. M. Petit, *Rev. Met.*, **23**, 418 (1926).  
357. B. Otani, *J. Inst. Metals*, **36**, 243 (1926).  
358. A. G. C. Gwyer and H. W. L. Phillips, *J. Inst. Metals*, **36**, 294 (1926).  
359. M. Bosshard and A. von Zeerleder, *Z. Metallkunde*, **19**, 461 (1927).  
360. W. Koester and F. Mueller, *Z. Metallkunde*, **19**, 52 (1927).  
361. M. L. V. Gayler, *J. Inst. Metals*, **38**, 157 (1927).  
362. E. H. Dix and A. C. Heath, *Trans. A.I.M.E.*, **78**, 164 (1928).  
363. G. Shinoda, *Suiyokwai-Shi*, [5] **5**, 422 (1927).  
364. L. Anastasiadis, *Z. anorg. Chem.*, **179**, 145 (1929).  
365. W. L. Fink and K. R. Van Horn, *Trans. A.I.M.E.*, **93**, 383 (1931).  
366. B. Otani, *Kinzoku-no-Kenkyu*, **7**, 666 (1930).  
367. H. Koto, *Sci. Rep. Tôhoku Univ.*, **Chikashige**, 303 (1930).  
368. L. Guillet and M. Ballay, *Rev. Met.*, **27**, 398 (1930).  
369. W. Fraenkel and R. Hahn, *Metallwirtschaft*, **10**, 643 (1931).  
370. L. Losana and R. Stratta, *Met. ital.*, **23**, 193 (1931).  
371. W. Brownieski and W. Smialowski, *Rev. Met.*, **29**, 542, 601 (1932).  
372. P. J. Saldau and M. V. Danilovitch, *Legkie Metal.*, **9**, 12 (1932).  
373. C. Schaarwaechter, *Z. Metallkunde*, **10**, 250 (1933).  
374. U. A. Klachko, *Kolloid Z.*, **69**, 215 (1934).  
375. S. Kishimo, *Nippon Kwagaku Kwaishi*, **55**, 1134 (1934).  
376. T. Harada, *Suiyokwai-Shi*, **8/9**, 882 (1935).  
377. H. Koto, *Mem. Coll. Eng. Kyoto Imp. Univ.*, **A18**, 17 (1935).  
378. J. Czocharlski and J. Kakzynski, *Viadamosci Inst. Metallurgii i Metaloznawstwa*, [4] **3**, 173 (1936).  
379. M. Goto and S. Sugiura, *Aluminum and Non-Ferrous Rev.*, [6] **2**, 223 (1937).  
380. M. S. Lipman, *Trudi Naukno Isled. Inst. Legkih Metallov Nisalumini*, **7**, 77 (1937); **8**, 86 (1937).  
381. M. I. Zaharova, *Izvest. Inst. Fiz. Khim. Anal.*, **10**, 113 (1938).  
382. H. Bauer and H. Winterhagen, *Aluminium*, **20**, 520 (1938).  
383. E. Pwowski and H. A. Nipper, *Aluminium*, **20**, 165 (1938).  
384. G. Guertler and E. Schultz, *Giesserei*, **26**, 537 (1939).  
385. W. Patterson, *Giesserei*, **26**, 461 (1939).

### Al-Sn

386. C. T. Heycock and F. H. Neville, *J. Chem. Soc.*, **57**, 385 (1890).  
387. L. Guillet, *Compt. rend.*, **133**, 935 (1902).  
388. W. Campbell and J. A. Mathews, *J. Am. Chem. Soc.*, **24**, 258 (1902).  
389. W. C. Anderson, *Proc. Roy. Soc. (London)*, **72**, 277 (1903).  
390. E. S. Shepherd, *J. Phys. Chem.*, **8**, 233 (1904).  
391. H. Pécheux, *Compt. rend.*, **140**, 1535 (1905).  
392. A. G. C. Gwyer, *Z. anorg. Chem.*, **49**, 311 (1906).  
393. W. Brownieski, *Ann. chim. phys.*, [5] **2**, 60 (1912).  
394. R. Lorenz and D. Plumbridge, *Z. anorg. Chem.*, **83**, 243 (1913).

395. E. Crepaz, *Gazz. chim. ital.*, **5**, 115 (1923).  
396. K. Kaneko and M. Kamiya, *Nippon Kogyo Kwaishi*, **40**, 509 (1924).  
397. J. F. Spencer and M. E. John, *Proc. Roy. Soc. (London)*, **116**, 68 (1927).  
398. Y. Shinizu, *Sci. Rep. Tôhoku Univ.*, **21**, 848 (1932).  
399. M. I. Zamotorin, *Metallurg*, **11**, 103 (1936).

#### Al-Sr

400. H. Nowotny and H. Wesenberg, *Z. Metallkunde*, **31**, 363 (1939).

#### Al-Ta

401. L. Maurignac, *Compt. rend.*, **66**, 180 (1868).  
402. H. Schirmeister, *Stahl u. Eisen*, **35**, 999 (1915).  
403. G. Brauer, *Naturwissenschaften*, [43] **26**, 710 (1938).

#### Al-Te

404. C. Whitehead, *J. Am. Chem. Soc.*, **17**, 849 (1895).  
405. M. Chikashige and J. Nose, *Mem. Coll. Eng. Kyoto Imp. Univ.*, **2**, 227 (1917).  
406. L. Moser and K. Ertl, *Z. anorg. Chem.*, **118**, 271 (1921).  
407. M. R. Whitmore and F. T. Sisco, *Ind. Eng. Chem.*, **16**, 838 (1924); **17**, 15 (1925).

#### Al-Th

408. O. Hoenigschmidt, *Compt. rend.*, **142**, 280 (1906).  
409. A. Von Leber, *Z. anorg. Chem.*, **166**, 16 (1927).  
410. J. D. Grogan and T. H. Schofield, *Aer. Res. Comm. Rep. & Mem., Rep.* 1253, 1929.  
411. G. Brauer, *Naturwissenschaften*, [43] **26**, 710 (1938).

#### Al-Ti

412. F. Woehler, *Ann. Chem. u. Pharm.*, **113**, 248 (1860).  
413. L. Guillet, *Bull. Soc. Encour. Ind. Nat.*, **103**, 244 (1902).  
414. W. Manchot and P. Richter, *Liebigs Ann.*, **357**, 140 (1907).  
415. L. Weiss and M. Kaiser, *Z. anorg. Chem.*, **65**, 238 (1910).  
416. E. Van Erkelen, *Metall u. Erz*, **20**, 206 (1923).  
417. W. Manchot and A. von Leber, *Z. anorg. Chem.*, **150**, 26 (1926).  
418. A. von Zeerleder and M. Bosshard, *Z. Metallkunde*, **19**, 288, 462 (1927).  
419. W. L. Fink, K. R. Van Horn, and P. M. Budge, *Trans. A.I.M.E.*, **93**, 421 (1931).  
420. H. Böhner, *Z. Metallkunde*, **26**, 268 (1934).  
421. H. Nishimura and N. Kagiwada, *Suiyokwai-Shi*, [2] **9**, 95 (1936).  
422. T. Harada, *Suiyokwai-Shi*, [6] **9**, 543 (1938).  
423. G. Brauer, *Naturwissenschaften*, [43] **26**, 710 (1938).  
424. H. Nishimura and E. Matumoto, *Nippon Kinzoku Gakkai Shi*, **4**, 339 (1940).

#### Al-Tl

425. F. Doerinckel, *Z. anorg. Chem.*, **48**, 188 (1906).

#### Al-U

426. L. Guillet, *Bull. Soc. Encour. Ind. Nat.*, **103**, 254 (1902).  
427. S. Heller and P. Heller, *Metall u. Erz*, **19**, 399 (1922).

## Al-V

428. C. Matignon and E. Monnet, *Compt. rend.*, **134**, 542 (1902).  
429. N. Czaco, *Compt. rend.*, **156**, 140 (1913).  
430. A. Roth, *Z. Metallkunde*, **32**, 356 (1940).

## Al-W

431. L. Guillet, *Compt. rend.*, **132**, 1112 (1901).  
432. H. List, *Edel Erden u. Erze*, **4**, 66 (1923).  
433. W. D. Clark, *J. Inst. Metals*, **66**, 271 (1940).

## Al-Y

434. W. Kroll, *Metals and Alloys*, **10**, 332 (1939).

## Al-Zn

435. H. Gautier, *Bull. Soc. Encour. Ind. Nat.*, **1**, 1308 (1896).  
436. C. T. Heycock and F. H. Neville, *J. Chem. Soc.*, **71**, 389 (1897).  
437. H. Pécheux, *Compt. rend.*, **138**, 1103 (1904).  
438. E. S. Shepherd, *J. Phys. Chem.*, **9**, 504 (1905).  
439. W. Guertler, *Z. anorg. Chem.*, **51**, 411 (1906).  
440. D. Ewen and T. Turner, *J. Inst. Metals*, **4**, 140 (1910).  
441. W. Rosenhain and S. L. Archbutt, *J. Inst. Metals*, **6**, 236 (1911).  
442. W. Brownieski, *Ann. chim. phys.*, **25**, 53 (1912).  
443. W. Smirnoff, *Compt. rend.*, **155**, 351 (1912).  
444. O. Bauer and O. Vogel, *Z. Metallkunde*, **8**, 101 (1916).  
445. A. S. Fedorow, *Z. Fizichi*, **49**, 394 (1917).  
446. A. Schulze, *Z. Physik*, **22**, 403 (1921).  
447. T. Hemmi, *Kōgyō Kwagaku Kwai*, **25**, 411 (1922).  
448. G. Holbein-Lechner, *Z. Metallkunde*, **14**, 76 (1922).  
449. W. Sanders and K. L. Meissner, *Z. Metallkunde*, **14**, 385 (1922).  
450. D. Hanson and M. L. V. Gayler, *J. Inst. Metals*, **27**, 267 (1922).  
451. H. Nishimura, *Mem. Coll. Eng. Kyoto Imp. Univ.*, **3**, 133 (1924).  
452. Ishihara, *Sci. Rep. Tōhoku Univ.*, **13**, 427 (1924).  
453. O. Bauer and W. Heidenhein, *Z. Metallkunde*, **16**, 221 (1924).  
454. T. Tanabe, *J. Inst. Metals*, **32**, 415 (1924).  
455. W. C. Phoebus and F. C. Blake, *Phys. Rev.*, **25**, 107 (1925).  
456. W. Fraenkel and W. Goetz, *Z. Metallkunde*, **17**, 12 (1925).  
457. T. Ishiware, *J. Inst. Metals*, **33**, 73 (1925).  
458. K. L. Meissner, *Z. Ver. deut. Ing.*, **70**, 394 (1926).  
459. O. Tiedemann, *Z. Metallkunde*, **18**, 18, 221 (1926).  
460. W. Fraenkel and J. Spanner, *Z. Metallkunde*, **18**, 189 (1926); **19**, 58 (1927).  
461. W. Fraenkel and W. Wachsmuth, *Z. Metallkunde*, **22**, 162 (1930).  
462. W. L. Fink and K. R. Van Horn, *Trans. A.I.M.E.*, **99**, 132 (1932).  
463. M. Schwarz and O. Summa, *Metallwirtschaftl.*, **11**, 369 (1932).  
464. H. Meyer, *Z. Physik*, **76**, 268 (1932); **78**, 854 (1932).  
465. V. Bugakow, *Z. Fizichi*, **3**, 632 (1933).  
466. R. G. Kennedy, *Metals and Alloys*, **5**, 106 (1934).  
467. E. Schmid and G. Wassermann, *Z. Metallkunde*, **26**, 145 (1934).  
468. H. Imai and M. Hagiya, *Mem. Ryojun Coll. Eng.*, **Inouye**, 83 (1934).  
469. E. A. Owen and J. Iball, *Phil. Mag.*, [7] **17**, 433 (1934).  
470. E. A. Owen and L. Pickup, *Phil. Mag.*, [7] **20**, 761 (1935).

471. G. F. Kosolapow and A. K. Trapeznikow, *Metallwirtschaft*, **14**, 45 (1935).  
472. M. Hagiya, I. Obinata, and S. Itimura, *Tetsu-to-Hagane*, [8] **22**, 622 (1936).  
473. W. L. Fink and L. A. Willey, *Trans. A.I.M.E.*, **122**, 244 (1936).  
474. W. Brownieski, J. Kucharski, and W. Winawer, *Rev. Met.*, **34**, 449 (1937).  
475. M. L. V. Gayler and E. G. Sutherland, *J. Inst. Metals*, **63**, 123 (1938).  
476. W. Guertler, H. Krause, and F. Voltz, *Metallwirtschaft*, **18**, 97 (1939).  
477. T. Morinaga, *Nippon Kinzoku Gakkai Shi*, [5] **3**, 216 (1939); [7] **4**, 216 (1940); [2] **5**, 49 (1941).  
478. E. C. Ellwood, *J. Inst. Metals*, **66**, 87 (1940).

#### Al-Zr

479. O. Hoenigschmidt, *Compt. rend.*, **143**, 224 (1906).  
480. L. Bradford, *Chem. Met. Eng.*, **19**, 684 (1918).  
481. J. W. Marden and M. N. Rich, *U. S. Bureau of Mines, Tech. Pap. Rep. Investigation*, **186**, 105 (1921).  
482. H. S. Cooper, *Trans. Am. Electrochem. Soc.*, **43**, 224 (1923).  
483. C. S. Sykes, *J. Inst. Metals*, **41**, 181 (1929).  
484. W. L. Fink and L. A. Willey, *Trans. A.I.M.E.*, **183**, 69 (1939).  
485. G. Brauer, *Z. anorg. Chem.*, **242**, 1 (1939).

#### Al-Ag-Bi

486. C. R. A. Wright, *Proc. Roy. Soc. (London)*, **52**, 11 (1892/3).

#### Al-Ag-Cu

487. M. Goto and T. Mishima, *Nippon Kogyo Kwai Shi*, [477] **41**, 1 (1925).  
488. S. Ueno, *Sci. Rep. Tôhoku Univ.*, **Chigashike**, 57 (1930).

#### Al-Ag-Mg

489. B. Otani, *Kinzoku-no-Kenkyu*, **10**, 262 (1933).

#### Al-Ag-Pb

490. C. R. A. Wright, *Proc. Roy. Soc. (London)*, **52**, 11 (1892/3).  
491. A. N. Campbell, L. Yaffe, W. G. Wallace, and R. W. Ashley, *Can. J. Res.*, [9] **B19**, 212 (1941).

#### Al-Ag-Si

492. M. Goto and T. Mishima, *Nippon Kogyo Kwai Shi*, [477] **41**, 1 (1925).

#### Al-Ag-Zn

493. S. Ueno, *Mem. Coll. Eng. Kyoto Imp. Univ.*, **8**, 91 (1930).

#### Al-Be-Mg

494. W. Kroll, *Metall u. Erz*, **23**, 613 (1926).  
495. G. Masing and O. Dahl, *Wiss. Veroeff. Siemens-Konz.*, **8**, 248 (1929).

#### Al-Be-Si

496. G. Masing and O. Dahl, *Wiss. Veroeff. Siemens-Konz.*, **8**, 248 (1929).  
497. W. Kroll, G. Masing, W. Koch, and E. Jess, *Wiss. Veroeff. Siemens-Konz.*, **10**, 15, 25 (1931).

**Al-Bi-Sb**

498. C. R. A. Wright, *Proc. Roy. Soc. (London)*, **55**, 130 (1894).

**Al-Bi-Sn**

499. C. R. A. Wright, *Proc. Roy. Soc. (London)*, **52**, 11 (1892/3).

**Al-Ca-Ni**

500. G. Shinoda, *J. Min. Inst. Japan*, **44**, 512 (1928).

**Al-Ca-Si**

501. G. Doan, *Z. Metallkunde*, **18**, 350 (1926).

502. J. D. Grogan, *J. Inst. Metals*, **37**, 77 (1927).

503. G. Shinoda, *J. Min. Inst. Japan*, **44**, 514 (1928).

**Al-Cd-Mg**

504. J. Valentin and G. Chaudron, *Compt. rend.*, **180**, 61 (1925); J. Valentin, *Rev. Met.*, **23**, 209 (1926).

505. S. Ishida, *J. Min. Inst. Japan*, **45**, 256, 611, 786 (1929).

506. E. Jaenecke, *Z. Metallkunde*, **30**, 424 (1938).

507. K. Riedlerer, *Z. Metallkunde*, **30**, 15 (1938).

**Al-Cd-Sn**

508. C. R. A. Wright, *Proc. Roy. Soc. (London)*, **55**, 130 (1894).

**Al-Cd-Zn**

509. N. F. Bugden, *J. Chem. Soc.*, **125**, 1642 (1924).

510. V. Jares, *Proc. A.I.M.E.*, **78A**, 65 (1927).

511. J. Ibarz, *Anales soc. españ. fís. chim.*, **33**, 140 (1935).

**Al-Ce-Fe**

512. K. L. Meissner, *Metall u. Erz*, **22**, 243 (1925).

513. J. Schulte, *Metall u. Erz*, **22**, 452 (1925).

**Al-Cr-Cu**

514. P. Roentgen and W. Koch, *Z. Metallkunde*, **26**, 9 (1934).

515. A. Knappwost and H. Nowotny, *Z. Metallkunde*, **33**, 153 (1941).

**Al-Cr-Fe**

516. C. Taillandier, *Rev. Met.*, **29**, 315, 348 (1932).

**Al-Cr-Mg**

517. F. Erdmann-Jesnitzer, *Alum. Archiv*, 1940, 29.

517b. H. Hanemann and A. Schrader, *Aluminium*, **22**, 378 (1940).

518. W. Hofmann and R. W. Herzer, *Metallwirtschaft*, **19**, 141 (1940).

**Al-Cr-Ni**

519. P. Roentgen and W. Koch, *Z. Metallkunde*, **26**, 9 (1934).

**Al-Cr-Si**

520. H. Bauer and H. Winterhagen, *Aluminium*, **20**, 520 (1938).

**Al-Cu-Fe**

521. V. Fuss, *Diss. Berlin*, 1922.  
522. M. Goto and T. Mishima, *Nippon Kogyo Kwaishi*, [477] **41**, 1 (1925).  
523. M. L. V. Gayler, *J. Inst. Metals*, **38**, 137 (1927).  
524. A. G. C. Gwyer, H. W. L. Phillips, and L. Mann, *J. Inst. Metals*, **40**, 297 (1928).  
525. K. Yamaguchi and I. Nakamura, *Rikwagaku-Kenkyu-Jo Ihō*, **11**, 815 (1932).  
526. W. Koch and F. V. Nothing, *Aluminium*, **17**, 535 (1935).  
527. M. Bosshard, *Aluminium*, **17**, 477 (1935).  
528. A. J. Bradley and H. J. Goldschmidt, *J. Inst. Metals*, **65**, 403 (1939).  
529. R. H. Brown, W. L. Fink, and M. S. Hunter, *Trans. A.I.M.E.*, **143**, 115 (1941).

**Al-Cu-Mg**

530. P. D. Merica, R. G. Waltenberg, and J. R. Freemann, *U. S. Bureau of Standards, Sci. Pap.* 337, 1919.  
531. R. Vogel, *Z. anorg. Chem.*, **107**, 265 (1919).  
532. M. L. V. Gayler, *J. Inst. Metals*, **29**, 507 (1923).  
533. B. Otani, *Kōgyō Kwagaku Kwai*, **26**, 427 (1923).  
534. V. Fuss, *Z. Metallkunde*, **16**, 24 (1924).  
535. S. Daniels, *Trans. A.I.M.E.*, **71**, 864 (1925).  
536. J. B. Friauf, *J. Am. Chem. Soc.*, **49**, 3107 (1927).  
537. E. H. Dix, G. F. Sager, and B. P. Sager, *Trans. A.I.M.E.*, **99**, 119 (1932).  
538. M. Bosshard, *Aluminium*, **17**, 477 (1935).  
539. F. Laves, K. Loehberg, and H. Witte, *Metallwirtschaft*, **14**, 793 (1935).  
540. F. Laves and S. Werner, *Z. Krist.*, **95**, 114 (1936).  
541. F. Laves and H. Witte, *Metallwirtschaft*, **15**, 15 (1936).  
542. W. Schuetz, *Metallwirtschaft*, **16**, 949 (1937).  
543. H. Nishimura, *Mem. Coll. Eng. Kyoto Imp. Univ.*, **10**, 18 (1937).  
544. V. G. Kuznetsov and L. N. Guseva, *Izvest. Akad. Nauk U.S.S.R., Khim.*, 928 (1940).  
545. I. Obinata and K. Mutuzaki, *Nippon Kinzoku Gakkai Shi*, **5**, 121 (1941).

**Al-Cu-Mn**

546. W. Rosenhain and F. C. A. H. Lantsberry, *Proc. Inst. Mech. Eng. (London)*, **74**, 119 (1910).  
547. W. Krings and W. Ostmann, *Z. anorg. Chem.*, **163**, 145 (1927).  
548. H. Sawamoto, *Suiyokwai-Shi*, **8**, 239 (1933).  
549. H. G. Petri, *Alum. Archiv*, 1938, p. 14.  
549b. H. Hanemann and A. Schrader, *Aluminium*, **21**, 381 (1939).

**Al-Cu-Ni**

550. A. A. Read and R. H. Greaves, *J. Inst. Metals*, **13**, 100 (1915).  
551. C. R. Austin and J. A. Murphy, *J. Inst. Metals*, **29**, 327 (1923).  
552. K. E. Bingham and J. L. Haughton, *J. Inst. Metals*, **29**, 71 (1923).  
553. I. Itaka, *Tetsu-to-Hagane*, [1] **10**, 1 (1924).  
554. M. Goto and T. Mishima, *Nippon Kogyo Kwaishi*, [477] **41**, 1 (1925).  
555. F. Roll, *Z. Metallkunde*, **20**, 444 (1928).  
556. H. Nishimura, *Suiyokwai-Shi*, [8] **5**, 616 (1928).  
557. M. Bosshard, *Aluminium*, **17**, 477 (1935).  
558. O. Quadrat and J. Jiriste, *Rev. Met.*, **33**, 489 (1936).  
559. W. Oelsen, *Z. Electrochem.*, **43**, 530 (1937).

560. A. J. Bradley and H. Lipson, *Proc. Roy. Soc. (London)*, **A167**, 421 (1938).  
561. A. Rapp, *Alum. Archiv*, 1940, p. 28.  
561b. H. Hanemann and A. Schrader, *Aluminium*, **22**, 378 (1940).

#### Al-Cu-Pb

562. L. W. Kempf and K. R. Van Horn, *Trans. A.I.M.E.*, **133**, 81 (1939).  
563. W. Claus and I. Herrmann, *Metallwirtschaft*, **18**, 957 (1939).

#### Al-Cu-Sb

564. T. Matsukawa, *Suiyokwai-Shi*, [8] **5**, 596 (1928).  
565. M. I. Zamotorin and L. N. Solaveva, *Metallurg*, **7**, 11 (1939).

#### Al-Cu-Si

566. E. H. Dix and A. J. Lyon, *Proc. Am. Soc. Testing Materials*, [2] **22**, 250 (1922).  
567. R. Steiner-Reiner, *Z. Metallkunde*, **16**, 362 (1924).  
568. M. Goto and T. Mishima, *Nippon Kogyo Kwaishi*, [477] **41**, 1 (1925).  
569. S. Daniels and D. M. Warner, *Trans. A.I.M.E.*, **73**, 464 (1926).  
570. A. G. C. Gwyer, H. W. L. Phillips, and L. Mann, *J. Inst. Metals*, **40**, 297 (1928).  
571. C. Hisatsune, *Suiyokwai-Shi*, [7] **5**, 559 (1928).  
572. G. Urasov and S. Pogodin, *Tsvetnye Met.*, **4**, 160 (1929).  
573. K. Matsuyama, *Kinzoku-no-Kenkyu*, [10] **11**, 461 (1934).  
574. C. Hisatsune, *Mem. Coll. Eng. Kyoto Imp. Univ.*, **9**, 18 (1935).  
575. W. Hofmann and H. Wiehr, *Aluminium*, **22**, 592 (1940).

#### Al-Cu-Sn

576. C. A. Edwards and J. H. Andrews, *J. Inst. Metals*, **2**, 29 (1909).  
577. M. Goto and T. Mishima, *Nippon Kogyo Kwaishi*, [464] **39**, 714 (1923).  
578. M. I. Zamotorin, *Metallurg*, **11**, 103 (1936).

#### Al-Cu-Ti

579. E. Bachemetew, N. G. Sevastinow, and N. I. Kotov, *Acta Physico-chim. U.S.S.R.*, **2**, 561 (1935).  
580. H. Nishimura and N. Kagiwada, *Suiyokwai-Shi*, **9**, 95 (1936).

#### Al-Cu-W

581. M. R. Whitmore and F. T. Sisco, *Ind. Eng. Chem.*, **17**, 15 (1925).

#### Al-Cu-Zn

582. H. C. H. Carpenter and C. A. Edwards, *Z. Metallkunde*, **2**, 209 (1911/2).  
583. V. Jares, *Z. Metallkunde*, **10**, 1 (1919).  
584. J. L. Haughton and K. E. Bingham, *Proc. Roy. Soc. (London)*, **A99**, 47 (1921).  
585. D. Hanson and M. L. V. Gayler, *J. Inst. Metals*, **34**, 125 (1925).  
586. H. Nishimura, *Mem. Coll. Eng. Kyoto Imp. Univ.*, **5**, 61 (1927).  
587. M. Hamasumi and S. Matoba, *Sci. Rep. Tôhoku Univ.*, **8**, 73 (1928).

#### Al-Fe-Mg

588. V. Fuss, *Metallographie des Aluminiums und seiner Legierungen*, Julius Sprir ger, Berlin, 1936.  
589. M. Barnick and H. Hanemann, *Aluminium*, **20**, 533 (1938).  
590. H. W. L. Phillips, *J. Inst. Metals*, **67**, 257 (1941).

**Al-Fe-Mn**

591. E. Degischer, *Alum. Archiv*, 1939, p. 18.  
591b. H. Hanemann and A. Schrader, *Aluminium*, **21**, 381 (1939).

**Al-Fe-Ni**

592. P. N. Lashchenko, *Zhur. Fiz. Khim.*, **46**, 311 (1914).  
593. V. Fuss, *Metallographie des Aluminiums und seiner Legierungen*, Julius Springer, Berlin, 1936.  
594. A. J. Bradley and A. Taylor, *Proc. Roy. Soc. (London)*, **A166**, 353 (1938); *J. Inst. Metals*, **66**, 53 (1940).  
595. H. W. L. Phillips, *J. Inst. Metals*, 1942, p. 27.

**Al-Fe-Si**

596. L. J. Wills, *J. Birmingham Soc.*, **7**, 475 (1920).  
597. E. H. Dix, *Trans. A.I.M.E.*, **69**, 957 (1923).  
598. J. Czochralski, *Z. Metallkunde*, **15**, 162 (1924).  
599. A. G. C. Gwyer and H. W. L. Phillips, *J. Inst. Metals*, **36**, 283 (1926).  
600. A. G. C. Gwyer and H. W. L. Phillips, *J. Inst. Metals*, **38**, 29 (1927).  
601. E. H. Dix and A. C. Heath, *Trans. A.I.M.E.*, **78**, 164 (1928).  
602. W. L. Fink and K. R. Van Horn, *Trans. A.I.M.E.*, **93**, 383 (1931).  
603. V. Fuss, *Z. Metallkunde*, **23**, 231 (1931).  
604. H. Nishimura, *Mem. Coll. Eng. Kyoto Imp. Univ.*, [5] **7**, 285 (1933).  
605. W. Jaeniche, *Alum. Archiv*, 1936, p. 5.  
606. G. Urasow and A. V. Shashin, *Metallurg*, [12] **41**, 27 (1937).  
607. L. N. Sergeev and B. I. Rimmer, *Metallurg*, [10] **41**, 112 (1937).  
608. H. Nishimura and E. Matumoto, *Suiyokwai-Shi*, [2] **10**, 105 (1939).  
609. G. Guertler and E. Schultz, *Giesserei*, **26**, 537 (1939).  
610. S. Takeda and K. Mutuzaki, *Tetsu-to-Hagane*, [5] **26**, 335 (1940).

**Al-Fe-Ti**

611. H. Nishimura and E. Matumoto, *Nippon Kinzoku Gakkai Shi*, [10] **4**, 339 (1940).

**Al-Fe-Zn**

612. V. Fuss, *Diss. Berlin*, 1922.

**Al-Ge-Mg**

613. W. Kroll, *Metall u. Erz*, **23**, 684 (1926).

**Al-Li-Si**

614. P. Assmann, *Z. Metallkunde*, **18**, 256 (1926).

**Al-Mg-Mn**

615. T. Ishiwara, *Sci. Rep. Tôhoku Univ.*, **1**, 19 (1930).  
616. W. G. Leemann, *Alum. Archiv*, 1938, p. 9.  
616b. H. Hanemann and A. Schrader, *Aluminium*, **20**, 771 (1938).

**Al-Mg-Ni**

617. V. Fuss, *Z. Metallkunde*, **16**, 24 (1924).



**Al-Mg-Pb**

618. H. Bauer, *Alum. Archiv*, 1939, p. 24.

**Al-Mg-Sb**

619. E. Loofs-Rassow, *Aluminium*, **3**, 20 (1931).  
620. W. Guertler and W. A. Bergmann, *Z. Metallkunde*, **25**, 81, 111 (1933).

**Al-Mg-Si**

621. D. Hanson and M. L. V. Gayler, *J. Inst. Metals*, **26**, 321 (1921).  
622. W. Sanders and K. L. Meissner, *Z. Metallkunde*, **16**, 12 (1924).  
623. V. Fuss, *Z. Metallkunde*, **16**, 24 (1924).  
624. B. Otani, *Kinzoku-no-Kenkyu*, **7**, 666 (1930).  
625. L. Losana, *Met. Ital.*, **23**, 375 (1931).  
626. E. H. Dix, F. Keller, and R. W. Graham, *Trans. A.I.M.E.*, **93**, 404 (1931).  
627. R. S. Archer and L. W. Kempf, *Trans. A.I.M.E.*, **93**, 448 (1931).  
628. A. A. Botchvar, K. W. Gorev, and A. M. Koralkov, *Metallurg*, [8] **1**, 7 (1931).  
629. S. Kishino, *Nippon Kwagaku Kwaishi*, **55**, 528 (1934).  
630. F. Keller and C. M. Craighead, *Trans. A.I.M.E.*, **122**, 315 (1936).  
631. G. Urasow and T. E. Shushpanova, *Izvest. Akad. Nauk U.S.S.R.*, **2**, 321 (1936).  
632. V. G. Kuznetsov and E. S. Makarov, *Doklady Akad. Nauk U.S.S.R.*, [3] **23**, 245 (1939).  
633. H. W. L. Phillips, *J. Inst. Metals*, **67**, 257 (1941).

**Al-Mg-Zn**

634. G. Eger, *Z. Metallkunde*, **4**, 29 (1913).  
635. W. Sanders and K. L. Meissner, *Z. Metallkunde*, **16**, 12 (1924).  
636. S. Nishihara, *Suiyokwai-Shi*, **5**, 783 (1929).  
637. S. Ishida, *J. Min. Inst. Japan*, **529**, 256 (1929); **532**, 611 (1929); **536**, 786 (1929).  
638. M. Haas, *Z. Metallkunde*, **21**, 58 (1929).  
639. G. Wassermann, *Z. Metallkunde*, **22**, 160 (1930).  
640. P. J. Saldau, V. S. Sokolov, and N. I. Korenev, *Trudi Naukno Isled., Inst. Legkih Metallov Nisalumini*, **1**, 57 (1932); **3**, 60 (1933).  
641. P. J. Saldau and M. I. Zamotorin, *Z. anorg. Chem.*, **213**, 377 (1933).  
642. A. A. Botchvar and V. G. Kuznetsov, *Metallurg*, **2**, 7 (1933).  
643. F. Laves, K. Loehberg, and H. Witte, *Metallwirtschaft*, **14**, 793 (1935).  
644. W. Koester, W. Dullenkopf, and W. Wolf, *Z. Metallkunde*, **28**, 155, 309, 363 (1936).  
645. K. Riederer, *Z. Metallkunde*, **28**, 312 (1936).  
646. M. Hamasumi, *Sci. Rep. Tôhoku Univ.*, **Honda**, 748 (1936).  
647. W. L. Fink and L. A. Willey, *Trans. A.I.M.E.*, **124**, 78 (1937).  
648. L. N. Sergeev, *Metallurg*, **3**, 79 (1937).

**Al-Mn-Si**

649. H. Bueckle, *Alum. Archiv*, 1938, p. 13.  
649b. H. Hanemann and A. Schrader, *Aluminium*, **20**, 771 (1938).

**Al-Mn-Sn**

650. A. Schueck, *Z. Metallkunde*, **27**, 11 (1935).

**Al-Na-Si**

651. B. Otani, *J. Inst. Metals*, **36**, 243 (1926).

**Al-Ni-Si**

652. V. Fuss, *Z. Metallkunde*, **16**, 24 (1924).  
653. C. Hisatsune, *Suiyokwai Shi*, [1] **5**, 52 (1926).  
654. B. Otani, *Kinzoku-no-Kenkyu*, **7**, 666 (1930).  
655. E. Weisse, *Alum. Archiv*, 1939, p. 26.  
655*b*. H. Hanemann and A. Schrader, *Aluminium*, **22**, 378 (1940).  
656. H. W. L. Phillips, *J. Inst. Metals*, 1942, p. 27.

**Al-Ni-Sn**

657. S. Kato, *Suiyokwai-Shi*, [6] **6**, 529 (1931).

**Al-Ni-Zn**

658. V. Fuss, *Z. Metallkunde*, **16**, 24 (1924).

**Al-Pb-Sb**

659. C. R. A. Wright, *Proc. Roy. Soc. (London)*, **55**, 130 (1894).

**Al-Pb-Sn**

660. C. R. A. Wright, *Proc. Roy. Soc. (London)*, **52**, 11 (1892).

**Al-Sb-Si**

661. T. Matsukawa, *Suiyokwai-Shi*, [8] **5**, 596 (1928).

**Al-Sb-Sn**

662. V. Fuss, *Metallographie des Aluminiums und seiner Legierungen*, Julius Springer, Berlin, 1934.

**Al-Si-Sn**

663. T. Matsukawa, *Suiyokwai-Shi*, [7] **5**, 567 (1928).

**Al-Si-Th**

664. J. D. Grogan and T. H. Schofield, *Aer. Res. Comm. Rep. Mem.*, **Rep. 1253**, 1929.

**Al-Si-Zn**

665. W. Sanders and K. L. Meissner, *Z. Metallkunde*, **15**, 180 (1923); **16**, 12 (1924).  
666. V. Fuss, *Z. Metallkunde*, **16**, 24 (1924).  
667. H. Nishimura, *Nippon Kinzoku Gakkai Shi*, **4**, 116 (1940).

**Al-Sn-Zn**

668. G. Hindricks, *Z. anorg. Chem.*, **59**, 514 (1908).  
669. L. Losana and E. Carrozzì, *Gazz. chim. ital.*, **53**, 546 (1923).  
670. H. Nishimura and O. Suzuki, *Suiyokwai-Shi*, [10] **4**, 1441 (1925).  
671. V. Jares, *Proc. A.I.M.E.*, **78A**, 65 (1927).

**Al-Cu-Fe-Mn**

672. F. Keller and G. W. Wilcox, *Metal Progress*, **23**, 45 (1933).

**Al-Cu-Fe-Si**

673. A. G. C. Gwyer, H. W. L. Phillips, and L. Mann, *J. Inst. Metals*, **40**, 297 (1928).  
674. M. L. V. Gayler, *J. Inst. Metals*, **59**, 75 (1937).

**Al-Cu-Mg-Ni**

675. K. E. Bingham, *J. Inst. Metals*, **36**, 137 (1926).

**Al-Cu-Mg-Si**

676. M. L. V. Gayler, *J. Inst. Metals*, **28**, 213 (1922); **30**, 139 (1923).  
677. E. H. Dix, G. F. Sager, and B. P. Sager, *Trans. A.I.M.E.*, **99**, 119 (1932).  
678. D. A. Petrov, *Acta Physico-chim. U.S.S.R.*, [4] **6**, 505 (1937).

**Al-Cu-Mg-Zn**

679. F. Laves, K. Loehberg, and H. Witte, *Metallwirtschaft*, **14**, 793 (1935).

**Al-Fe-Mg-Si**

680. H. Perlitz and A. Westgren, *Arkiv Kemi Mineral. Geol.*, **15B**, 16 (1942).

**Al-Mg-Si-Zn**

681. W. Sanders and K. L. Meissner, *Z. Metallkunde*, **16**, 12 (1924).

## PART II

**General**

682. O. F. Hudson, *J. Inst. Metals*, **13**, 193 (1915).  
683. R. J. Anderson, *J. Franklin Inst.*, **187**, 47 (1919).  
684. C. Panseri, *Alluminio*, **1**, 279 (1932); **2**, 59 (1933).  
685. F. Keller and G. W. Wilcox, *Metal Progress*, **23**, 45 (1933).  
686. E. Orosco and H. B. Orosco, *Metalografia das ligas de aluminio*, Inst. nacional de tecnologia, min. do trab. ind. comm., Rio de Janeiro, 1940.

**Macro-etching**

687. J. Czochralski, *Stahl u. Eisen*, **35**, 1073, 1129, 1915 (1915).  
688. D. Hanson and S. L. Archbutt, *J. Inst. Metals*, **21**, 291 (1919).  
689. F. B. Flick, *Trans. A.I.M.E.*, **71**, 816 (1925).  
690. E. Dorn and M. Skiegil, *Z. Metallkunde*, **17**, 133 (1925).  
691. R. Genders, *J. Inst. Metals*, **35**, 259 (1926).  
692. C. M. Tucker, *Metals and Alloys*, **1**, 655 (1930).  
693. W. Hume-Rothery, *J. Inst. Metals*, **46**, 239 (1931).  
694. Kraetsch and Shenk, *Aluminium*, **23**, 239 (1941).

**Polishing**

695. E. H. Dix, *Chem. Met. Eng.*, **27**, 1217 (1922).  
696. H. T. Roberts, *Met. Ind. London*, **21**, 450 (1923).  
697. F. F. Lucas, *Trans. A.I.M.E.*, **27**, 481 (1927).  
698. R. L. Dowdell and M. J. Wahll, *Metals and Alloys*, **4**, 181 (1933).  
699. G. T. Williams, *Metal Progress*, **27**, 58 (1935).  
700. F. L. Robbins, *Metal Progress*, **29**, 74 (1936).

- 701. E. H. Erdmann, *Metals and Alloys*, **8**, 27 (1937).
- 702. J. L. Everhard, *Metals and Alloys*, **8**, 115 (1937).
- 703. G. Mann, *Metallurgia*, [106] **18**, 121 (1938).
- 704. K. Altmannsberger, *Tech. Z. prakt. Metallbearbeit.*, [9-10] **48**, 394 (1938).
- 705. L. L. Wyman, *Proc. Am. Soc. Testing Materials*, [1] **38**, 511 (1938).

### Electrolytic Polishing

- 706. P. Jacquet, *Compt. rend.*, **205**, 1232 (1937).
- 707. R. F. Mehl, G. A. Pellissier, and A. Markins, *Metal Progress*, [1] **37**, 554 (1940).
- 708. A. L. De Sy and H. Haemers, *Stahl u. Eisen*, **61**, 185, 777 (1941).
- 709. H. Roehrig and W. Schneider, *Aluminium*, **23**, 281 (1941).
- 710. F. Keller, *Iron Age*, [2] **147**, 23 (1941).

### Etching

- 711. J. Czochralski, *Stahl u. Eisen*, **35**, 1073, 1129, 1915 (1915).
- 712. D. Hanson and S. L. Archbutt, *J. Inst. Metals*, **21**, 291 (1919).
- 713. R. J. Anderson, *Met. Ind. New York*, **19**, 69 (1921).
- 714. F. Adcock, *J. Inst. Metals*, **26**, 361 (1921).
- 715. A. Meyer, *Z. Metallkunde*, **15**, 257 (1923).
- 716. F. B. Flick, *Trans. A.I.M.E.*, **71**, 816 (1925).
- 717. J. R. Vilella, *Iron Age*, **117**, 761, 834, 903, 1926 (1926).
- 718. E. H. Dix and W. D. Keith, *Proc. Am. Soc. Testing Materials*, **24**, 2, 317 (1926).
- 719. E. H. Dix and F. Keller, *Mining and Metallurgy*, **9**, 327 (1928).
- 720. H. Choulant, *Z. Metallkunde*, **21**, 197 (1929).
- 721. J. G. S. De Haan, *Die Gieterii*, **5**, 50 (1931).
- 722. T. Berglund, *Metallographers Handbook of Etching*, Sir Isaac Pitman and Sons, London, 1931.
- 723. F. Keller, *Mining and Metallurgy*, **12**, 513 (1935).
- 724. E. Moeckel, *Aluminium*, **19**, 433 (1937).
- 725. A. Portevin and P. Bastien, *Reactifs d'attaque metallographique*, Dunod Frères, Paris, 1937.
- 726. M. Bosshard and H. Hug, *Metallwirtschaft*, **17**, 708 (1938).
- 727. H. Winterhagen, *Aluminium*, **20**, 704 (1938).
- 728. A. Schrader, *Aetzheft*, Borntraeger Geb., Berlin, 1939.
- 729. *Berglunds Handbuch der metallographischen Schleif-, Polier-, und Aetzverfahren*, revised by A. Meyer, Berlin, 1940.
- 730. F. Keller and T. W. Bossert, *Metal Progress*, January, 1942, p. 63.

### Constituents

- 731. R. J. Anderson, *Met. Chem. Eng.*, **18**, 172 (1918).
- 732. P. D. Merica, *Met. Chem. Eng.*, **19**, 135 (1918).
- 733. *U. S. Bureau of Standards, Sci. Pap.* 337, 1919.
- 734. D. Hanson and S. L. Archbutt, *J. Inst. Metals*, **21**, 291 (1919).
- 735. L. J. Wills, *J. Birmingham Soc.*, **7**, 475 (1920).
- 736. G. Guzzoni, *Met. ital.*, **22**, 747 (1930).
- 737. H. Nishimura, *Kinzoku-no-Kenkyu*, **4**, 179 (1934).
- 738. M. Bosshard, *Aluminium*, **17**, 477 (1935).
- 739. E. Copernick, *Aluminium*, **18**, 433 (1936).
- 740. H. Hanemann, *Aluminium*, **19**, 7 (1937).

## PART III

**General**

- 741. R. J. Anderson, *U. S. Bureau of Mines, Circ.* 14, 1919.
- 742. R. Steiner-Reiner, *Metallwirtschaft*, **7**, 1228 (1928).
- 743. C. Panseri, *Met. ital.*, **23**, 500, 624, 732 (1931).
- 744. J. S. Baron, *Métaux*, **11**, 297 (1936).
- 745. R. Hinzmann, *Metallwirtschaft*, **16**, 477 (1937).
- 746. H. Bohner, *Aluminium*, **19**, 131 (1937).
- 747. H. Koestner, *Aluminium*, **19**, 140 (1937).
- 748. M. Schwarz, *Metallwirtschaft*, **16**, 771 (1937).
- 749. E. Boehm, *Aluminium*, **20**, 168 (1938).

**Master Alloys**

- 750. R. J. Anderson, *Chem. Met. Eng.*, **23**, 317 (1920).
- 751. R. J. Anderson, *Am. Met. Market*, [137] **34**, 4 (1927).
- 752. E. T. Richards, *Das Metall*, **16**, 65 (1930).
- 753. E. R. Thews, *Metallurgist*, **10**, 162 (1934).
- 754. S. S. Stroeve and S. G. Glazunov, *Technika Vozdushnogo Flota*, **5**, 49 (1933).
- 755. H. Roehrig and E. Copernick, *Aluminium*, **19**, 428 (1937).

**Aluminum-Copper Alloys**

- 756. M. Levi-Malvano and M. Marantonio, *Gazz. chim. ital.*, **42**, 353 (1912).
- 757. R. J. Anderson, *Chem. Met. Eng.*, **23**, 883 (1920).
- 758. L. Guillet, *Génie civil*, **79**, 52 (1921).
- 759. E. H. Dix and A. J. Lyon, *U. S. Air Serv. Inf. Circ.*, **4**, 385 (1923).
- 760. S. R. Archer and Z. Jeffries, *Trans. A.I.M.E.*, **71**, 828 (1925).
- 761. V. Fuss, *Z. Metallkunde*, **19**, 19 (1927).
- 762. M. J. Suhr, *Rev. Aluminium*, **27**, 695 (1928).
- 763. A. G. C. Gwyer, H. W. L. Phillips, and L. Mann, *J. Inst. Metals*, **40**, 297 (1928).
- 764. M. J. Suhr, *Rev. Aluminium*, **48**, 1669 (1932).
- 765. G. H. Starmann, *Met. Ind. New York*, **30**, 181 (1932).
- 766. F. O. Ribkin, *Technika Vozdushnogo Flota*, **3**, 29 (1935).
- 767. A. Vivanti and R. Guastalla, *Alluminio*, **4**, 271 (1935).
- 768. J. Castel, *Congrès Internat. Fonderie, Paris, Preprint*, 1937.
- 769. M. L. V. Gayler, *J. Inst. Metals*, **59**, 75 (1937).
- 770. M. Schwarz, *Metallwirtschaft*, **16**, 771 (1937).

**Aluminum-Silicon Alloys**

- 771. G. Welter, *Z. Metallkunde*, **15**, 107 (1922).
- 772. R. S. Archer and L. W. Kempf, *Trans. A.I.M.E.*, **73**, 581 (1926).
- 773. M. Petit, *Rev. Met.*, **23**, 418 (1926).
- 774. G. Welter, *J. Inst. Metals*, **36**, 269 (1926).
- 775. J. Dornauf, *Aluminium*, **17**, 26 (1934).
- 776. E. Scheuer and E. Schultz, *Aluminium*, **18**, 545 (1936).
- 777. V. O. Gagentorn and M. M. Nazarova, *Legkie Metal.*, [6] **5**, 9 (1937).
- 778. W. Straumanis and N. Brakss, *Z. physik. Chem.*, **B38**, 2, 3, 140 (1937).
- 779. H. Bohner and H. Winterhagen, *Aluminium*, **20**, 520 (1938).
- 780. H. Nishimura and E. Matumoto, *Suiyokwai-Shi*, **10**, 105 (1939).
- 781. G. Guertler and E. Schultz, *Giesseret*, **26**, 537 (1939).
- 782. H. Roehrig and E. Copernick, *Aluminium*, **23**, 235 (1941).

**Corrosion-Resistant Alloys**

783. H. Pécheux, *Compt. rend.*, **138**, 1606 (1904).
784. M. Haas, *Giesserei-Ztg.*, **23**, 328 (1926).
785. S. Daniels, *Ind. Eng. Chem.*, **18**, 1280 (1926).
786. E. Dusaughey, *Trans. Am. Soc. Steel Treat.*, **11**, 810 (1927).
787. W. Fuchs, *Z. Metallkunde*, **19**, 361 (1927).
788. S. Daniels, *Ind. Eng. Chem.*, **18**, 2 (1927).
789. R. Steiner-Reiner, *Z. Metallkunde*, **19**, 282 (1927).
790. H. Roehrig and E. Copernick, *Metallwirtschaft*, **13**, 591 (1934).
791. E. Hermann, *Aluminium-Magnesium Legierungen*, Aluminium Zentrale, Berlin, 1937.
792. H. C. Hall, *Met. Ind. London*, **50**, 705 (1937); **51**, 9 (1937).
793. E. Moeckel, *Aluminium*, **19**, 433 (1937).
794. C. Panseri, *J. Inst. Metals*, **63**, 15 (1938).
795. W. Geller, *Z. Metallkunde*, **31**, 9 (1939).
796. M. Bosshard and H. Hug, *Metallwirtschaft*, **18**, 6 (1939).
797. H. Roehrig and J. Roch, *Aluminium*, **22**, 21 (1940).
798. P. Bastien, *Compt. rend.*, **210**, 248 (1940).
799. F. Bollenhart and W. Bungardt, *Z. Metallkunde*, **32**, 303 (1940).

**Duralumin**

800. A. Lennartz and W. Henniger, *Z. Metallkunde*, **18**, 213 (1926).
801. P. L. Teed, *Duralumin and Its Heat Treatment*, C. Griffin and Co., Ltd., London, 1937.
802. D. A. Petrov, *J. Inst. Metals*, **61**, 81 (1938).
803. G. Shinoda, *Nippon Kinzoku Gakkai Shi*, [9] **2**, 475 (1938).
804. D. A. Petrov, *Metallurg*, **3**, 88 (1938).
805. Fry, Wiederholt, and Bochme, *Z. Metallkunde*, **31**, 3 (1939).
806. M. Hansen and G. Dreyer, *Aluminium*, **22**, 134 (1940).
807. H. Nishimura and K. Yamaguchi, *Suiyokwai-Shi*, **8**, 471 (1941).

**Aluminum-Copper-Nickel Alloys**

808. W. Rosenhain, S. L. Archbutt, and S. A. E. Wells, *J. Inst. Metals*, **19**, 191 (1923).
809. A. J. Lyon and S. Daniels, *Soc. Automotive Engrs.*, **14**, 173 (1924).
810. H. Hyman, *J. Inst. Metals*, **34**, 207 (1925).
811. A. J. Lyon, *Aero. Eng.*, **2**, 257 (1930).
812. S. L. Archbutt, *Nickel Bull.*, **3**, 211 (1930).
813. C. Panseri, *Alluminio*, **7**, 303 (1938).
814. H. Nishimura, *Nippon Kinzoku Gakkai Shi*, **3**, 3, 108 (1939).
815. H. Nishimura and E. Matumoto, *Suiyokwai-Shi*, **11**, 281 (1940).
816. H. Nishimura, *Japan Nickel Rev.*, **8**, 8 (1940).

## PART IV

**Melting and Inclusions**

817. R. J. Anderson, *U. S. Bureau of Mines, Tech. Pap.* 241, 1919; 290, 1922.
818. J. Czochralski, *Z. Metallkunde*, **15**, 273 (1923).
819. A. J. Lyon, *Foundry*, **52**, 396 (1924).
820. L. Northcott, *J. Inst. Metals*, **36**, 265 (1926).

821. Stendel, *Z. Metallkunde*, **19**, 127 (1927).
822. R. J. Anderson, *Met. Ind. London*, **30**, 337 (1927).
823. N. F. Bugden, *J. Inst. Metals*, **42**, 119 (1929).
824. W. Rosenhain, J. D. Grogan, and T. H. Schofield, *J. Inst. Metals*, **46**, 331 (1930).
825. D. Hanson and I. G. Slater, *J. Inst. Metals*, **46**, 187 (1931).
826. W. Geller, *Metallwirtschaft*, **15**, 141 (1936).
827. P. Roentgen and H. Winterhagen, *Metallwirtschaft*, **17**, 1045 (1938).
828. W. Bourklah and F. Oesterlen, *Z. Metallkunde*, **30**, 386 (1938).
829. Kraetsch and Shenk, *Aluminium*, **23**, 239 (1941).

### Casting

830. A. J. Lyon and S. Daniels, *U. S. Air Serv. Inf. Circ.* 449, 1924.
831. L. Guillet, J. Galibourg, and M. Ballay, *Rev. Met.*, **22**, 253 (1925).
832. R. Genders, *J. Inst. Metals*, **37**, 241 (1927).
833. F. C. Nix and E. Schmid, *Z. Metallkunde*, **21**, 286 (1929).
834. E. Scheil, *Z. Metallkunde*, **21**, 121 (1929).
835. L. M. V. Gayler, *J. Inst. Metals*, **44**, 97 (1930).
836. H. Hanemann and A. Schrader, *Z. Metallkunde*, **23**, 269 (1931).
837. D. Hanson and I. G. Slater, *J. Inst. Metals*, **46**, 187 (1931).
838. H. Bohner, *Aluminium*, **3**, 3 (1931); **4**, 24 (1932).
839. G. Masing and E. Scheuer, *Z. Metallkunde*, **25**, 173 (1933).
840. A. von Zeerleder, *Schweiz. Tech. Z.*, 1933, p. 233.
841. I. G. Slater, *J. Inst. Metals*, **54**, 103 (1934).
842. J. A. Vero, *Kgl. Ung. Palatin Joseph Univ. Tech. Wirtschaftswiss. Sopron.*, **8**, 194 (1936).
843. W. Schnorrenberg, *Aluminium*, **18**, 422 (1936).
844. H. Roehrig, *Z. Metallkunde*, **28**, 43 (1936).
845. P. I. Baranov, *Tsvetnye Met.*, **7/8**, 102 (1936); **9**, 86 (1936).
846. R. Irman, *Aluminium*, **19**, 635 (1937).
847. A. Vaeth, *Giesserei*, **25**, 177 (1938).
848. A. A. Botchvar and Wagana, *Sbornik Nauk Trud. Moscow Inst. Tsventnykh. Met.*, 1938, p. 45.
849. R. Irman, *Aluminiumguss in Sand und Kokille*, Akad. Verlag. Ges. m.b.H., Leipzig, 1939.
850. A. von Zeerleder, *Aluminium*, **21**, 192 (1939).
851. H. Kostron, *Z. Metallkunde*, **31**, 14 (1939).
852. P. Brenner and A. Roth, *Z. Metallkunde*, **32**, 10 (1940).
853. T. Tanabe and H. Nakata, *Nippon Kinzoku Gakkai Shi*, **9**, 290 (1940).
854. W. Helling and H. Schick, *Aluminium*, **22**, 223 (1940).
855. Parker, *J. Inst. Metals*, **67**, 101 (1941).

### Working

856. G. Sachs and E. Schiebolt, *Z. Ver. deut. Ing.*, **17**, 1557, 1601 (1925).
857. E. Seids and E. Schiebolt, *Z. Metallkunde*, **17**, 221 (1925).
858. V. Goler and G. Sachs, *Z. Physik*, **41**, 873, 889 (1927).
859. E. Seidl, *Mining and Met.*, **8**, 454 (1927).
860. H. Stendel, *Z. Metallkunde*, **19**, 129 (1927).
861. G. S. Shdanow and L. Altshuler, *Z. Techn. Fiziki*, **3**, 1331 (1933).
862. H. A. J. Stelljes, *Aluminium*, **18**, 601 (1936); **21**, 297 (1939).

863. E. Sceil and Siebert, *Z. Metallkunde*, **32**, 288 (1940).  
864. T. Tanabe and H. Nakata, *Nippon Kinzoku Gakkai Shi*, **10**, 324 (1940).

### Heat Treatment

865. Anon., *J. Ind. Eng. Chem.*, **11**, 155 (1919).  
866. L. Guillet, *Compt. Rend.*, **173**, 979 (1921).  
867. E. Wetzel, *Mitt. Kaiser Wilhelm Inst. Metallforschung.*, **1**, 24 (1922).  
868. I. Iytaka, *J. Chem. Ind. Jap.*, **27**, 61 (1924).  
869. A. Lennartz and W. Henninger, *Z. Metallkunde*, **18**, 213 (1926).  
870. N. F. Bugden, *The Heat Treatment and Annealing of Aluminium and Its Alloys*, Chapman & Hall, London, 1932.  
871. H. H. Richardson, *Aluminium*, **5**, 166 (1936).  
872. M. I. Zamotorin and G. N. Pokrovskaya, *Metallurg*, 1938, p. 114.  
873. C. Panseri and L. Monticelli, *Alluminio*, **8**, 183 (1939).  
874. I. Obinata and Tabata, *Nippon Kinzoku Gakkai Shi*, **10**, 324 (1940).

### Age Hardening

875. F. Wilm, *Metallurgie*, **8**, 225 (1911).  
876. P. D. Merica, R. G. Waltenburg, and V. H. Scott, *Trans. A.I.M.E.*, **64**, 3 (1920).  
877. W. Fraenkel and Seng, *Z. Metallkunde*, **12**, 225 (1920).  
878. W. Fraenkel, *Z. Metallkunde*, **12**, 427 (1920).  
879. T. Kikuta, *Sci. Rep. Tôhoku Univ.*, **10**, 139 (1921).  
880. Z. Jeffries and R. S. Archer, *Chem. Met. Eng.*, **24**, 1057 (1921); **26**, 449 (1922).  
881. W. Fraenkel and E. Scheuer, *Z. Metallkunde*, **14**, 49, 111 (1922).  
882. P. D. Merica, *Chem. Met. Eng.*, **26**, 881 (1922).  
883. S. Konno, *Sci. Rep. Tôhoku Univ.*, **11**, 4, 269 (1922).  
884. P. Chevenard and A. Portevin, *Compt. rend.*, **176**, 296 (1923); *J. Inst. Metals*, **30**, 329 (1923).  
885. P. Portevin and H. Le Chatelier, *Compt. rend.*, **176**, 311 (1923).  
886. G. Igarasi, *Sci. Rep. Tôhoku Univ.*, **12**, 333 (1923).  
887. K. L. Meissner, *Z. Ges. Giesserei-Praxis: Das Metall*, **46**, 209 (1925).  
888. T. Tanabe, *Tetsu-to-Hagane*, [6] **11**, 437 (1925).  
889. W. Fraenkel, *Z. Metallkunde*, **18**, 189 (1926).  
890. E. Schmid and G. Wassermann, *Naturwissenschaften*, **14**, 980 (1926).  
891. W. Kroll, *Metall u. Erz*, **23**, 555 (1926).  
892. E. H. Dix and H. H. Richardson, *Trans. A.I.M.E.*, **73**, 560 (1926).  
893. R. S. Archer, *Trans. Am. Soc. Steel Treat.*, **10**, 718 (1926).  
894. W. Guertler, *Z. Metallkunde*, **19**, 488 (1927).  
895. H. Nishimura, *Mem. Coll. Eng. Kyoto Imp. Univ.*, **5**, 61 (1927).  
896. P. Chevenard and A. Portevin, *Compt. rend.*, **186**, 144 (1928).  
897. R. Hay, *Met. Ind. London*, **32**, 12 (1928).  
898. K. L. Meissner, *Z. Metallkunde*, **20**, 16 (1928).  
899. E. Schmid and G. Wassermann, *Metallwirtschaft*, **7**, 1329 (1928).  
900. M. L. V. Gayler and G. D. Preston, *J. Inst. Metals*, **41**, 191 (1929).  
901. A. Portevin, P. Chevenard, and X. Waché, *J. Inst. Metals*, **42**, 337 (1929).  
902. W. Fraenkel and L. Marx, *Z. Metallkunde*, **21**, 2 (1929).  
903. H. Bohner, *Aluminium*, **1**, 30 (1929).  
904. M. Haas and H. Hecker, *Z. Metallkunde*, **21**, 166 (1929).  
905. F. Goeler and G. Sachs, *Metallwirtschaft*, **8**, 671 (1929); *Naturwissenschaften*, **17**, 309 (1929); *Z. Metallkunde*, **22**, 142 (1930).



906. L. Guillet and M. Ballay, *Rev. Met.*, **27**, 398 (1930); *Compt. rend.*, **190**, 1473 (1930).
907. N. Ageew, M. Hansen, and G. Sachs, *Z. Physik*, **66**, 350 (1930).
908. G. Wassermann, *Z. Metallkunde*, **21**, 160 (1930).
- 908b. E. Schmid and G. Wassermann, *Metallwirtschaft*, **9**, 421 (1930).
909. K. L. Meissner, *Metallwirtschaft*, **9**, 661 (1930); *J. Inst. Metals*, **44**, 207 (1930).
910. G. Tammann, *Z. Metallkunde*, **22**, 78 (1930).
911. A. Portevin and P. Chevenard, *Compt. rend.*, **192**, 252 (1930); *Rev. Met.*, **27**, 412 (1930).
912. W. Fraenkel, *Z. Metallkunde*, **22**, 84 (1930).
913. S. Kokubo, *Kinzoku-no-Kenkyu*, **7**, 343 (1930).
914. S. Kokubo and K. Honda, *Sci. Rep. Tôhoku Univ.*, **19**, 365 (1930); *J. Inst. Metals*, **47**, 266 (1931).
915. S. Kokubo, *Sci. Rep. Tôhoku Univ.*, **20**, 268 (1931).
916. W. Fraenkel, *Z. Metallkunde*, **23**, 72 (1931).
917. R. F. Mehl and C. S. Barrett, *Trans. A.I.M.E.*, **93**, 78 (1931).
918. J. Hengstenberg and G. Wassermann, *Z. Metallkunde*, **23**, 114 (1931).
919. W. Stenzel and J. Weerts, *Z. Metallkunde*, **24**, 139 (1932).
920. R. S. Mehl, C. S. Barrett, and F. N. Rhines, *Trans. A.I.M.E.*, **99**, 203 (1932).
921. R. Hay, *J. Roy. Tech. Coll. Glasgow*, **4**, 601 (1932).
922. K. L. Meissner, *Z. Metallkunde*, **24**, 88 (1932).
923. Y. Matsuyama, *Sci. Rep. Tôhoku Univ.*, **21**, 242 (1932).
924. M. L. V. Gayler and G. D. Preston, *J. Inst. Metals*, **48**, 197 (1932).
925. P. D. Merica, *Trans. A.I.M.E.*, **99**, 13 (1932).
926. H. Roehrig, *Z. Metallkunde*, **24**, 231 (1932).
927. W. Fraenkel and R. Hahn, *Z. Metallkunde*, **25**, 185 (1933).
928. W. Fraenkel, *Metallwirtschaft*, **12**, 582 (1933).
929. H. O'Neil, *Phil. Mag.*, **16**, 913 (1933).
930. G. Masing and W. Koch, *Z. Metallkunde*, **25**, 137 (1933).
931. W. Stenzel and J. Weerts, *Metallwirtschaft*, **12**, 353 (1933).
932. G. V. Akimov and A. S. Oleshko, *Z. Tech. Fizichi*, **4**, 547 (1934).
933. J. L. Burns, *Trans. Am. Soc. Metals*, **22**, 728 (1934).
934. H. Auer and W. Gerlach, *Metallwirtschaft*, **13**, 871 (1934).
935. A. Phillips and R. M. Bricks, *Trans. A.I.M.E.*, **111**, 94 (1934).
936. E. Soenchen, *Metallwirtschaft*, **13**, 655 (1934); **14**, 205 (1935).
937. G. Wassermann and J. Weerts, *Metallwirtschaft*, **14**, 605 (1935).
938. P. L. Teed, *J. Inst. Metals*, **58**, 113 (1936).
939. H. Auer, *Z. Metallkunde*, **28**, 164 (1936).
940. H. Kosaki, *Kinzoku-no-Kenkyu*, [8] **13**, 342 (1936).
941. W. Swietolawski and J. Czocharlski, *Wiadamosci Inst. Metallurgii i Metaloznawstwa*, **3**, 59 (1936).
942. W. L. Fink and D. W. Smith, *Trans. A.I.M.E.*, **122**, 284 (1936).
943. H. Lay, *Z. Metallkunde*, **28**, 376 (1936).
944. S. Kokubo, *Sci. Rep. Tôhoku Univ.*, **Honda**, 694 (1936).
945. S. M. Voronv and I. A. Deutsch, *Aviopromishlemnost*, [5] **6**, 22 (1937); [6] 29 (1937).
946. H. Nishimura, *Nippon Kinzoku Gakkai Shi*, **1**, 59 (1937).
947. M. L. V. Gayler, *J. Inst. Metals*, **60**, 249 (1937).
948. R. Becker, *Z. Metallkunde*, **29**, 245 (1937).
949. P. Brenner and H. Kostron, *Z. Metallkunde*, **29**, 374 (1937).

950. R. Michaud, *Compt. rend.*, **205**, 1399 (1937).
951. M. Cohen, *Trans. A.I.M.E.*, **124**, 113 (1937).
952. W. L. Fink and D. W. Smith, *Trans. A.I.M.E.*, **124**, 162 (1937); **128**, 233 (1938).
953. G. D. Preston, *Proc. Roy. Soc. (London)*, **A167**, 526 (1938); *Nature*, **142**, 569 (1938); *Phil. Mag.*, **26**, 855 (1938); *Proc. Phys. Soc.*, **52**, 77 (1940).
954. N. Swindell and C. Sykes, *Proc. Roy. Soc. (London)*, **A168**, 237 (1938).
955. G. Wassermann, *Z. Metallkunde*, **30**, 62 (1938).
956. W. Koester and A. Durer, *Z. Metallkunde*, **30**, 311 (1938).
957. W. Hartnagel, *Z. Metallkunde*, **30**, 81 (1938).
958. H. Nishimura, *Nippon Kinzoku Gakkai Shi*, **2**, 557 (1938).
959. W. Koester and K. Kam, *Z. Metallkunde*, **30**, 320 (1938).
960. P. Lacombe and G. Chaudron, *Compt. rend.*, **207**, 860 (1938).
961. A. Guinier, J. Calvet, P. Jacquet, *Compt. rend.*, **206**, 1641, 1972 (1938).
962. G. Shinoda, *Nippon Kinzoku Gakkai Shi*, **2**, 475 (1938); **3**, 211 (1939).
963. A. Guinier, J. Calvet, and P. Jacquet, *J. Inst. Metals*, **45**, 121 (1939); *Compt. rend.*, **208**, 1903 (1939).
964. P. Lacombe and G. Chaudron, *Compt. rend.*, **208**, 1731 (1939); **209**, 306 (1939).
965. M. Cohen, *Trans. A.I.M.E.*, **133**, 95 (1939).
966. H. Sawamoto, *Suiyokwai-Shi*, **9**, 821 (1939).
967. K. L. Dreyer, *Z. Metallkunde*, **31**, 147 (1939).
968. L. Guillet and L. Guillet, Jr., *Compt. rend.*, **209**, 79 (1939).
969. M. L. V. Gayler, *Proc. Roy. Soc. (London)*, **A173**, 83 (1939).
970. H. Nishimura, *Nippon Kinzoku Gakkai Shi*, **3**, 108 (1939).
971. K. Honda, *Nippon Kinzoku Gakkai Shi*, **3**, 359 (1939).
972. J. Calvet and P. Jacquet, *J. Inst. Metals*, **65**, 121 (1939).
973. H. Kostron, *Aluminium*, **21**, 687 (1939); *Z. Metallkunde*, **31**, 329 (1939).
974. P. Brenner and H. Kostron, *Z. Metallkunde*, **31**, 89 (1939).
975. M. Hansen and K. L. Dreyer, *Z. Metallkunde*, **31**, 204 (1939).
976. R. W. Lindsay and J. T. Norton, *Trans. A.I.M.E.*, **133**, 111 (1939).
977. H. J. Seemann, *Aluminium*, **21**, 588 (1939).
978. H. Auer and W. Gerlach, *Naturwissenschaften*, **27**, 299 (1939).
979. V. G. Kuznetsov and E. S. Makarov, *Doklady Akad. Nauk U.S.S.R.*, **23**, 245 (1939).
980. W. L. Fink, D. W. Smith, and L. A. Willey, *Am. Soc. Metals, Age Hardening of Metals*, Tower Press, Cleveland, Ohio, 1940.
981. H. Y. Hunsicker, *Am. Soc. Metals, Age Hardening of Metals*.
982. R. F. Mehl and L. K. Jetter, *Am. Soc. Metals, Age Hardening of Metals*.
983. C. H. Samans, *Trans. A.I.M.E.*, **137**, 85 (1940).
984. W. L. Fink and D. W. Smith, *Trans. A.I.M.E.*, **137**, 95 (1940).
985. M. L. V. Gayler, *J. Inst. Metals*, 1940, pp. 67 and 311.
986. F. R. N. Nabarro, *Proc. Roy. Soc. (London)*, **A175**, 519 (1940).
987. F. R. N. Nabarro, *Proc. Phys. Soc.*, **52**, 90 (1940).
988. F. R. N. Nabarro and N. F. Mott, *Proc. Phys. Soc.*, **52**, 86 (1940).
989. U. Asakura, *Nippon Kinzoku Gakkai Shi*, **4**, 304 (1940).
990. C. S. Barrett, A. H. Geisler, R. F. Mehl, *Trans. A.I.M.E.*, **143**, 134 (1941).

### Corrosion and Cladding

991. G. W. Akimov and A. S. Oleshko, *Z. Fiz. Khim.*, **5**, 434 (1934).
992. A. Burkhardt and G. Sachs, *Metallwirtschaft*, **14**, 1 (1935).

- 993. F. Bollenhart and H. Groeber, *Aluminium*, **19**, 349 (1937).
- 994. P. Lacombe and E. Laurent, *Métaux et corrosion*, 1938, p. 216.
- 995. M. Bosshard and H. Hug, *Aluminium*, **20**, 389 (1938).
- 996. P. Brenner, *Aluminium*, **21**, 846 (1939).
- 997. T. Nishihara and T. Kori, *Trans. Soc. Mech. Eng. Japan*, 1939, p. 89.
- 998. M. Bosshard, *Schweiz. Arch.*, **10**, 265 (1940).
- 999. P. Brenner, *Metallwirtschaft*, **19**, 283, 1272 (1940).
- 1000. E. H. Dix, *Trans. A.I.M.E.*, **137**, 11 (1940).
- 1001. H. U. Von Vogel, *Korrosion u. Metallschutz*, **16**, 259 (1940).
- 1002. H. L. Logan, *U. S. Bureau of Standards, Sci. Pap.* 1378, 1941.
- 1003. H. Kostron, *Aluminium*, **23**, 195 (1941).
- 1004. W. Huenlich, *Aluminium*, **23**, 86 (1941).

## INDEX

- Age hardening, 302
  - etching for detection, 169
  - practice, *see* specific alloy
- Alumina, 155
- Aluminum, commercial, 237
- Ammonium persulfate, 167
- Annealing, 297
- Antimony, alloys containing, 232, 240
  - equilibrium diagram, 37
- Antimony-bismuth, equilibrium diagram, 58
- Antimony-copper, equilibrium diagram, 85
- Antimony-lead, equilibrium diagram, 117
- Antimony-magnesium, equilibrium diagram, 103
- Antimony-silicon, equilibrium diagram, 118
- Antimony-tin, equilibrium diagram, 119
- Arsenic, equilibrium diagram, 2
- Artificial aging, 302
  - etching for detection, 169
  - practice, *see* specific alloy
- Barium, equilibrium diagram, 6
- Beryllium, equilibrium diagram, 7
- Beryllium-magnesium, equilibrium diagram, 56
- Beryllium-silicon, equilibrium diagram, 57
- Bichromate etching reagent, 150
- Bismuth, alloys containing, 217
  - constituent, 174
  - equilibrium diagram, 8
- Bismuth-antimony, equilibrium diagram, 58
- Bismuth-silver, equilibrium diagram, 53
- Bismuth-tin, equilibrium diagram, 59
- Blistering, 309
  - in clad material, 313
- Boron, equilibrium diagram, 4
- Buffing polishing, 158
- Cadmium, equilibrium diagram, 10
- Cadmium-magnesium, equilibrium diagram, 63
- Cadmium-tin, equilibrium diagram, 64
- Cadmium-zinc, equilibrium diagram, 65
- Caesium, equilibrium diagram, 15
- Calcium, equilibrium diagram, 9
- Calcium-nickel, equilibrium diagram, 60
- Calcium-silicon, equilibrium diagram, 61
- Castability, *see* specific alloy
- Casting, die, 271
  - ingot, cold mold, 279
  - water-cooled, 280
  - permanent mold, 271
  - sand, 271
- Cerium, alloys containing, 260
  - equilibrium diagram, 11
- Cerium-iron, equilibrium diagram, 66
- Chromic acid, 166
- Chromium, alloys containing, 211, 214, 232, 240, 245, 260
  - constituents, 174
  - equilibrium diagram, 13
- Chromium alloys, master, 205
- Chromium-copper, equilibrium diagram, 69
- Chromium-iron, constituent, 183
  - equilibrium diagram, 70
- Chromium-iron-silicon, constituent, 196
- Chromium-magnesium, constituent, 183
  - equilibrium diagram, 71
- Chromium-nickel, equilibrium diagram, 73
- Chromium-silicon, constituent, 185
  - equilibrium diagram, 74
- Cladding, 310
  - blisters, 313
  - defective, 313
  - excessive diffusion, 313
- Cobalt, alloys containing, 229, 232
  - constituent, 174
  - equilibrium diagram, 12
- Cobalt alloys, master, 205
- Cobalt-copper, equilibrium diagram, 66

- Cobalt-iron, constituent, 183
  - equilibrium diagram, 66
- Cobalt-magnesium, equilibrium diagram, 67
- Cobalt-silicon, equilibrium diagram, 68
- Cobalt-silicon alloys, master, 210
- Columbium, alloys containing, 214, 260
  - equilibrium diagram, 10
- Columnar grain, 288
- Copper, alloys containing, 211, 214, 217, 220, 222, 226, 232, 237, 245, 249, 257, 260
  - constituent, 176
  - equilibrium diagram, 16
- Copper alloys containing 4-6% Cu, 217
  - 6-8% Cu, 214
  - more than 10% Cu, 211
  - effect of annealing, 212, 297
  - casting, 212, 215, 217, 271
  - extrusion, 219
  - solution treatment, 298
  - master, 203
  - oxide inclusions, 296
  - shrinkage, 279
- Copper-antimony, equilibrium diagram, 85
- Copper chloride, 145
- Copper-chromium, equilibrium diagram, 69
- Copper-cobalt, equilibrium diagram, 66
- Copper-iron, constituent, 185
  - equilibrium diagram, 75
- Copper-iron alloys, master, 210
- Copper-iron-manganese, constituent, 196
  - equilibrium diagram, 123
- Copper-iron-nickel, constituent, 196
- Copper-iron-silicon, constituent, 198
  - equilibrium diagram, 123
- Copper-lead, equilibrium diagram, 84
- Copper-magnesium, constituents, 186
  - equilibrium diagram, 77
- Copper-magnesium-nickel, equilibrium diagram, 131
- Copper-magnesium-silicon, constituent, 198
  - equilibrium diagram, 132
- Copper-magnesium-zinc, equilibrium diagram, 138
- Copper-manganese, constituent, 189
  - equilibrium diagram, 79
- Copper-manganese alloys, master, 207
- Copper-nickel, constituent, 189
  - equilibrium diagram, 82
- Copper-nickel alloys, defective forging, 284
  - effect of casting, 258, 261, 269
  - extrusion, 290
  - solution treatment, 299
  - eutectic melting, 305
  - high iron, 260
  - intergranular corrosion, 310
  - low iron, 257
  - porosity, 289
  - segregation, 277, 283
  - shrinkage, 279
  - successive etchings, 172
- Copper-silicon, equilibrium diagram, 86
- Copper-silicon alloys, 220
  - effect of casting, 221
- Copper-silver, equilibrium diagram, 54
- Copper-tin, equilibrium diagram, 87
- Copper-titanium, equilibrium diagram, 88
- Copper-tungsten, equilibrium diagram, 89
- Copper-zinc, equilibrium diagram, 89
- Copper-zinc alloys, 222
- Corrosion, 159, 310
- Corrosion resistance, *see* specific alloy
- Cracks, 269, 279, 288, 289
  - etching, 147
- Defective heat treatment, 302
- Defective polishing, 156
- Die casting, 271
- Diffusion in clad, 313
- Duralumin, blistering, 309
  - cladding, 313
  - defective, 313
  - corrosion, 159, 310
  - cracks, 289
  - defects from extrusion, 294
  - effect of annealing, 298
  - casting, 280
  - extrusion, 252, 290
  - rolling, 255, 290
  - solution treatment, 298
  - etching, 169
  - eutectic melting, 305
  - hardening constituent  $\text{Cu}_2\text{Mg}_2\text{Al}_5$ , 250
  - $\text{CuAl}_2 + \text{Mg}_2\text{Si}$ , 252
  - $\text{CuMg}_5\text{Si}_4\text{Al}_4$ , 254

- Duralumin, high temperature deterioration, 305  
incomplete solution, 302  
intergranular corrosion, 159, 310  
inverse segregation, 283  
effect on rolling, 288  
oxide inclusions, 269  
effect on rolling, 269  
pitting corrosion, 159, 310  
segregation, 283  
effect on extrusion, 283  
twinning, 289
- Electrolytic polishing, 162
- Etching characteristics, table, 200
- Etching reagent, for checking heat treatment, 165  
for detection of precipitate in aging, 169  
for grain size examination, 142 ff., 167, 168  
for iron constituents, 166  
for macro-etching, 142 ff.  
for silicon alloys, 145  
selection of, 169
- Eutectic melting, 305
- Excessive diffusion in clad, 313
- Extrusion, 290  
defects, 294
- Ferric nitrate, 165
- Ferrocyanide solution, 166
- Ferrous sulfate, 165
- Fiber direction, etching, 147
- Flick's solution, for macro-etching, 143  
for micro-etching, 168
- Forging, 290  
defective, 294
- Gallium, equilibrium diagram, 20
- Gas inclusions, 266
- Germanium, equilibrium diagram, 20
- Germanium-magnesium, equilibrium diagram, 99
- Gold, equilibrium diagram, 3
- Grain, columnar, 288  
effect of annealing, 298  
extrusion, 294  
working, 290  
large, 288  
refining, 47
- Grain size, macro-etching, 145, 147  
micro-etching, 167, 188
- Grinding polishing, 151
- Heat treatment, etching reagent for checking, 165  
practice, *see* specific alloy
- High temperature deterioration, 305
- Hume-Rothery's reagent, 145
- Hydrofluoric acid, for macro-etching, 143  
for micro-etching, 168
- Inclusions, gas, 266  
oxide, 266, 294  
effect on rolling, 269
- Incomplete solution, 302
- Ingot casting, cold mold, 279  
water-cooled, 280
- Intergranular corrosion, 159, 310
- Inverse segregation, 283  
effect on rolling, 288
- Iron, alloys containing, 211, 214, 217, 220, 222, 226, 229, 232, 237, 240, 243, 247, 249, 257, 260  
constituents, 179  
equilibrium diagrams, 18
- Iron alloys, master, 207
- Iron-cerium, equilibrium diagram, 66
- Iron-chromium, constituent, 183  
equilibrium diagram, 70
- Iron-cobalt, constituent, 183  
equilibrium diagram, 66
- Iron-chromium-silicon, constituent, 196
- Iron-copper, constituent, 185  
equilibrium diagram, 75
- Iron-copper alloys, master, 210
- Iron-copper-manganese, constituent, 196  
equilibrium diagram, 123
- Iron-copper-nickel, constituent, 196
- Iron-copper-silicon, constituent, 198  
equilibrium diagram, 123
- Iron-magnesium, equilibrium diagram, 90
- Iron-magnesium-silicon, constituent, 198  
equilibrium diagram, 139
- Iron-manganese, constituent, 191  
equilibrium diagram, 92
- Iron-manganese-silicon, constituents, 198  
equilibrium diagram, 139
- Iron-nickel, constituent, 191

- Iron-nickel, equilibrium diagram, 93
- Iron-silicon, constituents, 191
  - equilibrium diagram, 95
- Iron-titanium, equilibrium diagram, 97
- Iron-zinc, equilibrium diagram, 98
- Keller's etching reagent, 168
- Lanthanum, equilibrium diagram, 23
- Lead, alloys containing, 211, 214, 217, 232
  - constituent, 174
  - equilibrium diagram, 33
- Lead-antimony, equilibrium diagram, 117
- Lead-copper, equilibrium diagram, 84
- Lead-magnesium, equilibrium diagram, 102
- Lead-silver, equilibrium diagram, 55
- Lead-tin, equilibrium diagram, 117
- Liquation, 283
  - effect on rolling, 288
- Lithium, equilibrium diagram, 24
- Lithium-silicon, equilibrium diagram, 99
- Machinability, *see* specific alloy
- Macro-etching, 142
- Macro-examination, preparation of the surface, 140
  - etching, 142
- Magnesia, 156
- Magnesium, alloys containing, 211, 222, 229, 232, 240, 245, 249, 257, 260
  - constituent, 179
  - equilibrium diagram, 25
- Magnesium alloys, 240
  - effect of annealing, 298
  - casting, 241, 275
    - extrusion, 241
  - eutectic melting, 305
  - high temperature deterioration, 305
  - intergranular corrosion, 310
  - master, 207
  - oxide inclusions, 269
  - segregation, 277
- Magnesium-antimony, equilibrium diagram, 103
- Magnesium-beryllium, equilibrium diagram, 56
- Magnesium-cadmium, equilibrium diagram, 63
- Magnesium-chromium, constituent, 183
  - equilibrium diagram, 71
- Magnesium-cobalt, equilibrium diagram, 67
- Magnesium-copper, constituents, 186
  - equilibrium diagram, 77
- Magnesium-copper-nickel, equilibrium diagram, 131
- Magnesium-copper-silicon, constituent, 198
  - equilibrium diagram, 132
- Magnesium-copper-zinc, equilibrium diagram, 138
- Magnesium-germanium, equilibrium diagram, 99
- Magnesium-iron, equilibrium diagram, 90
- Magnesium-iron-silicon, constituent, 198
  - equilibrium diagram, 139
- Magnesium-lead, equilibrium diagram, 102
- Magnesium-manganese, equilibrium diagram, 100
- Magnesium-nickel, equilibrium diagram, 101
- Magnesium silicide alloys, 245
  - effect of rolling, 290
  - solution treatment, 298
- Magnesium-silicon, constituent, 181
  - equilibrium diagram, 104
- Magnesium-silicon-zinc, equilibrium diagram, 139
- Magnesium-silver, equilibrium diagram, 54
- Magnesium-zinc, constituents, 183, 193
  - equilibrium diagram, 107
- Magnesium-zinc alloys, 240
  - effect of extrusion, 241
- Manganese, alloys containing, 211, 214, 222, 229, 232, 240, 245, 247, 249
  - constituents, 181
  - equilibrium diagram, 28
- Manganese alloys, 247
  - effect of rolling, 247
  - master, 205
  - pitting corrosion, 310
- Manganese-copper, constituent, 189
  - equilibrium diagram, 79
- Manganese-copper alloys, master, 207

- Manganese-copper-iron, constituent, 196  
     equilibrium diagram, 123  
 Manganese-iron, constituent, 191  
     equilibrium diagram, 92  
 Manganese-iron-silicon, constituents, 198  
     equilibrium diagram, 139  
 Manganese-magnesium, equilibrium diagram, 100  
 Manganese-silicon, constituents, 193 ff.  
     equilibrium diagram, 110  
 Manganese-tin, equilibrium diagram, 112  
 Mechanical properties, *see* specific alloys  
 Mercury, equilibrium diagram, 21  
 Modification, 32, 41, 113, 266 ff.  
     defective, 269  
 Molybdenum, alloys containing, 211,  
     214, 232, 260  
     equilibrium diagram, 30  
 Mounting specimen, 152  
  
 Neodimium, equilibrium diagram, 32  
 Nickel, alloys containing, 211, 214, 222,  
     229, 232, 240, 257, 260  
     constituent, 181  
     equilibrium diagram, 32  
 Nickel alloys, master, 205  
 Nickel-calcium, equilibrium diagram, 60  
 Nickel-chromium, equilibrium diagram,  
     73  
 Nickel-copper, constituents, 189  
     equilibrium diagram, 82  
 Nickel-copper alloys, *see* copper-nickel  
     alloys  
 Nickel-copper-iron, constituent, 196  
 Nickel-copper-magnesium, equilibrium  
     diagram, 131  
 Nickel-iron, constituent, 191  
     equilibrium diagram, 93  
 Nickel-magnesium, equilibrium diagram,  
     101  
 Nickel-silicon, equilibrium diagram, 113  
 Nickel-silicon alloys, master, 210  
 Nickel-tin, equilibrium diagram, 115  
 Nickel-zinc, equilibrium diagram, 116  
 Niobium, equilibrium diagram, 10  
 Nitric acid, for macro-etching, 143  
     for micro-etching, 164  
  
 Oxide inclusions, 266, 294  
     effect on rolling, 269  
  
 Panseri's solution, 168  
 Permanent mold casting, 271  
 Phosphoric acid, 166  
 Picric acid, 166  
 Pinhole porosity, 266, 279  
 Pitting corrosion, 159, 310  
 Platinum, equilibrium diagram, 35  
 Porosity, 266, 279, 289  
     etching, 147  
 Potassium, equilibrium diagram, 22  
 Praseodymium, equilibrium diagram, 34  
 Properties of alloys, *see* specific alloy  
  
 Rolling, 290  
     effect of inclusions, 269  
 Rubidium, equilibrium diagram, 36  
  
 Sand casting, 271  
 Selection of etching reagent, 169  
 Segregation, 275, 283  
     effect on extrusion, 283  
     inverse, 283  
     effect on rolling, 288  
     macro-etching, 143  
 Selenium, equilibrium diagram, 38  
 Shrinkage, 278  
 Silicon, alloys containing, 211, 214, 217,  
     220, 222, 226, 229, 232, 237, 240,  
     245, 247, 249, 257, 260  
     constituent, 174  
     equilibrium diagram, 39  
 Silicon alloys, containing Cu, Mg, etc.,  
     232  
     Mg, 229  
     effect of annealing, 298  
     casting, 227, 229, 233, 271  
     solution treatment, 298  
     eutectic melting, 305  
     macro-etching, 145  
     master, 203  
     modification, 32, 41, 113, 226 ff.  
     defective, 269  
     oxide inclusions, 269  
     segregation, 277  
     straight, 226  
 Silicon-antimony, equilibrium diagram,  
     118  
 Silicon-beryllium, equilibrium diagram,  
     57  
 Silicon-calcium, equilibrium diagram, 61



- Silicon-chromium, constituent, 185
  - equilibrium diagram, 74
- Silicon-cobalt, equilibrium diagram, 68
- Silicon-cobalt alloys, master, 210
- Silicon-copper, equilibrium diagram, 86
- Silicon-copper alloys, 220
  - effect of casting, 221
- Silicon-copper-iron, constituent, 198
  - equilibrium diagram, 123
- Silicon-copper-magnesium, constituent, 198
  - equilibrium diagram, 132
- Silicon-iron, constituents, 191
  - equilibrium diagram, 95
- Silicon-chromium-iron, constituent, 196
- Silicon-iron-magnesium, constituent, 198
  - equilibrium diagram, 139
- Silicon-iron, manganese, constituents, 198
  - equilibrium diagram, 139
- Silicon-lithium, equilibrium diagram, 99
- Silicon-magnesium, constituent, 181
  - equilibrium diagram, 104
- Silicon-magnesium-zinc, equilibrium diagram, 139
- Silicon-manganese, constituents, 193 ff.
  - equilibrium diagram, 110
- Silicon-nickel, equilibrium diagram, 113
- Silicon-nickel alloys, master, 210
- Silicon-silver, equilibrium diagram, 56
- Silicon-sodium, equilibrium diagram, 113
- Silicon-thorium, equilibrium diagram, 121
- Silicon-tin, equilibrium diagram, 120
- Silicon-zinc, equilibrium diagram, 121
- Silver, equilibrium diagram, 1
- Silver-bismuth, equilibrium diagram, 53
- Silver-copper, equilibrium diagram, 54
- Silver-lead, equilibrium diagram, 55
- Silver-magnesium, equilibrium diagram, 54
- Silver-silicon, equilibrium diagram, 56
- Silver-zinc, equilibrium diagram, 56
- Sodium, equilibrium diagram, 31
- Sodium hydroxide, for macro-etching, 142
  - for micro-etching, 167
- Sodium-silicon, equilibrium diagram, 113
- Solution, incomplete, 302
- Solution treatment, 298
  - Solution treatment, etching reagent for checking, 165
    - practice, *see* specific alloy
  - Stabilization, 297
  - Strontium, equilibrium diagram, 42
  - Successive etching, 172
  - Sulfuric acid, 165
- Table of etching characteristics, 200
- Tantalum, equilibrium diagram, 43
- Tellurium, equilibrium diagram, 44
- Thallium, equilibrium diagram, 47
- Thorium, equilibrium diagram, 44
- Thorium-silicon, equilibrium diagram, 121
- Three acids mixture, for macro-etching, 143
  - for micro-etching, 168
- Tin, alloys containing, 211, 214, 217, 232
  - equilibrium diagram, 41
- Tin-antimony, equilibrium diagram, 119
- Tin-bismuth, equilibrium diagram, 59
- Tin-cadmium, equilibrium diagram, 64
- Tin-copper, equilibrium diagram, 87
- Tin-lead, equilibrium diagram, 117
- Tin-manganese, equilibrium diagram, 112
- Tin-nickel, equilibrium diagram, 115
- Tin-silicon, equilibrium diagram, 120
- Tin-zinc, equilibrium diagram, 122
- Titanium, alloys containing, 211, 214, 217, 226, 232, 237, 240, 260
  - constituent, 181
    - equilibrium diagram, 45
- Titanium alloys, master, 207
- Titanium-copper, equilibrium diagram, 88
- Titanium-iron, equilibrium diagram, 97
- Tungsten, equilibrium diagram, 49
- Tungsten-copper, equilibrium diagram, 89
- Twinning, 289
- Uranium, equilibrium diagram, 48
- Uses of alloys, *see* specific alloy
- Vanadium, alloys containing, 211, 214, 232, 237
  - equilibrium diagram, 48
- Vanadium alloys, master, 207

- Vanadium alloys, oxide inclusions, 269  
Vilella's etching reagent, 168  
Yttrium, equilibrium diagram, 50  
Zinc, alloys containing, 211, 214, 217, 222, 232, 240  
    equilibrium diagram, 50  
Zinc-cadmium, equilibrium diagram, 65  
Zinc-copper, equilibrium diagram, 89  
Zinc-copper alloys, 222  
Zinc-copper-magnesium, equilibrium diagram, 138  
Zinc-iron, equilibrium diagram, 98  
Zinc-magnesium, constituents, 183, 193  
    equilibrium diagram, 107  
Zinc-magnesium alloys, 240  
    effect of extrusion, 241  
Zinc-magnesium-silicon, equilibrium diagram, 139  
Zinc-nickel, equilibrium diagram, 116  
Zinc-silicon, equilibrium diagram, 121  
Zinc-silver, equilibrium diagram, 56  
Zinc-tin, equilibrium diagram, 122  
Zirconium, equilibrium diagram, 51











